frontiers

RESEARCH TOPICS

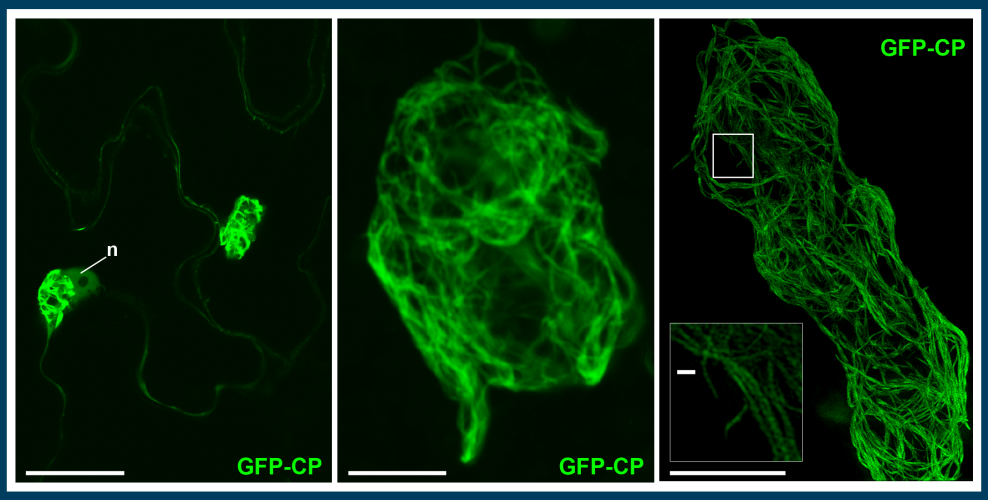

PLANT VIRUS INFECTION – A CELL BIOLOGY PERSPECTIVE

Topic Editors
Jean-François Laliberté, Peter Moffett, Helene Sanfacon, Aiming Wang, Richard Nelson and James Schoelz

frontiers in PLANT SCIENCE

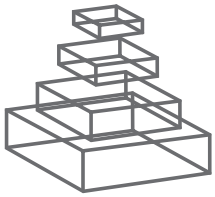

frontiers

ISSN 1664-8714
ISBN 978-2-88919-165-9
DOI 10.3389/978-2-88919-165-9

ABOUT FRONTIERS

Frontiers is more than just an open-access publisher of scholarly articles: it is a pioneering approach to the world of academia, radically improving the way scholarly research is managed. The grand vision of Frontiers is a world where all people have an equal opportunity to seek, share and generate knowledge. Frontiers provides immediate and permanent online open access to all its publications, but this alone is not enough to realize our grand goals.

FRONTIERS JOURNAL SERIES

The Frontiers Journal Series is a multi-tier and interdisciplinary set of open-access, online journals, promising a paradigm shift from the current review, selection and dissemination processes in academic publishing.
All Frontiers journals are driven by researchers for researchers; therefore, they constitute a service to the scholarly community. At the same time, the Frontiers Journal Series operates on a revolutionary invention, the tiered publishing system, initially addressing specific communities of scholars, and gradually climbing up to broader public understanding, thus serving the interests of the lay society, too.

DEDICATION TO QUALITY

Each Frontiers article is a landmark of the highest quality, thanks to genuinely collaborative interactions between authors and review editors, who include some of the world's best academicians. Research must be certified by peers before entering a stream of knowledge that may eventually reach the public - and shape society; therefore, Frontiers only applies the most rigorous and unbiased reviews.
Frontiers revolutionizes research publishing by freely delivering the most outstanding research, evaluated with no bias from both the academic and social point of view.
By applying the most advanced information technologies, Frontiers is catapulting scholarly publishing into a new generation.

WHAT ARE FRONTIERS RESEARCH TOPICS?

Frontiers Research Topics are very popular trademarks of the Frontiers Journals Series: they are collections of at least ten articles, all centered on a particular subject. With their unique mix of varied contributions from Original Research to Review Articles, Frontiers Research Topics unify the most influential researchers, the latest key findings and historical advances in a hot research area!
Find out more on how to host your own Frontiers Research Topic or contribute to one as an author by contacting the Frontiers Editorial Office: researchtopics@frontiersin.org

PLANT VIRUS INFECTION – A CELL BIOLOGY PERSPECTIVE

Topic Editors:
Jean-François Laliberté, Institut National de la Recherche Scientifique, Canada
Peter Moffett, Université de Sherbrooke, Canada
Helene Sanfacon, Pacific Agri-Food Research Centre, Agriculture and Agri-Food Canada, Canada
Aiming Wang, Agriculture and Agri-Food Canada, Canada
Richard Nelson, Samuel Roberts Noble Foundation, Inc., USA
James Schoelz, University of Missouri, USA

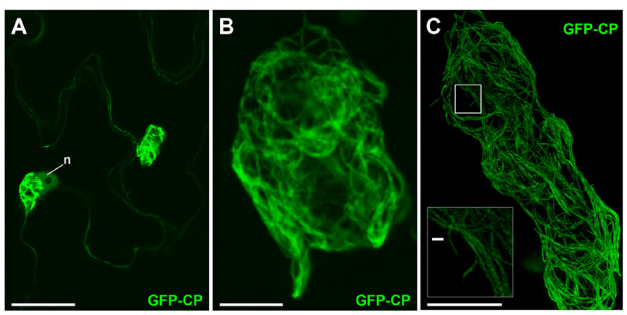

PVX virion "cages" encasing the X-body. Figure taken from Linnik O, Liesche J, Tilsner J and Oparka KJ (2013) Unraveling the structure of viral replication complexes at super-resolution. *Front. Plant Sci.* 4:6. doi: 10.3389/fpls.2013.00006.

It has long been known that viruses induce extensive remodeling of infected cells. These structural alterations include reshaping of large organelles (e.g., chloroplast, mitochondria), proliferation of membranes and membranous vesicles and modification of the plasmodesmata structure. These alterations have a profound impact on the plant physiology and development. However, it is only more recently that studies have investigated the biogenesis of virus-induced structures and their biological function(s).

The induction of cellular remodeling is conceivably the result of interactions between plant and virus components. A large body of recent literature has been focused on the study of these interactions at the molecular level; in particular, the interaction of viral proteins or nucleic acids with host factors (proteins, nucleic acids, carbohydrates, lipids and metabolites). Concurrent to these molecular studies, an avenue of investigation at the interface of molecular virology and plant cell biology has emerged. Techniques allowing easy expression of viral proteins or modified viral genomes in plants combined with powerful visualization tools (e.g., confocal microscopy, electron microscopy tomography) have shed a new light on the study of cellular remodeling in virus-infected plant cells. We now know that some of these

novel sub-cellular structures are virus-induced organelles or "factories" that house the RNA replication complex. Other morphological changes (e.g. membrane vesicles, alteration of the plasmodesmata, cell wall-associated tubular structures) are related to the intracellular and intercellular movement of the virus. Finally, induction of autophagosomes and modification of large organelles have been observed in association with the innate immune response.

A recent focus of plant virology is to dissect the molecular and cellular requirements that underlie the biogenesis of virus-induced structures. One avenue of research investigates how the host secretory pathway is involved in viral replication. The trafficking of viral entities from their site of origin to the plasmodesmata for cell-to-cell movement is another area of intensive research. Finally, one can forecast that the cellular biology of host defense responses (including the innate immune response and RNA silencing mechanisms) to be a rapidly developing field of investigation. Many challenges lie ahead. A high definition of viral factory architecture is required to better understand the interplay between virus replication and various cellular processes (e.g., translation). The dynamics and mechanisms of how these virus-induced structures are released from or integrated into host organelles need to be further investigated. It is with these issues in mind that we invite interested individuals to contribute their expertise for an encyclopedic coverage of this Research Topic. All types of contributions are welcomed. We need Original Research Articles and "State-of-the-Art" reviews, for instance on what plant viruses do to the host cell interior (either directly or indirectly) and what parallel can be made with other plant pathogens or with animal viruses. We want commentaries on important questions that have still not been addressed and how they can be answered. Technology is also an all-important component for any area of investigation and we wish to have "Technical Advances" articles describing the panoply of tools available to follow viruses from a cell biology perspective.

Table of Contents

06 ***E-Book on Plant Virus Infection - A Cell Biology Perspective***
Jean-François Laliberté, Peter Moffett, Hélène Sanfaçon, Aiming Wang, Richard S. Nelson and James E. Schoelz

08 ***Cytopathic Effects Incited by Viroid RNAs and Putative Underlying Mechanisms***
Francesco Di Serio, Angelo De Stradis, Sonia Delgado, Ricardo Flores and Beatriz Navarro

15 ***Hijack It, Change It: How do Plant Viruses Utilize the Host Secretory Pathway for Efficient Viral Replication and Spread?***
Camilo Patarroyo, Jean-François Laliberté and Huanquan Zheng

23 ***Investigating the Role of Viral Integral Membrane Proteins in Promoting the Assembly of Nepovirus and Comovirus Replication Factories***
Hélène Sanfaçon

30 ***The Cell Biology of Tobacco Mosaic Virus Replication and Movement***
Chengke Liu and Richard S. Nelson

40 ***Recent Advances in Research of Plant Virus Movement Mediated by Triple Gene Block***
Andrey G. Solovyev, Natalia O. Kalinina and Sergey Y. Morozov

48 ***Unraveling the Structure of Viral Replication Complexes at Super-Resolution***
Olga Linnik, Johannes Liesche, Jens Tilsner and Karl J. Oparka

61 ***Insights into Alternanthera Mosaic Virus TGB3 Functions: Interactions With Nicotiana Benthamiana PsbO Correlate With Chloroplast Vesiculation and Veinal Necrosis Caused by TGB3 Over-Expression***
Chanyong Jang, Eun-Young Seo, Jiryun Nam, Hanhong Bae, Yeong Guk Gim, Hong Gi Kim, In Sook Cho, Zee-Won Lee, Gary R. Bauchan, John Hammond and Hyoun-Sub Lim

76 ***The Potato Mop-Top Virus TGB2 Protein and Viral RNA Associate With Chloroplasts and Viral Infection Induces Inclusions in the Plastids***
Graham H. Cowan, Alison G. Roberts, Sean N. Chapman, Angelika Ziegler, Eugene I. Savenkov and Lesley Torrance

91 ***Role of Rice Stripe Virus NSvc4 in Cell-to-Cell Movement and Symptom Development in Nicotiana Benthamiana***
Yi Xu and Xueping Zhou

103 ***The Induction of Stromule Formation by a Plant DNA-Virus in Epidermal Leaf Tissues Suggests a Novel Intra- and Intercellular Macromolecular Trafficking Route***
Björn Krenz, Holger Jeske and Tatjana Kleinow

115 ***Cellular Chaperones and Folding Enzymes are Vital Contributors to Membrane Bound Replication and Movement Complexes During Plant RNA Virus Infection***
Jeanmarie Verchot

127 ***Virus-Induced ER Stress and the Unfolded Protein Response***
Lingrui Zhang and Aiming Wang

143 ***Genetic Recombination in Plant-Infecting Messenger-Sense RNA Viruses: Overview and Research Perspectives***
Jozef J. Bujarski

frontiers in
PLANT SCIENCE

EDITORIAL
published: 17 June 2013
doi: 10.3389/fpls.2013.00203

e-Book on plant virus infection—a cell biology perspective

Jean-François Laliberté[1]*, Peter Moffett[2], Hélène Sanfaçon[3], Aiming Wang[3], Richard S. Nelson[4] and James E. Schoelz[5]

[1] INRS-Institut Armand-Frappier, Institut National de la Recherche Scientifique, Laval, QC, Canada
[2] Département de biologie, Université de Sherbrooke, Sherbrooke, QC, Canada
[3] Pacific Agri-Food Research Centre, Agriculture and Agri-Food Canada, Summerland, BC, Canada
[4] Samuel Roberts Noble Foundation, Inc., Ardmore, OK, USA
[5] Division of Plant Sciences, University of Missouri, Columbia, MO, USA
*Correspondence: jean-francois.laliberte@iaf.inrs.ca

Edited by:
Mary B. Mudgett, Stanford University, USA

Plant viruses cause extensive remodeling of infected cells. These structural alterations include reshaping of large organelles (e.g., chloroplast, mitochondria, peroxisomes), proliferation of membranes and membranous vesicles and modification of the plasmodesmata (PD) structure. These alterations have a profound impact on plant physiology and development. However, it is only recently that studies have deeply investigated the biogenesis of virus-induced structures and their biological function(s).

Novel techniques that allow easy expression of viral proteins or modified viral genomes in plants combined with powerful visualization tools [e.g., confocal microscopy, electron microscopy (EM) tomography] offer a new perspective on cellular remodeling in virus-infected plant cells. We now know that some of these novel sub-cellular structures are virus-induced organelles or "factories" that house the RNA replication complex. Other morphological changes (e.g., membrane vesicles, alteration of the PD, cell wall-associated tubular structures) are related to the intracellular and intercellular movement of the virus. Finally, induction of autophagosomes and modification of large organelles have been observed in association with the innate immune response.

This e-Book on Plant Virus Infection—a Cell Biology Perspective aims at providing the latest information on the molecular and cellular requirements that underlie the biogenesis of these virus-induced structures.

First, we have a look at a non-virus pathogen: the viroid. In contrast to a virus, the viroid genome is composed of a tiny circular RNA (250–400 nt) that does not code for proteins. Nevertheless, viroid infections are accompanied by cellular and developmental disorders that sometimes have dramatic economic consequences, for instance the cadang-cadang disease of coconut palms. Di Serio et al. (2013) look at the cytopathic effects incited by viroid RNAs and propose mechanisms that may lead to these morphological changes.

"Hijack it, change it" is applicable to the description of many viral processes, given the propensity of viruses to commandeer the host machinery for their own purposes. In their review, Patarroyo et al. (2013) discuss this concept as applied to the secretory system. They provide an overview of the plant secretory pathway and discuss recent advances in our understanding of how viruses utilize and alter this system in order to permit such processes as replication, intra- and inter-cellular movement.

Sanfaçon (2013) summarizes the membrane-localization characteristics of proteins encoded by members of the *Secoviridae*, She further reviews and discusses literature demonstrating the ability of these proteins to induce membrane proliferation and perhaps alter membrane structure (e.g., curvature) and integrity (formation of pores through oligomerization) in the host cell. The membrane often targeted by these viral proteins is the endoplasmic reticulum.

In reviewing the latest cell biological studies describing tobacco mosaic virus (TMV) replication and movement, Liu and Nelson (2013) highlight how a divergent function of two orthologous proteins may explain different infection requirements by two tobamoviruses. The authors review the many publications showing influences or interactions of proteins encoded by TMV as infections develop. The complexity of the interactions and their proposed functions for just this one virus are striking. The findings from multiple laboratories strongly suggest that the host membrane is a primary vehicle for tobamovirus intercellular movement and that the cytoskeleton has a role in modulating movement for only some members. A theory that cytoskeletal-dependent trafficking of a TMV complex from the PD is necessary for TMV, but not the related *Turnip vein clearing virus* is presented.

The triple gene block (TBG) proteins are the focus of several contributions. First, Solovyev et al. (2012) introduce the reader to the complex story of viral cell-to-cell movement mediated by TGB proteins of potex- and hordei-like viruses. The authors provide links between virus cell-to-cell trafficking and replication, silencing suppression, virus systemic spread over the plant, and the roles of the nucleus in plant virus movement.

Indeed, TGB proteins may have multiple functions in the viral infection process. Linnik et al. (2013) contribute a research article on how three-dimensional structured illumination microscopy (3D-SIM) can provide a novel high definition view of the potato virus X (PVX) factory architecture. They show previously unrecognized membrane structures induced by the PVX TGB proteins. Specifically, they found that previously observed granular structures produced by TGB2 and TGB3 proteins are fine membrane doughnut-shaped loops of remodeled tubular ER containing the viral proteins. These loops form dense arrays wrapped around the TGB1 protein inclusions. These findings provide new insights into the structural organization of a PVX complex considered as a virus factory.

Interestingly, a second research paper studying a different *Potexvirus* genus member, alternanthera mosaic virus (AltMV), provides insight into how its TGB3 protein may function to

modify its target, the chloroplast and its membranes. In this study, Jang et al. (2013) further solidified a previously observed influence of AltMV TGB3 protein on chloroplast structure through EM studies. They also found that TGB3 interacts with a nuclear-encoded chloroplast protein that may result in a destabilization of the thylakoid membranes. While shedding light on an influence of a viral protein on another membrane system, this and the previous study on PVX indicate how conserved proteins may have diverged in function.

In addition to TGB3, TGB2 seems also to play a role in targeting the virus to chloroplasts. In another research paper, Cowan et al. (2012) demonstrated that TGB2 protein of potato mop-top virus (PTMV), the type virus of the genus *Pomovirus*, interacts with the ER, mobile granules, small round structures, and chloroplast envelops. Protein-lipid interaction assays confirmed the association of TGB2 with lipids of chloroplasts. Consistently, EM data revealed abnormal chloroplasts with cytoplasmic inclusions and terminal projections. Viral coat protein (CP), genomic RNA, and labeled TGB2 were colocalized to chloroplasts in PTMV-infected tissues.

Viral cell-to-cell movement remains a hot topic for plant virologists. Xu and Zhou (2012) studied NSvc4, the movement protein of rice stripe virus (RSV), the type member of the *Tenunivirus* genus. They showed that NSvc4 traffics on the actin filament and ER network and that targeting of NSvc4 to PD requires the functional cytoskeleton. They also found that NSvc4 contains a chloroplast-targeting signal and localizes to chloroplasts in infected cells, suggesting NSvc4 may also be a multi-functional protein.

In their hypothesis and theory article, Krenz et al. (2012) discuss alteration in chloroplast structure induced by geminiviruses. They provide evidence that abutilon mosaic virus (AbMV) infection induces a network of stromules that extend from the plastid to the cellular periphery. The stromules contain heat shock cognate 70 kDa protein, a plant chaperone that interacts with the AbMV movement protein. The authors discuss a model in which AbMV traffics along the stromule network to move into neighboring cells.

Cellular remodeling is also the consequence of molecular pathways being overpowered by viruses. Verchot (2012) explores the recruitment of host proteins, such as cellular chaperones, to membrane bound sites required for virus replication and cell-to-cell movement. She discusses the possibilities that cellular chaperones are acting within their normal context to enable viral protein folding, trafficking, and functioning, or whether they are diverted from their normal activities to provide novel contributions to virus infection.

Zhang and Wang (2012) summarize current knowledge about the unfolded protein response (UPR) in cells, which is a reaction to ER stress triggered by the accumulation of unfolded or misfolded proteins in the lumen of the endoplasmic reticulum. The UPR is an attempt by the cell to return to ER homeostasis. Both animal and plant viruses are capable of redirecting the cell to produce large amounts of viral proteins, which causes ER stress and sets in motion the UPR signaling pathways. Zhang and Wang (2012) discuss how viral infections activate the UPR and implications for host physiology.

Bujarski (2013) gives an overview of genetic recombination in plant positive-sense RNA viruses. Questions being raised are the identity of the host factors involved in RNA recombination and the intracellular location of this RNA–RNA template switching.

REFERENCES

Bujarski, J. J. (2013). Genetic recombination in plant-infecting messenger-sense RNA viruses: overview and research perspectives. *Front. Plant Sci.* 4:68. doi: 10.3389/fpls.2013.00068

Cowan, G. H., Roberts, A. G., Chapman, S. N., Ziegler, A., Savenkov, E. I., and Torrance, L. (2012). The potato mop-top virus TGB2 protein and viral RNA associate with chloroplasts and viral infection induces inclusions in the plastids. *Front. Plant Sci.* 3:290. doi: 10.3389/fpls.2012.00290

Di Serio, F., De Stradis, A., Delgado, S., Flores, R., and Navarro, B. (2013). Cytopathic effects incited by viroid RNAs and putative underlying mechanisms. *Front. Plant Sci.* 3:288. doi: 10.3389/fpls.2012.00288

Jang, C., Seo, E.-Y., Nam, J., Bae, H., Gim, Y. G., Kim, H. G., et al. (2013). Insights into Alternanthera mosaic virus TGB3 functions: interactions with Nicotiana benthamiana PsbO correlate with chloroplast vesiculation and veinal necrosis caused by TGB3 overexpression. *Front. Plant Sci.* 4:5. doi: 10.3389/fpls.2013.00005

Krenz, B., Jeske, H., and Kleinow, T. (2012). The induction of stromule formation by a plant DNA-virus in epidermal leaf tissues suggests a novel intra- and intercellular macromolecular trafficking route. *Front. Plant Sci.* 3:291. doi: 10.3389/fpls.2012.00291

Linnik, O., Liesche, J., Tilsner, J., and Oparka, K. J. (2013). Unraveling the structure of viral replication complexes at super-resolution. *Front. Plant Sci.* 4:6. doi: 10.3389/fpls.2013.00006

Liu, C., and Nelson, R. S. (2013). The cell biology of Tobacco mosaic virus replication and movement. *Front. Plant Sci.* 4:12. doi: 10.3389/fpls.2013.00012

Patarroyo, C., Laliberté, J.-F., and Zheng, H. (2013). Hijack it, change it: how do plant viruses utilize the host secretory pathway for efficient viral replication and spread? *Front. Plant Sci.* 3:308. doi: 10.3389/fpls.2012.00308

Sanfaçon, H. (2013). Investigating the role of viral integral membrane proteins in promoting the assembly of nepovirus and comovirus replication factories. *Front. Plant Sci.* 3:313. doi: 10.3389/fpls.2012.00313

Solovyev, A. G., Kalinina, N. O., and Morozov, S. Y. (2012). Recent advances in research of plant virus movement mediated by triple gene block. *Front. Plant Sci.* 3:276. doi: 10.3389/fpls.2012.00276

Verchot, J. (2012). Cellular chaperones and folding enzymes are vital contributors to membrane bound replication and movement complexes during plant RNA virus infection. *Front. Plant Sci.* 3:275. doi: 10.3389/fpls.2012.00275

Xu, Y., and Zhou, X. (2012). Role of rice stripe virus NSvc4 in cell-to-cell movement and symptom development in *Nicotiana benthamiana*. *Front. Plant Sci.* 3:269. doi: 10.3389/fpls.2012.00269

Zhang, L., and Wang, A. (2012). Virus-induced ER stress and the unfolded protein response. *Front. Plant Sci.* 3:293. doi: 10.3389/fpls.2012.00293

Received: 22 May 2013; accepted: 31 May 2013; published online: 17 June 2013.

Citation: Laliberté J-F, Moffett P, Sanfaçon H, Wang A, Nelson RS and Schoelz JE (2013) e-Book on plant virus infection—a cell biology perspective. Front. Plant Sci. 4:203. doi: 10.3389/fpls.2013.00203

This article was submitted to Frontiers in Plant-Microbe Interaction, a specialty of Frontiers in Plant Science.

frontiers in
PLANT SCIENCE

MINI REVIEW ARTICLE
published: 07 January 2013
doi: 10.3389/fpls.2012.00288

Cytopathic effects incited by viroid RNAs and putative underlying mechanisms

Francesco Di Serio[1]*, Angelo De Stradis[1], Sonia Delgado[2], Ricardo Flores[2] and Beatriz Navarro[1]

[1] *Istituto di Virologia Vegetale, UOS Bari, Consiglio Nazionale delle Ricerche, Bari, Italy*
[2] *Instituto de Biología Molecular y Celular de Plantas, Universidad Politécnica de Valencia-Consejo Superior de Investigaciones Científicas, Valencia, Spain*

Edited by:
Jean-François Laliberté, Institut National de la Recherche Scientifique, Canada

Reviewed by:
Martin Pelchat, University of Ottawa, Canada
Biao Ding, The Ohio State University, USA
Andrea Genre, University of Turin, Italy

****Correspondence:***
Francesco Di Serio, Istituto di Virologia Vegetale, UOS Bari, Consiglio Nazionale delle Ricerche, Via Amendola 165/A, 70126 Bari, Italy.
e-mail: f.diserio@ba.ivv.cnr.it

Viroids are infectious agents identified only in plants so far. In contrast to viruses, the genome of viroids is composed of a tiny circular RNA (250–400 nt) not coding for proteins, but containing in its compact structure all the information needed for parasitizing the transcriptional and RNA trafficking machineries of their hosts. Viroid infections are frequently accompanied by cellular and developmental disorders that ultimately result in macroscopic symptoms. The molecular events linking the structural domains of viroid RNAs with cellular and macroscopic alterations remain largely unexplored, although significant progress has been lately achieved in one specific viroid-host combination, highlighting the ability of viroids to strongly interfere with their host RNA regulatory networks. Cytopathic effects induced by nuclear-replicating viroids, which were investigated since early studies on viroids, consist in irregular proliferations of cell membranes (paramural bodies or plasmalemmasomes), cell wall distortions, and chloroplast malformations. Different alternatives have been proposed regarding how these cytological alterations may influence the onset of macroscopic symptoms. Recently, the cytopathology and histopathology incited by a chloroplast-replicating viroid have been investigated in depth, with defects in chloroplast development having been related to specific molecular events that involve RNA silencing and impairment of chloroplast ribosomal RNA maturation. On this basis, a tentative model connecting specific cytopathologic alterations with symptoms has been put forward. Here, early and more recent studies addressing this issue will be reviewed and reassessed in the light of recent advances in the regulatory roles of small RNAs.

Keywords: cell wall, chloroplast, non-coding RNAs, pathogenesis, plasmalemmasome, RNA silencing

INTRODUCTION

Viroids are infectious agents composed exclusively of a small (246–401 nt), circular, and highly structured RNA able to replicate autonomously and move systemically in their host plants, wherein they frequently elicit macroscopic symptoms (Flores et al., 2005; Ding, 2009). The approximately 30 viroid species reported so far have been assigned to the taxonomic families *Pospiviroidae*, grouping the type species *Potato spindle tuber viroid* (PSTVd) and many others that replicate and accumulate in the nucleus, and *Avsunviroidae*, clustering the type species *Avocado sunblotch viroid* (ASBVd) and three other viroids replicating and accumulating in plastids (mainly chloroplasts; Owens et al., 2011). Members of both families induce severe diseases in certain hosts, although in some viroid-host combinations the infection remains latent (Flores et al., 2011). Viroid diseases are characterized by macroscopic symptoms that may include stunting, alterations affecting leaves (epinasty, vein clearing, distortion, discoloration, mottling, and necrosis) and bark (cankers, scaling, cracking), and malformations of tubers, flowers, and fruits (in the last two organs frequently accompanied with color breaking). In rare cases viroids may cause the death of the plant.

In contrast to viruses, all the available data support that viroids do not code for any protein and, therefore, their replication, trafficking, and pathogenesis rely on the interplay between the invading RNA and host factors. There is evidence for members of both families supporting the direct interaction of viroid RNAs with host proteins (Daròs and Flores, 2002; Martínez de Alba et al., 2003; see for a review Owens and Hammond, 2009). These interactions are most likely mediated by structural domains that, mimicking those contained in cellular RNAs, allow viroid RNAs to usurp and redirect enzymes and other host components to their replication and trafficking. Structural elements in the genomic viroid RNA and their proposed role(s) in conferring functional properties to these infectious agents have been recently reviewed (Flores et al., 2012). Some of these elements have been shown to regulate specifically cell-to-cell (Qi et al., 2004; Takeda et al., 2011) and long distance (Zhong et al., 2007, 2008) movement of PSTVd through the plasmodesmata and phloem, respectively, while others have been implicated in replication or in pathogenesis (see for a review Navarro et al., 2012a).

Whether the macroscopic symptoms result from interaction(s) between the genomic viroid RNA and host factor(s) detracted from their physiological functions is not known. Alternatively, post-translational triggering of signaling cascades by RNA-activated phosphorylation of host proteins has been proposed as the primary event of viroid pathogenesis (Hiddinga et al., 1988; see for a

review Owens and Hammond, 2009). In addition to many studies supporting the ability of viroids to modify host gene expression during infection (Conejero et al., 1990; Itaya et al., 2002; Tessitori et al., 2007; Wang et al., 2011; Owens et al., 2012; Rizza et al., 2012; see for a review Owens and Hammond, 2009), other hypotheses based on the interference of viroid RNAs with the plant RNA silencing machinery have been proposed for their pathogenesis in the last few years (see below). Models on how viroids may elicit macroscopic symptoms have been described in previous reviews (Flores et al., 2005; Ding, 2009; Owens and Hammond, 2009; Navarro et al., 2012a). Here, we will address viroid pathogenesis from a different perspective, focusing on the cytological alterations induced by viroids in infected cells and taking into account recent advances in the plant-viroid interplay achieved by genome-wide technologies.

VIROID INFECTION IS FREQUENTLY ACCOMPANIED BY CYTOLOGICAL ALTERATIONS

Cytopathic effects of viroid infections were first reported by Semancik and Vanderwoude (1976) in the experimental host *Gynura aurantiaca* infected by *Citrus exocortis viroid* (CEVd), a member of family *Pospiviroidae*. Using electron microscopy, these authors identified in symptomatic leaves paramural bodies with electron density similar to plasma membranes that they termed plasmalemmasomes (PSs), which later on were also observed in tomato infected by PSTVd (Hari, 1980; **Figure 1A**). These invaginations of the plasmalemma into the cytoplasm were rare in asymptomatic leaves of infected plants, and absent in leaves that had reached maturity before viroid infection and in uninfected controls. Therefore, PSs were considered the primary cytopathic effect of CEVd infection (Semancik and Vanderwoude, 1976). They were found in all cell types, including mesophyll, epidermis, companion cells, and phloem and xylem parenchyma of vascular bundles, and were closely associated with the leaf epinasty and blistering caused by the viroid. The morphology of PSs was largely variable, with those from mature cells being prevalently located at the cell wall-plasma membrane interface and displaying multiple membrane layers. In contrast, PSs from immature cells were of smaller size and contained roundish granules. In some instances, PSs were also observed in contact with plasmodesmata, occasionally in opposite positions separated by the cell wall (Semancik and Vanderwoude, 1976).

A few years later, these data were questioned because PSs were recognized in both symptomatic and uninfected *G. aurantiaca* plants (Wahn et al., 1980). In particular, PSs were detected with the same frequency in CEVd-infected and healthy controls. Moreover, a distinction was made between vesicular and tubular PSs depending on their ultrastructure. Formation of PSs as the primary cytopathic effect induced by CEVd in *G. aurantiaca* was excluded in this study, but the shape and internal structure of both vesicular and tubular PSs were different in CEVd-infected and healthy leaf tissues (Wahn et al., 1980). In particular, PSs from diseased tissues contained vesicles strikingly irregular in their shape, size, and number, while tubular PSs contained malformed tubules; similar alterations were never observed in healthy controls and therefore appeared viroid-induced. Moreover, another interesting cytopathic effect of CEVd infection in *G. aurantiaca* was identified in this same study: the conspicuous distortion and irregular thickness of cell walls, which produced irregular cell shapes in symptomatic tissues (Wahn et al., 1980; see also below). Intriguingly, malformed PSs were only found in cells with altered walls, suggesting a correlation between these two subcellular alterations.

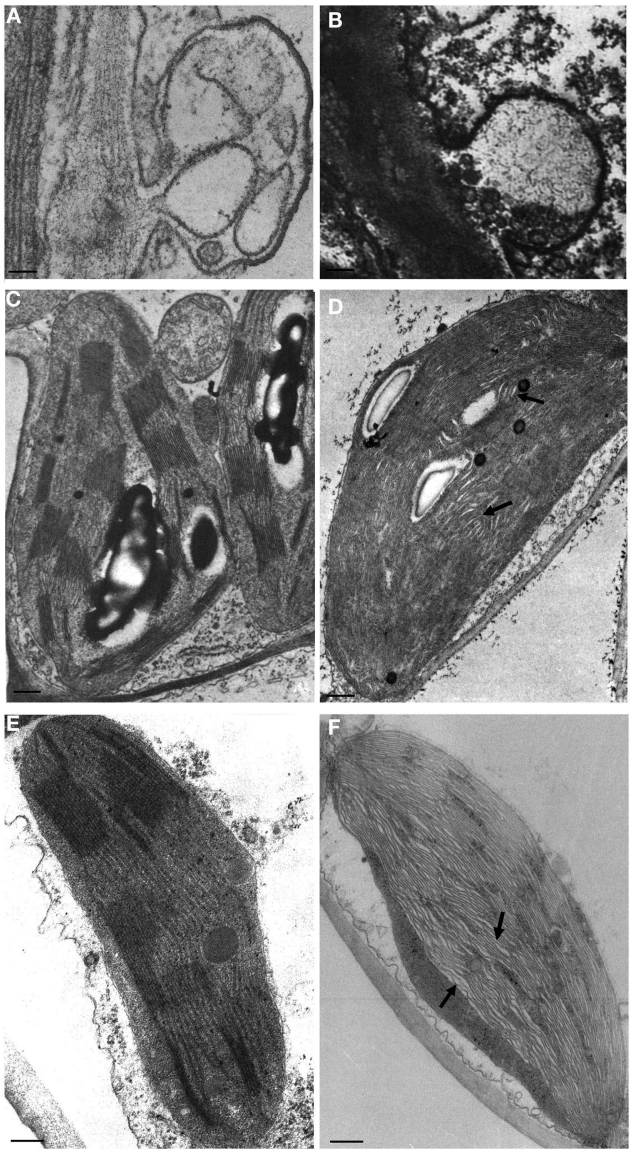

FIGURE 1 | Cytopathic effects associated to viroid infection. Plasmalemmasomes in tomato infected by PSTVd **(A)**, and in avocado infected by ASBVd **(B)**. Normal and malformed chloroplasts with irregularly stacked thylakoids and wide interspaces (denoted with arrows) in healthy and PSTVd-infected tomato [**(C,D)** respectively], and in peach healthy and infected with a PLMVd latent variant [**(E,F)** respectively). Bar = 50 nm. **(A,C,D)** have been reproduced (with modifications) from Hari (1980; Copyright The American Phytopathological Society), and **(B)** from Da Graça and Martin, 1981; Copyright John Wiley and Sons), in all cases with permission.

The role of PSs in viroid pathogenesis remains controversial. As indicated above, paramural bodies were subsequently reported as a cytopathic effect of PSTVd infection in tomato leaves (**Figure 1A**; Hari, 1980), thus extending their presence to viroid-host combinations other than CEVd and *G. aurantiaca.* PSs were later observed also in chlorotic tissues of chrysanthemum infected by *Chrysanthemum stunt viroid* (CSVd), another member of the family *Pospiviroidae* (Rosenberg de Gómez et al., 1985). On the other hand, Marton et al. (1982) observed in CEVd-infected tomato callus cells a significantly higher frequency of PSs that was not regarded as viroid-specific but rather a secondary (and non-specific) effect of viroid infection. Similarly, the higher number of PSs detected by Gruner and Santore (1991) in PSTVd-infected tomato leaves with respect to healthy controls was considered as a non-specific physiological response to diverse abiotic and biotic stresses. Interestingly, an increase in the number and size of paramural bodies with respect to healthy controls was also reported in ASBVd-infected avocado tissues (**Figure 1B**; Da Graça and Martin, 1981), thus showing that alterations in PSs are not restricted to infections by nuclear-replicating viroids.

The discrepancies regarding PSs do not apply to the cell wall alterations first reported in *G. aurantiaca* infected by CEVd (Wahn et al., 1980). Similar distorted, undulated cell walls with variable thickness were also observed in tomato infected by CEVd (Marton et al., 1982), chrysanthemum infected by CSVd (Rosenberg de Gómez et al., 1985), and hop and cucumber infected by *Hop stunt viroid* (HSVd; Momma and Takahashi, 1982), indicating that this is the most common cytopathic effect induced by several members of the family *Pospiviroidae*. In hop plants, these structural alterations were absent in shoot tips (0.2 mm long, consisting of the apical meristem and two pairs of primordial leaves), but present starting from the third leaf primordium, showing that they appear at early leaf developmental stages (Momma and Takahashi, 1983). Anomalies in cell wall structures are also consistent with: (i) modifications in wall composition of CEVd-infected tomato cells with respect to their healthy counterparts (Wang et al., 1986), and (ii) a marked reduction in the number of protoplasts, released from CEVd-containing tomato tissues and non-differentiated calli treated with enzymes for disrupting cell walls, with respect to healthy controls (Marton et al., 1982). However, no clear differences between the cell walls of healthy and PSTVd-infected tomato leaves were observed by Gruner and Santore (1991).

Early studies on viroid cytopathology also showed structural defects in chloroplasts induced by nuclear-replicating viroids, including PSTVd (Hari, 1980), CSVd (Rosenberg de Gómez et al., 1985), and HSVd (Momma and Takahashi, 1982). These findings suggest that viroids with preferential accumulation in one specific organelle can interfere with the development and presumably the function of other cell organella. When compared to healthy controls (**Figure 1C**), abnormal development and organization of the chloroplast membranes, with distorted and irregularly stacked thylakoids, were observed in PSTVd-infected cells (**Figure 1D**). Interestingly, similar alterations have been also reported in the chloroplasts from asymptomatic tissues infected by a chloroplast-replicating viroid, *Peach latent mosaic viroid* (PLMVd; **Figure 1F**), but not in the healthy controls (**Figure 1E**; Rodio et al., 2007). Whether this structural defect is induced specifically by viroid infection or is a more general plant response to biotic stresses remains an open question.

LINKING VIROID-INDUCED CYTOPATHIC EFFECTS WITH MACROSCOPIC SYMPTOMS AND THE UNDERLYING BIOCHEMICAL PATHWAYS

Among nuclear-replicating viroids, a correlation between subcellular alterations and macroscopic symptoms was proposed for certain viroid-infected hosts, such as *G. aurantiaca,* hop, and cucumber, in which cell wall defects were accompanied by leaf distortions (Wahn et al., 1980; Momma and Takahashi, 1982). However, the most conspicuous evidence that cytopathic effects may have a direct link with macroscopic symptoms has been obtained for the chloroplast-replicating PLMVd (for a review see Flores et al., 2006). Some variants of this viroid, which contain a specific pathogenic determinant consisting of an inserted hairpin of 12 nt (**Figure 2A**), cause peach calico (PC), a severe disease characterized by an extreme chlorosis (albinism) of leaves (**Figure 2C**), stems, and fruits (Malfitano et al., 2003; Rodio et al., 2006). In albino leaf tissues from PLMVd-infected peach trees, altered plastids with irregular shape and size and with rudimentary thylakoids, thus resembling proplastids, were observed by electron microscopy (**Figure 2D**; Rodio et al., 2007). Further analyses revealed that structural alterations, namely rudimentary thylakoids and presence of vesicles, are already evident in most proplastids from meristematic cells of the albino shoot apices, supporting the notion that an early step of chloroplast development is specifically impaired by PLMVd variants inducing PC. These alterations have never been found in green leaf tissue and shoot apices of plants infected by PC-inducing variants or by other mosaic-inducing or latent variants, thus confirming their close association with the albino phenotype (Rodio et al., 2007). In addition, these structural alterations have been closely associated with impaired processing and accumulation of plastid rRNAs in the albino tissues (**Figure 2B**), a molecular defect also reported in variegated mutants of some plants (Rodio et al., 2007). Therefore, a macroscopic symptom, the corresponding cytological defects, and the possible biochemical pathway, have been closely related to the presence of a specific structural domain (the inserted hairpin) in the infecting viroid RNA.

Interestingly, another chloroplast-replicating viroid, ASBVd, may induce a severe chlorosis (bleaching) in its natural host avocado. This symptomatology, which resembles closely PC (**Figure 2E**), has been associated with plastid ultrastructural defects partially similar to those reported in PC, but with rudimentary thylakoid membranes slightly more organized (Da Graça and Martin, 1981; **Figure 2F**). Moreover, ASBVd sequence variants from bleached tissues are slightly different from those accumulating in non-symptomatic tissues (Semancik and Szychowski, 1994) and, based on our preliminary results, accumulation of plastid rRNA appears also impaired in bleached tissues (Di Serio and Flores, unpublished data). Altogether, these data establish a particularly intriguing parallelism between PLMVd and ASBVd pathogenesis.

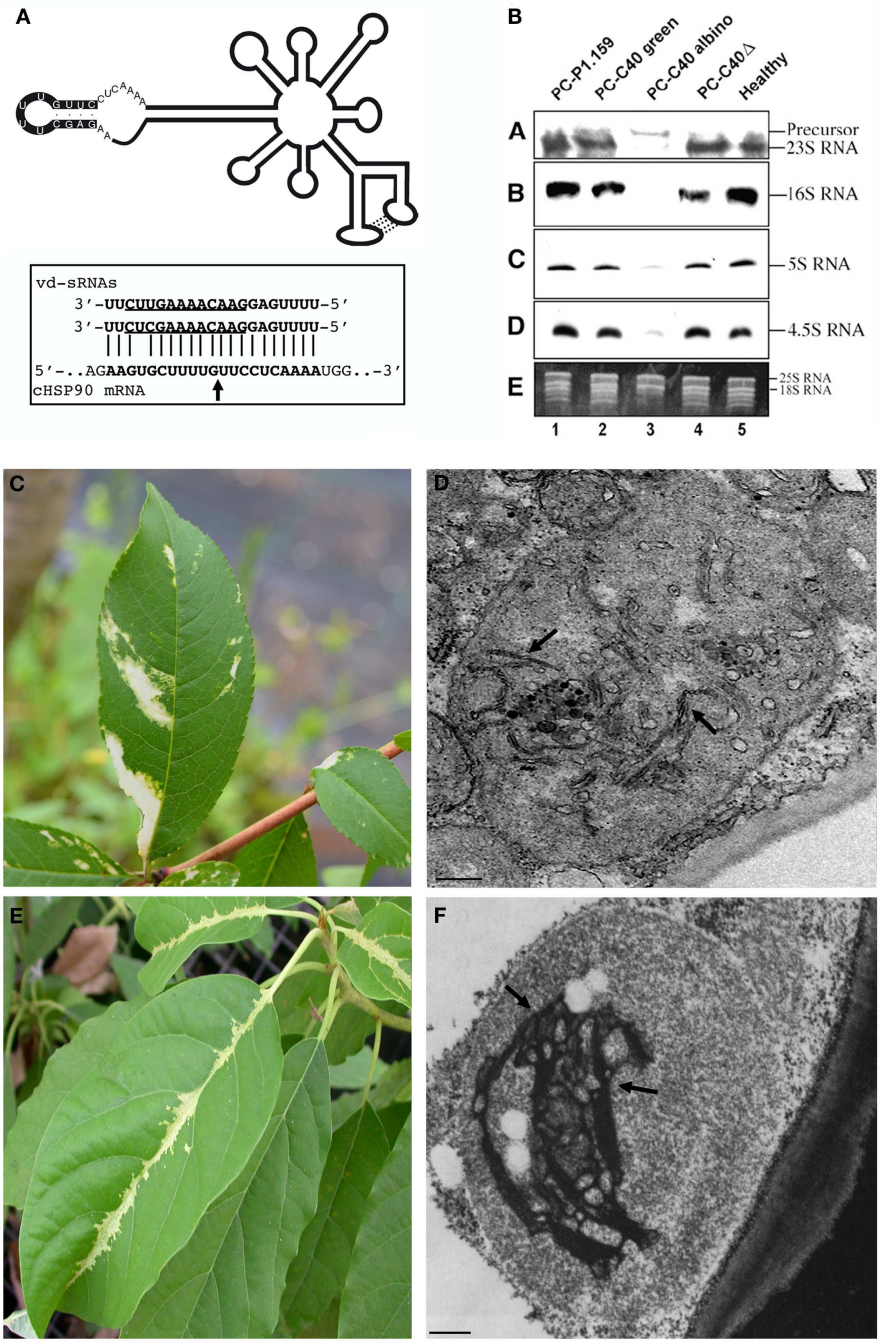

FIGURE 2 | Association of cytopathic effects and biochemical lesions with macroscopic symptoms in viroid infections. (A) Schematic representation of the secondary structure predicted for a PLMVd variant inducing PC, with the nucleotides forming the PC-associated insertion denoted by a black background. (Inset) Two PLMVd (-) sRNAs mapping at this insertion target for cleavage the mRNA coding for the chloroplastic heat-shock protein 90 (cHSP90) as predicted by RNA silencing; arrow marks the predicted and validated cleavage site (Navarro et al., 2012b). **(B)** Accumulation of plastid rRNAs in GF-305 peach leaves infected by latent (PC-P1.149 and PC-C40Δ) and PC-inducing (PC-C40) variants as revealed by Northern-blot hybridizations with cDNA probes specific for 23, 16, 5, and 4.5S rRNAs; the impaired accumulation and processing of plastid rRNAs is associated with the albino phenotype (Rodio et al., 2007). **(C)** Severe chlorosis induced by a PC-inducing variant of PLMVd and **(D)** altered plastid with rudimentary thylakoid membranes (arrows) observed in chlorotic areas. **(E)** Severe chlorosis induced by ASBVd and **(F)** altered plastid with rudimentary thylakoid structures (arrows), slightly more organized than in PC, in the corresponding bleached areas. Bar = 50 nm. **(A,B,F)** have been reproduced with permissions from Navarro et al., 2012b; Copyright John Wiley and Sons), Rodio et al., 2007; Copyright American Society of Plant Biologists, www.plantcell.org) and Da Graça and Martin (1981), respectively, in all cases with permission.

CYTOPATHIC EFFECTS ARE ASSOCIATED WITH MODIFICATIONS IN GENE EXPRESSION

The triggering events and molecular mechanisms underlying viroid pathogenesis are still largely unknown, but it is generally accepted that these RNAs induce modifications of host gene expression that, ultimately, lead to macroscopic symptoms through activation of cross-talking signaling cascades. Altered accumulation and phosphorylation of host proteins were identified in early studies (for a review see Navarro et al., 2012a), which more recently have been complemented by genome-wide transcriptome analyses (Qi and Ding, 2003; Wang et al., 2011; Owens et al., 2012; Rizza et al., 2012). Although it remains to be conclusively established whether the genes with altered expression are actually involved in symptom elicitation, these studies have supplied interesting information for further dissecting the molecular interplay between viroids and their hosts.

In the last decade, new hints on possible mechanisms by which non-protein-coding RNAs, like viroids, could modify host gene expression have been derived from dissection of RNA silencing pathways in plants (for reviews see Chen, 2009; Parent et al., 2012). Since early identification in infected tissues of viroid-derived small RNAs of 21–24 nt (vd-sRNAs) with structural features similar to the small interfering RNA (siRNAs) and micro RNAs (miRNAs; Itaya et al., 2001; Papaefthimiou et al., 2001; Martínez de Alba et al., 2002), RNA silencing has been proposed as a regulatory network by which viroids may modify host gene expression eventually resulting in macroscopic symptoms. In particular, it was proposed that, similarly to miRNAs and siRNAs, vd-sRNAs could be incorporated into Argonaute (AGO) complexes and target host mRNAs for cleavage or translation inhibition. The correlation between symptom severity and vd-sRNAs accumulation (Markarian et al., 2004; Wang et al., 2004; Matoušek et al., 2007; Gómez et al., 2008), and the identification of pre-miRNAs or mRNAs potentially targeted by vd-sRNAs (Diermann et al., 2010; Wang et al., 2011), provided circumstantial support for this hypothesis. However, compelling evidence that vd-sRNAs, mimicking miRNAs, indeed target host mRNAs for sequence-specific cleavage has been supplied only recently by dissecting the molecular mechanisms potentially involved in the induction of PC by PLMVd (Navarro et al., 2012b). More explicitly, two PLMVd-sRNAs containing the insertion strictly associated with PC were identified by vd-sRNAs deep sequencing and bioinformatics tools. RNA ligase-mediated rapid amplification of cDNA ends (RACE) has shown that these vd-sRNAs target for cleavage the mRNAs coding for the chloroplastic heat-shock protein 90 (cHSP90) as predicted by RNA silencing (**Figure 2A** inset). Interestingly, this protein is involved in chloroplast biogenesis and plastid-to-nucleus-signaling, which appear compromised in the albino tissues characteristic of PC (Rodio et al., 2007). In these tissues accumulation of the mRNA encoding for cHSP90 is significantly lowered with respect to the green adjacent tissues. Altogether these data strongly support a role for cHSP90 down-regulation in PC macroscopic symptoms and the closely associated cytopathic effects, although involvement of additional factors cannot be excluded at this stage (Navarro et al., 2012b). In addition, based on the previous observation that rRNA maturation is impaired in altered plastids from albino sectors of leaves expressing PC (**Figure 2B**; Rodio et al., 2007), it can be speculated that cHSP90, a chaperone, could mediate directly or indirectly this biochemical pathway.

Are the other ultrastructural defects induced by viroids also due to misregulation of specific host genes? Some years ago, the stunting and restricted cell wall expansion induced by PSTVd in tomato was correlated to the down-regulation of an expansin gene *(LeExp2*; Qi and Ding, 2003). More recently, genome-wide analyses have shown important transcriptional changes in response to infections by CEVd in Etrog citron (Rizza et al., 2012) and PSTVd in tomato (Owens et al., 2012). Notwithstanding the different viroid-host combinations and experimental designs of these studies, it is worth noting that overexpression of genes coding for proteins involved in cell wall remodeling (i.e., pectinesterases) and down-regulation of genes involved in chloroplast metabolism and biogenesis, were observed in both cases. Even if it is not known whether modulation of these genes can be directly related to the ultrastructural alterations in cell wall and chloroplast induced by CEVd and PSTVd, these data are intriguing. In addition, the identification of genes consistently overexpressed in viroid-infected hosts points to the existence of mechanisms, apart from RNA silencing mediated by vd-sRNAs, by which viroids could interfere with host gene expression.

CONCLUDING REMARKS

Ultrastructural defects induced by viroids in their hosts were prevalently investigated by biochemical and electron microscopy techniques in the 70s and 80s of the last century. However, the beginning of the 90s witnessed a change of focus and, since then, studies on viroid pathogenesis have been dominated by molecular approaches, leaving almost completely aside cellular and histological studies. Nowadays, current technologies based on genome-wide analyses, including deep sequencing, are being increasingly applied for dissecting viroid-host interactions at the molecular level, and it can be anticipated that they will be more and more used in the future. However, the studies on PC induced by PLMVd (Rodio et al., 2007; Navarro et al., 2012b) exemplify that data on cytopathic effects must be integrated when trying to characterize the biochemical pathways and regulatory networks involved in plant responses to viroid infections. At the same time, new studies on viroid-induced cytopathic alterations appear particularly stimulating if they are included in a wider experimental design aimed at exploring by high-throughput technologies the concurrent modifications in host gene expression. This combined multidisciplinary strategy should be instrumental for generating a broader view of how these fascinating non-coding RNAs manipulate their hosts.

ACKNOWLEDGMENTS

Research in Beatriz Navarro and Francesco Di Serio laboratory is supported by a dedicated grant (CISIA) of the Ministero dell'Economia e Finanze Italiano to the CNR (Legge n. 191/2009). Research in Ricardo Flores laboratory is presently supported by grant BFU2011-28443 from the Ministerio de Ciencia e Innovacion of Spain. We apologize for not quoting the original work of many authors due to space limitations.

REFERENCES

Chen, X. (2009). Small RNAs and their roles in plant development. *Annu. Rev. Cell Dev. Biol.* 25, 21–44.

Conejero, V., Belles, J. M., Garcia-Breijo, F., Garro, R., Hernandez-Yago, J., Rodrigo, I., et al. (1990). "Signalling in viroid pathogenesis," in *Recognition and Response in Plant-Virus Interactions, NATO ASI Series H 41*, ed. R. S. S. Fraser (Springer-Verlag: Berlin), 233–261.

Da Graça, J. V., and Martin, M. M. (1981). Ultrastructural changes in avocado leaf tissue infected with avocado sunblotch. *J. Phytopathol.* 102, 195–194.

Daròs, J. A., and Flores, R. (2002). A chloroplast protein binds a viroid RNA in vivo and facilitates its hammerhead-mediated self-cleavage. *EMBO J.* 21, 749–759.

Diermann, N., Matoušek, J., Junge, M., Riesner, D., and Steger, G. (2010). Characterization of plant miRNAs and small RNAs derived from potato spindle tuber viroid (PSTVd) in infected tomato. *Biol. Chem.* 391, 1379–1390.

Ding, B. (2009). The biology of viroid-host interactions. *Annu. Rev. Phytopathol.* 47, 105–131.

Flores, R., Delgado, S., Rodio, M. E., Ambrós, S., Hernández, C., and Di Serio, F. (2006). Peach latent mosaic viroid: not so latent. *Mol. Plant Pathol.* 7, 209–222.

Flores, R., Di Serio, F., Navarro, B., Duran-Vila, N., and Owens, R. A. (2011). "Viroids and viroid diseases of plants," in *Studies in Viral Ecology: Microbial and Botanical Host Systems*, Vol. 1, ed. C. J. Hurst (Hoboken, NJ: John Wiley & Sons), 311–346.

Flores, R., Hernández, C., Martínez de Alba, E., Daròs, J. A., and Di Serio, F. (2005). Viroids and viroid-host interactions. *Annu. Rev. Phytopathol.* 43, 117–139.

Flores, R., Serra, P., Minoia, S., Di Serio, F., and Navarro, B. (2012). Viroids: from genotype to phenotype just relying on RNA sequence and structural motifs. *Front. Microbiol.* 3:217. doi:10.3389/fmicb.2012.00217

Gómez, G., Martínez, G., and Pallás, V. (2008). Viroid-induced symptoms in *Nicotiana benthamiana* plants are dependent on RDR6 activity. *Plant Physiol.* 148, 414–423.

Gruner, R., and Santore, U. J. (1991). Comparative ultratructural observations of plasmalemmasomes in PSTVd-infected, healthy and artificially stunted tomato leaves. *J. Phytopathol.* 131, 243–252.

Hari, V. (1980). Untrastructure of potato spindle tuber viroid-infected tomato leaf tissues. *Phytopathology* 70, 385–387.

Hiddinga, H. J., Crum, C. J., Hu, J., and Roth, D. A. (1988). Viroid-induced phosphorylation of a host protein related to a dsRNA-dependent protein kinase. *Science* 241, 451–453.

Itaya, A., Folimonov, A., Matsuda, Y., Nelson, R. S., and Dig, B. (2001). Potato spindle tuber viroid as inducer of RNA silencing in infected tomato. *Mol. Plant Microbe Interact.* 14, 1332–1334.

Itaya, A., Matsuda, Y., Gonzales, R. A., Nelson, R. S., and Ding, B. (2002). Potato spindle tuber viroid strains of different pathogenicity induces and suppresses expression of common and unique genes in infected tomato. *Mol. Plant Microbe Interact.* 15, 990–999.

Malfitano, M., Di Serio, F., Covelli, L., Ragozzino, A., Hernández, C., and Flores, R. (2003). Peach latent mosaic viroid variants inducing peach calico contain a characteristic insertion that is responsible for this symptomatology. *Virology* 313, 492–501.

Markarian, N., Li, H. W., Ding, S. W., and Semancik, J. S. (2004). RNA silencing as related to viroid induced symptom expression. *Arch. Virol.* 149, 397–406.

Martínez de Alba, A. E., Flores, R., and Hernández, C. (2002). Two chloroplastic viroids induce the accumulation of the small RNAs associated with post-transcriptional gene silencing. *J. Virol.* 76, 13094–13096.

Martínez de Alba, A. E., Sägesser, R., Tabler, M., and Tsagris, M. (2003). A bromodomain-containing protein from tomato specifically binds potato spindle tuber viroid RNA in vitro and in vivo. *J. Virol.* 77, 9685–9694.

Marton, L., Duran-Vila, N., Lin, J. J., and Semancik, J. S. (1982). Properties of cell cultures containing the citrus exocortis viroid. *Virology* 122, 229–238.

Matoušek, J., Kozlová, P., Orctová, L., Schmitz, A., Pesina, K., Bannach, O., et al. (2007). Accumulation of viroid-specific small RNAs and increase of nucleolytic activities linked to viroid-caused pathogenesis. *Biol. Chem.* 388, 1–13.

Momma, T., and Takahashi, T. (1982). Ultrastructural of hop stunt viroid-infected leaf tissue. *J. Phytopathol.* 104, 201–221.

Momma, T., and Takahashi, T. (1983). Cytopathology of shoot apical meristem of hop plants infected with hop stunt viroid. *J. Phytopathol.* 106, 272–280.

Navarro, B., Gisel, A., Rodio, M. E., Delgado, S., Flores, R., and Di Serio, F. (2012a). Viroids: how to infect a host and cause disease without encoding proteins. *Biochimie* 94, 1474–1480.

Navarro, B., Gisel, A., Rodio, M. E., Delgado, S., Flores, R., and Di Serio, F. (2012b). Small RNAs containing the pathogenic determinant of a chloroplast-replicating viroid guide the degradation of a host mRNA as predicted by RNA silencing. *Plant J.* 70, 991–1003.

Owens, R. A., Flores, R., Di Serio, F., Li, S. F., Pallás, V., Randles, J. W., et al. (2011). "Viroids," in *Virus Taxonomy: Ninth Report of the International Committee on Taxonomy of Viruses*, eds A. M. Q. King, M. J. Adams, E. B. Carstens, and E. J. Lefkowitz (London: Elsevier Academic Press), 1221–1234.

Owens, R. A., and Hammond, R. W. (2009). Viroid pathogenicity: one process, many faces. *Viruses* 1, 298–316.

Owens, R. A., Tech, K. B., Shao, J. Y., Sano, T., and Baker, C. J. (2012). Global analysis of tomato gene expression during Potato spindle tuber viroid infection reveals a complex array of changes affecting hormone signaling. *Mol. Plant Microbe Interact.* 25, 582–598.

Papaefthimiou, I., Hamilton, A. J., Denti, M. A., Baulcombe, D. C., Tsagris, M., and Tabler, M. (2001). Replicating potato spindle tuber viroid RNA is accompanied by short RNA fragments that are characteristic of post-transcriptional gene silencing. *Nucleic Acids Res.* 29, 2395–2400.

Parent, J. S., Martínez de Alba, A. E., and Vaucheret, H. (2012). The origin and effect of small RNA signaling in plants. *Front. Plant Sci.* 3:179. doi:10.3389/fpls.2012.00179

Qi, Y., and Ding, B. (2003). Inhibition of cell growth and shoot development by a specific nucleotide sequence in a non coding viroid RNA. *Plant Cell* 15, 1360–1374.

Qi, Y., Pélissier, T., Itaya, A., Hunt, E., Wassenegger, M., and Ding, B. (2004). Direct role of a viroid RNA motif in mediating directional RNA trafficking across a specific cellular boundary. *Plant Cell* 16, 1741–1752.

Rizza, S., Conesa, A., Juarez, J., Catara, A., Navarro, L., Duran-Vila, N., et al. (2012). Microarray analysis of Etrog citron (*Citrus medica L.*) reveals changes in chloroplast, cell wall, peroxidase and symporter activities in response to viroid infection. *Mol. Plant Pathol.* 13, 852–864.

Rodio, M. E., Delgado, S., De Stradis, A. E., Gómez, M. D., Flores, R., and Di Serio, F. (2007). A viroid RNA with a specific structural motif inhibits chloroplast development. *Plant Cell* 19, 3610–3626.

Rodio, M. E., Delgado, S., Flores, R., and Di Serio, F. (2006). Variants of peach latent mosaic viroid inducing peach calico: uneven distribution in infected plants and requirements of the insertion containing the pathogenicity determinant. *J. Gen. Virol.* 87, 231–240.

Rosenberg de Gómez, F., Wahn, K., and Sänger, H. L. (1985). Cytopathologie von viroid-infiziertem Pflanzengewebe. II. Licht- und elektronenmikroskopische Untersuchungen an Blattgewebe von Chrysanthemum morifolium der Sorte "Mistletoe" nach Infektion mit dem Viroid der Stauchekrankheit der Chrysantheme (CSV). *Phytopath. Z.* 114, 41–68.

Semancik, J. S., and Szychowski, J. A. (1994). Avocado sunblotch disease: a persistent viroid infection in which variants are associated with differential symptoms. *J. Gen. Virol.* 75, 1543–1549.

Semancik, J. S., and Vanderwoude, W. J. (1976). Exocortis viroid: cytopathic effects at plasma membrane in association with pathogenic RNA. *Virology* 69, 719–726.

Takeda, R., Petrov, A. I., Leontis, N. B., and Ding, B. (2011). A three-dimensional RNA motif in potato spindle tuber viroid mediates trafficking from palisade mesophyll to spongy mesophyll in *Nicotiana benthamiana*. *Plant Cell* 23, 258–272.

Tessitori, M., Maria, G., Capasso, C., Catara, G., Rizza, S., De Luca, V., et al. (2007). Differential display analysis of gene expression in Etrog citron leaves infected by Citrus viroid III. *Biochim. Biophys. Acta* 1769, 228–235.

Wahn, K., Rosenberg de Gómez, F., and Sänger, H. L. (1980). Cytopathic changes in leaf tissue of *Gynura aurantiaca* infected with the viroid

of citrus exocortis disease. *J. Gen. Virol.* 49, 356–365.

Wang, M. B., Bian, X. Y., Wu, L. M., Liu, L. X., Smith, N. A., Isenegger, D., et al. (2004). On the role of RNA silencing in the pathogenicity and evolution of viroids and viral satellites. *Proc. Natl. Acad. Sci. U.S.A.* 101, 3275–3280.

Wang, M. G., Lin, J. J., Duran-Vila, N., and Semancik, J. S. (1986). Alteration in cell wall composition and structure in viroid-infected cells. *Physiol. Mol. Plant Pathol.* 28, 107–124.

Wang, Y., Shibuya, M., Taneda, A., Kurauchi, T., Senda, M., Owens, R. A., et al. (2011). Accumulation of potato spindle tuber viroid-specific small RNAs is accompanied by specific changes in gene expression in two tomato cultivars. *Virology* 413, 72–83.

Zhong, X., Archual, A. J., Amin, A. A., and Ding, B. (2008). A genomic map of viroid RNA motifs critical for replication and systemic trafficking. *Plant Cell* 20, 35–47.

Zhong, X., Tao, X., Stombaugh, J., Leontis, N., and Ding, B. (2007). Tertiary structure and function of an RNA motif required for plant vascular entry to initiate systemic trafficking. *EMBO J.* 26, 3836–3846.

Conflict of Interest Statement: The authors declare that the research was conducted in the absence of any commercial or financial relationships that could be construed as a potential conflict of interest.

Received: 17 October 2012; paper pending published: 02 November 2012; accepted: 03 December 2012; published online: 07 January 2013.

Citation: Di Serio F, De Stradis A, Delgado S, Flores R and Navarro B (2013) Cytopathic effects incited by viroid RNAs and putative underlying mechanisms. Front. Plant Sci. ***3****:288. doi: 10.3389/fpls.2012.00288*

This article was submitted to Frontiers in Plant-Microbe Interaction, a specialty of Frontiers in Plant Science.

frontiers in
PLANT SCIENCE

REVIEW ARTICLE
published: 11 January 2013
doi: 10.3389/fpls.2012.00308

Hijack it, change it: how do plant viruses utilize the host secretory pathway for efficient viral replication and spread?

Camilo Patarroyo[1], Jean-François Laliberté[2] and Huanquan Zheng[1]*

[1] *Department of Biology, McGill University, Montreal, QC, Canada*
[2] *INRS-Institut Armand-Frappier, Institut National de la Recherche Scientifique, Laval, QC, Canada*

Edited by:
Peter Moffett, Université de Sherbrooke, Canada

Reviewed by:
Keiko Yoshioka, University of Toronto, Canada
Vicente Pallas, Instituto de Biología Molecular y Celular de Plantas (Universidad Politécnica de Valencia - Consejo Superior de Investigaciones Científicas), Spain

***Correspondence:**
Huanquan Zheng, Department of Biology, McGill University, 1205 Doctor Penfield Avenue, Montreal, QC, Canada H3A 1B1.
e-mail: hugo.zheng@mcgill.ca

The secretory pathway of eukaryotic cells has an elaborated set of endomembrane compartments involved in the synthesis, modification, and sorting of proteins and lipids. The secretory pathway in plant cells shares many features with that in other eukaryotic cells but also has distinct characteristics important for fundamental cell and developmental processes and for proper immune responses. Recently, there has been evidence that the remodeling of this pathway, and often the formation of viral-induced organelles, play an important role in viral replication and spread. The modification of the host secretory pathway seems to be a common feature among most single-stranded positive ss(+)RNA and even some DNA viruses. In this review, we will present the recent advances in the understanding of the organization and dynamics of the plant secretory pathway and the molecular regulation of membrane trafficking in the pathway. We will also discuss how different plant viruses may interact with the host secretory pathway for their efficient replication and spread, with a focus on tobacco mosaic virus and turnip mosaic virus.

Keywords: ER, Golgi, endosomes, virus replication, virus transport

INTRODUCTION

Like any other eukaryotic cells, plant cells are characterized by an elaborated secretory pathway composed of a complex network of organelles including the endoplasmic reticulum (ER), the Golgi apparatus, the *trans*-Golgi network (TGN), various endosomes, and vacuoles (Hanton et al., 2005; Bassham et al., 2008). This pathway is involved in the synthesis, modification and transport of proteins, lipids and polysaccharides (Bassham et al., 2008). Proteins made in the ER can be transported, via Golgi, toward the plasma membrane; on the other hand, proteins outside of the cells can also be internalized, via endocytosis. The proper organization and the dynamics of the secretory pathway are vital for normal cell development and physiology (Hanton et al., 2005).

In animal cells, it is known that efficient replication of many viruses involves a modification of the secretory pathway in host cells that generates a membrane structure designated as virosome, virus inclusion, virus factory, or viroplasm (for review, see Novoa et al., 2005; Netherton et al., 2007; Miller and Krijnse-Locker, 2008). Most animal viruses are membrane enveloped and it is known that the modification of the secretory pathway in host cells is also crucial for viral assembly (Netherton et al., 2007), intracellular and intercellular movement of viral complexes (Brandenburg and Zhuang, 2007), and inhibition of cellular secretion to reduce host immune response (Netherton et al., 2007). Different animal viruses modify the secretory pathway in many different ways for efficient viral replication, assembly, and spread along the secretory pathway (Netherton et al., 2007). For example, picornaviruses modify the early secretory pathway for RNA replication and inhibition of cellular secretion by interfering with the function of Arf1 and its guanine nucleotide exchange factor GBF1 in the formation of COPI vesicles (Hsu et al., 2010), while Norwalk virus inhibits cellular secretion through an interaction with COPII vesicles (Sharp et al., 2010). It is interesting that, although much less is known about how plant viruses modify the plant secretory pathway, recent data indicate that many plant viruses also utilize the plant secretory pathway for efficient replication and probably for cell-to-cell spread (Laliberte and Sanfacon, 2010; Schoelz et al., 2011; Verchot, 2011).

In this review, we will first highlight the recent progress in the organization and dynamics of the plant secretory pathway, we will then present the recent findings on how plant viruses may utilize the host secretory pathway for replication and intracellular and intercellular transport, with a focus on the recent advances on how the secretory pathway may be utilized by tobacco mosaic virus (TMV) and turnip mosaic virus (TuMV) for successful virus infection.

THE ORGANIZATION AND DYNAMICS OF THE ER–GOLGI INTERFACE IN PLANT CELLS

The ER is an extensive membrane network that extends throughout the cytoplasm. The ER is the largest membranous structure in the eukaryotic cell; it is the site where proteins and lipids are synthesized and modified. The Golgi apparatus, with *cis*-Golgi facing the ER and *trans*-Golgi away from the ER, is the central station in the secretory pathway. In Golgi, proteins and lipids received from the ER will be further modified and sorted to the proper destination in the secretory pathway. Despite the fact that in animal cells the ER is mainly aligned with microtubules (Du et al., 2004) and in plant cells with microfilaments (Boevink et al., 1998), the morphology of the ER in plants is quite similar to that in animal cells. The ER in both mature animal and plant cells exhibits a labyrinth-like morphology composed of membranous tubules and cisternae (Hu et al., 2009; Orso et al., 2009; Chen et al., 2011, 2012). In addition, the mechanisms that mediate the tubulation of

the ER (Voeltz et al., 2006; Sparkes et al., 2010) as well as the generation of interconnected ER network also appear to be conserved across different eukaryotic cells (Hu et al., 2009; Orso et al., 2009; Chen et al., 2011; Zheng and Chen, 2011). On the other hand, the organization of the Golgi apparatus is quite different between mammalian and plant cells. In mammalian cells, Golgi stacks form a single large perinuclear ribbon at the microtubule organization center peripheral to the nucleus (Ladinsky et al., 1999); in plant cells, the Golgi apparatus is present in the form of numerous individual cisternal stacks that move rapidly along the actin/ER cable in the cytoplasm (Boevink et al., 1998). As such, the morphology of the protein transport in the ER–Golgi interface appears very different between mammalian and plant cells.

Transport of proteins from the ER to the Golgi apparatus in both animal and plant cells starts from a transitional ER domain called ER export site (ERES). In mammalian cells, the ERESs are relatively stationary (Hammond and Glick, 2000), which are linked with the *cis*-Golgi by ERGIC, an ER–Golgi intermediate compartment made by the fusion of COPII vesicles formed at the ERESs (will be discussed below). In plant cells, individual ERESs are believed to be motile and tightly associated with Golgi stacks (daSilva et al., 2004). The ERES works together with individual Golgi stacks as a single functional unit (daSilva et al., 2004); no intermediate ERGIC has been revealed in plant cells. Yet it appears that the molecular mechanisms underlying protein transport in the ER–Golgi interface are very conserved between animal and plant kingdoms (Lee and Miller, 2007; Hsu and Yang, 2009; Hwang and Robinson, 2009; Marti et al., 2010; Chen et al., 2012).

In animal cells, transport from the ER to the Golgi apparatus is mediated by COPII vesicles (Lee and Miller, 2007). The proteins required for the formation of COPII vesicles from the ER include small Sar1 GTPase, membrane anchored **g**uanine **e**xchange **f**actor (GEF) Sec12, Sec23/Sec24 heterodimers for cargo selection and initiation of ER membrane curving (Bickford et al., 2004), and Sec13/Sec31 for the final formation of cage-like spherical vesicle (Lee and Miller, 2007). The fusion of COPII vesicles to generate ERGIC, which will further mature into *cis*-Golgi cisternae, requires small Rab1 GTPase and ER-localized SNARE (**s**oluble ***N***-ethylmaleimide-sensitive-factor **a**daptor-protein **re**ceptors) proteins (Bonifacino and Glick, 2004). In plant cells, despite the morphological difference in the ER–Golgi interface, all these key proteins exist (Bassham et al., 2008; Marti et al., 2010). It has been experimentally demonstrated that AtSEC24a as well as Rab-D proteins, homologs of Rab1, are required for ER-to-Golgi transport in plant cells (Batoko et al., 2000; Faso et al., 2009; Qi and Zheng, 2011). In mammalian cells, the retrograde Golgi transport, essential for recycling of proteins and lipids back to the ER in order to maintain equilibrium with the COPII-dependent transport, occurs mainly through COPI vesicles (Hsu and Yang, 2009). The COPI coatomer is composed by two protein complexes, F- and B-COP. The formation of COPI vesicles in Golgi cisternae requires small Arf1 GTPase, whose activity is regulated by Sec7-domain Arf1-GEFs (Hsu and Yang, 2009). Brefeldin A (BFA), a fungal metabolite, has been found to be a specific inhibitor that interferes with the interaction between Sec7-domain Arf-GEF and Arf proteins (Nebenfuhr et al., 2002). In *Arabidopsis thaliana*, electron tomography analysis have shown the existence of two types of COPI coated vesicles, the COPIa vesicles derived from *cis*-Golgi and the COPIb vesicles derived from the *trans*-Golgi (Hwang and Robinson, 2009).

THE ORGANIZATION AND DYNAMICS OF POST-GOLGI TRAFFIC NETWORK IN PLANT CELLS

Proteins and lipids, after being transported and modified in the Golgi apparatus, are further transported to either the plasma membrane, or to the lysosome/vacuole (in plant cells). In mammalian cells, cargo molecules modified in the Golgi apparatus are usually delivered to the TGN where they are sorted into either secretory vesicles that move to the plasma membrane, or clathrin-coated vesicles to deliver cargoes to the endosomes and then the lysosome (Traub and Kornfeld, 1997). This anterograde protein transport to the plasma membrane is usually balanced by various clathrin-coated vesicle mediated endocytic pathways (Gruenberg and Maxfield, 1995; Clague and Urbe, 2001). After being formed in the plasma membrane, clathrin-coated endocytic vesicles are first delivered to the early endosome (EE), a compartment that can be marked by Rab5, a small GTPase required for the fusion of clathrin-coated vesicles to the EE (Gorvel et al., 1991; Rink et al., 2005). At the EE, proteins can be either recycled back to the plasma membrane via recycling endosomes (RE; Grant and Donaldson, 2009), or further sorted to the late endosomes (LE) and the lysosome. It is thought that the protein recycling at the EE via the RE is mediated by Rab11 (Grant and Donaldson, 2009). The LE is believed to mature by the fusion of different EEs mediated by small Rab7 GTPase and LE-specific SNARE proteins (Bonifacino and Glick, 2004; Rink et al., 2005). At the LE, ESCRT (the endosomal sorting complexes required for transport) at the surface can selectively pick ubiquitinated membrane proteins to be directed to the lysosomes for further degradation (Katzmann et al., 2001).

In plant cells, initially the TGN was thought to be absent, but recent evidence suggests that the TGN may be a motile organelle derived from the Golgi apparatus (Dettmer et al., 2006; Kang et al., 2011; Qi et al., 2011). It has been demonstrated that the plant TGN could act as a sorting station and simultaneously release two types of vesicles: secretory vesicles heading to the plasma membrane and the cell wall (Preuss et al., 2006; Szumlanski and Nielsen, 2009; Qi et al., 2011), and clathrin-coated vesicles mediating transport to vacuoles (Kang et al., 2011). The organization of the dynamics of the post-Golgi traffic network in plant cells is, however, not well studied. It appears that protein transport in the plant post-Golgi traffic network is quite distinct from that in mammalian cells. There are several lines of evidence suggesting that the TGN in plants also serves as an EE (Dettmer et al., 2006; Qi et al., 2011). At the TGN/EE, proteins can be either recycled back to the plasma membrane (Ueda et al., 2001), or further transported to multivesicular bodies (MVB) or prevacuolar compartments (PVC), a compartment equivalent to the LE in animal cells (Spitzer et al., 2009). In plant cells, no RE has been identified. Different from mammalian cells, in plant cells the TGN/EE is highlighted by the presence of different Rab-A proteins (Szumlanski and Nielsen, 2009; Kang et al., 2011; Qi et al., 2011), homologs of the animal Rab11 protein; the MVB/PVC is marked by Rab-F proteins (Ueda et al., 2001), homologs of the Rab5 in animal cells. MVB/PVC

bearing ESCRT that can selectively pick ubiquitinated membrane proteins has also been reported (Spitzer et al., 2009).

THE ROLE OF THE HOST SECRETORY PATHWAY IN PLANT VIRAL REPLICATION

Viruses are obligate intracellular parasites that depend on cellular materials for their replication and spread. As mentioned in the introduction, replication and assembly of many membrane enveloped animal viruses occur in an intracellular compartment termed virus factory, viral inclusion, viroplasm, or virosome whose generation requires the modification of the host secretory pathway (Novoa et al., 2005; Netherton et al., 2007; Miller and Krijnse-Locker, 2008). Despite the fact that most plant viruses are not membrane enveloped, recent research revealed that plant viruses also utilize the host secretory pathway for viral replication (Laliberte and Sanfacon, 2010; Verchot, 2011).

Studies with TMV, an extensively studied member of *tobamoviruses*, showed that TMV infection causes severe modifications of the ER, converting it into large irregular aggregates early in infection (Reichel and Beachy, 1998). This ER-derived structure contains virus particles, the virus-encoded 183 and 126 kDa replicases, movement protein (MP), vRNA, ribosomes, and host translation elongation factor EF1-α (Beachy and Zaitlin, 1975; Heinlein et al., 1998; Reichel and Beachy, 1998; Mas and Beachy, 1999; Figueira et al., 2002). Therefore it is believed that this ER-derived structure is the site for TMV replication, which is often termed as viral replication complex (VRC; Heinlein et al., 1998). However, how exactly these TMV replication complexes are formed is not yet clear. The MP and the replicase components 126 and 183-kDa proteins are associated with the ER (Reichel and Beachy, 1998; Hagiwara et al., 2003). The MP, when expressed ectopically, can induce modifications in the ER (Reichel and Beachy, 1998) and the 126-kDa replicase, when expressed ectopically, can also induce the formation of cytoplasmic inclusion bodies (Ding et al., 2004). Therefore it is possible that these viral proteins are involved in the formation of TMV replication complexes. Furthermore, the TMV replication complexes are found to be associated with the host transmembrane proteins TOM1 (Yamanaka et al., 2000; Hagiwara et al., 2003) and ARL8, a small GTP-binding protein (Nishikiori et al., 2011). Both proteins are required for efficient TMV RNA replication (Nishikiori et al., 2011). This suggests that host proteins also play important roles in the formation of TMV replication complexes in the secretory pathway. It will be interesting to study how exactly these viral and host proteins are involved in the process.

In the case of *potyviruses*, TuMV infection induces the formation of small vesicular compartments that move rapidly along the microfilaments and the ER (Beauchemin et al., 2007; Cotton et al., 2009; Grangeon et al., 2012). The polyprotein $6K_2$-VPg-Pro, through its hydrophobic $6K_2$ domain, is responsible for the formation of these motile structures (Beauchemin et al., 2007). The presence of viral dsRNA, an obligate intermediate in the replication of the ssRNA viruses, as well as the host eukaryotic initiation factor iso4E (eIF(iso)4E), poly-A binding protein, heat shock cognate 70-3 protein (Hsc70-3), and the eukaryotic elongation factor 1A (eEF1A; Beauchemin and Laliberte, 2007; Beauchemin et al., 2007; Dufresne et al., 2008; Thivierge et al., 2008; Cotton et al., 2009) in the $6K_2$-induced vesicles suggests that the viral genome replication takes place in these structures (Cotton et al., 2009). Interestingly, in cells infected by the *potyvirus* tobacco etch virus (TEV), the motile $6K_2$ vesicular compartments are ER-derived and are associated with ERESs. The formation of the structure is COPII- and COPI-dependent (Wei and Wang, 2008). The motile $6K_2$ vesicles in TuMV-infected cells are associated but not perfectly with COPII vesicles as well as Golgi stacks (Grangeon et al., 2012). BFA can enhance the association of $6K_2$ vesicles with COPII and Golgi stacks (Grangeon et al., 2012). The interpretation of these facts is that the formation as well as the transport (will be discussed further) of the motile $6K_2$ structures requires an interaction between $6K_2$ and host proteins involved in the formation and transport of COPII and COPI vesicles.

Recently, we reported that TuMV induces the formation of a perinuclear globular structure with an amalgamation of viral $6K_2$, ER, Golgi, and COPII membranes as well as the presence of chloroplasts within the structure (Grangeon et al., 2012). This globular structure maintains a dynamic connection with the cortical ER and the Golgi apparatus; additionally the motile $6K_2$ vesicles may originate from the globular structure (Grangeon et al., 2012). We hypothesize that this globular structure could provide an extended platform for viral replication and protein synthesis (Grangeon et al., 2012). Indeed, the formation of large perinuclear ER-derived structures has also been observed in several other plant viruses. For example, cowpea mosaic virus (CPMV) induces the proliferation of ER membranes (de Zoeten et al., 1974; Carette et al., 2000, 2002a) that are often next to the nuclei. By the incorporation of H^3-uridine in the infected leaves, newly synthesized viral RNA can be found in the perinuclear membranous structures induced by CPMV (de Zoeten et al., 1974). Grapevine fanleaf virus (GFLV) induces the formation of a punctate-spongy perinuclear structure composed of reorganized ER membranes and active synthesis of RNA is found in these ER-derived structures (Ritzenthaler et al., 2002). Potato virus X (PVX) also forms an ER-contained perinuclear structure called X-body (Tilsner et al., 2012) where the viral replicase and TGB1 are located.

The exact mechanism by which these globular structures are formed remains unclear. It is known in plant cells that disruption of the formation of COPII vesicles also induces the formation of perinuclear clusters of the ER and Golgi membranes (Faso et al., 2009). The 60K helicase of CPMV interacts with the ER localized v-SNARE-like protein VAP27 in the proliferation of ER membranes (Carette et al., 2002b), suggesting that an interaction of viral and host ER proteins may be required in the process. It is interesting, however, in TuMV infected cells, the BFA treatment does not inhibit the formation of the perinuclear globular structure nor viral replication (Grangeon et al., 2012). Although the perinuclear structure in TuMV-infected cells contains the ER and Golgi membranes, it seems that the formation of the structure does not require a functional early secretory pathway. Similarly, BFA seems not affect replication of melon necrotic spot virus but it may have a negative impact on viral cell-to-cell movement (Genoves et al., 2010). On the other hand, in GFLV-infected cells, although it is not known if the BFA treatment inhibits the formation of the perinuclear structure, such treatment results in a significant reduction of the replication efficiency of the virus (Ritzenthaler

et al., 2002). It is highly likely that different viruses use different strategies to generate membranous structures for their efficient replication.

In animal cells, the generation of the virus factory containing the membranous structures of the host secretory pathway is also thought to be a mechanism for viruses to hide from host cell anti-viral defenses (Novoa et al., 2005; Miller and Krijnse-Locker, 2008). With regards to this, it is interesting to note that in *N. benthamiana* cells expressing a dominant-negative Vps23, Vps24, Snf7p, and Vps4p, components of ESCRT complexes, the replication of the tomato bushy stunt virus (TBSV), a member of *tombusvirus*, is impaired (Barajas et al., 2009). In addition, in yeast *vps23*Δ or *vps24*Δ cells, the activity of the viral replicase p92 is reduced and the (−) stranded viral RNA is more accessible to ribonucleases (Barajas et al., 2009). How the absence of ESCRT complexes in host cells could lead to a reduced activity of p92 and less stable viral RNA remains unknown. As mentioned previously, the ESCRT complexes are required for the recognition and sorting of ubiquitin-modified cargo proteins into MVBs and eventually to the vacuole (Katzmann et al., 2001; Spitzer et al., 2009). It is possible that ESCRT complexes are recruited into the viral replicase complex at some stages to help the virus to evade the recognition by host defense proteins and/or to avoid the degradation by the gene silencing machinery. Indeed, the p33 replication protein of TBSV interacts with Vps23p (Barajas et al., 2009), suggesting that the viral protein may be involved in the recruitment of ESCRT into the virus factory, or regulate the activity of ESCRT in the factory.

Although most plant viruses are not membrane enveloped, it is interesting to note that there is a small group of plant viruses such as the tomato spotted wilt virus (TSWV) that are membrane enveloped (Mumford et al., 1996). TSWV is a plant-infecting counterpart of the animal infecting viruses within the arthropod-borne Bunyaviridae. It is known that *bunyaviruses* that infect animal cells are replicated in tubular viral factories that are built around Golgi stacks but are connected to both mitochondria and the rough ER (Walter and Barr, 2011). After the final virion assembly in the lumen of swollen Golgi stacks, viruses bud into secretory vesicles in which they migrate toward the plasma membrane and are then secreted (Walter and Barr, 2011). However, it is not clear if this is also the case for TSWV. TSWV is replicated in infected plant cells in association with a membrane modification of the ER and Golgi (Ribeiro et al., 2008). The viral particles are assembled within the infected plant cells when ribonucleoprotein complexes (RNPs) are enwrapped by Golgi cisternae. The Golgi membrane wrapped RNPs then fuse with each other and with ER membranes, producing a singly enveloped vesicle where virus particles are retained until uptake by its insect vector (Kitajima et al., 1992; Kikkert et al., 1999). It was recently shown that the TSWV glycoproteins Gn and Gc induce the formation of ER- and Golgi-derived membranous structures upon ectopic expression in plant protoplasts (Ribeiro et al., 2008). The Gn glycoprotein localizes to both the ER and Golgi and is able to redirect the ER-arrested glycoprotein Gc to Golgi in a COPII-dependent manner upon co-expression (Ribeiro et al., 2009). In addition, both Gn and Gc interact with the TSWV nucleocapsid protein (N) and RNPs in ER and Golgi (Ribeiro et al., 2009). Therefore it seems that viral Gn and Gc glycoproteins, transported within the ER and Golgi, play an important role in the generation of the hybrid ER–Golgi structure where the virus is replicated and assembled. As one of the few plant viruses that are enveloped by lipid membranes, it will be interesting to examine how TSWV migrates, once assembled in the cytoplasmatic vesicles, to the neighboring cells. Likely, TSWV moves cell-to-cell differently from its animal counterpart, because the viral NSm protein, which was shown to restore the cell-to-cell and long distance movement of a movement-defective TMV clone (Lewandowski and Adkins, 2005), forms tubules in association with plasmodesmata (PD) upon TSWV infection of *N. rustica* (Storms et al., 1995).

ROLE OF THE HOST SECRETORY PATHWAY IN INTRA- AND INTER-CELLULAR TRANSPORT OF VIRUSES

As described above, many plant viruses replicate in infected cells in association with membranous structures derived from the host secretory pathway (Laliberte and Sanfacon, 2010; Verchot, 2011). Consequently, virions or viral nucleic acid–protein complexes must travel from the site where they are replicated to the neighboring cells to start the replication cycle again in order to cause a systemic infection. It has been generally accepted that plant viruses move from an infected cell to its neighboring cells through PD (Schoelz et al., 2011; Ueki and Citovsky, 2011). However, the virions and even the naked genome of plant viruses are too large to fit through unaltered PD. To facilitate the spread of viral particles or replication complexes, most plant viruses encode at least one dedicated protein termed movement protein (Lucas, 2006) to modify the structure of PD (Lucas, 2006; Schoelz et al., 2011; Ueki and Citovsky, 2011).

How could viral particles or replication complexes generated in the virus factory move to PD? Studies of various plant viruses over the past decades indicated that host cytoskeletal elements provide viruses the means to move from their sites of replication to PD from where they travel to the neighboring cells (Schoelz et al., 2011; Ueki and Citovsky, 2011). However, recent studies of some plant viruses indicate that the host secretory pathway and protein transport machineries may also be hijacked by viruses for their efficient transport to PD and cell-to-cell movement. In TMV, the MP and the 126 kDa replicase proteins are required for its efficient movement (Reichel and Beachy, 1998; Hirashima and Watanabe, 2001). Both proteins as well as TMV replication complexes are found to be associated with the ER (Heinlein et al., 1998; Yamanaka et al., 2000; Hagiwara et al., 2003). However, it is interesting that lower concentrations of BFA (10 μg/ml) or overexpression of dominant negative Sar1 does not inhibit intercellular transport of neither the MP of TMV nor the TMV replication complexes to PD (Tagami and Watanabe, 2007), while a higher concentration of BFA (>50 μg/ml) did inhibit the movement of the TMV MP to PD (Heinlein et al., 1998; Wright et al., 2007). The higher concentration of BFA is known to disrupt interconnected ER network (Zheng et al., 2004). Thus the interpretation of the different effect of different BFA concentrations could be that the transport of TMV to PD requires a networked ER but does not require the COPII-/COPI-dependent molecular machinery. Considering the fact that ER tubules traverse through PD to the neighboring cells, it is possible that ER tubules are used directly

by TMV as a transport conduit for both intra- and inter-cellular transport.

In the case of the members of the genus *Potyviruses*, it appears that intracellular transport of virus replication complexes from the site where they replicate to PD requires the classic COPII/COPI vesicle trafficking machinery in the secretory pathway. As described in the previous section, in both TuMV- and TEV-infected cells, motile $6K_2$ vesicular structures are identified as a site where viral genome can be replicated (Beauchemin et al., 2007; Cotton et al., 2009; Grangeon et al., 2012). Yet the formation of these motile $6K_2$ vesicles is COPII- and COPI-dependent (Wei and Wang, 2008). They are generated from ERESs, move to Golgi stacks, and are transported along the actin and the ER to the cell periphery (Beauchemin et al., 2007; Wei and Wang, 2008; Cotton et al., 2009; Grangeon et al., 2012). Furthermore, the movement of $6K_2$ and the cell-to-cell movement of TuMV can be inhibited by BFA at 10 μM (Grangeon et al., 2012). For *potyviruses*, the proteins VPg, CI, CP, and P3N-PIPO have been implicated in inter-cellular movement of viruses through PD (Nicolas et al., 1997; Rojas et al., 1997; Carrington et al., 1998; Wei and Wang, 2008; Wei et al., 2010). It is interesting that recently, Wei et al. (2010) demonstrated that the trafficking of P3N-PIPO and CI to PD requires a COPII-/COPI-dependent protein transport machinery, but not the actomyosin system (Wei et al., 2010) as the localization of P3N-PIPO and CI to PD is abolished in infected cells treated with BFA, or in cells expressing a mutant version of Sar1 [Sar1(H74L)], but not by actin disrupting agents. It seems that the transport of the *potyvirus* replication complex to the cell periphery requires the classic COPII/COPI vesicle trafficking machinery in the secretory pathway and the actomyosin system, but the transport of the viral proteins to PD for the subsequent modification of PD only requires the classic COPII/COPI vesicle trafficking machinery in the secretory pathway. However, NSvc4, the putative MP of rice strip virus (RSV) and MP17, the MP of potato leaf roll virus (PLRV), when expressed alone, are targeted to PD in COPII- and actin-dependent manners (Vogel et al., 2007; Yuan et al., 2011). Similarly, the MP protein p7B of *melon necrotic spot virus* is found to localize to the ER, Golgi, and PD when ectopically expressed (Genoves et al., 2010). Genoves et al. (2010) show that both BFA and latrunculin B inhibit the transport of p7B to Golgi and PD at the level the ER. However, it is generally accepted that in plant cells the actomyosin system is not required for protein transport from the ER to Golgi (Brandizzi et al., 2002).

As mentioned previously, in plant virus infected cells, PD has to be modified, either with an increase in SEL or formation of tubules (reviewed by Schoelz et al., 2011), to allow viral particles or replication complexes to spread. Recent data suggested that, in addition to movement-related proteins encoded by various viruses, some host proteins, for example, PDLP1, a type-I membrane protein located to PD, appear to be required for successful modification of PD (Huang et al., 2001; Thomas et al., 2008; Amari et al., 2010). When *Arabidopsis* plants expressing mutant versions of *PDLP1*, *PDLP2*, and *PDLP3* are inoculated with cauliflower mosaic virus (CaMV), a *Caulimovirus* that induces tubules through which CaMV virions move, significantly fewer plants present systemic infections (Amari et al., 2010). The replication of CaMV in the protoplasts carrying the triple mutation is, however, comparable to the replication in wild type *Arabidopsis* (Amari et al., 2010). This suggests that the PDLP1 protein plays a vital role in the movement of the virus, possibly in the modification of PD for the formation of tubules. It is interesting that the targeting of PDLP1 to PD is COPII-dependent (Thomas et al., 2008). However, in CaMV-infected cells, it appears that targeting of the MP of the virus to the cell periphery is not abolished by the treatment of BFA (Huang et al., 2000). It seems that transport of viral proteins of CaMV and host proteins to PD relies on different transport routes.

In addition to the above mentioned roles that the host secretory pathway may play in the transport of virus replication complexes and viral and host proteins required for efficient spread of viruses, it is worth noting that the TGB2 protein of potato mot top virus (PMTV), which is located to both the ER and PD and is probably involved in the modification of PD for intercellular virus movement (Cowan et al., 2002), can also be found in vesicles marked by FM4-64 (Haupt et al., 2005), a fluorescent dye that is widely used to track endocytosis in plant cells (Qi et al., 2011). TGB2 interacts with a J-domain chaperone essential for the endocytic protein transport and is also co-localized with Ara7, a Rab-F protein localized to the PVC/MVB (Haupt et al., 2005). In addition to this, the MP of TMV and a DNA virus, cabbage leaf curl virus (CaLCuV), physically interact with the clathrin-associated SNARE-interacting protein synaptotagmin (Lewis and Lazarowitz, 2010). Synaptotagmin is a Ca^{2+} sensor and down-regulation of this protein inhibits endocytosis and intercellular spread of TMV and CaLCuV (Lewis and Lazarowitz, 2010). However, the exact role that this endocytic protein transport pathway may play in the virus multiplication is yet to be determined. Endocytosis is known to be a mechanism for cells to regulate the localization and/or function of some plasma membrane localized proteins (Gruenberg and Maxfield, 1995), perhaps the accumulation and function of proteins required for modification of PD for efficient virus spread needs to be regulated by endocytosis.

CONCLUDING REMARKS

Plant cells have a sophisticated secretory pathway that is vital for their growth and survival in response for prevailing environmental conditions. In recent years, there has been an explosion of information regarding the organization of the plant secretory pathway and the molecular mechanisms that regulate protein transport in the plant secretory pathway. For successful infection of host plant cells, it seems that plant viruses have developed different yet highly host-adapted strategies to take advantage of the molecular machineries provided by the host secretory pathway to replicate and move from infected to uninfected cells. However, how plant viruses interplay with their host secretory pathway is not well understood. It is highly likely that different plant viruses interact differently with the host secretory pathway for efficient virus multiplication. To unravel the exact mechanisms by which different viruses are replicated, and transported to and through PD to neighboring cells, we need to identify more of the host factors required for the multiplication of different viruses. We need to understand how these host factors interact with different viral factors and to figure out the functional significance of these interactions in viral

infection. We believe that a further understanding of these issues is important for those who wish to develop plant cultivars that resist to virus infection. On the other hand, such research could also serve as a way to unlock the secrets of the host secretory pathway in plant cells.

ACKNOWLEDGMENTS

This study was supported by the National Science and Engineering Research Council of Canada and from Le Fonds de la Recherche sur la Nature et les Technologies from the Government of Québec to Jean-François Laliberté and Huanquan Zheng.

REFERENCES

Amari, K., Boutant, E., Hofmann, C., Schmitt-Keichinger, C., Fernandez-Calvino, L., Didier, P., et al. (2010). A family of plasmodesmal proteins with receptor-like properties for plant viral movement proteins. *PLoS Pathog* 6:e1001119. doi: 10.1371/journal.ppat.1001119

Barajas, D., Jiang, Y., and Nagy, P. D. (2009). A unique role for the host ESCRT proteins in replication of tomato bushy stunt virus. *PLoS Pathog* 5:e1000705. doi: 10.1371/journal.ppat.1000705

Bassham, D. C., Brandizzi, F., Otegui, M. S., and Sanderfoot, A. A. (2008). The secretory system of *Arabidopsis*. *Arabidopsis Book* 6:e0116. doi: 10.1199/tab.0116

Batoko, H., Zheng, H. Q., Hawes, C., and Moore, I. (2000). A Rab1 GTPase is required for transport between the endoplasmic reticulum and Golgi apparatus and for normal Golgi movement in plants. *Plant Cell* 12, 2201–2218.

Beachy, R. N., and Zaitlin, M. (1975). Replication of tobacco mosaic virus: VI. Replicative intermediate and TMV-RNA-related RNAs associated with polyribosomes. *Virology* 63, 84–97.

Beauchemin, C., Boutet, N., and Laliberte, J. F. (2007). Visualization of the interaction between the precursors of VPg, the viral protein linked to the genome of turnip mosaic virus, and the translation eukaryotic initiation factor iso 4E in planta. *J. Virol.* 81, 775–782.

Beauchemin, C., and Laliberte, J. F. (2007). The poly(A) binding protein is internalized in virus-induced vesicles or redistributed to the nucleolus during turnip mosaic virus infection. *J. Virol.* 81, 10905–10913.

Bickford, L. C., Mossessova, E., and Goldberg, J. (2004). A structural view of the COPII vesicle coat. *Curr. Opin. Struct. Biol.* 14, 147–153.

Boevink, P., Oparka, K., Santa Cruz, S., Martin, B., Betteridge, A., and Hawes, C. (1998). Stacks on tracks: the plant Golgi apparatus traffics on an actin/ER network. *Plant J.* 15, 441–447.

Bonifacino, J. S., and Glick, B. S. (2004). The mechanisms of vesicle budding and fusion. *Cell* 116, 153–166.

Brandenburg, B., and Zhuang, X. (2007). Virus trafficking – learning from single-virus tracking. *Nat. Rev. Microbiol.* 5, 197–208.

Brandizzi, F., Snapp, E. L., Roberts, A. G., Lippincott-Schwartz, J., and Hawes, C. (2002). Membrane protein transport between the endoplasmic reticulum and the Golgi in tobacco leaves is energy dependent but cytoskeleton independent: evidence from selective photobleaching. *Plant Cell* 14, 1293–1309.

Carette, J. E., Stuiver, M., Van Lent, J., Wellink, J., and Van Kammen, A. (2000). Cowpea mosaic virus infection induces a massive proliferation of endoplasmic reticulum but not Golgi membranes and is dependent on de novo membrane synthesis. *J. Virol.* 74, 6556–6563.

Carette, J. E., Van Lent, J., Macfarlane, S. A., Wellink, J., and Van Kammen, A. (2002a). Cowpea mosaic virus 32- and 60-kilodalton replication proteins target and change the morphology of endoplasmic reticulum membranes. *J. Virol.* 76, 6293–6301.

Carette, J. E., Verver, J., Martens, J., Van Kampen, T., Wellink, J., and Van Kammen, A. (2002b). Characterization of plant proteins that interact with cowpea mosaic virus '60K' protein in the yeast two-hybrid system. *J. Gen. Virol.* 83, 885–893.

Carrington, J. C., Jensen, P. E., and Schaad, M. C. (1998). Genetic evidence for an essential role for potyvirus CI protein in cell-to-cell movement. *Plant J.* 14, 393–400.

Chen, J., Qi, X., and Zheng, H. (2012). Subclass-specific localization and trafficking of *Arabidopsis* p24 proteins in the ER–Golgi interface. *Traffic* 13, 400–415.

Chen, J., Stefano, G., Brandizzi, F., and Zheng, H. (2011). *Arabidopsis* RHD3 mediates the generation of the tubular ER network and is required for Golgi distribution and motility in plant cells. *J. Cell Sci.* 124, 2241–2252.

Clague, M. J., and Urbe, S. (2001). The interface of receptor trafficking and signalling. *J. Cell Sci.* 114, 3075–3081.

Cotton, S., Grangeon, R., Thivierge, K., Mathieu, I., Ide, C., Wei, T., et al. (2009). Turnip mosaic virus RNA replication complex vesicles are mobile, align with microfilaments, and are each derived from a single viral genome. *J. Virol.* 83, 10460–10471.

Cowan, G. H., Lioliopoulou, F., Ziegler, A., and Torrance, L. (2002). Subcellular localisation, protein interactions, and RNA binding of potato mop-top virus triple gene block proteins. *Virology* 298, 106–115.

daSilva, L. L., Snapp, E. L., Denecke, J., Lippincott-Schwartz, J., Hawes, C., and Brandizzi, F. (2004). Endoplasmic reticulum export sites and Golgi bodies behave as single mobile secretory units in plant cells. *Plant Cell* 16, 1753–1771.

Dettmer, J., Hong-Hermesdorf, A., Stierhof, Y. D., and Schumacher, K. (2006). Vacuolar H+-ATPase activity is required for endocytic and secretory trafficking in *Arabidopsis*. *Plant Cell* 18, 715–730.

de Zoeten, G. A., Assink, A. M., and Van Kammen, A. (1974). Association of cowpea mosaic virus-induced double-stranded RNA with a cytopathological structure in infected cells. *Virology* 59, 341–355.

Ding, X. S., Liu, J. Z., Cheng, N. H., Folimonov, A., Hou, Y. M., Bao, Y., et al. (2004). The tobacco mosaic virus 126-kDa protein associated with virus replication and movement suppresses RNA silencing. *Mol. Plant Microbe Interact.* 17, 583–592.

Du, Y., Ferro-Novick, S., and Novick, P. (2004). Dynamics and inheritance of the endoplasmic reticulum. *J. Cell Sci.* 117, 2871–2878.

Dufresne, P. J., Thivierge, K., Cotton, S., Beauchemin, C., Ide, C., Ubalijoro, E., et al. (2008). Heat shock 70 protein interaction with turnip mosaic virus RNA-dependent RNA polymerase within virus-induced membrane vesicles. *Virology* 374, 217–227.

Faso, C., Chen, Y. N., Tamura, K., Held, M., Zemelis, S., Marti, L., et al. (2009). A missense mutation in the *Arabidopsis* COPII coat protein Sec24A induces the formation of clusters of the endoplasmic reticulum and Golgi apparatus. *Plant Cell* 21, 3655–3671.

Figueira, A. D., Golem, S., Goregaoker, S. P., and Culvert, J. N. (2002). A nuclear localization signal and a membrane association domain contribute to the cellular localization of the tobacco mosaic virus 126-kDa replicase protein. *Virology* 301, 81–89.

Genoves, A., Navarro, J. A., and Pallas, V. (2010). The intra- and intercellular movement of melon necrotic spot virus (MNSV) depends on an active secretory pathway. *Mol. Plant Microbe Interact.* 23, 263–272.

Gorvel, J. P., Chavrier, P., Zerial, M., and Gruenberg, J. (1991). rab5 controls early endosome fusion in vitro. *Cell* 64, 915–925.

Grangeon, R., Agbeci, M., Chen, J., Grondin, G., Zheng, H., and Laliberte, J. F. (2012). Impact on the endoplasmic reticulum and Golgi apparatus of turnip mosaic virus infection. *J. Virol.* 86, 9255–9265.

Grant, B. D., and Donaldson, J. G. (2009). Pathways and mechanisms of endocytic recycling. *Nat. Rev. Mol. Cell Biol.* 10, 597–608.

Gruenberg, J., and Maxfield, F. R. (1995). Membrane transport in the endocytic pathway. *Curr. Opin. Cell Biol.* 7, 552–563.

Hagiwara, Y., Komoda, K., Yamanaka, T., Tamai, A., Meshi, T., Funada, R., et al. (2003). Subcellular localization of host and viral proteins associated with tobamovirus RNA replication. *EMBO J.* 22, 344–353.

Hammond, A. T., and Glick, B. S. (2000). Dynamics of transitional endoplasmic reticulum sites in vertebrate cells. *Mol. Biol. Cell* 11, 3013–3030.

Hanton, S. L., Bortolotti, L. E., Renna, L., Stefano, G., and Brandizzi, F. (2005). Crossing the divide – transport between the endoplasmic reticulum and Golgi apparatus in plants. *Traffic* 6, 267–277.

Haupt, S., Cowan, G. H., Ziegler, A., Roberts, A. G., Oparka, K. J., and Torrance, L. (2005). Two plant-viral movement proteins traffic in the endocytic recycling pathway. *Plant Cell* 17, 164–181.

Heinlein, M., Padgett, H. S., Gens, J. S., Pickard, B. G., Casper, S. J., Epel, B. L., et al. (1998). Changing patterns of localization of the tobacco mosaic virus movement protein and replicase to the endoplasmic reticulum and microtubules during infection. *Plant Cell* 10, 1107–1120.

Hirashima, K., and Watanabe, Y. (2001). Tobamovirus replicase coding region is involved in cell-to-cell movement. *J. Virol.* 75, 8831–8836.

Hsu, N. Y., Ilnytska, O., Belov, G., Santiana, M., Chen, Y. H., Takvorian, P. M., et al. (2010). Viral reorganization of the secretory pathway generates distinct organelles for RNA replication. *Cell* 141, 799–811.

Hsu, V. W., and Yang, J. S. (2009). Mechanisms of COPI vesicle formation. *FEBS Lett.* 583, 3758–3763.

Hu, J., Shibata, Y., Zhu, P. P., Voss, C., Rismanchi, N., Prinz, W. A., et al. (2009). A class of dynamin-like GTPases involved in the generation of the tubular ER network. *Cell* 138, 549–561.

Huang, Z., Andrianov, V. M., Han, Y., and Howell, S. H. (2001). Identification of *Arabidopsis* proteins that interact with the cauliflower mosaic virus (CaMV) movement protein. *Plant Mol. Biol.* 47, 663–675.

Huang, Z., Han, Y., and Howell, S. H. (2000). Formation of surface tubules and fluorescent foci in *Arabidopsis thaliana* protoplasts expressing a fusion between the green fluorescent protein and the cauliflower mosaic virus movement protein. *Virology* 271, 58–64.

Hwang, I., and Robinson, D. G. (2009). Transport vesicle formation in plant cells. *Curr. Opin. Plant Biol.* 12, 660–669.

Kang, B. H., Nielsen, E., Preuss, M. L., Mastronarde, D., and Staehelin, L. A. (2011). Electron tomography of RabA4b- and PI-4Kbeta1-labeled *trans* Golgi network compartments in *Arabidopsis*. *Traffic* 12, 313–329.

Katzmann, D. J., Babst, M., and Emr, S. D. (2001). Ubiquitin-dependent sorting into the multivesicular body pathway requires the function of a conserved endosomal protein sorting complex, ESCRT-I. *Cell* 106, 145–155.

Kikkert, M., Van Lent, J., Storms, M., Bodegom, P., Kormelink, R., and Goldbach, R. (1999). Tomato spotted wilt virus particle morphogenesis in plant cells. *J. Virol.* 73, 2288–2297.

Kitajima, E. W., Deavila, A. C., Resende, R. D., Goldbach, R. W., and Peters, D. (1992). Comparative cytological and immunogold labeling studies on different isolates of tomato spotted wilt virus. *J. Submicrosc. Cytol. Pathol.* 24, 1–14.

Ladinsky, M. S., Mastronarde, D. N., Mcintosh, J. R., Howell, K. E., and Staehelin, L. A. (1999). Golgi structure in three dimensions: functional insights from the normal rat kidney cell. *J. Cell Biol.* 144, 1135–1149.

Laliberte, J. F., and Sanfacon, H. (2010). Cellular remodeling during plant virus infection. *Annu. Rev. Phytopathol.* 48, 69–91.

Lee, M. C., and Miller, E. A. (2007). Molecular mechanisms of COPII vesicle formation. *Semin. Cell Dev. Biol.* 18, 424–434.

Lewandowski, D. J., and Adkins, S. (2005). The tubule-forming NSm protein from tomato spotted wilt virus complements cell-to-cell and long-distance movement of tobacco mosaic virus hybrids. *Virology* 342, 26–37.

Lewis, J. D., and Lazarowitz, S. G. (2010). *Arabidopsis* synaptotagmin SYTA regulates endocytosis and virus movement protein cell-to-cell transport. *Proc. Natl. Acad. Sci. U.S.A.* 107, 2491–2496.

Lucas, W. J. (2006). Plant viral movement proteins: agents for cell-to-cell trafficking of viral genomes. *Virology* 344, 169–184.

Marti, L., Fornaciari, S., Renna, L., Stefano, G., and Brandizzi, F. (2010). COPII-mediated traffic in plants. *Trends Plant Sci.* 15, 522–528.

Mas, P., and Beachy, R. N. (1999). Replication of tobacco mosaic virus on endoplasmic reticulum and role of the cytoskeleton and virus movement protein in intracellular distribution of viral RNA. *J. Cell Biol.* 147, 945–958.

Miller, S., and Krijnse-Locker, J. (2008). Modification of intracellular membrane structures for virus replication. *Nat. Rev. Microbiol.* 6, 363–374.

Mumford, R. A., Barker, I., and Wood, K. R. (1996). The biology of the tospoviruses. *Ann. Appl. Biol.* 128, 159–183.

Nebenfuhr, A., Ritzenthaler, C., and Robinson, D. G. (2002). Brefeldin A: deciphering an enigmatic inhibitor of secretion. *Plant Physiol.* 130, 1102–1108.

Netherton, C., Moffat, K., Brooks, E., and Wileman, T. (2007). A guide to viral inclusions, membrane rearrangements, factories, and viroplasm produced during virus replication. *Adv. Virus Res.* 70, 101–182.

Nicolas, O., Dunnington, S. W., Gotow, L. F., Pirone, T. P., and Hellmann, G. M. (1997). Variations in the VPg protein allow a potyvirus to overcome va gene resistance in tobacco. *Virology* 237, 452–459.

Nishikiori, M., Mori, M., Dohi, K., Okamura, H., Katoh, E., Naito, S., et al. (2011). A host small GTP-binding protein ARL8 plays crucial roles in Tobamovirus RNA replication. *PLoS Pathog* 7:e1002409. doi: 10.1371/journal.ppat.1002409

Novoa, R. R., Calderita, G., Arranz, R., Fontana, J., Granzow, H., and Risco, C. (2005). Virus factories: associations of cell organelles for viral replication and morphogenesis. *Biol. Cell* 97, 147–172.

Orso, G., Pendin, D., Liu, S., Tosetto, J., Moss, T. J., Faust, J. E., et al. (2009). Homotypic fusion of ER membranes requires the dynamin-like GTPase atlastin. *Nature* 460, 978–983.

Preuss, M. L., Schmitz, A. J., Thole, J. M., Bonner, H. K., Otegui, M. S., and Nielsen, E. (2006). A role for the RabA4b effector protein PI-4Kbeta1 in polarized expansion of root hair cells in *Arabidopsis thaliana*. *J. Cell Biol.* 172, 991–998.

Qi, X., Kaneda, M., Chen, J., Geitmann, A., and Zheng, H. (2011). A specific role for *Arabidopsis* TRAPPII in post-Golgi trafficking that is crucial for cytokinesis and cell polarity. *Plant J.* 68, 234–248.

Qi, X., and Zheng, H. (2011). *Arabidopsis* TRAPPII is functionally linked to Rab-A, but not Rab-D in polar protein trafficking in *trans*-Golgi network. *Plant Signal. Behav.* 6, 1679–1683.

Reichel, C., and Beachy, R. N. (1998). Tobacco mosaic virus infection induces severe morphological changes of the endoplasmic reticulum. *Proc. Natl. Acad. Sci. U.S.A.* 95, 11169–11174.

Ribeiro, D., Borst, J. W., Goldbach, R., and Kormelink, R. (2009). Tomato spotted wilt virus nucleocapsid protein interacts with both viral glycoproteins Gn and Gc in planta. *Virology* 383, 121–130.

Ribeiro, D., Foresti, O., Denecke, J., Wellink, J., Goldbach, R., and Kormelink, R. J. (2008). Tomato spotted wilt virus glycoproteins induce the formation of endoplasmic reticulum- and Golgi-derived pleomorphic membrane structures in plant cells. *J. Gen. Virol.* 89, 1811–1818.

Rink, J., Ghigo, E., Kalaidzidis, Y., and Zerial, M. (2005). Rab conversion as a mechanism of progression from early to late endosomes. *Cell* 122, 735–749.

Ritzenthaler, C., Laporte, C., Gaire, F., Dunoyer, P., Schmitt, C., Duval, S., et al. (2002). Grapevine fanleaf virus replication occurs on endoplasmic reticulum-derived membranes. *J. Virol.* 76, 8808–8819.

Rojas, M. R., Zerbini, F. M., Allison, R. F., Gilbertson, R. L., and Lucas, W. J. (1997). Capsid protein and helper component-proteinase function as potyvirus cell-to-cell movement proteins. *Virology* 237, 283–295.

Schoelz, J. E., Harries, P. A., and Nelson, R. S. (2011). Intracellular transport of plant viruses: finding the door out of the cell. *Mol. Plant* 4, 813–831.

Sharp, T. M., Guix, S., Katayama, K., Crawford, S. E., and Estes, M. K. (2010). Inhibition of cellular protein secretion by norwalk virus nonstructural protein p22 requires a mimic of an endoplasmic reticulum export signal. *PLoS ONE* 5:e13130. doi: 10.1371/journal.pone.0013130

Sparkes, I., Tolley, N., Aller, I., Svozil, J., Osterrieder, A., Botchway, S., et al. (2010). Five *Arabidopsis* reticulon isoforms share endoplasmic reticulum location, topology, and membrane-shaping properties. *Plant Cell* 22, 1333–1343.

Spitzer, C., Reyes, F. C., Buono, R., Sliwinski, M. K., Haas, T. J., and Otegui, M. S. (2009). The ESCRT-related CHMP1A and B proteins mediate multivesicular body sorting of auxin carriers in *Arabidopsis* and are required for plant development. *Plant Cell* 21, 749–766.

Storms, M. M., Kormelink, R., Peters, D., Van Lent, J. W., and Goldbach, R. W. (1995). The nonstructural NSm protein of tomato spotted wilt virus induces tubular structures in plant and insect cells. *Virology* 214, 485–493.

Szumlanski, A. L., and Nielsen, E. (2009). The Rab GTPase RabA4d regulates pollen tube tip growth in *Arabidopsis thaliana*. *Plant Cell* 21, 526–544.

Tagami, Y., and Watanabe, Y. (2007). Effects of brefeldin A on the localization of Tobamovirus movement protein and cell-to-cell movement of the virus. *Virology* 361, 133–140.

Thivierge, K., Cotton, S., Dufresne, P. J., Mathieu, I., Beauchemin, C., Ide, C., et al. (2008). Eukaryotic elongation factor 1A interacts with turnip mosaic virus RNA-dependent RNA polymerase and VPg-Pro in virus-induced vesicles. *Virology* 377, 216–225.

Thomas, C. L., Bayer, E. M., Ritzenthaler, C., Fernandez-Calvino, L., and Maule, A. J. (2008). Specific targeting of a plasmodesmal protein affecting cell-to-cell communication. *PLoS Biol.* 6:e7. doi: 10.1371/journal.pbio.0060007

Tilsner, J., Linnik, O., Wright, K. M., Bell, K., Roberts, A. G., Lacomme, C., et al. (2012). The TGB1 movement protein of potato virus X reorganizes actin and endomembranes into the X-body, a viral replication factory. *Plant Physiol.* 158, 1359–1370.

Traub, L. M., and Kornfeld, S. (1997). The *trans*-Golgi network: a late secretory sorting station. *Curr. Opin. Cell Biol.* 9, 527–533.

Ueda, T., Yamaguchi, M., Uchimiya, H., and Nakano, A. (2001). Ara6, a

plant-unique novel type Rab GTPase, functions in the endocytic pathway of *Arabidopsis thaliana*. *EMBO J.* 20, 4730–4741.

Ueki, S., and Citovsky, V. (2011). To gate, or not to gate: regulatory mechanisms for intercellular protein transport and virus movement in plants. *Mol. Plant* 4, 782–793.

Verchot, J. (2011). Wrapping membranes around plant virus infection. *Curr. Opin. Virol.* 1, 388–395.

Voeltz, G. K., Prinz, W. A., Shibata, Y., Rist, J. M., and Rapoport, T. A. (2006). A class of membrane proteins shaping the tubular endoplasmic reticulum. *Cell* 124, 573–586.

Vogel, F., Hofius, D., and Sonnewald, U. (2007). Intracellular trafficking of potato leafroll virus movement protein in transgenic *Arabidopsis*. *Traffic* 8, 1205–1214.

Walter, C. T., and Barr, J. N. (2011). Recent advances in the molecular and cellular biology of bunyaviruses. *J. Gen. Virol.* 92, 2467–2484.

Wei, T., and Wang, A. (2008). Biogenesis of cytoplasmic membranous vesicles for plant potyvirus replication occurs at endoplasmic reticulum exit sites in a COPI- and COPII-dependent manner. *J. Virol.* 82, 12252–12264.

Wei, T., Zhang, C., Hong, J., Xiong, R., Kasschau, K. D., Zhou, X., et al. (2010). Formation of complexes at plasmodesmata for potyvirus intercellular movement is mediated by the viral protein P3N-PIPO. *PLoS Pathog* 6:e1000962. doi: 10.1371/journal.ppat.1000962

Wright, K. M., Wood, N. T., Roberts, A. G., Chapman, S., Boevink, P., Mackenzie, K. M., et al. (2007). Targeting of TMV movement protein to plasmodesmata requires the actin/ER network: evidence from FRAP. *Traffic* 8, 21–31.

Yamanaka, T., Ohta, T., Takahashi, M., Meshi, T., Schmidt, R., Dean, C., et al. (2000). TOM1, an *Arabidopsis* gene required for efficient multiplication of a tobamovirus, encodes a putative transmembrane protein. *Proc. Natl. Acad. Sci. U.S.A.* 97, 10107–10112.

Yuan, Z. J., Chen, H. Y., Chen, Q., Omura, T., Xie, L. H., Wu, Z. J., et al. (2011). The early secretory pathway and an actin–myosin VIII motility system are required for plasmodesmatal localization of the NSvc4 protein of rice stripe virus. *Virus Res.* 159, 62–68.

Zheng, H., and Chen, J. (2011). Emerging aspects of ER organization in root hair tip growth: lessons from RHD3 and Atlastin. *Plant Signal. Behav.* 6, 1710–1713.

Zheng, H., Kunst, L., Hawes, C., and Moore, I. (2004). A GFP-based assay reveals a role for RHD3 in transport between the endoplasmic reticulum and Golgi apparatus. *Plant J.* 37, 398–414.

Conflict of Interest Statement: The authors declare that the research was conducted in the absence of any commercial or financial relationships that could be construed as a potential conflict of interest.

Received: 03 October 2012; paper pending published: 06 November 2012; accepted: 21 December 2012; published online: 11 January 2013.

*Citation: Patarroyo C, Laliberté J-F and Zheng H (2013) Hijack it, change it: how do plant viruses utilize the host secretory pathway for efficient viral replication and spread? Front. Plant Sci. **3**:308. doi: 10.3389/fpls.2012.00308*

This article was submitted to Frontiers in Plant-Microbe Interaction, a specialty of Frontiers in Plant Science.

frontiers in
PLANT SCIENCE

MINI REVIEW ARTICLE
published: 29 January 2013
doi: 10.3389/fpls.2012.00313

Investigating the role of viral integral membrane proteins in promoting the assembly of nepovirus and comovirus replication factories

Hélène Sanfaçon*

Pacific Agri-Food Research Centre, Agriculture and Agri-Food Canada, Summerland, BC, Canada

Edited by:
Richard Nelson, Samuel Roberts Noble Foundation, Inc., USA

Reviewed by:
Michael Goodin, University of Kentucky, USA
George A. Belov, University of Maryland, USA

****Correspondence:***
Hélène Sanfaçon, Pacific Agri-Food Research Centre, Agriculture and Agri-Food Canada, 4200 Highway 97, Summerland, BC, Canada V0H 1Z0.
e-mail: helene.sanfacon@agr.gc.ca

Formation of plant virus membrane-associated replication factories requires the association of viral replication proteins and viral RNA with intracellular membranes, the recruitment of host factors and the modification of membranes to form novel structures that house the replication complex. Many viruses encode integral membrane proteins that act as anchors for the replication complex. These hydrophobic proteins contain transmembrane domains and/or amphipathic helices that associate with the membrane and modify its structure. The comovirus Co-Pro and NTP-binding (NTB, putative helicase) proteins and the cognate nepovirus X2 and NTB proteins are among the best characterized plant virus integral membrane replication proteins and are functionally related to the picornavirus 2B, 2C, and 3A membrane proteins. The identification of membrane association domains and analysis of the membrane topology of these proteins is discussed. The evidence suggesting that these proteins have the ability to induce membrane proliferation, alter the structure and integrity of intracellular membranes, and modulate the induction of symptoms in infected plants is also reviewed. Finally, areas of research that need further investigation are highlighted.

Keywords: integral membrane proteins, viral replication complexes, intracellular membranes, protein–membrane interactions, secoviridae, picornavirales, plant–virus interactions, membrane remodeling

CHARACTERIZATION OF COMOVIRUS AND NEPOVIRUS REPLICATION COMPLEXES AND IDENTIFICATION OF PUTATIVE MEMBRANE ANCHORS

Positive-strand RNA viruses replicate in large complexes that are associated with host intracellular membranes (Salonen et al., 2005; Sanfacon, 2005; Miller and Krijnse-Locker, 2008; den Boon and Ahlquist, 2010; Laliberte and Sanfacon, 2010; Nagy and Pogany, 2012). Some viruses require host membrane proteins to target their replication proteins to the membranes (Yamanaka et al., 2000). However, many viruses encode proteins that interact with membranes directly and modify their intrinsic structure. These proteins have membrane association domains and contain protein–protein and/or protein–RNA interaction domains that allow them to recruit the viral RNA, other viral replication proteins, or host factors to the membranes. Well-characterized plant virus membrane proteins include the tombusvirus 33–36 kDa proteins, bromovirus 1a protein, potyvirus 6K protein, and tymovirus 140 kDa protein (Schaad et al., 1997; den Boon et al., 2001; Weber-Lotfi et al., 2002; Prod'Homme et al., 2003; Turner et al., 2004).

The family Secoviridae (order Picornavirales) includes the genera *Comovirus*, *Fabavirus*, *Nepovirus*, *Sequivirus*, *Waikavirus*, *Cheravirus*, *Sadwavirus*, and *Torradovirus* (Sanfacon et al., 2011). The best characterized members of the family are Cowpea mosaic virus (CPMV, comovirus), Grapevine fanleaf virus (GFLV, nepovirus), and Tomato ringspot virus (ToRSV, nepovirus; Pouwels et al., 2002a; Sanfacon et al., 2006). These viruses use a polyprotein strategy to express their proteins and have a replication block consisting of a nucleotide-binding protein (NTB), a genome-linked protein (VPg), a proteinase (Pro), and an RNA-dependent RNA polymerase (Pol; **Figure 1C**). Although they share these properties with picornaviruses (including the well-characterized poliovirus), nepo- and comoviruses differ in that they have bipartite genomes. The RNA1-encoded polyprotein contains all protein domains necessary for replication and RNA1 can replicate independently of RNA2 (Vos et al., 1988; Viry et al., 1993).

Plant cells infected by como- and nepoviruses are characterized by the presence of numerous membraneous vesicles, which are derived from the endoplasmic reticulum (ER; Carette et al., 2000; Ritzenthaler et al., 2002; Han and Sanfacon, 2003). In CPMV-infected cells, vesicles first appear throughout the cytoplasm, but later coalesce in a large perinuclear structure (Carette et al., 2002a). Actin microfilaments are probably involved in this process (Carette et al., 2002a). Perinuclear membrane aggregates are also observed in ToRSV- and GFLV-infected cells (Ritzenthaler et al., 2002; Han and Sanfacon, 2003). Viral replication proteins, *de novo* RNA synthesis and dsRNA intermediates co-localize with these structures, indicating that they are the site of viral replication (de Zoeten et al., 1974; Carette et al., 2000, 2002a; Ritzenthaler et al., 2002; Han and Sanfacon, 2003).

Vesicles induced in como- and nepovirus-infected cells are irregularly shaped, vary in size and are usually surrounded by a single-membrane (Carette et al., 2000; Ritzenthaler et al., 2002; **Figure 1A**). These vesicles are similar to those observed in early

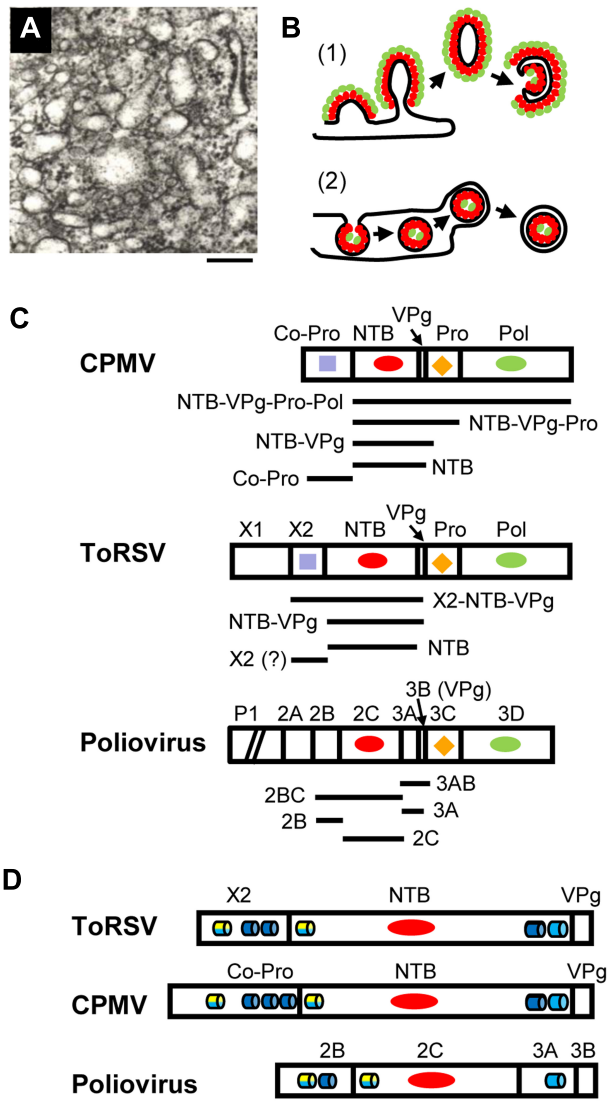

FIGURE 1 | Membrane replication proteins encoded by CPMV, ToRSV and poliovirus. (A) Electron micrograph showing the proliferation of single-membrane vesicles in ToRSV-infected *Nicotiana clevelandii* plants. The bar indicates 200 nm. **(B)** Models for the formation of viral replication complexes. (1) In cells infected with poliovirus or coxsackie B3 virus, viral integral membrane proteins (red ovals) induce positive curvature of the membrane allowing the budding of tubular structures. Other viral replication proteins (e.g., polymerase, green ovals) interact with the viral membrane proteins. Host factors and viral RNA (not shown) associate with the replication complex by protein–protein and protein–RNA interactions. Single-membrane vesicles may bud out and form double-membrane vesicles after the internal collapse of the single-membrane vesicle and subsequent membrane fusion to allow its circularization. Late in infection, double-membrane vesicles are predominant in picornavirus-infected cells. This model is based on electron tomography observations from Belov et al. (2012) and Limpens et al. (2011). (2) In cells infected with many plant and animal viruses, induction of negative membrane curvature results in membrane invagination and formation of spherules in the lumen of the membrane. In plant, spherules have been observed in association with membranes from the ER (brome mosaic virus), chloroplast (turnip yellow mosaic virus), peroxisome (tomato bushy stunt virus) and mitochondria (carnation Italian ringspot virus). The spherules are connected to the cytoplasm by a neck. Viral integral membrane proteins (red ovals) line the *(Continued)*

FIGURE 1 | Continued
interior of the spherule. The viral polymerase (green ovals) as well as other viral proteins, host factors and the viral RNA (not shown) are enclosed in the spherule. Release of the vesicle in the lumen of the membrane may be followed by budding of a double-membrane vesicle into the cytoplasm. This model has been discussed in recent reviews (den Boon and Ahlquist, 2010; Laliberte and Sanfacon, 2010; Nagy and Pogany, 2012). **(C)** Organization of replication protein domains in the polyproteins of CPMV, ToRSV, and poliovirus. The RNA1-encoded polyproteins of CPMV and ToRSV are shown. For poliovirus, the polyprotein encoded by the single genomic RNA is shown, although the P1 region (containing the structural proteins) is truncated as indicated by the diagonal bars. Vertical lines represent the protease cleavage sites. Conserved motifs are: RNA-dependent RNA polymerase (Pol, green ovals), protease (Pro, orange diamond), nucleotide-binding protein (NTB, red oval), Co-Pro and X2 (purple square). Horizontal bars under each polyprotein represent integral membrane proteins that have been detected in virus-infected cells. The mature ToRSV X2 protein is shown with a question mark. Although likely, its presence in infected cells could not be confirmed due to the lack of antibodies. **(D)** The regions of the polyprotein containing the putative membrane anchors are shown for each virus. Predicted membrane-association domains are indicated with blue barrels (hydrophobic helices) or with yellow/blue barrels (amphipathic helices, with the yellow half representing the polar/charged hydrophilic side of the helix and the blue half representing the hydrophobic side of the helix).

stages of infection by poliovirus and coxsackie B3 virus (both picornaviruses). Three-dimensional reconstruction of these early picornavirus-induced structures revealed that they are branching tubular structures rather than closed vesicles (Limpens et al., 2011; Belov et al., 2012). Positive membrane curvature induced by viral membrane proteins allows budding of tubular structures from the surface of the membrane. Replication proteins accumulate on the outside of the single-membrane structures (**Figure 1B**, model 1). That GFLV- and poliovirus-induced vesicles are immunoprecipitated by antibodies against viral replication proteins, is consistent with this model (Bienz et al., 1994; Carette et al., 2000). In contrast, membrane structures induced by many plant viruses (including bromo-, tombus-, and tymoviruses) are formed by membrane invagination and require negative membrane curvature. These replication complexes are sheltered inside spherules that are connected to the cytoplasm by a neck (**Figure 1B**, model 2).

Of the replication proteins encoded by como- or nepovirus RNA1, two contain obvious hydrophobic regions: the comovirus Co-Pro and NTB proteins and the cognate nepovirus X2 and NTB proteins (**Figure 1D**). In infected cells, mature proteins co-exist with stable intermediate polyproteins (**Figure 1C**). The CPMV Co-Pro is only detected as a mature protein due to efficient cleavage between Co-Pro and NTB. However, NTB is found either as a mature protein or within various intermediates (NTB–VPg, NTB–VPg–Pro, and NTB–VPg–Pro–Pol; Wellink et al., 1986). In contrast, processing at the nepovirus X2–NTB cleavage site is inefficient *in vitro* leading to the accumulation of X2–NTB and X2–NTB–VPg in addition to X2 and NTB (Wang and Sanfacon, 2000; Wetzel et al., 2008). In ToRSV-infected cells, NTB, NTB–VPg, and X2–NTB–VPg are tightly associated with ER membranes active in viral replication (Han and Sanfacon, 2003). In contrast, only a sub-population of a polyprotein containing the VPg, Pro, and Pol domains (VPg–Pro–Pol') is associated with replication-competent membranes and this association is peripheral, suggesting that it requires an interaction between

VPg–Pro–Pol' and a membrane protein (Chisholm et al., 2007). Similarly, only a fraction of VPg–Pro–Pol is membrane-bound in CPMV-infected cells (Dorssers et al., 1984). When expressed individually, the ToRSV X2, NTB and NTB–VPg and the CPMV Co-Pro and NTB–VPg associate with ER membranes, while proteins containing the ToRSV or CPMV VPg, Pro, and Pol domains remain in the soluble cytoplasmic fraction (Carette et al., 2002b; Zhang et al., 2005; Zhang and Sanfacon, 2006;Chisholm et al., 2007). Thus, the CPMV Co-Pro and NTB and ToRSV X2 and NTB and/or intermediate polyproteins containing these protein domains are likely to act as membrane anchors for the replication complex.

The nucleotide-binding motif of the nepo- and comovirus NTB is related to that of the poliovirus 2C protein (**Figure 1C**). The nepo- and comovirus NTB also contain a hydrophobic C-terminal domain, which is absent in 2C (**Figure 1D**). The poliovirus 3A protein (immediately downstream of 2C in the polyprotein) has a hydrophobic domain that corresponds to the C-terminal region of the nepo- and comovirus NTB, although polyproteins containing both 2C and 3A are not detected in infected cells (**Figure 1C**; Cameron et al., 2010). The ToRSV X2, and CPMV Co-Pro are highly hydrophobic and share a signature sequence (F-x_{27}-W-x_{11}-L-x_{23}-E; Rott et al., 1995), which is also found in the cognate proteins of nepo-, como-, faba-, and cheraviruses (Sanfacon et al., 2011). Co-Pro is a protease co-factor that slows the processing of the CPMV RNA1 polyprotein (Peters et al., 1992). However, there is no experimental evidence that X2 regulates the nepovirus protease activity (Wang and Sanfacon, 2000; Wetzel et al., 2008). Thus, the conserved motif may be important for another common activity of Co-Pro and X2. The poliovirus 2B protein is located immediately upstream of 2C (**Figure 1D**) but does not share sequence motifs with X2 and Co-Pro, other than a general hydrophobicity.

MEMBRANE MODIFICATIONS AND SYMPTOMS INDUCED BY THE COMOVIRUS Co-Pro AND NTB–VPg

When overexpressed from a viral vector, the CPMV NTB–VPg or Co-Pro induces the formation of small ER-derived perinuclear bodies (Carette et al., 2002b). Proliferation of the cortical ER is also observed after overexpression of Co-Pro. These structures resemble the ER modifications observed in early stages of natural CPMV infections but differ from the large perinuclear structures present later in infection. Thus, both proteins may act together to induce the larger structures in natural infections. NTB and NTB-containing intermediate polyproteins co-immunoprecipitate with Co-Pro, suggesting that Co-Pro and NTB interact with each other (Wellink et al., 1986). This situation is reminiscent of that observed with poliovirus membrane proteins. While 3A, 2C, and 2BC each induce ER modifications, co-expression of 3A and 2BC together is required to induce vesicles that are similar to those observed in natural poliovirus infections (Suhy et al., 2000). Protein–protein interactions among these proteins are well-documented (Teterina et al., 2006; Yin et al., 2007).

Ectopic overexpression of CPMV Co-Pro or NTB–VPg induces local necrosis in plant (Carette et al., 2002b). Interestingly, CPMV does not cause necrosis in natural infection, even though Co-Pro and NTB–VPg accumulate in infected cells. Accumulation of these proteins in electron-dense bodies, which are probable sites of protein aggregation, may help reduce their toxicity (Carette et al., 2002b). Comparison of the symptomatology induced by chimeric constructs of two isolates of bean pod mosaic virus (another comovirus) also points to Co-Pro and NTB as symptom severity determinants (Gu and Ghabrial, 2005). Chimeric constructs containing Co-Pro or NTB from the severe isolate induce increased symptomatology and accumulate to higher level than the mild isolate. Co-Pro and NTB may regulate the rate of virus replication, in agreement with their proposed role in replication complex assembly. Although the severe symptoms may be due to increased accumulation of viral products, possibly triggering plant defense responses, it may be a direct consequence of the membrane alterations induced by NTB and Co-Pro. Poliovirus 2B and 3A induce apoptosis when overexpressed (Madan et al., 2008). At least for 2B, the induction of apoptosis was correlated with its viroporin activity, which affects the integrity of various membranes, including mitochondrial membranes (Madan et al., 2008, 2010). Although a sub-population of the CPMV NTB–VPg targets chloroplast membranes (Carette et al., 2002b), there is no experimental evidence that mitochondria are targeted. Further studies will be necessary to investigate possible correlations between membrane alterations and symptomatology induced by the comovirus NTB and Co-Pro proteins and to determine whether the nepovirus X2 and NTB proteins can alter membrane structures and induce symptoms.

MEMBRANE TOPOLOGY OF THE ToRSV X2 AND NTB: EVIDENCE FOR OLIGOMERIZATION AND VIROPORIN ACTIVITY

Membrane association of integral membrane proteins can be directed by transmembrane α-helices, which are highly hydrophobic, or by amphipathic α-helices. Amphipathic helices initially insert parallel to the membranes with their hydrophobic face inserted in the lipid bilayer (**Figures 2A,B**). Oligomerization of amphipathic helices can lead to the formation of aqueous pores whereby the hydrophilic faces of the helices orient toward the pore and the hydrophobic faces interact within the membrane environment (Gonzalez and Carrasco, 2003; **Figure 2B**). Hydrophobic intra- and intermolecular interactions among amphipathic and adjacent hydrophobic helices can stabilize the oligomers (**Figure 2B**), as suggested for the poliovirus 2B protein (Agirre et al., 2002; Martinez-Gil et al., 2011).

The hydrophobic C-terminal domain and a predicted N-terminal amphipathic helix of the ToRSV NTB protein (**Figure 1D**) are each sufficient to target GFP fusion proteins to ER membranes in plant cells or to direct the insertion of NTB or NTB–VPg into canine microsomal membranes *in vitro* (Wang et al., 2004; Zhang et al., 2005). These domains are conserved in the sequence of NTB from other nepo- and comoviruses (**Figure 1D**). The C-terminal hydrophobic region of the ToRSV NTB contains a highly hydrophobic α-helix, which traverses the membrane. The VPg domain of NTB–VPg is translocated in the membrane lumen (topology 1, **Figure 2C**), allowing the recognition of a naturally occurring N-glycosylation site (Wang et al., 2004; Zhang et al., 2005). The luminal orientation of the C-terminal region of NTB–VPg was confirmed by proteinase K protection assays using

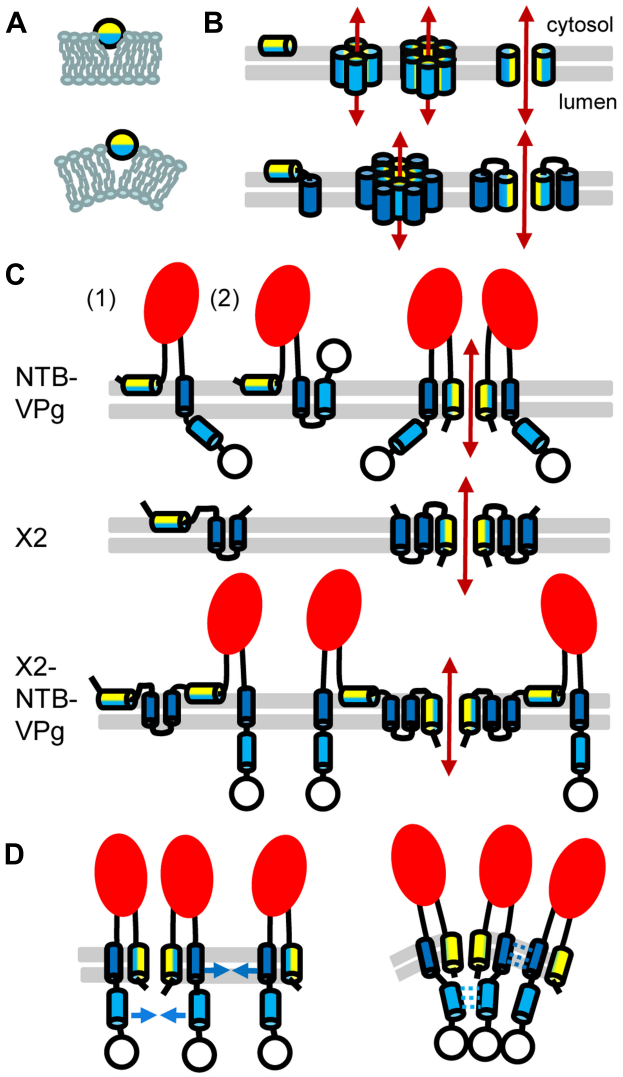

FIGURE 2 | Topology model for ToRSV membrane replication proteins. **(A)** Model for the parallel insertion of an amphipathic helix. The hydrophobic side of the helix (blue) inserts in one leaflet of the lipid bilayer while the polar/charged hydrophilic side of the helix (yellow) is exposed to the cytosolic face of the membrane. This insertion displaces the lipid headgroup, causing the acyl chain to reorient and inducing positive membrane curvature. **(B)** Model for the oligomerization of amphipathic helices and formation of an aqueous pore. In the top panel, an amphipathic helix is inserted parallel to the lipid bilayer (horizontal gray lines) of the membrane (left). Formation of an aqueous pore (double-ended red arrow) requires oligomerization of four or six amphipathic helices (middle). In the aqueous pore, the hydrophilic side of the helix (yellow) is exposed toward the pore, while its hydrophobic side (blue) is oriented toward the membrane lipid bilayer. A simplified representation of the pore shows only two molecules to better visualize each side of the amphipathic helix relative to the pore (right). In the bottom panel, a membrane protein consisting of an amphipathic helix and a hydrophobic helix (blue) is shown. After initial membrane insertion of the monomer with the amphipathic helix parallel to the membrane (left), an aqueous pore is formed by oligomerization of the amphipathic helix (middle). The hydrophobic helix of each molecule is located on the outside of the pore alongside the amphipathic helix (model shown for a hexamer). Hydrophobic interactions between the hydrophobic side of the amphipathic helix and the hydrophobic helix stabilize pore formation. A simplified representation of the pore shows only two

(Continued)

FIGURE 2 | Continued
molecules (right). **(C)** Predicted topologies for NTB–VPg, X2, and X2–NTB–VPg shown for monomers (left) or oligomers (right). Two possible topologies are shown for NTB–VPg monomers (1 and 2, see text). To simplify the figure, only two molecules are shown in the oligomer models. However, at least four molecules would be necessary to form an aqueous pore (as shown in B). The open circle represents the VPg domain and the red oval indicates the conserved NTB motif. **(D)** Model for the induction of positive membrane curvature by hydrophobic interactions of membrane proteins oligomers, shown for NTB–VPg. On the left, blue arrows represent possible hydrophobic interactions. These interactions (shown by broken blue lines on the right) would induce positive membrane curvature. Similar hydrophobic interactions are predicted to occur in X2 or X2–NTB–VPg oligomers (not shown).

membrane-fractions of ToRSV-infected cells (Han and Sanfacon, 2003). However, these results do not exclude the possibility that a sub-population of the protein adopt an alternate topology. *In vitro*, a second weakly predicted transmembrane α-helix traverses the membranes when the first transmembrane helix is deleted (Wang et al., 2004). In an alternate topology (topology 2, **Figure 2C**), the NTB C-terminal hydrophobic region traverses the membrane twice allowing a cytosolic orientation of the VPg. Experiments are required to determine whether this alternate topology exists in infected cells. Alternative topologies for NTB–VPg could regulate the presentation of the VPg to the cytoplasmic face of the membrane where protein–protein interactions and viral replication take place.

The N-terminus of NTB is translocated in the membrane lumen, suggesting oligomerization of the amphipathic helix and pore formation (Zhang et al., 2005; **Figure 2C**). Pore formation may be enhanced by hydrophobic interactions between the N-terminal amphipathic helix and the C-terminal transmembrane helix. Denaturing SDS-polyacrylamide gel electrophoresis (SDS-PAGE) of NTB–VPg or of fragments containing the amphipathic or transmembrane helices revealed the presence of additional bands that correspond in size to oligomers. Membrane proteins can conserve their oligomeric structure in the presence of denaturing agents, due to strong hydrophobic interactions (DeGrado et al., 2003). The potential NTB–VPg oligomers were glycosylated, suggesting that oligomerization occurred within the membranes (Wang et al., 2004; Zhang et al., 2005). Although the topology model of NTB–VPg oligomers suggests the formation of an aqueous pore, further experimentation is required to test whether the protein affects the membrane integrity *in vivo*.

In plant cells, ER-targeting of ToRSV X2 is directed by two strongly predicted transmembrane helices and a putative amphipathic helix (Zhang and Sanfacon, 2006; **Figure 1D**). These features are conserved in the X2 from other nepoviruses. Similarly, three transmembrane helices and one amphipathic helix are predicted in the CPMV Co-Pro (Carette et al., 2002b; Zhang and Sanfacon, 2006; **Figure 1D**). The topology of ToRSV X2 was examined *in vitro* (Zhang and Sanfacon, 2006). The two predicted transmembrane helices were found to traverse the membrane, forming a hairpin and resulting in a cytosolic orientation of the C-terminus of X2 (**Figure 2C**). The N-terminus of X2 was translocated to the membrane lumen. Analysis by SDS-PAGE of full-length or truncated X2 suggests that, as for NTB–VPg,

protein oligomerization occurs through hydrophobic interactions (Zhang and Sanfacon, 2006). A topology model of X2 oligomers implies the formation of an aqueous pore by oligomerization of the amphipathic helix (**Figure 2C**). However, *in vivo* evidence in support of this model is still lacking. Due to its highly hydrophobic nature, it has not been possible to produce antibodies against X2. Thus, although the presence of mature X2 in ToRSV-infected cells is likely, it could not be confirmed. However, polyproteins corresponding to the expected molecular mass for X2–NTB–VPg were detected with anti-NTB and anti-VPg antibodies (Han and Sanfacon, 2003). Efforts are underway to develop ToRSV infectious clones, which may allow the insertion of epitope tags in X2 to confirm its presence in ToRSV-infected cells and examine its topology *in vivo* (Chisholm and Sanfacon, unpublished). Although insertion of hydrophilic epitope tags into hydrophobic membrane proteins can hinder their function, a recent study described tolerated insertion sites in poliovirus membrane proteins (Teterina et al., 2011a).

The topology models for X2 and NTB–VPg pose some problems when applied to the X2–NTB–VPg polyprotein. The cytosolic orientation of the C-terminus of X2 is in apparent conflict with the luminal orientation of the N-terminus of NTB. However, the presence of two strong transmembrane domains in the X2 domain of X2–NTB–VPg may prevent the membrane translocation of the NTB amphipathic helix, forcing it to insert parallel to the membranes (**Figure 2C**). Thus, processing at the X2–NTB cleavage site may influence the orientation of the NTB amphipathic helix and alter the ability of NTB and/or X2 to modify intracellular membranes. The impact of proteolytic cleavage on membrane topology was demonstrated for the poliovirus 3A and 3AB (Fujita et al., 2007). Using a fluorescence quenching method, 3AB was shown to adopt a single topology, in which the hydrophobic domain is parallel to the membrane. In contrast, 3A adopts two possible orientations, one of which traverses the membrane. It was suggested that the hydrophilic VPg domain prevents the membrane translocation of the 3A hydrophobic domain in 3AB. Regulated cleavage of the poliovirus 2BC also impacts its membrane-modification activities. Although 2B, 2C, and 2BC can target to membranes, only 2BC induces a proliferation of membraneous vesicles (Suhy et al., 2000). On the other hand, poliovirus mutants with decreased processing efficiency at the 2BC cleavage site have reduced membrane permeabilization activity, suggesting that the release of mature 2B from 2BC is essential for its viroporin function (van Kuppeveld et al., 1996).

INTERACTION OF VIRAL MEMBRANE PROTEINS WITH HOST FACTORS: TOWARD A MECHANISM FOR MEMBRANE MODIFICATION

The experimental evidence points to a role for como- and nepovirus membrane replication proteins in altering host membranes and assembling the replication complexes. Positive membrane curvature can be induced by parallel insertion of amphipathic helices (**Figure 2A**) or by intra- and intermolecular hydrophobic interactions among membrane protein oligomers (as shown for NTB–VPg, **Figure 2D**; McMahon and Gallop, 2005).

Host factors are also likely to play an important role. The secretory pathway is hijacked by poliovirus to help the formation of membraneous vesicles, resulting in an inhibition of host protein transport (Hsu et al., 2010). The 2B and 3A proteins inhibit the secretory pathway (Doedens and Kirkegaard, 1995). 3A interacts with several components of the secretory pathway, including ACBD3, a Golgi adaptor protein (Greninger et al., 2012; Sasaki et al., 2012) and GBF1, a guanine nucleotide exchange factor that activates Arf1, a cellular GTPase and regulator of the secretory pathway (Wessels et al., 2006; Belov et al., 2008; Teterina et al., 2011b). Arf1 is also the known target of brefeldin A, an inhibitor of the secretory pathway that blocks poliovirus infection (Irurzun et al., 1992; Maynell et al., 1992). The 3A–GBF1 and 3A–ACBD3 interactions may assist in the recruitment of P1KIIIβ, an enzyme involved in phospholipid synthesis, to the replication complex (Hsu et al., 2010; Greninger et al., 2012; Sasaki et al., 2012). P1KIIIβ would alter the membrane lipid composition, possibly affecting the membrane curvature and facilitating the formation of virus factories. However, the sensitivity of picornaviruses to brefeldin A varies greatly and the GBF1–3A interaction is not conserved for all picornaviruses, suggesting that the interaction between viruses and the host secretory pathway varies.

How do these findings apply to como- and nepoviruses? Replication of CPMV and GFLV is hindered by cerulenin (Carette et al., 2000; Ritzenthaler et al., 2002), an inhibitor of type II fatty acid synthase, suggesting that *de novo* phospholipid synthesis is required for membrane proliferation, possibly involving changes in membrane lipid composition. GFLV and CPMV replication is inhibited by brefeldin A (Pouwels et al., 2002b; Ritzenthaler et al., 2002). However, the interaction of nepo- and comoviruses with the secretory pathway is not well understood and their ability to block protein secretion has not been investigated. Two SNARE-like proteins from *Arabidopsis thaliana* were shown to interact with the CPMV NTB–VPg (Carette et al., 2002c). Although their function is not known, they may regulate membrane fusion and vesicle formation. Identification of additional interaction partners of the nepo- and comovirus membrane proteins will be essential to better understand membrane remodeling directed by these proteins.

ACKNOWLEDGMENTS

This work was supported in part by an NSERC discovery grant. I wish to thank Joan Chisholm for critical reading of the manuscript and Andrew Wieczorek for taking the EM picture (shown in **Figure 2A**), while he was in my lab.

REFERENCES

Agirre, A., Barco, A., Carrasco, L., and Nieva, J. L. (2002). Viroporin-mediated membrane permeabilization. Pore formation by nonstructural poliovirus 2B protein. *J. Biol. Chem.* 277, 40434–40441.

Belov, G. A., Feng, Q., Nikovics, K., Jackson, C. L., and Ehrenfeld, E. (2008). A critical role of a cellular membrane traffic protein in poliovirus RNA replication. *PLoS Pathog.* 4:e1000216. doi:10.1371/journal.ppat.1000216

Belov, G. A., Nair, V., Hansen, B. T., Hoyt, F. H., Fischer, E. R., and Ehrenfeld, E. (2012). Complex dynamic development of poliovirus membranous replication complexes. *J. Virol.* 86, 302–312.

Bienz, K., Egger, D., and Pfister, T. (1994). Characteristics of the poliovirus replication complex. *Arch. Virol. Suppl.* 9, 147–157.

Cameron, C. E., Oh, H. S., and Moustafa, I. M. (2010). Expanding knowledge of P3 proteins in the poliovirus lifecycle. *Future Microbiol.* 5, 867–881.

Carette, J. E., Stuiver, M., Van Lent, J., Wellink, J., and Van Kammen, A. (2000). Cowpea mosaic virus infection induces a massive proliferation of endoplasmic reticulum but not Golgi membranes and is dependent on de novo membrane synthesis. *J. Virol.* 74, 6556–6563.

Carette, J. E., Guhl, K., Wellink, J., and Van Kammen, A. (2002a). Coalescence of the sites of cowpea mosaic virus RNA replication into a cytopathic structure. *J. Virol.* 76, 6235–6243.

Carette, J. E., van Lent, J., MacFarlane, S. A., Wellink, J., and van Kammen, A. (2002b). Cowpea mosaic virus 32- and 60-kilodalton replication proteins target and change the morphology of endoplasmic reticulum membranes. *J. Virol.* 76, 6293–6301.

Carette, J. E., Verver, J., Martens, J., van Kampen, T., Wellink, J., and van Kammen, A. (2002c). Characterization of plant proteins that interact with cowpea mosaic virus '60K' protein in the yeast two-hybrid system. *J. Gen. Virol.* 83, 885–893.

Chisholm, J., Zhang, G., Wang, A., and Sanfacon, H. (2007). Peripheral association of a polyprotein precursor form of the RNA-dependent RNA polymerase of Tomato ringspot virus with the membrane-bound viral replication complex. *Virology* 368, 133–144.

DeGrado, W. F., Gratkowski, H., and Lear, J. D. (2003). How do helix–helix interactions help determine the folds of membrane proteins? Perspectives from the study of homo-oligomeric helical bundles. *Protein Sci.* 12, 647–665.

den Boon, J. A., Chen, J., and Ahlquist, P. (2001). Identification of sequences in Brome mosaic virus replicase protein 1a that mediate association with endoplasmic reticulum membranes. *J. Virol.* 75, 12370–12381.

den Boon, J. A., and Ahlquist, P. (2010). Organelle-like membrane compartmentalization of positive-strand RNA virus replication factories. *Annu. Rev. Microbiol.* 64, 241–256.

de Zoeten, G. A., Assink, A. M., and van Kammen, A. (1974). Association of cowpea mosaic virus-induced double-stranded RNA with a cytopathological structure in infected cells. *Virology* 59, 341–355.

Doedens, J. R., and Kirkegaard, K. (1995). Inhibition of cellular protein secretion by poliovirus proteins 2B and 3A. *EMBO J.* 14, 894–907.

Dorssers, L., Van der Kroll, S., Van der Meer, J., Van Kammen, A., and Zabel, P. (1984). Purification of cowpea mosaic virus RNA replication complex: identification of a virus-encoded 110,000-dalton polypeptide responsible for RNA chain elongation. *Proc. Natl. Acad. Sci. U.S. A.* 81, 1951–1955.

Fujita, K., Krishnakumar, S. S., Franco, D., Paul, A. V., London, E., and Wimmer, E. (2007). Membrane topography of the hydrophobic anchor sequence of poliovirus 3A and 3AB proteins and the functional effect of 3A/3AB membrane association upon RNA replication. *Biochemistry* 46, 5185–5199.

Gonzalez, M. E., and Carrasco, L. (2003). Viroporins. *FEBS Lett.* 552, 28–34.

Greninger, A. L., Knudsen, G. M., Betegon, M., Burlingame, A. L., and Derisi, J. L. (2012). The 3A protein from multiple picornaviruses utilizes the golgi adaptor protein ACBD3 to recruit PI4KIIIbeta. *J. Virol.* 86, 3605–3616.

Gu, H., and Ghabrial, S. A. (2005). The Bean pod mottle virus proteinase cofactor and putative helicase are symptom severity determinants. *Virology* 333, 271–283.

Han, S., and Sanfacon, H. (2003). Tomato ringspot virus proteins containing the nucleoside triphosphate binding domain are transmembrane proteins that associate with the endoplasmic reticulum and cofractionate with replication complexes. *J. Virol.* 77, 523–534.

Hsu, N. Y., Ilnytska, O., Belov, G., Santiana, M., Chen, Y. H., Takvorian, P. M., et al. (2010). Viral reorganization of the secretory pathway generates distinct organelles for RNA replication. *Cell* 141, 799–811.

Irurzun, A., Perez, L., and Carrasco, L. (1992). Involvement of membrane traffic in the replication of poliovirus genomes: effects of brefeldin A. *Virology* 191, 166–175.

Laliberte, J. F., and Sanfacon, H. (2010). Cellular remodeling during plant virus infection. *Annu. Rev. Phytopathol.* 48, 69–91.

Limpens, R. W., van der Schaar, H. M., Kumar, D., Koster, A. J., Snijder, E. J., van Kuppeveld, F. J., et al. (2011). The transformation of enterovirus replication structures: a three-dimensional study of single- and double-membrane compartments. *MBio* 2:e00166-11. doi: 10.1128/mBio.00166-11

Madan, V., Castello, A., and Carrasco, L. (2008). Viroporins from RNA viruses induce caspase-dependent apoptosis. *Cell. Microbiol.* 10, 437–451.

Madan, V., Sanchez-Martinez, S., Carrasco, L., and Nieva, J. L. (2010). A peptide based on the pore-forming domain of pro-apoptotic poliovirus 2B viroporin targets mitochondria. *Biochim. Biophys. Acta* 1798, 52–58.

Martinez-Gil, L., Bano-Polo, M., Redondo, N., Sanchez-Martinez, S., Nieva, J. L., Carrasco, L., et al. (2011). Membrane integration of poliovirus 2B viroporin. *J. Virol.* 85, 11315–11324.

Maynell, L. A., Kirkegaard, K., and Klymkowsky, M. W. (1992). Inhibition of poliovirus RNA synthesis by brefeldin A. *J. Virol.* 66, 1985–1994.

McMahon, H. T., and Gallop, J. L. (2005). Membrane curvature and mechanisms of dynamic cell membrane remodelling. *Nature* 438, 590–596.

Miller, S., and Krijnse-Locker, J. (2008). Modification of intracellular membrane structures for virus replication. *Nat. Rev. Microbiol.* 6, 363–374.

Nagy, P. D., and Pogany, J. (2012). The dependence of viral RNA replication on co-opted host factors. *Nat. Rev. Microbiol.* 10, 137–149.

Peters, S. A., Voorhorst, W. G., Wery, J., Wellink, J., and van Kammen, A. (1992). A regulatory role for the 32K protein in proteolytic processing of cowpea mosaic virus polyproteins. *Virology* 191, 81–89.

Pouwels, J., Carette, J. E., Van Lent, J., and Wellink, J. (2002a). Cowpea mosaic virus: effects on host cell processes. *Mol. Plant Pathol.* 3, 411–418.

Pouwels, J., Van Der Krogt, G. N., Van Lent, J., Bisseling, T., and Wellink, J. (2002b). The cytoskeleton and the secretory pathway are not involved in targeting the cowpea mosaic virus movement protein to the cell periphery. *Virology* 297, 48–56.

Prod'Homme, D., Jakubiec, A., Tournier, V., Drugeon, G., and Jupin, I. (2003). Targeting of the turnip yellow mosaic virus 66K replication protein to the chloroplast envelope is mediated by the 140K protein. *J. Virol.* 77, 9124–9135.

Ritzenthaler, C., Laporte, C., Gaire, F., Dunoyer, P., Schmitt, C., Duval, S., et al. (2002). Grapevine fanleaf virus replication occurs on endoplasmic reticulum-derived membranes. *J. Virol.* 76, 8808–8819.

Rott, M. E., Gilchrist, A., Lee, L., and Rochon, D. (1995). Nucleotide sequence of tomato ringspot virus RNA1. *J. Gen. Virol.* 76, 465–473.

Salonen, A., Ahola, T., and Kaariainen, L. (2005). Viral RNA replication in association with cellular membranes. *Curr. Top. Microbiol. Immunol.* 285, 139–173.

Sanfacon, H. (2005). Replication of positive-strand RNA viruses in plants: contact points between plant and virus components. *Can. J. Bot.* 83, 1529–1549.

Sanfacon, H., Zhang, G., Chisholm, J., Jafarpour, B., and Jovel, J. (2006). "Molecular biology of Tomato ringspot nepovirus, a pathogen of ornamentals, small fruits and fruit trees," in *Floriculture, Ornamental and Plant Biotechnology: Advances and Topical Issues* (1st Edn), ed. J. Teixeira da Silva (London: Global Science Books), 540–546.

Sanfacon, H., Iwanami, T., Karasev, A., Van der Vlugt, R., Wellink, J., Wetzel, T., et al. (2011). "Family Secoviridae". in *Virus Taxonomy: Classification and Nomenclature of Viruses.* Ninth Report of the International Committee on the Taxonomy of Viruses, eds. A. M. Q. King, M. J. Adams, E. B. Carstens, and E. J. Lefkowitz (San Diego: Elsevier), 881–899.

Sasaki, J., Ishikawa, K., Arita, M., and Taniguchi, K. (2012). ACBD3-mediated recruitment of PI4KB to picornavirus RNA replication sites. *EMBO J.* 31, 754–766.

Schaad, M. C., Jensen, P. E., and Carrington, J. C. (1997). Formation of plant RNA virus replication complexes on membranes: role of an endoplasmic reticulum-targeted viral protein. *EMBO J.* 16, 4049–4059.

Suhy, D. A., Giddings, T. H. Jr., and Kirkegaard, K. (2000). Remodeling the endoplasmic reticulum by poliovirus infection and by individual viral proteins: an autophagy-like origin for virus-induced vesicles. *J. Virol.* 74, 8953–8965.

Teterina, N. L., Levenson, E., Rinaudo, M. S., Egger, D., Bienz, K., Gorbalenya, A. E., et al. (2006). Evidence for functional protein interactions required for poliovirus RNA replication. *J. Virol.* 80, 5327–5337.

Teterina, N. L., Lauber, C., Jensen, K. S., Levenson, E. A., Gorbalenya, A. E., and Ehrenfeld, E. (2011a). Identification of tolerated insertion sites in poliovirus non-structural proteins. *Virology* 409, 1–11.

Teterina, N. L., Pinto, Y., Weaver, J. D., Jensen, K. S., and Ehrenfeld, E. (2011b). Analysis of poliovirus protein 3A interactions with viral and

cellular proteins in infected cells. *J. Virol.* 85, 4284–4296.

Turner, K. A., Sit, T. L., Callaway, A. S., Allen, N. S., and Lommel, S. A. (2004). Red clover necrotic mosaic virus replication proteins accumulate at the endoplasmic reticulum. *Virology* 320, 276–290.

van Kuppeveld, F. J., van den Hurk, P. J., Zoll, J., Galama, J. M., and Melchers, W. J. (1996). Mutagenesis of the coxsackie B3 virus 2B/2C cleavage site: determinants of processing efficiency and effects on viral replication. *J. Virol.* 70, 7632–7640.

Viry, M., Serghini, M. A., Hans, F., Ritzenthaler, C., Pinck, M., and Pinck, L. (1993). Biologically active transcripts from cloned cDNA of genomic grapevine fanleaf nepovirus RNAs. *J. Gen. Virol.* 74, 169–174.

Vos, P., Jaegle, M., Wellink, J., Verver, J., Eggen, R., Van Kammen, A., et al. (1988). Infectious RNA transcripts derived from full-length DNA copies of the genomic RNAs of cowpea mosaic virus. *Virology* 165, 33–41.

Wang, A., and Sanfacon, H. (2000). Proteolytic processing at a novel cleavage site in the N-terminal region of the tomato ringspot nepovirus RNA-1-encoded polyprotein in vitro. *J. Gen. Virol.* 81, 2771–2781.

Wang, A., Han, S., and Sanfacon, H. (2004). Topogenesis in membranes of the NTB–VPg protein of tomato ringspot nepovirus: definition of the C-terminal transmembrane domain. *J. Gen. Virol.* 85, 535–545.

Weber-Lotfi, F., Dietrich, A., Russo, M., and Rubino, L. (2002). Mitochondrial targeting and membrane anchoring of a viral replicase in plant and yeast cells. *J. Virol.* 76, 10485–10496.

Wellink, J., Rezelman, G., Goldbach, R., and Beyreuther, K. (1986). Determination of the proteolytic processing sites in the polyprotein encoded by the bottom-component RNA of cowpea mosaic virus. *J. Virol.* 59, 50–58.

Wessels, E., Duijsings, D., Lanke, K. H., van Dooren, S. H., Jackson, C. L., Melchers, W. J., et al. (2006). Effects of picornavirus 3A Proteins on Protein Transport and GBF1-dependent COP-I recruitment. *J. Virol.* 80, 11852–11860.

Wetzel, T., Chisholm, J., Bassler, A., and Sanfacon, H. (2008). Characterization of proteinase cleavage sites in the N-terminal region of the RNA1-encoded polyprotein from Arabis mosaic virus (subgroup A nepovirus). *Virology* 375, 159–169.

Yamanaka, T., Ohta, T., Takahashi, M., Meshi, T., Schmidt, R., Dean, C., et al. (2000). TOM1, an Arabidopsis gene required for efficient multiplication of a tobamovirus, encodes a putative transmembrane protein. *Proc. Natl. Acad. Sci. U.S.A.* 97, 10107–10112.

Yin, J., Liu, Y., Wimmer, E., and Paul, A. V. (2007). Complete protein linkage map between the P2 and P3 non-structural proteins of poliovirus. *J. Gen. Virol.* 88, 2259–2267.

Zhang, G., and Sanfacon, H. (2006). Characterization of membrane-association domains within the tomato ringspot nepovirus X2 protein, an endoplasmic reticulum-targeted polytopic membrane protein. *J. Virol.* 80, 10847–10857.

Zhang, S. C., Zhang, G., Yang, L., Chisholm, J., and Sanfacon, H. (2005). Evidence that insertion of tomato ringspot nepovirus NTB–VPg protein in endoplasmic reticulum membranes is directed by two domains: a C-terminal transmembrane helix and an N-terminal amphipathic helix. *J. Virol.* 79, 11752–11765.

Conflict of Interest Statement: The author declares that the research was conducted in the absence of any commercial or financial relationships that could be construed as a potential conflict of interest.

Received: 25 September 2012; accepted: 31 December 2012; published online: 29 January 2013.

Citation: Sanfaçon H (2013) Investigating the role of viral integral membrane proteins in promoting the assembly of nepovirus and comovirus replication factories. Front. Plant Sci. ***3****:313. doi: 10.3389/fpls.2012.00313*

This article was submitted to Frontiers in Plant-Microbe Interaction, a specialty of Frontiers in Plant Science.

frontiers in
PLANT SCIENCE

REVIEW ARTICLE
published: 11 February 2013
doi: 10.3389/fpls.2013.00012

The cell biology of *Tobacco mosaic virus* replication and movement

Chengke Liu and Richard S. Nelson*

Plant Biology Division, The Samuel Roberts Noble Foundation, Inc., Ardmore, OK, USA

Edited by:
Jean-François Laliberté, Institut National de la Recherche Scientifique, Canada

Reviewed by:
Xueping Zhou, Zhejiang University, China
Yule Liu, Tsinghua University, China

***Correspondence:**
Richard S. Nelson, Plant Biology Division, The Samuel Roberts Noble Foundation, Inc., 2510 Sam Noble Parkway, Ardmore, OK 73401, USA.
e-mail: rsnelson@noble.org

Successful systemic infection of a plant by *Tobacco mosaic virus* (TMV) requires three processes that repeat over time: initial establishment and accumulation in invaded cells, intercellular movement, and systemic transport. Accumulation and intercellular movement of TMV necessarily involves intracellular transport by complexes containing virus and host proteins and virus RNA during a dynamic process that can be visualized. Multiple membranes appear to assist TMV accumulation, while membranes, microfilaments and microtubules appear to assist TMV movement. Here we review cell biological studies that describe TMV-membrane, -cytoskeleton, and -other host protein interactions which influence virus accumulation and movement in leaves and callus tissue. The importance of understanding the developmental phase of the infection in relationship to the observed virus-membrane or -host protein interaction is emphasized. Utilizing the latest observations of TMV-membrane and -host protein interactions within our evolving understanding of the infection ontogeny, a model for TMV accumulation and intracellular spread in a cell biological context is provided.

Keywords: membrane transport, microfilaments, microtubules, plant virus, vesicle trafficking, tobamovirus

INTRODUCTION

Viruses, as obligate organisms, utilize host factors to accumulate and spread in their host. A successful infection by a plant virus includes entry and accumulation in the first cell, movement into neighboring uninfected cells, and systemic infection through the plant vascular tissue (Boevink and Oparka, 2005; Epel, 2009; Harries and Ding, 2011; Niehl and Heinlein, 2011; Schoelz et al., 2011; Tilsner et al., 2011). Plant viruses have varying strategies for infecting hosts which reflect their use of existing functionally redundant host developmental pathways. Therefore an understanding of virus infection processes also offers insight into normal host physiological processes. *Tobacco mosaic virus* (TMV) encodes four known functional proteins: the 126 and 183 kDa replication-associated proteins, the movement protein (MP), and the structural capsid or coat protein (CP). In order to have a successful infection, these four multifunctional proteins cooperate with many host components. The host membrane and cytoskeleton are sub-cellular structures important for TMV infection. TMV-induced granules or inclusion bodies that contain membranes also contain host proteins. In this review, we discuss the changing roles of host membranes, cytoskeleton, and inclusion body-associated proteins as infection progresses. Findings reported in the literature are first presented in the section(s) where the effect on virus physiology was observed rather than where it may additionally influence this activity. For example, the influence of synaptotagmin on TMV physiology (Lewis and Lazarowitz, 2010) was reported as an inhibition of intercellular spread of the TMV MP, although it likely influences the intracellular transport of this protein. This was done to clearly indicate what is in the published literature rather than what a reader may interpret the results to indicate. In some instances, however, the presumed influence of the observed outcome on the mechanism of virus movement is noted. As pertinent, findings from other tobamoviruses are mentioned to indicate the generality or specificity of a conclusion for the genus.

INITIAL INFECTION

Tobacco mosaic virus enters plant cells only through mechanical wounds which either transiently open the plasma membrane or allow pinocytosis (Palukaitis and Zaitlin, 1986; Shaw, 1999; **Figure 1**). TMV begins to disassemble within 3 min after entry and disassembly of CP from the capsid is associated with translation of viral RNA (vRNA; Wu et al., 1994; reviewed in Shaw, 1999). TMV vRNA labeled with cyanine 3-UTP forms small granules in cytoplasm less than 5 min after entering the cell (Christensen et al., 2009). The vRNA-containing granules form where CP and vRNA co-localize as well as in the absence of CP, suggesting that although CP was not needed for granule formation the disassembly of TMV capsids occurred at the site of granule formation. Removal or mutation of *cis* and *trans* elements necessary for virus replication (i.e., the vRNA 3′ untranslated region and replicase) did not prevent granule formation, although they were smaller and less stable. The granules were shown to associate with fluorescently labeled ER. The 5′ methylguanosine cap on the vRNA was necessary to anchor vRNA to the ER/actin complex: absence of the cap leading to vRNA degradation and no granules (Christensen et al., 2009). Considering that uncoating of vRNA may make it accessible to the silencing surveillance system (reviewed in Niehl and Heinlein, 2011), it will be important to determine to which host factors viral proteins are attached during granule formation and transport to cortical and perinuclear replication sites. Identifying host factors in the granules will be difficult due to their presumed low

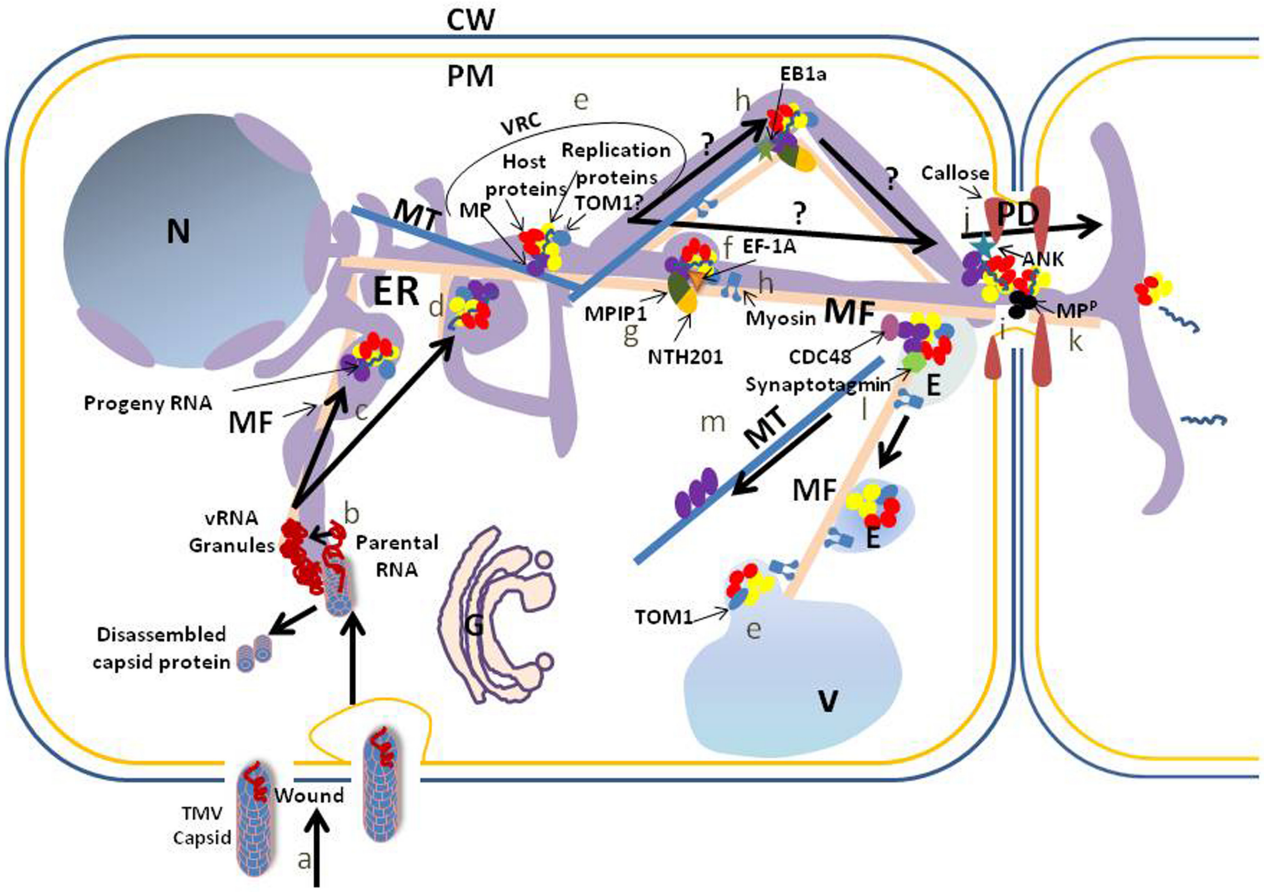

FIGURE 1 | Schematic of a proposed accumulation and movement pathway for TMV within cells. To simplify the model we do not address the possibility that the MP or any other viral protein moves within the cell, with or without viral RNA, independently of the virus replication complex. Also, we do not address the possibility that host proteins involved in virus accumulation and movement traffic independently from the virus complexes to support these activities. TMV capsid enters through an opening within the cell wall (CW) and plasma membrane (PM) or through pinocytosis after wounding (a). TMV RNA is released from the capsid at the site of viral RNA (vRNA) granule formation (b). The granules are associated with the endoplasmic reticulum (ER), which may serve as the replication site on transport of the vRNA to cortical vertices or perinuclear regions of the ER. Transport to these locations requires microfilaments (MF) (c). Other membranes such as the vacuolar (V) membrane may serve as a scaffold for virus replication, but this requires further analysis. A virus replication complex (VRC) is formed in the cortical vertices or perinuclear region of the ER (d). VRCs contain vRNA, movement protein (MP), replication proteins and host proteins. TOM1, a membrane protein, interacts with replication proteins and serves as an anchor between the replication proteins and a host membrane, which may be ER (TOM1?), vacuole (TOM1) or another membrane (e). For TMV intercellular movement, VRCs move from sites of replication to plasmodesmata (PD). Elongation factor 1A (EF-1A) interacts with vRNA, replication proteins, MFs and microtubules (MTs) and influences TMV movement. It is unclear if this influence is on sustained movement associated with clearance of virus components within the cell, or with initial movement: we have placed it with initial movement and with the MF (f). An interaction between two host proteins, a class II KNOTTED 1-like protein (NTH201) and a DnaJ-like protein (MPIP1), and the TMV MP also may aid transport of virus to the PD (g), although again it is unclear if this interaction aids initial or sustained movement. Movement of the VRC to the PD requires membrane, and may be influenced by actomyosin (MF and myosin) and MT (h). The influence of the MT end-binding protein (EB1a) on virus movement is placed during transport to the PD (h). MP microfilament severing activity at the PD is proposed to eliminate F-actin-like structures at the PD to increase the PD size exclusion limit SEL (i). In addition, interaction between the MP and the ankyrin repeat containing protein (ANK) is correlated with an increase of the PD SEL through a decrease in callose at the PD neck (j). vRNA transports through PD within a VRC or simply with vRNA and MP, the latter being phosphorylated (MP^P) in the PD to release the vRNA for translation in the next cell (k; Karpova et al., 1997; Lee et al., 2005). After vRNA transfer to the neighboring cell, VRC remnants associate with endosomes (E; possibly pre-vacuolar vesicles) for transport to vacuoles, potentially through interaction of the vesicle fusing protein, synaptotagmin, with the MP (l). Transport is proposed to involve the actomyosin network. Likely prior to this transport, CELL-DIVISION CYCLE protein48 (CDC48) extracts the MP from the ER-associated VRC for attachment to the MT and later degradation (m). N, nucleus.

quantities, but will be necessary to understand the steps prior to virus replication.

REPLICATION

Tobacco mosaic virus and the very closely related *Tomato mosaic virus* (ToMV) use their parental genomes to synthesize complementary negative strands which serve as templates for the synthesis of progeny full-length positive strands and subgenomic mRNAs containing MP and CP open reading frames (ORFs; Ishikawa and Okada, 2004; Ishibashi et al., 2010). Although the 183 kDa protein encoded by the 5′ ORF of these viruses can replicate the genome, the 126 kDa protein, produced by termination

of translation at an amber stop codon within the 183 kDa protein ORF, is necessary for maximum progeny RNA production (Ishikawa et al., 1986; Ishikawa et al., 1991; Lewandowski and Dawson, 2000). The 126 and 183 kDa proteins contain methyltransferase and helicase domains, while the 183 kDa protein alone contains the C-terminal domain encoding an RNA-dependent RNA polymerase. The 126 and 183 kDa proteins together will be referred to as the replication proteins in this review. TMV/ToMV replication is believed to occur in a membrane-associated complex containing the replication proteins, MP, vRNA, and host proteins (Hagiwara et al., 2003; Heinlein et al., 1998; Más and Beachy, 1999; reviewed in Ishibashi et al., 2010; Laliberté and Sanfaçon, 2010; de Castro et al., 2012; **Figure 1**). The ER was implicated as a site for virus replication complex (VRC) formation through co-localization of an ER marker, BiP, with MP-GFP and in turn, MP-GFP co-localization with replication proteins during immunofluorescence studies (Heinlein et al., 1998). Reichel and Beachy (1998), using transgenic plants expressing an ER-targeted GFP, determined that the ER formed large cortical aggregates at reticulate vertices and fewer membrane tubules during TMV accumulation, but returned to a normal structure after replication ended. However, later studies with ToMV using both fluorescence microscopy and biochemical fractionation methods determined that the replication proteins and replicase activity were associated predominantly with the vacuolar membrane, although they also showed some localization and activity with other less defined membrane fractions which included the ER (Hagiwara et al., 2003). Interestingly, ToMV can replicate in cells that are vacuole-diminished (Nishikiori et al., 2006). This finding supports the notion that although the tonoplast may function to support ToMV/TMV accumulation, other membranes such as the ER are important for this activity. Clearly, additional work is necessary to determine which membranes are essential for tobamovirus accumulation (**Figure 1**).

Regardless of the membrane used for tobamovirus accumulation, it is clear that a characteristic VRC is not uniformly induced by tobamoviruses. TMV, ToMV, and *Tobacco mild green mosaic virus* (TMGMV), form different subcellular structures containing replication proteins late in the infection cycle: TMV forming X-bodies and ToMV and TMGMV forming virus bundles when analyzed through immunocytochemical EM studies (Das and Hari, 1992). For a fourth tobamovirus, *Turnip vein clearing virus* (TVCV), X-bodies are rare (Resconich, 1961). Early fluorescence localization studies determined that for strains of TMV the size of the VRCs varied and was positively correlated with the level of disease observed (Liu et al., 2005, 2006). Recently, however, it was determined that silencing expression of the gamma subunit of ATP synthase, a nuclear-encoded chloroplast protein, resulted in smaller but more numerous VRCs and severe disease symptoms (Bhat et al., 2012). Thus, the size of the VRC is not a perfect indicator of disease intensity and the number of VRCs may influence this phenotype.

The form of inclusions induced by tobamoviruses is correlated with differences in the replication protein sequences (Liu et al., 2005; Harries et al., 2009). While ectopically expressed 126 kDa protein from TMV fused with GFP forms intracellular inclusions, the 125 kDa protein homolog from TVCV does not form inclusions (Harries et al., 2009). Interestingly, the intracellular inclusions formed by the TMV 126 kDa protein co-localized with microfilaments, as observed for the TMV VRC (Liu et al., 2005). Domain(s) within the 126 kDa protein necessary for inclusion body formation are not identified, however, it is known that the helicase domain when expressed alone is able to form octomers *in vitro* (Goregaoker and Culver, 2003) and thus may be a domain important for this activity. In addition, a 126 kDa protein-GFP construct expressing only the N terminal 781 amino acids of the 126 kDa protein associated with the ER and formed inclusions (dos Reis Figueira et al., 2002). The 781 amino acid protein includes the methyltransferase and non-conserved bridge domain that previously was determined to influence the RNA silencing suppression function of this protein. There is unpublished data indicating that the methyltransferase domain alone can form inclusions (Knapp et al., 2007). More work is needed to further identify the domains responsible for inclusion formation and the relevance of inclusion formation to tobamovirus physiology.

Ectopically expressed TMV MP fused with fluorescent reporter proteins also can form cytoplasmic inclusion bodies (Heinlein et al., 1998; Reichel and Beachy, 1998; Sambade et al., 2008). These small inclusions are similar to those visualized in the cortical periphery during infection with tobamoviruses expressing an MP-GFP fusion (Padgett et al., 1996; Heinlein et al., 1998; Reichel and Beachy, 1998; Boyko et al., 2007). The cortical MP-GFP inclusions that appear during virus infection likely represent the inclusions containing replication proteins and MP observed by Szécsi et al. (1999), but this requires confirmation. Inclusions containing MP-GFP associate with microtubules both early and late in the infection cycle (Heinlein et al., 1998; Boyko et al., 2007; Sambade et al., 2008). Studies with cellular markers and an MP-mRFP construct containing a downstream non-viral stemloop-forming RNA aptamer that can be fluorescently labeled determined that MP-mRFP associates with ER and its own RNA (Sambade et al., 2008). In this regard, it will be important to determine if multiple types of inclusions are formed independently during infection or are always part of a continuum, with progeny inclusions appearing from parental inclusions.

The host proteins within VRCs or inclusions that contain them are not fully identified. Late in infection, TMV-induced X-bodies have been shown to contain the microtubule component, β-tubulin, through immunocytochemical EM studies (X. S. Ding and R. S. Nelson, personal communication). The function of this protein in X-bodies is unknown, but perhaps it could be to aid the degradation of body components analogous to the suggested function of microtubules during TMV MP turnover (Kragler et al., 2003). The host translation factor, elongation factor 1A (EF-1A), is present in the membrane-associated fraction where viral replicase activity was observed (Osman and Buck, 1996; Watanabe et al., 1999) and in X-bodies produced by TMV (Ding et al., 1998). It also interacts with the 3′-UTR of genomic vRNA and with the methyltransferase domain of the replication proteins (Zeenko et al., 2002; Yamaji et al., 2006). EF-1A has additional activities beyond supporting translation including forming complexes with tubulin and actin, the actin interaction possibly linking the cytoskeleton to protein synthesis, and ubiquitin-mediated degradation (Durso and Cyr, 1994; Gonen et al., 1994; Kim and Coulombe, 2010).

The function of EF-1A during TMV accumulation was hypothesized to aid minus strand synthesis (Yamaji et al., 2006). However, down-regulation of EF-1A through virus-induced gene silencing resulted in the reduced size of green fluorescent lesions induced by TMV-expressing GFP, but no reduction in lesion numbers or translation activity in the silenced leaves (Yamaji et al., 2010). This result suggests that the function of EF-1A is not for translation or virus accumulation, but for virus movement that may, in some manner, be linked to the cytoskeleton (**Figure 1**).

Tobamovirus multiplication 1 (TOM1) is a predicted multipass transmembrane protein required for tobamovirus accumulation (Ishikawa et al., 1993; Yamanaka et al., 2000). Surprisingly, over-expression of TOM1 decreases ToMV multiplication (Hagiwara-Komoda et al., 2008). This observation is associated with the finding that accumulation of the ToMV replication proteins in membrane-free (soluble) fractions was lower for plants over-expressing TOM1 compared with those not over-expressing this protein (Hagiwara-Komoda et al., 2008). This result indicates that the level of the soluble form or the ratio of soluble and membrane-bound forms of the replication proteins is critical for normal virus accumulation. It was hypothesized that the soluble form is important for RNA silencing suppressor activity and it was shown that the loss of suppressor activity is correlated with diminished accumulation of the virus (Kubota et al., 2003; Hagiwara-Komoda et al., 2008). TOM1 interacts with the helicase domain of the 130 kDa protein from the related tobamovirus, *Tobacco mosaic virus-Cg* (crucifer-infecting virus), in a yeast two-hybrid screen (Yamanaka et al., 2000). This interaction was shown to be with the helicase core region based on predictions from the crystal structure of the helicase domain (Nishikiori et al., 2012). The replication proteins from ToMV and TOM1 share similar subcellular fractionation pattern in extracts from infected BY-2 cells, residing mostly in the tonoplast-containing fractions, but also in fractions with other membranes, including the ER (Hagiwara et al., 2003). It is hypothesized that TOM1 forms a link between the host membrane in which it resides and the tobamovirus replication proteins (**Figure 1**). This interaction is likely important for VRC formation, but the co-localization of TOM1 and tobamovirus replication proteins in live cells has not been reported.

INTRACELLULAR MOVEMENT

For TMV to establish a systemic infection, the virus or its components must move within a cell to establish an infection site, multiply and finally position for movement to the next cell. The granules of vRNA that form on initial infection, the VRCs that form during infection and the 126 kDa protein- and MP/vRNA-containing inclusions observed during ectopic expression all move within the cell (e.g., Kawakami et al., 2004; Liu et al., 2005; Sambade et al., 2008; Christensen et al., 2009). These complexes may change their form and constituents with time.

During initial infection, granules containing vRNA anchor to cortical ER and move to cortical ER vertices and the perinuclear ER where virus replication and translation occurs (Reichel and Beachy, 1998; Christensen et al., 2009; **Figure 1**). Indeed, vRNA has been visualized in the perinuclear bodies by bimolecular fluorescence complementation using a modified sequence-specific RNA-binding protein, Pumilio1, or by classical *in situ* RNA labeling (Tilsner et al., 2008). The vRNA must contain a sequence that targets the ER membrane directly or through a protein that targets the ER. Why the vRNA moves to particular cortical ER vertices or the perinuclear ER for replication is unknown. However, considering that most of the ribosome-containing, or rough, ER is present in the perinuclear region (Carrasco and Meyer, 2011) it is likely that this location, or a cortical ER vertex also containing ribosomes, is best suited for virus protein synthesis. Neither cytochalasin D nor latrunculin B (LatB) treatment, both microfilament antagonists, affect granule formation suggesting that microfilaments are not involved in this initial activity (Christensen et al., 2009). However, disruption of microfilaments results in granules hovering in the cortical ER, suggesting microfilaments help transport the granules in the cell. In contrast, depolymerizing microtubules does not stop vRNA granule movement along the tubular cortical ER (Christensen et al., 2009).

Membranes may be involved in intracellular trafficking of TMV components and the virus itself, as a VRC or vRNP, during virus accumulation and later spread. TMV replication occurs in association with ER and other membranes and both the MP and the replication proteins associate intrinsically or through a protein linker with membranes (Brill et al., 2000; Hagiwara et al., 2003; Fujiki et al., 2006). Interestingly, however, interruption of ER to Golgi secretory transport, mediated by the host coat complex II (COP-II) with brefeldin A (BFA) or through over-expression of a dominant-negative GTPase, Sar1p, did not alter targeting of ectopically expressed, fluorescently labeled MP to plasmodesmata (PD; Boutant et al., 2009; Genovés et al., 2010). This result, as well as BFA studies with infectious virus (see below), indicates that the COP-II-mediated transport system is not utilized by TMV MP or TMV to target viral products to the cell periphery. The actual pathway used by the virus, however, likely includes ER since that membrane is present in early- and late-formed virus inclusions (by fluorescence microscopy and EM), with early forming inclusions paired at the cell wall (e.g., Esau and Cronshaw, 1967; Heinlein et al., 1998; Szécsi et al., 1999; see below).

Much information is available on the movement of inclusion bodies containing the viral replication proteins. Several laboratories pursued EM-based immunocytolocalization studies of TMV infections with antibody against the replication proteins (Hills et al., 1987; Saito et al., 1987). They noted that the structure of the inclusions likely changed during development, going from smoothly granular to containing electron-dense rope-like structures, composed at least partly of 126 kDa protein, in a ribosome-rich matrix. Saito et al. (1987) referred to the former as viroplasms and the latter as X-bodies. Szécsi et al. (1999) showed through light and EM immunocytolocalization studies that TMV-induced inclusion bodies with viroplasm and X-body characteristics changed position and content as infections within cells developed. Near the infection front the inclusion bodies were paired on either side of the cell wall and contained both the replication proteins and MP, while four to six cells back from the front the bodies were not paired, had moved away from the cell wall and only contained the replication proteins. Through fluorescence microscopy of cells near the infection front, Tilsner et al. (2008) observed vRNA in small cortical bodies in the peripheral cytoplasm. They suggested these cortical bodies may represent the

inclusions at the cell periphery observed by Szécsi et al. (1999). Motionless small fluorescent bodies in the cell were detected at 12 h post-inoculation and these bodies were moving by 14 h post-inoculation when tracking TMV expressing an MP-GFP fusion: a period when both MP and the replication proteins would co-localize (Kawakami et al., 2004). Movement of the fluorescent inclusions early in infection, when both replication proteins and MP would be present, was aligned with microfilaments, and through pharmacological and gene-silencing studies, the inclusions (also referred to as VRCs) were shown to require these intact microfilaments for their intracellular movement (Kawakami et al., 2004; Liu et al., 2005). The degradation of the microfilaments was not sufficient to decrease virus accumulation to levels that would prevent virus movement or VRC formation and thus the influence of microfilaments on TMV intracellular movement was not confounded by a significant inhibition of virus replication (Liu et al., 2005). Treatment with a general myosin motor inhibitor, 2,3-butanedione monoxime (BDM), impaired the intracellular movement of VRCs (Kawakami et al., 2004).

Boyko et al. (2007), using a chimeric TMV expressing the MP from the Ob tobamovirus (Padgett et al., 1996), determined that MP-GFP inclusions at the infection front likely representing VRCs were associated with and typically trafficked along cortical microtubules for short distances in a stop-and-go manner (microtubules labeled with a microtubule-associated protein fused with GFP). Later studies obtained similar findings using the native MP of TMV fused with mRFP (Sambade et al., 2008). It was hypothesized that microtubules serve to anchor and then, through polymerization, release the VRC for movement (Sambade and Heinlein, 2009; reviewed in Peña and Heinlein, 2012). A second hypothesis, to be discussed further in the section on TMV intercellular movement, was that microtubule polymerization pushes the VRC along the ER (Peña and Heinlein, 2012). Other research, however, found that disruption of microtubules through pharmacological treatment with aminoprophos-methyl, colchicine, or oryzalin, or by silencing α-tubulin, had no significant effect on the transport of the MP-GFP within cells or to the PD area during infection (Gillespie et al., 2002; Kawakami et al., 2004; Wright et al., 2007). Regarding microfilaments, early studies indicated an association of TMV MP with rhodamine-conjugated phalloidin microfilaments after probing cells with polyclonal antibody against the MP and fluorescein-conjugated secondary antibody (McLean et al., 1995). Wright et al. (2007) utilized fluorescence recovery after photobleaching (FRAP) to observe MP-GFP movement and found that microfilament antagonists, LatB and cytochalasin B, inhibited MP targeting to the PD. However, a later study determined that the MP-GFP expressed during virus infection was not observed to co-align with fluorescently labeled microfilaments (Hofmann et al., 2009). Lastly, in studying membrane-mediated transport of the MP, inhibition of ER–Golgi membrane trafficking with BFA at low concentration (10 μg/ml) did not inhibit MP targeting (Tagami and Watanabe, 2007; Wright et al., 2007), but did influence the structure of the MP-GFP inclusion bodies (Tagami and Watanabe, 2007). At high concentration of BFA (100 μg/ml), which disrupts cortical ER structure, there was a significant effect on MP targeting to the PD (Wright et al., 2007). Thus, during virus infection the trafficking of the MP within the cell likely requires intact ER and may require microfilaments and microtubules (**Figure 1**), although evidence against a direct action for microfilaments exists and microtubules may not be in an intact form or the required microtubule array is unusual in that it is impervious to certain pharmacological agents (Seemanpillai et al., 2006).

Although the TMV VRC moves within cells, the replication proteins and the MP, independent of one another and in the absence of vRNA, also can transport within the cell. Their independent transport may have physiological relevance. Expression of a fusion of the TMV 126 kDa protein with GFP yields an intracellular inclusion body that, like the VRC, co-aligns with and traffics along microfilaments (Liu et al., 2005). As observed for the VRC, disruption of microfilaments ends intracellular transport of the 126 kDa protein-GFP inclusion body. Furthermore, normal intracellular movement of the 126 kDa-GFP inclusion body, like TMV sustained intercellular movement, requires myosin XI-2 (see section on "INTERCELLULAR MOVEMENT" for discussion of myosin influence on TMV physiology; Harries et al., 2009; C. Liu, and R. S. Nelson, personal communication). Whether the 126 kDa protein directly interacts with microfilaments or myosin XI-2 requires further study. If there is no direct interaction between these proteins, trafficking of virus proteins may be through interaction of myosin XI-2 with host components associated with a virus-host protein complex or through the creation of a bulk flow network of cytoplasmic constituents (i.e., cytoplasmic streaming). Considering that the viral replication proteins may transport independently of the MP or other viral components to complete their functions, additional studies of their ectopic transport in relationship to their transport during virus infection are needed. The difficulty in pursuing studies on the viral replication proteins is that no fusion between the replication proteins and a fluorescent marker has been developed that yields a viable virus. This needs to be addressed for further progress to occur.

Transient expression of the MP fused with fluorescent markers results in the formation of inclusions that associate with RNA and associate with and traffic along the ER, perhaps interacting with a microtubule scaffold necessary for movement (Sambade and Heinlein, 2009). Both microfilament and microtubule antagonists inhibited intracellular transport of the MP-fluorescent marker fusion, the results from the latter treatment (using aminoprophos-methyl) being a different finding from many during virus infection where MP-GFP fusion movement was not impeded by microtubule antagonists. To complicate this situation further, additional research determined that neither oryzalin or aminoprophos-methyl, both antagonists of microtubules, nor LatB, a microfilament antagonist, inhibited the formation of MP-GFP inclusions or their localization to the cell periphery or PD in cultured cells or leaves (Prokhnevsky et al., 2005; Boutant et al., 2009). These apparently conflicting results highlight the difficulty interpreting findings from pharmacological studies. Clearly, additional work is required to determine, in real time and through methods using non-pharmacological techniques, the influence of the cytoskeleton on transiently expressed MP intracellular trafficking. Assuming MP trafficking independent of the VRC has physiological relevance, findings from these additional studies would provide further insight into the mechanism of TMV intracellular movement. Some work investigating the influence of MP

transport in the absence of pharmacological treatment has been published. For example, Kotlizky et al. (2001) determined that an ectopically expressed MP mutant-GFP fusion, MP^{NT-1}-GFP, which inhibits TMV spread when expressed in transgenic plants, was able to associate with microtubules but did not target PD or move between cells. This suggests that the microtubule binding domain resides in a different location from the region important for PD localization and supports the pharmacological studies indicating that MP PD localization and initial virus spread requires more than microtubule association by the MP.

INTERCELLULAR MOVEMENT

As for intracellular movement, our understanding of TMV intercellular movement is fragmented. It is certain, however, that TMV utilizes PD to move between cells. PD are bounded by the plasma membrane and contain a cytoplasmic sleeve between this membrane and intact ER, the ER referred to as the desmotubule in this tissue (Lucas et al., 2009; Benitez-Alfonso et al., 2010; White and Barton, 2011; **Figure 1**). Callose is present in the neck region of the PD (Northcote et al., 1989; see Benitez-Alfonso et al., 2010). Actin and myosin are among multiple protein components in the cytoplasmic sleeve (Fernandez-Calvino et al., 2011; White and Barton, 2011). The size exclusion limit (SEL) of PD allows the passive diffusion of small molecules ∼1 kDa in size. This presents an impediment to virus movement because virus structures that are hypothesized to move between cells require a far larger SEL. The MP of TMV modifies the SEL of the PD to facilitate virus movement through PD and fluorescently labeled MP is observed in PD after virus spread has occurred (reviewed in Benitez-Alfonso et al., 2010; Niehl and Heinlein, 2011). The MP itself also can move between cells when ectopically expressed (reviewed in Niehl and Heinlein, 2011). The increase in PD SEL during TMV spread is transient, returning to a restricted size after passage of the infection front as measured by fluorescence expressed from the TMV-GFP genome (Oparka et al., 1997). Microfilament antagonists lead to a significant increase in the PD SEL while those that stabilize microfilaments prevent the MP from increasing the PD SEL (White et al., 1994; Ding et al., 1996; Su et al., 2010). The TMV MP exhibits microfilament severing activity (Su et al., 2010). These findings, in total, suggest a mechanism for virus spread where TMV MP opens PD through its microfilament severing activity, mimicking the phenotype induced with microfilament antagonists (**Figure 1**). Su et al. (2010) hypothesized that the severing activity of the TMV MP was limited to the PD area by analogy with findings from a mutant MP of *Cucumber mosaic virus* altered in its ability to target the PD. This mutant MP, which also has severing activity, fragments microfilaments in the cytoplasm (Su et al., 2010). Besides the MP, evidence for the VRC moving between cells has been published (Kawakami et al., 2004), but there have been no subsequent reports supporting this finding. The 126 kDa protein fused with GFP has not been reported to move between cells during ectopic expression, suggesting that VRC intercellular movement requires expression of additional viral proteins (likely the MP) or the presence of the vRNA.

In addition to innate actin severing activity by the TMV MP that may enlarge PD, the TMV MP interacts with ankyrin repeat-containing protein, ANK, at the PD and this association is correlated with an increase the PD SEL (Ueki et al., 2010). ANK has multiple activities, including binding to and delivering chloroplasts to their destination, supporting disease resistance against bacteria and virus challenge and participating in reactive oxygen scavenging, but it does not have callose degrading activity. Over-expressing ANK in transgenic plants resulted in more extensive MP-YFP and TMV-DsRed spread between cells. During transient expression of ANK and MP, the level of callose in the neck region of the PD decreased. Previously it was shown that enhanced TMV intercellular spread was correlated with enhanced expression of the callose-degrading enzyme, β -1, 3-glucanase (Bucher et al., 2001). Whether predominantly cytoplasmic ANK, through its MP interaction and the MP interaction with membrane, targets β -1, 3-glucanase in ER-derived vesicles to the cell wall or if ANK functions directly to inhibit callose synthase activity, remains to be determined (Ueki et al., 2010; **Figure 1**). Interactions of the TMV MP with other host proteins that influence TMV spread have been described (e.g., pectin methyl-esterase; Chen et al., 2000). However, in many instances cell biological studies to observe the interaction between the MP and host proteins within a live cell have not been conducted to further determine the location where the interaction may influence intercellular spread.

Regarding microtubules and TMV intercellular movement, there is evidence that MP interaction with the microtubule end-binding protein 1a (EB1a) is important for TMV spread. Brandner et al. (2008) determined that EB1a-GFP and MP-GFP form complexes both *in vitro* and *in vivo*. EB1a-GFP sub-cellular localization during TMV infection was altered from end labeling comet-like structures representing growing microtubules to labeling the length of microtubules. The length-wise decoration of microtubules was associated with a co-localization of MP-RFP. This unexpected re-localization of the EB1a protein at the infection front was correlated with an inhibition of virus intercellular spread. Ouko et al. (2010) determined that a mutant tobacco expressing a detyrosinated α-tubulin had a slower moving GFP-EB1 and inhibited intercellular spread by TMV. These studies suggest that modified microtubule dynamics inhibits TMV intercellular spread, perhaps by inhibiting microtubule polymerization that normally would push the VRC along the ER during intracellular transport (reviewed in Peña and Heinlein, 2012; **Figure 1**). These findings support those using a mutant strain of TMV whose temperature sensitive intercellular movement is correlated with the temperature sensitive localization of MP with microtubules (Boyko et al., 2007). However, other studies using pharmacological agents or silencing of the α-tubulin gene found no effect of these treatments on TMV intercellular spread or on the presence of MP in PD (Gillespie et al., 2002). Additionally, a virus expressing a modified MP with limited affinity for microtubules displayed enhanced intercellular spread (Gillespie et al., 2002). These and other findings from studies of a microtubule-binding protein, MPB2C, which binds to the MP and when overexpressed has a negative effect on intercellular movement of a related tobamovirus (Ruggenthaler et al., 2009), led to the suggestion that the function of microtubules in TMV spread is for degradation of the MP. Recently, it was determined that a CELL-DIVISION CYCLE protein48 (CDC48) from *Arabidopsis*, which localizes in the cytoplasm near the cortical ER network, interacts with the TMV MP to extract

it from ER for its subsequent accumulation on microtubules (Niehl et al., 2012). These authors also determined that overexpression of CDC48 in infected tissue inhibited virus spread. Thus, it appears that removal of the MP from the ER at the infection front and its movement to the microtubules through CDC48 activity is directed toward processing and possibly, degrading, the MP (**Figure 1**).

Microfilaments have been shown to be important for TMV intercellular movement, but the interpretation of their involvement in this activity is evolving. Findings from early studies using a GFP-labeled virus showed that disruption of microfilaments, through pharmacological methods or by silencing actin, inhibited sustained (2 days and beyond post-inoculation) virus intercellular movement (Kawakami et al., 2004; Liu et al., 2005). This inhibition in sustained intercellular spread was not associated with a decrease in virus accumulation per cell that would affect virus movement or prevent VRC formation (Liu et al., 2005). In addition, the sustained virus intercellular movement was not correlated with VRC size (Liu et al., 2005). This movement required myosin motor activity and specifically myosin XI-2 motor activity (Kawakami et al., 2004; Harries et al., 2009). Surprisingly, intercellular movement of the related tobamovirus, TVCV, was unaffected by disruption of microfilaments or silencing of any myosin studied to date (Harries et al., 2009). During this time, it also was shown that TMV was not inhibited in spread early after LatB treatment (i.e., movement up to 24 h after treatment; Hofmann et al., 2009). In addition, these researchers determined that actin binding domain 2 (ABD2)-GFP, expressed in transgenic plants, inhibited TMV movement. They concluded that this disruption in virus movement was primarily due to a loss of membrane fluidity caused by the ABD2-GFP marker and that TMV intercellular movement was predominantly influenced by membrane diffusion characteristics. Thus, results from studies of both TVCV and early TMV intercellular movement suggest membranes as the predominant vehicle controlling tobamovirus intercellular movement. These findings also support those from a previous study showing that both the viral replication proteins and MP are necessary to allow maximum diffusion through PD of GFP-fused probes representing soluble ER membrane-bound proteins (Guenoune-Gelbart et al., 2008). It was concluded that the results best support a model in which the virus complex, perhaps consisting of viral RNA, MP and other proteins, diffuses on the ER membrane within the PD from infected to uninfected cells driven by a concentration gradient (Guenoune-Gelbart et al., 2008). The involvement of the ER directly in virus movement, without prior transport through Golgi, is supported by the finding that inhibition of the COP II transport system through expression of a dominant negative GTPase mutant protein, Sar1, did not inhibit sustained TMV intercellular movement (Genovés et al., 2010).

Irrespective of the mechanism of early movement between cells by TMV, an explanation of this virus's requirement for microfilaments for sustained movement is required. Harries et al. (2010) suggested that the influence of microfilaments on this activity may be in preventing a stress response from occurring at the PD that later signaled to cells in advance of virus spread. These cells would then modify their metabolism in preparation for the arrival of the virus. Here we hypothesize that it is the transport of the VRC from the cell wall/PD area to an internal subcellular location on the actomyosin array that is necessary to prevent the stress signal from moving to the next cell (**Figure 1**). On treatment with LatB or silencing of myosin XI-2, the TMV VRCs would remain at the cell wall/PD interface, inhibiting normal cell–cell communications. This stress would be signaled to the cells in advance of the virus spread and modify these cells to inhibit subsequent virus spread. This hypothesis is supported by the finding that the VRCs of TMV move away from the cell wall as the infection passes (Szécsi et al., 1999). This interpretation would also accommodate the finding that early TMV movement is unaffected by actomyosin inhibitors since it would take some time to signal in advance of the infection front to stop virus movement. In addition, it would explain the lack of effect of LatB on TVCV movement since the 125 kDa protein, the homolog of the 126 kDa protein of TMV, does not form intracellular inclusions that associate with microfilaments (Harries et al., 2009) and the virus itself produces few visible VRCs (Resconich, 1961). The transport of the TMV VRC or its remnants from the wall may require membranes and vesicles since the TMV MP binds with a plant synaptotagmin *in vitro* (Lewis and Lazarowitz, 2010). Synaptogamins are a family of Ca^{2+}- and lipid-binding proteins that modulate, through interaction with SNARE proteins, the fusion of vesicles with membranes (Chapman, 2008). A dominant negative synaptotagmin mutant caused depletion of endosomes and inhibited intercellular trafficking of the MP-GFP fusion (Lewis and Lazarowitz, 2010). The direct influence of synaptotagmin on virus physiology appears to be on the endocytic pathway, implying that the effect of the dominant negative synaptotagmin on virus movement is through blocking the recycling of membrane used by the virus to reach the cell wall/PD area, thus backing up the system (**Figure 1**). This hypothesis, suggesting a requirement for actomyosin-mediated vesicle trafficking of the VRC or VRC components from the wall membranes for sustained virus movement, can be evaluated through cell biological studies.

Regarding non-cytoskeletal or membrane-associated proteins and TMV intercellular movement, a gene encoding a class II KNOTTED1-like protein, NTH201, was cloned from *Nicotiana tabacum* and its expression levels were positively correlated with MP accumulation, VRC numbers and virus spread (Yoshii et al., 2008). NTH201 has no ability to traffic between cells or traffic GFP, unlike class I KNOX-like plant proteins, and the authors speculated that NTH201 may function as a transcription factor that helps to stabilize or fold MP and VRCs through its regulation of other genes. This mystery was partially explained when a second host factor, MPIP1, a DnaJ-like protein with potential chaperone activity, was determined to interact with TMV MP and NTH201 in a yeast-three hybrid screen (Shimizu et al., 2009). Silencing MPIP1 inhibits TMV spread, as determined by GFP fluorescence, and thus its silencing phenocopies observations of TMV spread when NTH201 expression was silenced. It is possible that an interaction between two host proteins and the TMV MP aid in transport of virus between cells (**Figure 1**).

CONCLUSION

Cell biological studies over the last 20 years have tremendously aided our understanding of TMV accumulation and spread. Without advanced molecular and biochemical technologies allowing

virus and virus component labeling and advanced imaging hardware our understanding of the individual processes during virus spread would be diminished. For example, if virus intercellular movement were studied by genetics alone the importance of the transport of TMV vRNA granules to the perinuclear region of the ER versus the transport of TMV VRCs and MPs to the PD could go unrecognized. This said, some cell biological studies have yielded conflicting or controversial results. This is especially true of pharmacological studies and researchers must carefully control as many variables in these studies as possible. In addition, conclusions from pharmacological studies should be verified using other methods. Use of novel virus labeling techniques and advanced microscopes will allow further advances in this area. For example, the identification of small fluorescent tags that do not influence the function of the viral protein to which it is fused will be helpful. The iLOV protein, derived from the blue light receptor phototropin and much smaller than GFP, has been available for some time and was a first step toward utilizing smaller fluorescent tags (Chapman et al., 2008). More recently a MYB-related transcription factor, Rosea 1, which is also smaller than GFP, has been placed in TMV as a marker for virus location (Bedoya et al., 2012). Advanced microscopes with super high resolution will allow us to more easily determine whether proteins are interacting or simply co-localizing (Tilsner and Oparka, 2010). Access to the *N. benthamiana* genome (Bombarely et al., 2012) will allow better identification of gene family members projected to influence virus transport and the ability to target individual members for knockdown, over-expression and labeling. Lastly, recent findings suggest that while transport of TMV to the PD is important, it is also important to understand what happens to the virus inclusions left in the cell after virus movement, since their proper degradation or storage may influence sustained intercellular movement by the virus. As an analogy, although humans can function well for a time in their home (i.e., cell) without working plumbing, a plugged drain, like a plugged PD, will eventually be noticed. With our improving technologies, resources, and knowledge the future is bright, literally, for cell biological studies on TMV accumulation and spread.

ACKNOWLEDGMENTS

The authors thank Elison Blancaflor and Liangfa Ge for critically reading the manuscript and Kim Cooper for reference preparation. This work was supported by the Agriculture and Food Research Initiative Competitive Grants Program Grant no. 2010-65108-20525 from the USDA National Institute of Food and Agriculture.

REFERENCES

Bedoya, L. C., Martínez, F., Orzáez, D., and Daròs, J. A. (2012). Visual tracking of plant virus infection and movement using a reporter MYB transcription factor that activates anthocyanin biosynthesis. *Plant Physiol.* 158, 1130–1138.

Benitez-Alfonso, Y., Faulkner, C., Ritzenthaler, C., and Maule, A. (2010). Plasmodesmata: gateways to local and systemic virus infection. *Mol. Plant Microbe Interact.* 23, 1403–1412.

Bhat, S., Folimonova, S. Y., Cole, A. B., Ballard, K. D., Lei, Z., Watson, B. S., et al. (2012). Influence of host chloroplast proteins on Tobacco mosaic virus accumulation and intercellular movement. *Plant Physiol.* 161, 134–147.

Boevink, P., and Oparka, K. J. (2005). Virus-host interactions during movement processes. *Plant Physiol.* 138, 1815–1821.

Bombarely, A., Rosli, H. G., Vrebalov, J., Moffett, P., Mueller, L. A., and Martin, G. B. (2012). A draft genome sequence of *Nicotiana benthamiana* to enhance molecular plant-microbe biology research. *Mol. Plant Microbe Interact.* 25, 1523–1530.

Boutant, E., Fitterer, C., Ritzenthaler, C., and Heinlein, M. (2009). Interaction of the Tobacco mosaic virus movement protein with microtubules during the cell cycle in tobacco BY-2 cells. *Protoplasma* 237, 3–12.

Boyko, V., Hu, Q., Seemanpillai, M., Ashby, J., and Heinlein, M. (2007). Validation of microtubule-associated Tobacco mosaic virus RNA movement and involvement of microtubule-aligned particle trafficking. *Plant J.* 51, 589–603.

Brandner, K., Sambade, A., Boutant, E., Didier, P., Mély, Y., Ritzenthaler, C., et al. (2008). Tobacco mosaic virus movement protein interacts with green fluorescent protein-tagged microtubule end-binding protein 1. *Plant Physiol.* 147, 611–623.

Brill, L. M., Nunn, R. S., Kahn, T. W., Yeager, M., and Beachy, R. N. (2000). Recombinant Tobacco mosaic virus movement protein is an RNA-binding, alpha-helical membrane protein. *Proc. Natl. Acad. Sci. U.S.A.* 97, 7112–7117.

Bucher, G. L., Tarina, C., Heinlein, M., Serio, F. D., Meins, F. J., and Iglesias, V. A. (2001). Local expression of enzymatically active class I β-1, 3-glucanase enhances symptoms of TMV infection in tobacco. *Plant J.* 28, 361–369.

Carrasco, S., and Meyer, T. (2011). STIM proteins and the endoplasmic reticulum-plasma membrane junctions. *Annu. Rev. Biochem.* 80, 973–1000.

Chapman, E. R. (2008). How does synaptotagmin trigger neurotransmitter release? *Annu. Rev. Biochem.* 77, 615–641.

Chapman, S., Faulkner, C., Kaiserli, E., Garcia-Mata, C., Savenkov, E. I., Roberts, A. G., et al. (2008). The photoreversible fluorescent protein iLOV outperforms GFP as a reporter of plant virus infection. *Proc. Natl. Acad. Sci. U.S.A.* 105, 20038–20043.

Chen, M. H., Sheng, J., Hind, G., Handa, A. K., and Citovsky, V. (2000). Interaction between the Tobacco mosaic virus movement protein and host cell pectin methylesterases is required for viral cell-to-cell movement. *EMBO J.* 19, 913–920.

Christensen, N., Tilsner, J., Bell, K., Hammann, P., Parton, R., Lacomme, C., et al. (2009). The 5′ cap of Tobacco mosaic virus (TMV) is required for virion attachment to the actin/endoplasmic reticulum network during early infection. *Traffic* 10, 536–551.

Das, P., and Hari, V. (1992). Intracellular distribution of the 126K/183K and capsid proteins in cells infected by some tobamoviruses. *J. Gen. Virol.* 73, 3039–3043.

de Castro, I. F., Volonté, L., and Risco, C. (2012). Virus factories: biogenesis and structural design. *Cell. Microbiol.* 15, 24–34.

Ding, B., Kwon, M. O., and Warnberg, L. (1996). Evidence that actin filaments are involved in controlling the permeability of plasmodesmata in tobacco mesophyll. *Plant J.* 10, 157–164.

Ding, X. S., Bao, Y., Carter, S. A., and Nelson, R. S. (1998). "Host factors involved in viurs replication and cell-to-cell movement," in *1997 Annual Report of the Samuel Rorberts Noble Foundation* (Ardmore, OK: Noble Foundation Communiations), 94–96.

dos Reis Figueira, A., Golem, S., Goregaoker, S. P., and Culver, J. N. (2002). A nuclear localization signal and a membrane association domain contribute to the cellular localization of the Tobacco mosaic virus 126-kDa replicase protein. *Virology* 301, 81–89.

Durso, N. A., and Cyr, R. J. (1994). A calmodulin-sensitive interaction between microtubules and a higher plant homolog of elongation factor-1α. *Plant Cell* 6, 893–905.

Epel, B. L. (2009). Plant viruses spread by diffusion on ER-associated movement-protein-rafts through plasmodesmata gated by viral induced host beta-1, 3-glucanases. *Semin. Cell Dev. Biol.* 20, 1074–1081.

Esau, K., and Cronshaw, J. (1967). Relation of Tobacco mosaic virus to the host cells. *J. Cell Biol.* 33, 665–678.

Fernandez-Calvino, L., Faulkner, C., Walshaw, J., Saalbach, G., Bayer, E., Benitez-Alfonso, Y., et al. (2011). *Arabidopsis* plasmodesmal proteome. *PLoS ONE* 6:e18880. doi: 10.1371/journal.pone.0018880

Fujiki, M., Kawakami, S., Kim, R. W., and Beachy, R. N. (2006). Domains of Tobacco mosaic virus movement protein essential for its membrane association. *J. Gen. Virol.* 87, 2699–2707.

Genovés, A., Navarro, J. A., and Pallás, V. (2010). The intra- and intercellular movement of Melon necrotic spot virus (MNSV) depends on an active secretory pathway. *Mol. Plant Microbe Interact.* 23, 263–272.

Gillespie, T., Boevink, P., Haupt, S., Roberts, A. G., Toth, R., Valentine, T., et al. (2002). Functional analysis of a DNA-shuffled movement protein reveals that microtubules are dispensable for the cell-to-cell movement of Tobacco mosaic virus. *Plant Cell* 14, 1207–1222.

Gonen, H., Smith, C. E., Siegel, N. R., Kahana, C., Merrick, W. C., Chakarburtty, K., et al. (1994). Protein synthesis elongation factor EF-1α is essential for ubiquitin-dependent degradation of certain Naα-acetylated proteins and may be substituted for by the bacterial elongation factor EF-Tu. *Proc. Natl. Acad. Sci. U.S.A.* 91, 7648–7652.

Goregaoker, S. P., and Culver, J. N. (2003). Oligomerization and activity of the helicase domain of the Tobacco mosaic virus 126- and 183-kilodalton replicase proteins. *J. Virol.* 77, 3549–3556.

Guenoune-Gelbart, D., Elbaum, M., Sagi, G., Levy, A., and Epel, B. L. (2008). Tobacco mosaic virus (TMV) replicase and movement protein function synergistically in facilitating TMV spread by lateral diffusion in the plasmodesmal desmotubule of *Nicotiana benthamiana*. *Mol. Plant Microbe Interact.* 21, 335–345.

Hagiwara-Komoda, Y., Hirai, K., Mochizuki, A., Nishiguchi, M., Meshi, T., and Ishikawa, M. (2008). Overexpression of a host factor TOM1 inhibits Tomato mosaic virus propagation and suppression of RNA silencing. *Virology* 376, 132–139.

Hagiwara, Y., Komoda, K., Yamanaka, T., Tamai, A., Meshi, T., Funada, R., et al. (2003). Subcellular localization of host and viral proteins associated with tobamovirus RNA replication. *EMBO J.* 22, 344–353.

Harries, P., and Ding, B. (2011). Cellular factors in plant virus movement: at the leading edge of macromolecular trafficking in plants. *Virology* 411, 237–243.

Harries, P. A., Park, J.-W., Sasaki, N., Ballard, K. D., Maule, A., and Nelson, R. S. (2009). Differing requirements for actin and myosin by plant viruses for sustained intercellular movement. *Proc. Natl. Acad. Sci. U.S.A.* 106, 17594–17599.

Harries, P. A., Schoelz, J. E., and Nelson, R. S. (2010). Intracellular transport of viruses and their components: utilizing the cytoskeleton and membrane highways. *Mol. Plant Microbe Interact.* 23, 1381–1393.

Heinlein, M., Padgett, H. S., Gens, J. S., Pickard, B. G., Casper, S. J., Epel, B. L., et al. (1998). Changing patterns of localization of the Tobacco mosaic virus movement protein and replicase to the endoplasmic reticulum and microtubules during infection. *Plant Cell* 10, 1107–1120.

Hills, G. J., Plaskitt, K. A., Young, N. D., Dunigan, D. D., Watts, J. W., Wilson, T. M. A., et al. (1987). Immunogold localization of the intracellular sites of structural and nonstructural Tobacco mosaic virus proteins. *Virology* 161, 488–496.

Hofmann, C., Niehl, A., Sambade, A., Steinmetz, A., and Heinlein, M. (2009). Inhibition of Tobacco mosaic virus movement by expression of an actin-binding protein. *Plant Physiol.* 149, 1810–1823.

Ishibashi, K., Nishikiori, M., and Ishikawa, M. (2010). Interactions between tobamovirus replication proteins and cellular factors: their impacts on virus multiplication. *Mol. Plant Microbe Interact.* 23, 1413–1419.

Ishikawa, M., Naito, S., and Ohno, T. (1993). Effects of the toml mutation of *Arabidopsis thaliana* on the multiplication of Tobacco mosaic virus RNA in protoplasts. *J. Virol.* 67, 5328–5338.

Ishikawa, M., and Okada, Y. (2004). Replication of tobamovirus RNA. *Proc. Jpn. Acad. Ser. B* 80, 215–224.

Ishikawa, M., Meshi, T., Motoyoshi, F., Takamatsu, N., and Okada, Y. (1986). *In vitro* mutagenesis of the putative replicase genes of Tobacco mosaic virus. *Nucleic Acids Res.* 14, 8291–8305.

Ishikawa, M., Meshi, T., Ohno, T., and Okada, Y. (1991). Specific cessation of minus-strand RNA accumulation at an early stage of tobacco mosaic virus infection. *J. Virol.* 65, 861–868

Karpova, O. V., Ivanov, K. I., Rodionova, N. P., Dorokhov, Y. L., and Atabekov, J. G. (1997). Nontranslatability and dissimilar behavior in plants and protoplasts of viral RNA and movement protein complexes formed *in vitro*. *Virology* 230, 11–21.

Kawakami, S., Watanabe, Y., and Beachy, R. N. (2004). Tobacco mosaic virus infection spreads cell to cell as intact replication complexes. *Proc. Natl. Acad. Sci. U.S.A.* 101, 6291–6296.

Kim, S., and Coulombe, P. A. (2010). Emerging role for the cytoskeleton as an organizer and regulator of translation. *Nat. Rev. Mol. Cell Biol.* 11, 75–81.

Knapp, E., Achor, D., and Lewandowski, D. J. (2007). Tobacco mosaic virus defective RNAs expressing C-terminal methyltransferase domain sequences are severely impaired in long-distance movement in *Nicotiana benthamiana*. *Virology* 367, 82–91.

Kotlizky, G., Katz, A., Van Der Laak, J., Boyko, V., Lapidot, M., Beachy, R. N., et al. (2001). A dysfunctional movement protein of Tobacco mosaic virus interferes with targeting of wild-type movement protein to microtubules. *Mol. Plant Microbe Interact.* 14, 895–904.

Kubota, K., Tsuda, S., Tamai, A., and Meshi, T. (2003). Tomato mosaic virus replication protein suppresses virus-targeted posttranscriptional gene silencing. *J. Virol.* 77, 11016–11026.

Kragler, F., Curin, M., Trutnyeva, K., Gansch, A., and Waigmann, E. (2003). MPB2C, a microtubule-associated plant protein binds to and interferes with cell-to-cell transport of Tobacco mosaic virus movement protein. *Plant Physiol.* 132, 1870–1883.

Laliberté, J. F., and Sanfaçon, H. (2010). Cellular remodeling during plant virus infection. *Annu. Rev. Phytopathol.* 48, 69–91.

Lee, J.-Y., Taoka, K.-I., Yoo, B.-C., Ben-Nissan, G., Kim, D.-J., and Lucas, D. J. (2005). Plasmodesmal-associated protein kinase in tobacco and *Arabidopsis* recognizes a subset of non-cell-autonomous proteins. *Plant Cell* 17, 2817–2831.

Lewandowski, D. J., and Dawson, W. O. (2000). Functions of the 126- and 183-kDa proteins of TMV. *Virology* 271, 90–98.

Lewis, J. D., and Lazarowitz, S. G. (2010). Arabidopsis synaptotagmin SYTA regulates endocytosis and virus movement protein cell-to-cell transport. *Proc. Natl. Acad. Sci. U.S.A.* 107, 2491–2496.

Liu, J. Z., Blancaflor, E. B., and Nelson, R. S. (2005). The Tobacco mosaic virus 126-kilodalton protein, a constituent of the virus replication complex, alone or within the complex aligns with and traffics along microfilaments. *Plant Physiol.* 138, 1853–1865.

Liu, J. Z., Blancaflor, E. B., and Nelson, R. S. (2006). "The structure of the Tobacco mosaic virus replication complex is modulated by the 126-kDa protein and complex and protein traffic along microfilaments," in *Biology of Plant–Microbe Interactions*, Vol. 5, eds F. Sánchez, C. Quinto, I. M. Lopez-Lara, and O. Geiger (St Paul: IS-MPMI Press), 410–415.

Lucas, W. J., Ham, B. K., and Kim, J. Y. (2009). Plasmodesmata - bridging the gap between neighboring plant cells. *Trends Cell Biol.* 19, 495–503.

Más, P., and Beachy, R. N. (1999). Replication of Tobacco mosaic virus on endoplasmic reticulum and role of the cytoskeleton and virus movement protein in intracellular distribution of viral RNA. *J. Cell Biol.* 147, 945–958.

McLean, B. G., Zupan, J., and Zambryski, P. C. (1995). Tobacco mosaic virus movement protein associates with the cytoskeleton in tobacco cells. *Plant Cell* 7, 2101–2114.

Niehl, A., and Heinlein, M. (2011). Cellular pathways for viral transport through plasmodesmata. *Protoplasma* 248, 75–99.

Niehl, A., Khalid, A., Dalya, G., Brandner, K., Mély, Y., and Heinlein, M. (2012). Control of *Tobacco mosaic virus* movement protein fate by CELL-DIVISION-CYCLE protein48. *Plant Physiol.* 160, 2093–2108.

Nishikiori, M., Dohi, K., Mori, M., Meshi, T., Naito, S., and Ishikawa, M. (2006). Membrane-bound tomato mosaic virus replication proteins participate in RNA synthesis and are associated with host proteins in a pattern distinct from those that are not membrane bound. *J. Virol.* 80, 8459–8468.

Nishikiori, M., Sugiyama, S., Xiang, H., Niiyama, M., Ishibashi, K., Inoue, T., et al. (2012). Crystal structure of the superfamily 1 helicase from Tomato mosaic virus. *J. Virol.* 86, 7565–7576.

Northcote, D. H., Davey, R., and Lay, J. (1989). Use of antisera to localize callose, xylan and arabinogalactan in the cell-plate, primary and secondary walls of plant cells. *Planta* 178, 353–366.

Oparka, K. J., Prior, D. A., Cruz, S. S., Padgett, H. S., and Beachy, R. N. (1997). Gating of epidermal plasmodesmata is restricted to the leading edge of expanding infection sites of Tobacco mosaic virus (TMV). *Plant J.* 14, 781–789.

Osman, T. A., and Buck, K. W. (1996). Complete replication in vitro of Tobacco mosaic virus RNA by a template-dependent, membrane-bound RNA polymerase. *J. Virol.* 70, 6227–6234.

Ouko, M. O., Sambade, A., Brandner, K., Niehl, A., Peña, E., Ahad, A., et al. (2010). Tobacco mutants with reduced microtubule dynamics are less susceptible to TMV. *Plant J.* 62, 829–839.

Padgett, H. S., Epel, B. L., Kahn, T. W., Heinlein, M., Watanabe, Y., and Beachy, R. N. (1996). Distribution of tobamovirus movement protein in infected cells and implications for cell-to-cell spread of infection. *Plant J.* 10, 1079–1088.

Palukaitis, P., and Zaitlin, M. (1986). "Tobacco mosaic virus: infectivity and replication," in *The Plant Viruses*, Vol. 2, eds M. H. V. Van Regenmortel and H. Fraenkel-Conrat (New York: Plenum), 105–131.

Peña, E. J., and Heinlein, M. (2012). RNA transport during TMV cell-to-cell movement. *Front. Plant Sci.* 3:193. doi: 10.3389/fpls.2012.00193

Prokhnevsky, A. I., Peremyslov, V. V., and Dolja, V. V. (2005). Actin cytoskeleton is involved in targeting of a viral Hsp70 homolog to the cell periphery. *J. Virol.* 79, 14421–14428.

Reichel, C., and Beachy, R. N. (1998). Tobacco mosaic virus infection induces severe morphological changes of the endoplasmic reticulum. *Proc. Natl. Acad. Sci. U.S.A.* 95, 11169–11174.

Resconich, E. C. (1961). Interpretation of the forms of inclusions in bean systemically infected with Tobacco mosaic virus. *Virology* 15, 16–21.

Ruggenthaler, P., Fichtenbauer, D., Krasensky, J., Jonak, C., and Waigmann, E. (2009). Microtubule-associated protein AtMPB2C plays a role in organization of cortical microtubules, stomata patterning, and tobamovirus infectivity. *Plant Physiol.* 149, 1354–1365.

Saito, T., Hosokawa, D., Meshi, T., and Okada, Y. (1987). Immunocytochemical localization of the 130K and 180K proteins (putative replicase components) of Tobacco mosaic virus. *Virology* 160, 477–481.

Sambade, A., Brandner, K., Hofmann, C., Seemanpillai, M., Mutterer, J., and Heinlein, M. (2008). Transport of TMV movement protein particles associated with the targeting of RNA to plasmodesmata. *Traffic* 9, 2073–2088.

Sambade, A., and Heinlein, M. (2009). Approaching the cellular mechanism that supports the intercellular spread of Tobacco mosaic virus. *Plant Signal. Behav.* 4, 35–38.

Schoelz, J. E., Harries, P. A., and Nelson, R. S. (2011). Intracellular transport of plant viruses: finding the door out of the cell. *Mol. Plant* 4, 813–831.

Seemanpillai, M., Elamawi, R., Ritzenthaler, C., and Heinlein, M. (2006). Challenging the role of microtubules in Tobacco mosaic virus movement by drug treatments is disputable. *J. Virol.* 80, 6712–6715.

Shaw, J. G. (1999). Tobacco mosaic virus and the study of early events in virus infections. *Philos. Trans. R. Soc. Lond. B Biol. Sci.* 354, 603–611.

Shimizu, T., Yoshii, A., Sakurai, K., Hamada, K., Yamaji, Y., Suzuki, M., et al. (2009). Identification of a novel tobacco DnaJ-like protein that interacts with the movement protein of Tobacco mosaic virus. *Arch. Virol.* 154, 959–967.

Su, S., Liu, Z., Chen, C., Zhang, Y., Wang, X., Zhu, L., et al. (2010). Cucumber mosaic virus movement protein severs actin filaments to increase the plasmodesmal size exclusion limit in tobacco. *Plant Cell* 22, 1373–1387.

Szécsi, J., Ding, X. S., Lim, C. O., Bendahmane, M., Cho, M. J., Nelson, R. S., et al. (1999). Development of Tobacco mosaic virus infection sites in *Nicotiana benthamiana*. *Mol. Plant Microbe Interact.* 12, 143–152.

Tagami, Y., and Watanabe, Y. (2007). Effects of brefeldin A on the localization of tobamovirus movement protein and cell-to-cell movement of the virus. *Virology* 361, 133–140.

Tilsner, J., Amari, K., and Torrance, L. (2011). Plasmodesmata viewed as specialised membrane adhesion sites. *Protoplasma* 248, 39–60.

Tilsner, J., Linnik, O., Christensen, N. M., Bell, K., Roberts, I. M., Lacomme, C., et al. (2008). Live-cell imaging of viral RNA genomes using a Pumilio-based reporter. *Plant J.* 57, 758–770.

Tilsner, J., and Oparka, K. J. (2010). Tracking the green invaders: advances in imaging virus infection in plants. *Biochem. J.* 430, 21–37.

Ueki, S., Spektor, R., Natale, D. M., and Citovsky, V. (2010). ANK, a host cytoplasmic receptor for the Tobacco mosaic virus cell-to-cell movement protein, facilitates intercellular transport through plasmodesmata. *PLoS Pathog.* 6:e1001201. doi: 10.1371/journal.ppat.1001201

Watanabe, T., Honda, A., Iwata, A., Ueda, S., Hibi, T., and Ishihama, A. (1999). Isolation from Tobacco mosaic virus-infected tobacco of a solubilized template-specific RNA-dependent RNA polymerase containing a 126K/183K protein heterodimer. *J. Virol.* 73, 2633–2640.

White, R. G., Badelt, K., Overall, R. L., and Vesk, M. (1994). Actin associated with plasmodesmata. *Protoplasma* 180, 169–184.

White, R. G., and Barton, D. A. (2011). The cytoskeleton in plasmodesmata: a role in intercellular transport? *J. Exp. Bot.* 62, 5249–5266.

Wright, K. M., Wood, N. T., Roberts, A. G., Chapman, S., Boevink, P., Mackenzie, K. M., et al. (2007). Targeting of TMV movement protein to plasmodesmata requires the actin/ER network: evidence from FRAP. *Traffic* 8, 21–31.

Wu, X. J., Xu, Z., and Shaw, J. G. (1994). Uncoating of Tobacco mosaic virus RNA in protoplasts. *Virology* 200, 256–262.

Yamaji, Y., Hamada, K., Yoshinuma, T., Sakurai, K., Yoshii, A., Shimizu, T., et al. (2010). Inhibitory effect on the Tobacco mosaic virus infection by a plant RING finger protein. *Virus Res.* 153, 50–57.

Yamaji, Y., Kobayashi, T., Hamada, K., Sakurai, K., Yoshii, A., Suzuki, M., et al. (2006). *In vivo* interaction between Tobacco mosaic virus RNA-dependent RNA polymerase and host translation elongation factor 1A. *Virology* 347, 100–108.

Yamanaka, T., Ohta, T., Takahashi, M., Meshi, T., Schmidt, R., Dean, C., et al. (2000). TOM1, an *Arabidopsis* gene required for efficient multiplication of a tobamovirus, encodes a putative transmembrane protein. *Proc. Natl. Acad. Sci. U.S.A.* 97, 10107–10112.

Yoshii, A., Shimizu, T., Yoshida, A., Hamada, K., Sakurai, K., Yamaji, Y., et al. (2008). NTH201, a novel class II KNOTTED1-like protein, facilitates the cell-to-cell movement of Tobacco mosaic virus in tobacco. *Mol. Plant Microbe Interact.* 21, 586–596.

Zeenko, V. V., Ryabova, L. A., Spirin, A. S., Rothnie, H. M., Hess, D., Browning, K. S., et al. (2002). Eukaryotic elongation factor 1A interacts with the upstream pseudoknot domain in the 3′ untranslated region of Tobacco mosaic virus RNA. *J. Virol.* 76, 5678–5691.

Conflict of Interest Statement: The authors declare that the research was conducted in the absence of any commercial or financial relationships that could be construed as a potential conflict of interest.

Received: 16 November 2012; paper pending published: 10 December 2012; accepted: 17 January 2013; published online: 11 February 2013.
Citation: Liu C and Nelson RS (2013) The cell biology of Tobacco mosaic virus replication and movement. Front. Plant Sci. ***4****:12. doi: 10.3389/fpls.2013.00012*
This article was submitted to Frontiers in Plant-Microbe Interaction, a specialty of Frontiers in Plant Science.

frontiers in
PLANT SCIENCE

MINI REVIEW ARTICLE
published: 12 December 2012
doi: 10.3389/fpls.2012.00276

Recent advances in research of plant virus movement mediated by triple gene block

Andrey G. Solovyev, Natalia O. Kalinina and Sergey Y. Morozov*

Belozersky Institute of Physico-Chemical Biology, Moscow State University, Moscow, Russia

Edited by:
Jean-François Laliberté, Institut National de la Recherche Scientifique, Canada

Reviewed by:
Igor Kovalchuk, University of Lethbridge, Canada
Jeanmarie Verchot, Oklahoma State University, USA
Andrew O. Jackson, University of California-Berkeley, USA

****Correspondence:***
Sergey Y. Morozov, Belozersky Institute of Physico-Chemical Biology, Moscow State University, Moscow 119992, Russia.
e-mail: morozov@genebee.msu.su

The aim of this short review was to summarize recent advances in the field of viral cell-to-cell movement mediated by the triple gene block (TGB). The growing body of new research has uncovered links between virus cell-to-cell trafficking and replication, silencing suppression, virus spread over the plant, as well as suggested the roles of nucleus/nucleolus in plant virus transport and revealed protein-membrane associations occurring during subcellular targeting and cell-to-cell movement. In this context, our review briefly summarized current views on several potentially important functions of TGB proteins and on the development of new experimental systems that improved understanding of the molecular events during TGB-mediated virus movement.

Keywords: plant virus, virus movement, movement protein, triple gene block, TGB

INTRODUCTION

In recent years, the molecular mechanism of triple gene block (TGB)-mediated cell-to-cell movement of plant viruses was extensively studied and reviewed (Morozov and Solovyev, 2003; Verchot-Lubicz et al., 2010; Hyun et al., 2011; Niehl and Heinlein, 2011; Schoelz et al., 2011; Torrance et al., 2011). Three overlapping TGB genes encode proteins designated TGB1, which contains the domain of RNA helicase of superfamily 1, TGB2 and TGB3, which are small membrane-associated proteins. Our previous reviews focused on common and distinct properties of two major classes of TGB modules, potex-like and hordei-like TGBs (Morozov and Solovyev, 2003; Verchot-Lubicz et al., 2010). The TGB2 protein is highly conserved in both TGB classes, whereas the structural properties of TGB1 and TGB3 proteins differ considerably between potex-like and hordei-like TGBs (**Figure 1**; Morozov and Solovyev, 2003).

The analysis of recently published sequences of new TGB-containing viruses allowed us to reveal two additional TGB classes, one included the TGB of *Beet necrotic yellow vein virus* (BNYVV) and several related viruses belonging to the unassigned genus *Benyvirus*, and the other was TGB of bacilliform *Hibiscus green spot virus* (HGSV; **Figure 1A**; Morozov and Solovyev, 2012). Similar to the hordei-like TGB3 proteins, the BNYVV TGB3 has two transmembrane domains. However, the BNYVV TGB3 protein differs from hordei-like proteins by the N-terminal transmembrane domain located close to the protein terminus and a conserved sequence signature found only in the genus *Benyvirus* (Morozov and Solovyev, 2003, 2012; **Figure 1B**). The HGSV TGB1 helicase is very distantly related to other TGB1 proteins and shows more similarity to the superfamily 1 replicative helicases of the genus *Benyvirus*; and HGSV TGB3 contains two long hydrophobic segments with extremely short central hydrophilic region and no similarity to any of three other groups of TGB3 proteins (**Figure 1B**; Melzer et al., 2012). Moreover, despite the highest conservation of TGB2 among hordei-, beny-, and potex-like TGB proteins (Morozov and Solovyev, 2003), the HGSV protein has the central hydrophilic segment only distantly related to other TGB2 proteins (Morozov and Solovyev, 2012; **Figure 1B**). The relation of the TGB1 protein to the replicative helicases of alpha-like positive-stranded RNA viruses (Koonin and Dolja, 1993), occurence of two helicase domains in the RNA replicase of an endornavirus (Koonin and Dolja, 2012) and the ability to suppress RNA silencing observed for helicase domains of viral replicases as well as TGB1 proteins (Bayne et al., 2005; Senshu et al., 2009, 2011) allowed us to put forward the hypothesis of a multi-step TGB evolution (Morozov and Solovyev, 2012).

In this review, only three directions of TGB research where considerable progress has been achieved in recent years were selected for detailed discussion. The advances in functional analysis of TGB-mediated virus movement are summarized in **Table 1** and **Figure 1C**.

TGB-MEDIATED SILENCING SUPPRESSION AND VIRUS MOVEMENT

The pioneering work of Bayne et al. (2005) proposed that the virus movement depends on multiple functions including silencing suppression. The idea that silencing suppression mediated by the *Potato virus X* TGB1 protein could be required for cell-to-cell PVX movement came from the finding that the movement function of some TGB1 mutants could be restored by the heterologous silencing suppressors P19 and HcPro provided *in trans*. However, at least one of the other functions of the potex-like TGB1 protein (the movement function *per se*) is essential

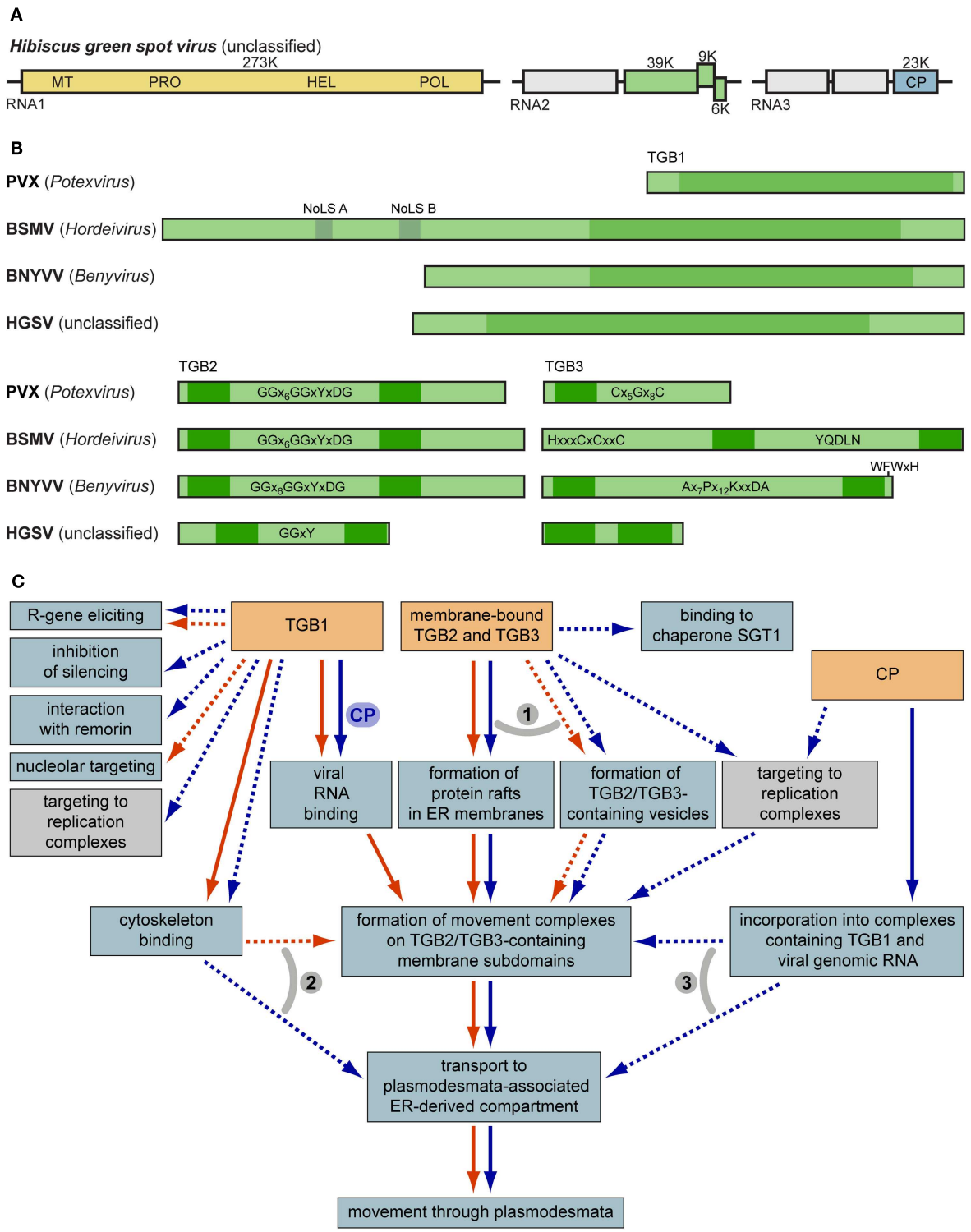

FIGURE 1 | (A) Genome organization of the new TGB-containing virus HGSV. Boxes represent genome-encoded open reading frames. Replicase gene domains are shown in the yellow box: MT, methyltransferase; PRO, protease; HEL, RNA helicase; POL, RNA-dependent RNA polymerase. Green boxes represent the TGB. Blue box specifies the viral coat protein (CP). **(B)** Molecular organization of TGB1, TGB2, and TGB3 proteins. Nucleolar localization sequences and helicase domain regions of TGB1 are shown above the BSMV TGB1. Characteristic signature sequences in TGB2 and TGB3 are shown. Dark green boxes indicate hydrophobic transmembrane sequence segments. **(C)** General scheme of TGB-mediated intracellular movement and interactions of macromolecules. Processes specific for potex-like and hordei-like TGBs are shown by blue and red arrows, respectively. Note that the box 'binding to chaperone SGT1' means a functional interaction between TGB3 and SGT1 (Ye et al., 2012). Transport steps common for both potex- and hordei-like TGBs are shown by parallel arrows. Processes that are

(Continued)

FIGURE 1 | Continued
not proved to be involved directly in virus cell-to-cell movement are shown by dashed arrows. Numbered gray arcs indicate alternative pathways of intracellular trafficking. (1) TGB2 and TGB3 may travel to their destinations in specific membrane containers such as vesicles formed in a COPII-independent manner, or ER-specific membrane rafts (Verchot-Lubicz et al., 2010; this review). (2) Trafficking to the cell periphery of the TGB1 protein (and TGB1-containing RNPs) may exploit the cytoskeleton-based pathway with the immediate movement to PD-associated compartment, or via binding to TGB2/TGB3-containing membrane subdomains involved in cytoskeleton-dependent transport (Verchot-Lubicz et al., 2010; this review). (3) TGB2/3-specific membrane containers may bind movement-competent RNPs containing TGBp1. On the other hand, these complexes may be delivered directly to the neck region of PD through interactions with cytoskeleton (see above; Verchot-Lubicz et al., 2010; this review). For further details, see text.

for virus movement, since several TGB1 protein mutants are movement-defective but fully competent as silencing suppressors, and strong silencing suppressors could not support movement of such TGB1-deficient PVX (Bayne et al., 2005). In accordance with these data, a specific mutation in TGB1 of *Alternanthera mosaic virus*, another potexvirus, proved to significantly reduce the TGB1 silencing suppression ability but retained the protein movement functions unaffected (Lim et al., 2010a). A similar effect of this particular TGB1 point mutation on silencing suppression is observed in other potexviruses too (Lim et al., 2010b).

Five different potexviruses exhibit strong variations in the ability to suppress RNA silencing in *Nicotiana benthamiana*, and these variations result from the differences in the suppressor activities of their TGB1 proteins (Senshu et al., 2009). Moreover, recent data demonstrate that some of the potexvirus TGB1 proteins suppress both intracellular silencing and the silencing spread through the plant, while others such as TGB1 encoded by potexvirus PVX and *Potato virus M*, a carlavirus, mainly suppress the spread of the silencing signal (Voinnet et al., 2000; Senshu et al., 2011). The clue to understanding the drastic functional differences observed in *N. benthamiana* for TGB1 proteins encoded by viruses with different natural hosts was made in the study where PVX, which is not competent for movement in *Arabidopsis thaliana*, was able to infect the *A. thaliana* triple dicer mutant (*dcl2*, *dcl3*, and *dcl4*). Moreover, the restriction of PVX systemic movement on *A. thaliana* also depended on AGO2 (RNAse H-like Argonaute protein; Jaubert et al., 2011). Thus, the ability of PVX to infect the *Arabidopsis* triple dicer mutant and AGO2 mutant suggests that the PVX TGB1 protein does not function as an effective silencing suppressor in this host (Alvarado and Scholthof, 2009; Jaubert et al., 2011). The specificity of TGB1 interaction with host and non-host proteins is one of the explanations of this phenomenon. Indeed, previous reports have shown that several viral silencing suppressors directly target AGO proteins and either prevent siRNA loading or induce AGO degradation (Alvarado and Scholthof, 2009; Csorba et al., 2010; Burgyán and Havelda, 2011; Shimura and Pantaleo, 2011; Schott et al., 2012). Recently, the PVX TGB1 protein was also reported to interact with AGO1, AGO2, AGO3, and AGO4 and destabilize AGO1 (Chiu et al., 2010).

Recently, Duan et al. (2012) demonstrated that the interaction of silencing suppressor 2b encoded by cucumoviruses with AGO proteins *in vivo* was required, in addition to the suppression function itself, for the nucleolar targeting of 2b and contributed to the re-distribution of both the 2b and AGO proteins in the nucleus. Therefore, TGB1 can be expected to be capable of trafficking to the nucleus and nucleolus. Indeed, the TGB1 proteins encoded by two potexviruses, *Alternanthera mosaic virus* and *Narcissus mosaic virus*, were shown to localize partly in the nucleus and nucleolus, and their nucleolar localization was experimentally proved to be essential for the efficient suppression of RNA silencing, probably through TGB1 interaction with nucleolar components of the host RNA silencing machinery (Lim et al., 2010b). However, the PVX TGB1 protein was localized to the nucleus but not to the nucleolus (Samuels et al., 2007).

POSSIBLE LINK BETWEEN THE TGB1 NUCLEOLAR LOCALIZATION AND VIRUS LONG-DISTANCE MOVEMENT

An increasing number of reports reveals that the proteins of many RNA viruses localize to the nucleus and its sub-compartments (mainly, to the nucleolus and the Cajal bodies), interact with nuclear/nucleolar proteins and divert host protein functions in order to exert novel role(s) during virus infection (Hiscox, 2007; Greco, 2009; Taliansky et al., 2010).

Analysis of TGB1 amino acid sequences employing the web service NoD, the nucleolar localization sequence detector (Scott et al., 2011), reveals nucleolar localization signals (NoLS) neither in HGSV, PVX, and other potex-like TGB1 proteins, nor in benyvirus-encoded proteins (our unpublished observations). On the other hand, all analyzed hordei-like TGB1 proteins are predicted to possess at least one NoLS: two NoLS sequences (NoLS A and B) were found in the proteins of all hordeiviruses, while a single NoLS was predicted in the pomovirus and pecluvirus proteins (**Figure 1B**). Therefore, we propose that the ability of the potexvirus TGB proteins to localize to the nucleolus can be due to their interactions with cell proteins (see above), whereas the transport of hordeivirus and pomovirus TGB1 proteins to the nucleolus can be directed by their own targeting signals.

In agreement with the NoLS predictions in hordei-like TGB1 proteins, several reports demonstrate the nuclear/nucleolar targeting of pomovirus and hordeivirus GFP-tagged TGB1 proteins observed along with their cytoplasmic localization (Wright et al., 2010; Semashko et al., 2012a). The NoLSs in TGB1 proteins encoded by viruses of both genera were predicted in the unstructured N-terminal domain (NTD; **Figure 1B**), which is present in all hordei-like TGB1 proteins (Makarov et al., 2009). These predictions are validated by the observation that the isolated N-terminal fragments of TGB1 can partly localize to the nucleolus (Wright et al., 2010; Semashko et al., 2012a). Moreover, mutations of basic residues in this region of the hordei-like pomovirus TGB1 protein abolish its nucleolar accumulation (Torrance et al., 2011). Similarly, mutagenesis of the basic amino acid residues in predicted hordeivirus NoLS A (aa107-136) and B

Table 1 | Overview of recent achievements in the cell biology studies of TGB.

Research directions	Novel advances	Reference
TGB-mediated silencing suppression and virus movement	Five different potexviruses exhibit strong variations in the ability to suppress RNA silencing in *Nicotiana benthamiana*	Senshu et al. (2009)
	A specific mutation in potexvirus TGB1 significantly reduces the TGB1 silencing suppression ability but retains the protein movement functions unaffected	Lim et al. (2010a,b)
	Carlavirus TGB1 suppresses systemic RNA silencing in *Nicotiana benthamiana*	Senshu et al. (2011)
	PVX is able to infect triple dicer and AGO2 mutants of the non-host plant *Arabidopsis thaliana*	Jaubert et al. (2011)
	PVX TGB1 protein interacts with and destabilizes AGO1	Chiu et al. (2010)
Localization of the TGB1 protein in the nucleus and nucleolus	Potexvirus TGB1 proteins are shown to localize partly in the nucleus and nucleolus	Samuels et al. (2007), Lim et al. (2010b)
	The isolated N-terminal fragments of hordei- and pomovirus TGB1 can partly localize to the nucleolus	Wright et al. (2010), Semashko et al. (2012a)
	Hordeivirus TGB1 interacts with nucleolar proteins fibrillarin and coilin	Semashko et al. (2012a,b)
Protein-membrane association in the TGB-mediated intracellular movement	Potexvirus TGB3 exhibits the affinity to highly curved subdomains of cortical ER	Lee et al. (2010), Wu et al. (2011)
	Potexvirus TGB3 protein is targeted to membrane bodies at the cell periphery of yeast and plant cells and directs the TGB2 protein to these structures	Wu et al. (2011)
	TGB3 multimer formation is required for the transport to specific peripheral compartments	Lee et al. (2010)
	Protein regions necessary for the multimerization and subcellular targeting are mapped in both potex- and hordeivirus TGB3 proteins	Wu et al. (2011), Shemyakina et al. (2011), Sun and Zhang (2012)
Interaction of the TGB proteins with the cytoskeleton	Pomovirus TGB1 interacts with microtubules, and this interaction is not required for virus movement	Wright et al. (2010), Torrance et al. (2011)
	Hordeivirus TGB1 interacts with microtubules, and this interaction is involved in protein trafficking to plasmodesmata and aggresomes	Shemyakina et al. (2011)
	Assembly of potexvirus TGB1 rod-like inclusions depends on actin microfilaments but not on microtubules	Yan et al. (2012)
	The potexvirus TGB1 protein remodels host actin	Tilsner et al. (2012)
	Actin cytoskeleton is important for BSMV cell-to-cell movement and for localization of TGB3	Lim et al. (2012)
Association of the TGB proteins with the sites of virus replication	The potexvirus TGB3 protein is co-localized with the viral replicase in the ER	Bamunusinghe et al. (2009)
	Potexvirus TGB1 is responsible for virus genome compartmentalization in infected cells	Tilsner et al. (2012)
The role of the virus coat protein in potexvirus movement	The interaction between the potexvirus replicase and the coat protein is critical for virus movement in plant hosts	Lee et al. (2011)
	Potexvirus CP mutants deficient in the interaction with TGB1 can form virus particles but is unable to move in plant tissues	Tilsner et al. (2012)
	The N-terminal region of the PlAMV potexvirus coat protein is required for cell-to-cell movement but is dispensable for virion assembly	Ozeki et al. (2009)
Genomic cis-elements involved in TGB-mediated movement	The stem-loop structure in the 5′-terminal region of potexvirus RNA controls viral movement by interacting with the several host proteins and the virus coat protein	Cho et al. (2012a,b,c)
TGB-induced ER stress	PVX TGB3 induces unfolded protein response	Ye et al. (2011), Ye and Verchot (2011)
	Hordeivirus TGB3 overexpression induces severe changes of endomembrane system	Solovyev et al. (2012), Lim et al. (2012)
Eliciting of hypersensitive response	Hordeivirus TGB1 elicits hypersensitive response and binds host Bsr1 R-protein	Cui et al. (2012), Lee et al. (2012)
TGB3 upregulates host chaperones	PVX TGB3 upregulates ER resident and ubiquitin ligase chaperones	Ye et al. (2011, 2012), Ye and Verchot (2011)
TGB1 and remorin	PVX TGB1 protein binds to plant membrane raft protein remorin. This interaction impairs cell-to-cell movement of the virus	Raffaele et al. (2009), Perraki et al. (2012)

(aa171-194) reveal that these protein regions are indeed involved in the protein localization to the nucleolus (Semashko et al., 2012a).

The hordeivirus TGB1 protein is able to bind fibrillarin, the major nucleolar protein, *in vitro*. The interaction of the two proteins, which involves the glycine-arginine-rich domain of fibrillarin and the 82 N-terminal amino acid residues of TGB1 protein, can also be detected by bimolecular fluorescence complementation upon transient coexpression in *N. benthamiana* plants (Semashko et al., 2012a). Additionally, the TGB1 NTD of two hordeiviruses is able to interact *in vitro* and *in vivo* with coilin, the major structural component of Cajal bodies, the subnuclear structures revealed in nuclei of many eukaryotes, including plants; and substitutions in the NoLS A resulted in an almost complete loss of the NTD ability to bind coilin (Semashko et al., 2012b; Kalinina and Guseinov, unpublished results). Fibrillarin is known to interact with the umbravirus ORF3 protein in the nucleolus, and this complex re-locates from the nuclei to the cytoplasm and takes part in the formation of viral cytoplasmic ribonucleoproteins (RNPs), which are capable of long-distance movement (Taliansky et al., 2010). In the hordeivirus and pomovirus TGB1 proteins, positively charged motifs corresponding to NoLS proved to be dispensable for the virus transport from cell-to-cell but necessary for the long-distance virus movement (Kalinina et al., 2001; Wright et al., 2010; Torrance et al., 2011). Collectively, these data suggest that, unlike viruses with the potex-like TGB where the nuclear localization of the TGB1 protein is due to its functions in suppression of RNA silencing, the localization of hordei-like TGB1 to the nucleus/nucleolus may result from its functions in virus long-distance movement. We hypothesize that this difference can be explained by different structure of the transport form of the viral genome in viruses with potex-like and hordei-like TGB, namely, the TGB1-modified virions in the former group and TGB1-formed non-virion RNPs in the latter one (Verchot-Lubicz et al., 2010). Presumably, the formation of transport-competent TGB1-containing virions does not require functions of cell nucleolar protein(s).

PROTEIN-MEMBRANE ASSOCIATION IN THE TGB-MEDIATED INTRACELLULAR MOVEMENT

Transport of the TGB1 protein to plasmodesmata is generally accepted to require the functions of the TGB2 and TGB3 proteins (Verchot-Lubicz et al., 2010). Previous data clearly demonstrated that the TGB3 protein contains signals of intracellular transport at least in viruses with the hordei-like TGB (Tilsner et al., 2010; Shemyakina et al., 2011; Sun and Zhang, 2012). Being capable of interaction with other TGB proteins, the TGB3 protein serves as a "driving force" of their intracellular transport to plasmodesmata-associated sites (Zamyatnin et al., 2004; Lim et al., 2008, 2009). Therefore, understanding the mechanism of TGB3 protein translocation from sites of its synthesis to plasmodesmata is of key importance for unraveling the details of the intracellular phase of TGB-mediated transport (**Figure 1C**).

In yeast cells, the behavior of the TGB3 protein encoded by *Bamboo mosaic virus* (BaMV), a potexvirus, is similar to that in plant cells: the protein is able to be targeted to the membrane bodies at the cell periphery and to direct the TGB2 protein to these structures (Lee et al., 2010). As in plant cells, the peripheral membrane TGB3-containing structures in yeast cells represent a subdomain of the cortical ER (Lee et al., 2010; Wu et al., 2011). Moreover, the TGB3-containing structures in yeast cells reside within discrete cortical ER regions enriched in cell reticulons Rtn1 and Yop1. These proteins belong to two families of integral ER membrane proteins necessary for the formation of highly curved membrane tubules of cortical ER in eukaryotic cells (Lee et al., 2010). The potexvirus TGB3 protein co-localized with a plant-encoded Rtn1-related protein in tobacco leaf cells as well, thus, validating the data obtained in yeast cells (Lee et al., 2010). Importantly, the desmotubule, an ER tubule, which locates in plasmodesmata and interconnects ER networks in neighboring cells, is extremely narrow and therefore has a high membrane curvature. Tilsner et al. (2011) recently suggested that the Rtn1- and Yop1-related proteins are required for the formation and stabilization of desmotubule, while the TGB3 protein can exhibit a high affinity to this specific plasmodesmal sub-structure. Indeed, the hordei-like TGB3 proteins of BSMV and *Potato mop-top virus* (PMTV) were shown to be retained within cell wall-embedded structures upon plasmolysis (Lim et al., 2009; Tilsner et al., 2010), which supports the hypothesis of their localization to the desmotubule.

As demonstrated for both potex-like and hordei-like TGBs, the TGB3 protein trafficking to plasmodesmata-associated membrane structures is COPII-independent and, thus, employs an unconventional mechanism, which does not involve the exit from ER in COPII-transport vesicles (**Figure 1C**; Schepetilnikov et al., 2005, 2008; Lee et al., 2010). The COPII-independent TGB3-specific trafficking to plasmodesmata-associated peripheral ER compartments requires specific signals in the TGB3 sequence. It was demonstrated that the targeting of hordei-like TGB3 protein was determined by a composite signal comprising the highly conserved sequence motif YQDLN located in the central hydrophilic protein region and the C-terminal transmembrane domain (Schepetilnikov et al., 2008; Tilsner et al., 2010; Lim et al., 2012). Recent studies show that these TGB3 regions play distinct roles. Analyses of the hordeivirus TGB3 protein demonstrate that the true signal of its intracellular transport resides in the protein C-terminal transmembrane segment, while the YQDLN motif is involved in protein oligomerization, which is essential for the functioning of targeting signal (Shemyakina et al., 2011; Sun and Zhang, 2012). Therefore, the hordeivirus TGB3 protein with the functional C-terminal targeting signal is able to enter its specific translocation pathway only in the form of multimeric complexes. Such TGB3-containing complexes represent the natural form of this protein found in hordeivirus-infected tissue (Shemyakina et al., 2011).

The residues responsible for specific targeting and self-interaction have been recently mapped in the BaMV TGB3 protein. The targeting to Rtn1/Yop-enriched cortical ER subdomains requires the C-terminal hydrophilic protein region, specifically, several critical residues conserved in the TGB3 proteins encoded by different potexviruses (Wu et al., 2011). Therefore, the functionally equivalent transport signals identified in the hordeivirus TGB3 protein (the transmembrane sequence domain) and the

potexvirus TGB3 protein (the hydrophilic sequence region) are strikingly different in their properties. The potexvirus TGB3 is capable of multimer formation, and the residues involved in protein self-interaction were mapped to the TGB3 region containing the protein sorting signal (Wu et al., 2011). It should be emphasized that, similarly to the hordeivirus TGB3 protein, the potexvirus TGB3 protein self-interaction is a pre-requisite for its correct subcellular targeting (Shemyakina et al., 2011; Wu et al., 2011).

The mechanism of TGB3 intracellular transport was hypothesized to involve either lateral translocation of TGB3-formed rafts, which also incorporate the TGB2 protein, in the plane of the ER membranes (Morozov and Solovyev, 2003; Wu et al., 2011) as postulated for the *Tobacco mosaic virus* MP (Epel, 2009), or vesicles of unknown nature tightly associated with the cortical tubular ER as observed for the PVX and PMTV TGB3 proteins (Samuels et al., 2007; Verchot-Lubicz et al., 2010).

Thus, the new data clearly show that the potex-like and hordei-like TGB3 proteins, which have markedly different structure (Morozov and Solovyev, 2003), nevertheless exhibit similar functional properties (**Figure 1C**) including the abilities for multimerization and multimerization-dependent subcellular targeting. Similar to hordeivirus TGB3 proteins, the BaMV TGB3 protein is found in discrete membrane bodies located at the cell periphery corresponding to highly curved subdomains of cortical ER (Wu et al., 2011) and is able to interact with the TGB2 protein, therefore ensuring the TGB2 co-targeting to TGB3-containing structures (Lee et al., 2010; Wu et al., 2011). Another parallel between the potex-like and hordei-like TGBs is provided by the recently shown interaction between the BaMV TGB2 and TGB1 proteins (Wu et al., 2011). This finding suggests that the complex containing the two membrane proteins encoded by potex-like TGB may direct the TGB1 protein to plasmodesmata-associated sites (**Figure 1C**). This hypothesis agrees with the reported ability of the hordei-like PMTV TGB2/TGB3 proteins to target the respective TGB1 protein to peripheral membrane compartments and to the plasmodesmata interior (Zamyatnin et al., 2004) as well as with the observed interactions of the BSMV TGB3 protein with both TGB2 and TGB1 proteins (Lim et al., 2008). The new findings make it possible to propose a general model of intracellular transport for hodeivirus and potexvirus TGB proteins (**Figure 1C**). This model includes common and specific events for both types of proteins as well as possible alternative pathways of trafficking process.

CONCLUSION

Studies carried out in the recent years reveal new aspects of the TGB-mediated virus movement, such as the accumulation of TGB3 protein in the cortical highly curved ER regions enriched in cell reticulons and involvement of the TGB1 protein in the interactions with the cellular RNA silencing machinery. The current research uncovers tight links between virus replication and cell-to-cell movement, the role of cytoskeleton, and the requirements for specific genomic RNA regions for TGB-mediated transport. In this short review we focused the reader's attention on the three trends in TGB studies to inspire further progress in the field.

ACKNOWLEDGMENTS

The work of N. Kalinina is funded by the Russian Foundation for Basic Research (grant 10-04-00522-a). The work of A. Solovyev and S. Morozov is funded by the Russian Foundation for Basic Research (grant 12-04-00139-a).

REFERENCES

Alvarado, V., and Scholthof, H. B. (2009). Plant responses against invasive nucleic acids: RNA silencing and its suppression by plant viral pathogens. *Semin. Cell Dev. Biol.* 20, 1032–1040.

Bamunusinghe, D., Hemenway, C. L., Nelson, R. S., Sanderfoot, A. A., Ye, C. M., Silva, M. A., et al. (2009). Analysis of potato virus X replicase and TGBp3 subcellular locations. *Virology* 393, 272–285.

Bayne, E. H., Rakitina, D. V., Morozov, S. Y., and Baulcombe, D. C. (2005). Cell-to-cell movement of potato potexvirus X is dependent on suppression of RNA silencing. *Plant J.* 44, 471–482.

Burgyán, J., and Havelda, Z. (2011). Viral suppressors of RNA silencing. *Trends Plant Sci.* 16, 265–272.

Chiu, M. H., Chen, I. H., Baulcombe, D. C., and Tsai, C. H. (2010). The silencing suppressor P25 of Potato virus X interacts with Argonaute1 and mediates its degradation through the proteasome pathway. *Mol. Plant Pathol.* 11, 641–649.

Cho, S. Y., Cho, W. K., and Kim, K. H. (2012a). Identification of tobacco proteins associated with the stem-loop 1 RNAs of Potato virus X. *Mol. Cells* 33, 379–384.

Cho, S. Y., Cho, W. K., Choi, H. S., and Kim, K. H. (2012b). Cis-acting element (SL1) of Potato virus X controls viral movement by interacting with the NbMPB2Cb and viral proteins. *Virology* 427, 166–176.

Cho, S. Y., Cho, W. K., Sohn, S. H., and Kim, K. H. (2012c). Interaction of the host protein NbDnaJ with Potato virus X minus-strand stem-loop 1 RNA and capsid protein affects viral replication and movement. *Biochem. Biophys. Res. Commun.* 417, 451–456.

Csorba, T., Lózsa, R., Hutvágner, G., and Burgyán, J. (2010). Polerovirus protein P0 prevents the assembly of small RNA-containing RISC complexes and leads to degradation of ARGONAUTE1. *Plant J.* 62, 463–472.

Cui, Y., Lee, M. Y., Huo, N., Bragg, J., Yan, L., Yuan, C., et al. (2012). Fine mapping of the Bsr1 barley stripe mosaic virus resistance gene in the model grass Brachypodium distachyon. *PLoS ONE* 7:e38333. doi:10.1371/journal.pone.0038333

Duan, C. G., Fang, Y. Y., Zhou, B. J., Zhao, J. H., Hou, W. N., Zhu, H., et al. (2012). Suppression of Arabidopsis ARGONAUTE1-mediated slicing, transgene-induced RNA silencing, and DNA methylation by distinct domains of the cucumber mosaic virus 2b protein. *Plant Cell* 24, 259–274.

Epel, B. L. (2009). Plant viruses spread by diffusion on ER-associated movement-protein-rafts through plasmodesmata gated by viral induced host beta-1,3-glucanases. *Semin. Cell Dev. Biol.* 20, 1074–1081.

Greco, A. (2009). Involvement of the nucleolus in replication of human viruses. *Rev. Med. Virol.* 19, 201–214.

Hiscox, J. A. (2007). RNA viruses: hijacking the dynamic nucleolus. *Nat. Rev. Microbiol.* 5, 119–127.

Hyun, T. K., Uddin, M. N., Rim, Y., and Kim, J. Y. (2011). Cell-to-cell trafficking of RNA and RNA silencing through plasmodesmata. *Protoplasma* 248, 101–116.

Jaubert, M., Bhattacharjee, S., Mello, A. F. S., Perry, K. L., and Moffett, P. (2011). ARGONAUTE2 mediates RNA-silencing antiviral defenses against Potato virus X in Arabidopsis. *Plant Physiol.* 156, 1556–1564.

Kalinina, N. O., Rakitina, D. A., Yelina, N. E., Zamyatnin, A. A. Jr., Stroganova, T. A., Klinov, D. V., et al. (2001). RNA-binding properties of the 63 kDa protein encoded by the triple gene block of poa semilatent hordeivirus. *J. Gen. Virol.* 82, 2569–2578.

Koonin, E. V., and Dolja, V. V. (1993). Evolution and taxonomy of positive-strand RNA viruses: implications of comparative analysis of amino acid sequences. *Crit. Rev. Biochem. Mol. Biol.* 28, 375–430.

Koonin, E. V., and Dolja, V. V. (2012). Expanding networks of RNA virus evolution. *BMC Biol.* 10:54. doi:10.1186/1741-7007-10-54

Lee, C. C., Ho, Y. N., Hu, R. H., Yen, Y. T., Wang, Z. C., Lee, Y. C., et al. (2011). The interaction between bamboo mosaic virus replication protein and coat protein is critical for virus movement in plant hosts. *J. Virol.* 85, 12022–12031.

Lee, M. Y., Yan, L., Gorter, F. A., Kim, B. Y., Cui, Y., Hu, Y., et al. (2012). Brachypodium distachyon Bd3-1 resistance is elicited by the Barley stripe mosaic virus Triple Gene Block 1 movement protein. *J. Gen. Virol.* 93, 2729–2739.

Lee, S.-C., Wu, C.-H., and Wang, C.-W. (2010). Traffic of a viral movement protein complex to the highly curved tubules of the cortical ER. *Traffic* 11, 912–930.

Lim, H. S., Bragg, J. N., Ganesan, U., Lawrence, D. M., Yu, J. L., Isogai, M., et al. (2008). Triple gene block protein interactions involved in movement of Barley stripe mosaic virus. *J. Virol.* 82, 4991–5006.

Lim, H. S., Bragg, J. N., Ganesan, U., Ruzin, S., Schichnes, D., Lee, M. Y., et al. (2009). Subcellular localization of the Barley stripe mosaic virus triple gene block proteins. *J. Virol.* 83, 9432–9448.

Lim, H. S., Lee, M. Y., Moon, J. S., Moon, J.-K., Yu, Y.-M., Cho, I. S., et al. (2012). Actin cytoskeleton and golgi involvement in barley stripe mosaic virus movement and cell wall localization of triple gene block proteins. *Plant Pathol. J.* 28 (in press).

Lim, H. S., Vaira, A. M., Reinsel, M. D., Bae, H., Bailey, B. A., Domier, L. L., et al. (2010a). Pathogenicity of alternanthera mosaic virus is affected by determinants in RNA-dependent RNA polymerase and by reduced efficacy of silencing suppression in a movement-competent TGB1. *J. Gen. Virol.* 91, 277–287.

Lim, H. S., Vaira, A. M., Domier, L. L., Lee, S. C., Kim, H. G., and Hammond, J. (2010b). Efficiency of VIGS and gene expression in a novel bipartite potexvirus vector delivery system as a function of strength of TGB1 silencing suppression. *Virology* 402, 149–163.

Makarov, V., Rybakova, E., Efimov, A., Dobrov, E., Serebryakova, M., Solovyev, A., et al. (2009). Domain organization of the N-terminal portion of hordeivirus movement protein TGBp1. *J. Gen. Virol.* 90, 3022–3032.

Melzer, M. J., Sether, D. M., Borth, W. B., and Hu, J. S. (2012). characterization of a virus infecting citrus volkameriana with citrus leprosis-like symptoms. *Phytopathology* 102, 122–127.

Morozov, S. Y., and Solovyev, A. G. (2003). Triple gene block: modular design of a multi-functional machine for plant virus movement. *J. Gen. Virol.* 84, 1351–1366.

Morozov, S. Y., and Solovyev, A. G. (2012). Did silencing suppression counter-defensive strategy contribute to origin and evolution of the triple gene block coding for plant virus movement proteins? *Front. Plant Sci.* 3:136. doi:10.3389/fpls.2012.00136

Niehl, A., and Heinlein, M. (2011). Cellular pathways for viral transport through plasmodesmata. *Protoplasma* 248, 75–99.

Ozeki, J., Hashimoto, M., Komatsu, K., Maejima, K., Himeno, M., Senshu, H., et al. (2009). The N-terminal region of the Plantago asiatica mosaic virus coat protein is required for cell-to-cell movement but is dispensable for virion assembly. *Mol. Plant Microbe Interact.* 22, 677–685.

Perraki, A., Cacas, J. L., Crowet, J. M., Lins, L., Castroviejo, M., German-Retana, S., et al. (2012). Plasma membrane localization of Solanum tuberosum remorin from group 1, homolog 3 is mediated by conformational changes in a novel C-terminal anchor and required for the restriction of potato virus X movement. *Plant Physiol.* 160, 624–637.

Raffaele, S., Bayer, E., Lafarge, D., Cluzet, S., German Retana, S., Boubekeur, T., et al. (2009). Remorin, a solanaceae protein resident in membrane rafts and plasmodesmata, impairs potato virus X movement. *Plant Cell* 21, 1541–1555.

Samuels, T. D., Ju, H. J., Ye, C. M., Motes, C. M., Blancaflor, E. B., and Verchot-Lubicz, J. (2007). Subcellular targeting and interactions among the Potato virus X TGB proteins. *Virology* 367, 375–389.

Schepetilnikov, M. V., Manske, U., Solovyev, A. G., Zamyatnin, A. A., Schiemann, J., and Morozov, S. Yu. (2005). The hydrophobic segment of Potato virus X TGBp3 is a major determinant of the protein intracellular trafficking. *J. Gen. Virol.* 86, 2379–2391.

Schepetilnikov, M. V., Solovyev, A. G., Gorshkova, E. N., Schiemann, J., Prokhnevsky, A. I., Dolja, V. V., et al. (2008). Intracellular targeting of a hordeiviral membrane-spanning movement protein: sequence requirements and involvement of an unconventional mechanism. *J. Virol.* 82, 284–1293.

Schoelz, J. E., Harries, P. A., and Nelson, R. S. (2011). Intracellular transport of plant viruses: finding the door out of the cell. *Mol. Plant* 4, 813–831.

Schott, G., Mari-Ordonez, A., Himber, C., Alioua, A., Voinnet, O., and Dunoyer, P. (2012). Differential effects of viral silencing suppressors on siRNA and miRNA loading support the existence of two distinct cellular pools of ARGONAUTE1. *EMBO J.* 31, 2553–2565.

Scott, M. S., Troshin, P. V., and Barton, G. J. (2011). NoD: a Nucleolar localization sequence detector for eukaryotic and viral proteins. *BMC Bioinformatics* 12:317. doi:10.1186/1471-2105-12-317

Semashko, M. A., González, I., Shaw, J., Leonova, O. G., Popenko, V. I., Taliansky, M. E., et al. (2012a). The extreme N-terminal domain of a hordeivirus TGB1 movement protein mediates its localization to the nucleolus and interaction with fibrillarin. *Biochimie* 94, 1180–1188.

Semashko, M. A., Rakitina, D. V., González, I., Canto, T., Kalinina, N. O., and Taliansky, M. E. (2012b). Movement protein of hordeivirus interacts in vitro and in vivo with coilin, a major structural protein of Cajal bodies. *Dokl. Biochem. Biophys.* 442, 57–60.

Senshu, H., Ozeki, J., Komatsu, K., Hashimoto, M., Hatada, K., Aoyama, M., et al. (2009). Variability in the level of RNA silencing suppression caused by triple gene block protein 1 (TGBp1) from various potexviruses during infection. *J. Gen. Virol.* 90, 1014–1024.

Senshu, H., Yamaji, Y., Minato, N., Shiraishi, T., Maejima, K., Hashimoto, M., et al. (2011). A dual strategy for the suppression of host antiviral silencing: two distinct suppressors for viral replication and viral movement encoded by potato virus M. *J. Virol.* 85, 10269–10278.

Shemyakina, E. A., Erokhina, T. N., Gorshkova, E. N., Schiemann, J., Solovyev, A. G., and Morozov, S. Y. (2011). Formation of protein complexes containing plant virus movement protein TGBp3 is necessary for its intracellular trafficking. *Biochimie* 93, 742–748.

Shimura, H., and Pantaleo, V. (2011). Viral induction and suppression of RNA silencing in plants. *Biochim. Biophys. Acta* 1809, 601–612.

Solovyev, A. G., Schiemann, J., and Morozov, S. Y. (2012). Microscopic analysis of severe structural rearrangements of the plant endoplasmic reticulum and Golgi caused by overexpression of Poa semilatent virus movement protein. *ScientificWorldJournal* 2012, 416076.

Sun, X., and Zhang, C. (2012). A conserved C-terminal motif is essential for self-interaction of Barley stripe mosaic virus China strain TGB3 protein. *Biochem. Biophys. Res. Commun.* 426, 153–157.

Taliansky, M. E., Brown, J. W., Rajamäki, M. L., Valkonen, J. P., and Kalinina, N. O. (2010). Involvement of the plant nucleolus in virus and viroid infections: parallels with animal pathosystems. *Adv. Virus Res.* 77, 119–158.

Tilsner, J., Amari, K., and Torrance, L. (2011). Plasmodesmata viewed as specialized membrane adhesion sites. *Protoplasma* 248, 39–60.

Tilsner, J., Cowan, G. H., Roberts, A. G., Chapman, S. N., Ziegler, A., Savenkov, E., et al. (2010). Plasmodesmal targeting and intercellular movement of Potato mop-top pomovirus is mediated by a membrane anchored tyrosine-based motif on the lumenal side of the endoplasmic reticulum and the C-terminal transmembrane domain in the TGB3 movement protein. *Virology* 402, 41–51.

Tilsner, J., Linnik, O., Wright, K. M., Bell, K., Roberts, A. G., Lacomme, C., et al. (2012). The TGB1 movement protein of Potato virus X reorganizes actin and endomembranes into the X-body, a viral replication factory. *Plant Physiol.* 158, 1359–1370.

Torrance, L., Wright, K. M., Crutzen, F., Cowan, G. H., Lukhovitskaya, N. I., Bragard, C., et al. (2011). Unusual features of pomoviral RNA movement. *Front. Microbiol.* 2:259. doi:10.3389/fmicb.2011.00259

Verchot-Lubicz, J., Torrance, L., Solovyev, A. G., Morozov, S. Y., Jackson, A. O., and Gilmer, D. (2010). Varied movement strategies employed by triple gene block-encoding viruses. *Mol. Plant Microbe Interact.* 23, 1231–1247.

Voinnet, O., Lederer, C., and Baulcombe, D. C. (2000). A viral movement protein prevents spread of the gene silencing signal in Nicotiana benthamiana. *Cell* 103, 157–167.

Wright, K. M., Cowan, G. H., Lukhovitskaya, N. I., Tilsner, J., Roberts, A. G., Savenkov, E. I., et al. (2010). The N-terminal domain of PMTV TGB1 movement protein is required for nucleolar localization, microtubule association, and long distance movement. *Mol. Plant Microbe Interact.* 11, 1486–1497.

Wu, C. H., Lee, S. C., and Wang, C. W. (2011). Viral protein targeting to the cortical endoplasmic reticulum is required for cell-cell spreading in plants. *J. Cell Biol.* 193, 521–535.

Yan, F., Lu, Y., Lin, L., Zheng, H., and Chen, J. (2012). The ability of PVX p25 to form RL structures in plant cells is necessary for its function in movement, but not for its suppression of

RNA silencing. *PLoS ONE* 7:e43242. doi:10.1371/journal.pone.0043242

Ye, C., Dickman, M. B., Whitham, S. A., Payton, M., and Verchot, J. (2011). The unfolded protein response is triggered by a plant viral movement protein. *Plant Physiol.* 156, 741–755.

Ye, C., and Verchot, J. (2011). Role of unfolded protein response in plant virus infection. *Plant Signal Behav.* 6, 2012–2015.

Ye, C. M., Kelly, V., Payton, M., Dickman, M. B., and Verchot, J. (2012). SGT1 is induced by the potato virus X TGBp3 and enhances virus accumulation in Nicotiana benthamiana. *Mol. Plant* 5, 1151–1153.

Zamyatnin, A. A., Solovyev, A. G., Savenkov, E. I., Germundsson, A., Sandgren, M., Valkonen, J. P. T., et al. (2004). Transient coexpression of individual genes encoded by the triple gene block of Potato mop-top virus reveals requirements for TGBp1 trafficking. *Mol. Plant Microbe Interact.* 17, 921–930.

Conflict of Interest Statement: The authors declare that the research was conducted in the absence of any commercial or financial relationships that could be construed as a potential conflict of interest.

Received: 20 September 2012; accepted: 23 November 2012; published online: 12 December 2012.

Citation: Solovyev AG, Kalinina NO and Morozov SY (2012) Recent advances in research of plant virus movement mediated by triple gene block. Front. Plant Sci. ***3****:276. doi: 10.3389/fpls.2012.00276*

This article was submitted to Frontiers in Plant-Microbe Interaction, a specialty of Frontiers in Plant Science.

frontiers in
PLANT SCIENCE

ORIGINAL RESEARCH ARTICLE
published: 31 January 2013
doi: 10.3389/fpls.2013.00006

Unraveling the structure of viral replication complexes at super-resolution

Olga Linnik[1], Johannes Liesche[2], Jens Tilsner[3,4] and Karl J. Oparka[1]*

[1] *Institute of Molecular Plant Sciences, University of Edinburgh, Edinburgh, UK*
[2] *Faculty of Life Sciences, University of Copenhagen, Frederiksberg C, Denmark*
[3] *Biomedical Sciences Research Complex, University of St Andrews, Fife, UK*
[4] *Cell and Molecular Sciences, The James Hutton Institute, Dundee, UK*

Edited by:
Jean-François Laliberté, Institut National de la Recherche Scientifique, Canada

Reviewed by:
Richard Nelson, Samuel Roberts Noble Foundation, Inc., USA
Tetsuro Okuno, Kyoto University, Japan

***Correspondence:**
Karl J. Oparka, Institute of Molecular Plant Sciences, University of Edinburgh, King's Buildings, Mayfield Road, Edinburgh EH9 3JR, UK.
e-mail: karl.oparka@ed.ac.uk

During infection, many RNA viruses produce characteristic inclusion bodies that contain both viral and host components. These structures were first described over a century ago and originally termed "X-bodies," as their function was not immediately appreciated. Whilst some inclusion bodies may represent cytopathic by-products of viral protein over-accumulation, X-bodies have emerged as virus "factories," quasi-organelles that coordinate diverse viral infection processes such as replication, protein expression, evasion of host defenses, virion assembly, and intercellular transport. Accordingly, they are now generally referred to as viral replication complexes (VRCs). We previously used confocal fluorescence microscopy to unravel the complex structure of X-bodies produced by Potato virus X (PVX). Here we used 3D-structured illumination (3D-SIM) super-resolution microscopy to map the PVX X-body at a finer scale. We identify a previously unrecognized membrane structure induced by the PVX "triple gene block" (TGB) proteins, providing new insights into the complex interplay between virus and host within the X-body.

Keywords: PVX, viral replication complex, 3D-SIM, super-resolution, TGB proteins, endoplasmic reticulum, Golgi

INTRODUCTION

VIRAL REPLICATION COMPLEXES

In the process of host invasion, many plant viruses induce the formation of characteristic inclusion bodies that were initially termed "X-bodies" due to their unclear role (Goldstein, 1924). Variously referred to as amorphous inclusions, amorphous bodies, amoeboid bodies, vacuolate bodies, or viroplasms, such inclusion bodies were described in early studies by Goldstein (1926), Sheffield (1939, 1949). Inclusion bodies have been valuable in the diagnosis of plant virus diseases (Martelli and Russo, 1977; Edwardson and Christie, 1978), and many detailed studies of their structure were conducted using electron microscopy (Esau, 1967; Shalla and Shepard, 1972; Christie and Edwardson, 1977). Although the observation of inclusion bodies during infection provided some insight into their role, their detailed structure and function was a mystery until the arrival of molecular tools.

Plant viruses predominantly have positive sense, single-stranded RNA genomes ((+)ssRNA; Hull, 2002). (+)ssRNA viruses replicate on the cytoplasmic surfaces of modified host cell membranes, and many viral inclusion bodies have been revealed to be "virus factories," i.e., replication sites (Miller and Krijnse-Locker, 2008; den Boon et al., 2010; Laliberté and Sanfaçon, 2010). Accordingly, these viral structures are now mostly referred to as viral replication complexes or VRCs (Asurmendi et al., 2004).

Viral RNA (vRNA)-dependent RNA polymerases ("replicases") are usually active as oligomeric arrays (Lyle et al., 2002; Kopek et al., 2007; Spagnolo et al., 2010), and the host membranes they occupy serve as scaffolds to assemble these complexes (Nishikiori et al., 2006). However, the functions of VRCs are more complex than simply functioning to anchor replicase proteins to membranes. In addition to vRNA and proteins, they often incorporate host components including rearranged host membranes (Schaad et al., 1997; Carette et al., 2000; Dunoyer et al., 2002; Ritzenthaler et al., 2002; Zamyatnin et al., 2002; Turner et al., 2004) that form a sheltered environment for the viral genome (Miller and Krijnse-Locker, 2008; den Boon et al., 2010; Laliberté and Sanfaçon, 2010). Besides being the primary centers of viral replication, VRCs may also facilitate viral access to essential host resources such as ribosomes, enzymes, and nucleotides. In animal RNA viruses, viral packaging may be closely linked to viral egress via the secretory pathway and budding from the plasma membrane (den Boon et al., 2010). Similarly in plant viruses, VRCs could be sites of assembly of movement-competent ribonucleoprotein complexes (RNPs) for intercellular transport via plasmodesmata (Schoelz et al., 2011; Tilsner and Oparka, 2012). With such a complex variety of processes coordinated in close proximity within VRCs, a detailed knowledge of the spatial organization of host and viral factors is crucial to understanding the functions of VRCs. Renewed ultrastructural investigations, using electron tomography, have yielded high-resolution "maps" of the VRCs of Flock house virus (FHV) and SARS corona virus (Kopek et al., 2007; Knoops et al., 2008). However, similar studies are lacking for plant viruses. In the case of FHV, combination of tomographic and biochemical data enabled estimations of the numbers of replicase molecules and (−)RNA replication templates in the membrane invaginations that harbor the replication machinery (Kopek et al., 2007). However, electron microscopy is limited in its ability to localize specific macromolecules within VRCs. This is more easily done

using fluorescence microscopy coupled to fluorescently labeled antibodies or fluorescent protein fusions.

Until recently, confocal laser scanning microscopy provided the highest resolution possible in fluorescence microscopy, with maximum resolutions of ∼200 nm in the focal plane (x-y) and ∼500 nm along the focal axis (z; Huang et al., 2009). Such ideal resolution is rarely achieved in heterogenous, living specimens, and for practical purposes confocal microscopy has approximately 50- to 100-fold lower resolution than electron microscopy, resulting in an inability to use confocal microscopy for structural mapping.

In recent years, various "super-resolution" microscopy (nanoscopy) approaches have been developed that overcome the diffraction barrier that limits conventional light microscopy, enabling fluorescence imaging at resolutions smaller than the wavelength of the emitted light (Huang et al., 2009; Schermelleh et al., 2010). Hence, these technologies are ideally suited to gain new insights into the structure-function relationships of VRCs (Horsington et al., 2012; Malkusch et al., 2012; Pereira et al., 2012). In practical terms, however, not all approaches are equally well suited to plants. In particular, the cell wall limits penetration of antibodies into plant cells. Therefore, the use of a genetically encoded fluorescent reporter fused with a protein of interest that is transcribed within the cell provides a better approach for intracellular studies. Additionally, the autofluorescence background created by chloroplasts and cell walls is particularly problematic for approaches that require single-molecule imaging such as photoactivation localization microscopy (PALM) and stochastic optical reconstruction microscopy (STORM; Tilsner and Flors, unpublished).

By contrast, three-dimensional structured illumination microscopy (3D-SIM) is a widefield imaging approach that is amenable to most specimens suitable for confocal microscopy. In 3D-SIM, a diffraction grating is superimposed upon the sample, and rotated during image acquisition. Sub-diffraction information is contained in the shifting diffraction patterns, and can be extracted by mathematical transformation, permitting image deconvolution with a resolution of ∼100 nm in x-y and 200 nm in z (Gustafsson et al., 2008; Huang et al., 2009). This constitutes an approximate two-fold increase in resolution over confocal microscopy, but in practical terms provides a significant increase in biological detail (Fitzgibbon et al., 2010; Phillips et al., 2012). We have previously used 3D-SIM to obtain super-resolution images of phloem sieve elements, including the localization of a viral movement protein to plasmodesmata (Fitzgibbon et al., 2010). To make the phloem accessible to 3D-SIM, we partially digested cell wall material and separated the cells of the tissue. Here, we employed 3D-SIM to analyze the X-body of a model virus, Potato virus X (PVX), and to demonstrate the suitability of the technique to imaging three-dimensional structures in leaf epidermal cells. This approach also should be suitable to a multitude of plant cell biology studies, including those conducted in the absence of virus infection.

THE POTATO VIRUS X-BODY

Potato virus X is a (+)ssRNA virus important for agriculture (Adams et al., 2004). It serves as a model virus for analysis of RNA silencing and virus movement, as a vector for protein overexpression and knockdown and as a virus-induced gene silencing model (Batten et al., 2003; Verchot-Lubicz et al., 2007). The mechanically transmitted PVX virions are flexuous filaments with a length of about 470–580 nm and are composed of the 6.4 kb vRNA and ∼1300 subunits of coat protein (CP; Atabekov et al., 2007).

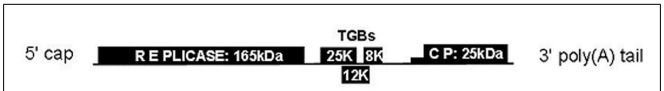

FIGURE 1 | Organization of the PVX genome (not to scale). TGB, triple gene block; CP, coat protein.

The PVX genome contains five open reading frames (ORFs) encoding five viral proteins (Batten et al., 2003): the 165 kDa replicase, which is the only viral protein required for replication (Doronin and Hemenway, 1996; Plante et al., 2000), a "triple gene block (TGB)" of three overlapping ORFs encoding the 25 kDa (TGB1), 12 kDa (TGB2), and 8 kDa (TGB3) movement proteins (MPs) responsible for cell-to-cell transport (Verchot-Lubicz et al., 2010; Solovyev et al., 2012 in this Research Topic), and the 25 kDa CP (**Figure 1**). All three TGBs and CP are needed for virus movement (Verchot-Lubicz et al., 2010) and CP is found in plasmodesmata and translocated between cells, indicating that it is a part of a movement-competent ribonucleoprotein complex (Oparka et al., 1996; Santa Cruz et al., 1998; Lough et al., 2000).

TGB1 is an RNA helicase that also functions as a translational activator (Atabekov et al., 2000; Rodionova et al., 2003) and silencing suppressor (Voinnet et al., 2000). TGB1 has been shown to be essential for forming the PVX X-body, and for recruiting actin filaments and host endomembranes [endoplasmic reticulum (ER) and Golgi] to this structure. TGB1 also recruits the two other viral MPs, TGB2, and TGB3 to the X-body (Tilsner et al., 2012). In contrast to TGB1, TGB2, and TGB3 are transmembrane proteins localized in the ER (Krishnamurthy et al., 2003; Ju et al., 2005). TGB2 induces the formation of ER-derived motile granules that also contain TGB3 (Ju et al., 2005, 2007; Samuels et al., 2007). The granules are associated with ribosomes, replicase, and virions (Ju et al., 2005; Bamunusinghe et al., 2009). As PVX replicates in association with the ER (Doronin and Hemenway, 1996), these granules may be replication sites.

Cells with mature PVX infections contain a perinuclear X-body. PVX X-bodies appear from about 1–2 days post-infection. They generally are circular or egg-shaped. The number and size of X-bodies per infected cell differs, but older infections typically contain only one. The X-body can be larger than the nucleus, ∼10–15 μm across, and is a complex amalgamation of host membranes including small vacuoles (Shalla and Shepard, 1972; Allison and Shalla, 1974; Santa Cruz et al., 1998; Tilsner et al., 2012). It also contains so-called "laminate inclusions" that are characteristic of PVX infection. In EM images, these inclusions consist of beaded or smooth sheets roughly 3 nm thick, firmly packed in several layers (Kozar and Sheludko, 1969; Stols et al., 1970; Shalla and Shepard, 1972; Allison and Shalla, 1974). Antibodies against TGB1 decorate the beaded sheets (Davies et al., 1993; Santa Cruz et al., 1998), and C-terminal fusions of fluorescent proteins (FPs) to TGB1 produce aggregates that morphologically resemble them (Tilsner et al., 2009, 2012). Thus, the inclusions contain large amounts of

TGB1, but it is not clear if they consist entirely of the TGB1 protein. It was proposed that the beaded sheets could be active sites of viral protein synthesis (Kozar and Sheludko, 1969; Shalla and Shepard, 1972). The smooth sheets had virus particles between the layers of the sheets (Shalla and Shepard, 1972), whereas the beaded sheets did not (Stols et al., 1970; Shalla and Shepard, 1972). Whilst the beaded sheets superficially resemble ribosome-studded ER membranes, no lipids were found to be present in them, but treatment with potassium permanganate destroyed them, indicating that they are proteinaceous. The beads, found on both surfaces of the sheets, are too small to be ribosomes (Shalla and Shepard, 1972). Surprisingly, more recent work on TGB1 does not refer to these early data on TGB1 beaded sheets. Fluorescent fusions of TGB2 and TGB3 also localized to the X-body (Samuels et al., 2007; Tilsner et al., 2012). Lastly, encapsidated PVX virions surround the X-body and when the CP is fused to GFP, virions appear as fluorescent cages around the inclusions (Oparka et al., 1996; Santa Cruz et al., 1998; Tilsner et al., 2012).

Recently, we undertook a detailed structural and functional analysis of the PVX X-body and its biogenesis (Tilsner et al., 2012). The X-body is formed by gradual accumulation of the ER-derived, TGB2/3-containing granules around the TGB1 beaded sheets. Non-encapsidated vRNA, visualized with a fluorescent reporter construct *in vivo*, localizes to whorls that tightly encircle the TGB1 inclusions. The presence of "naked" RNA inside the X-body, and encapsidated virions at its periphery, along with the association of TGB2/3 granules with replicase, strongly suggested that the X-body is indeed a replication site, i.e., a VRC. In the absence of TGB1, no X-body is formed. Without an X-body, PVX still accumulates, but fewer virion aggregates are observed, indicating that the X-body may play a role in efficient virus encapsidation (Tilsner et al., 2012). In uninfected cells, ectopically expressed TGB1 can recruit TGB2 and TGB3 into a "pseudo-VRC," which has a similar structure to the X-body.

In order to analyze the reorganized membrane structures of the PVX X-body at higher resolution, we turned to 3D-SIM microscopy. Here, we present results utilizing this technology to reveal new details of membrane organization within the PVX VRC and we demonstrate the applicability of 3D-SIM to general studies of plant subcellular structures.

MATERIALS AND METHODS

FLUORESCENT REPORTER AND VIRUS CONSTRUCTS

Bombardment vectors for expression of TGB1-mCherry, GFP-TGB2, and TGB3-GFP, and binary vectors for agroinfiltration of TGB1-TagRFP, GFP-TGB2, TGB3-GFP, and unfused TGB2 and TGB3, as well as a binary vector for expression of a complete PVX genome with an endogenous TGB1-mCherry fusion were previously described (Ju et al., 2005; Tilsner et al., 2009, 2012). PVX.GFP-CP and PVX.mCherry-CP constructs were previously described (Santa Cruz et al., 1996; Tilsner et al., 2009). In some cases, a 35S promoter-driven PVX.GFP-CP bombardment construct (Christophe Lacomme, unpublished) was used for infections. A transgenic *Nicotiana benthamiana* line expressing ER-GFP (Haseloff et al., 1997), and a transgenic *Nicotiana tabacum* line expressing Golgi (ST)-GFP (Boevink et al., 1998), were described previously.

EXPRESSION IN PLANTS

Infectious PVX RNA was obtained by T7 *in vitro* transcription from plasmid constructs containing PVX.GFP-CP and PVX.mCherry-CP modified cDNA copies, as described in Santa Cruz et al. (1996). Combinations of agrobacteria carrying binary expression constructs were infiltrated into *N. benthamiana* leaves at an OD_{600} of 0.15 or 0.25 each, as described previously (Tilsner et al., 2012). Microprojectile bombardments were carried out with a custom built gene gun according to the description in Gaba and Gal-On (2006).

IMAGING AND IMAGE PROCESSING

Confocal microscopy was performed as described in Tilsner et al. (2009, 2012). For super-resolution imaging, lower epidermal peels were prepared using a pair of fine forceps to peel carefully but quickly an epidermal peel from the lower epidermis of *N. benthamiana* or *N. tabacum* plants. Along the length of the peels, thickness varied from a few cells to a single cell layer. Immediately after peeling, the epidermal peels were fixed by floating them in a fixative solution for 30–45 min at room temperature (for details see Fitzgibbon et al., 2010). The epidermal peels were assembled on a cover slip, not on a glass slide, in order to have the peel as close as possible to the cover slip. Finally, the peels were mounted in Citifluor AF1 antifade medium (Agar Scientific), pressing gently to remove residual Citifluor from under the cover slip. The samples were sealed with nail varnish, and viewed through a cover slip for 3D-SIM imaging with an OMX version 2 microscope (Applied Precision) as described in (Fitzgibbon et al., 2010). GFP was excited at 488 nm and TagRFP and mCherry were excited at 594 nm. Image processing was done as described in Fitzgibbon et al. (2010). Figures were assembled with Adobe Photoshop and ImageJ software. TGB2 and TGB3 membrane hoops and Golgi dimensions were measured using softWoRx (Applied Precision) software. Mean outer and inner diameters of the membrane hoops were compared by one-way ANOVA followed by Least Significant Difference and Duncan's Multiple Range Tests using SPSS software (IBM).

RESULTS

FIBRILLAR VIRION BUNDLES SURROUND THE X-BODY

"Overcoat" PVX, in which viral CP is fused with a fluorescent protein via a 2A peptide linker, produces fluorescent virions in which a significant proportion (∼80%) of the virus coat is fluorescently labeled (Santa Cruz et al., 1996). The 2A peptide causes partial release of incomplete polypeptide without termination of translation, resulting in the production of both fluorescent protein-fused and unfused CP, thus enabling encapsidation. The fluorescent virions are found in fibrillar "cages" surrounding the X-body (**Figure 2**; Santa Cruz et al., 1998; Tilsner et al., 2012). In confocal images (**Figures 2A,B**), we observed large bundles of virus filaments but were unable to resolve the fine structure of the virion cages. Using 3D-SIM, we were able to resolve a fine network of virus bundles, the smallest of which were about 100 nm in diameter (**Figure 2C** insert). The diameter of individual PVX particles is 13 nm (Atabekov et al., 2007), suggesting that some of the small bundles that we resolved contained no more than eight virus particles aligned side-by-side. In three dimensions (Movie

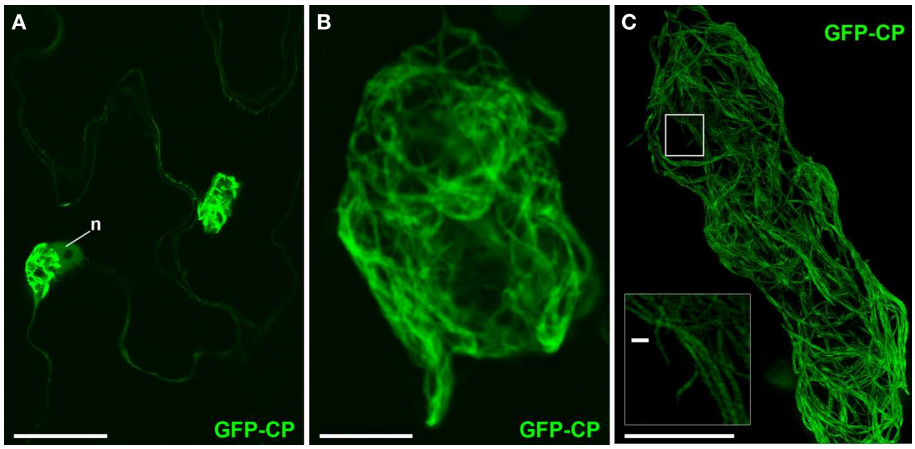

FIGURE 2 | PVX virion "cages" encasing the X-body. (A) Live-cell confocal overview of PVX.GFP-CP-infected cells with two perinuclear (n: nucleus) X-bodies. **(B)** Higher magnification confocal image of a virion cage surrounding the X-body from a fixed sample. **(C)** High-resolution 3D-SIM image. The insert shows an enlargement of the area in the rectangle in which individual virion filaments are resolved to <100 nm diameter. Bars **(A)**: 50 μm; **(B,C)**: 10 μm; [insert in **(C)**]: 500 nm.

S1 in Supplementary Materials), the viral cages formed a complex interconnected network of virions that surrounded host and viral structures at its center.

SUPER-RESOLUTION IMAGING OF TGB1 AGGREGATES AT THE CENTER OF THE X-BODY

TGB1 lies at the core of the X-body where it appears as walnut-shaped inclusions, each comprised of sickle-shaped aggregates (**Figure 3**; Tilsner et al., 2009, 2012). These correspond well to the circularly arranged TGB1 beaded sheets reported earlier from EM studies (Kozar and Sheludko, 1969; Stols et al., 1970; Shalla and Shepard, 1972; Davies et al., 1993; Santa Cruz et al., 1998). Using 3D-SIM we were able to resolve the fibrillar composition of the TGB1 aggregates, showing even more clearly their correspondence with the beaded sheets observed in EM (**Figures 3B–D**; Movie S2 in Supplementary Materials). Many of the TGB1 inclusions appeared to be arranged as flattened, undulating "ribbons" within the X-body (**Figures 3C,D**).

FINE-SCALE ARCHITECTURE OF THE TGB2 AND TGB3-INDUCED MEMBRANE COMPARTMENTS WITHIN THE X-BODY

As previously reported (Tilsner et al., 2012), TGB2 and TGB3 surround TGB1 aggregates within the X-body. In confocal images GFP-TGB2 is broadly localized around the TGB1 inclusions, and this localization resembles the granulated morphology of the recruited ER membranes (**Figure 4A**; see also Tilsner et al., 2012). Unlike TGB2, the TGB3-GFP fluorescence is concentrated in isolated patches or clusters in the X-body (**Figure 4F**; see also Tilsner et al., 2012). The isolated patches of TGB3 probably correspond to the aggregated TGB2/3 granules of earlier infection stages (Bamunusinghe et al., 2009; Tilsner et al., 2012). Similar compartments were observed with ER-GFP and Golgi-GFP markers (Tilsner et al., 2012). We speculated previously that these compartments were comprised of densely stacked membrane sheets or tubules because both Golgi and TGB2/3 transmembrane markers labeled them completely, and not just their surface, as would be expected for vesicle- or vacuole-like membrane structures.

Using 3D-SIM, we now show that the "granules" produced by TGB2 and TGB3 are in fact fine membrane hoops of remodeled tubular ER. In confocal images, these structures had the characteristic granular appearance (**Figures 4A,F**) but under 3D-SIM they appeared as donut-shaped loops (**Figures 4B–E,G,H**) with an outer diameter of 296 ± 37 nm and an inner diameter of 123 ± 15 nm for TGB2 ($n = 8$; **Figures 4D,E**) or 296 ± 49 nm (outer) and 134 ± 31 nm (inner) for TGB3 ($n = 21$; **Figure 4H**), respectively. Outer and inner diameters of the TGB2 and TGB3 hoops were not significantly different ($p > 0.05$, **Figure 5**; see Appendix). The clear separation of the two membrane tubes on opposite sides of the hoops, with apparent diameters of ca. 80–90 nm, and separated by only ∼120–130 nm, indicates that a lateral resolution of less than 100 nm was achieved by 3D-SIM in these images. TGB2 hoops formed dense arrays resembling "chain mail" in the center of X-bodies, wrapped around the TGB1 inclusions (**Figures 4B–E**). TGB3 hoops were more concentrated in patches around the TGB1 inclusions (**Figures 4G,H**; Movie S3 in Supplementary Materials). We have previously shown that TGB2 is more dispersed over the ER within the X-body, but also co-localizes with TGB3, which is confined to granules or aggregates (Tilsner et al., 2012). These findings are corroborated here and the 3D-SIM data indicate that these different modified ER compartments are all comprised of dense arrays of membrane hoops containing either only TGB2 or both TGB2 and TGB3. We could detect these hoops also on the peripheral cortical ER (arrowed in **Figure 4C**), and these probably correspond to the previously reported TGB2-induced, ER-derived granules (Ju et al., 2005).

REORGANIZATION OF ENDOMEMBRANES WITHIN THE X-BODY

Changes in the morphology of host ER and Golgi membranes were also more clearly resolved by 3D-SIM than in previous confocal images (**Figure 6**, see also Tilsner et al., 2012). The

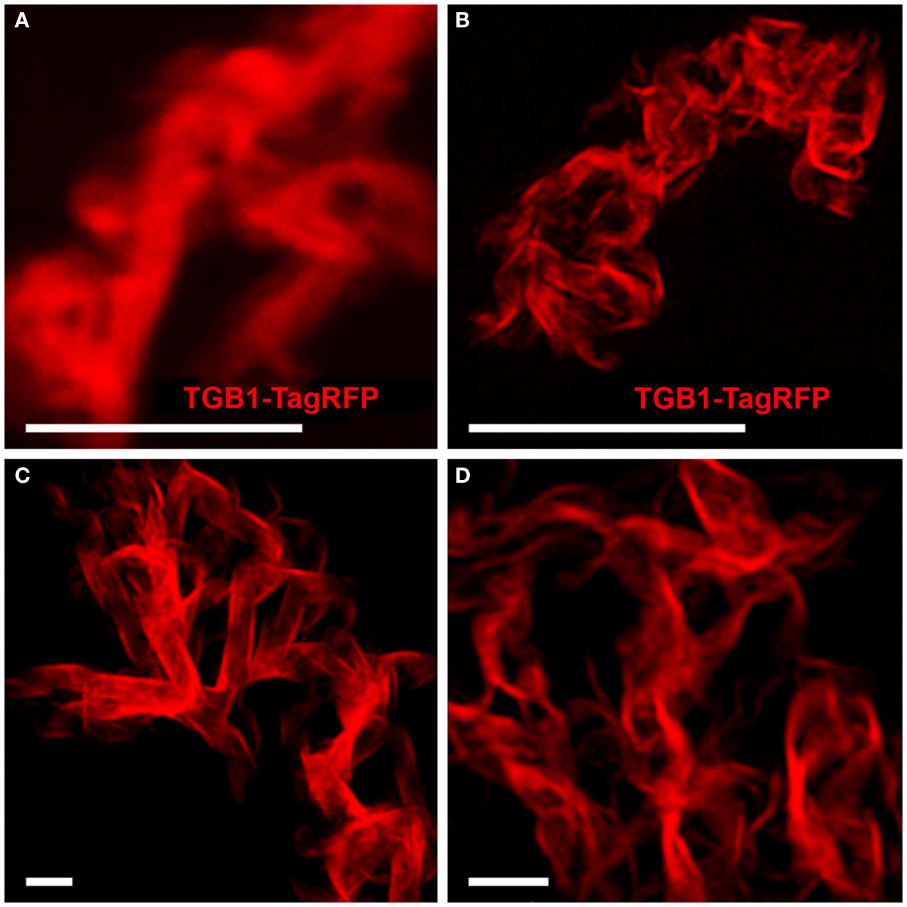

FIGURE 3 | TGB1 inclusions in the X-body. (A) Aggregates of TGB1-TagRFP co-expressed with TGB2 and TGB3 (not shown) in pseudo-VRCs (Tilsner et al., 2012) from fixed, uninfected tissue, resolved by confocal microscopy. **(B–D)** 3D-SIM super-resolution images of the same material. **(A,B)** Shown at the same scale. Bars **(A,B)**: 5 μm; **(C,D)**: 1 μm.

individual tubules of the ER network are barely discernible in the X-body even though they are unaltered in the surrounding cytoplasm (**Figure 6A**). However, at high magnification, the diffuse membrane aggregations within the X-body consist of the same membrane hoops observed for TGB2 and TGB3 (**Figures 6B,C**), in agreement with the previously demonstrated ER-association of these proteins (Krishnamurthy et al., 2003; Ju et al., 2005).

3D-SIM also resolved individual Golgi bodies labeled with a sialyl transferase (ST)-GFP membrane marker (Boevink et al., 1998) and revealed a ring-shaped structure (**Figures 6E,F**). Such details of this organelle are not visible in conventional confocal microscopy (**Figure 6D**). ST-GFP is a trans-Golgi marker (Boevink et al., 1998) and the ring structure probably corresponds to the outer rim of *trans*-Golgi compartments viewed along the *trans-cis* axis (Staehelin and Kang, 2008). However the Golgi rings were clearly different from the ER-derived membrane hoops observed with TGB2 and TGB3. They had larger outer (478 ± 44 nm) and inner (221 ± 31 nm) diameters (**Figure 5**; $n = 17$; statistically significant at $p < 0.001$; see Appendix) which correspond well to EM observations (Staehelin and Kang, 2008), and did not form linked "chain mail" structures or large arrays. This is in agreement with previous biochemical and microscopical findings that there is no direct association between the TGB proteins and the Golgi apparatus (Ju et al., 2005; Bamunusinghe et al., 2009).

DISCUSSION

POSSIBLE ROLES OF REMODELED ENDOMEMBRANES WITHIN THE X-BODY

In previous work we described the essential role of the TGB1 protein in generating the PVX X-body, and presented a model of the layered structure of this virus "factory" (Tilsner et al., 2012). The increased resolution provided by 3D-SIM enabled us to analyze in greater detail the TGB2 and TGB3 sub-compartments and the role of these proteins in organizing the X-body, and allowed us to update our previous model of the PVX "factory" (**Figure 7**). Our new data show that TGB2-labeled ER membranes consist of small hoops, which cluster within the X-body to form an extremely dense network. Since TGB2 and 3 are integral membrane proteins, the hoops are expected to be membrane structures. In previous studies (Boevink et al., 1996; Krishnamurthy et al., 2003; Mitra et al., 2003; Ju et al., 2005; Samuels et al., 2007; Wu et al., 2011) ER

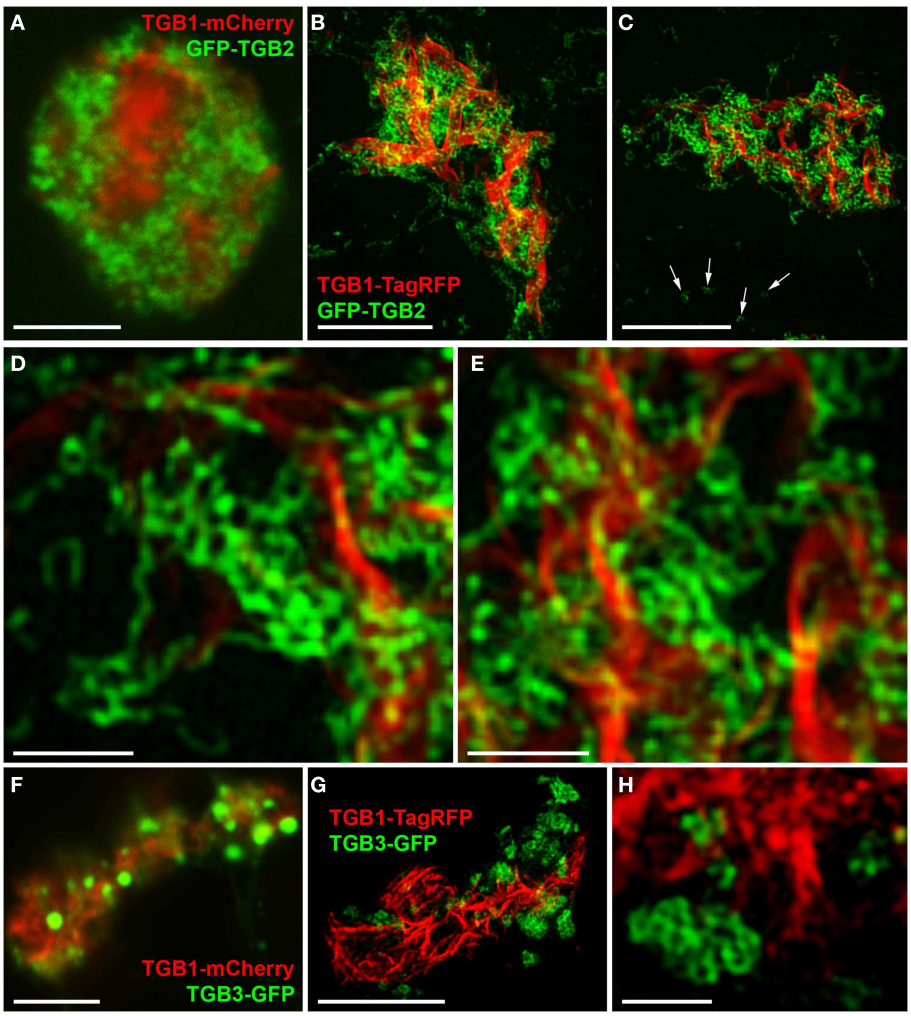

FIGURE 4 | TGB2- and TGB3-labeled membrane compartments in the X-body. (A) Live-cell confocal image of co-bombarded TGB1-mCherry and GFP-TGB2 in PVX-infected cell. GFP-TGB2 signal is spread around the TGB1 aggregates. The granular appearance of the reorganized ER-derived membranes is not further resolved. **(B–E)** High-resolution 3D-SIM images of TGB1-TagRFP and GFP-TGB2 in a pseudo-VRC in an uninfected cell. GFP-TGB2-labeled membrane hoops form "chain mail"-like ribbons and dense arrays in the X-body, but are also observed on the cortical ER (arrows in **C**). At higher magnification **(D,E)**, the hoop dimensions are apparent and the hoops can be seen winding around the TGB1 aggregates. **(F)** Live-cell confocal image of TGB1-mCherry and TGB3-GFP (co-bombarded into PVX-infected cells) show the occurrence of TGB3 granules or aggregates within the X-body. **(G,H)** In 3D-SIM images of TGB1-TagRFP and TGB3-GFP in a pseudo-VRC in an uninfected cell, the TGB3 structures are resolved as hoops similar in size to those labeled by TGB2 and concentrated in clusters or patches outside of the TGB1 inclusion. Bars **(A–C)**: 5 μm; **(D,E)**: 1 μm; **(F,G)**: 5 μm; **(H)**: 1 μm.

markers closely mirrored the locations of the TGB2 and 3 proteins, and we found that a lumenal ER marker also labeled small hoops in the X-body (**Figures 6B,C**). It can therefore be assumed that the TGB2/3 hoops remain within and are identical with the densely reticulated ER network within the X-body. The previously observed ER-derived TGB2/3 granules (Boevink et al., 1996; Ju et al., 2005) may in fact also be individual or small clusters of hoops branching out from the cortical ER (**Figure 4C** arrows). Within the resolution limits there is currently no evidence that the membrane tubules differ from those of the normal ER, however the "knitting" of the hoops is far more dense than in the unmodified cortical ER network, where three-way junctions are typically spaced a few μm apart, although reticulation of a similar density to the TGB2/3 hoops can also occur, for instance in meristematic cells (Boevink et al., 1998; Sparkes et al., 2009a,b). These observations suggest that TGB2 may remodel the ER by inducing a localized increase of network branching. The ability of the transmembrane TGB2/3 proteins of potexviruses to influence the structure of the ER requires further study. Recently, it was shown that a specific class of host proteins, the reticulons, is involved in the formation of VRCs by Brome mosaic virus replicating in yeast (Diaz et al., 2010; Diaz and Ahlquist, 2012). It will be interesting to see if this class of proteins is recruited to the X-body during PVX accumulation and whether reticulons, and other host proteins associated with ER-remodeling, operate in tandem with TGB2/3 type proteins.

Modification of host organelles and their redirection to, and involvement in, X-body organization is likely to be a vital event in the PVX infection process. One possible role of recruited host elements is to protect the virus from the host plant defense mechanisms by wrapping it in plant membranes and creating a unique isolated environment for the replicating virus in which it is more difficult for the plant to recognize and degrade the vRNA through the plant RNA silencing machinery. In addition, it is possible that the recruited host membranes enlarge the surface area for the replicating virus, making replication more efficient because of the production of increased concentrations of important viral components (Dunoyer et al., 2002; Schwartz et al., 2002, 2004; Sanfaçon, 2005; Laliberté and Sanfaçon, 2010). The dense arrays of membrane hoops observed by 3D-SIM are in agreement with this hypothesis. For a conclusive interpretation regarding the membrane surface utilized for replication, super-resolution localization of the PVX replicase will be required, and these methods are currently being developed in our lab. The organization of X-bodies is also thought to create a subcellular environment in which host resources required by the virus, e.g., translation factors, are readily available (Schwartz et al., 2002, 2004; Sanfaçon, 2005), and the reorganization of ER membranes may play a role in this. Detailed analyses of the interaction partners of the TGB2 and TGB3 proteins might corroborate this hypothesis for the PVX X-body. It is also possible that containment of viral replication in the X-body minimizes damage to the host cell (Sanfaçon, 2005). Lastly, endomembranes and cytoskeletal elements also provide the routes for viral cell-to-cell transport (Harries et al., 2009; Schoelz et al., 2011) and their reorganization by TGB proteins within the X-body probably reflects the movement-related activities of these proteins at earlier infection stages.

The accumulation of encapsidated virions on the cytoplasmic side of the X-body (Oparka et al., 1996; Santa Cruz et al., 1998; Tilsner et al., 2012; current study) suggests that CP synthesis and packaging of vRNA take place at the periphery of the X-body, whereas the location of the TGB proteins, in particular TGB1, may

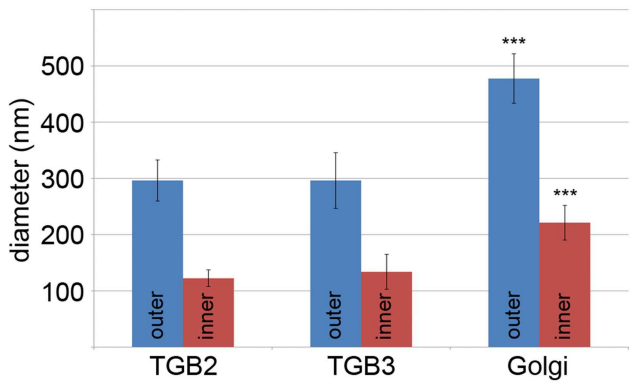

FIGURE 5 | Sizes of TGB2 and TGB3 membrane hoops and *trans*-Golgi rings. Means with standard deviations are shown (TGB2: $n = 8$; TGB3: $n = 21$; Golgi: $n = 17$). Blue: outer diameter, red: inner diameter. TGB2 and TGB3 hoops outer and inner diameters, respectively, are not significantly different ($p > 0.05$), but both outer and inner diameter of Golgi rings are significantly different from both TGB2 and TGB3 ($p < 0.001$) (see Appendix for results of statistical analysis).

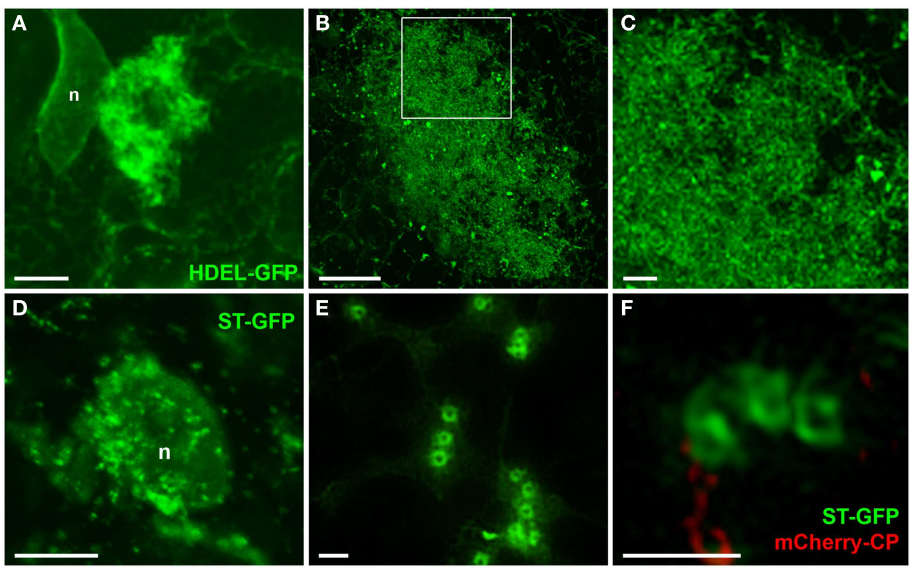

FIGURE 6 | Reorganized host endomembranes in the X-body. (A) Confocal image of densely reticulated host ER within the PVX X-body and unmodified cortical ER network outside of the X-body in fixed tissue. ER is labeled with lumenally targeted HDEL-GFP (Haseloff et al., 1997). n: nucleus. **(B,C)**, Super-resolution images of remodeled ER in the X-body of cells infected with PVX. TGB1-mCherry (not shown). The area in the rectangle in **(B)** is enlarged in **(C)** and shows the dense arrays of ER membranes to consist of membrane hoops similar to those labeled by the TGB2 and TGB3 proteins. **(D)** Confocal image of Golgi stacks labeled with ST-GFP (Boevink et al., 1998) recruited to a nascent X-body of a PVX-infected, fixed cell. **(E,F)**, Super-resolution images of Golgi stacks in cells infected with PVX.mCherry-CP [not shown in **(E)**] resolve the trans-Golgi as a membrane circle with a larger diameter than the TGB2/3-containing ER hoops [note **(C,E)** have almost identical scales]. Bars **(A,B)**: 5 μm; **(C)**: 1 μm; **(D)**: 10 μm; **(E,F)**: 1 μm.

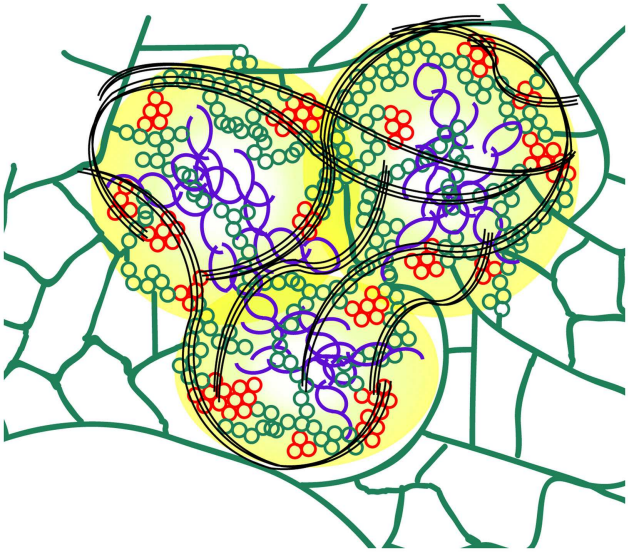

FIGURE 7 | Schematic model of the PVX X-body (not to scale). The TGB1 "beaded sheets" (purple) are localized in the center of the X-body. As shown previously, non-encapsidated vRNA (yellow) surrounds the TGB1 inclusions (Tilsner et al., 2009, 2012). Host ER (green) is remodeled into arrays of small membrane hoops by TGB2 which are wrapped around the TGB1 aggregates within the X-body. Some patches of these TGB2 loops also contain TGB3 (red) and may constitute the replication sites of the virus (Bamunusinghe et al., 2009). Bundles of encapsidated virions (black) accumulate at the periphery and form "cages" around the X-body sub-compartments.

be influenced by both their targeting properties and their site of synthesis within the X-body (Tilsner and Oparka, 2012). To fully address these questions, the distribution of the subgenomic messenger RNAs required for translation of these proteins requires to be analyzed within the VRC. However, this is beyond the technical limits of current localization techniques. The distinct localization of PVX CP and TGB1 in the X-body and their putative production (and isolation) in separate sub-compartments is probably essential for PVX infection (Karpova et al., 2006). Because TGB1 destabilizes PVX virions *in vitro* (Rodionova et al., 2003), it needs to be sequestered away from those progeny virions destined for mechanical transmission to other host plants.

CONCLUSION

3D-SIM "super-resolution" has enabled us to gain new insights into the structural organization of the replication "factory" of a model plant virus and develop new hypotheses about its functions. This highlights the value of super-resolution approaches for the analysis of other viruses, including those that infect animal cells. The study of viral inclusions is an area within cell biology that lends itself to the practical application of super-resolution microscopy, bringing its powers to bear on important biological questions. To obtain 3D-SIM images does not require complicated embedding and sectioning techniques but only mild fixation and the use of antifade reagents, ensuring a low degree of sample disruption. Imaging was conducted on intact epidermal cells in single- and even multi-cell layer epidermal peels, showing the versatility of 3D-SIM for complex biological specimens. Due to their greater photostability, we found GFP fusions better suited to 3D-SIM imaging than RFP constructs, but the rapid development of new FPs is likely to overcome such limitations in the near future, and others have successfully imaged RFP fusions with 3D-SIM (Horsington et al., 2012). The increased resolution gained, for example on Golgi bodies, demonstrates the utility of this approach outside virology. In the future, correlative super-resolution light and electron microscopy approaches (Fridman et al., 2012) should enable a complete mapping of virus "factories" and other complex cellular structures at near-molecular resolution.

ACKNOWLEDGMENTS

We thank Dr. Markus Posch for help with the 3D-SIM microscopy and image processing, Dr. Christophe Lacomme for the PVX.GFP-CP bombardment vector, and Dr. Jeanmarie Verchot for the GFP-TGB2 and TGB3-GFP bombardment constructs. This work was funded by Biotechnology and Biomedical Sciences Research Council grant BB/H018719/1.

SUPPLEMENTARY MATERIAL

The Supplementary Material for this article can be found online at http://www.frontiersin.org/Plant-Microbe_Interaction/10.3389/fpls.2013.00006/abstract

REFERENCES

Adams, M. J., Antoniw, J. F., Bar-Joseph, M., Brunt, A. A., Candresse, T., Foster, G. D., et al. (2004). The new plant virus family Flexiviridae and assessment of molecular criteria for species demarcation. *Arch. Virol.* 149, 1045–1060.

Allison, A. V., and Shalla, T. A. (1974). The ultrastructure of local lesions induced by potato virus X: a sequence of cytological events in the course of infection. *Phytopathology* 64, 784–793.

Asurmendi, S., Berg, R. H., Koo, J. C., and Beachy, R. N. (2004). Coat protein regulates formation of replication complexes during tobacco mosaic virus infection. *Proc. Natl. Acad. Sci. U.S.A.* 101, 1415–1420.

Atabekov, J., Dobrov, E., Karpova, O., and Rodionova, N. (2007). Potato virus X: structure, disassembly and reconstitution. *Mol. Plant Pathol.* 8, 667–675.

Atabekov, J. G., Rodionova, N. P., Karpova, O. V., Kozlovsky, S. V., and Poljakov, V. Y. (2000). The movement protein-triggered in situ conversion of potato virus X virion RNA from a nontranslatable into a translatable form. *Virology* 271, 259–263.

Bamunusinghe, D., Hemenway, C. L., Nelson, R., Sanderfoot, A. A., Ye, C. M., Silva, M. A. T., et al. (2009). Analysis of potato virus X replicase and TGBp3 subcellular locations. *Virology* 393, 272–285.

Batten, J. S., Yoshinari, S., and Hemenway, C. (2003). Potato virus X: a model system for virus replication, movement and gene expression. *Mol. Plant Pathol.* 4, 125–131.

Boevink, P., Oparka, K. J., Santa Cruz, S., Martin, B., Betteridge, A., and Hawes, C. (1998). Stacks on tracks: the plant Golgi apparatus traffics on an actin/ER network. *Plant J.* 15, 441–447.

Boevink, P., Santa Cruz, S., Hawes, C., Harris, N., and Oparka, K. J. (1996). Virus-mediated delivery of the green fluorescent protein to the endoplasmic reticulum of plant cells. *Plant J.* 10, 935–941.

Carette, J. E., Stuiver, M., Van Lent, J., Wellink, J., and Van Kammen, A. (2000). Cowpea mosaic virus infection induces a massive proliferation of endoplasmic reticulum but not Golgi membranes and is dependent on de novo membrane synthesis. *J. Virol.* 74, 6556–6563.

Christie, R. G., and Edwardson, J. R. (1977). Light and electron microscopy of plant virus inclusions. *Fla. Agric. Exp. Stn. Monogr.* 9, 155pp.

Davies, C., Hills, G., and Baulcombe, D. C. (1993). Sub-cellular localization of the 25-kDa protein encoded in the triple gene block of potato virus X. *Virology* 197, 166–175.

den Boon, J. A., Diaz, A., and Ahlquist, P. (2010). Cytoplasmic viral replication complexes. *Cell Host Microbe* 8, 77–85.

Diaz, A., and Ahlquist, P. (2012). Role of host reticulon proteins in rearranging membranes for positive-strand RNA virus replication. *Curr. Opin. Microbiol.* 15, 519–524.

Diaz, A., Wang, X., and Ahlquist, P. (2010). Membrane-shaping host reticulon proteins play crucial roles in viral RNA replication compartment formation and function. *Proc. Natl. Acad. Sci. U.S.A.* 107, 16291–16296.

Doronin, S. V., and Hemenway, C. (1996). Synthesis of potato virus X RNAs by membrane-containing extracts. *J. Virol.* 70, 4795–4799.

Dunoyer, P., Ritzenthaler, C., Hemmer, O., Michler, P., and Fritsch, C. (2002). Intracellular localization of the peanut clump virus replication complex in tobacco BY-2 protoplasts containing green fluorescent protein-labeled endoplasmic reticulum or Golgi apparatus. *J. Virol.* 76, 865–874.

Edwardson, J. R., and Christie, R. G. (1978). Use of virus-induced inclusions in classification and diagnosis. *Annu. Rev. Phytopathol.* 16, 31–55.

Esau, K. (1967). Anatomy of plant virus infections. *Annu. Rev. Phytopathol.* 5, 45–76.

Fitzgibbon, J., Bell, K., King, E., and Oparka, K. (2010). Super-resolution imaging of Plasmodesmata using three-dimensional structured illumination microscopy. *Plant Physiol.* 153, 1453–1463.

Fridman, K., Mader, A., Zwerger, M., Elia, N., and Medalia, O. (2012). Advances in tomography: probing the molecular architecture of cells. *Nat. Rev. Mol. Cell Biol.* 13, 736–742.

Gaba, V., and Gal-On, A. (2006). Inoculation of plants using bombardment. *Curr. Protoc. Microbiol.* 16B.3.1–16B.3.14.

Goldstein, B. (1924). Cytological study of living cells of tobacco plants affected with mosaic disease. *Bull. Torrey Botan. Club* 51, 261–272.

Goldstein, B. (1926). A cytological study of the leaves and growing points of healthy and mosaic diseased tobacco plants. *Bull. Torrey Botan. Club* 53, 499–600.

Gustafsson, M. G. L., Shao, L., Carlton, P. M., Wang, C. J. R., Golubovskaya, I. N., Cande, W. Z., et al. (2008). Three-dimensional resolution doubling in wide-field fluorescence microscopy by structured illumination. *Biophys. J.* 94, 4957–4970.

Harries, P. A., Park, J. W., Sasaki, N., Ballard, K. D., Maule, A. J., and Nelson, R. S. (2009). Differing requirements for actin and myosin by plant viruses for sustained intercellular movement. *Proc. Natl. Acad. Sci. U.S.A.* 106, 17594–17599.

Haseloff, J., Siemering, K. R., Prasher, D. C., and Hodge, S. (1997). Removal of a cryptic intron and subcellular localization of green fluorescent protein are required to mark transgenic Arabidopsis plants brightly. *Proc. Natl. Acad. Sci. U.S.A.* 94, 2122–2127.

Horsington, J., Turnbull, L., Whitchurch, C. B., and Newsome, T. P. (2012). Sub-viral imaging of vaccinia virus using super-resolution microscopy. *J. Virol. Methods* 186, 132–136.

Huang, B., Bates, M., and Zhuang, X. (2009). Super-resolution fluorescence microscopy. *Annu. Rev. Biochem.* 78, 993–1016.

Hull, R. (2002). *Matthews' Plant Virology*, 4th Edn. San Diego, CA: Academic Press.

Ju, H. J., Brown, J. E., Ye, C. M., and Verchot-Lubicz, J. (2007). Mutations in the central domain of potato virus X TGBp2 eliminate granular vesicles and virus cell-to-cell trafficking. *J. Virol.* 81, 1899–1911.

Ju, H.-J., Samuels, T. D., Wang, Y.-S., Blancaflor, E., Payton, M., Mitra, R., et al. (2005). The potato virus X TGBp2 movement protein associates with endoplasmic reticulum-derived vesicles during virus infection. *Plant Physiol.* 138, 1877–1895.

Karpova, O. V., Zayakina, O. V., Arkhipenko, M. V., Sheval, E. V., Kiselyova, O. I., Poljakov, V. Y., et al. (2006). Potato virus X RNA-mediated assembly of single-tailed ternary 'coat protein-RNA-movement protein' complexes. *J. Gen. Virol.* 87, 2731–2740.

Knoops, K., Kikkert, M., Worm, S. H. E., Zevenhoven-Dobbe, J. C., van der Meer, Y., Koster, A. J., et al. (2008). SARS-Coronavirus replication is supported by a reticulovesicular network of modified endoplasmic reticulum. *PLoS Biol.* 6:e226. doi:10.1371/journal.pbio.0060226

Kopek, B. G., Perkins, G., Miller, D. J., Ellisman, M. H., and Ahlquist, P. (2007). Three-dimensional analysis of a viral rna replication complex reveals a virus-induced mini-organelle. *PLoS Biol.* 5:e220. doi:10.1371/journal.pbio.0050220

Kozar, F. E., and Sheludko, Y. M. (1969). Ultrastructure of potato and Datura stramonium plant cells infected with potato virus X. *Virology* 38, 220–229.

Krishnamurthy, K., Heppler, M., Mitra, R., Blancaflor, E., Payton, M., Nelson, R. S., et al. (2003). The Potato virus X TGBp3 protein associates with the ER network for virus cell-to-cell movement. *Virology* 309, 135–151.

Laliberté, J. F., and Sanfaçon, H. (2010). Cellular remodeling during plant virus infection. *Annu. Rev. Phytopathol.* 48, 69–91.

Lough, T. J., Netzler, N. E., Emerson, S. J., Sutherland, P., Carr, F., Beck, D. L., et al. (2000). Cell-to-cell movement of potexviruses: evidence for a ribonucleoprotein complex involving the coat protein and first triple gene block protein. *Mol. Plant Microbe Interact.* 13, 962–974.

Lyle, J. M., Bullitt, E., Bienz, K., and Kirkegaard, K. (2002). Visualization and functional analysis of RNA-dependent RNA polymerase lattices. *Science* 296, 2218–2222.

Malkusch, S., Muranyi, W., Müller, W., Kräusslich, H.-G., and Heilemann, M. (2012). Single-molecule coordinate-based analysis of the morphology of HIV-1 assembly sites with near-molecular spatial resolution. *Histochem. Cell Biol.* 139, 173–179.

Martelli, G. P., and Russo, M. (1977). Plant virus inclusion bodies. *Adv. Virus Res.* 21, 175–266.

Miller, S., and Krijnse-Locker, J. (2008). Modification of intracellular membrane structures for virus replication. *Nat. Rev. Microbiol.* 6, 363–374.

Mitra, R., Krishnamurthy, K., Blancaflor, E., Payton, M., Nelson, R. S., and Verchot-Lubicz, J. (2003). The Potato virus X TGBp2 protein association with the endoplasmic reticulum plays a role in but is not sufficient for viral cell-to-cell movement. *Virology* 312, 35–48.

Nishikiori, M., Dohi, K., Mori, M., Meshi, T., Naito, S., and Ishikawa, M. (2006). Membrane-bound tomato mosaic virus replication proteins participate in RNA synthesis, and are associated with host proteins in a pattern distinct from those that are not membrane bound. *J. Virol.* 80, 8459–8468.

Oparka, K. J., Roberts, A. G., Roberts, I. M., Prior, D. A. M., and Santa Cruz, S. (1996). Viral coat protein is targeted to, but does not gate, plasmodesmata during cell-to-cell movement of potato virus X. *Plant J.* 10, 805–813.

Pereira, C. F., Rossy, J., Owen, D. M., Mak, J., and Gaus, K. (2012). HIV taken by STORM: super-resolution fluorescence microscopy of a viral infection. *Virol. J.* 9, 84.

Phillips, D., Nibau, C., Wnetrzak, J., and Jenkins, G. (2012). High resolution analysis of meiotic chromosome structure and behaviour in barley (*Hordeum vulgare* L.). *PLoS ONE* 7:e39539. doi:10.1371/journal.pone.0039539

Plante, C. A., Kim, K. H., Pillai-Nair, N., Osman, T. A. M., Buck, K. W., and Hemenway, C. L. (2000). Soluble, template-dependent extracts from *Nicotiana benthamiana* plants infected with potato virus X transcribe both plus- and minus-strand RNA templates. *Virology* 275, 444–451.

Ritzenthaler, C., Laporte, C., Gaire, F., Dunoyer, P., Schmitt, C., Duval, S., et al. (2002). Grapevine fanleaf virus replication occurs on endoplasmic reticulum-derived membranes. *J. Virol.* 76, 8808–8819.

Rodionova, N. P., Karpova, O. V., Kozlovsky, S. V., Zayakina, O. V., Arkhipenko, M. V., and Atabekov, J. G. (2003). Linear remodeling of helical virus by movement protein binding. *J. Mol. Biol.* 333, 565–572.

Samuels, T. D., Ju, H.-J., Ye, C.-M., Motes, C. M., Blancaflor, E. B., and Verchot-Lubicz, J. (2007). Subcellular targeting and interactions among the potato virus X TGB proteins. *Virology* 367, 375–389.

Sanfaçon, H. (2005). Replication of positive-strand RNA viruses in plants: contact points between plant and virus components. *Can. J. Bot.* 83, 1529–1549.

Santa Cruz, S., Chapman, S., Roberts, A. G., Roberts, I. M., Prior, D. A. M., and Oparka, K. J. (1996). Assembly and movement of a plant virus carrying a green fluorescent protein overcoat. *Proc. Natl. Acad. Sci. U.S.A.* 93, 6286–6290.

Santa Cruz, S., Roberts, A. G., Prior, D. A. M., Chapman, S., and Oparka, K. J. (1998). Cell-to-cell and phloem-mediated transport of potato virus X: the role of virions. *Plant Cell* 10, 495–510.

Schaad, M. C., Jensen, P. E., and Carrington, J. C. (1997). Formation of plant RNA virus replication complexes on membranes: role of an endoplasmic reticulum-targeted viral protein. *EMBO J.* 16, 4049–4059.

Schermelleh, L., Heintzmann, R., and Leonhardt, H. (2010). A guide to super-resolution fluorescence microscopy. *J. Cell Biol.* 190, 165–175.

Schoelz, J. E., Harries, P. A., and Nelson, R. S. (2011). Intracellular transport of plant viruses: finding the door out of the cell. *Mol. Plant* 4, 813–831.

Schwartz, M., Chen, J., Janda, M., Sullivan, M., Den Boon, J., and Ahlquist, P. (2002). A positive-strand RNA virus replication complex parallels form and function of retrovirus capsids. *Mol. Cell* 9, 505–514.

Schwartz, M., Chen, J., Lee, W.-M., Janda, M., and Ahlquist, P. (2004). Alternate, virus-induced membrane rearrangements support positive-strand RNA virus genome replication. *Proc. Natl. Acad. Sci. U.S.A.* 101, 11263–11268.

Shalla, T. A., and Shepard, J. F. (1972). The structure and antigenic analysis of amorphous inclusion bodies induced by potato virus X. *Virology* 49, 654–667.

Sheffield, F. M. L. (1939). Micrurgical studies on virus-infected plants. *Proc. R. Soc. Lond. B Biol. Sci.* 126, 529–538.

Sheffield, F. M. L. (1949). The virus in the plant cell. *Exptl. Cell Res. Suppl.* 1, 178–182.

Solovyev, A. G., Kalinina, N. O., and Morozov, S. Y. (2012). Recent advances in research of plant virus movement mediated by triple gene block. *Front. Plant Sci.* 3:276. doi:10.3389/fpls.2012.00276

Spagnolo, J. F., Rossignol, E., Bullitt, E., and Kirkegaard, K. (2010). Enzymatic and nonenzymatic functions of viral RNA-dependent RNA polymerases within oligomeric arrays. *RNA* 16, 382–393.

Sparkes, I. A., Frigerio, L., Tolley, N., and Hawes, C. (2009a). The plant endoplasmic reticulum: a cell-wide web. *Biochem. J.* 423, 145–155.

Sparkes, I. A., Runions, J., Hawes, C., and Griffing, L. (2009b). Movement and remodeling of the endoplasmic reticulum in nondividing cells of tobacco leaves. *Plant Cell* 21, 3937–3949.

Staehelin, L. A., and Kang, B.-H. (2008). Nanoscale architecture of endoplasmic reticulum export sites and of Golgi membranes as determined by electron tomography. *Plant Physiol.* 147, 1454–1468.

Stols, A. L. H., Hill-van der Meulen, G. W., and Toen, M. K. I. (1970). Electron microscopy of Nicotiana glutinosa leaf cells infected with potato virus X. *Virology* 40, 168–170.

Tilsner, J., Linnik, O., Christensen, N. M., Bell, K., Roberts, I. M., Lacomme, C., et al. (2009). Live-cell imaging of viral RNA genomes using a pumilio-based reporter. *Plant J.* 57, 758–770.

Tilsner, J., Linnik, O., Wright, K. M., Bell, K., Roberts, A. G., Lacomme, C., et al. (2012). The TGB1 movement protein of potato virus X re-organises actin and endomembranes into the 'X-body' a viral replication factory. *Plant Physiol.* 158, 1359–1370.

Tilsner, J., and Oparka, K. J. (2012). Missing links? – The connection between replication and movement of plant RNA viruses. *Curr. Opin. Virol.* 2, 699–705.

Turner, K. A., Sit, T. L., Callaway, A. S., Allen, N. S., and Lommel, S. A. (2004). Red clover necrotic mosaic virus replication proteins accumulate at the endoplasmic reticulum. *Virology* 320, 276–290.

Verchot-Lubicz, J., Torrance, L., Solovyev, A. G., Morozov, S. Y., Jackson, A. O., and Gilmer, D. (2010). Varied movement strategies employed by triple gene block-encoding viruses. *Mol. Plant Microbe Interact.* 23, 1231–1247.

Verchot-Lubicz, J., Ye, C. M., and Bamunusinghe, D. (2007). Molecular biology of potexviruses: recent advances. *J. Gen. Virol.* 88, 1643–1655.

Voinnet, O., Lederer, C., and Baulcombe, D. C. (2000). A viral movement protein prevents spread of the gene silencing signal in Nicotiana benthamiana. *Cell* 103, 157–167.

Wu, C.-H., Lee, S.-C., and Wang, C.-W. (2011). Viral protein targeting to the cortical endoplasmic reticulum is required for cell-cell spreading in plants. *J. Cell Biol.* 193, 521–535.

Zamyatnin, A. A., Solovyev, A. G., Sablina, A. A., Agranovsky, A. A., Katul, L., Vetten, H. J., et al. (2002). Dual-colour imaging of membrane protein targeting directed by poa semilatent virus movement protein TGBp3 in plant and mammalian cells. *J. Gen. Virol.* 83, 651–662.

Conflict of Interest Statement: The authors declare that the research was conducted in the absence of any commercial or financial relationships that could be construed as a potential conflict of interest.

Received: 15 November 2012; accepted: 09 January 2013; published online: 31 January 2013.

Citation: Linnik O, Liesche J, Tilsner J and Oparka KJ (2013) Unraveling the structure of viral replication complexes at super-resolution. Front. Plant Sci. ***4****:6. doi: 10.3389/fpls.2013.00006*

This article was submitted to Frontiers in Plant-Microbe Interaction, a specialty of Frontiers in Plant Science.

APPENDIX

DESCRIPTIVES

	N	Mean (μm)	SD	SE	95% Confidence interval for mean		Minimum	Maximum
					Lower bound	Upper bound		
OUTER DIAMETER								
TGB2	8	0.2963	0.03662	0.01295	0.2656	0.3269	0.25	0.34
TGB3	21	0.2962	0.04944	0.01079	0.2737	0.3187	0.20	0.37
Golgi	16	0.4775	0.04405	0.01101	0.4540	0.5010	0.41	0.56
Total	45	0.3607	0.09843	0.01467	0.3311	0.3902	0.20	0.56
INNER DIAMETER								
TGB2	8	0.1225	0.01488	0.00526	0.1101	0.1349	0.11	0.14
TGB3	21	0.1338	0.03106	0.00678	0.1197	0.1479	0.10	0.20
Golgi	16	0.2213	0.03074	0.00769	0.2049	0.2376	0.17	0.28
Total	45	0.1629	0.05229	0.00780	0.1472	0.1786	0.10	0.28

TEST OF HOMOGENEITY OF VARIANCES

	Levene statistic	df1	df2	Sig.
Outer diameter	0.198	2	42	0.821
Inner diameter	1.420	2	42	0.253

ANOVA

	Sum of squares	df	Mean square	*F*	Sig.
OUTER DIAMETER					
Between groups	0.339	2	0.169	81.444	0.000
Within groups	0.087	42	0.002		
Total	0.426	44			
INNER DIAMETER					
Between groups	0.085	2	0.043	51.153	0.000
Within groups	0.035	42	0.001		
Total	0.120	44			

***POST HOC* TESTS, $P < 0.001$.**

Multiple comparisons

Dependent Variable		(I) Factor	(J) Factor	Mean difference (I-J)	SE	Sig.	99.9% Confidence interval	
							Lower bound	Upper bound
Outer diameter	LSD	TGB2	TGB3	0.00006	0.01895	0.998	−0.0670	0.0671
			Golgi	−0.18125*	0.01975	0.000	−0.2511	−0.1114
		TGB3	TGB2	−0.00006	0.01895	0.998	−0.0671	0.0670
			Golgi	−0.18131*	0.01514	0.000	−0.2349	−0.1278
		Golgi	TGB2	0.18125*	0.01975	0.000	0.1114	0.2511
			TGB3	0.18131*	0.01514	0.000	0.1278	0.2349
Inner diameter	LSD	TGB2	TGB3	−0.01131	0.01200	0.351	−0.0538	0.0311
			Golgi	−0.09875*	0.01250	0.000	−0.1430	−0.0545
		TGB3	TGB2	0.01131	0.01200	0.351	−0.0311	0.0538
			Golgi	−0.08744*	0.00958	0.000	−0.1213	−0.0535
		Golgi	TGB2	0.09875*	0.01250	0.000	0.0545	0.1430
			TGB3	0.08744*	0.00958	0.000	0.0535	0.1213

**The mean difference is significant at the 0.001 level. The highlight emphasizes the numbers that show that Golgi does significantly differ from TGB2 and TGB3 at this significance level.*

HOMOGENEOUS SUBSETS

Outer diameter

	Factor	N	Subset for alpha = 0.001	
			1	2
Duncan[a,b]	TGB3	21	0.2962	
	TGB2	8	0.2963	
	Golgi	16		0.4775
	Sig.		0.997	1.000

Means for groups in homogeneous subsets are displayed. The highlight emphasizes the numbers that show that Golgi does significantly differ from TGB2 and TGB3 at this significance level.

[a] Uses harmonic mean sample size = 12.759.

[b] The group sizes are unequal. The harmonic mean of the group sizes is used. Type I error levels are not guaranteed.

Inner diameter

	Factor	*N*	Subset for alpha = 0.001	
			1	2
Duncan[a,b]	TGB2	8	0.1225	
	TGB3	21	0.1338	
	Golgi	16		0.2213
	Sig.		0.328	1.000

Means for groups in homogeneous subsets are displayed. The highlight emphasizes the numbers that show that Golgi does significantly differ from TGB2 and TGB3 at this significance level.

[a] Uses harmonic mean sample size = 12.759.

[b] The group sizes are unequal. The harmonic mean of the group sizes is used. Type I error levels are not guaranteed.

POST HOC TESTS, $P < 0.05$

Dependent variable		(I) Factor	(J) Factor	Mean difference (I-J)	SE	Sig.	95% Confidence interval	
							Lower bound	Upper bound
Outer diameter	LSD	TGB2	TGB3	0.00006	0.01895	0.998	−0.0382	0.0383
			Golgi	−0.18125*	0.01975	0.000	−0.2211	−0.1414
		TGB3	TGB2	−0.00006	0.01895	0.998	−0.0383	0.0382
			Golgi	−0.18131*	0.01514	0.000	−0.2119	−0.1508
		Golgi	TGB2	0.18125*	0.01975	0.000	0.1414	0.2211
			TGB3	0.18131*	0.01514	0.000	0.1508	0.2119
Inner diameter	LSD	TGB2	TGB3	−0.01131	0.01200	0.351	−0.0355	0.0129
			Golgi	−0.09875*	0.01250	0.000	−0.1240	−0.0735
		TGB3	TGB2	0.01131	0.01200	0.351	−0.0129	0.0355
			Golgi	−0.08744*	0.00958	0.000	−0.1068	−0.0681
		Golgi	TGB2	0.09875*	0.01250	0.000	0.0735	0.1240
			TGB3	0.08744*	0.00958	0.000	0.0681	0.1068

**The mean difference is significant at the 0.05 level. The highlight emphasizes the numbers that show that TGB2 and TGB3 do not differ significantly from each other even at this significance level.*

HOMOGENEOUS SUBSETS

Outer diameter

	Factor	*N*	Subset for alpha = 0.05	
			1	2
Duncan[a,b]	TGB3	21	0.2962	
	TGB2	8	0.2963	
	Golgi	16		0.4775
	Sig.		0.997	1.000

Means for groups in homogeneous subsets are displayed. The highlight emphasizes the numbers that show that TGB2 and TGB3 do not differ significantly from each other even at this significance level.

[a] Uses harmonic mean sample size = 12.759.

[b] The group sizes are unequal. The harmonic mean of the group sizes is used. Type I error levels are not guaranteed.

Inner diameter

	Factor	*N*	Subset for alpha = 0.05	
			1	2
Duncan[a,b]	TGB2	8	0.1225	
	TGB3	21	0.1338	
	Golgi	16		0.2213
	Sig.		0.328	1.000

Means for groups in homogeneous subsets are displayed. The highlight emphasizes the numbers that show that TGB2 and TGB3 do not differ significantly from each other even at this significance level.

[a] Uses Harmonic Mean Sample Size = 12.759.

[b] The group sizes are unequal. The harmonic mean of the group sizes is used. Type I error levels are not guaranteed.

frontiers in
PLANT SCIENCE

ORIGINAL RESEARCH ARTICLE
published: 31 January 2013
doi: 10.3389/fpls.2013.00005

Insights into *Alternanthera mosaic virus* TGB3 functions: interactions with *Nicotiana benthamiana* PsbO correlate with chloroplast vesiculation and veinal necrosis caused by TGB3 over-expression

Chanyong Jang[1], Eun-Young Seo[1], Jiryun Nam[1], Hanhong Bae[2], Yeong Guk Gim[1], Hong Gi Kim[1], In Sook Cho[3], Zee-Won Lee[4], Gary R. Bauchan[5], John Hammond[6]* and Hyoun-Sub Lim[1]*

[1] *Department of Applied Biology, Chungnam National University, Daejeon, South Korea*
[2] *School of Biotechnology, Yeungnam University, Gyeongsan, South Korea*
[3] *National Institute of Horticultural and Herbal Science, Rural Development Administration, Suwon, South Korea*
[4] *Division of Life Science, Korea Basic Science Institute, Daejeon, South Korea*
[5] *Electron and Confocal Microscopy Unit, Beltsville Agricultural Research Center, Agricultural Research Service, United States Department of Agriculture, Beltsville, MD, USA*
[6] *Floral and Nursery Plants Research Unit, US National Arboretum, Agricultural Research Service, United States Department of Agriculture, Beltsville, MD, USA*

Edited by:
Richard Nelson, Samuel Roberts Noble Foundation, Inc., USA

Reviewed by:
Jens Tilsner, University of St Andrews, UK
Na-Sheng Lin, Academia Sinica, Taiwan

****Correspondence:***
John Hammond, Floral and Nursery Plants Research Unit, US National Arboretum, United States Department of Agriculture, Agricultural Research Service, 10300 Baltimore Avenue, B-010A, Beltsville, MD 20705, USA.
e-mail: john.hammond@ars.usda.gov;
Hyoun-Sub Lim, Department of Applied Biology, Chungnam National University, 79 Daehangno, Yuseong-gu, Daejeon 305-764, South Korea.
e-mail: hyounlim@cnu.ac.kr

Alternanthera mosaic virus (AltMV) triple gene block 3 (TGB3) protein is involved in viral movement. AltMV TGB3 subcellular localization was previously shown to be distinct from that of *Potato virus X* (PVX) TGB3, and a chloroplast binding domain identified; veinal necrosis and chloroplast vesiculation were observed in *Nicotiana benthamiana* when AltMV TGB3 was over-expressed from PVX. Plants with over-expressed TGB3 showed more lethal damage under dark conditions than under light. Yeast-two-hybrid analysis and bimolecular fluorescence complementation (BiFC) reveal that *Arabidopsis thaliana* PsbO1 has strong interactions with TGB3; *N. benthamiana* PsbO (NbPsbO) also showed obvious interaction signals with TGB3 through BiFC. These results demonstrate an important role for TGB3 in virus cell-to-cell movement and virus-host plant interactions. The Photosystem II oxygen-evolving complex protein PsbO interaction with TGB3 is presumed to have a crucial role in symptom development and lethal damage under dark conditions. In order to further examine interactions between AtPsbO1, NbPsbO, and TGB3, and to identify the binding domain(s) in TGB3 protein, BiFC assays were performed between AtPsbO1 or NbPsbO and various mutants of TGB3. Interactions with C-terminally deleted TGB3 were significantly weaker than those with wild-type TGB3, and both N-terminally deleted TGB3 and a TGB3 mutant previously shown to lose chloroplast interactions failed to interact detectably with PsbO in BiFC. To gain additional information about TGB3 interactions in AltMV-susceptible plants, we cloned 12 natural AltMV TGB3 sequence variants into a PVX expression vector to examine differences in symptom development in *N. benthamiana*. Symptom differences were observed on PVX over-expression, with all AltMV TGB3 variants showing more severe symptoms than the WT PVX control, but without obvious correlation to sequence differences.

Keywords: AltMV, *potexvirus*, TGB3, chloroplast, PsbO

INTRODUCTION

The chloroplast has for many years been recognized as susceptible to damage during plant virus infections. Infection with *Tobacco mosaic virus* (TMV) was shown to interfere with starch mobilization in local lesions on tobacco (Holmes, 1931). Later, TMV particles were observed in association with chloroplasts (Esau and Cronshaw, 1967; Granett and Shalla, 1970), while Reinero and Beachy (1986) showed that TMV coat protein (CP) accumulated within chloroplasts of infected tobacco. Schoelz and Zaitlin (1989) demonstrated that TMV genomic RNA, but not subgenomic RNA, enters tobacco chloroplasts, and suggested that the CP detected may be translated by chloroplast ribosomes from the genomic RNA due to the presence of a Shine–Dalgarno sequence upstream of the CP initiation codon.

Other viruses have also been shown to associate with chloroplasts. Both CP and the HC-Pro of *Potato virus Y* (PVY) were detected in chloroplasts (Gunasinghe and Berger, 1991). The 6K2 protein of the potyvirus *Turnip mosaic virus* (TuMV) is an integral membrane protein that first forms vesicles at the endoplasmic reticulum (ER), and then traffics to the periphery of the chloroplasts, where large invaginations appear to result from chloroplast extrusions engulfing aggregated vesicles (Wei et al., 2010). The

Triple Gene Block (TGB) 2 (TGB2) protein of *Barley stripe mosaic virus* also accumulates in chloroplasts (Torrance et al., 2006), as does the CP of *Cucumber necrosis virus* (Xiang et al., 2006). We have recently shown that the CP of *Lolium latent virus* (LoLV) has a chloroplast transit peptide, and that blocking cleavage of the transit peptide has a dramatic effect on LoLV systemic movement (Vaira et al., 2012).

Turnip yellow mosaic virus (TYMV) has been known for many years to induce vesicles in the exterior of the chloroplasts (Chalcroft and Matthews, 1966), which were assumed to be the site of viral RNA synthesis (Ushiyama and Matthews, 1970), and have more recently been demonstrated to harbor the TYMV replicase proteins (Prod'Homme et al., 2001, 2003). Cells in areas of white (severe) mosaic were observed to have enlarged chloroplasts with numerous vesicles, including more very large vesicles than in yellow-green areas; disintegrated chloroplasts were also observed in such areas (Chalcroft and Matthews, 1966).

A number of studies have identified responses of Photosystem II (PS II) to infection with various viruses, including differential effects on components of the Oxygen-evolving complex (OEC); Abbink et al. (2002) utilized the yeast two-hybrid (Y2H) system to show that the RNA helicase domain of the 126-kDa replicase of TMV-U1 (but not of TMV-Ob) interacted with the 33-kDa subunit of the OEC, also known as PsbO. Virus-Induced Gene Silencing (VIGS) of *Nicotiana benthamiana psbO* (NbPsbO) with the *Tobacco rattle virus* (TRV) system resulted in a 10-fold increase in TMV accumulation, and also increased accumulation of *Potato virus X* (PVX; *Potexvirus*) and *Alfalfa mosaic virus* several-fold; inhibition of PS II with the herbicide [3-(3,4-Dichlorophenyl)-1,1-dimethyurea] (DCMU) also increased accumulation of TMV (Abbink et al., 2002). Other tobamoviruses and *Cucumber mosaic virus* have been reported to differentially affect components of PS II, reducing the levels of the 24-kDa (PsbP) and 16-kDa (PsbQ) subunits but not PsbO (Takahashi et al., 1991; Takahashi and Ehara, 1992; Rahoutei et al., 2000; Pérez-Bueno et al., 2004; Sui et al., 2006).

Specific interactions of other virus proteins with chloroplast proteins include those observed between the CP of PVX and the chloroplast transit peptide of plastocyanin; VIGS of plastocyanin using the TRV system reduced both the severity of PVX symptoms and the accumulation of PVX CP (Qiao et al., 2009). Chloroplast phosphoglycerate kinase (cPGK) was found to interact with the 3′-untranslated region (UTR) of *Bamboo mosaic virus* (BaMV), another member of the genus *Potexvirus*; when cPGK was silenced by VIGS with TRV, accumulation of BaMV CP was also reduced, suggesting that the replication site of BaMV is associated with the chloroplast and that cPGK may target the RNA to the chloroplast membrane (Lin et al., 2007). *Tomato mosaic virus* CP interacts with a thylakoid membrane protein IP-L (Zhang et al., 2008), while PVY (*Potyvirus*) CP has been shown to interact with the large subunit of Rubisco (Feki et al., 2005), and PVY HC-Pro with the domain of the nuclear-encoded chloroplast-division related protein MinD required for dimerization (Jin et al., 2007). TuMV CP interacts with an otherwise unidentified 37 kDa chloroplast protein (McClintock et al., 1998). HC-Pro of another potyvirus, *Sugarcane mosaic virus*, interacts in the cytoplasm with the chloroplast transit peptide of maize ferredoxin-5 (Fd V), possibly disturbing chloroplast import of mature Fd V (Cheng et al., 2008). The replication-associated CI protein of *Plum pox virus* (PPV) interacts with nuclear-encoded photosystem I (PS I) protein PSI-K of *N. benthamiana*, and down-regulation of the gene encoding PSI-K increased PPV accumulation; PPV infection itself results in reduced levels of PSI-K protein (Jiménez et al., 2006). The P1 protein of *Soybean mosaic virus* interacts with both the chloroplast transit peptide and the mature nuclear-encoded chloroplast Rieske Fe/S protein of several host species, but only weakly with the corresponding protein of the non-host *Arabidopsis thaliana* (Shi et al., 2007).

We have previously shown that the triple gene block 3 (TGB3) of the potexvirus *Alternanthera mosaic virus* (AltMV) localizes to the chloroplast, whereas TGB3 of PVX, the type member of the genus *Potexvirus*, accumulates at the ER (Lim et al., 2010a). We also used deletion mutants and site-directed mutagenesis to demonstrate that chloroplast localization is due to a signal in the N-terminal domain, and that mutation of VL(17,18)AR in the N-terminal domain was sufficient to both prevent chloroplast localization, and to severely limit virus movement to a few cells within the epidermal layer (Lim et al., 2010a). Over-expression of AltMV TGB3 as an additional gene from either AltMV or from a PVX vector resulted in veinal-associated necrosis, chloroplast malformation and vesicular invaginations of chloroplast membranes, and cytoplasmic membrane proliferation (Lim et al., 2010a). Fluorescence *in situ* hybridization showed that AltMV RNA was closely associated with the chloroplasts, which combined with chloroplast invagination when TGB3 was over-expressed suggests that the chloroplast is the site of AltMV replication (Lim et al., 2010a). In related preliminary work, we have shown that AltMV TGB1 interacts with chloroplast β-ATPase of both *A. thaliana* and *N. benthamiana* (Nam et al., 2012).

Here we examine the interactions of AltMV TGB3 with host PS II OEC protein PsbO of both *A. thaliana* and *N. benthamiana*, using deletion mutants to determine the TGB3 domains involved in the interactions, and demonstrate significant chloroplast damage when plants over-expressing TGB3 are grown under dark conditions. We have also examined over-expression of a series of natural AltMV TGB3 sequence variants, and determined that all variants induced chloroplast damage under dark conditions.

MATERIALS AND METHODS

VIRUS ISOLATES, cDNA CLONES, AND PLANT MAINTENANCE

Alternanthera mosaic virus 3–7 (AltMV 3–7) is derived from an infectious clone prepared from *Phlox stolonifera* isolate AltMV-SP, and was used for all experiments unless otherwise noted; AltMV 3–1 and AltMV 4–7 are also derived from AltMV-SP, and share an identical TGB3 amino acid sequence (Lim et al., 2010b). *P. stolonifera* isolates AltMV-BR and AltMV-PA, and *Portulaca grandiflora* isolate AltMV-Po have been described previously (Hammond et al., 2006a,b). Complementary DNA clones of the 3′-terminal region of AltMV-PGL (from *P. carolina*), AltMV-PLR (from hybrid annual phlox), AltMV-Po57 (from *P. grandiflora*), AltMV-NAN (from *Nandina domestica*), and AltMV-CIN (from hybrid *Pericallis*) were produced and sequenced essentially as reported for AltMV-BR and AltMV-Po (Hammond et al., 2006a,b). The TGB3 of all isolates except AltMV-MU (see below)

were amplified using primers *Xho*I-F-TGB3 and *Bam*HI-R-TGB3 (**Table 1**). The full sequence of European portulaca isolate AltMV-MU was reported by Ivanov et al. (2011), and the amino acid sequence of AltMV-MU TGB3 was derived by polymerase chain reaction (PCR) from an AltMV-Po template using *Xho*I-F-TGB3 paired with a reverse primer *Bam*HI-R-TGB3-MU (**Table 1**) to introduce the substitution R62K which differentiates the TGB3 of these isolates. The *Xho*I and *Bam*HI sites were introduced to allow cloning of the PCR products into pGD, pGDG, or pGDR (Goodin et al., 2002) for transient expression by agroinfiltration. The sequences of all TGB3 constructs were verified by sequencing.

Triple gene block 3 sequences of the various AltMV isolates were also separately introduced into infectious clone PVX-MCS as an additional gene, essentially as described (Lim et al., 2010a), forming PVX(TGB3 AltMV+) variants. Infectious RNA transcripts of wild-type (WT) PVX and the PVX(TGB3 AltMV+) variants were transcribed *in vitro* after linearization with *Spe*I, and inoculated to young plants of *N. benthamiana* as described (Petty et al., 1989; Lim et al., 2010a). Seven days post inoculation (dpi) plants inoculated with AltMV 4–7, WT PVX, or PVX(TGB3 AltMV+) variants were separately incubated under either light (16 h light/8 h dark) or continuous dark conditions at 16°C.

Alternanthera mosaic virus was maintained by mechanical inoculation on *N. benthamiana* using 1% K_2HPO_4 and carborundum powder as an abrasive. Plants were grown in 10 cm pots in an insect-proof greenhouse at 25°C, under a 14-h light regime. Plants of *A. thaliana* and *N. benthamiana* for agroinfiltration were grown under similar conditions, and were fully imbibed by standing pots in water for 4–5 h prior to agroinfiltration.

YEAST TWO-HYBRID ASSAYS

Alternanthera mosaic virus 3–7 TGB3 was subcloned into pGBKT7 at *Eco*RI and *Bam*HI sites, in fusion with the Gal4 DNA-BD, and the resulting plasmid (pGBKT-TGB3) was used to transform yeast competent cells (strain AH109) for bait protein expression (Becker et al., 1991). *A. thaliana* cDNA library (CD4–30, Arabidopsis Biological Resource Center, www.abrc.osu.edu) in pAD-GAL4-2.1 (in fusion with Gal4 DNA-AD) plasmid was used to transform yeast competent cells containing pGBKT-TGB3. Transformant cells were screened on SD agar His-, Leu-, Trp- plus Aureobasidin A. Yeast colonies obtained were grown on the same media including the chromogenic substrate X-α-galactosidase; only colonies developing blue color were considered positive. *A. thaliana* genes encoding proteins identified as binding TGB3 were amplified from the selected yeast colonies using appropriate primers, sequenced, and identified by BLAST analysis against the NCBI database (Lim et al., unpublished data).

Arabidopsis thaliana PsbO1 gene (oxygen-evolving enhancer protein 1-1, TAIR: AT5G66570, Acc. No. NM126055) and the homologous gene in *N. benthamiana* (NbPsbO; Acc. No. AY952375; Sui et al., 2006) were examined in this study. The corresponding NbPsbO gene (about 1000 bp), was amplified from *N. benthamiana* total RNA using primers *Xho*I-F-NbPsboI and *Kpn*I-R-NbPsboI (**Table 1**) based on the NbPsbO sequence, following cDNA synthesis with a polyT primer, sequenced, and fused to the C-terminus of the *Discosoma* sp. red fluorescent protein (DsRed) in pGDR for agroinfiltration. NbPsbO was also cloned into pGDG as a fusion to the C-terminus of the Green Fluorescent Protein (GFP), and pSPYCE/pSPYNE vector variants (Waadt et al., 2008) for subcellular localization and bimolecular fluorescence complementation (BiFC) assays, respectively.

The insertion gene fragment of NbPsbO for BiFC was derived from PCR using cDNA of *N. benthamiana* which was synthesized from *N. benthamiana* total mRNA. Primers *Spe*I-F-NbPSBOI BiFC and *Xho*I-R-NbPSBOI BiFC (**Table 1**) were used to amplify the 999-bp PCR product of NbPsbO with oligo(dT)-primed *N. benthamiana* cDNA as template. The primer set were synthesized based on the sequence of *N. benthamiana* chloroplast photosynthetic oxygen-evolving protein 33 kDa subunit (PsbO) mRNA (GenBank ID: AY952375.1; Sui et al., 2006).

BIMOLECULAR FLUORESCENCE COMPLEMENTATION ASSAYS

The pSPYCE(M), pSPYCE(MR), pSPYNE173, and pSPYNE(R)173 vectors (Waadt et al., 2008) were used for insertion of TGB3 variants, *A. thaliana* PsbBO1 (AtPsbO1), and NbPsbO, as fusions with the C-terminal (SPYCE constructs) and N-terminal (SPYNE constructs) domains of the enhanced Yellow Fluorescent Protein (eYFP), respectively, using the primers shown in **Table 1**. Binary plasmids were transformed into *Agrobacterium tumefaciens* strain EHA105 by standard protocols (Johansen and Carrington, 2001), and agroinfiltrated in each combination of TGB3 and PsbO, as well as homologous TGB3 combinations. Transient expression in *N. benthamiana* was performed by agroinfiltration (at $OD_{600} = 0.6$) with each pSPYCE and pSPYNE variant; pGD-p19 (Bragg and Jackson, 2004) was included at 1:10 ratio in all infiltrations as described (Lim et al., 2009). AtPsbO1 combinations were examined by agroinfiltration of *A. thaliana*, and all other combinations by agroinfiltration of *N. benthamiana*. For all combinations, eYFP fluorescence was observed at 3 days post-agroinfiltration (dpa) by laser scanning confocal microscopy (LSCM; see below).

INTERACTION OF GFP:PsbO AND DsRed:TGB3 FUSIONS

Nicotiana benthamiana PsbO was fused to the C-terminus of GFP, and TGB3 to the C-terminus of DsRed, in the vectors pGDG and pGDR (Goodin et al., 2002), respectively. Transient expression by agroinfiltration of *N. benthamiana* was performed as for BiFC assays, and fluorescent protein localization and interactions observed by LSCM (see below) at 3 dpa.

DETECTION OF FLUORESCENT PROTEIN EXPRESSION IN *N. BENTHAMIANA*

Laser scanning confocal microscopy using a Zeiss LSM 710 microscope was used for detection of GFP, DsRed, and chloroplast autofluorescence as described by Lim et al. (2010a). For BiFC, eYFP was excited at 514 nm (Argon laser, MBS458/514 filter set) and the emission detected at 514–550 nm. When required, nuclei were stained with 4′-6-diamidino-2-phenylindole dihydrochloride (DAPI) essentially as described by Deng et al. (2007). DAPI fluorescence was excited with a 405-nm laser, with emission detected at 410–475 nm.

Zeiss Zen™2009 software was used to obtain images with maximum intensity projection (MIP) of *Z*-stacks (1 μm slices, 2–80 focal planes) of leaves from the top of the epidermis into the mesophyll, or within the mesophyll.

Table 1 | Primers used in this study.

Clone	5′-Oligo	5′-Oligo sequence	3′-Oligo	3′-Oligo sequence	Feature
PRIMERS USED IN BINARY VECTORS CONSTRUCTS FOR *AGROBACTERIUM* INFILTRATION EXPERIMENTS					
AltMV TGB3	*Xho*I-F-TGB3	CTCGAGAAATGCCCTATCTTGTAGAG	*Bam*HI-R-TGB3	CAAACGGATCCTAAAACCTAAGCCCG	*Xho*I and *Bam*HI
AltMV TGB3 MU	*Xho*I-F-TGB3	CTCGAGAAATGCCCTATCTTGTAGAG	*Bam*HI-R-TGB3-MU	CAAACGGATCCTAAAACTTAAGCCCG	*Xho*I and *Bam*HI
NbPsbOI	*Xho*I-F-NbPsbol	GAGCTCGAGAAATGGCTGCCTCTCTACAAGCAGCTG	*Kpn*I-R-NbPsbol	GAGGGTACCCCCTTCAAGTTGGGCATACCAGATACC	*Xho*I and *Kpn*I
PRIMERS USED FOR YEAST-TWO-HYBRID EXPRESSION OF AltMV TGB3					
pGBKT7-TGB3	*Eco*RI F	GAGAGAATTCATGCCCTATCTTGTAGAG	*Bam*HI R	GAGAGGATCCCTAAAACCTAAGCCAAAGCA	*Eco*RI and *Bam*HI
AltMV TGB3 CONSTRUCTS IN BiFC VECTORS					
BiFC: AltMV TGB3	*Xho*I-F-TGB3 BiFC	GAGCTCGAGATGCCCTATCTTGTAGAGGCGGCC	*Xma*I-R-TGB3 BiFC	GAGCCCGGGCCCAAACCTAAGCCCGGTTAAATAGTCTCC	*Xho*I and *Xma*I
BiFC: AltMV TGB3-ΔN15	*Xho*I-F- TGB3-ΔN15 BiFC	GAGCTCGAGATGGTCCTTGCTGCTCTTAGGCCA	*Xma*I-R-TGB3 BiFC	GAGCCCGGGCCCAAACCTAAGCCCGGTTAAATAGTCTCC	*Xho*I and *Xma*I
BiFC: AltMV TGB3-ΔC15	*Xho*I-F-TGB3 BiFC	GAGCTCGAGATGCCCTATCTTGTAGAGGCGGCC	*Xma*I-R-TGB3-ΔC15 BiFC	GAGCCCGGGCCCTGGTGCGACGGGTCCACAATCT	*Xho*I and *Xma*I
PsbOI CONSTRUCTS IN BiFC VECTORS					
BiFC: AtPsbOI	*Xho*I-F-AtPsbol BiFC	GAGCTCGAGATGGCAGCCTCTCTCCAATCCACC	*Xma*I-R-AtPsbol BiFC	GAGCCCGGGCCCCTCAAGTTGACCATACCAC	*Xho*I and *Xma*I
BiFC: NbPsbOI	*Spe*I-F-NbPsbol BiFC	GAGACTAGTATGGCTGCCTCTCTACAAGC	*Xho*I-R-NbPsbol BiFC	GAGCTCGAGCCCTTCAAGTTGGGCATACC	*Spe*I and *Xho*I
TGB3 OVER-EXPRESSION EXPERIMENTS					
PVX(AltMV TGB3+)	*Bam*HI-F-TGB3	GAGAGGATCCATGCCCTATCTTGTAGAG	*Mlu*I-R-TGB3	GAGAACGCGTCTACCTGATGGTCTCTGGTGCG	*Bam*HI and *Mlu*I
PVX(AltMV TGB3 MU+)	*Bam*HI-F-TGB3	GAGAGGATCCATGCCCTATCTTGTAGAG	*Mlu*I-R-TGB3-MU	GAGAACGCGTCTACTTGATGGTCTCTGGTGCG	*Bam*HI and *Mlu*I

ELECTRON MICROSCOPY

Tissue samples (ca. 2 mm × 1 mm) were excised from leaves of *N. benthamiana* infected with WT PVX, PVX over-expressing AltMV TGB3 or AltMV 3–1 over-expressing TGB3 (Lim et al., 2010a), and processed for embedding according to Lawson and Hearon (1973). Ultrathin sections were examined with a JEOL 100CX II transmission electron microscope (JEOL Ltd.) equipped with an AMT HR digital camera system (Advanced Microscopy Techniques Corp.).

RESULTS

YEAST TWO-HYBRID INTERACTIONS

Several proteins were identified by screening of an *Arabidopsis* cDNA library with AltMV TGB3 as bait; because the PS II OEC protein, AtPsbO1, showed the strongest interaction (data not shown), and because we had previously shown that TGB3 localizes to the chloroplast (Lim et al., 2010a), we selected PsbO for detailed examination. The interactions detected by screening of the *Arabidopsis* cDNA library were confirmed using the full-length AtPsbBO1 and NbPsbO proteins for BiFC.

BIMOLECULAR FLUORESCENCE COMPLEMENTATION ASSAYS

Reciprocal interactions between AltMV TGB3 and AtPsbO1 were detected by BiFC only when both constructs were expressed with the eYFP fragment fused to the N-terminus of the test protein. No interaction was observed when either TGB3 or PsbO1 was fused upstream of the eYFP fragment, and no homologous TGB3 interaction was observed in any combination (**Table 2**).

Similar interactions were observed between AltMV TGB3 and both AtPsbO1 and NbPsbO, in *A. thaliana* and *N. benthamiana*, respectively, in both epidermal and mesophyll layers (**Figures 1A,D,H,I**; and data not shown). As we had previously demonstrated that N-terminal TGB3 deletions of as much as 16 residues, and C-terminal deletions of at least 11 residues were still directed to the chloroplast (Lim et al., 2010a), we utilized N-terminal and C-terminal mutants of TGB3 (**Figure 2**) in BiFC experiments to determine which domains of TGB3 were responsible for interaction with both AtPsbBO1 and NbPsbO. In each case, deletion of the C-terminal 15 residues reduced but did not eliminate the interaction (**Figures 1A,E,J,K**), whereas deletion of N-terminal residues 2–16 essentially eliminated the interaction with either PsbO (**Figures 1C,F**).

The interactions of PsbO and either TGB3 (**Figures 1D,I**) or C-terminally deleted TGB3 (**Figures 1E,K**) were clearly localized around the chloroplasts in the mesophyll layer, with additional fluorescence at the periphery of the cell. The intimacy of the association with chloroplasts varied between cells; in some cells the BiFC interaction was clearly localized to the chloroplast envelope, as well as in the cytoplasm surrounding the chloroplasts [**Figures 1Iii, Kii**]. Interaction with some chloroplasts showed a more punctate appearance [**Figure 1Iii**] similar to that previously observed with GFP:TGB3 and DsRed:TGB3 fusions (Lim et al., 2010a), but other chloroplasts in the same cell appeared to be surrounded by the interaction as seen with C-terminal fusions of GFP and DsRed to full-length TGB3, TGB3ΔN9, and TGB3ΔN16ΔC11 (Lim et al., 2010a). Interestingly, epidermal cells were also labeled by $eYFP_{C155}$-TGB3/$eYFP_{N173}$-PsbO interactions (**Figures 1A,B,D,E,H,J**) although GFP:TGB3 and DsRed:TGB3 fusions were previously found to be essentially absent from epidermal tissue (Lim et al., 2010a).

Table 2 | Interactions of AltMV TGB3 and AtPsbO1 as detected by BiFC.

Combination	Interaction
TGB3-$eYFP_{C155}$/AtPsbO1-$eYFP_{N173}$	−
TGB3-$eYFP_{N173}$/AtPsbO1-$eYFP_{C155}$	−
$eYFP_{C155}$-TGB3/$eYFP_{N173}$-AtPsbO1	+
$eYFP_{N173}$-TGB3/$eYFP_{C155}$-AtPsbO1	+
TGB3-$eYFP_{C155}$/$eYFP_{N173}$-AtPsbO1	−
TGB3-$eYFP_{N173}$/$eYFP_{C155}$-AtPsbO1	−
$eYFP_{C155}$-TGB3/AtPsbO1-$eYFP_{N173}$	−
$eYFP_{N173}$-TGB3/AtPsbO1-$eYFP_{C155}$	−
TGB3-$eYFP_{C155}$/TGB3-$eYFP_{N173}$	−
$eYFP_{N173}$-TGB3/$eYFP_{N173}$-TGB3	−
$eYFP_{C155}$-TGB3/TGB3-$eYFP_{N173}$	−
TGB3-$eYFP_{N173}$/TGB3-$eYFP_{C155}$	−

In the epidermal cells, the distribution of the BiFC signal was more dispersed at the periphery of the cells (**Figures 1A,E,H,J**). Although globular accretions of BiFC signal observed in epidermal cells (**Figures 1B,E**) appear to be nuclei, no association of BiFC signal with nuclei could be identified in leaf pieces infiltrated with DAPI; epidermal aggregations of BiFC signal were instead observed primarily in curves of the cell wall (**Figures 1H,J**). These epidermal aggregates of $eYFP_{N173}$-PsbO and $eYFP_{C155}$-TGB3 were therefore presumed to result from over-expression, rather than to reflect a specific association with a cellular component, and no nuclear association could be confirmed. Little PsbO would normally be expected in the epidermal layer, due to the low frequency of chloroplasts in this tissue, and no nuclear association of TGB3 has been identified.

Overall, these results suggested that it is the N-terminal domain of TGB3 which interacts with PsbO. As we have previously demonstrated that the region between residues 16 and 20 is critical for chloroplast targeting, and that mutation VL(17,18)AR (**Figure 2**) ablates direct chloroplast interaction (Lim et al., 2010a), we next examined the interaction of $TGB3_{VL(17,18)AR}$ with PsbO. We hoped to determine whether chloroplast localization is a prerequisite for interaction with PsbO, or alternatively, whether interaction with PsbO is required for chloroplast localization of TGB3. No interaction was observed between NbPsbO and $TGB3_{VL(17,18)AR}$ in *N. benthamiana* (**Figure 1G**), suggesting that these TGB3 residues (or at least L18; see below) are critical for the interaction with PsbO as well as chloroplast localization.

INTERACTION OF GFP:PsbO AND DsRed:TGB3 FUSIONS

GFP:PsbO (NbPsbO) expressed by agroinfiltration of *N. benthamiana* (with pGDG:PsbO) in the absence of DsRed:TGB3 localized around the chloroplasts of mesophyll cells (**Figure 3A**, upper), whereas DsRed:TGB3 (from pGDR:TGB3) localized to the chloroplasts as punctate spots (**Figure 3A**, lower). When GFP:PsbO and DsRed:TGB3 were co-expressed, almost complete co-localization was observed in mesophyll cells, apparently at points where two chloroplasts were in close contact (**Figures 3B–D**), confirming the interactions visualized by BiFC. The GFP:PsbO/DsRed:TGB3

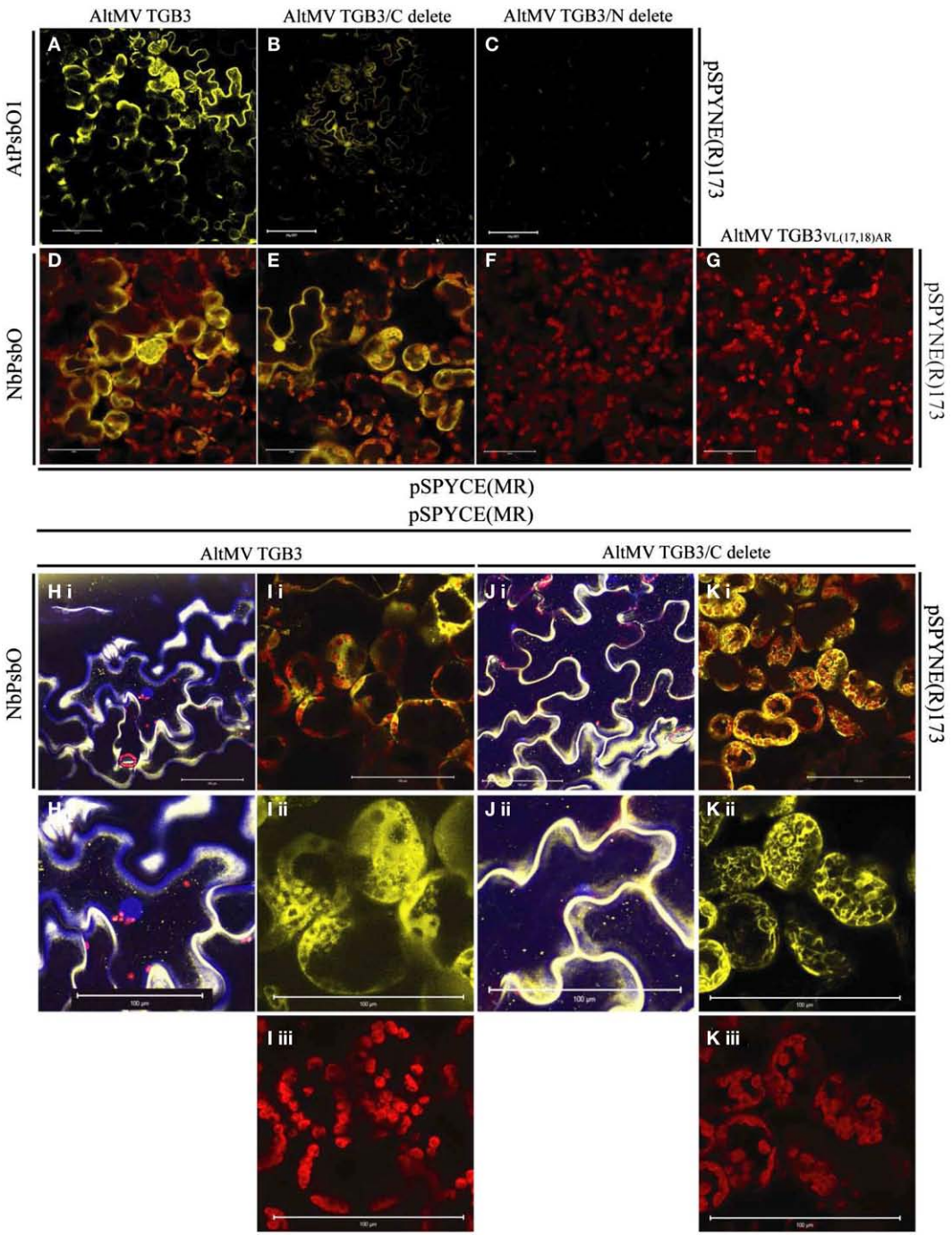

FIGURE 1 | BiFC interactions between AtPsbO1 or NbPsbO and variants of AltMV TGB3. (A–C) Reactions of AtPsbO1 with TGB3 in epidermal cells of *A. thaliana*. **(D–K)** Reactions of NbPsbO with TGB3 in mesophyll cells of *N. benthamiana*. **(A,D,H,I)** Full-length TGB3. **(B,E,J,K)** C-terminal deleted TGB3. **(C,F)** N-terminal deleted TGB3. **(G)** $TGB3_{VL(17,18)AR}$. **(H)**, **(i)** Full-length TGB3 in epidermal cells, with nuclei revealed by DAPI staining; and **(ii)** enlargement of central area of **(i)**, showing BiFC interaction along cell wall, and absence of interaction associated with central nucleus (blue). **(I)** Full-length TGB3 in mesophyll cells, showing **(i)**, BiFC interaction around chloroplasts; **(ii)**, BiFC (yellow) channel image of enlarged area of **(i)** showing punctate interaction on some chloroplasts, interaction surrounding envelope of other chloroplasts, and in cytoplasm around chloroplasts; **(iii)**, Red channel, showing chloroplast autofluorescence of same enlarged area as **(ii)**. **(J)**, **(i)** C-terminal deleted TGB3 in epidermal cells, with nuclei revealed by DAPI staining; and **(ii)** enlargement of lower left area of **(i)**, showing nucleus (blue) appressed to cell wall with absence of nuclear-associated BiFC interaction. **(K)** C-terminal deleted TGB3 in mesophyll cells, showing **(i)** BiFC interaction around chloroplasts; **(ii)**, BiFC (yellow) channel image of enlarged area of **(i)**, showing interaction at chloroplast envelope as well as in cytoplasm around chloroplasts; **(iii)**, Red channel (chloroplast autofluorescence) of same enlarged area as **(ii)**. Note BiFC reaction with full-length and C-terminal deleted TGB3, and absence of interaction with N-terminal deleted TGB3 or $TGB3_{VL(17,18)AR}$. AtPsbO1 and NbPsbO were fused with the N-terminal domain of YFP in pSPYNE(R)173, while TGB3 variants were fused to the C-terminal domain of YFP in pSPYCE(MR). Red is chloroplast autofluorescence from mesophyll cells. Bars = 100 μm.

```
TGB3-WT      MPYLVEAAITVLACIGVLAALRPGSHPCTILLTGHSATISGNCGPVAPETIRALGDYLTGLRF
C-del        MPYLVEAAITVLACIGVLAALRPGSHPCTILLTGHSATISGNCGPVAP---------------
N-del        ---------------MVLAALRPGSHPCTILLTGHSATISGNCGPVAPETIRALGDYLTGLRF
VL(17,18)AR  MPYLVEAAITVLACIGARAALRPGSHPCTILLTGHSATISGNCGPVAPETIRALGDYLTGLRF
```

FIGURE 2 | Amino acid sequence of mutants of AltMV TGB3 used for BiFC reactions. Altered residues are shown in bold and underlined.

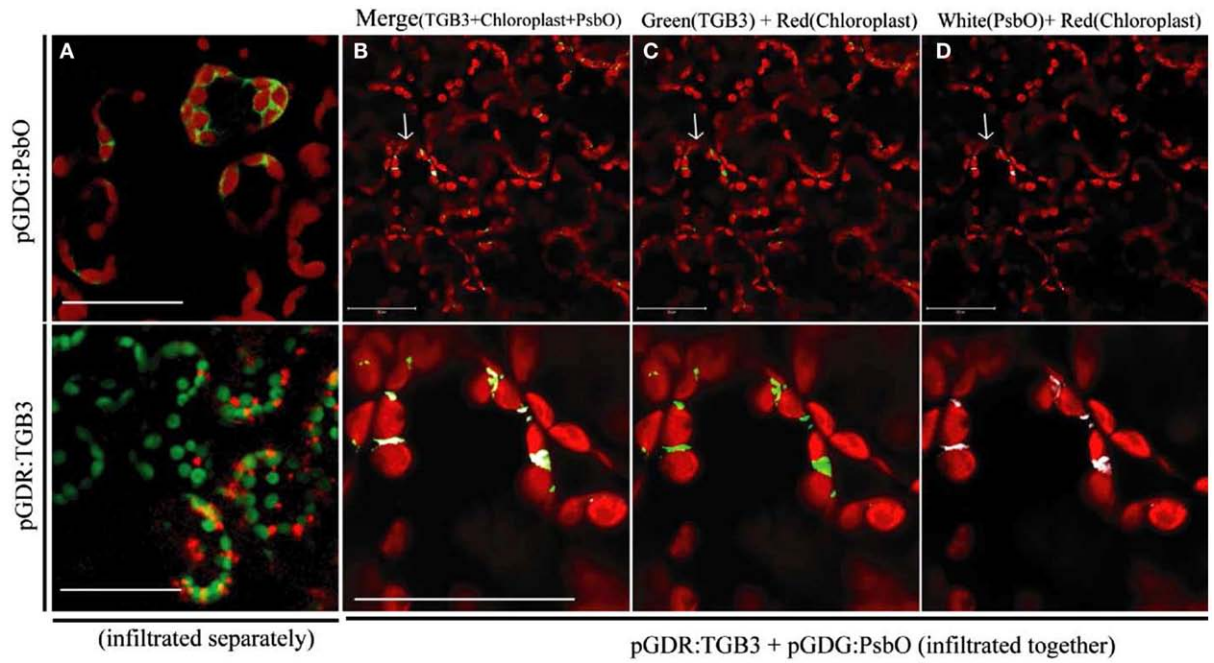

FIGURE 3 | Interaction between GFP:PsbO (NbPsbO) and DsRed:TGB3 in mesophyll tissue of *Nicotiana benthamiana*. Constructs pGDG:PsbO and pGDR:TGB3 were infiltrated separately **(A)**, or co-agroinfiltrated **(B–D)** into leaves of *N. benthamiana* and examined by LSCM at 3 dpa. **(A)** Upper, GFP:PsbO (shown as green) expressed alone, showing localization around the chloroplasts, with chloroplast autofluorescence shown in red; lower, DsRed:TGB3 (shown as red) showing punctate spots associated with chloroplasts, with chloroplast autofluorescence shown in green. **(B–D)** The upper row shows multiple cells with typical morphology of the mesophyll layer, and red chloroplast autofluorescence. The lower row shows a magnified image of the area indicated by an arrow in the upper panel. **(B)** Merge of DsRed:TGB3 (shown as green) with GFP:PsbO (shown as white) and chloroplast autofluorescence (red). **(C)** DsRed:TGB3 (green) and chloroplast autofluorescence (red). **(D)** GFP:PsbO (white) and chloroplast autofluorescence (red). Note co-localization of DsRedD:TGB3 and GFP:PsbO at areas where chloroplasts appear to be in close contact. Scale bar = 50 μm.

interaction was predominantly punctate, by comparison to the BiFC interaction, which displayed a mix of punctate spots at the chloroplast surface, distribution surrounding the chloroplast, and in the adjacent cytoplasm and cell periphery (**Figure 1**). This suggests that localization of TGB3 predominates in the GFP:PsbO/DsRed:TGB3 interaction, whereas PsbO localization may be dominant in the BiFC interaction.

ELECTRON MICROSCOPY

Plants infected with WT PVX had essentially normal chloroplasts (**Figure 4A**), whereas in plants infected with PVX over-expressing AltMV TGB3, abnormal chloroplasts with approximately spherical vesicular invaginations at the peripheral membrane could frequently be found (**Figures 4B,C**). Similar vesicles were also observed in chloroplasts of plants infected with AltMV over-expressing TGB3 (**Figure 4D**), as could some much larger vesicles (**Figure 5**).

Additional types of abnormal chloroplasts were frequently observed in plants infected with AltMV over-expressing TGB3. Significant invaginations of cytoplasmic material were found, typically toward the ends of chloroplasts (**Figures 5A–C,E**), and in some instances combined with significant quantities of irregular small vesicles lacking apparent connection to the chloroplast peripheral membrane (**Figures 5A,D,F**). The large invaginations could either be apparently totally enclosed within the chloroplast (**Figures 5A,C,E,F**), or still obviously connected to the cytoplasm (**Figures 5B,E**). In some instances spheroidal microbodies with a paracrystalline appearance were observed in close proximity to invaginated chloroplasts (**Figure 5A**); these may represent peroxisomes. Osmiophilic globules or plastoglobules were

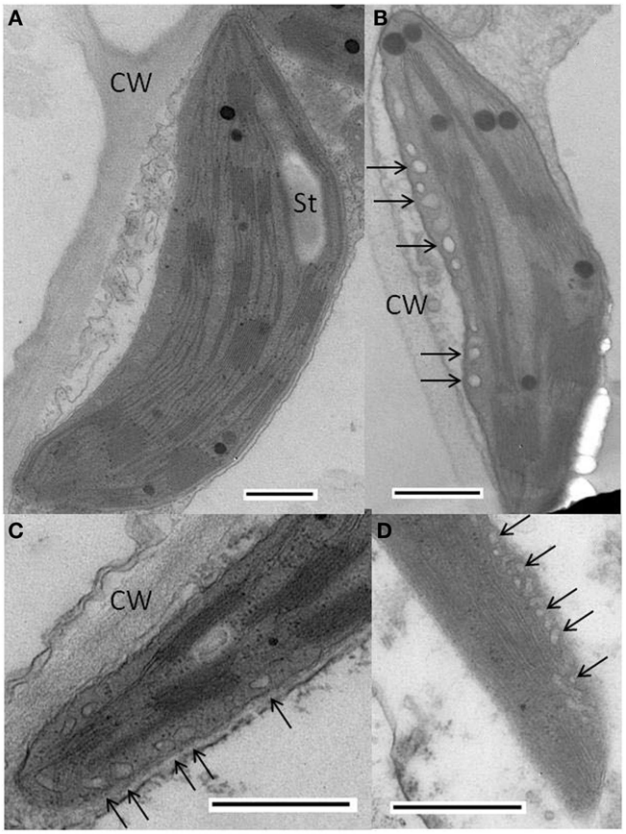

FIGURE 4 | Cytopathology associated with AltMV TGB3 over-expression. (A) Normal chloroplast in thin section of *N. benthamiana* infected with PVX. **(B,C)** Vesicles (arrows) observed in chloroplast of *N. benthamiana* infected with PVX over-expressing AltMV TGB3 as an added gene. **(D)** Vesicles (arrows) in chloroplast of *N. benthamiana* infected with AltMV over-expressing AltMV TGB3 as an added gene. CW, cell wall; St, starch. Scale bars in each panel = 500 nm.

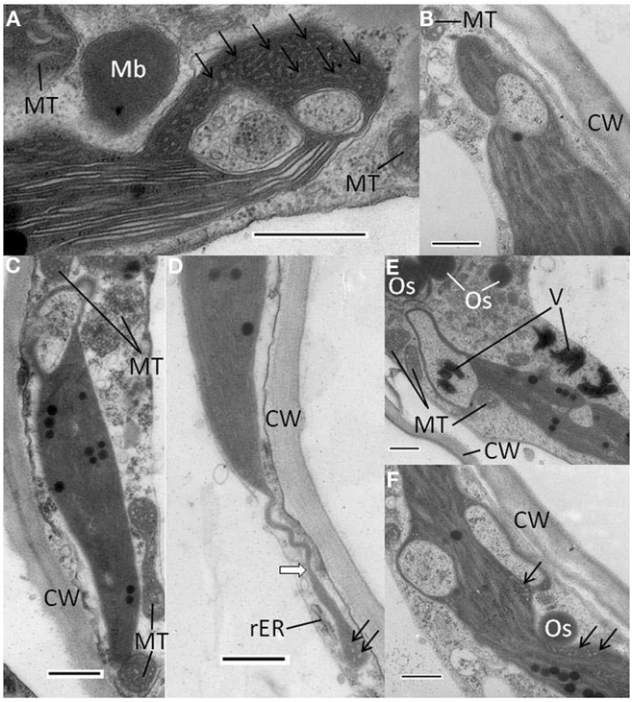

FIGURE 5 | Abnormal chloroplast morphology observed in *N. benthamiana* infected with AltMV over-expressing TGB3 as an added gene. (A) Large invagination and multiple vesicles present at end of a chloroplast, with an adjacent paracrystalline microbody that may be a peroxisome. **(B)** Large invagination open to cytoplasm near one end of a chloroplast. **(C)** Large apparent cytoplasmic invagination at one end of a chloroplast. **(D)** Stromule-like extension (white arrow) from the end of a chloroplast. **(E)** Two large invaginations of cytoplasmic material into a chloroplast. Note apparent virion aggregates inside apparently fully enclosed area, and larger virion aggregates near invagination open to cytoplasm. **(F)** Chloroplast with two large apparently closed cytoplasmic invaginations, and multiple small vesicles in constricted region adjacent to possible TGB1 aggregate. CW, cell wall; Mb, microbody or peroxisome; MT, mitochondrion; Os, osmiophilic globule or plastoglobule; rER, rough endoplasmic reticulum; V, virion aggregates: arrows indicate areas of small vesicles. Scale bars in each panel = 500 nm.

frequently observed close to abnormal chloroplasts (**Figures 5E,F**). In rare instances, chloroplasts with significant long terminal extensions resembling stromules were observed (**Figure 5D**). Aggregates of virions were occasionally observed near chloroplasts with large cytoplasmic inclusions, and rarely inside apparently totally enclosed invaginations (**Figure 5E**).

SEQUENCE VARIANTS OF TGB3 IN NATURAL AltMV ISOLATES

We have sequenced the TGB3 region of a number of AltMV isolates from various hosts (Hammond et al., 2006a,b; Lim et al., 2010b; J. Hammond and M. D. Reinsel, unpublished data) and the full sequence of a European portulaca isolate is also available (Ivanov et al., 2011). There are multiple TGB3 amino acid differences between these isolates (**Figure 6**), so we expressed each variant TGB3 sequence as an added gene from a PVX vector as previously described (Lim et al., 2010a) in *N. benthamiana*. Plants infected with AltMV 4–7 (Lim et al., 2010b), WT PVX, or PVX separately expressing each TGB3 variant were transferred at 7 dpi to be grown in either light (16 h/8 h diurnal cycle) or constant dark conditions for six further days. Plants infected with AltMV showed somewhat more severe symptoms after dark growth than in light (**Figure 7A**), while plants infected with PVX over-expressing TGB3 variants grown under dark conditions showed significantly more severe symptoms than plants maintained in the light (**Figures 7B–G**); plants infected with WT PVX showed milder, similar symptoms than AltMV-infected plants under both light and dark conditions (**Figure 7H**). As previously noted (Lim et al., 2010a) with plants infected with PVX(TGB3 AltMV+) and grown under normal light conditions, more severe symptoms including veinal-associated necrosis occurred (**Figure 8A**). Significantly fewer chloroplasts were observed by confocal microscopy in plants in which AltMV TGB3 variants were over-expressed, compared to plants infected with PVX (**Figures 8B,C**); the difference was greater for plants grown in the dark, but no correlation with specific amino acid substitutions was obvious (data not shown).

Comparison of the TGB3 sequences of different AltMV isolates revealed that AltMV-CIN (from cineraria) and AltMV-PLR (from

```
AltMV 3-1    MPYLVEAAITVLACIGVLAALRPGSHPCTILLTGHSATISGNCGPVAPETIRALGDYLTGLRF
AltMV 4-7    MPYLVEAAITVLACIGVLAALRPGSHPCTILLTGHSATISGNCGPVAPETIRALGDYLTGLRF
AltMV-SP     MPYLVEAAITVLACIGVLAALRPGSHPCTILLTGHSATISGNCGPVAPETIRALGDYLTGLRF
AltMV-BR     MPYLVEAAITVLACIGVLAALRPGSHPCTILLTGHSATISGNCGPVAPETIRALGDYLTGLRF
AltMV-PA     MPYLVEAAITVLACIGVLAALRPGSHPCTILLTGHSATISGDCGPVAPETIRALGDYLTGLRF
AltMV-PGL    MPYLVEAAITVLACIGVLAALRPGSHPCTILLTGHSATISGDCGPVAPETIRALGDYLTGLRF
AltMV-NAN    MPYLVEAAITVLACIGVLAALRPGFHPCTILLTGHSATISGDCGPVAPETIRALGDYLTGLRF
AltMV-CIN    MPYLVEAAIAVLVCIGALAALRPGSHPCTILLTGHSATISGDCGPVAPETIRALGEHLTGLRF
AltMV-PLR    MPYLVEAAIAVLVCIGALAALRPGSHPCTILLTGHSATISGDCGPVAPETIRALGEHLTGLRF
AltMV-Po57   MPYLVEAAIAVLVCIGVLAALRPGSHPCTILLTGHSATISGDCGPVAPETIRALGEHLTGLRF
AltMV-MU     MPYLVEAAIAVLACIGVLAALRPGSHPCTILLTGHSATISGDCGPVAPETIRALGEHLTGLKF
AltMV-Po     MPYLVEAAIAVLACIGVLAALRPGSHPCTILLTGHSATISGDCGPVAPETIRALGEHLTGLRF
             *********:**.***.******* ****************:*************::****:*
```

FIGURE 6 | Alignment of TGB3 amino acid sequences of different AltMV isolates. Residues that differ from the consensus of phlox-derived isolates are highlighted; AltMV isolates CIN, PLR, Po57, MU, and Po are "portulaca-type" isolates that are also differentiated from "phlox-type" isolates by differences in the CP amino acid sequence (J. Hammond and M. Reinsel, unpublished data). The GenBank accession numbers of the isolates are: AltMV 3–1, GQ179646; AltMV 4–7, GQ179647; AltMV-SP, AY850931; AltMV-BR, AY850628; AltMV-PA, AY863024; AltMV-PGL, JQ405265; AltMV-NAN, JQ405267; AltMV-CIN, JQ405268; AltMV-PLR, JQ405266; AltMV-Po57, JQ405269; AltMV-MU, FJ822136; AltMV-Po, AY850930.

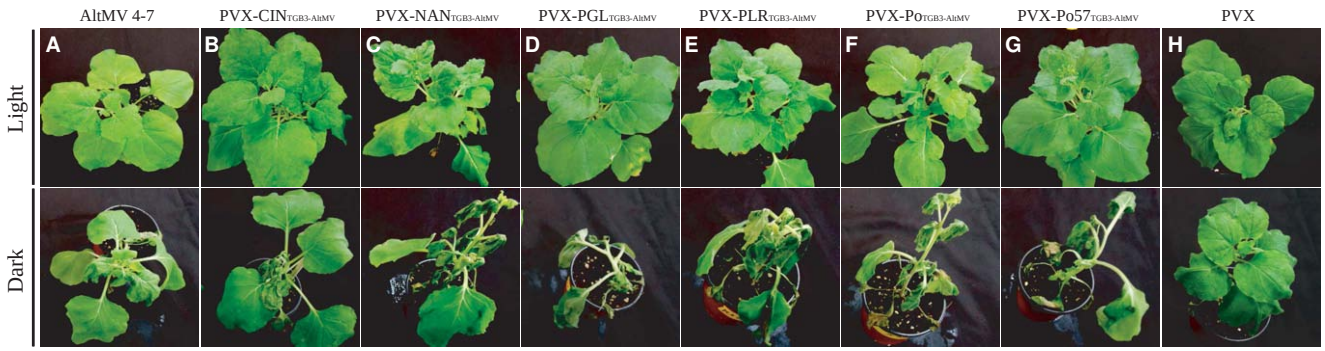

FIGURE 7 | Effect of growth in the dark on symptom severity in plants over-expressing AltMV TGB3 variants from a PVX vector. Starting at 7 days after inoculation, *N. benthamiana* plants infected with AltMV 4–7, WT PVX, or PVX(TGB3 AltMV+) variants were incubated for 6 days under either diurnal light or constant dark conditions. Upper row – plants grown in light; Lower row – plants grown in dark. **(A)** AltMV 4–7 (positive control). **(B)** PVX-CIN$_{TGB3\text{-}AltMV}$. **(C)** PVX-NAN$_{TGB3\text{-}AltMV}$. (**D**) PVX-PGL$_{TGB3\text{-}AltMV}$. **(E)** PVX-PLR$_{TGB3\text{-}AltMV}$. **(F)** PVX-Po$_{TGB3\text{-}AltMV}$. **(G)** PVX-Po57$_{TGB3\text{-}AltMV}$. **(H)** WT PVX (negative control). Note increased severity of symptoms in dark-grown plants over-expressing AltMV TGB3 variants, with collapse of apical leaves, whereas AltMV 4–7 **(A)** shows slightly more severe symptoms, and WT PVX **(H)** shows minimal increase in symptom severity compared to light-grown plants.

hybrid annual phlox) both have an alanine residue at position 17 (**Figure 6**). This is of interest because mutant TGB3$_{VL(17,18)AR}$ (see **Figure 2**) failed to accumulate at the chloroplast (Lim et al., 2010a), and failed to interact detectably with PsbO in BiFC (**Figure 3**). The occurrence of A17 in these two isolates suggests that it is L18 that is critical to chloroplast localization.

DISCUSSION

AltMV TGB3 LOCALIZATION

Alternanthera mosaic virus TGB3 is a multifunctional protein, associated with both intra- and intercellular local movement, and with systemic movement; an infectious clone unable to produce TGB3 as a result of a premature stop codon is able to replicate and spread to a few adjacent epidermal cells, but not to move to the mesophyll (Lim et al., 2010a). TGB3 is therefore not absolutely required for replication, but the limited epidermal movement distinguishes the TGB3 mutant from clones unable to express either TGB2, or CP, which were unable to spread beyond the initially infected cell (Lim et al., 2010a), as previously noted for similar mutants of *White clover mosaic virus*, PVX, and BaMV (Beck et al., 1991; Lough et al., 2000; Lin et al., 2006). It has yet to be demonstrated whether AltMV TGB2 and TGB3 interact, as has been demonstrated with those of PVX (Samuels et al., 2007), BaMV (Lee et al., 2010), and some other TGB-expressing viruses (e.g., Solovyev et al., 2000; Cowan et al., 2002; Lim et al., 2008). PVX TGB3 has been shown to co-localize with the viral replicase at the ER in membrane-bound structures (Bamunusinghe et al., 2009), while AltMV TGB3 localizes to chloroplast membranes which may be the main site of AltMV replication, as the chloroplast membrane is the preferential site of virus accumulation (Lim et al., 2010a).

Whereas PVX TGB3 has been shown to localize to granular vesicles that also contain TGB2 (Schepetilnikov et al., 2005;

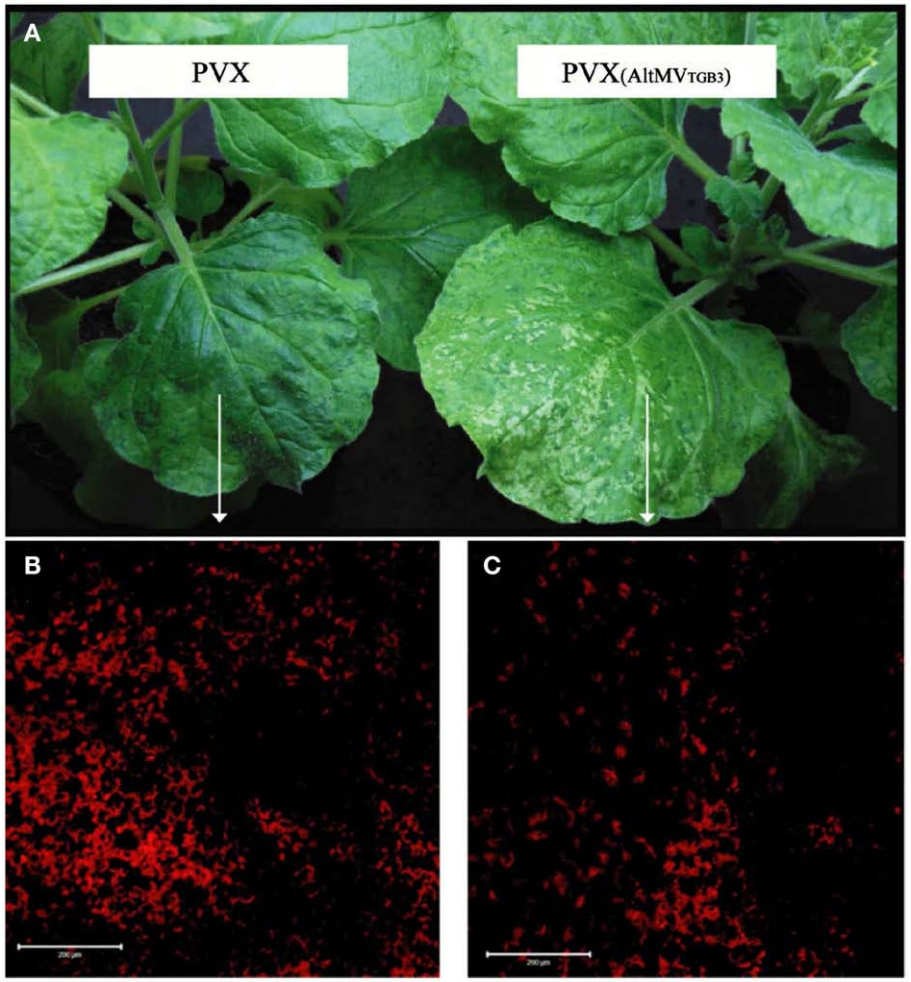

FIGURE 8 | Reduced chloroplast survival in plants with AltMV TGB3 over-expressed from the PVX genome. Plants of *N. benthamiana* were inoculated with WT PVX, or PVX over-expressing AltMV TGB3, and grown under normal diurnal lighting. **(A)** Mild mosaic symptoms of WT PVX (left) and more severe symptoms including veinal necrosis induced by PVX over-expressing AltMV TGB3 (right). **(B)** LSCM visualization of chloroplast autofluorescence in the mesophyll layer of indicated area of leaf infected with PVX. **(C)** Significantly reduced chloroplast autofluorescence in indicated region of leaf infected with PVX over-expressing AltMV TGB3. Scale bar = 200 μm.

Samuels et al., 2007; Ju et al., 2008) and with replicase at spherical bodies along the ER (Bamunusinghe et al., 2009), both N- and C-terminal AltMV TGB3 fluorescent fusion proteins localized to the chloroplast, and localization was not affected by co-expression of free TGB2, TGB3, or TGB2 + TGB3 (Lim et al., 2010a). Similarly, no TGB3 self-interaction was detected in BiFC (this study); thus unlike BaMV TGB3 (Lee et al., 2010), there is as yet no evidence for AltMV TGB3 self-interaction. Agroinfiltrated PVX GFP:TGB3 and DsRed:TGB3 were localized primarily at the periphery of epidermal cells, while AltMV TGB3 fusions were observed almost exclusively in the mesophyll in association with the chloroplasts when agroinfiltrated under the same conditions (Lim et al., 2010a). It is the N-terminal domain of AltMV TGB3 that is critical for chloroplast targeting, even when fused downstream of GFP or DsRed. Mutation of TGB3 residues VL(17,18)AR was sufficient to ablate chloroplast targeting and allow accumulation at the periphery of epidermal cells, and in the context of an infectious clone yielded a virus unable to move beyond the epidermal layer (Lim et al., 2010a). There was therefore strong evidence of a link between TGB3 and the chloroplast, which is necessary for systemic movement of AltMV.

The chloroplast association was further demonstrated by over-expression of AltMV TGB3 from either AltMV or PVX; plants infected with either virus over-expressing TGB3 developed more severe symptoms, including veinal necrosis. In *N. tabacum*, a non-host of AltMV, PVX over-expressing AltMV TGB3 induced necrotic local lesions rather than the chlorotic local lesions induced by WT PVX, whereas PVX TGB3 over-expressed from AltMV in *N. benthamiana* did not increase symptom severity (Lim et al., 2010a). Chloroplast invaginations similar to those reported with plants infected by TYMV (Ushiyama and Matthews, 1970) were observed in *N. benthamiana* infected with either AltMV or PVX over-expressing AltMV TGB3, and fewer intact chloroplasts were observed in plants infected with PVX over-expressing AltMV

TGB3 than in controls infected with WT PVX (Lim et al., 2010a; and this study); the observed chloroplast destruction mirrors that reported for TYMV under normal light conditions by Chalcroft and Matthews (1966).

PsbO LOCALIZATION AND FUNCTIONS

It was therefore of considerable interest when we identified an interaction between AltMV TGB3 and AtPsbO1 by screening an *A. thaliana* cDNA library by the Y2H method, as PsbO is a nuclear-encoded major component of the chloroplast-localized OEC of PS II (Tyagi et al., 1987). We also cloned a PsbO gene from *N. benthamiana*, based on the sequence determined by Sui et al. (2006), and confirmed interaction between TGB3 and both AtPsbO1 and NbPsbO by BiFC; the BiFC results clearly demonstrate co-localization of TGB3 and PsbO surrounding chloroplasts in mesophyll cells.

The chloroplast-localized interaction of TGB3 and PsbO observed by BiFC was confirmed by the co-localization of DsRed:TGB3 with GFP:PsbO; interestingly the siting of the interaction between appressed chloroplasts is similar to the observation of chloroplast clumping caused by TYMV infection (Chalcroft and Matthews, 1966), although in the current instance in the absence of viral infection and other viral proteins. As DsRed:TGB3 expressed alone induced punctuate spots, whereas GFP:PsbO expressed alone accumulated surrounding the chloroplasts, perhaps the interaction draws the chloroplasts together and creates a more favorable environment for replication complexes to be protected from host defenses.

While Sui et al. (2006) were aware that *N. tabacum* has multiple copies of the *psbO* gene, only one copy was cloned from *N. benthamiana* until Pérez-Bueno et al. (2011) cloned four isoforms and demonstrated that only three amino acids differ between the mature forms of NbPsbO1 and NbPsbO2; two further residues differ between the 85-residue signal peptides of these isoforms. The NbPsbO of Sui et al. (2006) is identical to NbPsbO2 (Pérez-Bueno et al., 2011) except for the third residue of the signal peptide (Ala, Val, and Thr in NbPsbO, NbPsbO1, and NbPsbO2, respectively), as a consequence of the NbPsbO PCR primer designed on the basis of *N. tabacum* PsbO (Sui et al., 2006); our construct is therefore essentially equivalent to NbPsbO2. NbPsbO1 and NbPsbO2 are presumed to have different functionality than NbPsbO3 and NbPsbO4 (Pérez-Bueno et al., 2011), as reported for AtPsbO1 and AtPsbO2 in *Arabidopsis* due to three specific amino acid differences in the C-terminal domain (Murakami et al., 2005; Lundin et al., 2007a,b). In *Arabidopsis*, PsbO2 has threefold higher GTPase activity that PsbO1, whereas PsbO1 is expressed at higher levels and supports PS II activity better under high light conditions; AtPsbO2 is also known to regulate dephosphorylation and turnover of PS II reaction center D1 protein (Lundin et al., 2007a, 2008). However, comparison of *Arabidopsis* and NbPsbO amino acid sequences shows multiple differences between both of the *Arabidopsis* proteins and all of the *N. benthamiana* homologs (Pérez-Bueno et al., 2011), such that functional differences between NbPsbO isoforms cannot be readily predicted from the sequences. Further work with different isoforms of NbPsbO will be necessary to identify possible differences in interaction with AltMV TGB3. It is possible that TGB3 may interact with all isoforms; there are limited amino acid differences between isoforms (95–96% identity), although some of these differences may affect binding between PsbO and PsbP, or GTP binding (Pérez-Bueno et al., 2011). Only one GTP motif residue, in motif G1, differentiates NbPsbO2 from the other isoforms, whereas the G2/G3 motif is identical in all isoforms, and the G4 motif is GKPE in NbPsbO1/2, and GKPD in NbPsbO3/4, as in AtPsbO1 and AtPsbO2, respectively.

The extrinsic proteins of PS II have recently been reviewed by Bricker et al. (2012): PsbO binds GTP with high affinity and functions as a GTPase; in this role it may control the phosphorylation state of D1 (the chloroplast-encoded core protein of PS II), which is coupled to efficient PS II cycling. PsbO may therefore impose important regulatory controls on photosynthesis; different isoforms may exert differential function, and depletion of one PsbO isoform may have a different effect than depletion of another. In *Arabidopsis*, PsbO1 primarily supports normal oxygen evolution, while PsbO2 regulates the phosphorylation state and turnover of D1; AtPsbO2 has substantially higher GTPase activity, while functioning poorly in support of oxygen evolution. PsbO is also generally assumed to be required for PsbP binding, while PsbP is required for the association of PsbQ to PS II. The chloroplast-encoded PS II intrinsic core protein D1 is light-regulated, and translation is controlled by signals initiated by both PS I and PS II (Trebitsh and Danon, 2001).

PsbO is nuclear-encoded, and is directed to the chloroplast by an 85-residue signal peptide which is cleaved from the mature protein prior to localization of PsbO in the thylakoid lumen. Within the thylakoid lumen, PsbO is proposed to stabilize the dimeric structure of the PS II complex, and also to bind and hydrolyze GTP. PsbO is known to dissociate from its docking site upon photoinactivation of PS II electron transport, and can be released under non-inhibitory light conditions as well as at pH 6.0 in darkness; GTP stimulates light-induced release of PsbO from inactivated PS II complexes, resulting in degradation of the PS II reaction center protein D1. GTP binding and hydrolysis occur readily in darkness, potentially releasing PsbO from the luminal surface of PS II (see Lundin et al., 2007b). The D1 protein is located in the thylakoid stromal membrane, and rapid turnover of dissociated D1 requires the incorporation of freshly synthesized D1 to rebuild PS II. PsbO is thus an important regulator of D1 protein turnover (Lundin et al., 2008), and is the minimal and most crucial luminal extrinsic component for an adequate function of water oxidation to molecular oxygen in PS II (Lundin et al., 2007b).

CAUSES AND EFFECTS OF CHLOROPLAST DAMAGE

In the current study we over-expressed multiple natural variants of AltMV TGB3 from PVX, and examined chloroplasts in leaves of plants grown either under diurnal lighting, or in continuous darkness. Whereas PVX-infected controls showed little difference between light- and dark-grown plants, all plants over-expressing AltMV TGB3 variants showed more severe symptoms than WT PVX in light conditions, and additionally caused significant chloroplast damage and tissue collapse under dark conditions. One possible explanation for this observation is that cytoplasmic interaction of TGB3 and PsbO interferes with the recruitment of fresh PsbO to the chloroplast and PS II, affecting turnover of D1, further destabilizing the thylakoids and PS II, and leading to

subsequent chloroplast disruption. Neither infection by WT PVX under either light or dark conditions, nor the over-expression of TGB3 under light conditions, is sufficient to cause severe symptoms or major chloroplast damage. The lack of light-induced expression of D1 when plants were grown in the dark, in combination with inhibition of PsbO recruitment to the thylakoids, is the probable cause of the observed severe symptoms and chloroplast destruction.

Further investigation is needed to examine the effects of these treatments on relative levels of different chloroplast proteins, and in particular on the ratios of PsbO to PsbP and PsbQ, and to D1. Differential effects on components of the PS II complex have been reported with other viruses, at least partially correlating with tobamovirus and cucumovirus symptom severity in *N. tabacum* and *N. benthamiana* (Takahashi et al., 1991; Takahashi and Ehara, 1992; Rahoutei et al., 2000; Pérez-Bueno et al., 2004; Sui et al., 2006); however, all components of the PS II complex were depleted in *N. tabacum* infected with the *flavum* (yellowing) strain of TMV (Lehto et al., 2003). Interestingly, silencing of *psbO* resulted in a 10-fold increase in TMV accumulation, whereas infection with TMV normally down-regulated PsbO mRNA levels suggesting the possibility that inhibition of the OEC and PS II optimizes conditions for infection by suppressing basal plant defense mechanisms (Abbink et al., 2002). It will be of interest to see whether VIGS of *psbO* will increase accumulation of AltMV as observed for TMV (Abbink et al., 2002), or decrease accumulation as reported with PVX when plastocyanin expression was reduced (Qiao et al., 2009), or for BaMV when *cPGK* was silenced (Lin et al., 2007).

Although over-expression of AltMV TGB3 clearly has a significant effect on chloroplast survival (causing veinal necrosis and reduced chloroplast numbers, especially under dark conditions), the mechanism is not clear. Damage to the chloroplasts may suppress the plant's basal defense mechanisms, allowing the virus to replicate unhindered; however, overall levels of virus replication appear little altered, as replication of neither AltMV nor PVX over-expressing AltMV TGB3 was obviously enhanced (Lim et al., 2010a). Whereas we have established a clear interaction between PsbO and TGB3, and demonstrated that the N-terminal domain of TGB3 is required for the interaction, we have yet to determine which domains of PsbO are involved, and exactly where the interaction occurs, as visualization at the chloroplast does not preclude PsbO from acting to transport TGB3 to the chloroplast. The N-terminal domain of TGB3 contains signals required for chloroplast localization, and mutation of VL(17,18)AR is sufficient to prevent both chloroplast attachment and to restrict movement of otherwise infectious AltMV to a few cells within the epidermis (Lim et al., 2010a), as well as essentially abolishing the BiFC interaction with PsbO (this work). It should be noted that the N-terminal domain of TGB3 containing the chloroplast localization sequence is highly constrained as it overlaps with the C-terminus of TGB2 in a different reading frame, and that the $TGB3_{VL(17,18)AR}$ mutant maintains the WT TGB2 amino acid sequence (Lim et al., 2010a). Because $TGB3_{VL(17,18)AR}$ neither localizes to the chloroplast (Lim et al., 2010a), nor interacts with PsbO, we were unable to distinguish between the possibilities that chloroplast localization of TGB3 is required for interaction with PsbO, or that PsbO interaction is necessary for targeting of TGB3 to the chloroplast. In future work we will determine whether TGB3 interacts with the PsbO signal peptide or with the mature protein.

POTENTIAL PsbO INTERACTION DOMAINS

Alignment of AtPsbO and NbPsbO variants shows that there are many differences within the signal peptide domain, except for 15 fully conserved residues immediately upstream of the cleavage site, whereas there is a high degree of identity throughout the mature PsbO peptide (Pérez-Bueno et al., 2011; and data not shown). It is therefore most likely that TGB3 interacts with the functional portion of PsbO rather than the signal peptide, although the localization of the interaction is not yet known. In contrast, it has been demonstrated that PVX CP interacts specifically with the transit peptide of plastocyanin (Qiao et al., 2009), a nuclear-encoded chloroplast protein involved in PS I and accumulating in the thylakoid lumen (Lawrence and Kindle, 1997); plastocyanin precursor protein may therefore target PVX CP to the chloroplast, but whether plastocyanin is also sufficient to act as a carrier to transport CP into the organelle is not clear (Qiao et al., 2009). Our evidence to date suggests that TGB3 remains outside the chloroplast membrane (Lim et al., 2010a). As TGB3 does not have a canonical signal sequence, it is possible that interaction of TGB3 with PsbO results in transport of TGB3 to the chloroplast, where electron microscopy suggests that invaginations result from TGB3 insertion forming protrusions into, rather than across, the chloroplast membrane (Lim et al., 2010a). It is notable that BaMV TGB3 has been shown to localize to curved domains of the cortical ER (Lee et al., 2010), and that a sorting signal critical for targeting of BaMV TGB3 to punctae within curved ER tubules has been identified; however, while BaMV TGB3 targets curved domains of the ER, it is unable to shape the ER (Wu et al., 2011).

FUNCTIONS OF VIRAL:CHLOROPLAST INTERACTIONS

The TGB proteins are often considered to interact with each other in order to transport viral RNA between cells via the plasmodesmata, supported by the ability to exchange the complete TGB to produce functional hybrid viruses, and multiple reports of co-localization of TGB2 and TGB3 (e.g., Solovyev et al., 2000; Morozov and Solovyev, 2003; Verchot-Lubicz, 2005; Samuels et al., 2007). TGB3 and the replicase of PVX have been shown to co-localize in membrane-bound spherical bodies including the ER marker BiP, at an early stage of infection (Bamunusinghe et al., 2009). More recently, PVX TGB1 has been demonstrated to reorganize actin and endomenbranes into the X-body, which was also shown to include CP, granular vesicles containing TGB2 and TGB3, and non-encapsidated viral RNA (Tilsner et al., 2012). While the presence of the replicase itself was not directly demonstrated, the TGB2/TGB3 granular vesicles have previously been associated with replicase and ribosomes (Ju et al., 2005; Bamunusinghe et al., 2009), and the X-body is presumed to be the viral replication "factory" (Tilsner et al., 2012). Whereas Golgi bodies were found within the X-bodies (Tilsner et al., 2012), the inclusion of chloroplasts was not noted. Yan et al. (2012) further examined aggregates of PVX TGB1/TGB2/TGB3, confirming the close association of the TGB proteins, without any chloroplast association. Chloroplasts were also not obviously associated with perinuclear ER-derived membrane aggregations in cells infected

with the comovirus *Cowpea mosaic virus* (CPMV; Carette et al., 2000) or the nepovirus *Grapevine fanleaf virus* (GFLV; Ritzenthaler et al., 2002).

In contrast to the situation with PVX, CPMV, and GFLV, the potyvirus TuMV has been shown to recruit ER membranes and chloroplasts sequentially through the action of 6K2-containing membranous vesicles, which aggregate and induce invaginations at the chloroplast membrane (Wei et al., 2010). Further examination of this system revealed perinuclear globular structures that included ER, Golgi bodies, COPII coatamers, and chloroplasts as well as viral proteins (Grangeon et al., 2012).

Manfre et al. (2011) summarize a number of studies suggesting that the chloroplast plays an important cellular role during viral invasion, which might include the location of viral replication, or activity in host defenses. As AltMV TGB3 is part of the viral movement complex, and AltMV replication is associated with the chloroplast (Lim et al., 2010a), both of these roles may be relevant. A number of viruses have been shown to repress expression of multiple nuclear-encoded chloroplast proteins (Dardick, 2007; Shimizu et al., 2007; Yang et al., 2007), and multiple chloroplast proteins interact with various potyviral proteins in Y2H screens, indicating that many viruses disrupt or modify chloroplast structure or function while establishing infection (Manfre et al., 2011). Whether such interactions interfere with host defenses to promote systemic susceptibility is still unclear, but it has been proposed that the chloroplast plays a critical role in host defense (Genoud et al., 2002; Griebel and Zeier, 2008) and that viral interactions with the chloroplast may interfere in defense signaling (Abbink et al., 2002; Lehto et al., 2003). Manfre et al. (2011) showed that silencing of several individual photosynthetic proteins led to increases in numbers of TuMV infection foci compared to controls, suggesting that a general effect on photosynthetic capacity or chloroplast function influences host susceptibility; infections under low light also resulted in increased numbers of infection foci and increased rate of systemic movement. Treatment with the chloroplast protein synthesis inhibitor Lin increased both numbers of foci and rate of systemic movement even under light conditions, indicating that the photosynthetic or energy-production functions of the chloroplast are essential for plant defense mechanisms (Manfre et al., 2011). Although salicylic acid (SA)-mediated host defense mechanisms are light-dependent, and SA is thought to be synthesized in the chloroplast, no direct relationship could be demonstrated between SA and numbers of TuMV infection foci; an alternative hypothesis that light and chloroplast function influence the ability of viruses to establish replication centers was considered (Manfre et al., 2011). TuMV has indeed recently been shown to establish replication complexes at the outer membrane of the chloroplast (Wei et al., 2010), as AltMV is also believed to do, in part through the interaction of TGB3 at the chloroplast (Lim et al., 2010a). The interaction of TGB3 with PsbO may thus both interfere with the host basal defenses, and establish the location for the AltMV replication complex at the chloroplast surface.

DIFFERENCES BETWEEN AltMV AND PVX

Alternanthera mosaic virus is a member of the genus *Potexvirus*, yet has several clear differences from the type member, PVX. AltMV TGB3 agroinfiltrated alone is targeted to the mesophyll and specifically to the chloroplast (Lim et al., 2010a), whereas PVX TGB3 is targeted to the ER (Ju et al., 2008), and accumulates primarily in the epidermis (Lim et al., 2010a). Fluorescence *in situ* hybridization to AltMV-infected leaf sections revealed that AltMV RNA was primarily associated with chloroplasts in the mesophyll, with little signal from either epidermis (Lim et al., 2010a), whereas PVX has no obvious reported association with chloroplasts. No beaded sheets of TGB1 are readily discernible in AltMV-infected tissue, whereas the beaded sheets of PVX TGB1 are characteristic and easily detected (e.g., Davies et al., 1993). In contrast, paracrystalline inclusions are frequently observed in both the nucleus and cytoplasm of AltMV-infected cells (J. Hammond, H.-S. Lim, and M. M. Dienelt, unpublished data) and these may represent aggregates of TGB1; GFP-TGB1 aggregates in both the cytoplasm and nucleus (Lim et al., 2010c). Further work will be required to determine whether AltMV replication complexes are indeed associated with the chloroplast rather than the nucleus (as for TYMV; Prod'Homme et al., 2001, 2003), or incorporate chloroplasts in association with the nucleus (as for TuMV; Grangeon et al., 2012). Considering the differences in subcellular localization of TGB3, in TGB2/TGB3 interactions, in TGB1 subcellular organization, and apparent sites of replication, there is much to be learned by further comparison of AltMV and PVX. It will also be of interest to further examine the host proteins interacting with the respective viral proteins, to determine the common features and further differences between these two members of the genus *Potexvirus*.

ACKNOWLEDGMENTS

We thank Margaret Dienelt for performing the electron microscopy and Dr. Autar Mattoo for useful discussions regarding the likely causes of chloroplast damage in the dark. This work supported by grants from the Next-Generation BioGreen 21 Program (PJ008063), Rural Development Administration, and the National Research Foundation of Korea (NRF No. 2012R1A1A2007417).

REFERENCES

Abbink, T. E., Peart, J. R., Mos, T. N., Baulcombe, D. C., Bol, J. F., and Linthorst, H. J. (2002). Silencing of a gene encoding a protein component of the oxygen-evolving complex of photosystem II enhances virus replication in plants. *Virology* 295, 307–319.

Bamunusinghe, D., Hemenway, C. L., Nelson, R. S., Sanderfoot, A. A., Ye, C. M., Silva, M. A. T., et al. (2009). Analysis of potato virus X replicase and TGBp3 subcellular locations. *Virology* 393, 272–285.

Beck, D. L., Guilford, P. J., Voot, D. M., Andersen, M. T., and Forster, R. L. (1991). Triple gene block proteins of white clover mosaic potexvirus are required for transport. *Virology* 183, 695–702.

Becker, D. M., Fikes, J. D., and Guarente, L. (1991). A cDNA encoding a human CCAAT-binding protein cloned by functional complementation in yeast. *Proc. Natl. Acad. Sci. U.S.A.* 88, 1968–1972.

Bragg, J. N., and Jackson, A. O. (2004). The C-terminal region of the Barley stripe mosaic virus gamma b protein participates in homologous interactions and is required for suppression of RNA silencing. *Mol. Plant Pathol.* 5, 465–481.

Bricker, T. M., Roose, J. L., Fagerlund, R. D., Frankel, L. K., and Eaton-Rye, J. J. (2012). The extrinsic proteins of Photosystem II. *Biochim. Biophys. Acta* 1817, 121–142.

Carette, J. E., Stuiver, M., Van Lent, J., Wellink, J., and Van Kammen, A. (2000). Cowpea mosaic virus infection induces a massive proliferation of endoplasmic reticulum but not Golgi membranes and is dependent on *de novo* membrane synthesis. *J. Virol.* 74, 6556–6563.

Chalcroft, J., and Matthews, R. E. (1966). Cytological changes induced by turnip yellow mosaic virus in Chinese cabbage leaves. *Virology* 28, 555–562.

Cheng, Y. Q., Liu, Z. M., Xu, J., Zhou, T., Wang, M., Chen, Y. T., et al. (2008). HC-Pro protein of sugar cane mosaic virus interacts specifically with maize ferredoxin-5 in vitro and in planta. *J. Gen. Virol.* 89, 2046–2054.

Cowan, G. H., Lioliopoulou, F., Ziegler, A., and Torrance, L. (2002). Subcellular localisation, protein interactions, and RNA binding of Potato mop-top virus triple gene block proteins. *Virology* 298, 106–115.

Dardick, C. (2007). Comparative expression profiling of *Nicotiana benthamiana* leaves systemically infected with three fruit tree viruses. *Mol. Plant Microbe Interact.* 20, 1004–1017.

Davies, C., Hills, G., and Baulcombe, D. C. (1993). Sub-cellular localization of the 25-kDa protein encoded in the triple gene block of potato virus X. *Virology* 197, 166–175.

Deng, M., Bragg, J. N., Ruzin, S., Schichnes, D., King, D., Goodin, M. M., et al. (2007). Role of the sonchus yellow net virus N protein in formation of nuclear viroplasms. *J. Virol.* 81, 5362–5374.

Esau, K., and Cronshaw, J. (1967). Relation of tobacco mosaic virus to the host cells. *J. Cell Biol.* 33, 665–678.

Feki, S., Loukili, M. J., Triki-Marrakchi, R., Karimova, G., Old, I., Ounouna, H., et al. (2005). Interaction between tobacco Ribulose-l,5-biphosphate Carboxylase/Oxygenase large subunit (RubisCO-LSU) and the PVY Coat Protein (PVY-CP). *Eur. J. Plant Pathol.* 112, 221–234.

Genoud, T., Buchala, A. J., Chua, N. H., and Métraux, J. P. (2002). Phytochrome signalling modulates the SA-perceptive pathway in Arabidopsis. *Plant J.* 31, 87–95.

Goodin, M. M., Dietzgen, R. G., Schichnes, D., Ruzin, S., and Jackson, A. O. (2002). pGD vectors: versatile tools for the expression of green and red fluorescent protein fusions in agroinfiltrated plant leaves. *Plant J.* 31, 375–383.

Granett, A. L., and Shalla, T. A. (1970). Discrepancies in the intracellular behavior of three strains of tobacco mosaic virus, two of which are serologically indistinguishable. *Phytopathology* 60, 419–425.

Grangeon, R., Agbeci, M., Chen, J., Grondin, G., Zheng, H., and Laliberté, J. F. (2012). Impact on the endoplasmic reticulum and Golgi apparatus of turnip mosaic virus infection. *J. Virol.* 86, 9255–9265.

Griebel, T., and Zeier, J. (2008). Light regulation and daytime dependency of inducible plant defenses in Arabidopsis: phytochrome signaling controls systemic acquired resistance rather than local defense. *Plant Physiol.* 147, 790–801.

Gunasinghe, U. B., and Berger, P. H. (1991). Association of potato virus Y gene products with chloroplasts in tobacco. *Mol. Plant Microbe Interact.* 4, 452–457.

Hammond, J., Reinsel, M. D., and Maroon-Lango, C. J. (2006a). Identification and full sequence of an isolate of Alternanthera mosaic potexvirus infecting Phlox stolonifera. *Arch. Virol.* 151, 477–493.

Hammond, J., Reinsel, M. D., and Maroon-Lango, C. J. (2006b). Identification of potexvirus isolates from phlox and portulaca as strains of Alternanthera mosaic virus. *Acta Hortic.* 722, 71–77.

Holmes, F. O. (1931). Local lesions of mosaic in Nicotiana tabacum L. *Contrib. Boyce Thompson Inst.* 3, 163–172.

Ivanov, P. A., Mukhamedzhanova, A. A., Smirnov, A. A., Rodionova, N. P., Karpova, O. G., and Atebekov, J. G. (2011). The complete nucleotide sequence of Alternanthera mosaic virus infecting Portulaca grandiflora represents a new strain distinct from phlox isolates. *Virus Genes* 42, 268–271.

Jiménez, I., López, L., Alamillo, J. M., Valli, A., and García, J. A. (2006). Identification of a plum pox virus CI-interacting protein from chloroplast that has a negative effect in virus infection. *Mol. Plant Microbe Interact.* 19, 350–358.

Jin, Y., Ma, D., Dong, J., Li, D., Deng, C., Jin, J., et al. (2007). The HC-pro protein of potato virus Y interacts with NtMinD of tobacco. *Mol. Plant Microbe Interact.* 20, 1505–1511.

Johansen, L. K., and Carrington, J. C. (2001). Silencing on the spot. Induction and suppression of RNA silencing in the Agrobacterium-mediated transient expression system. *Plant Physiol.* 126, 930–938.

Ju, H. J., Samuels, T. D., Wang, Y. S., Blancaflor, E., Payton, M., Mitra, R., et al. (2005). The potato virus X TGBp2 movement protein associates with endoplasmic reticulum-derived vesicles during virus infection. *Plant Physiol.* 138, 1877–1895.

Ju, H. J., Ye, C. M., and Verchot-Lubicz, J. (2008). Mutational analysis of PVX TGBp3 links subcellular accumulation and protein turnover. *Virology* 375, 103–117.

Lawrence, S. D., and Kindle, K. L. (1997). Alterations in the Chlamydomonas plastocyanin transit peptide have distinct effects on in vitro import and in vivo protein accumulation. *J. Biol. Chem.* 272, 20357–20363.

Lawson, R. H., and Hearon, S. S. (1973). Ultrastructure of Carnation etched ring virus-infected Saponaria vaccaria and Dianthus caryophyllus. *J. Ultrastruct. Res.* 48, 201–215.

Lee, S. C., Wu, C. H., and Wang, C. W. (2010). Traffic of a viral movement protein complex to the highly curved tubules of the cortical endoplasmic reticulum. *Traffic* 11, 912–930.

Lehto, K., Tikkanen, M., Hiriart, J. B., Paakkarinen, V., and Aro, E. M. (2003). Depletion of the photosystem II core complex in mature tobacco leaves infected by the flavum strain of tobacco mosaic virus. *Mol. Plant Microbe Interact.* 16, 1135–1144.

Lim, H. S., Bragg, J. N., Ganesan, U., Lawrence, D. M., Yu, J., Isogai, M., et al. (2008). Triple gene block protein interactions involved in movement of Barley stripe mosaic virus. *J. Virol.* 82, 4991–5006.

Lim, H. S., Bragg, J. N., Ganesan, U., Ruzin, S., Schichnes, D., Lee, M. Y., et al. (2009). Subcellular localization of the Barley Stripe Mosaic Virus Triple Gene Block proteins. *J. Virol.* 83, 9432–9448.

Lim, H.-S., Vaira, A. M., Bae, H., Bragg, J. N., Ruzin, S. E., Bauchan, G. R., et al. (2010a). Mutation of a chloroplast targeting signal in Alternanthera mosaic virus TGB3 impairs cell-to-cell movement and eliminates long distance virus movement. *J. Gen. Virol.* 91, 2102–2115.

Lim, H.-S., Vaira, A. M., Reinsel, M. D., Bae, H., Bailey, B. A., Domier, L. L., et al. (2010b). Pathogenicity of Alternanthera mosaic virus pathogenicity is affected by determinants in RNA-dependent RNA polymerase and by reduced efficacy of silencing suppression in a movement-competent TGB1. *J. Gen. Virol.* 91, 277–287.

Lim, H.-S., Vaira, A. M., Domier, L. L., Lee, S. C., Kim, H. G., and Hammond, J. (2010c). Efficiency of VIGS and gene expression in a novel bipartite potexvirus vector delivery system as a function of strength of TGB1 silencing suppression. *Virology* 402, 149–163.

Lin, J. W., Ding, M. P., Hsu, Y. H., and Tsai, C. H. (2007). Chloroplast phosphoglycerate kinase, a gluconeogenetic enzyme, is required for efficient accumulation of Bamboo mosaic virus. *Nucleic Acids Res.* 35, 424–432.

Lin, M. K., Hu, C. C., Lin, N. S., Chang, B. Y., and Hsu, Y. H. (2006). Movement of potexviruses requires species-specific interactions among the cognate triple gene block proteins, as revealed by a trans-complementation assay based on the bamboo mosaic virus satellite RNA-mediated expression system. *J. Gen. Virol.* 87, 1357–1367.

Lough, T. J., Netzler, N. E., Emerson, S. J., Sutherland, P., Carr, F., Beck, D. L., et al. (2000). Cell-to-cell movement of potexviruses: evidence for a ribonucleoprotein complex involving the coat protein and first triple gene block protein. *Mol. Plant Microbe Interact.* 13, 962–974.

Lundin, B., Hansson, M., Schoefs, B., Vener, A. V., and Spetea, C. (2007a). The Arabidopsis PsbO2 protein regulates dephosphorylation and turnover of the photosystem II reaction centre D1 protein. *Plant J.* 49, 528–539.

Lundin, B., Thuswaldner, S., Shutova, T., Eshaghi, S., Samuelsson, G., Barber, J., et al. (2007b). Subsequent events to GTP binding by the plant PsbO protein: structural changes, GTP hydrolysis and dissociation from the photosystem II complex. *Biochim. Biophys. Acta* 1767, 500–508.

Lundin, B., Nurmi, M., Rojas-Stuetz, M., Aro, E. M., Adamska, I., and Spetea, C. (2008). Towards understanding the functional difference between the two PsbO isoforms in Arabidopsis thaliana – insights from phenotypic analyses of psbo knockout mutants. *Photosyn. Res.* 98, 405–414.

Manfre, A., Glenn, M., Nuñez, A., Moreau, R. A., and Dardick, C. (2011). Light quantity and photosystem function mediate host susceptibility to Turnip mosaic virus via a salicylic acid-independent mechanism. *Mol. Plant Microbe Interact.* 24, 315–327.

McClintock, K., Lamarre, A., Parsons, V., Laliberté, J. F., and Fortin, M. G. (1998). Identification of a 37 kDa plant protein that interacts with the turnip mosaic potyvirus capsid protein using anti-idiotypic-antibodies. *Plant Mol. Biol.* 37, 197–204.

Morozov, S. Y., and Solovyev, A. G. (2003). Triple gene block: modular design of a multifunctional machine for plant virus movement. *J. Gen. Virol.* 84, 1351–1366.

Murakami, R., Ifuku, K., Takabayashi, A., Shikanai, T., Endo, T., and Sato, F.

(2005). Functional dissection of two Arabidopsis PsbO proteins: PsbO1 and PsbO2. *FEBS J.* 272, 2165–2175.

Nam, J., Jang, C., Li, M., Kim, H., Cho, S., Kim, H., et al. (2012). Alternanthera mosaic virus TGB1 interaction with chloroplast β ATPase is necessary for viral replication. *Phytopathology* 102(Suppl. 4), S4.85.

Pérez-Bueno, M. L., Barón, M., and García-Luque, I. (2011). PsbO, PsbP, and PsbQ of photosystem II are encoded by gene families in *Nicotiana benthamiana*. Structure and functionality of their isoforms. *Photosynthetica* 49, 573–580.

Pérez-Bueno, M. L., Rahoutei, J., Sajnani, C., García-Luque, I., and Barón, M. (2004). Proteomic analysis of the oxygen-evolving complex of photosystem II under biotec stress: studies on *Nicotiana benthamiana* infected with tobamoviruses. *Proteomics* 4, 418–425.

Petty, I. T., Hunter, B. G., Wei, N., and Jackson, A. O. (1989). Infectious barley stripe mosaic virus RNA transcribed in vitro from full-length genomic cDNA clones. *Virology* 171, 342–349.

Prod'Homme, D., Jakubiec, A., Tournier, V., Drugeon, G., and Jupin, I. (2003). Targeting of the turnip yellow mosaic virus 66K replication protein to the chloroplast envelope is mediated by the 140K protein. *J. Virol.* 77, 9124–9135.

Prod'Homme, D., Le Panse, S., Drugeon, G., and Jupin, I. (2001). Detection and subcellular localization of the turnip yellow mosaic virus 66K replication protein in infected cells. *Virology* 281, 88–101.

Qiao, Y., Li, H. F., Wong, S. M., and Fan, Z. F. (2009). Plastocyanin transit peptide interacts with Potato virus X coat protein, while silencing of plastocyanin reduces coat protein accumulation in chloroplasts and symptom severity in host plants. *Mol. Plant Microbe Interact.* 22, 1523–1534.

Rahoutei, J., García-Luque, I., and Barón, M. (2000). Inhibition of photosynthesis by viral infection: effect on PSII structure and function. *Physiol. Plant.* 110, 286–292.

Reinero, A., and Beachy, R. N. (1986). Association of TMV coat protein with chloroplast membranes in virus-infected leaves. *Plant Mol. Biol.* 6, 291–301.

Ritzenthaler, C., Laporte, C., Gaire, F., Dunoyer, P., Schmitt, C., Duval, S., et al. (2002). Grapevine fanleaf virus replication occurs on endoplasmic reticulum-derived membranes. *J. Virol.* 76, 8808–8819.

Samuels, T. D., Ju, H. J., Ye, C. M., Motes, C. M., Blancaflor, E. B., and Verchot-Lubicz, J. (2007). Subcellular targeting and interactions among the Potato virus X TGB proteins. *Virology* 367, 375–389.

Schepetilnikov, M. V., Manske, U., Solovyev, A. G., Zamyatnin, A. A. Jr., Schiemann, J., and Morozov, S. Y. (2005). The hydrophobic segment of Potato virus X TGBp3 is a major determinant of the protein intracellular trafficking. *J. Gen. Virol.* 86, 2379–2391.

Schoelz, J. E., and Zaitlin, M. (1989). Tobacco mosaic virus RNA enters chloroplasts in vivo. *Proc. Natl. Acad. Sci. U.S.A.* 86, 4496–4500.

Shi, Y., Chen, J., Hong, X., Chen, J., and Adams, M. J. (2007). A potyvirus P1 protein interacts with the Rieske Fe/S protein of its host. *Mol. Plant Pathol.* 8, 785–790.

Shimizu, T., Satoh, K., Kikuchi, S., and Omura, T. (2007). The repression of cell wall- and plastid-related genes and the induction of defense-related genes in rice plants infected with Rice dwarf virus. *Mol. Plant Microbe Interact.* 20, 247–254.

Solovyev, A. G., Stroganova, T. A., Zamyatnin, A. A. Jr, Fedorkin, O. N., Schiemann, J., and Morozov, S. Y. (2000). Subcellular sorting of small membrane-associated triple gene block proteins: TGBp3-assisted targeting of TGBp2. *Virology* 269, 113–127.

Sui, C., Fan, Z., Wong, S.-M., and Li, H. (2006). Cloning of cDNAs encoding the three subunits of oxygen evolving complex in *Nicotiana benthamiana* and gene expression changes in tobacco leaves infected with Tobacco mosaic virus. *Physiol. Mol. Plant Pathol.* 68, 61–68.

Takahashi, H., and Ehara, Y. (1992). Changes in the activity and the polypeptide composition of the oxygen-evolving complex in photosystem II of tobacco leaves infected with cucumber mosaic virus strain Y. *Mol. Plant Microbe Interact.* 5, 269–272.

Takahashi, H., Ehara, Y., and Hirano, H. (1991). A protein in the oxygen-evolving complex in the chloroplast is associated with symptom expression on tobacco leaves infected with cucumber mosaic virus strain Y. *Plant Mol. Biol.* 16, 689–698.

Tilsner, J., Linnik, O., Wright, K. M., Bell, K., Roberts, A. G., Lacomme, C., et al. (2012). The TGB1 movement protein of Potato virus X reorganizes actin and endomembranes into the X-body, a viral replication factory. *Plant Physiol.* 158, 1359–1370.

Torrance, L., Cowan, G. H., Gillespie, T., Ziegler, A., and Lacomme, C. (2006). Barley stripe mosaic virus-encoded proteins triple-gene block 2 and gamma-b localize to chloroplasts in virus-infected monocot and dicot plants, revealing hitherto-unknown roles in virus replication. *J. Gen. Virol.* 87, 2403–2411.

Trebitsh, T., and Danon, A. (2001). Translation of chloroplast psbA mRNA is regulated by signals initiated by both photosystems II and I. *Proc. Natl. Acad. Sci. U.S.A.* 98, 12289–12294.

Tyagi, A., Hermans, J., Steppuhn, J., Jansson, C., Vater, F., and Herrmann, R. G. (1987). Nucleotide sequence of cDNA clones encoding the complete "33 kDa" precursor protein associated with the photosynthetic oxygen-evolving complex from spinach. *Mol. Gen. Genet.* 207, 288–293.

Ushiyama, R., and Matthews, R. E. (1970). The significance of chloroplast abnormalities associated with infection by turnip yellow mosaic virus. *Virology* 42, 293–303.

Vaira, A. M., Lim, H. S., Bauchan, G. R., Owens, R. A., Natilla, A., Dienelt, M. M., et al. (2012). Lolium latent virus (Alphaflexiviridae) coat proteins: expression and functions in infected plant tissue. *J. Gen. Virol.* 93, 1814–1824.

Verchot-Lubicz, J. (2005). A new cell-to-cell transport model for Potexviruses. *Mol. Plant Microbe Interact.* 18, 283–290.

Waadt, R., Schmidt, L. K., Lohse, M., Hashimoto, K., Bock, R., and Kudla, J. (2008). Multicolor bimolecular fluorescence complementation reveals simultaneous formation of alternative CBL/CIPK complexes in planta. *Plant J.* 56, 505–516.

Wei, T., Huang, T. S., McNeil, J., Laliberté, J. F., Hong, J., Nelson, R. S., et al. (2010). Sequential recruitment of the endoplasmic reticulum and chloroplasts for plant potyvirus replication. *J. Virol.* 84, 799–809.

Wu, C. H., Lee, S. C., and Wang, C. W. (2011). Viral protein targeting to the cortical endoplasmic reticulum is required for cell-cell spreading in plants. *J. Cell Biol.* 193, 521–535.

Xiang, Y., Kakani, K., Reade, R., Hui, E., and Rochon, D. (2006). A 38-amino-acid sequence encompassing the arm domain of the cucumber necrosis virus coat protein functions as a chloroplast transit peptide in infected plants. *J. Virol.* 80, 7952–7964.

Yan, F., Lu, Y., Lin, L., Zheng, H., and Chen, J. (2012). The ability of PVX p25 to form RL structures in plant cells is necessary for its function in movement, but not for its suppression of RNA silencing. *PLoS ONE* 7:e43242. doi:10.1371/journal.pone.0043242

Yang, C., Guo, R., Jie, F., Nettleton, D., Peng, J., Carr, T., et al. (2007). Spatial analysis of Arabidopsis thaliana gene expression in response to Turnip mosaic virus infection. *Mol. Plant Microbe Interact.* 20, 358–370.

Zhang, C., Liu, Y., Sun, X., Qian, W., Zhang, D., and Qiu, B. (2008). Characterization of a specific interaction between IP-L, a tobacco protein localized in thylakoid membranes, and Tomato mosaic virus coat protein. *Biochem. Biophys. Res. Commun.* 374, 253–257.

Conflict of Interest Statement: The authors declare that the research was conducted in the absence of any commercial or financial relationships that could be construed as a potential conflict of interest.

Received: 14 October 2012; accepted: 08 January 2013; published online: 31 January 2013.

Citation: Jang C, Seo E-Y, Nam J, Bae H, Gim YG, Kim HG, Cho IS, Lee Z-W, Bauchan GR, Hammond J and Lim H-S (2013) Insights into Alternanthera mosaic virus TGB3 functions: interactions with Nicotiana benthamiana PsbO correlate with chloroplast vesiculation and veinal necrosis caused by TGB3 overexpression. Front. Plant Sci. ***4****:5. doi: 10.3389/fpls.2013.00005*

This article was submitted to Frontiers in Plant-Microbe Interaction, a specialty of Frontiers in Plant Science.

frontiers in
PLANT SCIENCE

ORIGINAL RESEARCH ARTICLE
published: 24 December 2012
doi: 10.3389/fpls.2012.00290

The potato mop-top virus TGB2 protein and viral RNA associate with chloroplasts and viral infection induces inclusions in the plastids

Graham H. Cowan[1], Alison G. Roberts[1], Sean N. Chapman[1], Angelika Ziegler[2], Eugene I. Savenkov[3] and Lesley Torrance[1]*

[1] *The James Hutton Institute, Invergowrie, Dundee, Scotland, UK*
[2] *Federal Research Centre for Cultivated Plants, Julius Kühn Institute, Institute for Epidemiology and Pathogen Diagnostics, Quedlinburg, Germany*
[3] *Department of Plant Biology and Forest Genetics, Swedish University of Agricultural Sciences, Uppsala, Sweden*

Edited by:
Aiming Wang, Agriculture and Agri-Food Canada, Canada

Reviewed by:
John Hammond, United Stated Department of Agriculture, USA
Ching-Hsiu Tsai, National Chung Hsing University, Taiwan

Correspondence:
Lesley Torrance, Cell and Molecular Sciences, The James Hutton Institute, Invergowrie, Scotland, DD2 5DA, UK.
e-mail: lesley.torrance@hutton.ac.uk

The potato mop-top virus (PMTV) triple gene block 2 (TGB2) movement proteins fused to monomeric red fluorescent protein (mRFP-TGB2) was expressed under the control of the PMTV subgenomic promoter from a PMTV vector. The subcellular localizations and interactions of mRFP-TGB2 were investigated using confocal imaging [confocal laser-scanning microscope, (CLSM)] and biochemical analysis. The results revealed associations with membranes of the endoplasmic reticulum (ER), mobile granules, small round structures (1–2 μm in diameter), and chloroplasts. Expression of mRFP-TGB2 in epidermal cells enabled cell-to-cell movement of a TGB2 defective PMTV reporter clone, indicating that the mRFP-TGB2 fusion protein was functional and required for cell-to-cell movement. Protein-lipid interaction assays revealed an association between TGB2 and lipids present in chloroplasts, consistent with microscopical observations where the plastid envelope was labeled later in infection. To further investigate the association of PMTV infection with chloroplasts, ultrastructural studies of thin sections of PMTV-infected potato and *Nicotiana benthamiana* leaves by electron microscopy revealed abnormal chloroplasts with cytoplasmic inclusions and terminal projections. Viral coat protein (CP), genomic RNA and fluorescently-labeled TGB2 were detected in plastid preparations isolated from the infected leaves, and viral RNA was localized to chloroplasts in infected tissues. The results reveal a novel association of TGB2 and vRNA with chloroplasts, and suggest viral replication is associated with chloroplast membranes, and that TGB2 plays a novel role in targeting the virus to chloroplasts.

Keywords: PMTV, TGB2, viral RNA, replication, chloroplasts, inclusions

INTRODUCTION

Plant viral genomes are relatively small and most comprise positive-sense, single-stranded RNAs that encode a few multi-functional proteins. RNA viruses replicate in association with various cellular membranes including those of the endoplasmic reticulum (ER), mitochondria, peroxisomes, vacuole, and chloroplasts (reviewed by Ahlquist et al., 2003; Salonen et al., 2005; Harries et al., 2010; Laliberté and Sanfaçon, 2010). Targeting of viral replication machinery to particular compartments by virus-encoded, non-structural proteins that associate with specific organellar membranes, can lead to the formation of membrane-bound, cytosolic viral replication complexes (VRCs). For those viruses, such as potato mop-top virus (PMTV), where the coat protein (CP) is not required for cell-to-cell or systemic movement (Torrance et al., 2009), different membranes may be involved in replication and movement of the viral ribonucleoprotein (vRNP) complex and virions. In addition, plant viruses encode one or more movement proteins to facilitate the spread of infection throughout the plant (reviewed by Lucas, 2006; Taliansky et al., 2008; Schoelz et al., 2011). It is becoming apparent that some movement proteins are multi-functional, playing additional roles in virus replication, counter defense and pathogenicity, as well as in viral genome transport (Scholthof, 2005; Lucas, 2006; Torrance et al., 2006).

PMTV, the type species of the genus *Pomovirus* is a tubular rod-shaped virus with a tripartite, positive-sense, single-stranded, RNA genome. The PMTV genome contains a module of three overlapping open reading frames (ORFs) encoding the triple gene block proteins (TGB), that are required for virus movement. The TGB module is found in nine genera of plant viruses and previously was classified into two broad groups: potex-like and hordei-like (reviewed by Morozov and Solovyev, 2003). However, research has shown that there are some differences in functional properties and this has led to a revision and re-classification into three groups: potex, hordei, and pomovirus (Verchot-Lubicz et al., 2010). The TGB of PMTV represents the Pomovirus group. In all groups, the three TGB movement proteins act in a coordinated manner, and all are required for cell-to-cell and systemic movement of the viral genomes. The hordei- and pomo-like TGB viruses are differentiated from the potex-like viruses by their

larger TGB1 containing an N-terminal domain of variable mass in addition to the helicase domain, the TGB3 which contains two predicted transmembrane domains and the CP is not needed for systemic movement. Furthermore, there is increasing evidence that there are subtle differences in the sub-cellular localizations of the TGB proteins between the hordei-, pomo-, and potex-like groups which may indicate differences in functional roles (Haupt et al., 2005; Ju et al., 2005, 2007; Verchot-Lubicz, 2005; Torrance et al., 2006; Lim et al., 2009; Tilsner et al., 2010; Wright et al., 2010). In this paper we focus on the pomovirus PMTV TGB2. The current model for the coordinated action of the TGB proteins is that TGB1 interacts with viral RNA, forming a ribonucleoprotein vRNP movement complex that exits the cell, and that the TGB1/vRNP complex requires the integral membrane proteins TGB2 and TGB3 for localization to the plasma membrane and plasmodesmata (PD; Zamyatnin et al., 2004; Lucas, 2006; Lim et al., 2008; Verchot-Lubicz et al., 2010). Studies using TGB2 and TGB3 fused to fluorescent proteins and expressed from the cauliflower mosaic virus 35S (35S) promoter have revealed that they co-localize in cellular membranes and mobile granules and utilize the actin-ER network to facilitate movement to the cell periphery and PD (Gorshkova et al., 2003; Haupt et al., 2005). PMTV TGB2 and TGB3 contain vesicle-targeting and PD-targeting signals respectively, enabling them to associate with components of the endocytic pathway (Haupt et al., 2005; Tilsner et al., 2010). Although TGB2 and TGB3 can both increase the size exclusion limit (SEL) of PD, there is no evidence that they are independently capable of trafficking between cells (Haupt et al., 2005). The properties of PMTV TGB2 differ from those of hordeivirus TGB2 proteins reported to date in that it binds RNA in a sequence non-specific manner (Cowan et al., 2002) but is not required for RNA replication, can increase PD SEL independently (Haupt et al., 2005), and it associates with components of the endosomal network (Haupt et al., 2005).

There have been many reports of plastids as possible sites of virus replication. The turnip mosaic potyvirus (TuMV) has been shown to sequentially recruit the ER and chloroplasts for genome replication, and the 6K protein, which induces ER-derived vesicles, viral RNA and replicase components have all been found associated with invaginations of the plastid envelope (Jakubiec et al., 2004; Wei et al., 2010). Chloroplasts are also amalgamated into perinuclear bodies containing other organelles and viral proteins in TuMV-infected tissue (Grangeon et al., 2012). For turnip yellow mosaic virus (TYMV), virus particles, the replicase protein, CP and viral RNA have all been found associated with cytoplasmic inclusions that form at the periphery of chloroplasts and have been proposed to be the sites of RNA replication and viral encapsidation (Ushiyama and Matthews, 1970; Hatta et al., 1973; Hatta and Matthews, 1974, 1976; Prod'homme et al., 2001, 2003). Barley stripe mosaic virus (BSMV), closely related to PMTV, also causes invaginations in chloroplast membranes which contain virions (Carroll, 1970; McMullen et al., 1978) and viral proteins TGB2 and γb (Torrance et al., 2006), suggesting that plastids are possible sites of BSMV replication and virion assembly (Lin and Langenberg, 1984, 1985). The TGB3 protein of *Alternanthera* mosaic virus (AltMV) has also been shown to target to chloroplasts and the targeting is required for both efficient cell-to-cell and long-distance movement of that virus (Lim et al., 2010). Ultrastructural changes and production of peripheral vesicles in chloroplasts have also been found for a wide range of other plant viruses although direct evidence of viral replication or assembly has not always been detected.

To date, the published experimental data describe the localizations of PMTV TGB2 when expressed from the 35S promoter. This paper presents results of localization studies of proteins expressed from a viral subgenomic promoter in a virus context and establishes the functionality of the mRFP-TGB2 fusion protein in facilitating cell-to-cell movement. The confocal laser-scanning microscopy results are supported by biochemical and ultra-structural studies of PMTV-infected tissues which reveal that PMTV infection induces chloroplast abnormalities and that viral CP, RNA, and TGB2 are associated with chloroplasts. Collectively, the results allow us to hypothesize that chloroplasts may be sites of virus replication and possibly encapsidation, and that TGB2 may play a role in directing movement of both viral RNP complexes and virions.

MATERIALS AND METHODS

PLANT MATERIAL

Nicotiana benthamiana plants were grown from virus-free seed stocks maintained at The James Hutton Institute (JHI, UK) and sown in 10 cm diameter pots in a compost mix containing: 66% (v/v) Irish moss peat, 28% (v/v) Vermiculite, 6% (v/v) Pavoir sand, 0.14% (w/v) magnesium limestone, 0.14% (w/v) calcium limestone, 0.17% (w/v) Sincrocell controlled release fertilizer (William Sinclair Horticulture Ltd, Lincoln, UK), 0.08% (w/v) Osmocote Start fertilizer (Scotts, Humberside, UK) and 0.03% (w/v) Celcote wetting agent (LBS Horticulture, Lancashire, UK) and growth of plants was maintained in a glasshouse with a daytime temperature of 26°C and night time of 22°C. The daytime light intensity varied between 400 and 1000 μmol m^{-2} sec^{-1} with a mean day length of 16 h. Transgenic *N. benthamiana* plants expressing ER-targeted GFP (35S::mGFP5ER-HDEL) were a gift from Jim Haseloff (Haseloff et al., 1997) and grown under the same conditions as above.

TRANSIENT EXPRESSION PLASMIDS

The 35S::mRFP-TGB2 vector used by Haupt et al. (2005) contained the gene encoding PMTV TGB2 fused to the 3′-end of the mRFP ORF and placed under control of the 35S promoter in the plasmid vector pRTL2. This plasmid was modified to prevent expression of the N-terminal portion of TGB3 by mutating the AUG initiation codon of the overlapping TGB3 ORF to ACG. A fusion of green fluorescent protein (GFP) to aspartate aminotransferase (GFP-AAT) was used as a marker for the plastid stroma (Kwok and Hanson, 2004).

INFECTIOUS CLONES AND TRANSCRIPT PREPARATION

Full-length cDNA clones of the three genomic RNAs of a Swedish isolate of PMTV ($PMTV_{Sw}$), named pPMTV-1, pPMTV-2, and pPMTV-3 (Savenkov et al., 2003) were used to produce run-off transcripts as follows: *Mlu*I-linearized (pPMTV-1 and pPMTV-2) or *Spe*I-linearized (pPMTV-3) plasmid DNA was used as template

in the RiboMax Large Scale RNA Production System (Promega). The transcripts were mixed with an equal volume of GKP buffer (50 mM Glycine, 30 mM K_2HPO_4, 3% (w/v) celite, 3% (w/v) bentonite) and mechanically inoculated onto leaves of 4-week old *N. benthamiana* plants. Three weeks post inoculation the systemically-infected leaves were examined or used as sources of inoculum.

EXPRESSION OF GFP-TGB2 FROM A TMV VECTOR

The recombinant TMV vector GFP-TGBp2 (Cowan et al., 2002) was used to infect 4-week old *N. benthamiana* plants. At 6 days post inoculation (dpi) systemically-fluorescing leaves were sampled and used for plastid preparation (see later).

PLASMID CONSTRUCTION TO CREATE PMTV REPORTER AND MUTANT CLONES

The plasmid pPMTV-3 (Savenkov et al., 2003; see above) was used to generate the constructs described in this study. To demonstrate that a 400 nt fragment upstream of the TGB2 gene could function as a subgenomic promoter for expression of a reporter protein, the putative subgenomic promoter fragment and YFP gene were inserted downstream of the TGB3 gene to produce pPMTV3.sgP2::YFP. First *Nco*I and *Apa*I restriction enzyme sites were inserted downstream of the TGB3 gene through PCR. The resulting plasmid was digested with *Nco*I and *Apa*I and ligated to a *Nco*I/*Apa*I-digested YFP PCR product obtained using primers (1) (5′-GCCACCATGGTGAGCAAGGGCGAGGAGC-3′) and (2) (5′-AAAGGGCCCTTACTTGTACAGCTCGTCCA-3′) to yield pPMTV3.YFP. Finally, an *Nco*I-digested PCR product, encompassing the putative subgenomic promoter (1361–1745 nt in RNA3), obtained using primers (3) (5′-CTGCCAT*GGATCC*GATTTGGTAAAGCTACAGC-3′) and (4) (5′-GGACCATGGCTGTCTGTTTGTGGTTGC-3′), was cloned into *Nco*I-digested pPMTV3.YFP. The correct orientation of the putative subgenomic promoter was verified using a unique *Bam*HI restriction site (in italics, above). Inoculation of RNA transcripts onto *N. benthamiana* leaves resulted in detectable YFP fluorescence, demonstrating that the putative subgenomic promoter was functional. To generate an RNA-based replicon with enhanced stability, the plasmid pPMTV3.sgP2::YFP was digested with *Mlu*I and *Bam*HI (removing a portion of the TGB1 gene and all of the TGB2 and TGB3 genes) prior to blunting and self-ligation to yield the replicon plasmid pR3.TGB1(5′).sgP2::YFP.

To substitute a mRFP-TGB2 gene fusion for the YFP gene, a *Nco*I/*Apa*I-digested mRFP-TGB2 PCR product, generated with primers (5) (5′-CGACCATGGCCTCCTCCGAGGACGTC-3′) and (6) (5′-TTTGGGCCCTCTAGATTAACCTCCATATGAC-3′), was cloned into *Nco*I/*Apa*I-digested pR3.TGB1 (5′).sgP2::YFP to produce pR3.sgP2::mRFP-TGB2. Subsequently, the start codon of the TGB1 gene was removed to prevent expression of a truncated TGB1. The 5′-UTR was amplified with primers (7) (5′-AAAGGTACCTAACAAGGAATCGTGAAACAATT-3′) and M13-Reverse, and digested with *Sac*I/*Kpn*I prior to cloning into *Sac*I/*Apa*I-digested pR3.sgP2::mRFP-TGB2 with a *Kpn*I/*Apa*I-digested PCR product comprising the entire cassette (5′ end of the TGB1 gene, subgenomic promoter and mRFP-TGB2 gene fusion) obtained with primers (6) (see above) and (8) (5′-AAAGGTACCGAAAGCGCATTCAACGGAAG-3′). The resulting plasmid, pR3.ΔATG.sgP2::mRFP-TGB2, was used in mRFP-TGB2 localization studies.

To construct pPMTV-3.YFP-TGB1, the plasmid pPMTV-3.GFP-TGBp1 (Zamyatnin et al., 2004) was digested with *Nco*I to remove the GFP gene and ligated to a *Nco*I-digested YFP PCR product obtained using primers (1) (see above) and (9) (5′-AAACCATG*GATCC*CTTGTACAGCTCGTCCATG-3′). The correct orientation of the YFP gene was verified using a unique *Bam*HI restriction site (in italic, above).

Primers PMTV13MutF (5′-CCGGCCAATATTAATTTGGTCGCGC-3′) and PMTV13MutR (5′-GCGCGACCAAATTAATATTGGCCGG-3′) were used to prepare the construct pPMTV-3.YFP-TGB1.ΔTGB2, in which the A at nucleotide 37 in the TGB2 coding sequence was converted to a T. This created an in-frame UAA stop codon and prevented expression of TGB2 without interfering with expression of TGB1 or TGB3.

MICROPROJECTILE BOMBARDMENT

Plasmid DNA and RNA transcripts were introduced into leaf epidermal cells by bombardment of gold particles as described previously by Haupt et al. (2005).

AGROBACTERIUM-BASED TRANSIENT EXPRESSION

The binary vector pGreen0229 (Hellens et al., 2000) was modified by insertion of the T-DNA cassette from pRTL2 to produce pGRAB (Petra Boevink, unpublished). The mRFP-TGB2 gene fusion was cloned into pGRAB for transformation of *Agrobacterium tumefaciens* strain LBA4404. Bacterial cultures were grown and, after testing across a wide range of optical densities ($OD_{600} = 0.01$–0.5) all of which gave the same phenotype, the cells were suspended at $OD_{600} = 0.2$ in 10 mM MES (pH 5.5), 10 mM $MgCl_2$ containing 0.15 mM acetosyringone for 1 h at room temperature (∼22°C) before infiltration through stomata on the abaxial surface of *N. benthamiana* source leaves.

CONFOCAL LASER-SCANNING MICROSCOPY

Confocal images were obtained using a Leica TCS SP2 spectral confocal laser-scanning microscope (CLSM) equipped with water-dipping lenses. GFP and YFP were excited at 488 nm, and emission collected between 505–530 and 515–535 nm, respectively. mRFP was excited at 561 nm and emission collected between 580–600 nm. Chlorophyll autofluorescence was excited at 488 nm and emission collected between 660–700 nm. Simultaneous imaging of GFP and mRFP fusions, or YFP and mRFP-fusions was possible, but imaging of chlorophyll in combination with mRFP was always performed sequentially.

CLSM IMAGE DECONVOLUTION

For deconvolution, images were collected using an active Z-galvo attachment for the Leica SP2 CLSM, 512 × 512 pixel resolutions and a voxel size of approximately 75 nm to suit the XY resolution of the Leica HCX PL APO 63x water-dipping lens. Images were recorded using a Z-step size equivalent to 0.5–1 times the z-resolution of the objective lens. Point spread functions (PSF) were calculated for each fluorophore by imaging fluorescent beads

with appropriate fluorescent characteristics (PS-Speck microscope point source kit; Molecular Probes) and processing the data using Amira 3D visualization software (Mercury Computer Systems Inc.). Deconvolution of the images was also carried out using Amira software, utilizing the appropriate PSFs. Multiple-channel, 3D deconvolved images were separated into single channels and transferred to Adobe Photoshop (Adobe Corporation) software to create the 2D projections shown in **Figure 3**.

PLASTID PREPARATIONS

Four week old *N. benthamiana* plants were inoculated with $PMTV_{Sw}$ and maintained in a growth cabinet providing a 14 h, 18°C light period with light intensity of 145 μmol m^{-2} s^{-1}, and a 10 h, 15°C dark period. Plastids were isolated essentially as described by Nivison et al. (1986) from plants 14–20 dpi following a 24 h dark period. Briefly, 1 g of leaves was triturated in seven volumes of grinding buffer (0.35 M Sorbitol, 0.05 M HEPES-KOH pH 7.5, 2 mM EDTA, 0.5 mM $MgCl_2$, 1 mM DTT, 10 mg/mL BSA) and filtered through muslin. The extract was centrifuged at 1000× g for 3 min (Eppendorf centrifuge 5417R; rotor F45-30-11) and the resulting pellets suspended in a total of 1 ml Sorbitol medium (0.35 M Sorbitol, 35 mM HEPES-KOH pH 8.3, 10 mM K_2HPO4, 0.5 mM $MgCl_2$, 1 mM DTT). A 0.5 ml aliquot of the preparation was layered onto a gradient comprising 1 ml of 40% and 1 ml 85% [v/v] Percoll (prepared in 40 mM HEPES-KOH pH 7.5, 0.05 mM $MgCl_2$, 0.35 M Sorbitol, 1 mM DTT) and centrifuged at 13,000× g for 7 min. The intact plastids were recovered from the interface between the 40% and 85% layers of Percoll, and a fraction containing broken chloroplasts was recovered from a single band in the 40% Percoll fraction. The plastid samples were washed twice by dilution with five volumes of Sorbitol medium and centrifugation at 4000× g for 5 min. The pellet containing the plastids was finally suspended in 0.5 ml Sorbitol medium.

WESTERN BLOTS

Samples of leaf extracts and plastid preparations were mixed with an equal volume of Laemmli buffer and electrophoresed in a 12.5% SDS-PAGE gel. The separated proteins were electroblotted onto Hybond ECL nitrocellulose (GE Healthcare) and the membrane subsequently incubated with antibody preparations essentially as described previously (Torrance, 1992) using the immunoglobulin fraction of a PMTV antiserum (Torrance et al., 1993) at 2 μg ml^{-1} and an anti-rabbit alkaline phosphatase conjugate (Sigma product no A8025) as the second antibody.

RT-PCR

Total RNA was extracted from leaf or plastid samples using the RNeasy Plant Mini Kit (Qiagen) following the manufacturer's instructions. First strand PMTV RNA1 cDNA was synthesized with the reverse primer (5′-CGATCGTGTCTTGATCGCAGC-3′) using one microgram of total RNA. The resulting cDNA was used as template (2 μl of a 1:10 and 1:100 dilution in a 25 μl reaction) in a PCR with the reverse primer (above) and forward primer 5′-CTTGTGGGAGAAGTCGCAGTG-3′ to amplify a product of 1057 bp.

DETECTION OF NEGATIVE-STRAND RNA ASSOCIATED WITH CHLOROPLASTS

Chloroplasts were isolated from PMTV-Swe-infected and non-infected *N. benthamiana* leaves and counted using a haemocytometer. Aliquots containing 4, 2, 1, 0.5, or 0.25 × 10^7 chloroplasts were taken and total RNA extracted using the RNeasy Kit (Qiagen) then 10 μl used as template to prepare cDNA using M-MLV reverse transcriptase (Promega) with 10 pmol of primer Nested1 (5′-GTGAATGCGATACTTCACAC-3′) in 20 μl reaction. 2 μl of cDNA was used as template in a 50 μl PCR reaction comprising 1× Green GoTaq Reaction buffer (Promega), 0.2 μM of primer Nested2 (5′CACTTACGCTATGAAGTGTG-3′) and 0.2 μM of primer Nested3 (5′-GTCACATACAACATCAACGAG-3′), 0.2 mM dNTPs, 2.5 mM $MgCl_2$, and 2.5 μl of GoTaq DNA Polymerase (Promega). The PCR conditions were 95°C for 2 min, then 30 cycles of 95°C for 30 s, 55°C for 30 s, 70°C for 30 s, followed by 70°C for 10 min. 2 μl of this reaction were used as template for a second PCR with primers Nested6 (5′-GACATCTTCAGTGCACAGAGG-3′) and Nested7 (5′-GTAAAACCCATTGACGCTAGG-3′) using the conditions 95°C for 2 min, then 35 cycles of 95°C for 30 s, 55°C for 30 s, 70°C for 30 s, followed by 70°C for 10 min. These PCR products were electrophoresed in 2% agarose gels and then stained with ethidium bromide.

In-situ RNA HYBRIDISATION

RNA probes were created by cloning a 950 bp fragment from the 3′ UTR of PMTV RNA1 into the pGEMT-Easy vector. PCR screening was used to identify clones containing the sequence in both orientations such that both sense and antisense RNA probes could be produced by running off transcripts from the T7 promoter, ensuring comparable quantity and quality of both probes. The *in-situ* hybridization protocol was a modified version of that used by Drea et al. (2005), brief details of which follow.

Tissue was fixed in 4% paraformaldehyde in PEM buffer (0.1 M PIPES pH 6.95, 1 mM EGTA, 1 mM $MgSO_4$), dehydrated through an ethanol series and then into xylene before being infiltrated with and then embedded in Paramat Extra wax (VWR International, Lutterworth, UK). Chloroplasts were prepared as previously described and embedded in 1% Agar No.1 (Oxoid Ltd., Basingstoke, UK) before being fixed and processed in parallel to the plant tissue. Tissue and chloroplasts were sectioned to 10 μm thick and mounted on Polysine slides (Menzel–Glaser, Braunschweig, Germany) before being de-waxed and pre-treated as follows: two washes in PBS buffer, two washes in Histoclear (Fisher Scientific, Loughborough, UK), for 20 min each; 100% ethanol for 10 min, then through a 95, 85, 50, and 30%, ethanol series (2 min each); PBS for 3–4 min; proteinase K treatment (2–3 μg/mL in 100 mM Tris and 10 mM EDTA, pH 7.5) for 30 min at 37°C; Glycine (0.2%, w/v) in PBS for 2 min; PBS for 3–4 min; acetic anhydride (0.5% [v/v] in 0.1 M triethanolamine, pH 8.0) for 10 min; PBS for 3–4 min; and then back through 30, 50, 85, 95, and 100% ethanol. Slides were dried at room temperature and stored at 4°C until hybridization.

In vitro transcription was performed for 2 h at 37°C incorporating digoxigenin-UTP nucleotides (0.35 mM), using T7 RNA polymerase (Promega) in the presence of 100 mM DTT, RNAsin

and 200 ng of PCR product as the DNA template. (The plasmid templates were cut using restriction enzyme *Pvu*II and then amplified using M13 forward and reverse primers). RNA probes were hydrolyzed immediately in 100 mM carbonate buffer, (60 mM Na_2CO_3, 40 mM $NaHCO_3$, pH 10.2), at 60°C for 30 min to reduce the probe to ∼200 bp fragments, and products were precipitated in 2.5 M ammonium acetate and three volumes of 100% ethanol for 1 h at 4°C. Following precipitation, transcripts were diluted in four times the volume of the original transcription reaction in RNAse-free water. To assess the incorporation of digoxigenin-UTP, probes were diluted and one microliter was spotted on nitrocellulose for a dot blot and processed as follows: 30 min in blocking buffer (Sigma–Aldrich, St. Louis, MO); 30 min in anti-digoxigenin–alkaline phosphatase-conjugated antibody (Roche, Herts, UK; diluted 1/5000 in TBS); 5-min wash in Tris-buffered saline (TBS; 10 mM Tris and 250 mM NaCl); 5 min in alkaline phosphatase buffer (100 mM Tris, 100 mM NaCl, pH 9.5, and 50 mM $MgCl_2$); and developed in alkaline phosphatase buffer containing nitroblue tetrazolium (0.1 mg/mL) and 5-bromo-4-chloro-3-indolyl phosphate salt (0.075 mg/mL) for ∼10 min.

Hybridization chambers (Grace Biolabs) were applied securely to the slides (after pretreatment). The probes were diluted 100 times in hybridization solution (300 mM NaCl, 10 mM Tris, pH 6.8, 10 mM $NaPO_4$, 5 mM EDTA, 50% [v/v] formamide, 5% [w/v] dextran sulfate, 0.5 mg/mL tRNA, 1× Denhardt's solution) and introduced into the chambers at 55°C after being heated to 85°C for 2 min to denature the probe. Hybridization was performed overnight in a 55°C incubator.

Chambers were removed and the slides were washed as follows: three 1 h washes in 0.2 × SSC (1 × SSC is 0.15 M NaCl and 0.015 M sodium citrate) at 50°C with constant agitation; 10 min in 1 × TBS at room temperature. The slides were then transferred into racks for anti-digoxigenin staining as follows: 1% blocking solution (Roche) in TBS for 1 h; 1 × TBS containing a 1:2500 dilution of anti-digoxigenin–alkaline phosphatase and 0.025% [v/v] Tween-20 for 2 h; four 10 min washes in 1 × TBS; and 5 min in alkaline phosphatase buffer (0.1 M Tris, 0.1 M NaCl, and 50 mM $MgCl_2$, pH 9.5). Then, the color reaction was developed in alkaline phosphatase buffer containing nitroblue tetrazolium (0.1 mg/mL) and 5-bromo-4-chloro-3-indolyl phosphate-*p*-toluidine salt (0.075 mg/mL) for up to 6 h. Slides were then washed several times in water to stop the reaction before being dried.

If necessary, tissue was lightly counterstained with 0.25% Alcian Blue 8GX (Sigma–Aldrich, Dorset, UK) in 3% acetic acid to show cellular structure before being mounted in DPX mountant (Sigma–Aldrich, Dorset, UK) under glass coverslips. Representative sections for each probe were photographed with a Leica DC500 digital camera on a Nikon Optiphot microscope under bright-field conditions.

PROTEIN-LIPID OVERLAY BLOTS

Protein lipid overlay assays were done using Membrane Lipid Strips™ (Echelon Biosciences Inc.) following the manufacturer's instructions. Briefly, blocked membranes were incubated overnight with up to 20 μg/mL preparations of either thioredoxin-TGB2 or thioredoxin (Cowan et al., 2002). The membranes were then incubated for 1 h with anti-thioredoxin-TGB2 rabbit polyclonal antiserum (Cowan et al., 2002) diluted to 1 μg/mL, followed by anti-rabbit horseradish peroxidase (HRP) conjugate (Invitrogen Ltd.) diluted 1:1000 and visualized with HRP ECL™ substrate (GE Healthcare) according to the manufacturer's instructions.

TRANSMISSION ELECTRON MICROSCOPY (EM)

Source material was obtained from PMTV-infected *N. benthamiana* plants with yellowing symptoms that had been maintained in the controlled environment conditions described above. Small segments of leaves were fixed, dehydrated and embedded in Araldite resin (Agar Scientific) as described by Taylor et al. (2000). In addition, leaves were taken from naturally infected potato, *cv* Scarborough, showing aucuba (yellow mosaic) symptoms which had tested positive for PMTV in ELISA and EM examination failed to detect the presence of any other virus. Segments of potato leaf were fixed and dehydrated as described in Oparka et al. (1999), and embedded in LR White resin (Agar Scientific). Ultrathin sections of both *N. benthamiana* and potato were mounted on pyroxylin-coated nickel grids, post-stained with uranyl acetate and lead citrate as described by Roberts (2002), and examined in a Jeol 1200EX electron microscope.

RESULTS

EXPRESSION OF mRFP-TGB2 IN EPIDERMAL CELLS FROM A MODIFIED VIRUS VECTOR

Previously, we studied the localization of mRFP-TGB2 expressed in epidermal cells from the 35S promoter following biolistic bombardment of plasmid DNA (Haupt et al., 2005) and we have confirmed these observed localizations through *Agrobacterium*-mediated expression (unpublished results). To investigate whether the localizations we observed were influenced by over-expression from the 35S promoter, the mRFP-TGB2 fusion protein was expressed from a PMTV vector (see **Figure 1** for a schematic of all constructs used in this study). A region of the PMTV TGB genetic module containing the putative subgenomic promoter for TGB2 and TGB3 was identified. A cDNA clone was modified to delete the ORFs and a mRFP-TGB2 fusion gene inserted downstream of the putative subgenomic promoter sequence. RNA transcripts from this construct were bombarded with RNA1 onto *N. benthamiana* leaves. In these experiments, the virally-expressed fusion protein was observed in epidermal cells, indicating that the promoter was functional. The distribution of the virally-expressed, red fluorescent TGB2-fusion protein was the same as when expressed from the 35S promoter revealing associations at first with membranes of the ER (**Figure 2A**) and mobile granules and later, the membranes of two populations of small (**Figure 2B**) and larger, ∼4 μm diameter, vesicular structures as reported previously (Haupt et al., 2005).

mRFP-TGB2 COMPLEMENTS VIRUS MOVEMENT

We previously showed that the mRFP-TGB2 fusion protein could function to increase the SEL of PD (Haupt et al., 2005). To test whether the mRFP-TGB2 could also complement virus movement, a PMTV reporter construct that expressed yellow

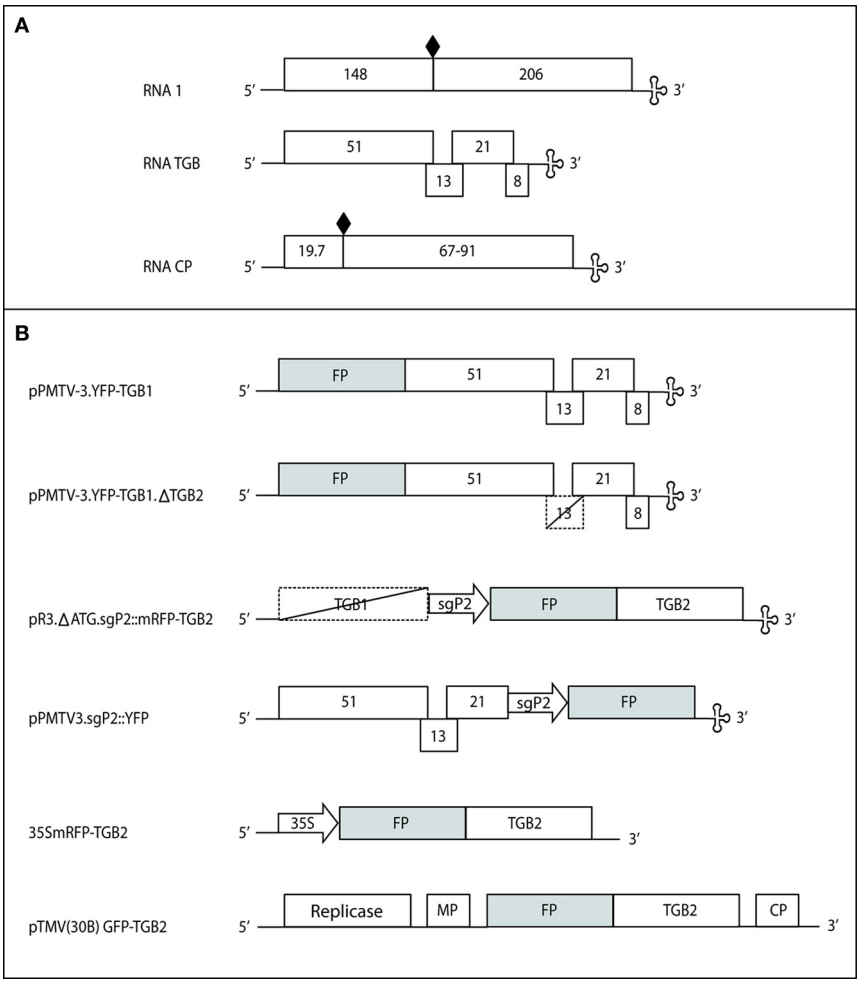

FIGURE 1 | PMTV genome (A) and constructs derived from RNA TGB (B). The viral RNA1 encodes the 148K replication protein and the 206K read-through (RT) product. RNA TGB encodes the three overlapping TGB proteins (51K, 13K, and 21K) and an 8K cysteine-rich protein. RNA CP encodes the 19.7K coat protein and its RT domain. Diamonds, leaky termination codons; clover-leaf motif, tRNA-like structure; solid boxes, expressed ORFs, dashed boxes, non-expressed ORFs, promoters are shown in arrows, FP, fluorescent protein. The 35S mRFP-TGB2 diagram shows the gene fusion expressed from the plasmid pRTL2 (used for microprojectile bombardment) or the binary vector pGRAB (used for *Agrobacterium*-mediated transient expression).

fluorescent protein (YFP) fused to the N-terminus of TGB1 (PMTV-3.YFP-TGB1) was prepared. When transcripts of this construct were inoculated together with RNA1, small, spreading, fluorescent lesions, ∼12 cells in size, were visible at 2 dpi (**Figure 2C**) and had spread to more than a hundred cells by 7 dpi. A derivative construct, PMTV-3.YFP-TGB1.ΔTGB2, was prepared in which a stop codon was introduced to prevent translation of TGB2. Inoculation of RNA transcripts from this derivative with RNA1 resulted in single fluorescent cells (**Figure 2D**), movement out of the initial cell never occurred, confirming that TGB2 is required for movement but not for replication. To test the functionality of the mRFP-TGB2 fusion protein, *N. benthamiana* leaves were infiltrated with *Agrobacterium* containing the binary vector with the 35S::mRFP-TGB2 cassette prior to bombardment of RNA transcripts of PMTV-3.YFP-TGB1.ΔTGB2 into the infiltrated area. Cells expressing both fusion proteins were rarely detected; a total of 27 cells in three experiments. Most of these cells showed aggregated (and probably non-functional) mRFP-TGB2 protein, but in the nine cells without aggregation the YFP reporter clone moved out of the initial cell (9/27 cells), often showing a halo surrounding the initial cell and occasionally moving over several cell boundaries (**Figures 2E,F**). These experiments indicate that mRFP-TGB2 can functionally complement for the TGB2 deletion in the mutated clone PMTV-3.YFP-TGB1.ΔTGB2.

mRFP-TGB2 LOCALISES TO THE CHLOROPLAST ENVELOPE

CLSM imaging revealed that the mRFP-TGB2, expressed from either the binary vector or a viral replicon, was localized in the bounding membrane of two populations of vesicles; one approximately 1–2 μm in diameter and a second population of ∼4 μm diameter vesicle-like compartments (Haupt et al., 2005). In the present study we investigated the 4 μm diameter structures in more detail. The vesicles were excited using 488 nm light and

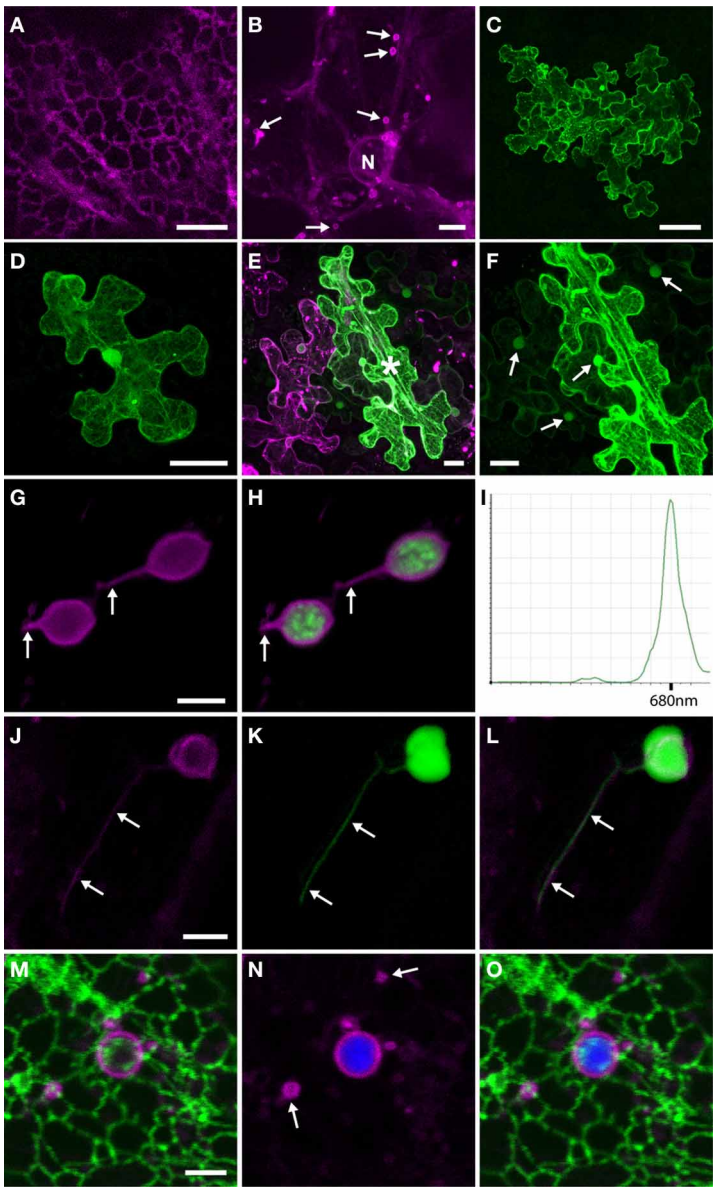

FIGURE 2 | Transient expression of TGB2 protein in epidermal cells. **(A)** Expression of sg::mRFP-TGB2 (magenta) from a PMTV vector in epidermal cells of *N. benthamiana*. Fluorescence is first visible throughout the ER network (typically 1 dpi). Bar = 10 μm. **(B)** Slightly later in the infection process (typically 2 dpi) than seen in **(A)**, mRFP-TGB2 labels the membranes of small mobile vesicles that are 2 μm in diameter (arrows). Bar = 10 μm. **(C)** Expression of PMTV reporter clone PMTV3.YFP-TGB1 in epidermal cells of *N. benthamiana* at 2 dpi; YFP fluorescence (green) is seen throughout a small lesion consisting of ∼12 cells. Bar = 50 μm. **(D)** Expression of PMTV reporter clone PMTV3.YFP-TGB1ΔTGB2 in epidermal cells of *N. benthamiana*. In the absence of a functional TGB2, the viral reporter clone (YFP fluorescence) is confined to a single cell. Bar = 20 μm. **(E)** Expression of PMTV reporter clone PMTV3.YFP-TGB1ΔTGB2 (green) in epidermal cells of *N. benthamiana* that are expressing 35S::mRFP-TGB2 (magenta); YFP fluorescence has spread out of the initial cell (marked with *) to surrounding cells; YFP can be seen in the cytosol and accumulated in the nuclei of neighboring cells. Bar = 10 μm. **(F)** Enlarged portion of the YFP signal shown in **(E)** to show the movement of the fluorescence out of the initial cell, and the accumulation of this YFP in nuclei of neighboring cells (arrowed). Bar = 10 μm. **(G,H)** Expression of sg::mRFP-TGB2 from PMTV vector in epidermal cells of *N. benthamiana*. Red fluorescence (magenta) is localized to the chloroplast envelope. Stromules are arrowed. Chlorophyll autofluorescence is shown in green in **(H)**. Bar in G = 4 μm for **(G** and **H)**. **(I)** The emission spectrum of the contents of a 4 μm diameter vesicle labeled with mRFP-TGB2 shows a peak at 680 nm (emission range shown is from 495 to 755 nm). **(J,K,L)** Co-expression of 35S::mRFP-TGB2 (magenta; **J**) with GFP-AAT (green; **K**) in a chloroplast in an epidermal cell of *N. benthamiana*. TGB2 is present in the membrane of the chloroplast and the stromule **(J)**, while GFP is visible throughout the stroma of both plastid and stromule **(K)**. The stromule is arrowed in each image and **(L)** shows an overlay of the two channels. Bar in J = 4 μm for **(J–L)**. **(M,N,O)** To ensure that the ER membrane was not contributing to the fluorescence seen on the chloroplast membrane, 35S::mRFP-TGB2 (magenta) was expressed in mGFP5-ER (green) transgenic *N. benthamiana*. The green ER does not surround the chloroplasts and the plastids sit internal to the cortical ER network. Strands of ER can be seen to cross the surface of the chloroplasts **(M** and **O)**. The membranes of both 2 μm diameter vesicles (arrows) and a 4 μm diameter chloroplast are labeled with mRFP-TGB2 **(M–O)**, with the chlorophyll autofluorescence from the interior of the plastid shown in blue **(N** and **O)**. Bar in M = 4 μm for **(M–O)**.

scanned over a wavelength range of 495–755 nm. We found mRFP fluorescence located in the membrane (**Figures 2G,H**) and the emission spectrum of the contents was found to match that of chlorophyll A (maximum at 680 nm; **Figure 2I**). Furthermore, when mRFP-TGB2 was co-expressed with GFP-aspartate aminotransferase (GFP-AAT; a marker for the plastid stroma), mRFP-TGB2 was seen to surround GFP fluorescence that was within the compartment. mRFP-TGB2 was also associated with GFP in stromules (**Figures 2J–L**), indicating that mRFP-TGB2 associates with membranes of the chloroplast envelope. It was noted that in the experiments where mRFP-TGB2 was expressed from the viral subgenomic promoter, the localization to chloroplasts occurred later than when expressed from the 35S promoter; typically 1–2 dpi from the 35 s promoter but 3–4 dpi from the viral promoter.

To eliminate the possibility that the mRFP-TGB2 fluorescence was in the ER surrounding the chloroplast, rather than in the chloroplast envelope, 35S::mRFP-TGB2 was expressed in transgenic *N. benthamiana* plants expressing ER-localized GFP (mGFP5-ER-HDEL; Haseloff et al., 1997). In these experiments, GFP was clearly associated with the ER network and, though in close proximity to the mRFP-TGB2-labeled vesicles, did not co-localize with the vesicle membrane (**Figures 2M–O**). The different fluorescent signals were also clearly distinguished when viewed over time (supplementary **Figure 1**; Movie).

To clarify further the relationship of TGB2 with chloroplasts, 3-dimensional image stacks were acquired using microscope settings that allow deconvolution, giving improved image resolution. Following deconvolution, the structures of the chlorophyll-containing vesicles were more clearly resolved; the internal autofluorescence was located in thylakoids and grana stacks, confirming these structures were chloroplasts (**Figures 3A–C**). Furthermore, it was clear from the deconvolved image stacks that, although the mRFP-TGB2 labeling was most intense on the peripheral membrane of the chloroplasts, there was some signal from within the plastid (**Figures 3A,C**), indicating that some TGB2 was also present inside chloroplasts. Deconvolution of these images also showed that the ER network is still faintly labeled with mRFP-TGB2 (arrows in **Figure 3A**) when the protein begins to accumulate in plastids; something that was not visible previously, and similarly, small bright spots could be distinguished on the ER network in the deconvolved image. These latter objects are assumed to be the mobile granules typically found early in infection (see Haupt et al., 2005), as they are the same size, but, like the ER network, have reduced in fluorescence intensity to a level undetectable without deconvolution at the later time point when TGB2 protein accumulates in chloroplasts.

PMTV RNA, CP, AND TGB2 WERE DETECTED IN PLASTID PREPARATIONS FROM *N. benthamiana* LEAVES

To investigate whether the chloroplast association occurred in the context of a natural viral infection, plastid preparations were made from leaves of uninfected and virus-infected *N. benthamiana* plants. Two fractions were obtained from Percoll step gradients; intact chloroplasts and a fraction containing membranes from disrupted plastids and other cellular membranes (membrane fraction). Western blots of the preparations revealed the presence of PMTV CP in samples of both the intact plastids (**Figure 3D** lane 3) and membrane fractions (also containing disrupted plastid membranes; **Figure 3D** lane 1); the band relating to the CP is arrowed. However, TGB2 could not be detected in these samples using antiserum prepared against TGB2 (data not shown).

Total RNA was prepared from each of the fractions and RT-PCR revealed the presence of viral genomic RNA in both intact plastids (**Figure 3E**, lanes 9 and 10) and membrane fractions (**Figure 3E**, lanes 11 and 12) as well as in total leaf extracts (**Figure 2E**, lanes 7 and 8). No viral RNA or CP was detected in negative control preparations from non-infected leaves (**Figure 3E**, lanes 1–6).

Chloroplasts were isolated from systemically-infected leaves of *N. benthamiana* infected with the tobacco mosaic virus (TMV) vector expressing GFP-TGB2 (Cowan et al., 2002). Western blot analysis of extracts from the isolated chloroplasts with the TGB2-specific antiserum failed to detect TGB2 accumulation. However, CLSM imaging of the intact isolated chloroplasts revealed that ∼5% of chloroplasts were labeled with GFP-TGB2 (**Figure 3F**) although this is likely to be an underestimation because large starch grains in infected plastids cause them to rupture during chloroplast preparation, making it difficult to isolate infected plastids intact. Deconvolved image stacks of these isolated chloroplasts reconfirmed that the fluorescent TGB2 fusion protein was associated with the bounding membranes of the plastids (**Figure 3G**). Furthermore, these higher resolution images revealed that a small amount of TGB2-associated fluorescence was also present inside the plastids, as was chlorophyll autofluorescence (**Figures 3G,H**). In combination, these results suggest that the available TGB2 antiserum is not sensitive enough to detect the chloroplast-associated TGB2. In control experiments, plastid preparations from PMTV-infected mGFP5-ER-HDEL *N. benthamiana* plants did not show any green fluorescence in the chloroplast envelope (**Figure 3I**) and western blots were negative for the presence of HDEL (a marker for the ER; **Figure 3J**), confirming that the TGB2 protein (**Figure 3F**) was indeed associated with the chloroplast envelope and not contaminating ER membranes.

DETECTION OF PMTV NEGATIVE STRAND RNA IN CHLOROPLASTS

In order to determine whether viral replication was occurring at chloroplasts, RT-PCR was used to detect the viral replicative intermediate, negative strand RNA in chloroplasts isolated from PMTV-Swe-infected plants. Non-infected *N. benthamiana* leaves were used as a negative control. No negative strand RNA was detected in healthy control chloroplasts, but was detected in each sample of PMTV-infected chloroplasts (**Figure 3K**) indicating that replication of viral RNA occurs in association with chloroplasts.

In-situ VIRAL RNA LOCALISATION

To further confirm the presence of viral RNA at chloroplasts, *in-situ* RNA labeling of PMTV-Swe-infected *N. benthamiana* leaves and isolated chloroplast preparations was conducted. Antisense and sense DIG-labeled RNA probes, designed to hybridize to and detect viral genomic RNA and the replicative

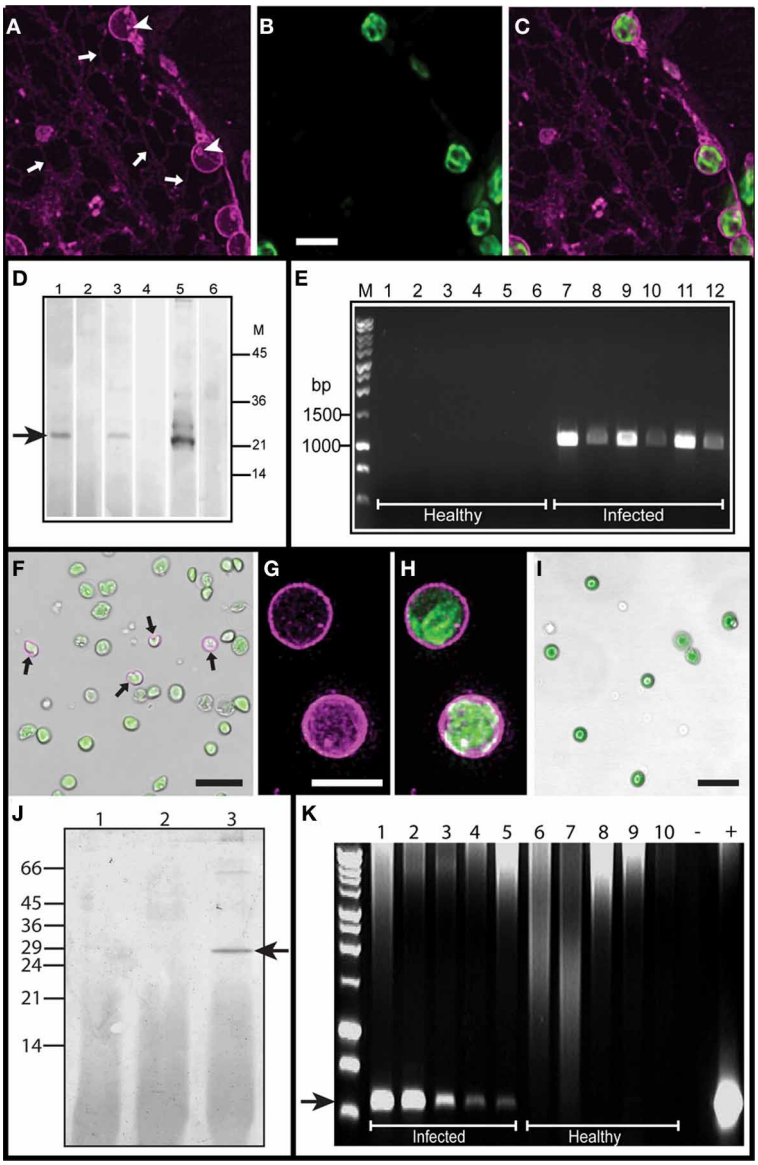

FIGURE 3 | Analysis of TGB2 protein associated with chloroplasts. **(A,B,C)** Deconvolved images showing mRFP-TGB2 (in magenta; **A**) in the membrane of chloroplasts, in strands of the ER network (arrows) and in small bodies on the ER. Chlorophyll autofluorescence is shown in green **(B)**. TGB2 is also present at a low level in the stroma of the chloroplasts and in some foci on the surface of the plastids (arrowheads; **A**). **(C)** shows an overlay of **(A)** and **(B)**. Bar in B = 5 μm for **(A–C)**. **(D)** Western blot of plastid preparations from PMTV-infected (lanes 1, 3, 5) and non-infected (lanes 2, 4, 6) *N. benthamiana* leaves; the blot was reacted with anti-PMTV CP serum. Lanes 1 and 2, disrupted plastids and membrane fraction; lanes 3 and 4, intact plastids and lanes 5 and 6, non-fractionated preparation. Reaction with CP arrowed; the positions of the size markers (kDa) indicated on right. **(E)** RT-PCR of plastid preparations from non-infected (lanes 1–6) and PMTV-infected (lanes 7–12) *N. benthamiana* leaves. Total RNA was prepared from leaves (lanes 1, 2, 7, 8), intact plastid fraction (lanes 3, 4, 9, 10) or disrupted plastid and membrane fraction (lanes 5, 6, 11, 12). cDNA preparations from each sample were tested at dilutions of 1/10 and 1/100. Size markers indicated on the left. **(F)** False transmission and fluorescence image overlay of plastid preparation from *N. benthamiana* leaves infected with the TMV vector expressing GFP-TGB2. Chlorophyll autofluorescence is shown in green, while GFP-TGB2 on the plastid membrane is shown in magenta. ~5% of all plastids showed TGB2 in the outer membrane (arrows). Bar = 15 μm. **(G,H)** Higher magnification and deconvolved images of purified plastids labeled with GFP-TGB2 expressed from the TMV vector. The TGB2 signal is visible on the membrane and in small internal speckles (magenta; **G** and **H**) while the chlorophyll signal (green; **H**) is located in the thylakoids. Bar in G = 5 μm for **(G** and **H)**. **(I)** False transmission and fluorescence image overlay of plastid preparation from mGFP5-ER-HDEL *N. benthamiana* leaves. Chlorophyll autofluorescence is shown in green. No GFP fluorescence was detected in association with the plastid envelope. Bar = 15 μm. **(J)** Detection of ER proteins retained in chloroplast preparations from transgenic *N.benthamiana* expressing mGFP5-ER-HDEL. Western blot of disrupted plastid and membrane fraction (lane 1), intact chloroplasts (lane 2) and whole leaf extract (lane 3) reacted with anti-HDEL monoclonal antibody. The positions of molecular mass markers (kDa) are indicated to the left of the blot. **(K)** Detection of negative strand PMTV RNA1 in chloroplasts. Lanes 1–5 represent products amplified in RT-PCR from templates derived from PMTV-infected chloroplasts (4,2,1,0.5 and 0.25 × 10^7 chloroplasts, respectively). Lanes 6–10 are controls showing no amplification from healthy chloroplasts (4,2,1,0.5 and 0.25 × 10^7 chloroplasts, respectively). "−" represents a no template PCR control; "+" represents a positive control PCR reaction. The size of the arrowed DNA molecular mass marker (M) is 500 bp.

intermediate respectively, were first tested on healthy and PMTV-infected leaf tissue. No viral RNA was detected using either probe in healthy tissue (data not shown). The sense probe did not detect any replicative intermediate (negative strand) RNA in sections of PMTV-infected leaf midrib and lamina (**Figure 4A**), but on adjacent serial sections, the antisense probe showed the presence of viral RNA in all infected cells. PMTV was found in a patchy manner throughout the tissue, but especially in the leaf lamina (**Figures 4B** and **C**), and although not high-resolution images, these micrographs suggested the probe was associated with chloroplasts.

Viral genomic RNA was also detected in association with isolated chloroplasts; eighty random fields of labeled chloroplasts were selected and between 2 and 15% of plastids in each field

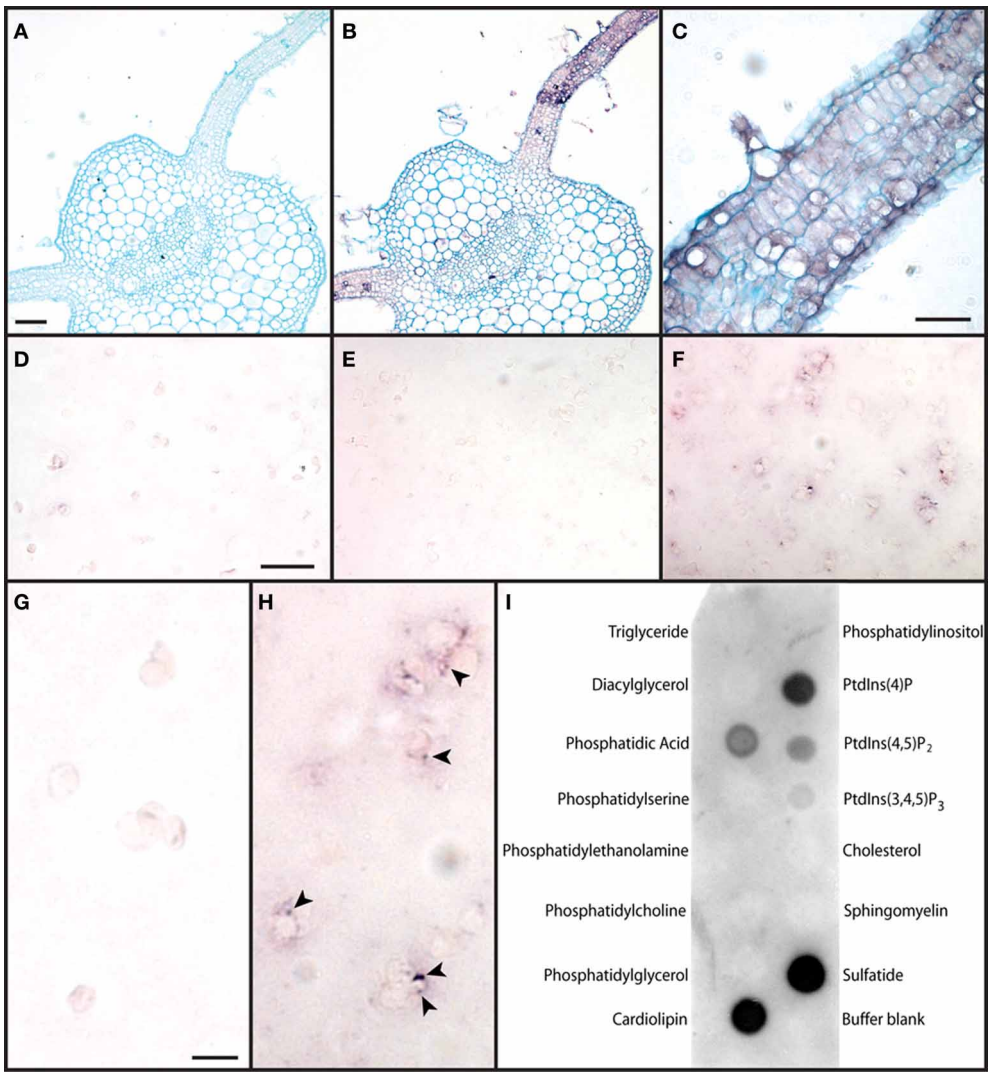

FIGURE 4 | Association of PMTV RNA with chloroplasts and TGB2 with lipids. (A) PMTV 3′UTR DIG-labeled sense RNA probe did not detect any viral RNA in a section of leaf infected with PMTV as shown by the lack of purple precipitate. The tissue has been counterstained with Alcian Blue to show cell structure. (Bar = 250 μm for **A** and **B**). **(B)** PMTV 3′UTR DIG-labeled antisense RNA probe detected viral RNA in the leaf lamina and in some parenchyma cells associated with the vascular trace in the midrib of the leaf, as shown by purple-coloration of infected cells with replicating virus. The tissue has been counterstained with Alcian Blue to show cell structure. **(C)** A higher magnification image of the tissue shown in **(B)** to show the purple coloration associated with viral RNA in many cell types in a patch of PMTV-infected leaf lamina (Bar = 100 μm). **(D)** Chloroplasts from control, healthy tissue did not label strongly with the PMTV DIG-labeled antisense probe showing that there was little non-specific labeling with this probe (Bar in D = 20 μm for **D–F**). **(E)** Chloroplasts from PMTV-infected tissue did not label strongly with the PMTV DIG-labeled sense probe showing that, if present, the viral negative strand RNA which is produced as a replicative intermediate was present at levels too low to be detected. **(F)** Chloroplasts from PMTV-infected tissue and labeled with the PMTV DIG-labeled antisense probe showed viral genomic RNA associated with the plastid membrane. Small purple spots can be seen in many chloroplasts in this image. **(G,H)** Show higher-magnification images of portions of **(D)** and **(F)** respectively. Some of the spots of viral RNA associated with the plastid membrane are marked with arrowheads in **(H)**. (Bar in G = 5 μm for **G** and **H**). **(I)** Membrane blot showing TGB2 interactions with a number of lipids. The strongest reactions were obtained with cardiolipin and sulfatide, but PtdIns(4)P, Phosphatidic acid, PtdIns(4,5)P_2 and PtdIns(3,4,5)P_3 also showed interactions of decreasing intensity with TGB2.

showed the presence of positive-strand RNA. The PMTV antisense probe did not react strongly with chloroplasts from healthy tissue (**Figures 4D** and **G**), nor did the sense probe with chloroplasts from PMTV-infected tissue (**Figure 4E**), but viral genomic RNA was associated with chloroplasts from PMTV-infected tissue as detected by the antisense probe (**Figures 4F** and **H**). In these chloroplasts the RNA appeared to be in punctate spots associated with the periphery of the chloroplasts (arrows in **Figure 4H**).

PROTEIN-LIPID ASSAYS

Since mRFP-TGB2 interacts with a number of different subcellular compartments we wanted to ascertain the specificity of membrane targeting. Membrane lipid arrays were incubated with preparations of recombinant thioredoxin-TGB2 fusion protein, which was subsequently detected with antiserum raised to the fusion protein. The results showed that TGB2 interacted with 6 of the 15 lipids tested: cardiolipin, 3-sulfogalactosylceramide (sulfatide), phosphatidic acid and the phosphoinositides PtdIns(4)P, PtdIns(4,5)P_2, and PtdIns(3,4,5)P_3. Reproducible results were obtained using TGB2 at either 20 $\mu g ml^{-1}$ or 2 $\mu g ml^{-1}$, and a representative assay is shown in **Figure 4I**. No reactions were seen in controls where the arrays were incubated with thioredoxin followed by the thioredoxin-TGB2 antiserum and anti-rabbit HRP, showing the binding was TGB2-specific (data not shown).

ELECTRON MICROSCOPY OF INFECTED PLANTS REVEALS THE PRESENCE OF ABNORMAL CYTOPLASMIC INCLUSIONS IN CHLOROPLASTS

Previous electron microscopical reports of PMTV infection have not shown detailed cytological effects of the virus and so ultra-structural studies were used to investigate the physical effects of virus infection on chloroplasts. Tissue samples from leaves of healthy or virus-infected *N. benthamiana* plants were fixed and embedded, and thin sections were examined in the electron microscope. PMTV infections in leaves typically have a low titre of virions and viral spread is sparse and patchy within leaves; tissue was sampled from uninfected leaves and infected leaves showing yellowing symptoms. The most marked difference between the samples was the presence of multiple large starch grains in chloroplasts in infected leaves, while chloroplasts in healthy leaves had none or a few small starch grains (**Figures 5A** and **B**). The chloroplasts showed extensive deformation and often had large cytoplasmic inclusions (**Figures 5B–D**) and abnormal terminal projections (**Figure 5D**). These inclusions occurred most frequently at the ends of chloroplasts and often encompassed organelles such as mitochondria (**Figures 5B** and **C**). The frequency of chloroplasts with inclusions and terminal projections was more prevalent in older infected tissue with yellow mosaic symptoms than in younger infected tissue. Such abnormalities were not found in uninfected tissue. The form of the cytoplasmic inclusions was assessed by examination of serial ultra-thin sections. They were found to be spheroidal in shape, with diameters of about 0.5–1 μm, but were also not true inclusions; rather they were flask-shaped, cytoplasmic invaginations, each being connected to the external cytoplasm by a narrow opening (**Figures 5C**,**E**,**F**). The incidence of virus particles in infected tissue was very low and particles were not observed in the flask-shaped invaginations.

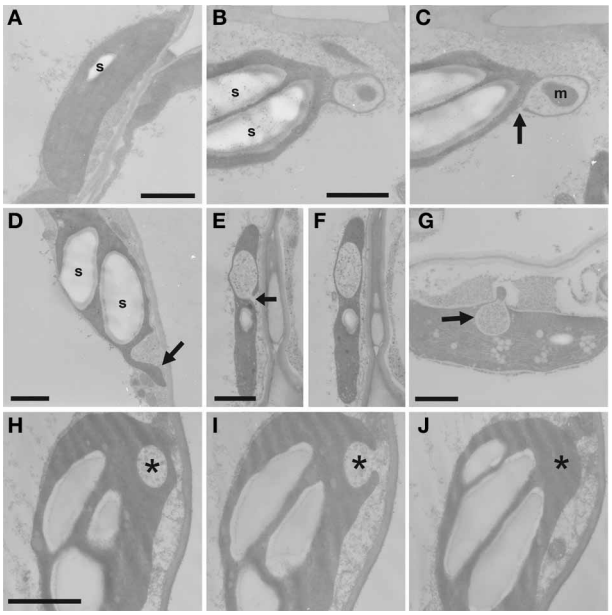

FIGURE 5 | Ultrastructural effects of PMTV infection on chloroplasts. Transmission electron microscope images of thin sections from a healthy N. *benthamiana* plant **(A)**, PMTV-infected *N. benthamiana* plants **(B–F)** and *S. tuberosum* cv. Scarborough **(G–J)**, the sections show ultrastructural changes in chloroplasts. **(A)** Example of a typical chloroplast from an uninfected *N. benthamiana* plant containing a single small starch grain (s). Bar = 1 μm. **(B,C)** Sequential sections through a distorted chloroplast, from a PMTV-infected plant, containing large starch grains (s) and with a terminal, cytoplasmic inclusion encompassing a mitochondrion (m): in **(B)** the inclusion appears enclosed, while in **(C)** it appears open with the aperture to the cytoplasm marked with an arrow. Bar in B = 1 μm for (**B** and **C**). **(D)** Chloroplast containing large starch grains (s) and with an abnormal, terminal extension (marked with arrow). Bar = 1 μm **(E,F)** Serial sections through a chloroplast of an epidermal cell with a cytoplasmic inclusion: the inclusion appears open in **(E)** (aperture marked with an arrow) and enclosed in **(F)**. Bar in E = 1 μm for **(E** and **F). (G)** Chloroplast with large cytoplasmic inclusion (marked with an arrow) from PMTV-infected potato plant. Bar = 1 μm. **(H,I,J)** Serial sections through a chloroplast from a potato plant infected with PMTV: in **(H)**, the inclusion (*) appears enclosed, while it is open in **(I)** and missing from **(J)**, indicating the open flask-shaped nature of these inclusions. (Bar in H = 1 μm for **H–J**).

Ultra-structural studies were also carried out on leaf tissue from the natural host, potato. As in the experimental host, the most pronounced abnormality was the presence of multiple, large starch grains in chloroplasts and some contained cytoplasmic inclusions (**Figure 5G**), which were most frequently found at the ends of chloroplasts. Examination of serial sections from infected potato tissue showed that these inclusions were also spheroidal and connected to the ground cytoplasm by a cytoplasmic bridge (**Figures 5H–J**).

DISCUSSION

It was previously shown that PMTV mRFP-TGB2 and GFP-TGB3 when expressed from a 35S promoter co-localized in cellular membranes and mobile granules, utilizing the ER-actin network

to facilitate movement to the cell periphery and PD. In addition, TGB2 and TGB3 associated with components of the endocytic pathway. The SEL was also increased in cells expressing either protein, suggesting that both proteins can interact with, and functionally gate, PD (Haupt et al., 2005). In this study the distribution of mRFP-TGB2 was examined after expression from a modified PMTV vector under the control of a viral subgenomic promoter to investigate whether the observed localizations were reproducible in a virus context. Identical results were obtained with the different expression systems used and a more detailed analysis of the images of the ∼4 μm-diameter spherical structures first published in Haupt et al. (2005) where they were simply referred to as large vesicles, revealed that they were chloroplasts. This finding was surprising because chloroplasts are typically ovoid or disc-shaped organelles (Esau, 1965), but this rounding-up of chloroplasts has also been seen before in BSMV-infected tissues (Torrance et al., 2006). Movement of a PMTV mutant clone that was deficient in TGB2 expression was functionally complemented by mRFP-TGB2, allowing the virus, as reported by YFP-TGB1 fluorescence, to move into neighboring cells. Following co-expression, YFP fluorescence was detected in cells surrounding the initial infected cell and occasionally more than one cell boundary distant. In these experiments, the proportion of co-expressing cells was low in comparison to the numbers of individual red- or yellow-fluorescent cells. This may be a result of exclusion of the virus due to a form of RNA silencing, since the PMTV-3.YFP-TGB1.ΔTGB2 mutant was created by mutation of the TGB2 initiation codon rather than by deletion of the gene. It is highly unlikely that cell-to-cell movement of the TGB2 deletion mutant was due to reversion since, in control bombardments of RNA1 and the mutant viral RNA, movement out of the initial cell never occurred. Furthermore, if the mutant had reverted, continued movement over many cell boundaries, resulting in larger fluorescent lesions of greater than 20–100 cells, would have been expected. The bombardment results confirm that TGB2 is not required for viral replication, although PMTV TGB2 is known to bind RNA (Cowan et al., 2002).

These data reveal subtle differences in the localizations of PMTV TGB2 protein compared to other TGB2 proteins. In the systems examined, TGB2 proteins are all observed in association with the ER and mobile granules, particularly at early time points in expression. However, unlike PMTV, the BSMV TGB2 localized later in the infection to chloroplasts only in the presence of viral RNA (Torrance et al., 2006) and PVX TGB2 has never been reported to associate with chloroplasts or with components of the endocytic pathway, accumulated instead in the cytosol and nucleus later in expression (Ju et al., 2005).

Chloroplasts labeled with mRFP-TGB2 were often seen surrounding the nucleus and mRFP-TGB2 also labeled stromules. In the experiments reported here, localization to the chloroplast envelope was consistent between different expression systems, although the timing varied slightly. The localizations described for TGB2 from a PMTV vector under the control of its own subgenomic promoter were all visible slightly later than from 35S promoter expression. Differences in the time at which localizations were observed may be due to different levels of expression between the various systems rather than an intrinsic effect of the expression system, however, we cannot rule out the possibility of temporal regulation by the virus infection process. Deconvolution has produced greater resolution of fine and faintly-labeled structures, showing additional detail and allowing imaging of compartments that were previously invisible without image processing. It was, for instance, interesting to note that, when deconvolved, the ER and small mobile structures were still visible at the later stage of chloroplast labeling. These sub-cellular structures are typically labeled with mRFP-TGB2 early in the infection process (see Haupt et al., 2005), but were previously considered to be unlabeled at the later, vesicle and chloroplast-associated stage.

TGB2 was undetectable in preparations of chloroplasts from PMTV-infected tissues using antisera raised against TGB2, and in a previous study we were unable to detect TGB2 in PMTV systemically-infected *N. benthamiana* tissue. However, TGB2 was detected in P1 and P30 fractions (enriched for nuclei, chloroplasts and cellular membranes) when it was over-expressed from a TMV-based vector (Cowan et al., 2002). In the present study, TGB2 was found, by CLSM imaging, to be present in ∼5% of the intact chloroplasts isolated from tissues that were systemically infected with TMV expressing GFP-TGB2. It seems likely therefore, that the level of expression of TGB2 in natural infections is below the limit of detection in Western blots. However, the distribution of mRFP-TGB2 fluorescence in chloroplasts was clear in the CLSM experiments reported here using three different expression systems. These results suggest that, in a natural infection, TGB2 is present on and in chloroplasts and that this localization is a functional part of the infection process, but that the levels required for this function are below the detection limits of the available antiserum. The technical difficulty in preparing chloroplasts for analysis is compounded by the presence of large starch grains in chloroplasts from PMTV-infected tissues (cf **Figure 4**): these tend to pass through the plastid membrane during centrifugation, rupturing the chloroplast and probably reducing the abundance of chloroplasts from infected cells in any preparation used for analysis.

RT-PCR detected the presence of viral negative strand RNA (the replicative intermediate), in chloroplasts isolated from PMTV-Swe-infected *N. benthamiana* leaves, indicating that replication of viral RNA occurs in association with chloroplasts. *In-situ* RNA labeling of both infected tissue and isolated chloroplasts from infected tissue showed that viral genomic (positive strand) RNA was associated with infected plastids. *In-situ* RNA labeling was unable to detect negative strand RNA above background labeling, but this is perhaps not surprising since it is assumed to be present in very small quantities; methods utilizing PCR amplification are likely to be of greatest utility. Detection of viral RNA in association with chloroplasts was also a relatively rare event; only a small percentage of isolated chloroplasts or small patches of leaf tissue showed hybridization with the PMTV probe which is consistent with the sporadic and patchy nature of a PMTV infection in foliar tissue. When detected, the viral genomic RNA was found to be in punctate spots associated with the plastid periphery; possibly corresponding to the membrane invaginations seen in the EM and the punctate spots of TGB2 seen with CLSM.

Because TGB2 was localized to several different subcellular compartments we wanted to investigate whether TGB2 displayed any binding specificity to membrane lipids. Lipids play important roles in the maintenance and activity of integral membrane proteins and function as signaling molecules in plant growth and development (reviewed by Martin et al., 2005), and can be involved in plant pathogen resistance (Takahashi et al., 2009) and viral replication (Lee and Ahlquist, 2003). Lipid interaction analysis revealed that TGB2 interacts with phosphatidic acid, a signaling phospholipid and biosynthetic precursor of cardiolipin. Phosphatidic acid is thought to be transported from the ER to chloroplast thylakoids (Awai et al., 2006), and cardiolipin is present in photosystem II fractions from chloroplast thylakoid membranes (Depalo et al., 2004), both providing additional supporting evidence for TGB2 association with plastids. The other lipids that TGB2 interacted with in the membrane blots, the phosphoinositides (PtdIns) and sulfatide are found in discrete domains of plasma membranes and are involved in signaling and host-pathogen interactions (Mongrand et al., 2004; Borner et al., 2005). These interactions are the subject of further study. The lipid binding experiments support the contention that TGB2 interacts with specific lipid domains since no reaction was found with phosphatidylcholine and phosphatidylethanolamine both of which are major constituents of plasma membranes.

There have been many reports of viruses inducing deformation and disruption of chloroplasts. For example, chloroplasts are known to be sites of replication of TYMV where the virus induces small spherules at the periphery (Prod'homme et al., 2001). The 6K protein of (TuMV) induces vesicles that target chloroplasts and induce chloroplast membrane invaginations (Wei et al., 2010) and virus infection causes plastids to accumulate in perinuclear structures containing other membraneous organelles and viral proteins that are required for genome replication (Grangeon et al., 2012). BSMV induces cytoplasmic invaginations and vesiculation in membranes of proplastids and chloroplasts (Carroll, 1970; Torrance et al., 2006). The CP and RNA of BSMV were detected in chloroplast preparations (Torrance et al., 2006) while double-stranded RNA was found in proplastids of wheat root tips (Lin and Langenberg, 1985), implicating plastids as sites of virus replication. AltMV TGB3 targets to chloroplasts, causes chloroplast malformation and vesicular membrane invaginations and the association is required for efficient cell-cell and systemic movement. As found for PMTV, viral RNA also associates with the chloroplast periphery (Lim et al., 2010). Viruses commonly cause chlorosis and have been reported to adversely affect photosystem II structure and function (Rahoutei et al., 2000; Lehto et al., 2003). Recently, it was shown that the potyvirus helper component proteinase (HC-Pro), a multifunctional protein with roles in RNA silencing suppression, movement and transmission by vector aphids, interacts with the tobacco MinD protein that plays a role in chloroplast division (Jin et al., 2007). It was suggested that HC-Pro binding may interfere with chloroplast division to promote virus pathogenicity.

A previous EM study of PMTV-infected potato tissue revealed an abundance of cytoplasmic membranous tubules and perforation and loss of both the plasma membrane and chloroplast envelope (Fraser, 1976). However, chloroplast ultra-structure was not reported in detail. In our study, we show for the first time that PMTV induces the formation of large cytoplasmic invaginations in chloroplasts and tests on chloroplast preparations from PMTV-infected *N. benthamiana* showed that viral genomic RNA and CP were associated with chloroplasts. Immunogold labeling of ultrathin sections with the anti-TGB2 antibody was unable to detect TGB2 protein in association with the chloroplasts, but this is perhaps unsurprising since the TGB2 antiserum did not work in western blots. However results presented here show TGB2 associated with plastid membranes and localized to spots on the surface of chloroplasts (possibly cytoplasmic invaginations) using a number of different methods. The additional association of viral RNA and CP with the spots on chloroplasts suggests these may be sites of virus replication, and it is possible that the plastid association of TGB2 reflects a role in viral replication by recruiting vRNP. Alternatively it is possible that TGB2 has a cytopathic effect, for example, blocking or subverting chloroplast receptors thereby inducing inclusions of cytoplasm for replication. A similar phenotype (cytoplasmic inclusions) has been observed in mutants defective in chloroplast import receptors (Kubis et al., 2004). Chloroplasts are sites of salicylic acid biosynthesis and are the target of virulence effectors in other host-pathogen interactions (Jelenska et al., 2007). Therefore, it is possible that chloroplast targeting by TGB2 is virus-mediated to promote pathogenesis. However, we do not know whether PMTV induces a salicylic acid mediated defense response. It may also be that TGB2 is required for intracellular transport of viral RNP complexes or assembled virions that are produced in association with plastids; TGB2 associates with TGB3 in a complex of defined stoichiometric ratio to associate with motile membrane compartments of the ER through protein-protein or protein-lipid interactions to achieve passage to and through PD (Tilsner et al., 2010). Although virus particles were not seen associated with the invaginations of chloroplasts in EM sections in this study, CP was detected in chloroplast preparations, suggesting that CP production could be associated with plastid membranes, or encapsidation could occur here. PMTV does not produce large quantities of virions in infected cells, but given that the virus can move as a vRNP complex, virions may not be important in leaf tissue. The one event that does require the viral CP is natural transmission by its plasmodiophorid vector, *Spongospora subterranea*, but this only occurs in root cells. This lack of necessity for virions to move systemically through the apical parts of the plant may explain their relative absence in infected leaf cells. Future research will be focused on establishing whether TGB2 plays a role in pathogenesis, vRNP and virion transmission and/or virus replication.

ACKNOWLEDGMENTS

We thank Petra Boevink for the pGRAB plasmid, Chris Hawes for the HDEL antibody preparation and David Baulcombe for the mGFP5-ER transgenic plants. This work was performed under HSE consent number GM250/07.1, Scottish Government plant health license PH/29/2007 and SCRI Risk assessment number 061202. Financial support to JHI from the Scottish Government,

Rural and Environment Science and Analytical Services Division is acknowledged and Eugene I. Savenkov was in receipt of a Wenner-Gren Foundation visiting fellowship to conduct research at JHI.

SUPPLEMENTARY MATERIAL

The Supplementary Material for this article can be found online at: http://www.frontiersin.org/Plant-Microbe_Interaction/10.3389/fpls.2012.00290/abstract

REFERENCES

Ahlquist, P., Noueiry, A. O., Lee, W.-M., Kushner, D. B., and Dye, B. T. (2003). Host factors in positive-strand RNA virus genome replication. *J. Virol.* 77, 8181–8186.

Awai, K., Xu, C., Lu, B., and Benning, C. (2006). Lipid trafficking between the endoplasmic reticulum and the chloroplast. *Biochem. Soc. Trans.* 34, 395–398.

Borner, G. H. H., Sherrier, D. J., Weimar, T., Michaelson, L. V., Hawkins, N. D., MacAskill, A., et al. (2005). Analysis of detergent-resistant membranes in Arabidopsis. Evidence for plasma membrane lipid rafts. *Plant Physiol.* 137, 104–116.

Carroll, T. W. (1970). Relation of barley stripe mosaic virus to plastids. *Virology* 42, 1015–1022.

Cowan, G. H., Lioliopoulou, F., Ziegler, A., and Torrance, L. (2002). Subcellular localisation, protein interactions and RNA binding of *Potato mop-top virus* triple gene block proteins. *Virology* 298, 106–115.

Depalo, N., Catucci, L., Mallarrdi, A., Corcelli, A., and Agostiano, A. (2004). Enrichment of cardiolipin content throughout the purification procedure of photosystem II. *Bioelectrochemistry* 63, 103–106.

Drea, S., Corsar, J., Crawford, B., Shaw, P., Dolan, L., and Doonan, J. H. (2005). A streamlined method for systematic, high resolution *in situ* analysis of mRNA distribution in plants. *Plant Methods* 1:8. doi: 10.1186/1746-4811-1-8

Esau, K. (1965). *Plant Anatomy.* 2nd Edn. London: John Wiley and Sons.

Fraser, T. W. (1976). Mop-top tubules. The ultrastructure of unusual tubular elements associated with two different leaf symptoms of potato mop-top virus infected potato plants. *Protoplasma* 90, 15–31.

Gorshkova, E. N., Erokhina, T. N., Stroganova, T. A., Yelina, N. E., Zamyatnin, A. A. Jr., Kalinina, N. O., et al. (2003). Immunodetection and fluorescent microscopy of transgenically expressed hordeivirus TGBp3 movement protein reveals its association with ER elements in close proximity to plasmodesmata. *J. Gen. Virol.* 84, 985–994.

Grangeon, R., Agbeci, M., Chen, J., Grondin, G., Zheng, H., and Laliberté, J.-F. (2012). Impact on the endoplasmic reticulum and golgi apparatus of turnip mosaic virus infection. *J. Virol.* 86, 9255–9265.

Harries, P. A., Schoelz, J. E., and Nelson, R. S. (2010). Intracellular transport of viruses and their components: utilizing the cytoskeleton and membrane highways. *Mol. Plant Microbe Interact.* 23, 1381–1393.

Haseloff, J., Siemering, K. R., Prasher, D. C., and Hodge, S. (1997). Removal of a cryptic intron and subcellular localisation of green fluorescent protein are required to mark *Arabidopsis* plants brightly. *Proc. Natl. Acad. Sci. U.S.A.* 94, 2122–2127.

Hatta, T., Bullivant, S., and Matthews, R. E. F. (1973). Fine structure of vesicles induced in chloroplasts of chinese cabbage leaves by infection with turnip yellow mosaic virus. *J. Gen. Virol.* 20, 37–50.

Hatta, T., and Matthews, R. E. F. (1974). The sequence of early cytological changes in chinese cabbage leaf cells following systemic infection with turnip yellow mosaic virus. *Virology* 59, 383–396.

Hatta, T., and Matthews, R. E. F. (1976). Sites of coat protein accumulation in turnip yellow mosaic virus-infected cells. *Virology* 73, 1–16.

Haupt, S., Cowan, G. H., Ziegler, A., Roberts, A. G., Oparka, K. J., and Torrance, L. (2005). Two plant-viral movement proteins traffic in the endocytic recycling pathway. *Plant Cell* 17, 164–181.

Hellens, R. P., Edwards, E. A., Leyland, N. R., Bean, S., and Mullineaux, P. M. (2000). pGreen: a versatile and flexible binary Ti vector for *Agrobacterium*-mediated plant transformation. *Plant Mol. Biol.* 42, 819–832.

Jakubiec, A., Notaise, J., Tournier, V., Héricourt, F., Block, M. A., Drugeon, G., et al. (2004). Assembly of turnip yellow mosaic virus replication complexes: interaction between the proteinase and polymerase domains of the replication proteins. *J. Virol.* 78, 7945–7957.

Jelenska, J., Yao, N., Vinatzer, B. A., Wright, C. M., Brodsky, J. L., and Greenberg, J. T. (2007). A J domain virulence effector of *Pseudomonas syringae* remodels host chloroplasts and suppresses defences. *Curr. Biol.* 17, 499–508.

Jin, Y., Ma, D., Dong, J., Li, D., Deng, C., Jin, J., et al. (2007). The HC-Pro protein of potato virus Y interacts with NtMinD of tobacco. *Mol. Plant Microbe Interact.* 20, 1505–1511.

Ju, H. J., Brown, J. E., Ye, C. M., and Verchot-Lubicz, J. (2007). Mutations in the central domain of potato virus X TGBp2 eliminate granular vesicles and virus cell-to-cell trafficking. *J. Virol.* 81, 1899–1911.

Ju, H. J., Samuels, T. D., Wang, Y. S., Blancaflor, E., Payton, M., Mitra, R., et al. (2005). The potato virus X TGBp2 movement protein associates with endoplasmic reticulum-derived vesicles during virus infection. *Plant Physiol.* 138, 1877–1895.

Kubis, S., Patel, R., Combe, J., Bedard, J., Kovacheva, S., Lilley, K., et al. (2004). Functional specialization amongst the Arabidopsis Toc 159 family of chloroplast protein import receptors. *Plant Cell* 16, 2059–2077.

Kwok, E. Y., and Hanson, M. R. (2004). Plastids and stromules interact with the nucleus and cell membrane in vascular plants. *Plant Cell Rep.* 23, 188–195.

Laliberté, J.-F., and Sanfaçon, H. (2010). Cellular remodeling during plant virus infection. *Annu. Rev. Phytopathol.* 48, 69–91.

Lee, W.-M., and Ahlquist, P. (2003). Membrane synthesis, specific lipid requirements, and localized lipid composition changes associated with a positive-strand RNA virus RNA replication protein. *J. Virol.* 77, 12819–12828.

Lehto, K., Tikkanen, M., Hiriart, J.-P., Paakkarinen, V., and Aro, E.-M. (2003). Depletion of the photosystem II core complex in mature tobacco leaves infected by the *Flavum* strain of *Tobacco mosaic virus*. *Mol. Plant Microbe Interact.* 16, 1135–1144.

Lim, H.-S., Bragg, J. N., Ganesan, U., Lawrence, D. M., Yu, J., Isogai, M., et al. (2008). Triple gene block protein interactions involved in movement of barley stripe mosaic virus. *J. Virol.* 82, 4991–5006.

Lim, H.-S., Bragg, J. N., Ganesan, U., Ruzin, S., Schichnes, D., Lee, M. Y., et al. (2009). Subcellular localization of the barley stripe mosaic virus triple gene block proteins. *J. Virol.* 83, 9432–9448.

Lim, H.-S., Vaira, A. M., Bae, H., Bragg, J. N., Ruzin, S. E., Bauchan, G. R., et al. (2010). Mutation of a chloroplast-targeting signal in *Alternanthera* mosaic virus TGB3 impairs cell-to-cell movement and eliminates long-distance virus movement. *J. Gen. Virol.* 91, 2102–2115.

Lin, N.-S., and Langenberg, W. G. (1984). Chronology of appearance of barley stripe mosaic virus protein in infected wheat cells. *J. Ultrastruct. Res.* 89, 309–323.

Lin, N.-S., and Langenberg, W. G. (1985). Peripheral vesicles in proplastids of barley stripe mosaic virus-infected wheat cells contain double-stranded RNA. *Virology* 142, 291–298.

Lucas, W. J. (2006). Plant viral movement proteins: agents for cell-to-cell trafficking of viral genomes. *Virology* 344, 169–184.

Martin, S. W., Glover, B. J., and Davies, J. M. (2005). Lipid microdomains – plant membranes get organized. *Trends Plant Sci.* 10, 263–265.

McMullen, C. R., Gardner, W. S., and Myers, G. A. (1978). Aberrant plastids in barley leaf tissue infected with barley stripe mosaic virus. *Phytopathology* 68, 317–325.

Mongrand, S., Morel, J., Laroche, J., Claverol, S., Carde, J.-P., Hartmann, M.-A., et al. (2004). Lipid rafts in higher plant cells. *J. Biol. Chem.* 279, 36277–36286.

Morozov, S. Y., and Solovyev, A. G. (2003). Triple gene block: modular design of a multifunctional machine for plant virus movement. *J. Gen. Virol.* 84, 1351–1366.

Nivison, H. T., Fish, L. E., and Jagendorf, A. T. (1986). Translation by isolated pea chloroplasts. *Meth. Enzymol.* 118, 282–295.

Oparka, K. J., Roberts, A. G., Boevink, P., Santa Cruz, S., Roberts, I., Pradel, K. S., et al. (1999). Simple, but not branched, plasmodesamata allow the nonspecific trafficking of proteins in developing tobacco leaves. *Cell* 97, 743–754.

Prod'homme, D., Jakubiec, A., Tournier, V., Drugeon, G., and Jupin, I. (2003). Targeting of the turnip yellow mosaic virus 66K replication protein to the chloroplast envelope is mediated

by the 140K protein. *J. Virol.* 77, 9124–9135.

Prod'homme, D., Le Panse, S., Drugeon, G., and Jupin, I. (2001). Detection and subcellular localization of the turnip yellow mosaic virus 66K replication protein in infected cells. *Virology* 281, 88–101.

Rahoutei, J., Garcia-Luque, I., and Baron, M. (2000). Inhibition of photosynthesis by viral infection: effect on PSII structure and function. *Physiol. Plant.* 110, 286–292.

Roberts, I. M. (2002). Iso-butanol saturated water: a simple procedure for increasing staining intensity of resin sections for light and electron microscopy. *J. Microsc.* 207, 97–107.

Salonen, A., Ahola, T., and Kaariainen, L. (2005). Viral RNA replication in association with cellular membranes. *Curr. Top. Microbiol. Immunol.* 285, 139–173.

Savenkov, E. I., Germundsson, A., Zamyatnin, A. A., Sandgren, S., Valkonen, J. P. T. (2003). *Potato mop-top virus*: the coat protein-encoding RNA and the gene for cysteine-rich protein are dispensable for systemic virus movement in *Nicotiana benthamiana*. *J. Gen. Virol.* 84, 1001–1005.

Schoelz, J. E., Harries, P. A., and Nelson, R. S. (2011). Intracellular transport of plant viruses; finding the door out of the cell. *Mol. Plant* 4, 813–831.

Scholthof, H. B. (2005). Plant virus transport: motions of functional equivalence. *Trends Plant Sci.* 10, 376–382.

Takahashi, Y., Berberich, T., Kanzaki, H., Matsumura, H., Saitoh, H., Kusano, T., et al. (2009). Serine palmitoyltransferase, the first step enzyme in sphingolipid biosynthesis, is involved in nonhost resistance. *Mol. Plant Microbe Interact.* 22, 31–38.

Taliansky, M. E., Torrance, L., and Kalinina, N. O. (2008). "Role of plant virus movement proteins," in *Plant Virology Protocols: From Virus Sequence to Protein Function. Methods in Molecular Biology, 2nd Edn*. eds G. Foster, Y. Hong, E. Johansen, and P. Nagy (New York, NY: The Humana Press Inc.), 33–54.

Taylor, M. A., Ross, H. A., McRae, D., Stewart, D., Roberts, I., Duncan, G., et al. (2000). A potato α-glucosidase gene encodes a glycoprotein-processing α-glucosidase II-like activity. Demonstration of enzyme activity and effects of down-regulation in transgenic plants. *Plant J.* 24, 305–316.

Tilsner, J., Cowan, G. H., Roberts, A. G., Chapman, S. N., Ziegler, A., Savenkov, E., et al. (2010). Plasmodesmal targeting and intercellular movement of potato mop-top pomovirus is mediated by a membrane anchored tyrosine-based motif on the luminal side of the endoplasmic reticulum and the C-terminal transmembrane domain in the TGB3 movement protein. *Virology* 402, 41–51.

Torrance, L. (1992). "Serological methods to detect plant viruses: production and use of monoclonal antibodies," in *Techniques for the Rapid Detection of Plant Pathogens,* eds J. M. Duncan and L. Torrance (Oxford: Blackwell Scientific Publications), 7–33.

Torrance, L., Cowan, G. H., Gillespie, T., Ziegler, A., and Lacomme, C. (2006). Barley stripe mosaic virus encoded proteins triple gene block 2 and γb localize to chloroplasts in virus-infected monocot and dicot plants revealing hitherto unknown roles in virus replication. *J. Gen. Virol.* 87, 2403–2411.

Torrance, L., Cowan, G. H., and Pereira, L. G. (1993). Monoclonal antibodies specific for potato mop-top virus, and a revised estimate of coat protein molecular weight. *Ann. Appl. Biol.* 122, 311–322.

Torrance, L., Lukhovitskaya, N. I., Schepetilnikov, M. V., Cowan, G. H., Ziegler, A., and Savenkov, E. I. (2009). Unusual long-distance movement strategies of potato mop-top virus RNAs in *Nicotiana benthamiana*. *Mol. Plant Microbe Interact.* 22, 381–390.

Ushiyama, R., and Matthews, R. E. (1970). The significance of chloroplast abnormalities associated with infection by turnip yellow mosaic virus. *Virology* 42, 293–303.

Verchot-Lubicz, J. (2005). A new cell-to-cell transport model for potexviruses. *Mol. Plant Microbe Interact.* 18, 283–290.

Verchot-Lubicz, J., Torrance, L., Solovyev, A. G., Morozov, S. Y., Jackson, A. O., and Gilmer, D. (2010). Varied movement strategies employed by triple gene block-encoding viruses. *Mol. Plant Microbe Interact.* 23, 1231–1247.

Wei, T., Huang, T.-S., McNeil, J., Laliberte, J.-F., Hong, J., Nelson, R. S., et al. (2010). Sequential recruitment of the endoplasmic reticulum and chloroplasts for plant potyvirus replication. *J. Virol.* 84, 799–809.

Wright, K. M., Cowan, G. H., Lukhovitskaya, N. I., Tilsner, J., Roberts, A. G., Savenkov, E. I., et al. (2010). The N-terminal domain of PMTV TGB1 movement protein is required for nucleolar localization, microtubule association and long-distance movement. *Mol. Plant Microbe Interact.* 23, 1486–1497.

Zamyatnin, A. A., Solovyev, A. G., Savenkov, E. I., Germundsson, A., Sandgren, M., Valkonen, J. P. T., et al. (2004). Transient coexpression of individual genes encoded by the triple gene block of *Potato mop-top virus* reveals requirements for TGBp1 trafficking. *Mol. Plant Microbe Interact.* 17, 921–930.

Conflict of Interest Statement: The authors declare that the research was conducted in the absence of any commercial or financial relationships that could be construed as a potential conflict of interest.

Received: 28 September 2012; accepted: 05 December 2012; published online: 24 December 2012.

Citation: Cowan GH, Roberts AG, Chapman SN, Ziegler A, Savenkov EI and Torrance L (2012) The potato mop-top virus TGB2 protein and viral RNA associate with chloroplasts and viral infection induces inclusions in the plastids. Front. Plant Sci. ***3****:290. doi: 10.3389/fpls.2012.00290*

This article was submitted to Frontiers in Plant-Microbe Interaction, a specialty of Frontiers in Plant Science.

frontiers in
PLANT SCIENCE

ORIGINAL RESEARCH ARTICLE
published: 07 December 2012
doi: 10.3389/fpls.2012.00269

Role of rice stripe virus NSvc4 in cell-to-cell movement and symptom development in *Nicotiana benthamiana*

Yi Xu and Xueping Zhou*

State Key Laboratory of Rice Biology, Institute of Biotechnology, Zhejiang University, Hangzhou, China

Edited by:
Aiming Wang, Agriculture and Agri-Food Canada, Canada

Reviewed by:
Taiyun Wei, Fujian Agriculture and Forestry University, China
Weimin Li, Chinese Academy of Agricultural Sciences, China
Andrew O. Jackson, University of California, Berkeley, USA

***Correspondence:**
Xueping Zhou, State Key Laboratory of Rice Biology, Institute of Biotechnology, Zhejiang University, Hangzhou, Zhejiang 310058, China.
e-mail: zzhou@zju.edu.cn

Our previous work has demonstrated that the NSvc4 protein of *Rice stripe virus* (RSV) functions as a cell-to-cell movement protein. However, the mechanisms whereby RSV traffics through plasmodesmata (PD) are unknown. Here we provide evidence that the NSvc4 moves on the actin filament and endoplasmic reticulum network, but not microtubules, to reach cell wall PD. Disruption of cytoskeleton using different inhibitors altered NSvc4 localization to PD, thus impeding RSV infection of *Nicotiana benthamiana*. Sequence analyses and deletion mutagenesis experiment revealed that the N-terminal 125 amino acids (AAs) of the NSvc4 determine PD targeting and that a transmembrane domain spanning AAs 106–125 is critical for PD localization. We also found that the NSvc4 protein can localize to chloroplasts in infected cells. Analyses using deletion mutants revealed that the N-terminal 73 AAs are essential for chloroplast localization. Furthermore, expression of NSvc4 from a Potato virus X (PVX) vector resulted in more severe disease symptoms than PVX alone in systemically infected *N. benthamiana* leaves. Expression of NSvc4 in *Spodoptera frugiperda* 9 cells did not elicit tubule formation, but instead resulted in punctate foci at the plasma membrane. These findings shed new light on our understanding of the movement mechanisms whereby RSV infects host plants.

Keywords: rice stripe virus, movement, chloroplast, tubules

INTRODUCTION

Rice stripe disease is the most devastating viral disease of rice in China, Japan, and Korea (Wei et al., 2009). The causal agent, *Rice stripe virus* (RSV), is the type member of the *Tenuivirus* genus and the viral genome consists of four single-stranded RNA segments (RNAs 1, 2, 3, and 4; Hibino, 1996). RNA 1 is negative-sense and encodes a putative RNA-dependent RNA polymerase. RNAs 2, 3, and 4 are ambisense, and each of which encodes two open reading frames (ORFs) with one on viral RNA (vRNA) and another on viral complementary RNA (vcRNA). RSV vRNA 2 encodes a membrane-associated protein that reportedly is an RNA silencing suppressor and interacts with SGS3 (Du et al., 2011). The vcRNA 2 encodes a glycoprotein with unidentified functions (Zhao et al., 2012). The vRNA 3 and vcRNA 3 encode a gene silencing suppressor and a nucleocapsid (NC) protein, respectively (Hibino, 1996; Xiong et al., 2009). RSV vRNA 4 encodes a disease-specific protein that accumulates in both infected plant and insect cells (Toriyama, 1986). The protein encoded by vcRNA 4 was identified as the RSV movement protein (MP; Xiong et al., 2008). RSV is transovarially transmitted by small brown planthopper (SBPH), *Laodelphax striatellus*, in a circulative-propagative manner (Falk and Tsai, 1998; Li et al., 2011). After RSV infection, rice plants often show chlorotic stripes in the newly expanded leaves, and the stripes progress into pale streaks in infected plant leaves. Because of global environment changes and the extensive increases in distribution of the transmission vector (*L. striatellus*) in the south and southeastern parts of China, RSV has caused significant losses in rice production in the past decade.

To infect a host plant successfully, viruses must overcome two obstacles; they must be capable of replicating in host cells and moving between cells and then be able to move systemically throughout the plant via the vasculature. To carry out these functions, viruses encode MPs that often interact with viral genomic (g) RNAs to form ribonucleoprotein complexes that mediate intra- and intercellular movement. At the plasmodesmata (PD), the MPs modify PD size exclusion limits to enable transit of the ribonucleoprotein complexes to adjacent cells. In some examples, the viral MPs form tubules that penetrate through the PD and serve as conduits for whole virus cell-to-cell transport. It has been shown that viruses often co-opt plant cellular processes to carry out specific functions required for infection (Scholthof, 2005; Shen et al., 2011). In addition to host factors that interact directly with viral MPs (Paape et al., 2006; Shimizu et al., 2009), host cytoskeleton, and endoplasmic reticulum (ER) networks also play critical roles in virus movement in hosts (Ashby et al., 2006; Harries et al., 2010). For example, both microtubules and microfilaments have been implicated in supporting cell-to-cell movement of *Tobacco mosaic virus* (TMV) in *Nicotiana benthamiana* (Brandner et al., 2008; Harries et al., 2009b, 2010). The MP of *Abutilon mosaic virus* (AbMV) is known to have an anchor domain that allows the MP to localize to the ER (Aberl et al., 2002). Association of viral MPs with the secretory pathway was also reported for viruses whose MPs form tubules. For example in cells infected with *Cowpea mosaic virus* or *Cauliflower mosaic virus*, tubule formation was independent of microtubules or microfilaments, but tubule formation required a functional secretory pathway (Huang

et al., 2000; Pouwels et al., 2002). Trafficking of P3N-PIPO and CI of *Turnip mosaic virus* (TuMV) to PD has also been shown to be dependent on the host secretory pathway (Wei et al., 2010b). Interestingly, in *Grapevine fanleaf virus* infected cells both the secretory pathway and the cytoskeleton networks were reported to be involved in tubule formation and in intra-cellular targeting of virions (Laporte et al., 2003). Thus, plant virus may utilize the host cytoskeleton, the ER network, or both for PD targeting. Genomes of plant viruses are small and each virus encodes only a few proteins. Consequently, virus-encoded proteins are often multi–functional proteins. For example, the coat protein of *Turnip crinkle virus* (TCV) not only functions in movement between cells and in virion assembly, but also functions as a suppressor of gene silencing (Qu et al., 2003; Cao et al., 2010). Viral MPs also have varied functions: BC1 of AbMV accumulates preferentially at the cell periphery or around the nucleus in plant cells, and hence may participate in distinct functions (Zhang et al., 2001, 2002). The *Barley stripe mosaic virus*-encoded triple-gene block (TGB) 1 protein has similar localization patterns, and TGB2 can localize to both ER membranes and chloroplasts, indicating it also has distinct functions (Torrance et al., 2006; Lim et al., 2009). Several other viral MPs have been reported to accumulate in chloroplasts and are considered to have important roles in virus replication, viral transport, or symptom development. For example, mutation of the chloroplast-targeting signal in the *Alternanthera mosaic virus* (AltMV) TGB3 impaired the virus cell-to-cell movement and eliminated the long distance movement of the virus (Lim et al., 2010). A number of biochemical and subcellular localization activities are associated with the TGB proteins of other flexiviruses, including intra-cellular targeting, gene silencing activities, and host membrane remodeling (Verchot-Lubicz et al., 2010; Tilsner et al., 2012). The 66 K protein of Turnip yellow mosaic virus (TYMV) was reported to localize to virus-induced chloroplastic membrane vesicles, which are thought to function as TYMV RNA replication factories (Prod'homme et al., 2003). The TuMV 6 K also has been shown to target chloroplasts to result in aggregation and elicitation of membrane invaginations (Wei et al., 2010a). Former work demonstrated that NSvc4 rely on the early secretory pathway and actin-myosin VIII motility system for plasmodesmatal localization and could induce foliar necrosis from a TMV-NSvc4 hybrid vector (Yuan et al., 2011; Zhang et al., 2012). Here we present new evidence indicating that NSvc4 exerts its movement functions by trafficking on actin filaments and ER networks to reach the PD and shown that the N-terminal 125 amino acids (AAs) determine the PD localization. We also demonstrate that the NSvc4 protein targets chloroplasts in infected cells and is a symptom determinant in plant.

MATERIALS AND METHODS

PLASMIDS CONSTRUCTIONS

The full length ORFs of NSvc4 protein and the N- and C-terminal deletion mutants were amplified from pBin438-NSvc4 (Xiong et al., 2008) using the Phusion High-Fidelity DNA polymerase (New England Biolabs, Ipswich, USA). The NSvc4 deletion mutant (lacking AAs 106–125) was first amplified via an overlap PCR method with the primers MP-Fol and MP-Rol (See **Table A1** in Appendix for all the primers used in this study). The resulting PCR fragments were ligated individually into the pCHF3-eGFP plasmid and used for agroinfiltration into *N. benthamiana* (Xiong et al., 2008). To construct Potato virus X (PVX) NSvc4 expression vectors, full length and deletion mutants of NSvc4 were PCR amplified with primers containing *Cla*I and *Sal*I restriction sites. The PCR fragments were cloned individually into the pGEM-Teasy vector. After digestion using the *Cla*I and *Sal*I enzymes, the resulting fragments were ligated individually to the PVX pgR107 vector (provided by Dr D. C. Baulcombe, Sainsbury Laboratory, John Innes Centre, Norwich Research Park, Norwich, UK). All the plasmids were verified by DNA sequencing before further use.

PLANT INOCULATION AND CONFOCAL MICROSCOPY

N. benthamiana plants were grown in a growth chamber set at $25 \pm 1^{\circ}$C and 16 h light and 8 h dark conditions. RSV infectivity trials were carried out by rub-inoculating leaves with crude extracts from RSV-infected *O. sativa* leaves ground in phosphate buffer (0.2 M). After a 12-h incubation in the dark, the plant were transferred to a culture room set at $25 \pm 1^{\circ}$C, 80% relative humidity, and 16 h light and 8 h dark cycle. Local and systemic leaf infections were evaluated at 3, 7, and 10 days post inoculation by RT-RCR (data not shown). Leaves of 4-week-old plants were infiltrated with *Agrobacterium tumefaciens* (strain GV3101) harboring either the full length NSvc4 sequence or one of the mutant NSvc4 plasmids using needleless syringes as described previously (Batoko et al., 2000). Leaf tissue was harvested at 48 h post agro-infiltration and examined for GFP fluorescence under a Leica TCS SP5 confocal microscope equipped with a 20× objective lens. Conditions set to excite GFP and monitor the emission were as described by Brandizzi et al. (2002). Chloroplast autofluorescence was detected using a 670-nm emission filter according to the manufacturer's instructions. Confocal images were processed using the LCS Lite Leica software.

INHIBITOR TREATMENTS

Latrunculin B (LatB), oryzalin, and brefeldin A (BFA) were purchased from Sigma-Aldrich (St. Louis, USA) and dissolved in dimethyl sulfoxide (DMSO) to make stock solutions at 10 mM, 2 mM, and 200 μg/ml, respectively. Immediately prior to use, the stocks were diluted to 5 μM LatB, 50 μM oryzalin, and 50 μg/ml BFA using double-distilled water (ddH_2O). Three hours before agroinfiltration, diluted LatB, oryzalin, or BFA solutions were infiltrated into *N. benthamiana* leaves using needleless syringes as described (Harries et al., 2009a). Diluted DMSO (1:1000 in ddH_2O) was infiltrated into *N. benthamiana* leaves and used as a control. The MAN1-RFP (from soybean, which is known to localize to cis-Golgi) was used to monitoring BFA in function in our system (data not shown).

For virus inoculation assays, leaves of six-to-eight leaf stage *N. benthamiana* were rub-inoculated with 5 μM LatB, 50 μM oryzalin, or diluted DMSO (1:1000 in ddH_2O). One day after the chemical treatments, the leaves were rub-inoculated as described previously with crude extracts prepared from RSV-infected *O. sativa* leaves (Xiong et al., 2008). After 12 h incubation in the dark, the plants were transferred to a culture room set at $25 \pm 1^{\circ}$C, 80% relative humidity, and 16 h light (5000 lux) and 8 h dark.

IMMUNOCYTOCHEMISTRY AND ELECTRON MICROSCOPY

Small tissues (approximately 1 mm wide and 3 mm long) were excised from *N. benthamiana* leaves agroinfiltrated with the bacteria harboring the pgR107 or pgR107-NSvc4 vectors. Harvested tissues were fixed with 50 mM phosphate-buffered saline (PBS), pH 6.8, containing 1% glutaraldehyde and 2% formaldehyde for 3 h at 4°C. After dehydration in a graded series of ethanol (30, 50, 70, 90, and 100%), the fixed samples were embedded in Lowicryl K4M resin as described previously (Xiong et al., 2008).

CONSTRUCTION OF BACULOVIRUS PLASMIDS AND TRANSFECTION OF Sf-9 CELLS

The full length *NSvc4* sequence was PCR amplified from the pgR107-NSvc4 using the primers MP-(BamH1)-F and MP-(Sal1)-R. The amplified fragments were digested with the *Bam*HI and *Sal*I restriction enzymes, and then inserted between the *Bam*HI and *Sal*I sites within the pFastBacHTGFPT transfection vector (kindly supplied by Chuanxi Zhang, Zhejiang University, Zhejiang, China) under the control of the polh promoter. The recombinant plasmid pFastBacHTGFPT-NSvc4 was transformed into *E. coli DH10Bac* as instructed (Invitrogen, Carlsbad, USA). After transformation, the gene cassette from the recombinant plasmid was transferred to the bacmid genome by site-specific transposition and the recombinant bacmid DNA was then isolated following the manufacturer's instructions.

Recombinant bacmid DNA was transfected into 1.0×10^6 cells *Spodoptera frugiperda* 9 (Sf-9) cell using Cellfectin Reagent (Invitrogen, Carlsbad, USA), and transfected cells were incubated at 27°C for 72 h. Supernatant of culture medium TNM-FH (Sigma-Aldrich, USA) was collected from the transfected Sf-9 cell cultures and transferred to fresh Sf-9 cells followed by an additional 48–72 h incubation period before confocal microscopy observations.

COMPUTATIONAL ANALYSES OF THE NSvc4 PROTEIN

The transmembrane helices of NSVc4 were predicted using the Membrane Protein Explorer (MPEx, version 3.2[1]) and the ΔG prediction server[2] (Hessa et al., 2007; Snider et al., 2009). The ΔG server provides predictions of the corresponding apparent free energy differences. In principle, a negative ΔG value by the Sec translocon predicts that a protein sequence has a TM helix and that proteins can integrate into membranes.

RESULTS

ACTIN FILAMENTS AND GOLGI APPARATUS DISRUPTION ABOLISH PD LOCALIZATION OF NSvc4 AND DELAY RSV SYSTEMIC INFECTIONS IN *N. BENTHAMIANA*

To investigate roles of the cytoskeleton and secretory membranes in NSvc4 intra-cellular transport and PD targeting, three pharmacological inhibitors were applied to *N. benthamiana* leaves before agroinfiltration-mediated transient expression of NSvc4-eGFP. LatB and oryzalin treatments were used to disrupt actin filaments and microtubules, as previously reported (Harries et al., 2009a; Yuan et al., 2011). Expression of NSvc4-eGFP under control of the PVX pgR107-NSvc4 vector in the DMSO (control) treated *N. benthamiana* leaves yielded punctate spots at the PD (**Figure 1A**). When NSvc4-eGFP was expressed in LatB treated *N. benthamiana* leaves, the number of punctate spots at the PD were clearly reduced, and fluorescence was more generally dispersed throughout the cell (**Figure 1B**), indicating that a functional actin cytoskeleton is important for targeting NSvc4-eGFP to punctate foci at the PDs. When the NSvc4-eGFP was expressed in the oryzalin treated *N. benthamiana* leaves, abundant punctate spots similar to those noted in the DMSO controls were evident at the PD (**Figure 1C**). These experiments indicate that depolymerizing microtubules does not have obvious interference on formation of punctate spot at the PD. BFA is known to interfere with the ER/Golgi secretory pathway by inhibiting COPI vesicle production (Tse et al., 2006). We therefore treated *N. benthamiana* leaves with BFA and noted the NSvc4-eGFP fluorescence was more generally distributed in the cytosol than in the DMSO treated controls and that the localization at the PD and the peripheral membranes was greated reduced (**Figures 2A,B**). These results thus suggest that an intact Golgi secretory system has a substantial positive effect on PD targeting of NSv4-eGFP.

In order to determine whether the pharmacological affects were correlated with RSV infection, we inoculated *N. benthamiana* leaves with extracts from RSV-infected rice. We had noted earlier (Xiong et al., 2008) that RSV results in systemic infections in *N. benthamiana* after mechanical inoculation. Therefore to test

[1]http://blanco.biomol.uci.edu/mpex/
[2]http://dgpred.cbr.su.se/index.php?p=home

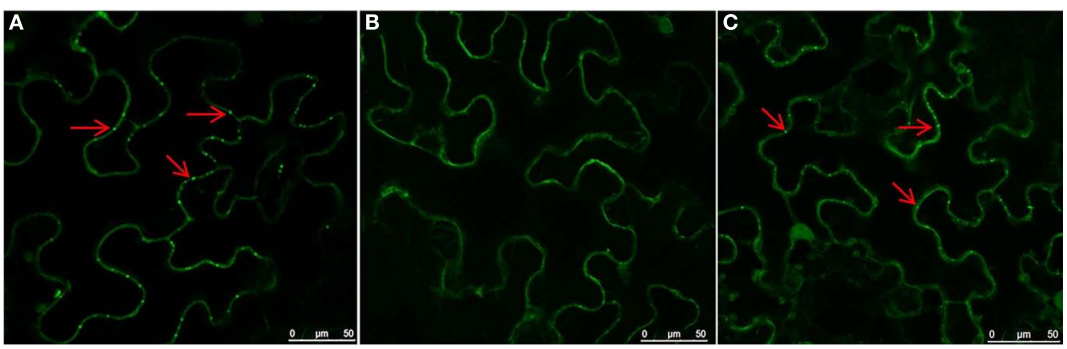

FIGURE 1 | Role of actin filaments in PD localization of NSvc4. *N. benthamiana* leaves were first infiltrated with DMSO **(A)**, LatB **(B)**, or oryzalin **(C)**. Three hours later, the leaves were agroinfiltrated with bacteria harboring the NSvc4-eGFP vector. Infiltrated leaves were sampled at 48 h after agro-infiltration and subjected to examination under the confocal microscopy. Arrows indicate PD localization of fusion proteins.

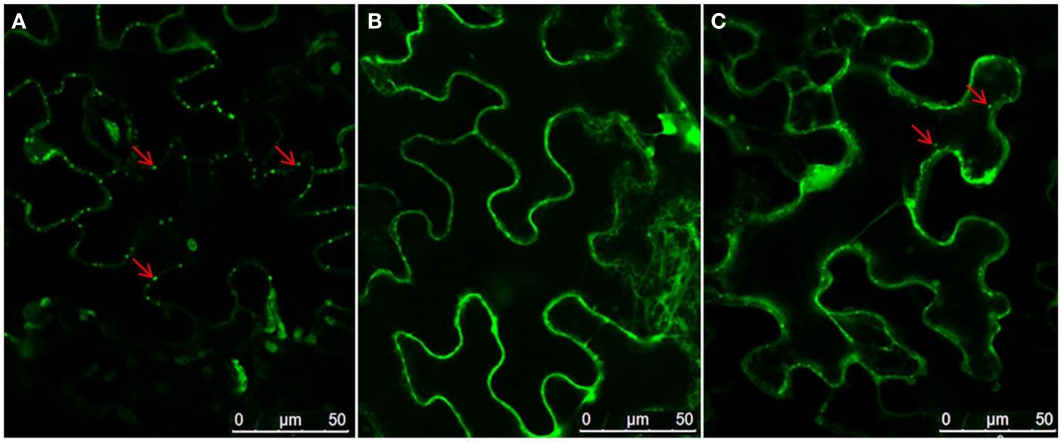

FIGURE 2 | Role of the ER-Golgi secretion pathway in PD localization of NSvc4. *N. benthamiana* leaves were infiltrated with DMSO **(A)** or BFA **(B)**. After 3 h, the leaves were agroinfiltrated for expression of NSvc4-eGFP. The leaf shown in **(C)** was agroinfiltrated with deletion mutant of NSvc4 ($NSvc4_{106–125}$-eGFP). Arrows indicate the localization of fusion protein.

the effects of the DMSO, LatB, and oryzalin treatments on RSV infection, we inoculated RSV from infected rice extracted to *N. benthamiana* leaves 1 day after application of the drug treatments. The results show that disruption of actin filaments using LatB strongly inhibits systemic infection of RSV, whereas oryzalin treatments were similar to those of DMSO on RSV systemic infection in *N. benthamiana* (**Table 1**).

Table 1 | Effect of different inhibitors on RSV infection in *N. benthamiana*.

Treatment	3 dpi[a] inoculation leaf	3 dpi systemic leaf	7 dpi systemic leaf	10 dpi systemic leaf
LatB	15/15[b]	0/15	3/15	3/15
Oryzalin	15/15	0/15	11/15	12/15
DMSO	15/15	0/15	13/15	15/15

[a] Days post inoculation of RSV in N. benthamiana. [b] The denominator shows the number of N. benthamiana plants used in these treatment; the numerator represents the number of N. benthamiana plants with symptom.

COMPUTATIONAL ANALYSIS OF NSvc4 AND DOMAINS RESPONSIBLE FOR NSvc4 PD LOCALIZATION

Using the Membrane Protein Explorer program, AAs spanning positions 106–125 of the NSvc4 protein have properties of a transmembrane domain (**Figure 3**). To confirm this prediction, we deleted AAs 106–125 from the NSvc4 to create $NSvc4_{\Delta 106–125}$-eGFP, and expressed the mutant transiently from the PVX vector in the epidermal cells of *N. benthamiana* leaves via agro-infiltration. Confocal microscopy observations revealed that PD localization by the deletion mutant was substantially reduced compared to the DMSO controls. Only a few apparently intact foci were evident and most of the fluorescence was diffuse and appeared to be associated with the cytosol (**Figure 2C**). These observations provide evidence suggesting that the predicted transmembrane region (AAs 106–125) in the NSvc4 protein provides an important anchor domain that is required for NSvc4 trafficking on the endomembrane network.

To determine the domain responsible for NSvc4 PD localization, a series of NSvc4 deletion mutants were constructed, inserted into the pCHF3 vector and expressed transiently by agroinfiltration into *N. benthamiana* leaf cells. The fluorescence patterns in cells at 48 h after infiltration revealed that the $NSvc4_{1–54}$-eGFP, $NSVc4_{1–73}$-eGFP, $NSvc4_{1–106}$-eGFP, and $NSvc4_{\Delta 125–286}$-eGFP mutant derivatives each elicited GFP expression patterns similar to those produced by pCHF3-eGFP, the GFP control vector (**Figure 4**). However, fluorescence from the $NSvc4_{1–125}$-eGFP deletion mutant protein accumulated in punctate foci at the PD that appeared to be similar to the fluorescence elicited in cells expressing NSvc4-eGFP (Compare **Figures 4B,G**). In marked contrast, the $NSvc4_{\Delta\ 106–125}$-eGFP proteins accumulated as small punctate bodies in the cytoplasm and were not observed at the PD (**Figure 4E**). These observations indicate that the N-terminal 1–125 AA fragment contains a PD localization signal that is sufficient for PD targeting.

LOCALIZATION OF NSvc4 IN SPHERE-LIKE COMPARTMENTS AND CHLOROPLAST

Image analysis indicated that as well as localizing at the PD, the NSvc4 protein also accumulated in discrete, sphere-like compartments of approximately 4 mm in diameter in cells (**Figure 5**). To determine the subcellular localization of these spheres, epidermal cells expressing NSvc4-eGFP were analyzed by confocal microscope. A lambda scan set at 5 nm intervals between 595 and 755 nm for analysis of the sphere-like compartments had emission peaks at 500–530 nm and at 650–700 nm (**Figure 5B**). The spectral characteristics of the 650–700 nm emission peak were similar to the chlorophyll spectrum (maximum at 680 nm). So, the fluorescence spectra were collected simultaneously, with one photon multiplier-tube bandwidth set at 500–530 nm and a second one at 660–700 nm, and the NSvc4-eGFP and chlorophyll

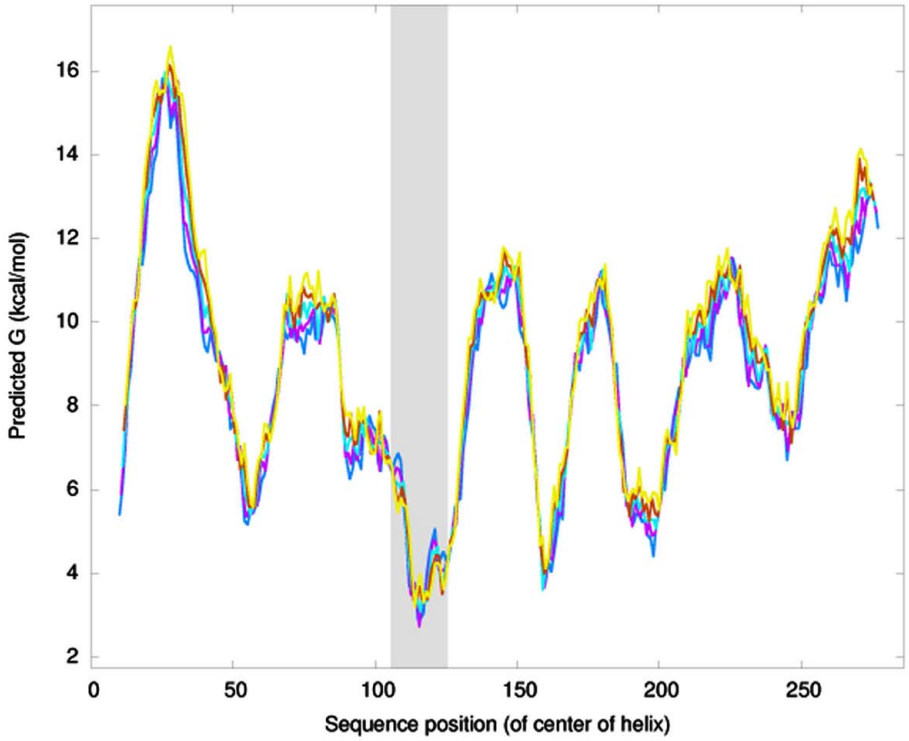

FIGURE 3 | NSVc4 transmembrane domain prediction. Prediction of transmembrane domain was carried out with the ΔG prediction server (http://dgpred.cbr.su.se/index.php?p=home). The *Y*-axis shows the predicted G value and the *x*-axis represents the amino acid sequence position. The dark region spanning amino acids 106–125 is predicted to be a transmembrane domain.

autofluorescence was merged to generate yellow fluorescent of the overlapping foci (**Figure 5**).

To confirm the presence of NSvc4 in the chloroplasts, NSvc4-eGFP was expressed in *N. benthamiana* leaf cells using the PVX vector (pgR107). By 7–8 days post agroinfiltration (dpi), leaves with systemic symptoms were sampled and examined by confocal microscopy. In cells expressing the NSvc4-eGFP, the GFP signal co-localized with the chlorophyll autofluorescence, suggesting that a fraction of the expressed NSvc4-eGFP protein accumulates in the chloroplasts (**Figure 6**).

To determine which region of NSvc4 is required for chloroplast-targeting, we agroinfiltrated plasmids harboring the wild type or mutant NSvc4-eGFP fusions (**Figure 7**). The results showed that $NSvc4_{1–73}$-eGFP accumulated in the sphere-like compartments and in the chloroplasts of the epidermal leaf cells (**Figure 7B**). However, $NSvc4_{1–54}$-eGFP and $NSvc4_{54–73}$-eGFP localized around the nuclei and in the cytoplasm, but were not obvious in the chloroplasts (**Figures 7A,E**). The remaining NSvc4 mutants localized exclusively in the cytoplasm. These observations suggest that the N-terminal 73 AAs contain a chloroplast-targeting signal.

THE NSvc4 PVX VECTOR INDUCES MORE SEVERE SYMPTOMS IN *N. BENTHAMIANA* THAN PVX

By 7 days after agroinfiltration of *N. benthamiana* plants for expression of the wtPVX vector (pgR107) or the NSvc4 (pgR-NSvc4), all plants developed systemic symptoms in the upper emerging leaves. Symptoms in plants infiltrated with pgR-NSvc4 were more severe than in plants infiltrated with the wtPVX vector. By 20 dpi, virus symptoms in plants infected with wtPVX vector disappeared, whereas symptoms in the PVX-NSvc4 infected plants remained intense and developed foliar necrosis (**Figure 8**). Reverse transcription PCR result showed that NSvc4 was accumulated in leaves of the PVX-NSvc4 infected plants in both the early and the late infection stages (data not shown). Examination of thin sections prepared from the PVX or PVX-NSvc4 infected *N. benthamiana* leaf tissues by electron microscopy revealed major malformations of chloroplast grana and electron lucent bodies beneath the membranes of PVX-NSvc4 infected cells, but similar malformations were not evident in wtPVX infected cells. In addition, proliferations radiating from the chloroplasts into the cytoplasm were observed in the PVX-NSvc4 and RSV rub-inoculating infected *N. benthamiana* leaves, but not in the cells infected with wtPVX (**Figure 9** and **Figure A1** in Appendix).

SYMPTOM DEVELOPMENT IS INDEPENDENT OF NSvc4 CHLOROPLAST LOCALIZATION

To determine the correlation between NSvc4 chloroplast localization and symptom development, PVX vectors expressing various mutants of NSvc4 were agroinfiltrated individually into *N. benthamiana* leaves. The results demonstrate that $NSvc4_{1–73}$ and $NSvc4_{1–106}$ are capable of targeting chloroplasts (**Figure 10**; **Table 2**). Interestingly, plants infected with two mutant viruses

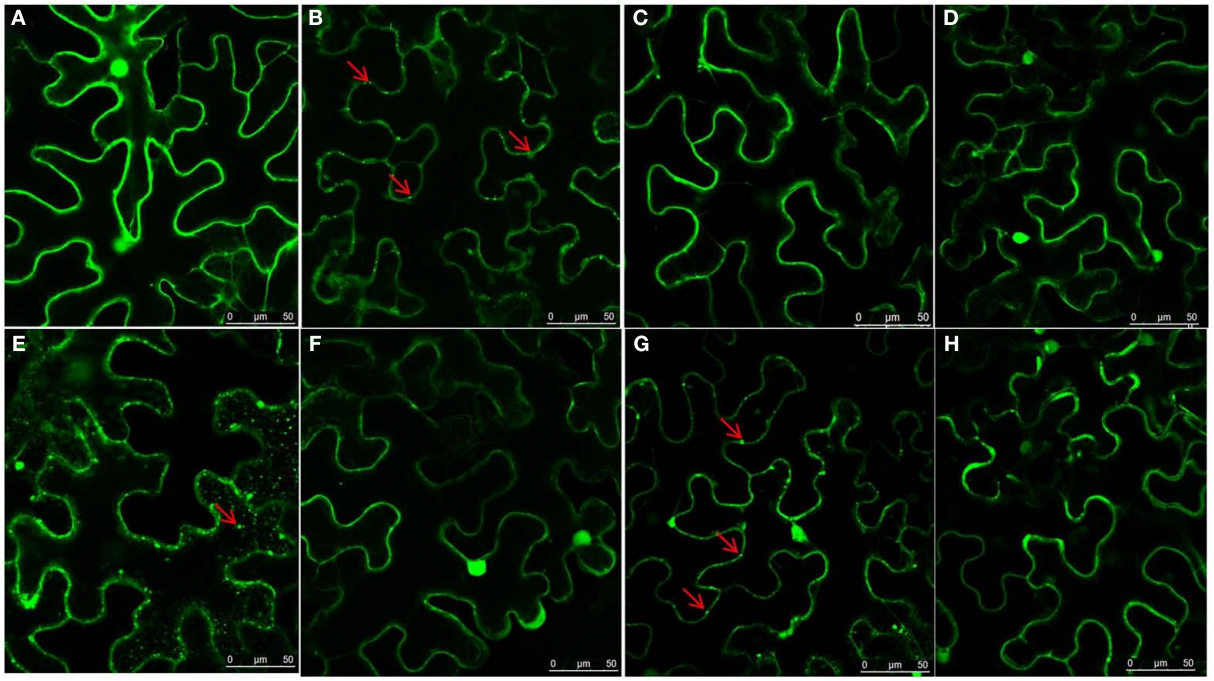

FIGURE 4 | Determination of domains within the NSvc4 that are responsible for PD localization. Tissue was collected from *N. benthamiana* leaves at 48 h after agroinfiltration with pCHF3-eGFP **(A)**, pCHF3-NSvc4-eGFP **(B)**, pCHF3-NSvc4$_{1–54}$-eGFP **(C)**, pCHF3-NSvc4$_{1–73}$-eGFP **(D)**, pCHF3-NSvc4$_{\Delta 106–125}$-eGFP **(E)**, pCHF3-NSvc4$_{1–106}$-eGFP **(F)**, pCHF3-NSvc4$_{1–125}$-eGFP **(G)**, and pCHF3-NSvc4$_{125–286}$-eGFP **(H)**. Harvested leaf samples were examined by confocal microscopy. Arrows indicate the localization of NSvc4 and its mutant fusion protein.

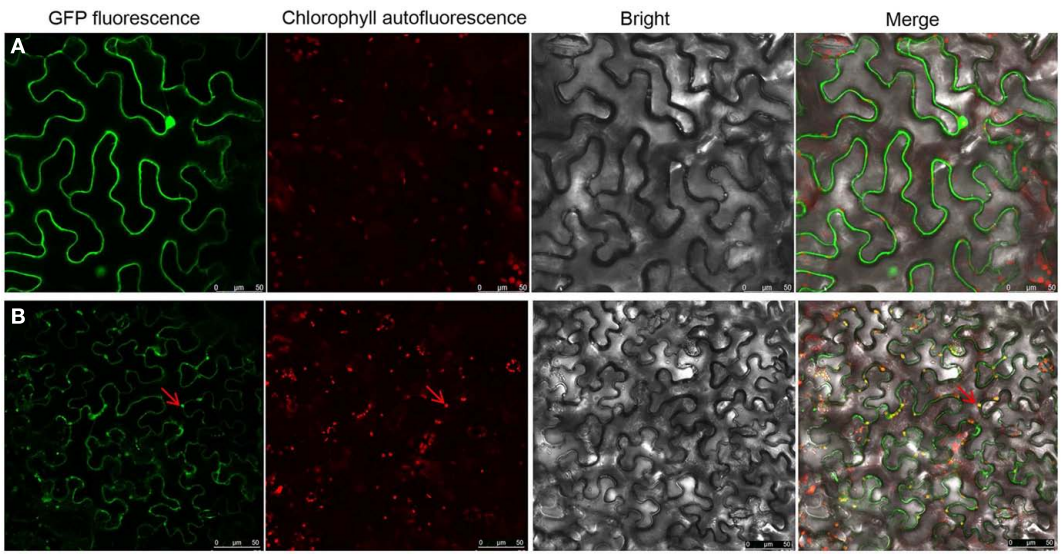

FIGURE 5 | Localization of NSvc4 proteins in chloroplast. Tissues were harvested from *N. benthamiana* leaves at 48 h after agroinfiltration with **(A)** pCHF3-eGFP or **(B)** pCHF3-NSvc4-eGFP. The harvested tissues were then examined under a confocal microscope. Fluorescence emissions were collected simultaneously, with a one photon multiplier-tube bandwidth set at 500–530 and 660–700 nm, respectively. Arrows indicate the sphere-like compartments formed by NSvc4-eGFP fusion protein.

developed phenotypes similar to those caused by the wild wtPVX at 7dpi, and the disease phenotype also recovered by 20 dpi. Interestingly, NSvc4$_{106–286}$ was predicted not to localize to chloroplasts, but, the mutant still elicited a severe symptom phenotype in infiltrated *N. benthamiana* plants that was maintained for up to 20 dpi. These results indicate that NSvc4 chloroplast localization

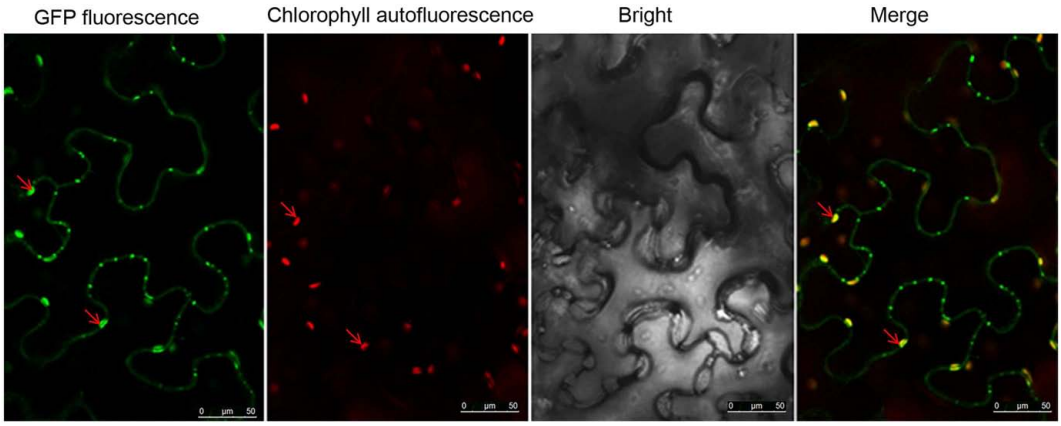

FIGURE 6 | NSvc4-eGFP expressed using the Potato virus X-based vector localized to chloroplasts. At 7 or 8 days post inoculation with pgR-NSvc4-eGFP, systemically infected leaves were sampled and examined by confocal microscope. Arrows indicate the sphere-like compartments formed by NSvc4-eGFP fusion protein.

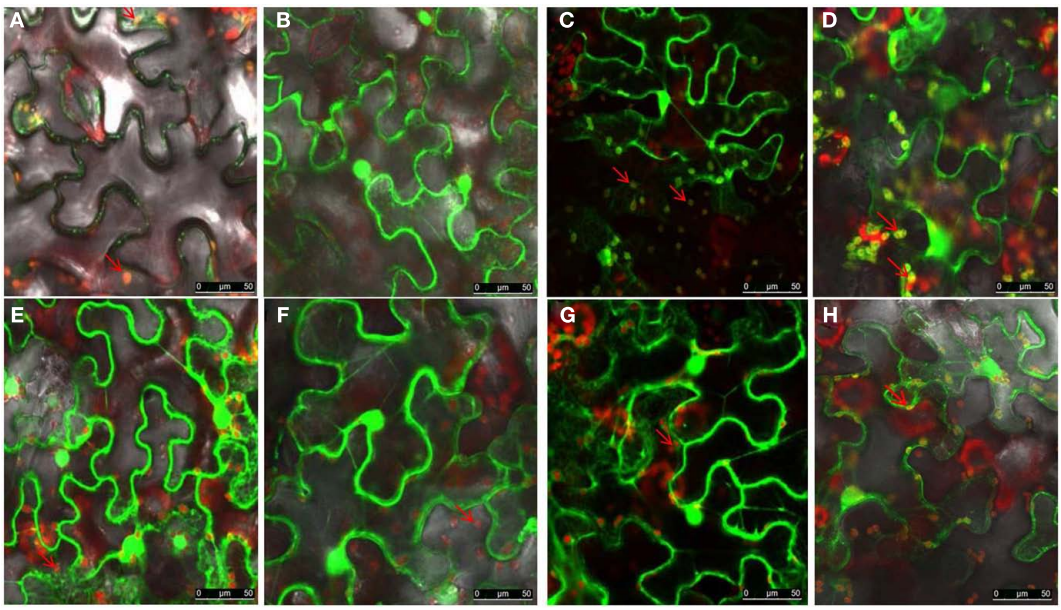

FIGURE 7 | The N-terminus 73 amino acids determine the chloroplast localization of NSvc4. *N. benthamiana* leaves were agroinfiltrated with pCHF3-NSvc4-eGFP **(A)**, pCHF3-NSvc4$_{1-54}$-eGFP **(B)**, pCHF3-NSvc4$_{1-73}$-eGFP **(C)**, pCHF3-NSvc4$_{1-125}$-eGFP **(D)**, pCHF3-NSvc4$_{54-73}$-eGFP **(E)**, pCHF3-NSvc4$_{125-286}$-eGFP **(F)**, pCHF3-NSvc4$_{106-125}$-eGFP **(G)**, pCHF3-NSvc4$_{\Delta 106-125}$-eGFP **(H)**. At 48 h post agroinfiltration the leaves were sampled and examined under a confocal microscope. The fluorescence emission was collected simultaneously, with one photon multiplier-tube bandwidth set at 500–530 and 660–700 nm, respectively. Arrows indicate the sphere-like compartments and the chloroplast.

is dispensable for the exacerbated symptoms. Hence, it is possible that the NSvc4 transmembrane domain has a role in chloroplast malformations, membrane proliferations from the chloroplasts and symptom development.

NSvc4 PROTEIN DID NOT MEDIATE TUBULE FORMATION IN Sf-9 CELLS

Our earlier research has shown that NSvc4 accumulated at PD in the walls of RSV-infected cells (Xiong et al., 2008). Because the NSm MP of *Tomato spotted wilt virus* (TSWV) formed tubule-like structures in insect cells (Storms et al., 1995), we decided to investigate the possibility of tubule formation by RSV NSvc4. In these experiments, the TSWV NSm (AcNPV/NSm-GFP) protein elicited numerous tubule-like extensions on Sf-9 cell surface by 36–48 h post transfection. However, Sf-9 cells transfected with the RSV NSvc4 protein (AcNPV/NSvc4-GFP), failed to develop similar tubules by 48 hpi. In contrast to the free GFP protein (AcNPV/GFP), which was distributed uniformly in the nuclei and in the cytoplasm, the NSvc4-GFP protein (AcNPV/NSvc4-GFP) accumulated as globular structures at the cell periphery and, in this regard, was similar to the localization patterns of NSvc4 in plant

cells (**Figure 11**). However, it has been reported in an abstract that the NS2 protein encoded by RSV vRNA 2 can induce tubule-like structures in insect cells (ITMGCM, 1999), but this report has not been verified in a peer reviewed paper. Nevertheless, it is possible that NS2 may interact with NSvc4 to facilitate RSV movement, so in future experiments, we plan to investigate possible roles of NS2 and NSvc4 protein interactions to determine whether they may act together to facilitate RSV cell-to-cell transport.

DISCUSSION

Our previous studies of RSV NSvc4 have indicated that NSvc4 belongs to the 30 K MP superfamily, and have shown experimentally that the protein interacts with single-stranded RNA *in vitro*, traffics to the PD of dicot cells and can move to adjacent cells after

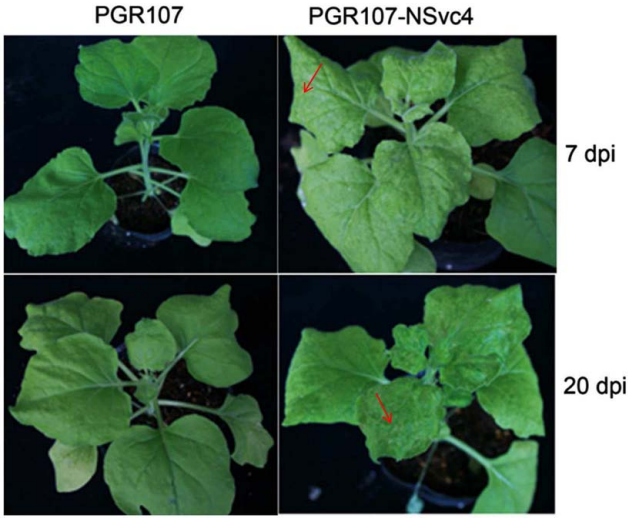

FIGURE 8 | Symptom expression in *N. benthamiana* plants after infection with the wild type PVX vector or the NSVc4 expressing PVX vector. *N. benthamiana* plants were infiltrated with pgR107 (wild type PVX) or pgR107-NSvc4 (PVX expressing NSvc4) at 7 or at 20 dpi. Allows showed the foliar necrosis in pgR107-NSvc4 infected *N. benthamiana*.

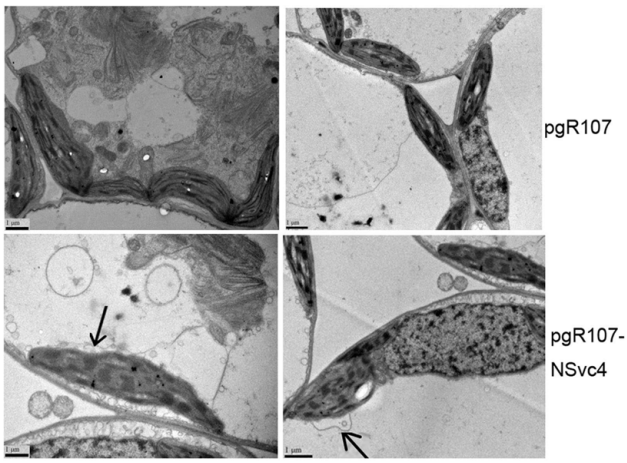

FIGURE 9 | Ultrastructural changes resulting from infection with wild type PVX or PVX-NSvc4. Tissue sections were prepared from the leaves infected with the wild type PVX or PVX expressing NSvc4. Morphological changes in chloroplast were only observed in plants infected with PVX expressing NSvc4. Arrows indicate alterations of chloroplast membrane.

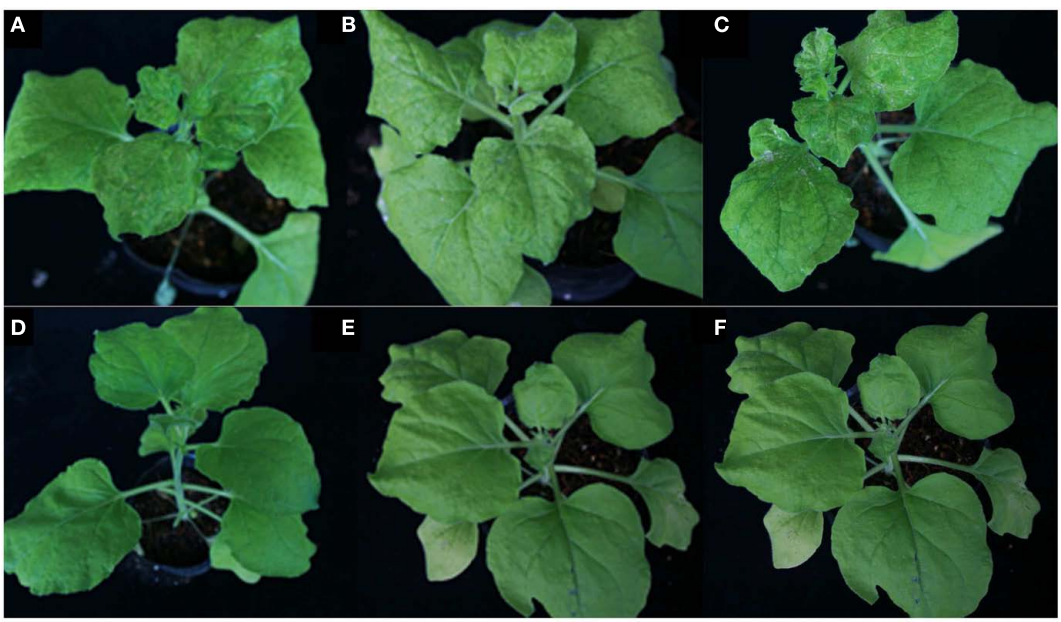

FIGURE 10 | Symptoms elicited by wild type PVX or PVX expressing mutants of NSvc4. *N. benthamiana* plants were agroinfiltrated with various PVX constructs. Plant infected with PVX-NSvc4 **(A)**, PVX-NSvc4$_{1–125}$ **(B)**, PVX-NSvc4$_{125–286}$ **(C)**, PVX **(D)**, PVX-NSvc4$_{1–53}$ **(E)**, and PVX-NSvc4$_{1–73}$ **(F)**. Photographs were taken at 20 days post agroinfiltration.

bombardment (Xiong et al., 2008). Within the 30 K superfamily, the TMV MP has been studied most intensively and is known to target PD via trafficking on cortical ER and actin cytoskeleton (Wright et al., 2007; Hofmann et al., 2009). A recently report indicates that targeting of NSvc4 to PDs utilizes the actin microfilament pathway and the myosin VIII rather than myosin XI motility system (Yuan et al., 2011). Our results complement and verify this study by demonstrating that actin microfilament dissociation by LatB and Golgi disruption by BFA interfere with PD targeting of the NSvc4-eGFP fusion protein, whereas disruption of microtubules by oryzalin has little effect on PD targeting. Moreover, microfilament disruption but not microtubule disruption inhibits infection of RSV in *N. benthamiana*, Thus, our combined results clearly suggest that targeting of NSvc4 to PDs depends on a functional ER and actin network.

Many viral MPs within the 30 K superfamily have a hydrophilic region at their C-termini. Deletion or alanine-scanning mutations within the C-termini of several viral MPs have demonstrated that this region is dispensable for cell-to-cell movement (Schoelz et al., 2011). We have now extended previous RSV studies through transient expression of wtNSvc4 and NSvc4 mutants in cells, and have determined that NSvc4 differs from the general MP rule because the N-terminal 125 AAs are sufficient to target the truncated fragment to the PD. Furthermore, we have shown that AAs 106–125 contain a predicted transmembrane domain and that deletion of this domain abolishes the PD targeting ability of NSvc4. These results strongly suggest that the 20 deleted residues serve as an integral membrane signal that facilitates insertion into the ER.

Several previous reports have shown that some viral MPs accumulated in chloroplast and thus might have an important role in virus replication, movement, and/or symptom development (Prod'homme et al., 2003; Torrance et al., 2006). For example AltMV TGB3 was shown to be responsible for AltMV movement between cells and contained a novel signal which was required for chloroplast membrane localization. Here we provide definitive evidence that RSV NSvc4 has a chloroplast-targeting signal within its N-terminal 73 residues, and that this signal targets the NSvc4-GFP chloroplast in both the agro-mediated and PVX-based expression systems. We anticipate further studies to elucidate the potential involvement of chloroplast-targeting in the RSV life cycle.

Expression of the NSvc4 through PVX-based vector exacerbated disease symptoms in *N. benthamiana* than the symptoms elicited by PVX alone. Electron microscope observations suggested that disease symptoms correlated with chloroplast malformations and cytoplasmic membrane proliferations in cells. However, expression of mutants of NSvc4 indicated no direct connection between chloroplast localization of NSvc4 and symptom development. We propose that the chloroplast-targeting phenomenon may be involved in RSV replication or other unidentified activities. Considering the chloroplast malformations and membrane proliferations in the PVX-NSvc4 infected *N. benthamiana* cells, it

Table 2 | Targeting of NSvc4 and its mutants to plasmodesmata and chloroplast and their roles in symptom development.

Localization/symptom	Plasmodesmata	Chloroplast	Symptom
NSvc4	+	+	+
$NSvc4_{1–54}$	–	–	–
$NSvc4_{1–73}$	–	+	–
$NSvc4_{1–106}$	–	+	n
$NSvc4_{1–125}$	+	+	+
$NSvc4_{125–286}$	–	–	+
$NSvc4_{106–286}$	–	–	+

n, The symptom data was not record.

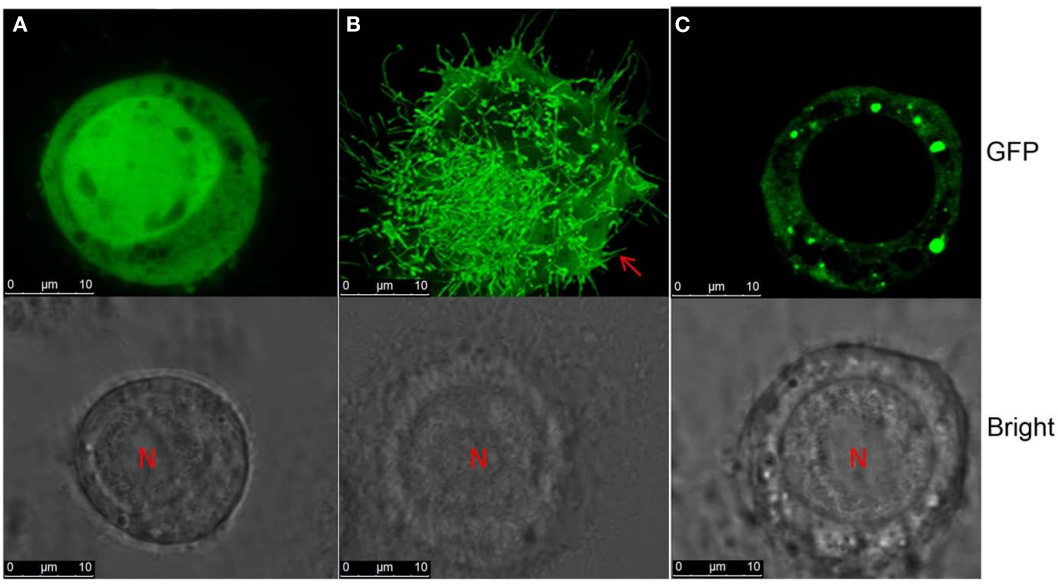

FIGURE 11 | Tubule formation in Sf-9 cells. *S. frugiperda* 9 cells were transinfected with recombinant baculovirus AcNPV/GFP **(A)**, AcNPV/NSm-GFP **(B)**, or AcNPV/NSvc4-GFP **(C)**. Images were taken at 72 h post transfection.

is reasonable to propose that the transmembrane activity of the NSvc4 may play a pivotal role in development of disease symptoms. Because viral MPs modify PD structures and increase PD size exclusion limits, transgenic plants expressing viral MPs often show alterations in plant development. Plant developmental anomalies have also been demonstrated through infection of *N. benthamiana* plants using TMV-based vector expression NSvc4 (Zhang et al., 2012), so the phenomena we have observed are not virus specific. The authors also found that region D17–K33 was recognized as a crucial domain for leaf necrosis response using TMV-based vector expression NSvc4 (Zhang et al., 2012). In our experiment, we also observed foliar necrosis expressed of PVX-NSvc4. More detailed work is needed to determine the regions responsible for formation of foliar necrosis expressed from PVX vector. From these accumulated data, we conclude that RSV NSvc4 is a symptom determinant that affects the host phenotype, but the mechanisms whereby the protein functions in symptom development remain to be elucidated.

One of the major questions unique to RSV movement is the form in which infectious entities might move from initial infection foci to adjacent cells. Because RSV is a negative strand "ambisense" virus, it is obvious that the NC must be involved in intra-cellular transit in order to facilitate nascent transcription and replication in newly invaded plant cells. Similar events also must function during RSV infections of planthopper vectors. Therefore, we carried out preliminary experiments to determine the location of NSvc4 and the TSWV NSm MP in insect cells. Our results show that in contrast to NSm, NSvc4 failed to produce tubule-like structures after plasmid transfection into Sf-9 cells, but instead formed large foci at the surface of the cells. We previously were unable to detect NSvc4 binding to the RSV NC protein, but have shown that NSvc4 exhibits non-specific RNA binding in gel shift assays. These results suggest that NSvc4 may be able to access RNA encapsidated in the NC, and such a mechanism is compatible with recent experimental data for Vesicular stomatitis virus (VSV), the most intensively studied negative strand virus (Green et al., 2011). Interestingly, the VSV NC (N) protein is thought to undergo conformational changes to permit access by the polymerase protein during transcription and replication. Moreover, the matrix protein of negative strand viruses has mechanisms to discriminate genomic NCs from antigenomic NCs during morphogenesis, and these likely are RNA sequence specific. Therefore, we posit that NSvc4 specifically recognizes RNA in RSV gNCs and ferries these complexes to the cell wall and then enlarges the PD complexes sufficiently to facilitate NC transit to adjacent cells. Although, different mechanisms, possibly cell fusion, may be involved in systemic spread in infected planthoppers, we envision that NSvc4:NC associations with NCs likely function during insect infection processes. Therefore, we are planning further investigations to elucidate the complicated mechanisms whereby RSV moves between plant and insect cells.

ACKNOWLEDGMENTS

This research was supported by the Hi-tech Research and Development Program of China (2012AA101505) and the National Natural Science Foundation of China (Grant No. 30870110). We thank Prof. Chuanxi Zhang in Zhejiang University for supply of pFastBacHT-eGFPT and *E. coli DH10Bac*, Qianli An for supplying Man1-RFP plasmids. We apologize to colleagues whose articles were not cited because of space limitations. TSWV NSm was kindly provided by Prof. Jian Hong in Zhejiang University.

REFERENCES

Aberl, H. J., Rutz, M. L., Karayavuz, M., Frischmuth, S., Wege, C., Hülser, D., et al. (2002). Localizing the movement proteins of abutilon mosaic geminivirus in yeast by subcellular fractionation and freeze-fracture immuno-labelling. *Arch. Virol.* 147, 103–117.

Ashby, J., Boutant, E., Seemanpillai, M., Groner, A., Sambade, A., Ritzenthaler, C., et al. (2006). Tobacco mosaic virus movement protein functions as a structural microtubule-associated protein. *J. Virol.* 80, 12433–12433.

Batoko, H., Zheng, H. Q., Hawes, C., and Moore, I. (2000). A rab1 GTPase is required for transport between the endoplasmic reticulum and Golgi apparatus and for normal Golgi movement in plants. *Plant Cell* 12, 2201–2218.

Brandizzi, F., Frangne, N., Marc-Martin, S., Hawes, C., Neuhaus, J. M., and Paris, N. (2002). The destination for single-pass membrane proteins is influenced markedly by the length of the hydrophobic domain. *Plant Cell* 14, 1077–1092.

Brandner, K., Sambade, A., Boutant, E., Didier, P., Mely, Y., Ritzenthaler, C., et al. (2008). Tobacco mosaic virus movement protein interacts with green fluorescent protein-tagged microtubule end-binding protein 1. *Plant Physiol.* 147, 611–623.

Cao, M., Ye, X., Willie, K., Lin, J., Zhang, X., Redinbaugh, M. G., et al. (2010). The capsid protein of turnip crinkle virus overcomes two separate defense barriers to facilitate systemic movement of the virus in Arabidopsis. *J. Virol.* 84, 7793–7802.

Du, Z., Xiao, D., Wu, J., Jia, D., Yuan, Z., Liu, Y., et al. (2011). p2 of Rice stripe virus (RSV) interacts with OsSGS3 and is a silencing suppressor. *Mol. Plant Pathol.* 12, 808–814.

Falk, B. W., and Tsai, J. H. (1998). Biology and molecular biology of viruses in the genus tenuivirus. *Annu. Rev. Phytopathol.* 36, 139–163.

Green, T. J., Rowse, M., Tsao, J., Kang, J., Ge, P., Zhou, Z. H., et al. (2011). Access to RNA encapsidated in the nucleocapsid of vesicular stomatitis virus. *J. Virol.* 85, 2714–2722.

Harries, P. A., Palanichelvam, K., Yu, W., Schoelz, J. E., and Nelson, R. S. (2009a). The cauliflower mosaic virus protein P6 forms motile inclusions that traffic along actin microfilaments and stabilize microtubules. *Plant Physiol.* 149, 1005–1016.

Harries, P. A., Park, J. W., Sasaki, N., Ballard, K. D., Maule, A. J., and Nelson, R. S. (2009b). Differing requirements for actin and myosin by plant viruses for sustained intercellular movement. *Proc. Natl. Acad. Sci. U.S.A.* 106, 17594–17599.

Harries, P. A., Schoelz, J. E., and Nelson, R. S. (2010). Intracellular transport of viruses and their components: utilizing the cytoskeleton and membrane highways. *Mol. Plant Microbe Interact.* 23, 1381–1393.

Hessa, T., Meindl-Beinker, N. M., Bernsel, A., Kim, H., Sato, Y., Lerch-Bader, M., et al. (2007). Molecular code for transmembrane-helix recognition by the Sec61 translocon. *Nature* 450, 1026–1030.

Hibino, H. (1996). Biology and epidemiology of rice viruses. *Annu. Rev. Phytopathol.* 34, 249–274.

Hofmann, C., Niehl, A., Sambade, A., Steinmetz, A., and Heinlein, M. (2009). Inhibition of tobacco mosaic virus movement by expression of an actin-binding protein. *Plant Physiol.* 149, 1810–1823.

Huang, Z., Han, Y., and Howell, S. H. (2000). Formation of surface tubules and fluorescent foci in Arabidopsis thaliana protoplasts expressing a fusion between the green fluorescent protein and the cauliflower mosaic virus movement protein. *Virology* 271, 58–64.

ITMGCM. (1999). Expression of rice stripe virus 228 k protein in insect cell. *Annu. Phytopathol. Soc. Jpn.* 65, 337.

Laporte, C., Vetter, G., Loudes, A. M., Robinson, D. G., Hillmer, S., Stussi-Garaud, C., et al. (2003). Involvement of the secretory pathway and the cytoskeleton in intracellular targeting and tubule assembly of grapevine fanleaf virus movement protein in tobacco BY-2 cells. *Plant Cell* 15, 2058–2075.

Li, S., Xiong, R. Y., Wang, X. F., and Zhou, Y. J. (2011). Five proteins of *Laodelphax striatellus* are potentially involved in the interactions between rice stripe virus and vector. *PLoS ONE* 6:e26585. doi:10.1371/journal.pone.0026585.

Lim, H. S., Bragg, J. N., Ganesan, U., Ruzin, S., Schichnes, D., Lee, M. Y., et al. (2009). Subcellular localization of the barley stripe mosaic virus triple gene block proteins. *J. Virol.* 83, 9432–9448.

Lim, H. S., Vaira, A. M., Bae, H., Bragg, J. N., Ruzin, S. E., Bauchan, G. R., et al. (2010). Mutation of a chloroplast-targeting signal in alternanthera mosaic virus TGB3 impairs cell-to-cell movement and eliminates long-distance virus movement. *J. Gen. Virol.* 91, 2102–2115.

Paape, M., Solovyev, A. G., Erokhina, T. N., Minina, E. A., Schepetilnikov, M. V., Lesemann, D. E., et al. (2006). At-4/1, an interactor of the tomato spotted wilt virus movement protein, belongs to a new family of plant proteins capable of directed intra- and intercellular trafficking. *Mol. Plant Microbe Interact.* 19, 874–883.

Pouwels, J., Van der Krogt, G. N. M., Van Lent, J., Bisseling, T., and Wellink, J. (2002). The cytoskeleton and the secretory pathway are not involved in targeting the cowpea mosaic virus movement protein to the cell periphery. *Virology* 297, 48–56.

Prod'homme, D., Jakubiec, A., Tournier, V., Drugeon, G., and Jupin, I. (2003). Targeting of the turnip yellow mosaic virus 66K replication protein to the chloroplast envelope is mediated by the 140K protein. *J. Virol.* 77, 9124–9135.

Qu, F., Ren, T., and Morris, T. J. (2003). The coat protein of turnip crinkle virus suppresses posttranscriptional gene silencing at an early initiation step. *J. Virol.* 77, 511–522.

Schoelz, J. E., Harries, P. A., and Nelson, R. S. (2011). Intracellular transport of plant viruses: finding the door out of the cell. *Mol. Plant* 4, 813–831.

Scholthof, H. B. (2005). Plant virus transport: motions of functional equivalence. *Trends Plant Sci.* 10, 376–382.

Shen, Q., Liu, Z., Song, F., Xie, Q., Hanley-Bowdoin, L., and Zhou, X. (2011). Tomato SlSnRK1 protein interacts with and phosphorylates betaC1, a pathogenesis protein encoded by a geminivirus beta-satellite. *Plant Physiol.* 157, 1394–1406.

Shimizu, T., Yoshii, A., Sakurai, K., Hamada, K., Yamaji, Y., Suzuki, M., et al. (2009). Identification of a novel tobacco DnaJ-like protein that interacts with the movement protein of tobacco mosaic virus. *Arch. Virol.* 154, 959–967.

Snider, C., Jayasinghe, S., Hristova, K., and White, S. H. (2009). MPEx: a tool for exploring membrane proteins. *Protein Sci.* 18, 2624–2628.

Storms, M. M., Kormelink, R., Peters, D., Van Lent, J. W., and Goldbach, R. W. (1995). The nonstructural NSm protein of tomato spotted wilt virus induces tubular structures in plant and insect cells. *Virology* 214, 485–493.

Tilsner, J., Linnik, O., Wright, K. M., Bell, K., Roberts, A. G., Lacomme, C., et al. (2012). The TGB1 movement protein of potato virus X reorganizes actin and endomembranes into the X-body, a viral replication factory. *Plant Physiol.* 158, 1359–1370.

Toriyama, S. (1986). Rice stripe virus: prototype of a new group of viruses that replicate in plants and insects. *Microbiol. Sci.* 3, 347–351.

Torrance, L., Cowan, G. H., Gillespie, T., Ziegler, A., and Lacomme, C. (2006). Barley stripe mosaic virus-encoded proteins triple-gene block 2 and gammab localize to chloroplasts in virus-infected monocot and dicot plants, revealing hitherto-unknown roles in virus replication. *J. Gen. Virol.* 87, 2403–2411.

Tse, Y. C., Lo, S. W., Hillmer, S., Dupree, P., and Jiang, L. (2006). Dynamic response of prevacuolar compartments to brefeldin a in plant cells. *Plant Physiol.* 142, 1442–1459.

Verchot-Lubicz, J., Torrance, L., Solovyev, A. G., Morozov, S. Y., Jackson, A. O., and Gilmer, D. (2010). Varied movement strategies employed by triple gene block-encoding viruses. *Mol. Plant Microbe Interact.* 23, 1231–1247.

Wei, T., Huang, T. S., McNeil, J., Laliberte, J. F., Hong, J., Nelson, R. S., et al. (2010a). Sequential recruitment of the endoplasmic reticulum and chloroplasts for plant potyvirus replication. *J. Virol.* 84, 799–809.

Wei, T. Y., Zhang, C. W., Hong, J. A., Xiong, R. Y., Kasschau, K. D., Zhou, X., et al. (2010b). Formation of complexes at plasmodesmata for potyvirus intercellular movement is mediated by the viral protein P3N-PIPO. *PLoS Pathog.* 6:e1000962. doi:10.1371/journal.ppat.1000962.

Wei, T. Y., Yang, J. G., Liao, F. R., Gao, F. L., Lu, L. M., Zhang, X.-T., et al. (2009). Genetic diversity and population structure of rice stripe virus in China. *J. Gen. Virol.* 90, 1025–1034.

Wright, K. M., Wood, N. T., Roberts, A. G., Chapman, S., Boevink, P., Mackenzie, K. M., et al. (2007). Targeting of TMV movement protein to plasmodesmata requires the actin/ER network: evidence from FRAP. *Traffic* 8, 21–31.

Xiong, R., Wu, J., Zhou, Y., and Zhou, X. (2008). Identification of a movement protein of the tenuivirus rice stripe virus. *J. Virol.* 82, 12304–12311.

Xiong, R., Wu, J., Zhou, Y., and Zhou, X. (2009). Characterization and subcellular localization of an RNA silencing suppressor encoded by rice stripe tenuivirus. *Virology* 387, 29–40.

Yuan, Z., Chen, H., Chen, Q., Omura, T., Xie, L., Wu, Z., et al. (2011). The early secretory pathway and an actin-myosin VIII motility system are required for plasmodesmatal localization of the NSvc4 protein of rice stripe virus. *Virus Res.* 159, 62–68.

Zhang, C., Pei, X., Wang, Z., Jia, S., Guo, S., Zhang, Y., et al. (2012). The rice stripe virus pc4 functions in movement and foliar necrosis expression in *Nicotiana benthamiana*. *Virology* 425, 113–121.

Zhang, S. C., Ghosh, R., and Jeske, H. (2002). Subcellular targeting domains of abutilon mosaic geminivirus movement protein BC1. *Arch. Virol.* 147, 2349–2363.

Zhang, S. C., Wege, C., and Jeske, H. (2001). Movement proteins (BC1 and BV1) of abutilon mosaic geminivirus are cotransported in and between cells of sink but not of source leaves as detected by green fluorescent protein tagging. *Virology* 290, 249–260.

Zhao, S. L., Dai, X. J., Liang, J. S., and Liang, C. Y. (2012). Surface display of rice stripe virus NSvc2 and analysis of its membrane fusion activity. *Virol. Sin.* 27, 100–108.

Conflict of Interest Statement: The authors declare that the research was conducted in the absence of any commercial or financial relationships that could be construed as a potential conflict of interest.

Received: 09 October 2012; accepted: 19 November 2012; published online: 07 December 2012.

Citation: Xu Y and Zhou X (2012) Role of rice stripe virus NSvc4 in cell-to-cell movement and symptom development in Nicotiana benthamiana. Front. Plant Sci. ***3****:269. doi: 10.3389/fpls.2012.00269*

This article was submitted to Frontiers in Plant-Microbe Interaction, a specialty of Frontiers in Plant Science.

APPENDIX

Table A1 | Primers used in our experiments.

MP(Kpn1)-F	5′-ggggtaccATGGCTTTGTCTCGACTTTTG-3′
MP(BamH1)-R	5′-CGGGATCCcatgatgacagaaacttcag-3′
MP(BamH1)-R54	5′-GGATCCtgtggcagcttggtcaatc-3′
MP(BamH1)-R73	5′-GGATCCATCATACTTGTTCACCTTGACAT-3′
MP(BamH1)-R106	5′-CGGGATCCatgggtgagaggttgatg-3′
MP(kpn1)-F125	5′-gggtaccATGagtggaataactaccctcc-3′
MP(Kpn1)-F106	5′-gggtaccATGtatccattctttagagtggc-3′
MP(BamH1)-R125	5′-CGGGATCCagctctacccttgattcct-3′
MP-FoI	5′-cctctcacccatagtggaataactaccctc-3′
MP-RoI	5′-agttattccactatgggtgagaggttgatg-3′
eGFP(Sal1)-R	5′-GTCGACTTACTTGTACAGCTCGTCCAT-3′
MP(sal1)-R54	5′-GTCGACCTAtgtggcagcttggtcaatc-3′
MP(sal1)-R73	5′-GTCGACCTAATCATACTTGTTCACCTTGACAT-3′
MP(sal1)-R125	5′-GTCGACCTAagctctacccttgattcct-3′
MP(Cla1)-F125	5′-CCATCGATATGagtggaataactaccctcc-3′
MP(Cla1)-F	5′-ATCGATATGGCTTTGTCTCGACTTTT-3′
MP(sal1)-R	5′-GTCGACCTACATGATGACAGAAACTTC-3′
MP-(BamH1)-F	5′-GGATCCATGGCTTTGTCTCGACTTTT-3′
MP-(Sal1)-R	5′-GTCGACCTACATGATGACAGAAACTTC-3′

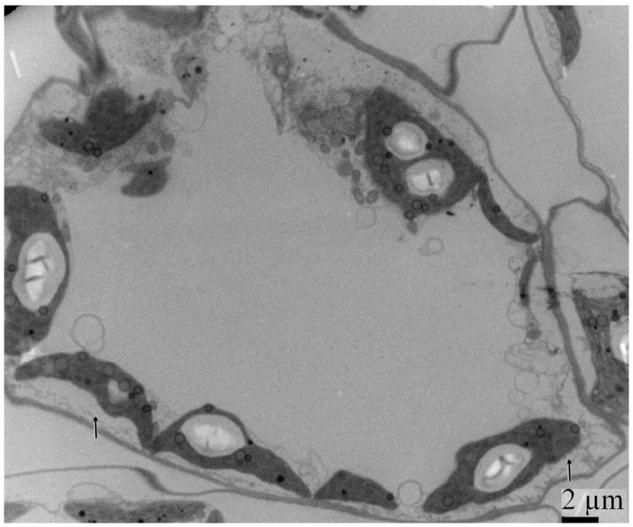

FIGURE A1 | Ultrastructural structures resulting from 20 days post rub-inoculating *N. benthamiana* leaves with crude extracts from RSV-infected *O. sativa* leaves. Allows showed that membrane proliferations radiating from the chloroplasts into the cytoplasm.

frontiers in
PLANT SCIENCE

HYPOTHESIS AND THEORY ARTICLE
published: 27 December 2012
doi: 10.3389/fpls.2012.00291

The induction of stromule formation by a plant DNA-virus in epidermal leaf tissues suggests a novel intra- and intercellular macromolecular trafficking route

Björn Krenz[1], Holger Jeske[2] and Tatjana Kleinow[2]*

[1] *Plant Pathology and Plant-Microbe Biology, Cornell University, Ithaca, NY, USA*
[2] *Molecular Biology and Plant Virology, Institute of Biology, Universität Stuttgart, Stuttgart, Germany*

Edited by:
Helene Sanfacon, Agriculture and Agri-Food Canada, Canada

Reviewed by:
Walter Gassmann, University of Missouri, USA
John Hammond, United States Department of Agriculture, USA
Ching-Hsiu Tsai, National Chung Hsing University, Taiwan
Handanahal Subbarao Savithri, Indian Institute of Science, India

***Correspondence:**
Tatjana Kleinow, Molecular Biology and Plant Virology, Institute of Biology, Universität Stuttgart, Pfaffenwaldring 57, 70569 Stuttgart, Germany.
e-mail: tatjana.kleinow@bio.uni-stuttgart.de

Stromules are dynamic thin protrusions of membrane envelope from plant cell plastids. Despite considerable progress in understanding the importance of certain cytoskeleton elements and motor proteins for stromule maintenance, their function within the cell has yet to be unraveled. Several viruses cause a remodulation of plastid structures and stromule biogenesis within their host plants. For RNA-viruses these interactions were demonstrated to be relevant to the infection process. An involvement of plastids and stromules is assumed in the DNA-virus life cycle as well, but their functional role needs to be determined. Recent findings support a participation of heat shock cognate 70 kDa protein (cpHSC70-1)-containing stromules induced by a DNA-virus infection (*Abutilon* mosaic virus, AbMV, *Geminiviridae*) in intra- and intercellular molecule exchange. The chaperone cpHSC70-1 was shown to interact with the AbMV movement protein (MP). Bimolecular fluorescence complementation confirmed the interaction of cpHSC70-1 and MP, and showed a homo-oligomerization of either protein *in planta*. The complexes were detected at the cellular margin and co-localized with plastids. In healthy plant tissues cpHSC70-1-oligomers occurred in distinct spots at chloroplasts and in small filaments extending from plastids to the cell periphery. AbMV-infection induced a cpHSC70-1-containing stromule network that exhibits elliptical dilations and transverses whole cells. Silencing of the *cpHSC70* gene revealed an impact of cpHSC70 on chloroplast stability and restricted AbMV movement, but not viral DNA accumulation. Based on these data, a model is suggested in which these stromules function in molecule exchange between plastids and other organelles and perhaps other cells. AbMV may utilize cpHSC70-1 for trafficking along plastids and stromules into a neighboring cell or from plastids into the nucleus. Experimental approaches to investigate this hypothesis are discussed.

Keywords: geminivirus, movement protein, plastid, chaperone, heat shock protein

INTRODUCTION

In plants, transport of endogenous macromolecules such as proteins and nucleic acids over cellular boundaries occurs in a highly selective and regulated manner (Oparka, 2004; Lee and Lu, 2011; Maule et al., 2011; Niehl and Heinlein, 2011; Zavaliev et al., 2011). These controlled intra- and intercellular pathways are exploited by plant viruses for their systemic spread within their hosts; viruses can thus be used as tools to study basic endogenous transport processes within plants (Lee et al., 2003; Lucas, 2006; Benitez-Alfonso et al., 2010; Harries and Ding, 2011; Harries et al., 2011; Niehl and Heinlein, 2011; Schoelz et al., 2011; Ueki and Citovsky, 2011). There is evidence accumulating that interactions of viruses with the cytoskeleton or the endomembrane system are involved in the targeting of viral nucleoprotein complexes and transport-mediating movement proteins (MPs) to plasmodesmata. However, it is still not possible to generate a complete model of intra- and intercellular movement for any known plant virus. Considering the diverse and sometimes contrasting reports on the roles of various cellular components in viral spread, it is conceivable that viruses use fundamentally different transport mechanisms within their hosts. This seems to be the case for members within one genus, as shown, for example by research into RNA-viruses of the genus *Tobamovirus* [turnip vein-clearing virus (TVCV) and tobacco mosaic virus (TMV); Harries et al., 2009] and the genus *Potexvirus* [*Alternanthera* mosaic virus (AltMV) and potato virus X (PVX); Lim et al., 2010].

TRANSPORT MODELS FOR THE PLANT DNA GEMINIVIRUSES

In contrast to RNA-viruses, plant-infecting DNA geminiviruses (family *Geminiviridae*) replicate within the nucleus, and systemic infection requires the crossing of two cellular barriers, the nuclear envelope via pores and the cell wall via plasmodesmata (Waigmann et al., 2004; Krichevsky et al., 2006; Lucas, 2006; Jeske, 2009). The geminiviruses have relatively small genomes (2.5–3.0 kb per single-stranded DNA circle) and with this limited coding capacity exhibit a strong dependency on host proteins to complete their life cycle. As a consequence, viral-encoded transport-mediating proteins have to interact with a variety of plant factors involved in

macromolecular trafficking to overcome cellular boundaries and transfer viral DNA (vDNA) from a nucleus through the cytoplasm and via plasmodesmata into an adjacent cell and into the nucleus of that cell. The genome of bipartite geminiviruses (genus *Begomovirus*) consists of two DNA molecules: DNA A and DNA B. The two DNA B-encoded proteins, nuclear-shuttle protein (NSP) and MP, mediate the viral transport processes (Gafni and Epel, 2002; Rojas et al., 2005; Wege, 2007; Jeske, 2009) and both proteins have an impact on viral pathogenicity (Rojas et al., 2005; Zhou et al., 2007; Jeske, 2009). Previous work showed the C-terminal domain of begomoviral MPs to be important for symptom development and pathogenicity (von Arnim and Stanley, 1992; Ingham and Lazarowitz, 1993; Pascal et al., 1993; Duan et al., 1997; Hou et al., 2000; Saunders et al., 2001; Kleinow et al., 2009a). The DNA A-encoded coat protein (CP) is not essential for systemic infection of bipartite begomoviruses, suggesting that the transport complex is distinct from virions (Rojas et al., 2005; Jeske, 2009). However, CP was able to complement defective NSP mutants, and is therefore regarded as a redundant element in viral movement (Qin et al., 1998). Several studies provide evidence that NSP facilitates trafficking of vDNA into and out of the nucleus, and that MP serves as a membrane adaptor and mediates cell-to-cell transfer via plasmodesmata as well as long-distance spread through the phloem (Rojas et al., 2005; Krichevsky et al., 2006; Wege, 2007; Jeske, 2009).

Two models are currently suggested for the role of NSP and MP during cell-to-cell transport of bipartite geminiviruses: the "couple-skating" and the "relay race" models (Rojas et al., 2005; Jeske, 2009). The "couple-skating" model is based on the experimental data of the phloem-limited begomoviruses squash leaf curl virus (SLCV; Pascal et al., 1994; Sanderfoot and Lazarowitz, 1995; Sanderfoot et al., 1996), cabbage leaf curl virus (CaLCuV; Carvalho et al., 2008a,b), and *Abutilon* mosaic virus (AbMV; Zhang et al., 2001; Aberle et al., 2002; Hehnle et al., 2004; Frischmuth et al., 2007). This model suggests that MP binds the NSP/vDNA complex at the cytoplasmic side of plasma membranes or microsomal vesicles, and transfers the nucleoprotein complex into the next cell either along the plasma membrane or via the endoplasmic reticulum (ER) that spans the plasmodesmata. In contrast, the "relay race" model predicts that after NSP-mediated nuclear export the vDNA is taken over by MP, which then transports the vDNA into the adjacent cell (Noueiry et al., 1994; Rojas et al., 1998, 2005). This model is based on experimental data of the mesophyll-invading begomovirus bean dwarf mosaic virus (BDMV; Levy and Tzfira, 2011). Nevertheless, details of how both proteins co-ordinate vDNA transfer from the nucleus to the cell periphery and further throughout the plant body, are mostly unknown.

For a controlled cycle of geminiviral replication, transcription, encapsidation, and movement, NSP and MP are most likely integrated into a regulatory network consisting of other viral proteins and plant factors. Several studies have characterized a set of interacting host proteins for NSP and MP. NSPs of CaLCuV, tomato golden mosaic virus (TGMV), and tomato crinkle leaf yellows virus (TCrLYV) were found to interact with two classes of receptor-like kinases from *Arabidopsis thaliana* (Fontes et al., 2004; Mariano et al., 2004; Florentino et al., 2006). The further analysis of the NSP/kinase interactions indicated that they play a role in infectivity and symptom development. NSP counters activation of defense signaling mediated by one kinase class via phosphorylation of an immediate downstream target, the ribosomal protein L10/QM (Fontes et al., 2004; Mariano et al., 2004; Florentino et al., 2006; Carvalho et al., 2008c; Rocha et al., 2008; Santos et al., 2010). Additionally, CaLCuV NSP was found to interact with an acetyltransferase (AtNSI; McGarry et al., 2003; Carvalho and Lazarowitz, 2004; Carvalho et al., 2006) and with a small GTPase (Carvalho et al., 2008a,b). AtNSI is proposed to regulate nuclear export of vDNA by acetylating histones and CP. Carvalho et al. (2008a,b) suggest a function for the small GTPase in nuclear export processes, probably as a co-factor of NSP.

Independent of the transport model, the begomoviral MPs have to mediate multiple functions during intra- and intercellular trafficking. The identification of three phosphorylation sites in the AbMV MP, which have an impact on symptom development and/or vDNA accumulation (Kleinow et al., 2009a), indicates a regulation of diverse MP functions by yet unknown host kinases. Currently, three interacting host factors of begomoviral MPs have been identified: a histone H3 (Zhou et al., 2011), a synaptotagmin (SYTA; Lewis and Lazarowitz, 2010), and a chaperone, the heat shock cognate 70 kDa protein cpHSC70-1 (Krenz et al., 2010). Gel overlay assays, and *in vitro* and *in vivo* co-immunoprecipitation (Co-IP) experiments showed an interaction of H3 with NSP and MP of BDMV as well as with CPs of different geminiviruses (Zhou et al., 2011). In *Nicotiana tabacum* protoplasts and *N. benthamiana* leaves, transiently expressed H3 co-localized with NSP in the nucleus and the presence of MP redirected H3 to the cell periphery and plasmodesmata. A complex composed of H3, NSP, MP, and vDNA was recovered by Co-IP from *N. benthamiana* leaves transiently expressing epitope-tagged H3. The data support a model in which histone H3 is a component of a geminiviral movement-competent vDNA complex that assembles in the nucleus and is transferred to the cell periphery and plasmodesmata. SYTA localized to endosomes in *Arabidopsis* cells, and interacted with MPs of the begomoviruses CaLCuV and SLCV as well as with the unrelated MP of the RNA-virus TMV (Lewis and Lazarowitz, 2010). Transgenic *Arabidopsis* lines with either a reduced SYTA level or expressing a dominant-negative SYTA mutant exhibited a delayed systemic infection and an inhibition of cell-to-cell trafficking of the different MPs. Consequently, Lewis and Lazarowitz (2010) proposed that: (i) SYTA regulates endocytosis and (ii) distinct viral MPs transport their cargo to plasmodesmata for cell-to-cell spread via an endocytotic recycling pathway. The chaperone cpHSC70-1 of *Arabidopsis* was shown to specifically interact with the N-terminal domain of AbMV MP in a yeast two-hybrid system (Krenz et al., 2010). Bi-molecular fluorescence complementation (BiFC) analysis provided further evidence for the chaperone/MP interaction, and revealed an MP as well as a cpHSC70-1 self-interaction *in planta* (Krenz et al., 2010). MP/cpHSC70-1 complexes and MP-oligomers were observed at the cell periphery and co-localized with chloroplasts. The detection of MP-homo-oligomers at the cellular margin is in agreement with other localization studies in plant cells (Zhang et al., 2001; Kleinow et al., 2009b) and with earlier yeast two-hybrid assays that showed an MP oligomerization via

the C-terminal domain (Frischmuth et al., 2004). MP-oligomer formation has also been detected at chloroplasts (Krenz et al., 2010). It is unknown whether BiFC results from MP imported into plastids or merely associated with the outer envelope of the chloroplast. No BiFC signal was seen in peri-nuclear sites as was previously found for AbMV MP transiently expressed as green fluorescent protein (GFP) fusion in plant cells (Zhang et al., 2001). Thus, MP/MP interaction may be restricted to chloroplasts and the cell periphery.

Bi-molecular fluorescence complementation showed that cpHSC70-1-oligomers were mainly associated with chloroplasts where they accumulated in distinct spots, and occurred to a lower extent in small filaments extending from plastids to the cell periphery and distributed at the periphery (Krenz et al., 2010). The localization of cpHSC70-1 was significantly influenced by AbMV-infection, accumulating in fluorescent foci on long filamental tubular structures reminiscent of plastid stromules, stroma-filled plastid tubules (Natesan et al., 2005; Hanson and Sattarzadeh, 2008). It remains uncertain whether cpHSC70-1 was maintained exclusively within the stroma or whether it was re-located to other structures upon geminiviral infection such as envelope membranes or the intermembrane space. Altogether, AbMV-infection seems to induce a prominent formation of stromules. To our knowledge the geminivirus AbMV is the only plant DNA-virus so far for which stromule biogenesis was documented. Silencing of the *cpHSC70* gene of *N. benthamiana* with the aid of an AbMV DNA A-derived gene silencing vector caused tiny white leaf sectors, which indicated an impact of cpHSC70 on chloroplast stability (Krenz et al., 2010). vDNA accumulated within these small chlorotic areas that were spatially restricted to small sectors adjacent to veins, suggesting a functional relevance of the MP/chaperone interaction for AbMV transport to symptom induction *in planta*.

CELLULAR FUNCTIONS OF HSP70 AND HSC70 AND THEIR PUTATIVE ROLES IN VIRAL INFECTION

The expression of chaperones from the heat shock protein 70 kDa (HSP70) family is induced in response to developmental signals and various abiotic and biotic stress stimuli (Escaler et al., 2000a,b; Maule et al., 2000; Sung et al., 2001; Aparicio et al., 2005; Brizard et al., 2006; Swindell et al., 2007). Some family members exhibit a low constitutive expression level and are therefore named heat shock cognate proteins 70 kDa (HSC70s) (Sung et al., 2001; Swindell et al., 2007). The cellular functions of this chaperone family are quite diverse. They assist newly translated proteins to obtain their active conformation, misfolded or aggregated proteins to refold, assist in membrane translocation of proteins, in assembly and disassembly of macromolecular complexes and in controlling the activity of regulatory factors (Kanzaki et al., 2003; Mayer and Bukau, 2005; Weibezahn et al., 2005; Bukau et al., 2006; Noel et al., 2007; Kampinga and Craig, 2010; Mayer, 2010; Flores-Pérez and Jarvis, 2012). In addition to their intracellular functions in different subcellular compartments, HSP70s play a role in cell-to-cell transport as indicated by two non-cell-autonomous cytoplasmic HSP70s from *Cucurbita maxima* (Aoki et al., 2002) and by closterovirus-encoded homologs of HSP70s which are essential for virus transport and plasmodesmata targeting (Alzhanova et al., 2007; Avisar et al., 2008, and references therein). For HSP70s and HSC70s, substrate binding and release is regulated by a conformational change that is driven by their ATPase activity. Co-chaperones (DNAJ-like/HSP40 type proteins) assist HSP70s and HSC70s functions with their delivery and release of substrates and by enhancing ATP hydrolysis activity.

HSP70s and HSC70s transcript and protein levels are up-regulated in plants upon an infection with RNA- or DNA-viruses (Escaler et al., 2000a,b; Maule et al., 2000; Aparicio et al., 2005; Brizard et al., 2006). Accumulation of viral proteins within the cell during the infection causes stress and might thereby induce the expression of this chaperone family. Several classes of chaperones and co-chaperones including HSP70s/HSC70s and their specific co-chaperones were identified to interact with viral proteins to facilitate the regulation of viral replication, transcription, encapsidation, and intra- and intercellular movement as well as to suppress pathogen responses (Noel et al., 2007; Benitez-Alfonso et al., 2010; Nagy et al., 2011). Recently, silencing of a cytosolic HSC70-1 was found to impair infection by the monopartite geminivirus tomato yellow leaf curl Sardinia virus (TYLCSV) in *N. benthamiana* (Lozano-Duran et al., 2011). However, none of these HSP70s and HSC70s involved in viral life cycles were located in the chloroplast stroma where cpHSC70-1 was identified to interact with the MP of the geminivirus AbMV (Krenz et al., 2010). In addition to the localization of cpHSC70-1 in the chloroplast stroma and stromules, it is also seen in mitochondria and as a nuclear protein in response to cold stress (Sung et al., 2001; Peltier et al., 2002, 2006; Bae et al., 2003; Ito et al., 2006; Su and Li, 2008, 2010; Krenz et al., 2010; Latijnhouwers et al., 2010). An analysis of an *Arabidopsis* knock-out mutant of cpHSC70-1 revealed that its deficiency caused severe developmental defects (Su and Li, 2008, 2010; Latijnhouwers et al., 2010), but the functions of cpHSC70-1 and other stroma-targeted HSP70s/HSC70s are not completely understood. Recent genetic and biochemical analyses indicated that cpHSC70-1 seems to play a role in protein translocation into the plastid stroma in early developmental stages of plants (Su and Li, 2010; Flores-Pérez and Jarvis, 2012). It is well known that HSP70s/HSC70s fulfill multiple functions in chloroplasts (Flores-Pérez and Jarvis, 2012), therefore the participation of cpHSC70-1 in protein transport across membranes might not be the only function it provides. What function of cpHSC70-1 is targeted by AbMV MP? It can be speculated that the virus exploits the ATPase activity of the chaperone as a driving force to mediate transport of the geminiviral nucleoprotein complexes.

PLASTIDS AND STROMULES IN VIRAL INFECTION

Several interactions of RNA-viruses with chloroplasts have been described which were important for the viral infection process (Reinero and Beachy, 1986; Schoelz and Zaitlin, 1989; Prod'homme et al., 2003; Jimenez et al., 2006; Torrance et al., 2006; Xiang et al., 2006; Lin et al., 2007; Lim et al., 2010). Virus–chloroplast interactions most likely facilitate viral replication or movement. The role of chloroplasts in the life cycle of plant DNA-viruses needs to be examined. In studies of cellular alterations induced by various geminiviruses in systemically infected plants, dramatic morphological changes in the ultrastructure of chloroplasts were identified, such as vesiculated entities, reduced

starch and chlorophyll content, accumulation of fibrillar inclusions, virus-like particles, and vDNA within plastids (Esau, 1933; Jeske and Werz, 1978, 1980a,b; Schuchalter-Eicke and Jeske, 1983; Jeske and Schuchalter-Eicke, 1984; Jeske, 1986; Gröning et al., 1987, 1990; Rushing et al., 1987; Channarayappa et al., 1992). For AbMV it was shown that the severity of chloroplast structure remodeling was dependent on light intensity, and diurnal and seasonal conditions. Geminivirus-induced plastid alterations have thus far been interpreted to be an indirect result of the interference of viral infection with carbohydrate metabolism, mainly through a disruption in translocation via the phloem (Jeske and Werz, 1978). Nevertheless, the detection of vDNA, fibrillar inclusions, or virus-like particles within chloroplasts, suggests other functions of this interplay. Until now, only AbMV vDNA was detected in purified plastids from infected plants (Gröning et al., 1987, 1990). An artificial co-purification was excluded by thermolysin and DNase I treatment. *In situ* hybridization detected high amounts of AbMV vDNA in a low number of purified plastids, which would not be expected for a non-specific co-purification. However, so far, *in situ* hybridization of infected *Abutilon sellovianum* tissue only revealed AbMV vDNA-specific signals on plastids in rare cases (Horns and Jeske, 1991). Furthermore, the finding that an outer envelope membrane protein (Crumpled leaf) is implicated in the CaLCuV infection process also supports an involvement of chloroplasts in the geminiviral life cycle (Trejo-Saavedra et al., 2009). An interesting plastid modification detected upon AbMV-infection, was the induction of stromule biogenesis (Krenz et al., 2010).

Stromules emanate from the main body of the plastid and are confined by the outer and inner envelope membranes (Natesan et al., 2005; Hanson and Sattarzadeh, 2008, 2011). They represent a highly dynamic structure which extends, retracts, branches, bends, and sometimes releases vesicles from their tip (Gunning, 2005; Natesan et al., 2005; Hanson and Sattarzadeh, 2008). The typical diameter is <1 μm and the length is extremely variable due to their dynamic properties (Gray et al., 2001; Kwok and Hanson, 2004b; Waters et al., 2004). Stromules are distinguished from other irregular shaped plastid protrusions by their specific shape index (Holzinger et al., 2007). The movement of stromules relies on the actin cytoskeleton and the motor protein myosin XI (Kwok and Hanson, 2003; Natesan et al., 2009; Sattarzadeh et al., 2009). Differentially shaped stromules have been identified by using expression of various stroma-targeted fluorescent proteins; these include straight or branched tubules which can exhibit either randomly localized elliptical dilations that transverse the tubule length or triangular areas of expansion (Köhler et al., 2000; Hanson and Sattarzadeh, 2008; Schattat et al., 2011, 2012). For the latter type, branch formation occurs in tandem with dynamic remodeling of contiguous ER tubules (Schattat et al., 2011). Schattat and colleagues suppose that this co-alignment might originate from membrane contact points or by an exploitation of the same cytoskeletal elements for development. Single or multiple stromules may arise in all plastid types present in higher plant tissues, but their frequency varies; for example their abundance is significantly higher for achlorophylic plastids in sink tissues than for chlorophyll-containing plastids in green tissues (Köhler et al., 1997; Köhler and Hanson, 2000; Natesan et al., 2005; Hanson and Sattarzadeh, 2008; Schattat et al., 2012). Analyses of the fruit ripening in tomato showed that the formation of stromules is influenced by the plastid differentiation status and is inversely correlated with the density and size of plastids within a cell (Waters et al., 2004). Consequently, a role of stromules in sensing the number of plastids in a cell is supposed. Various abiotic and biotic stress conditions including heat (Holzinger et al., 2007), subcellular redox stress (Itoh et al., 2010), application of extracellular sucrose or glucose (Schattat and Klösgen, 2011), treatment with abscisic acid (Gray et al., 2012), colonization by an arbuscular mycorrhizal fungus (Fester et al., 2001; Hans et al., 2004; Lohse et al., 2005), and infiltration of agrobacteria (Schattat et al., 2012) were described as inducers of stromules. The formation of a dense plastid network in cells close to the main symbiotic structure during mycorrhizae formation supports a putative correlation between plastid metabolic activity and stromule biogenesis. An induction of stromules was detected as well upon viral infections (Esau, 1944; Shalla, 1964; Caplan et al., 2008; Krenz et al., 2010). RNA-virus infected sugar beets exhibit mosaic disease symptoms including mottling and yellow-green sectoring of leaves. Plastids within these yellow areas showed vesiculation and an amoeboid shape resembling stromules (Esau, 1944). Shalla (1964) described the appearance of "long appendages which extend and contracted within a few seconds" from the plastid body and vesicle formation inside chloroplasts of TMV-infected tomato leaflets. TMV-infected tobacco plants exhibited a strong induction of stromule formation (Caplan et al., 2008) just as for *N. benthamiana* plants locally infected with the DNA-virus AbMV (Krenz et al., 2010).

Although several inducers of stromules have been identified, their functional role remains to be determined. They were proposed to participate in plastid motility and in facilitating transport of various molecules, e.g., proteins, metabolites and signaling components, into and out of a plastid, among plastids and even between plastids and other organelles (Köhler et al., 1997, 2000; Kwok and Hanson, 2004a; Natesan et al., 2005; Hanson and Sattarzadeh, 2008, 2011). Chlorophyll, thylakoid membranes, plastid DNA, and ribosomes have not been detected within stromules (Hanson and Sattarzadeh, 2008, 2011; Newell et al., 2012). Nevertheless, the possibility of a rare movement of plastid DNA and ribosomes or the transfer of much smaller DNA molecules, e.g., plastid transformation vectors, via stromules cannot be completely excluded. Exchange of stroma-targeted GFP between two plastids interconnected by stromules was observed using fluorescence recovery after photobleaching (FRAP) experiments in tobacco and *Arabidopsis* (Köhler et al., 1997; Tirlapur et al., 1999). Moreover, two-photon excitation fluorescence correlation spectroscopy revealed two different transport modes through stromules in tobacco suspension cells (Köhler et al., 2000). A simple diffusion of single stroma-targeted GFP molecules was observed in addition to an active ATP-dependent batch movement of GFP "packets." Köhler and colleagues supposed that these GFP bodies represent an accumulation of GFP in small vesicles. Stromules may carry several of these GFP "packets" leading to a beaded appearance (Köhler and Hanson, 2000; Pyke and Howells, 2002; Hanson and Sattarzadeh, 2008, 2011). The stromules induced by AbMV-infection and containing the MP-interacting chaperone

cpHSC70-1 exhibited a related appearance like pearls on a string (Krenz et al., 2010; **Figures 1 and 2**). It is hypothesized that cpHSC70-1 is present in the same type of "packet" structure as GFP in the preceding experiments, probably associated with vesicles and actively transported.

The data obtained by Kwok and Hanson (2004a) suggested that stromules may serve as pathways between nuclei and more distant regions of the cell and possibly even other cells. They observed that clusters of plastids around nuclei are capable of extending stromules both outward, to the cell membrane, as well as inward, through nuclear grooves. Close contact between plastids and the nuclei and the plasma membrane of plant cells suggests that physical interactions may enhance functional interactions between these organelles. Furthermore, Kwok and Hanson (2004a) found that stromules from two adjacent cells appeared to meet at either side of an adjoining cell wall. Consequently, the stromule's structure seems to be suitable for the exchange of molecules between plastids and other organelles or the trafficking of plastidal proteins and metabolites to diverse regions of the plant cell. Remarkably, the cpHSC70-1-containing stromules detected upon an AbMV-infection arose not only on plastids clustered around and in close association with the nucleus, but also appeared to interconnect plastids and extend from plastids outward to the cell periphery (Krenz et al., 2010; **Figures 1 and 2**).

By contrast, in non-infected tissues only short cpHSC70-1-containing filaments were found which extended solely from cortex positioned plastids to the cell periphery. However, molecular transfer from the plastids to the nucleus or vice versa with the aid of stromules remains to be confirmed. That a retrograde protein exchange between plastids and the nucleus can occur was demonstrated recently. Plastid-encoded HA-tagged Whirly1 protein was translocated to the nucleus in transplastomic tobacco plants, where it stimulated pathogen-related gene expression (Isemer et al., 2012). The chloroplast-localized NRIP1 (N receptor-interacting protein 1) was redirected to the cytoplasm and to the nucleus in presence of the p50 effector, a 50 kDa helicase domain encoded by TMV (Caplan et al., 2008). Upon this recruitment to the nucleus and the cytoplasm NRIP1 binds to the N innate immunity receptor to initiate effector recognition and pathogen defense mechanisms. TMV-infection causes a strong increase in stromule formation, and a localization of fluorescent protein-tagged NRIP1 within stromules was observed (Caplan et al., 2008). Thus, the authors speculated about an involvement of stromules in the nuclear re-localization of NRIP1.

Schattat et al. (2012) do not support a function of stromules in trafficking of macromolecules between plastids. In this thoroughly performed work, interconnectivity of independent plastids was tested with the aid of a photoconvertible stroma-targeted fluorescent protein. Despite the strong microscopic impression of interplastid connectivity via stromules, an exchange of the stroma marker protein could not be visualized by high quality confocal imaging. Various plant materials (e.g., *N. benthamiana* and *Arabidopsis*) were comprehensively analyzed for plastid morphology and marker protein transfer. Although the differently colored plastids and stromules were in very close proximity, the labeled organelles remained separate as indicated by the absence

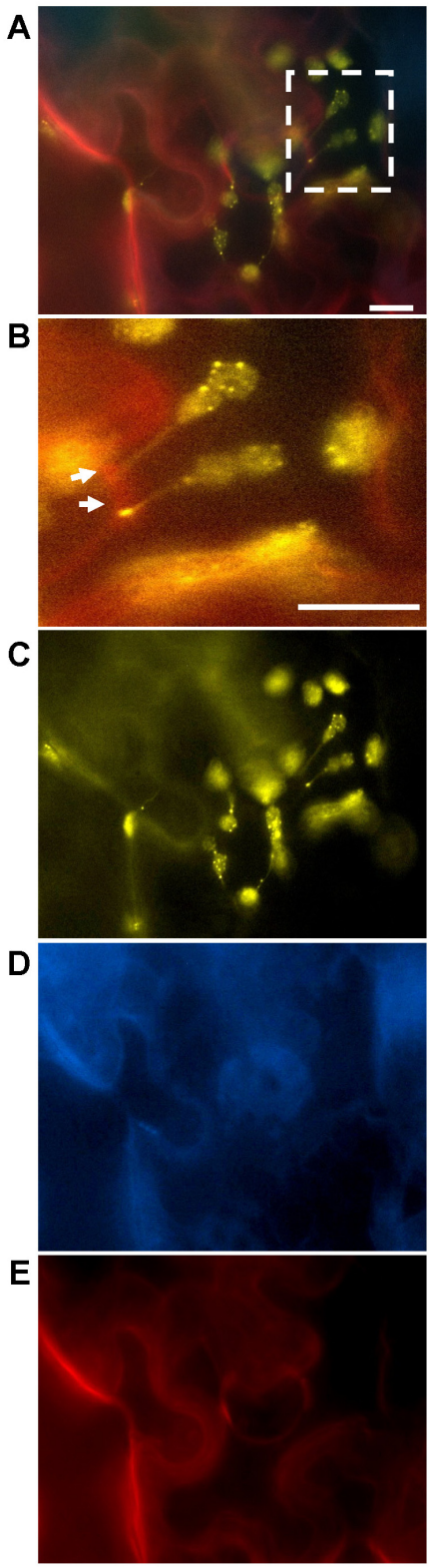

FIGURE 1 | *Abutilon* mosaic virus-induced cpHSC70-1-containing stromules extending from plastids to the cell periphery. Transient co-expression of test constructs in leaf tissues of locally AbMV-infected

(Continued)

FIGURE 1 | Continued
N. benthamiana and epi-fluorescence microscopy were carried out according to Krenz et al. (2010, 2011). AbMV infection was established by simultaneous agro-infiltration of infectious DNA A and DNA B clones with the fluorescent protein expression constructs. **(A)** Merged image of cells expressing NSP:cyan fluorescent protein (CFP), the two split yellow fluorescent protein (YFP)/BiFC constructs of cpHSC70-1 and the plasmodesmata marker PDCB1:mCherry (callose binding protein 1, Simpson et al., 2009) for 4 days post agro-infiltration (dpai). The square in **(A)** highlights cpHSC70-1-oligomers at chloroplasts and stromules (yellow, arrows) anchoring at the cell periphery (red: PDCB1:mCherry), and is magnified in **(B)**. The separate fluorescence signals superimposed in **(A)** are shown in **(C)** YFP, **(D)** CFP, and **(E)** mCherry. Note: The plasmodesmata marker PDCB1:mCherry lost its extracellular localization at the neck region of plasmodesmata upon AbMV-infection (compare **Figure 3**) and is probably distributed throughout the apoplast. NSP:CFP is redirected from the nucleus to the cell periphery, probably the plasma membrane, by presence of MP or AbMV-infection (Zhang et al., 2001; Frischmuth et al., 2007). Bar: 10 μm.

of color mixing. That the method applied in these studies is suitable to detect an exchange of material between organelles upon a fusion was confirmed by analogous experiments using a mitochondria-targeted version of the fluorescent protein. In contrast to our observations from geminivirus-infected plants, the results of Schattat et al. (2012) were obtained working with uninfected plants. Whether these conflicting results are caused by the different experimental set-up, plastid types, and plant material used, or whether indeed a macromolecular trafficking of stroma-proteins through interconnecting stromules is not feasible under any conditions, needs to be elucidated by further experimentation.

In addition to the induction of stromule biogenesis, AbMV-infection influences the localization of a plasmodesmata-associated protein. The plasmodesmata callose binding protein 1 (PDCB1) fused to mCherry was investigated as a marker for plasmodesmata by Simpson et al. (2009). PDCB1 is a glycosylphosphatidylinositol (GPI)-linked protein that exhibits callose binding activity and localizes to the neck region of plasmodesmata in the apoplast. Here it possibly acts as a structural anchor between the plasma membrane component spanning the plasmodesmata and the cell wall. The available data support a function for PDCB1 in plasmodesmata flux control by influencing the callose deposition in the cell wall and as a consequence the aperture of plasmodesmata. Due to its extracellular localization PDCB1 was not expected to interfere with viral proteins like AbMV MP, which is likely to accumulate in the central symplastic cavity region of complex plasmodesmata (Kleinow et al., 2009b; Lee and Lu, 2011). The fluorescence microscopic analyses showed punctate structures in the cell periphery after transient expression of PDCB1:mCherry in epidermal leaf tissues, which are in agreement with the expected plasmodesmata localization (**Figure 3**).

Surprisingly, upon AbMV-infection PDCB1:mCherry signals were still distributed at the cell periphery, most likely the cell wall (**Figures 1–3**), but no punctate structures were detected anymore. Thus, the protein seems to have lost the plasmodesmata localization. We hypothesize this as an AbMV-induced remodeling of the plasmodesmata aperture by callose depletion in the neck region.

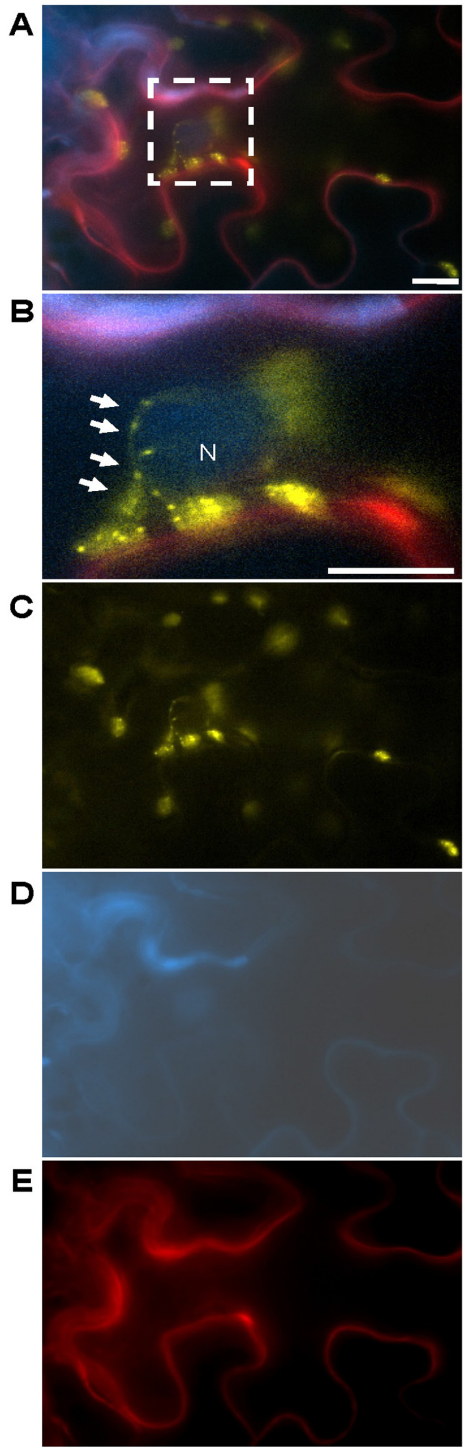

FIGURE 2 | *Abutilon* mosaic virus-induced cpHSC70-1-containing stromules grabbing a nucleus. The experimental set-up is the same as stated in **Figure 1**. **(A)** Merged image of cells expressing the three test proteins for 4 dpai and **(B)** magnification of the square in **(A)** which marks cpHSC70-1-oligomers at chloroplasts and stromules (yellow, arrows) which closely associate to a nucleus (blue: NSP:CFP) near to the cell periphery (blue: NSP:CFP, likely plasma membrane and red: PDCB1:mCherry, apoplast), magnified in **(B)**. The separate emissions merged in **(A)** are shown in **(C)** YFP, **(D)** CFP, and **(E)** mCherry. N, nucleus; bar: 10 μm.

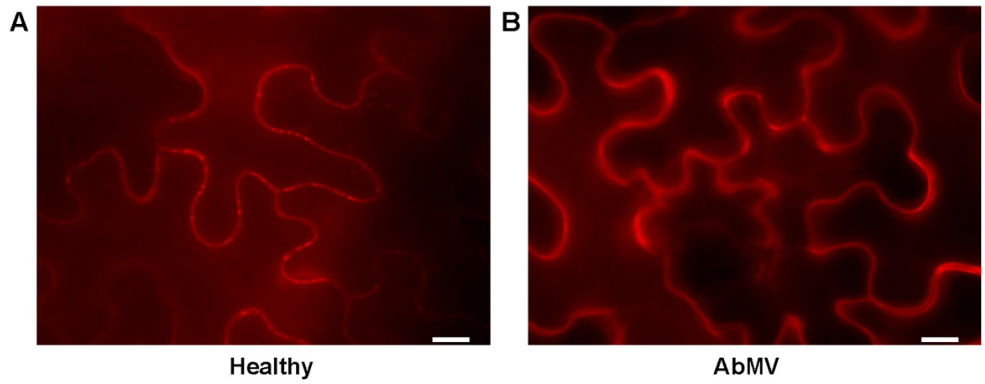

FIGURE 3 | Influence of AbMV-infection on localization of the plasmodesmata marker PDCB1. PDCB1:mCherry (Simpson et al., 2009) was expressed in epidermal tissues of *N. benthamiana* plants either **(A)** healthy or **(B)** locally infected with AbMV for 4 days. The experiment was performed as described in **Figure 1**. **(A)** Punctate mCherry signals indicate the targeting of PDCB1 to the apoplastic part of the neck region from plasmodesmata according to Simpson et al. (2009). **(B)** Upon AbMV-infection these plasmodesmata-specific signals disappeared and PDCB1 emerged homogenously in the apoplast. These results showed a virus-induced alteration of the subcellular localization of PDCB1, probably by modifying callose deposition at plasmodesmata. Bar: 10 μm.

AbMV MOVEMENT ALONG STROMULES WITH THE HELP OF A CHAPERONE

A cellular function in plant endogenous macromolecular trafficking is suspected for stromules and chaperones like HSC70s and in addition an involvement for chaperones in viral movement. However, their combined participation in these processes has thus far not been examined. The accumulated data for the geminivirus AbMV indicate that for both factors there is a joint involvement in the viral life cycle, very likely the movement process (Krenz et al., 2010). In the studies of Krenz et al. (2010) stromules were visualized on chlorophyll-containing plastids by BiFC experiments using the chaperone cpHSC70-1. Here, two different types of cpHSC70-1-containing stromules were monitored. Only short stromules extending from plastids to the cell periphery have been found in healthy epidermal tissues, whereas upon AbMV-infection long stromules forming a network between plastids, nucleus, and the cell periphery were detected. For the latter ones, the BiFC signals of cpHSC70-oligomers highlighted mainly stromule structures with elliptical dilations giving them a beaded appearance. This significant difference created by the geminivirus infection might indicate additional functions of cpHSC70 in association with the two stromule types observed. The cpHSC70-containing stromules may function in macromolecule transfer, perhaps just under certain cellular conditions, e.g., a virus infection. This transport may happen intracellulary among plastids and between plastids and other organelles, or even intercellularly through plasmodesmata.

A prerequisite for the traveling of stromal proteins via stromules from an individual plastid to another plastid or organelle (e.g., nucleus) might be the fusion of the outer and inner envelope membrane with the target membrane. AbMV-infection might create a cellular environment that allows such a fusion event of stromules and the consequent transposition of quantities of stromal components. Alternatively, a transfer process might be initiated, which does not comprise a fusion of the inner envelope membrane or the envelope at all. This might consist of transport along the cytoplasmic leaflet of the outer envelope membrane, through the intermembrane space after fusion of the outer envelope with the target membrane or via envelope-coated vesicles released from stromules (Gunning, 2005; Krause and Krupinska, 2009). Irrespective of the underlying mechanism, a movement of a geminiviral nucleoprotein complex in association with interacting plastid stromules and cpHSC70, even with a low efficiency, might be sufficient for intra- and intercellular viral spread. A transport event in close association with membranes or vesicles would be consistent with the geminiviral MP being a membrane-associated protein. AbMV MP was localized to the protoplasmic face of plasma membranes and vesicles, where its C- and N-terminal domains most likely protrude into the cytoplasm (Aberle et al., 2002; Frischmuth et al., 2004, 2007). The central part of MP probably forms an amphipathic helix structure which inserts into one leaflet of the target membrane (Zhang et al., 2002). It has been observed that insertion of amphipathic helices into a monolayer induces bending and generates local curvature (Kozlov et al., 2010; McMahon et al., 2010). Such protein-mediated membrane stresses were found to trigger fusion, fission, and budding events of membranes. Presumably, AbMV MP may be capable of inducing and/or enhancing such membrane remodeling. However, it cannot be excluded that the close association of AbMV MP with plastid structures represents a targeting of the cytoskeletal elements, to which chloroplasts and stromules are usually attached, for cellular transit of viral nucleoprotein complexes. The result of cpHSC70 silencing in *N. benthamiana* revealed that the chaperone/MP interaction is not essential for the systemic spread of AbMV (Krenz et al., 2010), suggesting it plays a role via an alternative path.

In summary, a model (**Figure 4**) can be proposed in which MP/cpHSC70 interaction and stromule induction facilitate intra- and intercellular macromolecular trafficking along plastids and stromules into the neighboring cell or in the other direction from plastids into the nucleus. Whether this represents an accidental event or is of major significance for AbMV propagation and/or symptom development remains to be investigated.

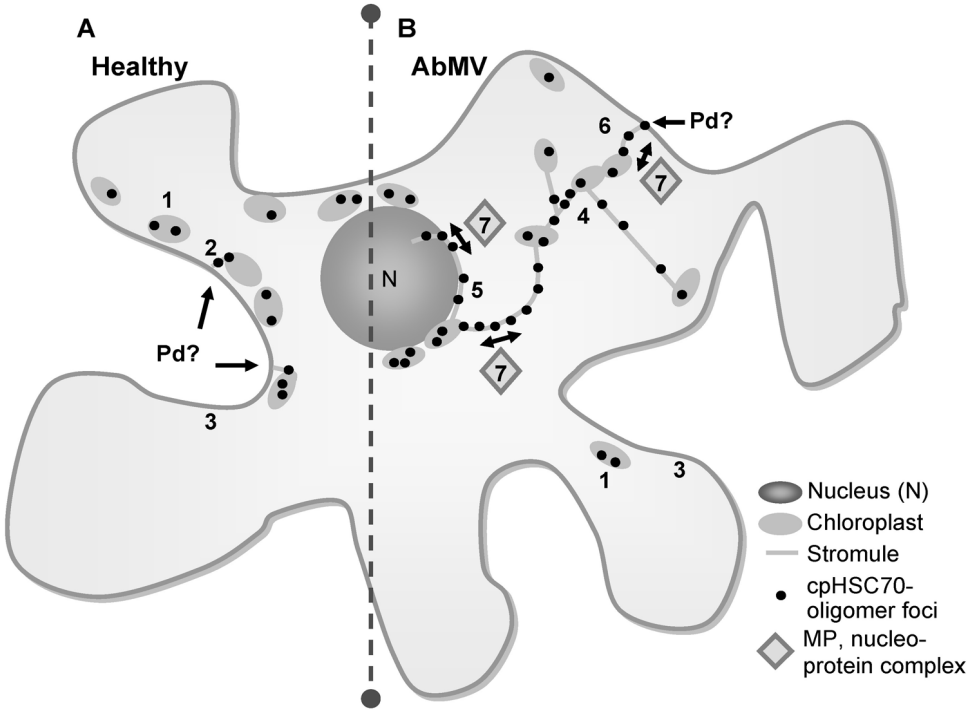

FIGURE 4 | Hypothetical model of AbMV intra- and intercellular trafficking via a plastid network. (A) In healthy plant cells oligomers of the chaperone cpHSC70 locate mainly in small spots at chloroplasts (1), to a lesser amount in small filaments extending from cortical chloroplasts toward the cell periphery (2) and distributed at the cellular margin (3). **(B)** In AbMV-infected cells homo-oligomers of cpHSC70-1 were found similar to non-infected cells at chloroplasts (1) and to a low extent at the cellular margin (3). However, AbMV-infection establishes the formation of a stromule network interconnecting different chloroplasts (4), but also extending from plastids inward to the nucleus, where they closely attach (5) and outward to the cell periphery/cell wall, assumedly to plasmodesmata (Pd) that transverse the cell wall (6). These stromules exhibit structures where cpHSC70-oligomers appeared mainly in elliptical dilations giving them a "pearls on a string"-appearance. The stromule network might function in intra- and intercellular trafficking of viral nucleoprotein complexes by the interaction of AbMV MP with the chaperone cpHSC70 within stromules (7). The potential underlying transport mechanism is yet unknown, but probably involves membrane fusions or a vesicle formation.

So far geminivirus replication and virion assembly were only detected within the nucleus of infected cells (Rojas et al., 2005; Jeske, 2007, 2009). Thus, it seems to be very unlikely that the observed interaction of AbMV with plastids and stromules plays a role in replication or virion assembly processes. Nevertheless, AbMV-induced stromule formation and/or cpHSC70-1 interaction might be also related to other cellular processes. Plastids were involved in the biosynthesis pathways of many essential compounds (e.g., carbohydrates, fatty acids, purines) and stromules might be important in facilitating metabolic exchanges within the cells (Fester et al., 2001; Hans et al., 2004; Kwok and Hanson, 2004b; Waters et al., 2004; Lohse et al., 2005; Schattat and Klösgen, 2011). Plant cells respond to various abiotic and biotic stress stimuli, causing disturbance in the cellular energy status, by complex changes, which include the carbohydrate metabolism and therefore also plastid activity. It is known that stromules occur more frequently and are longer in plant cells with disturbed metabolism (Hanson and Sattarzadeh, 2008), e.g., cells cultured in liquid medium, callus or suspension culture that shed chlorophyll in their chloroplast. That stromule emergence is triggered by an increased plastid metabolic capacity resulting from biotic stress, is supported by the findings of their strong induction upon symbiotic interaction of root cells with mycorrhiza (Fester et al., 2001; Hans et al., 2004; Lohse et al., 2005). Interestingly, geminiviral proteins other than MP have an impact on a regulatory key component of the stress and glucose signal transduction, the sucrose non-fermenting 1-related (SnRK1) protein kinase (Kong and Hanley-Bowdoin, 2002; Hao et al., 2003; Shen and Hanley-Bowdoin, 2006). Plastids and HSP70s were previously concluded to be involved in the onset of a virus-pathogen response (Noel et al., 2007; Caplan et al., 2008; Nagy et al., 2011); therefore, the interaction of AbMV with the plastidal cpHSC70-1 might depict a counteraction of an antiviral defense mechanism.

Recently, a mutant screen identified a plastid- and a mitochondria-localized RNA helicase to be necessary for plastid development, embryogenesis and unexpectedly for cell-to-cell trafficking (Burch-Smith et al., 2011; Burch-Smith and Zambryski, 2012). For both knock-out plants profound changes in the transcriptome were observed, e.g., a dramatic down-regulation of nucleus-encoded plastid-related genes. Although the proteins are located exclusively in plastids and mitochondria, respectively, loss of one of the RNA helicase functions causes formation of twinned and branched plasmodesmata in *Arabidopsis*. Thus, disruption of the plastid function seems to induce an increased molecule exchange, possibly metabolites or signaling factors, among neighboring cells. The data supports a pathway linking

intra- to intercellular communication and therefore a signaling from organelles to the nucleus and plasmodesmata. It can be speculated that viral interactions with plastids also targets this novel regulatory pathway to enhance plasmodesmata trafficking.

CONCLUSION AND FUTURE PERSPECTIVES

The AbMV data on movement is consistent with cell-to-cell transport according to the "couple-skating" model. However, the results of Krenz et al. (2010) may demand to widen this concept of geminiviral cellular transfer for AbMV: it may opportunistically hijack different pathways for intracellular transport and plasmodesmata targeting including an alternative route via chloroplasts and stromules with the aid of a plastidal chaperone. It is clear, in any case, that further research is needed to elucidate this hypothesis.

A functional characterization of AbMV MP and the host factor cpHSC70-1 in the assumed transport processes could start with comprehensive analyses of their localization in subcellular compartments and membrane structures. The following points should be considered: (i) To resolve the geometric relation of the different cellular structures high resolution confocal imaging and time lapse imaging is required. (ii) Test protein expression should be done in combination with a set of fluorescent marker proteins, probably photoconvertible, for different compartments to monitor the subcellular distribution, temporal activities, and macromolecular trafficking events. A cytoplasmic marker would be needed to investigate if AbMV-induced stromules actively associate with the nucleus or are just pressed by other organelles, like a large vacuole, toward the nucleus. (iii) Careful controls should be included to account for stresses (including agro-infiltration) that are known to influence stromule formation. (iv) To minimize the influence of agro-infiltration, transgenic plants expressing required fluorescent test proteins and alternate methods to introduce AbMV (biolistic bombardment of vDNA) should be applied. To investigate the precise molecular function of cpHSC70-1 on AbMV infection and presumably macromolecular trafficking, the impact of the following scenarios on AbMV spread could be investigated: (i) transgenic plants overexpressing wild-type cpHSC70-1 or a non-MP-interacting, dominant-negative cpHSC70-1 variant and (ii) infection with AbMV DNA encoding a non-cpHSC70-1-interacting MP mutant. Finally, the relevance of the findings should be tested for additional geminiviruses other than AbMV. This knowledge gained will contribute significantly to the elucidation of the geminiviral intra- and intercellular movement process.

ACKNOWLEDGMENTS

The authors thank Gabi Kepp for excellent technical assistance and Diether Gotthardt and Marvin Müller for taking care of experimental plants. We are grateful to Keith Lloyd Perry (Cornell University, USA) for critical reading of the manuscript, Karin Krupinska (Christian-Albrechts-University of Kiel, Germany) for helpful discussions on stromules and Emmanuelle Bayer and Andrew Maule (John Innes Centre, UK) for providing the expression construct for PDCB1:mCherry. This work was supported by a trilateral ERA-PG/BMBF project (BMBF 0313986) and by Deutsche Forschungsgemeinschaft DFG (KL1366/3-1).

REFERENCES

Aberle, H. J., Rütz, M. L., Karayavuz, M., Frischmuth, S., Wege, C., Hülser, D., et al. (2002). Localizing BC1 movement proteins of Abutilon mosaic geminivirus in yeasts by subcellular fractionation and freeze-fracture immunolabelling. *Arch. Virol.* 147, 103–107.

Alzhanova, D. V., Prokhnevsky, A. I., Peremyslov, V. V., and Dolja, V. V. (2007). Virion tails of beet yellows virus: coordinated assembly by three structural proteins. *Virology* 359, 220–226.

Aoki, K., Kragler, F., Xoconostle-Cazares, B., and Lucas, W. J. (2002). A subclass of plant heat shock cognate 70 chaperones carries a motif that facilitates trafficking through plasmodesmata. *Proc. Natl. Acad. Sci. U.S.A.* 99, 16342–16347.

Aparicio, F., Thomas, C. L., Lederer, C., Niu, Y., Wang, D., and Maule, A. J. (2005). Virus induction of heat shock protein 70 reflects a general response to protein accumulation in the plant cytosol. *Plant Physiol.* 138, 529–536.

Avisar, D., Prokhnevsky, A. I., and Dolja, V. V. (2008). Class VIII myosins are required for plasmodesmatal localization of a closterovirus HSP70 homolog. *J. Virol.* 82, 2836–2843.

Bae, M. S., Cho, E. J., Choi, E. Y., and Park, O. K. (2003). Analysis of the Arabidopsis nuclear proteome and its response to cold stress. *Plant J.* 36, 652–663.

Benitez-Alfonso, Y., Faulkner, C., Ritzenthaler, C., and Maule, A. J. (2010). Plasmodesmata: gateways to local and systemic virus infection. *Mol. Plant Microbe Interact.* 23, 1403–1412.

Brizard, J. P., Carapito, C., Delalande, F., Van Dorsselaer, A., and Brugidou, C. (2006). Proteome analysis of plant-virus interactome: comprehensive data for virus multiplication inside their hosts. *Mol. Cell. Proteomics* 5, 2279–2297.

Bukau, B., Weissman, J., and Horwich, A. (2006). Molecular chaperones and protein quality control. *Cell* 125, 443–451.

Burch-Smith, T. M., Brunkard, J. O., Choi, Y. G., and Zambryski, P. C. (2011). Organelle-nucleus cross-talk regulates plant intercellular communication via plasmodesmata. *Proc. Natl. Acad. Sci. U.S.A.* 108, E1451–E1460.

Burch-Smith, T. M., and Zambryski, P. C. (2012). Plasmodesmata paradigm shift: regulation from without versus within. *Annu. Rev. Plant Biol.* 63, 239–260.

Caplan, J. L., Mamillapalli, P., Burch-Smith, T. M., Czymmek, K., and Dinesh-Kumar, S. P. (2008). Chloroplastic protein NRIP1 mediates innate immune receptor recognition of a viral effector. *Cell* 132, 449–462.

Carvalho, C. M., Fontenelle, M. R., Florentino, L. H., Santos, A. A., Zerbini, F. M., and Fontes, E. P. (2008a). A novel nucleocytoplasmic traffic GTPase identified as a functional target of the bipartite geminivirus nuclear shuttle protein. *Plant J.* 55, 869–880.

Carvalho, C. M., Machado, J. P., Zerbini, F. M., and Fontes, E. P. (2008b). NSP-interacting GTPase: a cytosolic protein as cofactor for nuclear shuttle proteins. *Plant Signal. Behav.* 3, 752–754.

Carvalho, C. M., Santos, A. A., Pires, S. R., Rocha, C. S., Saraiva, D. I., Machado, J. P., et al. (2008c). Regulated nuclear trafficking of rpL10A mediated by NIK1 represents a defense strategy of plant cells against virus. *PLoS Pathog.* 4:e1000247. doi: 10.1371/journal.ppat.1000247

Carvalho, M. F., and Lazarowitz, S. G. (2004). Interaction of the movement protein NSP and the Arabidopsis acetyltransferase AtNSI is necessary for cabbage leaf curl geminivirus infection and pathogenicity. *J. Virol.* 78, 11161–11171.

Carvalho, M. F., Turgeon, R., and Lazarowitz, S. G. (2006). The geminivirus nuclear shuttle protein NSP inhibits the activity of AtNSI, a vascular-expressed Arabidopsis acetyltransferase regulated with the sink-to-source transition. *Plant Physiol.* 140, 1317–1330.

Channarayappa, V. M., Schwegler-Berry, D., and Shivashankar, G. (1992). Ultrastructural changes in tomato infected with tomato leaf curl virus, a whitefly-transmitted geminivirus. *Can. J. Bot.* 70, 1747–1753.

Duan, Y. P., Powell, C. A., Purcifull, D. E., Broglio, P., and Hiebert, E. (1997). Phenotypic variation in transgenic tobacco expressing mutated geminivirus movement/pathogenicity (BC1) proteins. *Mol. Plant Microbe Interact.* 10, 1065–1074.

Esau, K. (1933). Pathologic changes in the anatomy of leaves of the sugar beet, *Beta vulgaris* L., affected by curly top. *Phytopathology* 23, 679–712.

Esau, K. (1944). Anatomical and cytological studies on beet mosaic. *J. Agric. Res.* 69, 95–117.

Escaler, M., Aranda, M. A., Roberts, I. M., Thomas, C. L., and Maule, A. J. (2000a). A comparison between virus replication and abiotic stress (heat) as

modifiers of host gene expression in pea. *Mol. Plant Pathol.* 1, 159–167.

Escaler, M., Aranda, M. A., Thomas, C. L., and Maule, A. J. (2000b). Pea embryonic tissues show common responses to the replication of a wide range of viruses. *Virology* 267, 318–325.

Fester, T., Strack, D., and Hause, B. (2001). Reorganization of tobacco root plastids during arbuscule development. *Planta* 213, 864–868.

Florentino, L. H., Santos, A. A., Fontenelle, M. R., Pinheiro, G. L., Zerbini, F. M., Baracat-Pereira, M. C., et al. (2006). A PERK-like receptor kinase interacts with the geminivirus nuclear shuttle protein and potentiates viral infection. *J. Virol.* 80, 6648–6656.

Flores-Pérez, U., and Jarvis, P. (2012). Molecular chaperone involvement in chloroplast protein import. *Biochim. Biophys. Acta*. doi: 10.1016/j.bbamcr.2012.1003.1019 [Epub ahead of print].

Fontes, E. P., Santos, A. A., Luz, D. F., Waclawovsky, A. J., and Chory, J. (2004). The geminivirus nuclear shuttle protein is a virulence factor that suppresses transmembrane receptor kinase activity. *Genes Dev.* 18, 2545–2556.

Frischmuth, S., Kleinow, T., Aberle, H.-J., Wege, C., Hülser, D., and Jeske, H. (2004). Yeast two-hybrid systems confirm the membrane-association and oligomerization of BC1 but do not detect an interaction of the movement proteins BC1 and BV1 of Abutilon mosaic geminivirus. *Arch. Virol.* 149, 2349–2364.

Frischmuth, S., Wege, C., Hülser, D., and Jeske, H. (2007). The movement protein BC1 promotes redirection of the nuclear shuttle protein BV1 of Abutilon mosaic geminivirus to the plasma membrane in fission yeast. *Protoplasma* 230, 117–123.

Gafni, Y., and Epel, B. L. (2002). The role of host and viral proteins in intra- and inter-cellular trafficking of geminiviruses. *Physiol. Mol. Plant Pathol.* 60, 231–241.

Gray, J. C., Hansen, M. R., Shaw, D. J., Graham, K., Dale, R., Smallman, P., et al. (2012). Plastid stromules are induced by stress treatments acting through abscisic acid. *Plant J.* 69, 387–398.

Gray, J. C., Sullivan, J. A., Hibberd, J. M., and Hansson, M. R. (2001). Stromules: mobile protrusions and interconnections between plastids. *Plant Biol.* 3, 223–233.

Gröning, B. R., Abouzid, A., and Jeske, H. (1987). Single-stranded DNA from Abutilon mosaic virus is present in the plastids of infected *Abutilon sellovianum*. *Proc. Natl. Acad. Sci. U.S.A.* 84, 8996–9000.

Gröning, B. R., Frischmuth, T., and Jeske, H. (1990). Replicative form DNA of Abutilon mosaic virus is present in plastids. *Mol. Gen. Genet.* 220, 485–488.

Gunning, B. E. (2005). Plastid stromules: video microscopy of their outgrowth, retraction, tensioning, anchoring, branching, bridging, and tip-shedding. *Protoplasma* 225, 33–42.

Hans, J., Hause, B., Strack, D., and Walter, M. H. (2004). Cloning, characterization, and immunolocalization of a mycorrhiza-inducible 1-deoxy-d-xylulose 5-phosphate reductoisomerase in arbuscule-containing cells of maize. *Plant Physiol.* 134, 614–624.

Hanson, M. R., and Sattarzadeh, A. (2008). Dynamic morphology of plastids and stromules in angiosperm plants. *Plant Cell Environ.* 31, 646–657.

Hanson, M. R., and Sattarzadeh, A. (2011). Stromules: recent insights into a long neglected feature of plastid morphology and function. *Plant Physiol.* 155, 1486–1492.

Hao, L., Wang, H., Sunter, G., and Bisaro, D. M. (2003). Geminivirus AL2 and L2 proteins interact with and inactivate SNF1 kinase. *Plant Cell* 15, 1034–1048.

Harries, P., and Ding, B. (2011). Cellular factors in plant virus movement: at the leading edge of macromolecular trafficking in plants. *Virology* 411, 237–243.

Harries, P. A., Park, J. W., Sasaki, N., Ballard, K. D., Maule, A. J., and Nelson, R. S. (2009). Differing requirements for actin and myosin by plant viruses for sustained intercellular movement. *Proc. Natl. Acad. Sci. U.S.A.* 106, 17594–17599.

Harries, P. A., Schoelz, J. E., and Nelson, R. S. (2011). Intracellular transport of viruses and their components: utilizing the cytoskeleton and membrane highways. *Mol. Plant Microbe Interact.* 23, 1381–1393.

Hehnle, S., Wege, C., and Jeske, H. (2004). Interaction of DNA with the movement proteins of geminiviruses revisited. *J. Virol.* 78, 7698–7706.

Holzinger, A., Buchner, O., Lutz, C., and Hanson, M. R. (2007). Temperature-sensitive formation of chloroplast protrusions and stromules in mesophyll cells of *Arabidopsis thaliana*. *Protoplasma* 230, 23–30.

Horns, T., and Jeske, H. (1991). Localization of Abutilon mosaic virus DNA within leaf tissue by *in situ* hybridization. *Virology* 181, 580–588.

Hou, Y. M., Sanders, R., Ursin, V. M., and Gilbertson, R. L. (2000). Transgenic plants expressing geminivirus movement proteins: abnormal phenotypes and delayed infection by tomato mottle virus in transgenic tomatoes expressing the bean dwarf mosaic virus BV1 or BC1 proteins. *Mol. Plant Microbe Interact.* 13, 297–308.

Ingham, D. J., and Lazarowitz, S. G. (1993). A single missense mutation in the BR1 movement protein alters the host range of the squash leaf curl geminivirus. *Virology* 196, 694–702.

Isemer, R., Mulisch, M., Schafer, A., Kirchner, S., Koop, H. U., and Krupinska, K. (2012). Recombinant Whirly1 translocates from transplastomic chloroplasts to the nucleus. *FEBS Lett.* 586, 85–88.

Ito, J., Heazlewood, J. L., and Millar, A. H. (2006). Analysis of the soluble ATP-binding proteome of plant mitochondria identifies new proteins and nucleotide triphosphate interactions within the matrix. *J. Proteome Res.* 5, 3459–3469.

Itoh, R. D., Yamasaki, H., Septiana, A., Yoshida, S., and Fujiwara, M. T. (2010). Chemical induction of rapid and reversible plastid filamentation in *Arabidopsis thaliana* roots. *Physiol. Plant* 139, 144–158.

Jeske, H. (1986). The detection of the Abutilon mosaic virus depends on the experimental daytime. *J. Phytopathol.* 115, 243–256.

Jeske, H. (2007). "Replication of geminiviruses and the use of rolling circle amplification for their diagnosis," in *Tomato Yellow Leaf Curl Virus Disease: Management, Molecular Biology, and Breeding for Resistance*, ed. H. Czosnek (Dordrecht: Springer Science Business Media), 141–156.

Jeske, H. (2009). Geminiviruses. *Curr. Top. Microbiol. Immunol.* 185–226.

Jeske, H., and Schuchalter-Eicke, G. (1984). The Abutilon mosaic virus (AbMV) in different leaf tissue of several host plant species of Malvaceae. *Phytopathol. Z.* 109, 353–362.

Jeske, H., and Werz, G. (1978). The influence of light intensity on pigment composition and ultrastructure of plastids in leaves of diseased *Abutilon sellowianum* Reg. *Phytopathol. Z.* 91, 1–13.

Jeske, H., and Werz, G. (1980a). Cytochemical characterization of plastidal inclusions in Abutilon mosaic-infected *Malva parviflora* mesophyll cells. *Virology* 106, 155–158.

Jeske, H., and Werz, G. (1980b). Ultrastructural and biochemical investigations on the whitefly transmitted Abutilon mosaic virus (AbMV). *Phytopathol. Z.* 97, 43–55.

Jimenez, I., Lopez, L., Alamillo, J. M., Valli, A., and Garcia, J. A. (2006). Identification of a plum pox virus CI-interacting protein from chloroplast that has a negative effect in virus infection. *Mol. Plant Microbe Interact.* 19, 350–358.

Kampinga, H. H., and Craig, E. A. (2010). The HSP70 chaperone machinery: J proteins as drivers of functional specificity. *Nat. Rev. Mol. Cell Biol.* 11, 579–592.

Kanzaki, H., Saitoh, H., Ito, A., Fujisawa, S., Kamoun, S., Katou, S., et al. (2003). Cytosolic HSP90 and HSP70 are essential components of INF1-mediated hypersensitive response and non-host resistance to *Pseudomonas cichorii* in *Nicotiana benthamiana*. *Mol. Plant Pathol.* 4, 383–391.

Kleinow, T., Nischang, M., Beck, A., Kratzer, U., Tanwir, F., Preiss, W., et al. (2009a). Three C-terminal phosphorylation sites in the Abutilon mosaic virus movement protein affect symptom development and viral DNA accumulation. *Virology* 390, 89–101.

Kleinow, T., Tanwir, F., Kocher, C., Krenz, B., Wege, C., and Jeske, H. (2009b). Expression dynamics and ultrastructural localization of epitope-tagged Abutilon mosaic virus nuclear shuttle and movement proteins in *Nicotiana benthamiana* cells. *Virology* 391, 212–220.

Köhler, R. H., Cao, J., Zipfel, W. R., Webb, W. W., and Hanson, M. R. (1997). Exchange of protein molecules through connections between higher plant plastids. *Science* 276, 2039–2042.

Köhler, R. H., and Hanson, M. R. (2000). Plastid tubules of higher plants are tissue-specific and developmentally regulated. *J. Cell Sci.* 113, 81–89.

Köhler, R. H., Schwille, P., Webb, W. W., and Hanson, M. R. (2000). Active protein transport through plastid tubules: velocity quantified by fluorescence correlation spectroscopy. *J. Cell Sci.* 113, 3921–3930.

Kong, L. J., and Hanley-Bowdoin, L. (2002). A geminivirus replication protein interacts with a protein kinase and a motor protein that display different expression patterns during plant development and infection. *Plant Cell* 14, 1817–1832.

Kozlov, M. M., McMahon, H. T., and Chernomordik, L. V. (2010).

Protein-driven membrane stresses in fusion and fission. *Trends Biochem. Sci.* 35, 699–706.

Krause, K., and Krupinska, K. (2009). Nuclear regulators with a second home in organelles. *Trends Plant Sci.* 14, 194–199.

Krenz, B., Neugart, F., Kleinow, T., and Jeske, H. (2011). Self-interaction of Abutilon mosaic virus replication initiator protein (Rep) in plant cell nuclei. *Virus Res.* 161, 194–197.

Krenz, B., Windeisen, V., Wege, C., Jeske, H., and Kleinow, T. (2010). A plastid-targeted heat shock cognate 70 kDa protein interacts with the Abutilon mosaic virus movement protein. *Virology* 401, 6–17.

Krichevsky, A., Kozlovsky, S. V., Gafni, Y., and Citovsky, V. (2006). Nuclear import and export of plant virus proteins and genomes. *Mol. Plant Pathol.* 7, 131–146.

Kwok, E. Y., and Hanson, M. R. (2003). Microfilaments and microtubules control the morphology and movement of non-green plastids and stromules in *Nicotiana tabacum*. *Plant J.* 35, 16–26.

Kwok, E. Y., and Hanson, M. R. (2004a). Plastids and stromules interact with the nucleus and cell membrane in vascular plants. *Plant Cell Rep.* 23, 188–195.

Kwok, E. Y., and Hanson, M. R. (2004b). Stromules and the dynamic nature of plastid morphology. *J. Microsc.* 214, 124–137.

Latijnhouwers, M., Xu, X. M., and Moller, S. G. (2010). Arabidopsis stromal 70-kDa heat shock proteins are essential for chloroplast development. *Planta* 232, 567–578.

Lee, J. Y., and Lu, H. (2011). Plasmodesmata: the battleground against intruders. *Trends Plant Sci.* 16, 201–210.

Lee, J. Y., Yoo, B. C., Rojas, M. R., Gomez-Ospina, N., Staehelin, L. A., and Lucas, W. J. (2003). Selective trafficking of non-cell-autonomous proteins mediated by NtNCAPP1. *Science* 299, 392–396.

Levy, A., and Tzfira, T. (2011). Bean dwarf mosaic virus: a model system for the study of viral movement. *Mol. Plant Pathol.* 11, 451–461.

Lewis, J. D., and Lazarowitz, S. G. (2010). Arabidopsis synaptotagmin SYTA regulates endocytosis and virus movement protein cell-to-cell transport. *Proc. Natl. Acad. Sci. U.S.A.* 107, 2491–2496.

Lim, H. S., Vaira, A. M., Bae, H., Bragg, J. N., Ruzin, S. E., Bauchan, G. R., et al. (2010). Mutation of a chloroplast-targeting signal in *Alternanthera* mosaic virus TGB3 impairs cell-to-cell movement and eliminates long-distance virus movement. *J. Gen. Virol.* 91, 2102–2115.

Lin, J. W., Ding, M. P., Hsu, Y. H., and Tsai, C. H. (2007). Chloroplast phosphoglycerate kinase, a gluconeogenetic enzyme, is required for efficient accumulation of bamboo mosaic virus. *Nucleic Acids Res.* 35, 424–432.

Lohse, S., Schliemann, W., Ammer, C., Kopka, J., Strack, D., and Fester, T. (2005). Organization and metabolism of plastids and mitochondria in arbuscular mycorrhizal roots of *Medicago truncatula*. *Plant Physiol.* 139, 329–340.

Lozano-Duran, R., Rosas-Diaz, T., Luna, A. P., and Bejarano, E. R. (2011). Identification of host genes involved in geminivirus infection using a reverse genetics approach. *PLoS ONE* 6:e22383. doi: 10.1371/journal.pone.0022383

Lucas, W. J. (2006). Plant viral movement proteins: agents for cell-to-cell trafficking of viral genomes. *Virology* 344, 169–184.

Mariano, A. C., Andrade, M. O., Santos, A. A., Carolino, S. M., Oliveira, M. L., Baracat-Pereira, M. C., et al. (2004). Identification of a novel receptor-like protein kinase that interacts with a geminivirus nuclear shuttle protein. *Virology* 318, 24–31.

Maule, A. J., Benitez-Alfonso, Y., and Faulkner, C. (2011). Plasmodesmata – membrane tunnels with attitude. *Curr. Opin. Plant Biol.* 14, 683–690.

Maule, A. J., Escaler, M., and Aranda, M. A. (2000). Programmed responses to virus replication in plants. *Mol. Plant Pathol.* 1, 9–15.

Mayer, M. P. (2010). Gymnastics of molecular chaperones. *Mol. Cell* 39, 321–331.

Mayer, M. P., and Bukau, B. (2005). HSP70 chaperones: cellular functions and molecular mechanism. *Cell. Mol. Life Sci.* 62, 670–684.

McGarry, R. C., Barron, Y. D., Carvalho, M. F., Hill, J. E., Gold, D., Cheung, E., et al. (2003). A novel Arabidopsis acetyltransferase interacts with the geminivirus movement protein NSP. *Plant Cell* 15, 1605–1618.

McMahon, H. T., Kozlov, M. M., and Martens, S. (2010). Membrane curvature in synaptic vesicle fusion and beyond. *Cell* 140, 601–605.

Nagy, P. D., Wang, R. Y., Pogany, J., Hafren, A., and Makinen, K. (2011). Emerging picture of host chaperone and cyclophilin roles in RNA virus replication. *Virology* 411, 374–382.

Natesan, S. K., Sullivan, J. A., and Gray, J. C. (2009). Myosin XI is required for actin-associated movement of plastid stromules. *Mol. Plant* 2, 1262–1272.

Natesan, S. K. A., Sullivan, J. A., and Gray, J. C. (2005). Stromules: a characteristic cell-specific feature of plastid morphology. *J. Exp. Bot.* 56, 787–797.

Newell, C. A., Natesan, S. K. A., Sullivan, J. A., Jouhet, J., Kavanagh, T. A., and Gray, J. C. (2012). Exclusion of plastid nucleoids and ribosomes from stromules in tobacco and Arabidopsis. *Plant J.* 69, 399–410.

Niehl, A., and Heinlein, M. (2011). Cellular pathways for viral transport through plasmodesmata. *Protoplasma* 248, 75–99.

Noel, L. D., Cagna, G., Stuttmann, J., Wirthmuller, L., Betsuyaku, S., Witte, C. P., et al. (2007). Interaction between SGT1 and cytosolic/nuclear HSC70 chaperones regulates Arabidopsis immune responses. *Plant Cell* 19, 4061–4076.

Noueiry, A. O., Lucas, W. J., and Gilbertson, R. L. (1994). Two proteins of a plant DNA virus coordinate nuclear and plasmodesmal transport. *Cell* 76, 925–932.

Oparka, K. J. (2004). Getting the message across: how do plant cells exchange macromolecular complexes? *Trends Plant Sci.* 9, 33–41.

Pascal, E., Goodlove, P. E., Wu, L. C., and Lazarowitz, S. G. (1993). Transgenic tobacco plants expressing the geminivirus BL1 protein exhibit symptoms of viral disease. *Plant Cell* 5, 795–807.

Pascal, E., Sanderfoot, A. A., Ward, B. M., Medville, R., Turgeon, R., and Lazarowitz, S. G. (1994). The geminivirus BR1 movement protein binds single-stranded DNA and localizes to the cell nucleus. *Plant Cell* 6, 995–1006.

Peltier, J. B., Cai, Y., Sun, Q., Zabrouskov, V., Giacomelli, L., Rudella, A., et al. (2006). The oligomeric stromal proteome of *Arabidopsis thaliana* chloroplasts. *Mol. Cell. Proteomics* 5, 114–133.

Peltier, J. B., Emanuelsson, O., Kalume, D. E., Ytterberg, J., Friso, G., Rudella, A., et al. (2002). Central functions of the lumenal and peripheral thylakoid proteome of Arabidopsis determined by experimentation and genome-wide prediction. *Plant Cell* 14, 211–236.

Prod'homme, D., Jakubiec, A., Tournier, V., Drugeon, G., and Jupin, I. (2003). Targeting of the turnip yellow mosaic virus 66K replication protein to the chloroplast envelope is mediated by the 140K protein. *J. Virol.* 77, 9124–9135.

Pyke, K. A., and Howells, C. A. (2002). Plastid and stromule morphogenesis in tomato. *Ann. Bot.* 90, 559–566.

Qin, S. W., Ward, B. M., and Lazarowitz, S. G. (1998). The bipartite geminivirus coat protein aids BR1 function in viral movement by affecting the accumulation of viral single-stranded DNA. *J. Virol.* 72, 9247–9256.

Reinero, A., and Beachy, R. N. (1986). Association of TMV coat protein with chloroplast membranes in virus-infected leaves. *Plant Mol. Biol.* 291–301.

Rocha, C. S., Santos, A. A., Machado, J. P., and Fontes, E. P. (2008). The ribosomal protein L10/QM-like protein is a component of the NIK-mediated antiviral signaling. *Virology* 380, 165–169.

Rojas, M. R., Hagen, C., Lucas, W. J., and Gilbertson, R. L. (2005). Exploiting chinks in the plant's armor: evolution and emergence of geminiviruses. *Annu. Rev. Phytopathol.* 43, 361–394.

Rojas, M. R., Noueiry, A. O., Lucas, W. J., and Gilbertson, R. L. (1998). Bean dwarf mosaic geminivirus movement proteins recognize DNA in a form- and size-specific manner. *Cell* 95, 105–113.

Rushing, A. E., Sunter, G., Gardiner, W. E., Dute, R. R., and Bisaro, D. M. (1987). Ultrastructural aspects of tomato golden mosaic virus infection in tobacco. *Phytopathology* 77, 1231–1236.

Sanderfoot, A. A., Ingham, D. J., and Lazarowitz, S. G. (1996). A viral movement protein as a nuclear shuttle. The geminivirus BR1 movement protein contains domains essential for interaction with BL1 and nuclear localization. *Plant Physiol.* 110, 23–33.

Sanderfoot, A. A., and Lazarowitz, S. G. (1995). Cooperation in viral movement: the geminivirus BL1 movement protein interacts with BR1 and redirects it from the nucleus to the cell periphery. *Plant Cell* 7, 1185–1194.

Santos, A. A., Lopes, K. V., Apfata, J. A., and Fontes, E. P. (2010). NSP-interacting kinase, NIK: a transducer of plant defence signalling. *J. Exp. Bot.* 61, 3839–3845.

Sattarzadeh, A., Krahmer, J., Germain, A. D., and Hanson, M. R. (2009). A myosin XI tail domain homologous to the yeast myosin vacuole-binding domain interacts with plastids and stromules in *Nicotiana benthamiana*. *Mol. Plant* 2, 1351–1358.

Saunders, K., Wege, C., Veluthambi, K., Jeske, H., and Stanley, J. (2001).

The distinct disease phenotypes of the common and yellow vein strains of tomato golden mosaic virus are determined by nucleotide differences in the 3′-terminal region of the gene encoding the movement protein. *J. Gen. Virol.* 82, 45–51.

Schattat, M., Barton, K., Baudisch, B., Klosgen, R. B., and Mathur, J. (2011). Plastid stromule branching coincides with contiguous endoplasmic reticulum dynamics. *Plant Physiol.* 155, 1667–1677.

Schattat, M. H., Griffiths, S., Mathur, N., Barton, K., Wozny, M. R., Dunn, N., et al. (2012). Differential coloring reveals that plastids do not form networks for exchanging macromolecules. *Plant Cell* 24, 1465–1477.

Schattat, M. H., and Klösgen, R. B. (2011). Induction of stromule formation by extracellular sucrose and glucose in epidermal leaf tissue of *Arabidopsis thaliana*. *BMC Plant Biol.* 11:115. doi: 10.1186/1471-2229-11-115

Schoelz, J. E., Harries, P. A., and Nelson, R. S. (2011). Intracellular transport of plant viruses: finding the door out of the cell. *Mol. Plant* 4, 813–831.

Schoelz, J. E., and Zaitlin, M. (1989). Tobacco mosaic virus RNA enters chloroplasts in vivo. *Proc. Natl. Acad. Sci. U.S.A.* 86, 4496–4500.

Schuchalter-Eicke, G., and Jeske, H. (1983). Seasonal changes in the chloroplast ultrastructure in Abutilon mosaic virus (AbMV) infected *Abutilon* spec. (Malvaceae). *Phytopathol. Z.* 108, 172–184.

Shalla, T. A. (1964). Assembly and aggregation of tobacco mosaic virus in tomato leaflets. *J. Cell Biol.* 21, 253–264.

Shen, W., and Hanley-Bowdoin, L. (2006). Geminivirus infection up-regulates the expression of two Arabidopsis protein kinases related to yeast SNF1 and mammalian AMPK activating kinases. *Plant Physiol.* 142, 1642–1655.

Simpson, C., Thomas, C., Findlay, K., Bayer, E., and Maule, A. J. (2009). An Arabidopsis GPI-anchor plasmodesmal neck protein with callose binding activity and potential to regulate cell-to-cell trafficking. *Plant Cell* 21, 581–594.

Su, P.-H., and Li, H.-M. (2008). Arabidopsis stromal 70-kD heat shock proteins are essential for plant development and important for thermotolerance of germinating seeds. *Plant Physiol.* 146, 1231–1241.

Su, P. H., and Li, H. M. (2010). Stromal Hsp70 is important for protein translocation into pea and Arabidopsis chloroplasts. *Plant Cell* 22, 1516–1531.

Sung, D. Y., Vierling, E., and Guy, C. L. (2001). Comprehensive expression profile analysis of the Arabidopsis HSP70 gene family. *Plant Physiol.* 126, 789–800.

Swindell, W. R., Huebner, M., and Weber, A. P. (2007). Transcriptional profiling of Arabidopsis heat shock proteins and transcription factors reveals extensive overlap between heat and non-heat stress response pathways. *BMC Genomics* 8:125. doi: 10.1186/1471-2164-8-125

Tirlapur, U. K., Dahse, I., Reiss, B., Meurer, J., and Oelmuller, R. (1999). Characterization of the activity of a plastid-targeted green fluorescent protein in Arabidopsis. *Eur. J. Cell Biol.* 78, 233–240.

Torrance, L., Cowan, G. H., Gillespie, T., Ziegler, A., and Lacomme, C. (2006). Barley stripe mosaic virus-encoded proteins triple-gene block 2 and γb localize to chloroplasts in virus-infected monocot and dicot plants, revealing hitherto-unknown roles in virus replication. *J. Gen. Virol.* 87, 2403–2411.

Trejo-Saavedra, D. L., Vielle-Calzada, J. P., and Rivera-Bustamante, R. F. (2009). The infective cycle of cabbage leaf curl virus (CaLCuV) is affected by CRUMPLED LEAF (CRL) gene in *Arabidopsis thaliana*. *Virol. J.* 6, 169.

Ueki, S., and Citovsky, V. (2011). To Gate, or not to gate: regulatory mechanisms for intercellular protein transport and virus movement in plants. *Mol. Plant* 4, 782–793.

von Arnim, A., and Stanley, J. (1992). Determinants of tomato golden mosaic virus symptom development located on DNA B. *Virology* 186, 286–293.

Waigmann, E., Ueki, S., Trutnyeva, K., and Citovsky, V. (2004). The ins and outs of nondestructive cell-to-cell and systemic movement of plant viruses. *Crit. Rev. Plant Sci.* 23, 195–250.

Waters, M. T., Fray, R. G., and Pyke, K. A. (2004). Stromule formation is dependent upon plastid size, plastid differentiation status and the density of plastids within the cell. *Plant J.* 39, 655–667.

Wege, C. (2007). "Movement and localization of tomato yellow leaf curl viruses in the infected plant," in *Tomato Yellow Leaf Curl Virus Disease: Management, Molecular Biology, and Breeding for Resistance*, ed. H. Czosnek (Dordrecht: Springer Science Business Media), 185–206.

Weibezahn, J., Schlieker, C., Tessarz, P., Mogk, A., and Bukau, B. (2005). Novel insights into the mechanism of chaperone-assisted protein disaggregation. *Biol. Chem.* 386, 739–744.

Xiang, Y., Kakani, K., Reade, R., Hui, E., and Rochon, D. (2006). A 38-amino-acid sequence encompassing the arm domain of the cucumber necrosis virus coat protein functions as a chloroplast transit peptide in infected plants. *J. Virol.* 80, 7952–7964.

Zavaliev, R., Ueki, S., Epel, B. L., and Citovsky, V. (2011). Biology of callose (beta-1,3-glucan) turnover at plasmodesmata. *Protoplasma* 248, 117–130.

Zhang, S. C., Ghosh, R., and Jeske, H. (2002). Subcellular targeting domains of Abutilon mosaic geminivirus movement protein BC1. *Arch. Virol.* 147, 2349–2363.

Zhang, S. C., Wege, C., and Jeske, H. (2001). Movement proteins (BC1 and BV1) of Abutilon mosaic geminivirus are cotransported in and between cells of sink but not of source leaves as detected by green fluorescent protein tagging. *Virology* 290, 249–260.

Zhou, Y., Rojas, M. R., Park, M.-R., Seo, Y.-S., Lucas, W. J., and Gilbertson, R. L. (2011). Histone H3 interacts and co-localizes with the nuclear shuttle protein and movement protein of a geminivirus. *J. Virol.* 85, 11821–11832.

Zhou, Y. C., Garrido-Ramirez, E. R., Sudarshana, M. R., Yendluri, S., and Gilbertson, R. L. (2007). The N-terminus of the begomovirus nuclear shuttle protein (BV1) determines virulence or avirulence in *Phaseolus vulgaris*. *Mol. Plant Microbe Interact.* 20, 1523–1534.

Conflict of Interest Statement: The authors declare that the research was conducted in the absence of any commercial or financial relationships that could be construed as a potential conflict of interest.

Received: 22 September 2012; accepted: 06 December 2012; published online: 27 December 2012.

Citation: Krenz B, Jeske H and Kleinow T (2012) The induction of stromule formation by a plant DNA-virus in epidermal leaf tissues suggests a novel intra- and intercellular macromolecular trafficking route. Front. Plant Sci. ***3****:291. doi: 10.3389/fpls.2012.00291*

This article was submitted to Frontiers in Plant-Microbe Interaction, a specialty of Frontiers in Plant Science.

frontiers in
PLANT SCIENCE

REVIEW ARTICLE
published: 06 December 2012
doi: 10.3389/fpls.2012.00275

Cellular chaperones and folding enzymes are vital contributors to membrane bound replication and movement complexes during plant RNA virus infection

Jeanmarie Verchot*

Department of Entomology and Plant Pathology, Oklahoma State University, Stillwater, OK, USA

Edited by:
Jean-François Laliberté, Institut National de la Recherche Scientifique, Canada

Reviewed by:
Michael Goodin, University of Kentucky, USA
Roger Wise, United States Department of Agriculture - Agricultural Research Service, USA

****Correspondence:***
Jeanmarie Verchot, Department of Entomology and Plant Pathology, Oklahoma State University, 127 Noble Research Center, Stillwater, OK 74075, USA.
e-mail: verchot.lubicz@okstate.edu

Cellular chaperones and folding enzymes play central roles in the formation of positive-strand and negative-strand RNA virus infection. This article examines the key cellular chaperones and discusses evidence that these factors are diverted from their cellular functions to play alternative roles in virus infection. For most chaperones discussed, their primary role in the cell is to ensure protein quality control. They are system components that drive substrate protein folding, complex assembly or disaggregation. Their activities often depend upon co-chaperones and ATP hydrolysis. During plant virus infection, Hsp70 and Hsp90 proteins play central roles in the formation of membrane-bound replication complexes for certain members of the tombusvirus, tobamovirus, potyvirus, dianthovirus, potexvirus, and carmovirus genus. There are several co-chaperones, including Yjd1, RME-8, and Hsp40 that associate with the bromovirus replication complex, pomovirus TGB2, and tospovirus Nsm movement proteins. There are also examples of plant viruses that rely on chaperone systems in the endoplasmic reticulum (ER) to support cell-to-cell movement. TMV relies on calreticulin to promote virus intercellular transport. Calreticulin also resides in the plasmodesmata and plays a role in calcium sequestration as well as glycoprotein folding. The pomovirus TGB2 interacts with RME-8 in the endosome. The potexvirus TGB3 protein stimulates expression of ER resident chaperones via the bZIP60 transcription factor. Up-regulating factors involved in protein folding may be essential to handling the load of viral proteins translated along the ER. In addition, TGB3 stimulates SKP1 which is a co-factor in proteasomal degradation of cellular proteins. Such chaperones and co-factors are potential targets for antiviral defense.

Keywords: RNA virus replicase, cellular chaperones, unfolded protein response, virus intercellular movement, HSP70 heat-shock proteins, HSP90 heat-shock proteins, DNAJ homologs

INTRODUCTION

Positive-strand RNA viruses are among the largest group of viruses infecting plants worldwide and contribute to some of the most critical issues in agriculture. Two types of cellular alterations that are essential for (+) strand RNA virus replication and cell-to-cell movement include: (1) discrete and well characterized changes in the endomembrane architecture, and (2) the recruitment of host factors into viral protein containing complexes. With regard to changes in membrane architecture, viruses typically create membrane bound environments, called virus factories, to protect replication and assembly complexes from cellular defenses. At the electron microscopic level viroplasms are large virus factories that are amorphous structures containing virion particles, viral RNAs, and non-structural proteins, but typically exclude organelles. The term viroplasm was first used to describe such perinuclear virus factories produced by large DNA viruses and some (+) strand RNA viruses such as poxvirus and poliovirus. Recent research indicates that many plant infecting (+) strand RNA create microenvironments that are sometimes referred to as miniorganelles and these can range in size from vesicles or invaginations along organelle membranes to slightly larger virus factories. Typically these various membrane bound virus factories are induced by non-structural viral proteins and serve to concentrate replication proteins, viral genomes, and host proteins needed for efficient virus replication. Such extensive rearrangement of host membrane compartments are a hallmark of (+) strand RNA virus infection and the specific structures produces by various virus species have been reviewed in prior publications and will not be explored in depth here (Heath et al., 2001; Netherton et al., 2007; Wileman, 2007; Verchot, 2011).

The second cellular alteration mentioned above is the recruitment of host proteins, including cellular chaperones, to membrane bound sites required for virus replication and cell-to-cell movement. Among these are the heat shock protein (Hsp) 40, 70, 90, and 100 families of protein chaperones which are highly conserved across eukaryotes and are vital factors in the quality control of cellular proteins and protein complexes contributing to a wide range of cellular processes (Mayer, 2010). Chaperones within the context of the cellular quality control machinery enable misfolded or aggregated proteins to be refolded (Tyedmers et al., 2010) or targeted for degradation by cellular proteases (Bukau et al., 2006). The ubiquitin ligase machinery is central to ubiquitin tagging

misfolded proteins and targeting them for degradation by cellular proteasomes. There are also reports that the ubiquitin ligase machinery is vital for regulating host immunity to infection. With regard to viral processes, there are few examples where the protein quality control machinery regulates viral proteins in the same way that it acts on cellular proteins. But there are also examples where viruses commandeer chaperones to become central components of replication complexes or drive virus egress into neighboring cells, providing activities that are outside of their normal cellular functions. Among these examples, it is not clear whether the entire machinery is dismantled or if there are an abundance of factors that can allow for some to be recruited without inhibiting normal cellular functions.

This review discusses the various contributions of cellular chaperones and folding enzymes, including a variety of Hsp, to the formation of viral multi-protein complexes. This article contrasts the cellular functions of such proteins to provide the reader with adequate information to consider whether cellular chaperones are acting within their normal context to enable viral protein folding, trafficking, and functioning, or whether they are diverted from their normal activities to provide novel contributions to virus infection. Understanding the various contributions of protein chaperones to cellular and viral activities could enable researchers to determine when and where such factors could be targeted by antiviral compounds to suppress disease. Given the rapid evolution of plant viral genomes and the slow evolution of Hsp proteins, it is reasonable to consider that therapeutic interventions targeting host components of the viral replication and transport machinery could offer a reliable approach to controlling disease.

THE CONTRASTING ROLES OF CYTOSOLIC Hsp70 AND J-DOMAIN PROTEINS IN CELLULAR PROTEIN FOLDING AND PLANT RNA VIRUS INFECTION

Hsp70 family of proteins can interact with a wide range of cofactors and folding substrates and contribute to diverse biological processes. The most common cofactors are J-domain proteins (also known as Hsp40) which identify and recruit substrates to Hsp70 through direct interactions (**Figure 1A**). Nucleotide exchange factors (NEFs) are another set of cellular partners which stimulate dissociation of ADP and this fosters client dissociation upon refolding (**Figure 1A**; Kampinga and Craig, 2010). Thus, the Hsp70 chaperones cycle between substrate bound and free states and rely on the energy of ATP to induce conformation changes in the substrates (**Figure 1A**). Hsp70 can also partner with Hsp90 or Hsp100 (or ClpB) family to solubilize and refold protein aggregates into the native state (Mayer and Bukau, 2005; Kampinga and Craig, 2010; Tyedmers et al., 2010).

The Hsp70 and J-domain proteins are mentioned first because they are most often reported to associate with plant virus infection (Aparicio et al., 2005; Chen et al., 2008). Importantly, Hsp70 and J-domain proteins are not always linked in their contributions to plant virus infection which leads to the speculation that these factors can be diverted from their normal cellular functions to contribute to crucial viral protein complexes. Cytosolic Hsp70s play crucial roles in the replication cycle, intercellular transport, and virion assembly of many positive-strand RNA viruses including potexviruses, tobamoviruses, potyviruses, cucumoviruses, tombusvirus, and carmoviruses. Hsp70 gene expression is induced by these same positive-strand RNA viruses as well as by plant rhabdoviruses and tospoviruses, which have negative-strand genomes (Aparicio et al., 2005; Senthil et al., 2005; Chen et al., 2008; Wang et al., 2009; Mathioudakis et al., 2012). For some plant viruses, there is research knowledge concerning how viral proteins interact with Hsp70 and which aspects of virus infection are aided by these interactions, but for many viruses there is much to learn about the vital roles that Hsp70 plays in pathogenesis. For example, the inhibition of Hsp70 activity or expression alters the replication of turnip crinkle carmovirus although the exact role within the viral replication complex is not known (Chen et al., 2008). Beyond fulfilling key needs in viral pathogenesis, Hsp70 overexpression can enhance abiotic stress tolerance in plants. Thus, understanding the contrasting roles of Hsp70 in plant virus infection can be critical for designing broad strategies to control disease and improve plant tolerance to abiotic stresses. For example, diverting Hsp70 from its normal function could compromise abiotic stress responses. However, if viruses enhance Hsp70 gene expression or if there are multiple homologs or redundancy in function amongst homologs then it is possible that subversion of the Hsp70 machinery by the plant virus might have no impact on the normative cellular processes or might even serve to enhance abiotic stress tolerance. There is no data yet on this topic to know the impact of plant virus infection on Hsp70 related abiotic stress tolerance.

Tombusvirus and bromovirus replication has been studied extensively using yeast as a host model system. Both viruses encode two protein components that comprise the core replicase. For Tomato bushy stunt virus and Cucumber necrosis virus (TBSV and CNV; tombusvirus) it is the p33 and p92 proteins. The p92 is produced by translational readthrough of the UAG stop codon at the end of the p33 domain. Both of the replicase proteins have membrane anchoring domains and assemble with viral RNA template along membrane sites (Panavas et al., 2005). Yeast Hsp70 and DNAJ homologs contribute to the assembly and activation of these viral replicases (**Figure 2A1**). Hsp70 plays a vital role in localizing the TBSV replicase to organellar membranes and in membrane insertion of the replication proteins *in vitro* and in *Nicotiana benthamiana* plants (Pogany et al., 2008; Wang et al., 2009). Two yeast Hsp70 proteins, named Ssa1p and Ssa2p, are present in purified TBSV replicase complexes and mutations in these genes cause cytosolic redistribution of the p33 and p92 replication proteins. With respect to Brome mosaic virus (BMV; bromovirus), the two viral protein components of the replicase are named 1a and 2a and are translated from separate genomic RNAs. The 1a multimerizes along endoplasmic reticulum (ER) membrane causing invaginations that lead to vesicle formation (Diaz et al., 2012). The 1a protein provides RNA capping and helicase activity. The 2a protein is the polymerase and recruits template RNA into the replication vesicles (Chen and Ahlquist, 2000). The yeast *Ydj1* encodes Ydj1p, which is a DNAJ homolog that normally interacts with the Ssa family of Hsp70, is vital for BMV replication (**Figure 2A2**) and interact with the 2a protein (Tomita et al., 2003). Mutations in *Ydj1* inhibit negative-strand RNA synthesis but do not inhibit 1a recruitment of 2a to membrane bound complexes. Thus, Ydj1p is proposed to play a role in the converting the complex to an active form that is capable of negative-strand RNA activation (Tomita

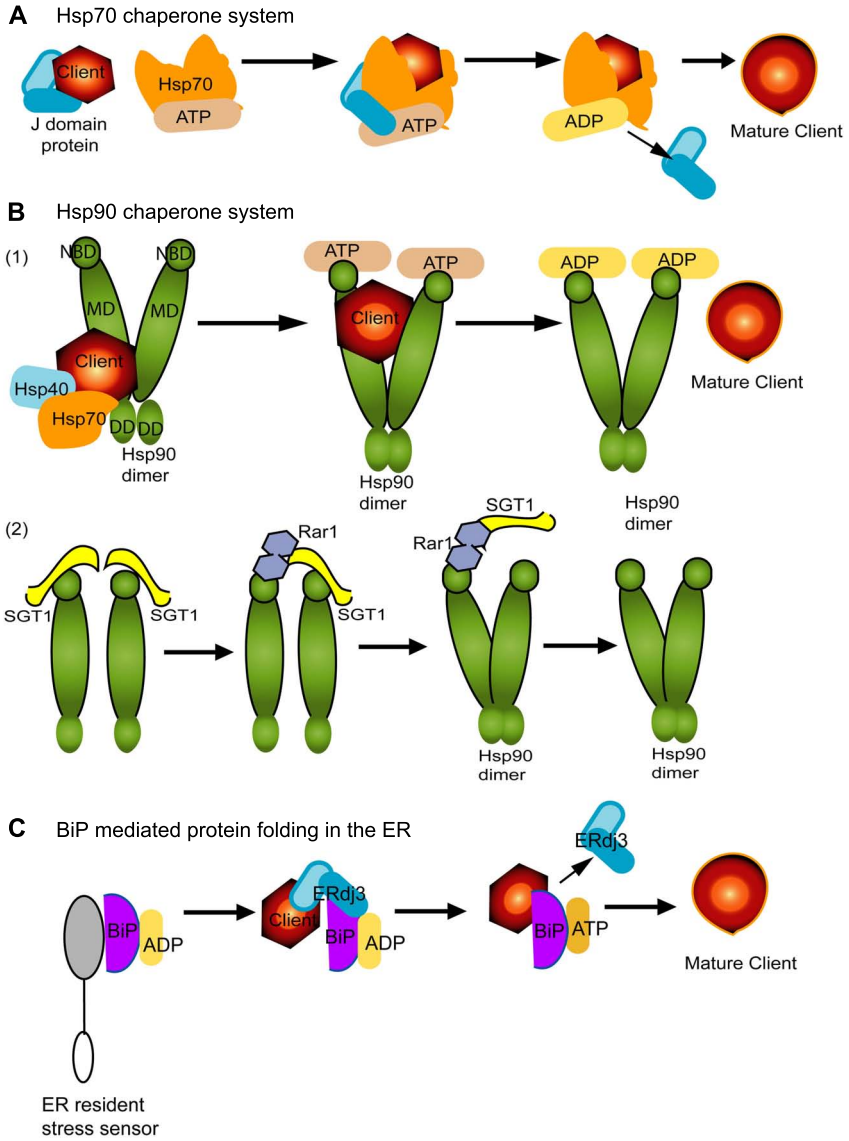

FIGURE 1 | The Hsp70, Hsp90, and BiP mediated protein folding systems are conserved across kingdoms and are vital contributors to plant virus infection and immunity. Misfolded proteins can be referred to as "substrates" or "clients." Hsp70 is shown in orange **(A,B)**. Hsp90 **(B)** is a dimer and has three domains which are represented in deep green and BiP **(C)** is shown in purple. Each chaperone in this figure depends upon ATP (beige) hydrolysis for client binding and release. ADP is depicted in yellow. J-domain proteins are a broad family of proteins that include Hsp40 and DNAJ-like homologs and are depicted in cyan in each panel. While each panel schematic shows a linear representation of the process for recruiting co-chaperones and clients for maturation, in fact the chaperone systems are dynamic and cycle between complex formation for maturation of a client followed, ATP hydrolysis, and disassembly. The cycles repeat in each example. **(A)** The J-domain protein binds to a misfolded protein client and delivers it to Hsp70. These proteins directly interact and it is ATP hydrolysis which enables the release of the J-domain protein. This is also followed by maturation and release of the client protein. **(B)** Hsp90 has a nucleotide-binding domain (NBD) at the N-terminus, the client and co-chaperone binding middle domain (MD), and the dimerization domain (DD) t the C-terminus. The NBD participates in ATP hydrolysis **(B1)** but, interestingly, also interacts with SGT1 and Rar1 **(B2)**. There are two types of co-factors represented in the figure: (1) Hsp40 and Hsp70 coordinate to recruit client proteins to Hsp90 dimers. The Hsp90 MD is primarily responsible for interactions with the misfolded client presented by the Hsp40/70 complex. ATP hydrolysis enables Hsp90 dimer conformational changes and client protein maturation. (2) Rar1-SGT1-Hsp90 are vital for folding and stabilization of NLR proteins. SGT1 and Rar1 are co-chaperones and function to assist the assembly of the Hsp90 dimer. The schematic shows the sequential binding and release of SGT1 and Rar1 to Hsp90. SGT1 binds to the ND domain of Hsp90. Two SGT1 proteins are drawn together bringing Hsp90 monomers into close proximity necessary for dimerization. Rar1 binds ND and interacts with SGT1, sequentially dissociating one and then the next SGT1. Thus, Rar1 enhances SGT1-Hsp90 interactions, but also aids dissociation of SGT1 from Hsp90. Thus the schematic attempts to represent the dynamics nature of their complex formation as proposed by Kadota et al. (2010). These associations are suggested by Shirasu (2009) to stabilize Hsp90 dimers for client substrate loading or release. **(C)** BiP is an Hsp70 homolog and vital contributor to the ERQC machinery. According to Kampinga and Craig (2010), an inactive BiP is bound to the ER luminal domain of a resident ER stress sensor, and to ADP. Upon recognition of misfolded proteins, ERdj3 is a J-domain protein with two domains for substrate and chaperone interactions. ERdj3 resides in the ER and recruits BiP and a misfolded client substrate into a complex. ADP conversion to ATP is necessary to release ERdj3 and subsequent client protein maturation by BiP in the ER.

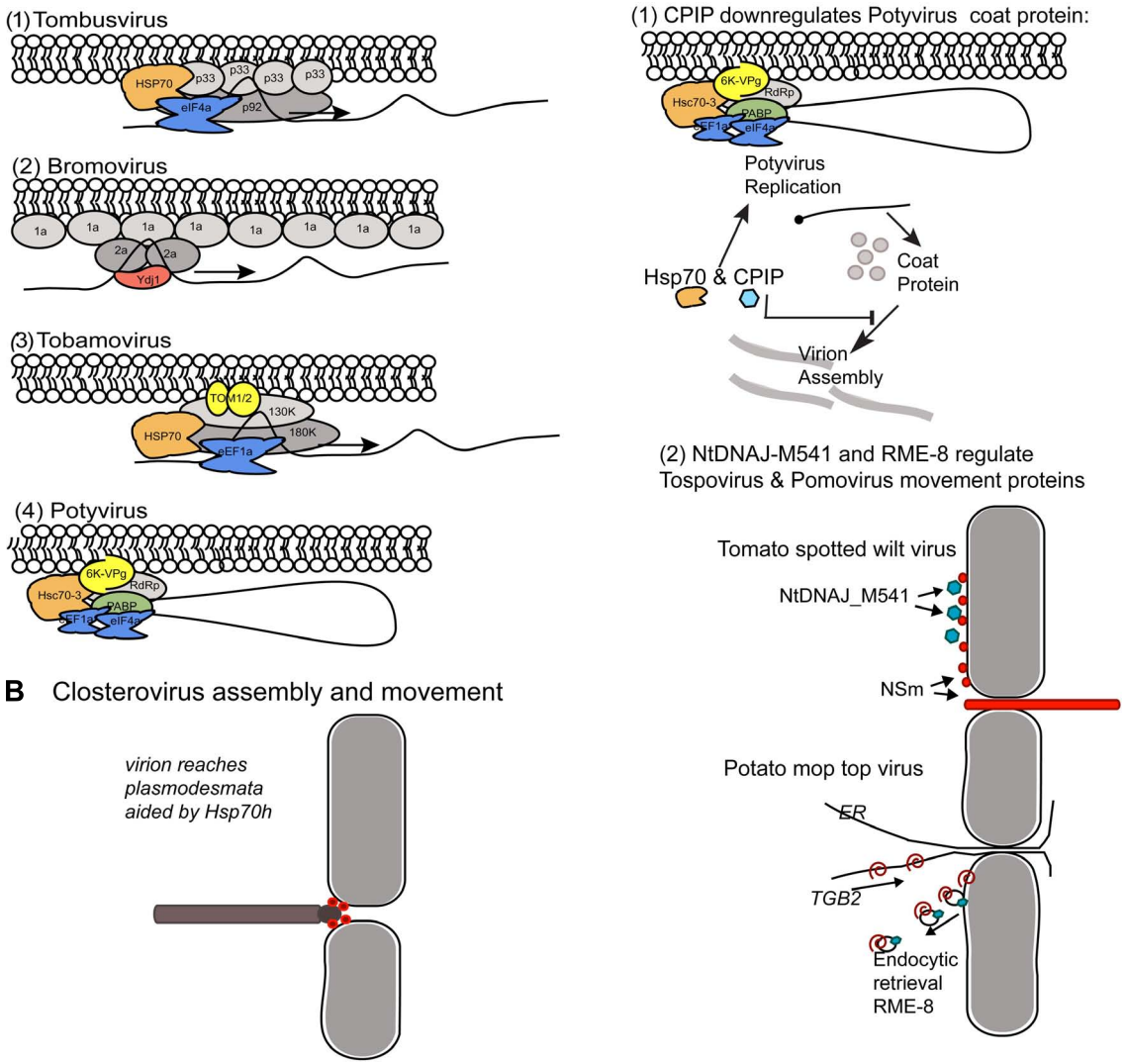

FIGURE 2 | Comparison of the host protein chaperones recruited to membrane bound viral complexes by unrelated (+) strand RNA viruses. Similar chaperones provide different roles in the viral protein complexes. **(A)** Comparison of Hsp70 and Ydj1 interactions with various viral replicases. **(A1,2)** The tombusvirus and bromovirus replicases assemble in spherules along the peroxisome and ER membranes, respectively. **(A3,4)** Tobamoviruses and Potyviruses replicate in ER derived structures. **(A1)** Tombusviruses encode p33 and p92 proteins required for replication. The Hsp70 (orange) recruits p33 to cellular membranes. eIF4e (blue) is another cellular component of the replication complex. **(A2)** Bromoviruses encode 1a and 2a proteins. 1a forms a shell along the membrane. Ydj1p is a J-domain protein involved in negative-strand synthesis which interacts with the 2a protein. **(A3)** Tobamovirus replicase consists of the 130K and 180K proteins and accumulates on ER membranes. TOM1 and TOM2 are host proteins which provide membrane anchoring. Hsp70 and eEF1a are host factors that associate with the viral replicase. **(A4)** The potyvirus replicase is anchored to ER membranes by the viral encoded 6K-VPg. The host PABP, eEF1a, eIF4a, and Hsc70-3 proteins associate with the viral replicase. It is likely that the PABP brings the 3′ end of the genome near the 5′ end and that replication is initiated along a circular RNA. **(B)** Closterovirus virions are long filamentous particles with structurally differentiated tail domain. The viral movement protein is an Hsp70 homolog (Hsp70h; red spheres) which functions to both stabilize the tail region of the virion and aid trafficking across plasmodesmata. **(C)** Role of DNAJ homologs in regulating virus encapsidation and egress. **(C1)** Depiction of the Hsc70-3 containing viral replicase and its relationship to another Hsp70 and CPIP protein. This describes another role for Hsp70 in the potyvirus life cycle, unlike its role in replication depicted in **(A4)**. The Hsp70 and CPIP depicted here suppresses coat protein accumulation and blocks virion assembly. Virion assembly also serves to suppress viral genome translation and therefore, suppression of CP accumulation can enhance genome expression. This machinery reduces the impact of CP on viral genome translation. In this model, proposed by Hafren et al. (2010), CPIP recruits the potyvirus coat protein to Hsp70 which serves to aid ubiquitination and CP degradation. CPIP recruits the CP and thereby reduces its impact on viral genome translation. **(C2)** Yeast two-hybrid assays carried out using the tospovirus NSm protein identified NtDNAJ_M541 protein as an interacting partner. NSm (red spheres) associates with the plasma membrane, binds nucleocapsids, weakly binds RNA, and forms tubules. Given the myriad of NSm activities it is not yet clear how NtDNAJ_M541 (blue octagons) contributes to its functions. Pomovirus TGB2 movement protein is a transmembrane protein that resides in the ER and interacts with RME-8. TGB2 binds viral RNA and potentially cargoes it along the ER to plasmodesmata to facilitate intercellular transport. Researchers proposed that RME-8 is an endocytic marker indicating TGB2 is recycled from the plasma membrane back to the ER where it can bind viral genomes for further rounds of transport to the plasmodesmata.

et al., 2003). While Ydj1p, Ssa1p, and Ssa2p are separately identified as factors in these virus replication cycles, the co-chaperone complex itself has not be identified so it is not clear whether the individual factors are highjacked independently or if the entire chaperone complex is needed to drive membrane insertion and conformational changes in both systems.

Flock house virus (FHV) is primarily an insect infecting virus and is not defined as a plant virus, but is important to consider alongside TBSV and BMV because there are key similarities with regard to the viral replicases, and in laboratory experiments FHV replicates in plant cells as well as yeast and *Drosophila*. In yeast, FHV requires Ydj1p and Hsp70 chaperones for virus replication (Weeks and Miller, 2008). Single deletions of *Ssa1* or *Ssa2* did not alter FHV RNA3 accumulation in yeast but deletion of *Ssz1* which encodes an atypical Hsp70 resulted in an abundant increase in FHV RNA3 accumulation. However, deletion of the *Ydj1* gene suppressed FHV RNA replication while deletion of other DNA J homologs (*JJJ1*, *JJJ2*, or *ZUO1*) increased FHV RNA3 accumulation (Weeks and Miller, 2008; Weeks et al., 2010). The combined data show that the Ssa family of Hsp70 chaperones are essential for replication of several positive-strand RNA viruses in yeast. The fact that viruses which normally infect either plants or an insect commonly require of Hsp70 and Ydj1p is remarkable and suggests that the need for the Hsp70 complex for the replication of some positive-strand RNA viruses are maintained through evolution of their hosts. However, the mechanistic contribution to virus replication varies for each virus. For example, deletion of *Ssa1* or *Ssa2* alters the membrane distribution of the tombusvirus replicase while similar deletions alter the post-translational stability of the FHV protein A polymerase (Weeks and Miller, 2008; Weeks et al., 2010). Thus, while the need for the Hsp70 complex for virus replication is well established, the mechanistic contributions cannot be broadly infer based on studies of a single plant virus.

Research conducted in plants has also identified Hsp70 associating with the tobamovirus and potyvirus replicase (**Figures 2A3,4**), although its role in these complexes is not yet described is such detail. Affinity purified Tomato virus mosaic virus (ToMV; tobamovirus) replicase identified Hsp70, eEF1A, TOM1, and TOM2A proteins associating with membrane bound complexes. TOM1 and TOM2A are integral membrane proteins normally associated with the vacuolar membrane but are highjacked by the ToMV replicase to the membrane site of virus replication (Nishikiori et al., 2006). Turnip mosaic virus (TuMV; potyvirus) RdRP co purifies with *Arabidopsis* Hsc70-3 and the poly(A) binding protein (PABP) in ER-derived vesicles (Dufresne et al., 2008).

Beyond aiding assembly of viral replication complexes, Hsp70 and DNAJ-like proteins contribute to virion assembly and cell-to-cell spread of viruses in other genera. Key examples of (+) strand RNA viruses include the potyviruses, closteroviruses, and pomoviruses. There is also evidence that the Hsp70 machinery contributes to the intercellular transport of (−) strand RNA genome containing tospoviruses.

With regard to viral coat protein (CP) interactions and virion assembly there are two examples. The first example is the closterovirus movement protein (MP) which is itself an Hsp70 homolog (Hsp70h). The Hsp70h plays dual roles in virion assembly and intercellular movement (**Figure 2B**) and its activities appear to be unlike the function of cellular Hsp70 that is depicted in **Figure 1**. Closteroviruses are filamentous viruses that have a long flexuous particles formed by the major capsid protein and a short tail formed by the minor capsid protein (CPm). For Citrus tristeza virus (CTV) and Beet yellows virus (BYV) Hsp70h combined with the viral encoded p61 protein enables the assembly of full-length virions by specifically enabling tail assembly by CPm (Satyanarayana et al., 2000, 2004; Alzhanova et al., 2007; Tatineni et al., 2010). The second function of Hsp70h is to traffic virions to plasmodesmata and enables intercellular transport. The closterovirus Hsp70h autonomously associates with the actin–myosin network and can move through plasmodesmata. Dominant negative mutants of class VIII myosins impede plasmodesmal localization of Hsp70h (Avisar et al., 2008). In *Cucurbita maxima*, Hsp70 homologs were identified to have the capacity to traffic through plasmodesmata and the combined data suggest that a subclass of Hsp70 chaperones engage the plasmodesmata trafficking machinery (Aoki et al., 2002). These data do not fit the current understanding of the roles for Hsp70 in protein folding and turnover, and suggests an alternative function in long distance trafficking that is worth further studying. It is reasonable to speculate the Hsp70 is a component of machinery that moves along the actin network or associates with myosins, but this topic requires further investigation to provide clear understand of this subclass of Hsp70 chaperones. However, these combined data of closterovirus Hsp70h and the *C. maxima* Hsp70s led researchers to speculate that there is a basic mechanism for filamentous virions to require chaperone activity to reach plasmodesmata and trigger viral RNA transfer to neighboring cells

Secondly, separate studies have reported the potyvirus CP interacting with Hsc70 and CPIP, which is a DNAJ-like protein (Hofius et al., 2007; Mathioudakis et al., 2012). In this example, the co-chaperone machinery appears to function in its normal role of client recruitment and modification. CPIP binds to the CP and delivers it to Hsp70 to aid ubiquitination and degradation (Hafren et al., 2010; **Figure 2C1**). Given the multimeric nature of CPs it is possible that the Hsp70 machinery ensures proper protein folding and prevents CP aggregation (Hafren et al., 2010). Beyond quality control regulation of the potyvirus CP, this mechanism also plays a significant role in regulating potyviral gene expression. Within the context of virus infection, the potyvirus CP functions to down-regulate viral gene expression and replication to enable genome encapsidation. As CPs build up in the cell, there becomes an increasing pressure toward suppressing viral genome expression and replication. Therefore, to prolong or increase the amount of genome translation and replication, the combined action of CPIP and Hsp70 serves to down-regulate CP-mediated effects on viral gene expression (**Figure 2C**; Hafren et al., 2010).

DNAJ proteins contribute to membrane bound events relating to virus intercellular movement and there are two well-studied examples (Soellick et al., 2000; **Figure 2C2**). First is RME-8, another DNAJ-like chaperone, which interacts with the pomovirus TGB2 MP (**Figure 2C2**). RME-8 localizes to endocytic vesicles and interacts with cytosolic Hsp70 to control clathrin-dependent endocytosis (Haupt et al., 2005). Thus, TGB2 may rely on

endosome for recycling proteins to the cell's interior where it can provide further rounds of transporting viral genomes from the site of replication to plasmodesmata. However, given the examples of TOM1 and TOM2A which are highjacked by TMV from the vacuolar membrane to viral replication complexes located on other membranes, it is possible that RME-8 is either a landmark for the endosome or plays a different role in TGB2 trafficking. Another example are the (−) strand RNA genome containing tospoviruses whose MP, named NSm, localizes to the plasma membrane and forms tubular extensions from the cell surface. Nsm also interacts with the nucleocapsid and genomic RNA and potentially functions to enable the tubule guided transport of the ribonucleoprotein complex across plasmodesmata. The tospovirus NSm MP interacts with a DNAJ-like protein (NtDnaJ_M541) from both *N. tabacum* and *A. thaliana* (Soellick et al., 2000; **Figure 2C2**). This factor belongs to a subclass of the DNAJ family that only contains the J-domain. Such factors contribute to protein translocation into the mammalian ER, plant peroxisomes, and microtubule formation. The particular role of the NtDnaJ_M541 protein is not known but researchers proposed that it either mediates Hsp70 dependent mechanism of virus movement or itself provides the motive force for ribonucleoprotein translocation to the plasmodesmata (Soellick et al., 2000).

Hsp100 CHAPERONES REGULATE CELLULAR PROTEIN AGGREGATES BUT Hsp101 PROMOTES TOBAMOVIRUS TRANSLATION

The Hsp100/Clp family of chaperones belongs to the superfamily of AAA+ domain containing ATPases and some members act solely in the protein quality control network, functioning in protein disaggregation. This superfamily is defined by direct nucleotide binding and the presence of highly conserved Walker A and B motifs. Most AAA+ domain proteins form ATP bound oligomers and it is the molecular scaffold that is essential for HSp100/Clp as well as nucleotide-binding domain leucine-rich repeat (NLR) protein functions (Mayer, 2010; Bonardi et al., 2012). Hsp100 proteins can cooperate with the Hsp70-Hsp40 system to solubilize and refold aggregated substrate proteins (Zhang and Guy, 2005; Sharma et al., 2009). In plants, Hsp101 is required for thermotolerance and oxidative stress (Tonsor et al., 2008; Kim et al., 2012).

In TMV infection, Hsp101 and eIF4G are recruited by the 68 nucleotide 5′ untranslated leader, known as Ω, and enhances translation of the genomic RNA (Wells et al., 1998; Gallie, 2002). Other tobamoviruses such as Oilseed rape mosaic virus (ORSV) which lack the Ω sequence, do not display the Hsp101-dependent enhancement (Carr et al., 2006), which emphasizes the role of Ω in Hsp101 recruitment. Furthermore, the *N. tabacum* Hsp101 enhances translation of Ω-containing constructs in yeast. Genetic analysis of Hsp101 interactions with the TMV 5′ leader showed that it binds to a poly(CAA) sequence within Ω and aids the recruitment of eIF4F (Gallie, 2002). It is interesting that the Ω -Hsp101 enhancement is not conserved among all tobamoviruses. One possible explanation is that the Ω functions overlap with the 5′ cap and poly(A) tail for recruiting eIF4G (which is a subunit of eIF4F) to the mRNA. The Ω is more effective following heat shock and its presence can reduce the effectiveness of the 5′-cap and poly(A) tail for recruiting eIF4G (Wells et al., 1998). Given that the 5′ cap and poly(A) tail synergistically operate to recruit eIF4G, the Ω may not be crucial in all tobamoviruses and this could explain why it is not highly conserved across members of this genus (Carr et al., 2006).

Hsp90 PLAYS ESSENTIAL ROLES IN HOST PLANT IMMUNITY AND VIRUS REPLICATION

Hsp90 is a highly conserved eukaryotic molecular chaperone. It contributes to the stabilization, or activation of proteins that are involved in signal transduction, protein trafficking, and immunity. Hsp90 typically forms a dimer and its associations with client proteins, as for Hsp70, are regulated by co-chaperones as well as ATP binding and hydrolysis (**Figure 1B1**). Its clients are often properly folded or are in a near native state. Hsp90 proteins have three functional domains: nucleotide-binding domain (NBD) at the N-terminus, the middle domain (MD) which is involved in client and co-chaperone binding, and the dimerization domain (DD) at the C-terminus (Zhang et al., 2010). Hsp90 forms an open homodimer mediated by interactions occurring through the DD domain. When the NBD binds ATP the N-terminal domains come into contact and for a closed conformation. Hsp90 cycles between open and closed conformations (**Figure 1B1**).

In mammalian cells, Hsp40, Hsp70, and Hsp90 are known to cooperate in the maturation of certain client proteins (**Figure 1B1**). The Hsp90 machinery also associates with ubiquitin-dependent degradation processes that contribute to immune regulation (Zhang et al., 2010). In plants and animals, *Hsp90*, *SGT1* (suppressor of G2 allele of skp1) and *Rar1* are essential to the function of many NLR proteins (**Figure 1B2**). NLR proteins are pathogen sensors which contribute to host immunity by activating disease defense responses (Azevedo et al., 2002; Shirasu, 2009; Kadota et al., 2010; Kadota and Shirasu, 2012). Mutations in *Hsp90* can lead to the loss of NLR-mediated defense responses in plants. Most NLR proteins exist in a cell in a near native state but upon recognition of a pathogen effector the NLR proteins are folded and may form dimer or multimeric complexes that are necessary for immune regulation. The Hsp90–SGT1–Rar1 machinery is needed for *Rx*- or *N*-mediated resistance to Potato virus X (PVX) or TMV (Boter et al., 2007; Takabatake et al., 2007), *RPM1* or *RPS2* resistance to *Pseudomonas syringae* (Cai et al., 2006; Kadota et al., 2010), *Mi-1* resistance to root knot nematodes (Bhattarai et al., 2007), *Mla*-resistance to powdery mildew in barley (Hein et al., 2005) among others. The Hsp90–SGT1–Rar1machinery is intriguing because the required partnership among these three factors differs from the Hsp40–Hsp70–Hsp90 partnership for client recruitment and folding. **Figure 1B2** shows that SGT1 and Rar1 bind to the N-terminal ATPase domain of Hsp90, but do not promote ATP hydrolysis. Instead, Rar1 enhances SGT1–Hsp90 interactions and form an asymmetric complex that holds the Hsp90 dimer to enable loading or release of the client protein. Both *Rar1* and *SGT1* are required for steady state accumulation of many NLR proteins and SGT1 plays an addition role in recruiting the NLR client to Hsp90 (Kadota et al., 2008, 2010; Shirasu, 2009; Kadota and Shirasu, 2012). This model is substantiated by yeast two-hybrid assays showing SGT1 and Rar1 proteins interact in the absence of Hsp90. Also mutations in Rar1 can reduce NLR protein accumulation but

the consequence is not as significant as mutations affecting SGT1 and Hsp90. Thus, the NLR stability is mediated by SGT1–Hsp90 complex and enhanced by the presence of *Rar1*.

The SGT1–Hsp90–Rar1 machinery is particularly intriguing because each of these factors provide additional roles in biological processes that are independent of each other (Shirasu and Schulze-Lefert, 2003). *Rar1* was shown in soybean and *Arabidopsis* to be essential for the induction of pathogenesis-related (PR) gene expression and contributes to PAMP-mediated immunity (Fu et al., 2009). While *SGT1* is required for *Rx*-steady state accumulation, it also negatively regulates some NLR proteins in *Arabidopsis* and helps to mediate systemic acquired resistance in soybean (Boter et al., 2007; Fu et al., 2009). With regard to plant virus infection, *SGT1* is specifically induced by SMV, PVX, and Plantago asiatica mosaic virus (PlAMV) infection in susceptible hosts (Komatsu et al., 2010; Ye et al., 2012b). PlAMV and PVX are both potexviruses and VIGS silencing *SGT1* enhanced virus accumulation relative to leaves treated with only the VIGS vector. *N. benthamiana* plants overexpressing SGT1 show enhanced systemic accumulation of PVX (Ye et al., 2012b). Unlike PVX, PlAMV infection causes systemic necrosis and silencing *SGT1* and *RAR1* reduces these symptoms (Komatsu et al., 2010). Thus, for potexviruses it appears that SGT1 contributes to the regulation of systemic virus accumulation. Moreover, SGT1 associates with *Hsc70* in Arabidopsis and this interaction contributes to basal resistance. Given that *Hsc70* is also a positive factor in plant virus infection this story may be quite complicated. More research is needed to uncover the various roles of SGT1 as a co-chaperone in events that modulate immunity and promote plant virus multiplication.

There are also reports showing Hsp90 plays a positive role in Bamboo mosaic virus (BaMV; a potexvirus), Red clover necrotic mosaic virus (RCNMV; a dianthovirus), and FHV infection and it appears to provide different partnerships with the various viral replicases (**Figure 3**). The *N. benthamiana* Hsp90 was reported by Huang et al. (2012) to interact specifically with the 3′ untranslated region of BaMV. Hsp90 does not associate with the 3′ region of the BaMV-associated satellite RNA, PVX (potexvirus genus) or Cucumber mosaic virus (CMV; cucumovirus genus) genomic RNAs suggesting that this is a unique interaction that promotes BaMV replication (**Figure 3**; Huang et al., 2012). In contrast, RCNMV encodes two replication associated proteins named p27 and p88. Hsp70 and Hsp90 interact with p27 and lead to the recruitment of RNA 2 to the ER. Hsp70 and Hsp90 also promote translation of p27 (Mine et al., 2010, 2012). FHV also requires Hsp90 for assembly of the viral replication complex and protein-A accumulation (Kampmueller and Miller, 2005). These very recent discoveries that Hsp90 contributes to the initiation of viral RNA synthesis in a virus species-specific manner is intriguing. While the interactions between component proteins of the viral replicase with Hsp90 seem to have little in common, it is possible that a common fold in the proteins is recognized by Hsp90 or that a viral RNA element first attracts Hsp90 which then recruits other of viral replication factors (Huang et al., 2012). Further investigations are needed to unlock the mechanism of replicase assembly and the role of Hsp90 for these and other plant viruses.

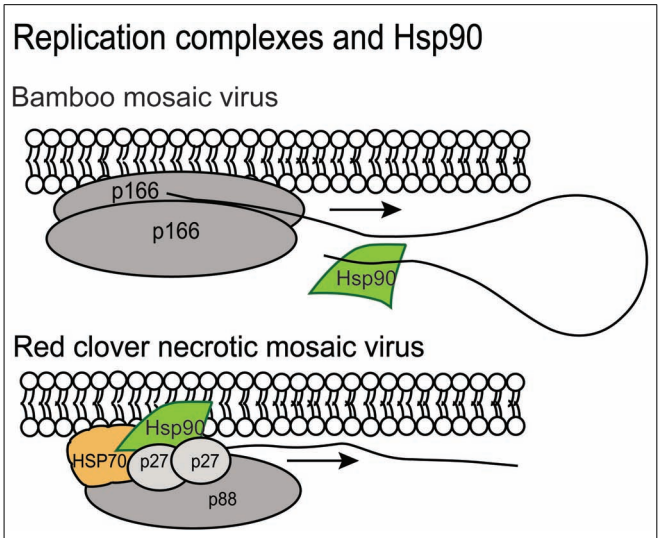

FIGURE 3 | Hsp90 contributes to the BaMV and RCNMV replication complexes. The gray spheres represent the membrane bound viral components of the replicase. The BaMV p166 protein is represented as a dimer. The RCNMV p88 and p27 are also represented. Hsp90 is indicated in green and binds to the 3′ end of the BaMV genome. It is not known to interact with other viral genomes making this observation unique. Hsp90 and hsp70 are also components of the RCNMV replicase and are essential for membrane recruitment of the complex.

ER CHAPERONE SYSTEM AND ITS EMERGING IMPORTANCE IN PLANT VIRUS INFECTION

A separate set of chaperones and folding enzymes exist in the ER and contribute to the ER quality control (ERQC) machinery which regulates the folding of newly synthesized proteins (Meunier et al., 2002). Proper folding and assembly is necessary for proteins entering the secretory pathway to reach their appropriate cellular destinations (Iwata and Koizumi, 2012). Key components of the ERQC include protein disulfide isomerase (PDI) which enables the formation of disulfide bonds in proteins, calreticulin (CRT) and calnexin (CNX) which are lectin-like chaperones that recognize and monitor N-linked glycan modifications (Meunier et al., 2002; Meusser et al., 2005), and the ER luminal-binding protein BiP, which is a member of the Hsp70 family that monitors protein folding and maturation in the ER. Glycoproteins can also be processed by ERp57 (a member of PDI family) which enable the formation of disulfide bonds (Ellgaard and Helenius, 2001, 2003).

Both the CRT/CNX and BiP chaperone systems sequester malformed proteins in the ER for refolding. N-linked glycosylation occurs through the transfer of a triglucosylated, branched chore oligosaccharide to a nascent polypeptide. The core oligosaccharide is trimmed by ER resident glucosidases to the monoglucosylated form. CNX and CRT recognize N-linked glycans attached to proteins which function to ensure the glucose is removed from the glycan. Improperly trimmed glycans can go through a reiterative process of transfers between the glucosidases and CNX/CRT to ensure proper maturation prior to ER export. BiP resembles other Hsp70 proteins in that its interactions with cofactors and substrates are regulated by the ATPase cycle (**Figure 1**). In this system

ERdj3, which is a member of the Hsp40 family, first binds to the unfolded proteins and recruits BiP (Kampinga and Craig, 2010). The binding and release of nascent chains is controlled by the cycle of ATP and ADP exchange (**Figure 1**). Similar to CRT/CNX system, BiP undergoes cylces of binding and release from unfolded proteins. Co-chaperones include ERdj3 which is an Hsp40 and PDI. When proteins fail to mature properly, they are directly cleared from the ER and degraded by the ubiquitin-proteasome system.

CRT also functions in Ca^{2+} sequestration and in plants, accumulates in plasmodesmata. CRT interacts directly with the TMV MP and is suggested to play a regulatory role in promoting virus intercellular transport. Overexpression of CRT interferes with TMV cell-to-cell movement and is suggested to direct TMV MP from plasmodesmata to microtubules. It is worth speculating that this could lead to TMV MP degradation (Chen et al., 2005). Interestingly, BiP, CRT, and PDIs including ERp57 are up-regulated during *N*-mediated resistance to TMV (Caplan et al., 2009). Silencing ERp57, CRT2, and CRT3 in *N*-gene expressing *N. benthamiana* led to partial restoration of systemic accumulation lending further support to earlier reports that up-regulating CRT blocks TMV movement. CRTs also regulate the folding of plasma membrane localized induced receptor-like kinase (IRK) that functions during *N*-mediated resistance (Caplan et al., 2009).

BiP is best known for its central role in ER stress and the unfolded protein response (UPR; **Figure 4**). In the absence of ER stress, BiP binds to the ER luminal domain of IRE1. Upon stress, BiP moves away from IRE1 and binds to the unfolded protein. IRE1 possesses a cytosolic endoribonuclease domain which is activated by the uncoupling of BiP and IRE1 (Iwata and Koizumi, 2012; Parmar and Schroder, 2012). IRE1then cleaves exon–intron junctions in the mRNA encoding the bZIP60 transcription factor. The bZIP60 is translocated to the nucleus where it activates expression of genes involved in the UPR. Overexpression of BiP suppresses the UPR because it increases the amount of protein binding IRE1 and enabling protein maturation. The PVX TGB3 protein is essential for virus movement and is an ER resident protein that appears to stimulate expression of the IRE1-major downstream effector *bZIP60* as well as BiP and CRT (Ye et al., 2011). Silencing bZIP60 also impairs PVX accumulation in protoplasts, indicating that activation of UPR related transcription factor is vital for PVX infection. Overexpression of TGB3 from a CaMV 35S promoter or from a TMV vector can cause HR-like lesions *N. benthamiana* leaves. Experiments also revealed that BiP plays a cytoprotective role in virus infected leaves and its overexpression can alleviate TGB3 or virus-induced cell death. These data argue that BiP and the UPR components of a pro-survival response that is activated by TGB3 to create a cellular environment that enables the spread of virus infection.

Another component of the ERQC machinery that works in conjunction with the ER resident chaperones is a mechanism to eliminate the malformed proteins from the ER. Such malformed proteins that cannot be refolded are recognized by Hrd1/Der3p which acts to ubiquitinate substrates to enable their dislocation and subsequent degradation. Hrd1p/Der3p resides in the ER and provides the essential ubiquitin ligase activity that precedes proteolytic breakdown of misfolded proteins. Hrd1p/Der3p is well described in mammal and yeast cells and was recently identified in plant cells (Meusser et al., 2005; Zhang and Kaufman, 2006; Su et al., 2011). The ubiquitinated substrates are transported out of the ER for degradation by the 26S proteasome.

Curiously there are other ubiquitin ligases that interact with the 26S proteinase, including SCF E3 ubiquitin ligase complex (**Figure 4**). This complex includes the co-chaperones SKP1 and Cullin. While TGBp3 is not known to induce Hrd1p/Der3p it has been shown to activate expression of SKP1 (Ye et al., 2011). Other plant viruses that are known to directly interact with SKP1 include the polerovirus P0 silencing suppressor protein and the nanovirus Clink. Both P0 and Clink have F-box like domains that can interact with SKP1 (Aronson et al., 2000; Pazhouhandeh et al., 2006; Bortolamiol et al., 2007). Up-regulation of SKP1 by PVX TGB3 or SKP1 interaction with P0 or Clink lead to enhanced virus accumulation. These combined data suggest that certain plant viruses stimulate chaperones or co-chaperones involved in protein turnover as a means to create a favorable environment for efficient replication. These factors might rely on SKP1-dependent machinery to degrade host factors that could impede replication or movement and may be involved in immunity.

CONCLUSION

This article provides examples where plant viruses subvert a few key cellular chaperones and cofactors from their normal cellular function into viral protein complexes and examples where certain chaperones are likely to function within their normal cellular context, and viral proteins are the recognized substrates. With regard to subversion of chaperones, the tombusvirus, tobamovirus, and potyviruses require Hsp70, while BaMV and dianthoviruses require Hsp90 to participate early in the formation of active membrane anchored replication complexes (Nishikiori et al., 2006; Wang et al., 2009; Hafren et al., 2010; Huang et al., 2012; Mine et al., 2012). It is possible that these viral replicases have a common fold that can be recognized by the Hsp70 or Hsp90 partner, however future research is needed to better understand how these two cellular chaperones participate in the replication of a wide range of unrelated viruses. *Ydj1*, *JJJ*, *JJ2*, and *ZOU1* are *Hsp40* homologs in yeast that act independently of Ssa1/2 to enable replication of either BMV or FHV (Tomita et al., 2003; Weeks and Miller, 2008; Weeks et al., 2010). The combined data among different plant viruses indicate that the mechanistic contributions of chaperones to RNA virus replication varies among viruses and that there is not one broad definition of how these viral replicases assemble with host factors. The requirement for *Ydj1* appears to be uncoupled from *Hsp70* for BMV replication. However, we do not yet understand whether these Hsp70 and Hsp40 separately or in combination regulate the folding and assembly or membrane anchoring of the viral replicases. It worth speculating that Hsp chaperones aid in recruiting essential host factors such as the PABP, eEF1a, or eIF4a into the replication complex or to stabilize associations between viral proteins that comprise the replication complexes (Leonard et al., 2004). They may also provide stability to the membrane anchor for the replication complex. Evidence that Hsp90 interacts with 3′ end of the BaMV RNA indicates that chaperones may be subverted to stabilize viral RNA.

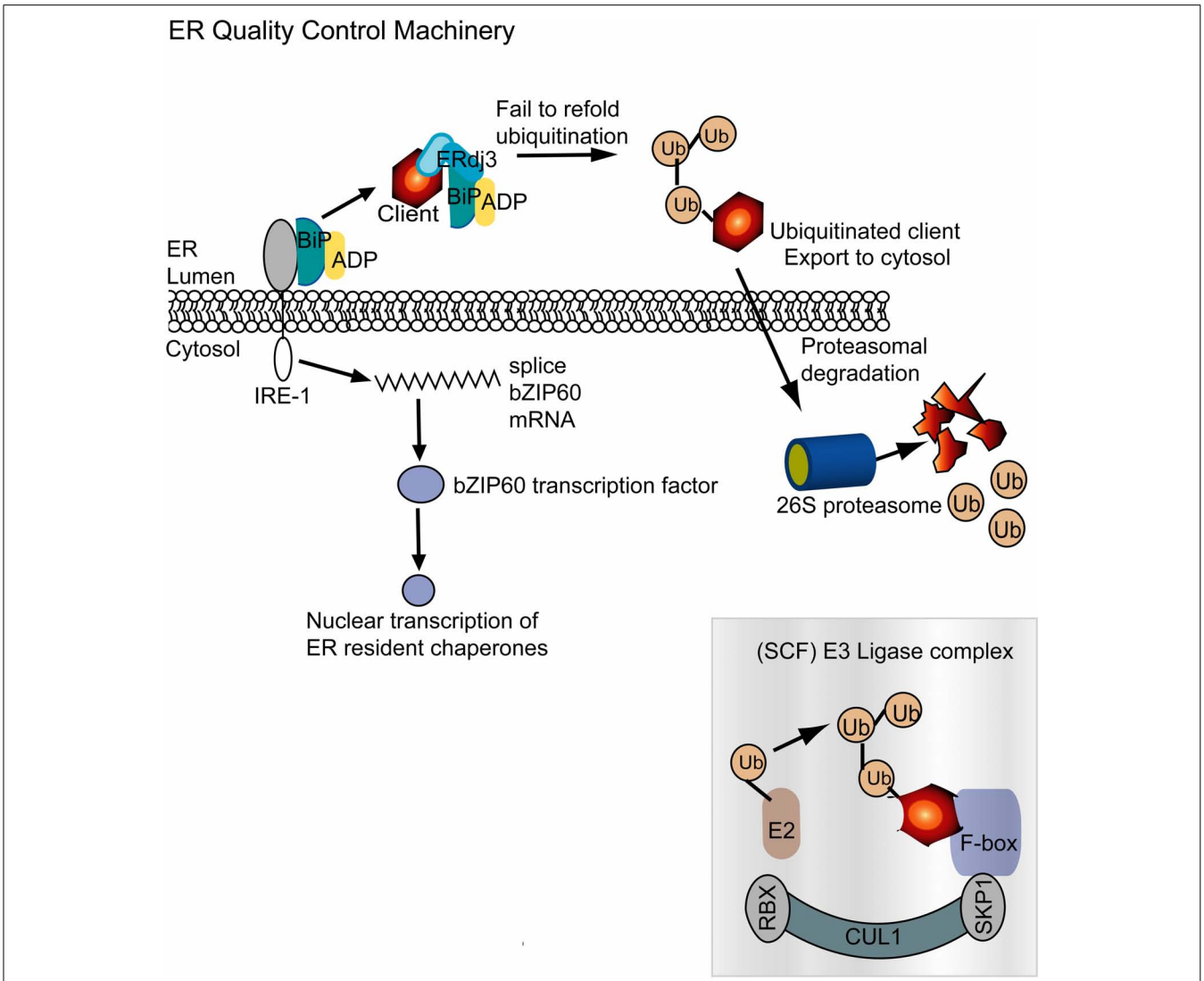

FIGURE 4 | The ER quality control machinery monitors protein folding in the ER following translation. BiP is an ER chaperone that in its resting state is bound to the ER stress transmembrane receptor IRE-1 and to ADP. A nascent or misfolded protein is identified and recruited by ERdj3, which is an Hsp40 homolog, and BiP is redirected to this complex. As seen in **Figure 1**, the role of BiP is to refold misfolded proteins. But in the event that this does not succeed, the misfolded client is ubiquitinated in the ER. Hrd1p/Der3p in mammals, yeast, and plants is responsible for substrate ubiquitination in the ER (Meusser et al., 2005; Zhang and Kaufman, 2006; Su et al., 2011). The ubiquitinated substrates degraded in the cytosol by the 26S proteasome. The SCF E3 ubiquitin ligase complex, depicted here, is a cytosolic complex often described to be associated with the plant NLR immune system. It is intriguing to see that plant viruses require or mimic components of the SCF complex. IRE-1 senses accumulation of misfolded proteins and splices bZIP60 mRNA. bZIP60 is a transcription factor that upon translation is transported to the nucleus and activates expression of ER resident chaperones, including BiP. Up-regulation of the network is designed to restore ER homeostasis by eliminating malformed proteins.

Furthermore, there is no evidence yet to indicate whether the ATPase activities are essential for the chaperone functions within the viral replication complexes (Huang et al., 2012). In summary, further research is needed to understand mechanistic contribution of these factors to virus replication. With regard to the roles of *Hsp70* and virus movement, there is evidence that Hsp70 overexpression enhances virus movement but mechanistically we know very little about its role in the plasmodesmata or interactions with viral MPs. It is intriguing that the closterovirus MP is an Hsp70 homolog which functions to stabilize the virion as well as direct plasmodesmata trafficking. Perhaps further studies with this protein will provide insight into the activities Hsp70 contributes to intercellular trafficking.

Ydp1, CPIP, RME-8, and NtDNAJ_M541 are J-domain proteins that are subverted by the plant viruses. Except for Ydp1 which associates with the BMV replicase, most interact with structural or MPs. CPIP is described as a factor that down-regulates the potyvirus CP, RME-8 is involved in endocytic trafficking of the pomovirus TGB2 protein from the plasma membrane toward the cell interior, and the role of the NtDNAJ_M541 protein is not yet defined (Haupt et al., 2005; Hafren et al., 2010). These factors are intriguing because they are known to identify client proteins for

partner chaperones. Thus, it is easy to imagine that they might identify the viral proteins clients, relying on their substrate binding sites for stabilizing interactions. The questions we are left with, is whether these proteins are highjacked by the virus and subverted for viral functions, or if they target these viral proteins for degradation. For example, we do not yet know the next step in CPIP led processes, but researchers proposed that CPIP targets the CP for degradation (Hafren et al., 2010). This activity promotes viral genome expression and replication but down regulates encapsidation. The tospovirus NSm protein is required for virus intercellular movement but the mechanism for virus transport is not fully understood. Nsm accumulates along the plasma membrane, forms tubules, and interacts with a viral ribonucleoprotein complex which is transported between cells. NtDNAJ_M541 might stabilize the tospovirus Nsm in tubules or in the plasma membrane, and it might also stabilize complexes involving the capsid and genomic RNA (Soellick et al., 2000). On the other hand, this DNAJ-like protein could target Nsm for degradation to alleviate stress on the plasma membrane or modulate the size of the tubules. The function of RME-8 interactions with the pomovirus TGB2 protein is also uncertain. Pomoviruses encode three MPs known as the "triple gene block" proteins. TGB2 binds viral RNA, inserts into the ER network and might be responsible for trafficking viral RNA toward the plasmodesmata. Upon delivering the genome cargo to its destination TGB2 might move along the plasma membrane where it is recycled back to the cells interior by the endocytic machinery for further rounds of RNA trafficking. It is also possible that TGB2 is directed by the endosome to the vacuole for degradation. Thus RME-8 might function as a chaperone either to stabilize and regenerate movement complexes, or aid in protein turnover. Thus, considering that we know so little about CPIP, NtDNAJ_M541, and RME-8 in viral processes, future research is likely to produce fascinating new insights into the machinery regulating viral encapsidation and egress.

Finally, the potexvirus TGB3 protein up-regulates the expression of ER resident chaperones via bZIP60 transcription factor indicates that the ERQC machinery plays a vital role in plant virus infection (Ye et al., 2011, 2012a). This is the first example of a plant viral MP that activates bZIP60 to induce host gene expression. Up-regulation of ERQC machinery could function to stimulate protein folding and maintain ER homeostasis during plant virus infection. This might be a necessary activity to promote virus replication and spread. It is also possible that TGB3 identifies host proteins, such as NLR proteins for degradation via the proteasome. The SCF E3 ligase complex contains SKP1 and F-box protein to aid client protein ubiquitination prior to proteasomal degradation. Given a report by Ye et al. (2011) that SKP1 is induced by TGB3 and is important for virus infection it is possible that the PVX TGB3 protein acts at the ER to redirect such factors to the E3 ligase complex for ubiquitin-proteasome pathway soon after translation as a means to block host immune responses (Ye et al., 2012a). Further research is needed to identify factors that are degraded in a manner that is TGB3 dependent.

While the above discussion of Hsp40, Hsp70, and Hsp90 supports the hypothesis that the chaperone machinery is somewhat dismantled and reconfigured to support virus replication, the newer data concerning CPIP, RME-8, and NtDNAJ_M541, and the ERQC could be viewed as evidence that the chaperone machinery is diverted to recognizing alternative substrates while their cellular functions are unaltered. In other words, the endocytic machinery and ERQC machinery appears to remain intact but the virus piggybacks onto the machinery to achieve a successful infection. This is important to consider because it could represent a manner in which the virus can evade defense within the host and avoid recognition by the immune system. Alternatively, we know so little about how plant viruses interact with the endocytic machinery or ERQC machinery but we do know that both systems can achieve protein degradation. Endosomes containing viral components could fuse with the vacuole to degrade viral components and ERQC machinery to down-regulate infection by identifying viral proteins as foreign or aberrant products that need to be degraded through the proteasome. Thus, these machineries could be part of an immune response. We do know from animal virus research that RNA viruses have mechanisms to cleverly evade recognition by the host immune system and this can include interacting with the host autophagic machinery in a manner that promotes infection. Future research is likely to examine the exciting possibilities that the ERQC machinery or endocytic machinery are natural extensions of the antiviral defense machinery or essential pathway to achieving successful infection. Understanding their roles in infection could be quite valuable for designing strategies for controlling virus disease which target host machinery that is vital for infection.

REFERENCES

Alzhanova, D. V., Prokhnevsky, A. I., Peremyslov, V. V., and Dolja, V. V. (2007). Virion tails of Beet yellows virus: coordinated assembly by three structural proteins. *Virology* 359, 220–226.

Aoki, K., Kragler, F., Xoconostle-Cazares, B., and Lucas, W. J. (2002). A subclass of plant heat shock cognate 70 chaperones carries a motif that facilitates trafficking through plasmodesmata. *Proc. Natl. Acad. Sci. U.S.A.* 99, 16342–16347.

Aparicio, F., Thomas, C. L., Lederer, C., Niu, Y., Wang, D., and Maule, A. J. (2005). Virus induction of heat shock protein 70 reflects a general response to protein accumulation in the plant cytosol. *Plant Physiol.* 138, 529–536.

Aronson, M. N., Meyer, A. D., Gyorgyey, J., Katul, L., Vetten, H. J., Gronenborn, B., et al. (2000). Clink, a nanovirus-encoded protein, binds both pRB and SKP1. *J. Virol.* 74, 2967–2972.

Avisar, D., Prokhnevsky, A. I., and Dolja, V. V. (2008). Class VIII myosins are required for plasmodesmatal localization of a closterovirus Hsp70 homolog. *J. Virol.* 82, 2836–2843.

Azevedo, C., Sadanandom, A., Kitagawa, K., Freialdenhoven, A., Shirasu, K., and Schulze-Lefert, P. (2002). The RAR1 interactor SGT1, an essential component of R gene-triggered disease resistance. *Science* 295, 2073–2076.

Bhattarai, K. K., Li, Q., Liu, Y., Dinesh-Kumar, S. P., and Kaloshian, I. (2007). The MI-1-mediated pest resistance requires Hsp90 and Sgt1. *Plant Physiol.* 144, 312–323.

Bonardi, V., Cherkis, K., Nishimura, M. T., and Dangl, J. L. (2012). A new eye on NLR proteins: focused on clarity or diffused by complexity? *Curr. Opin. Immunol.* 24, 41–50.

Bortolamiol, D., Pazhouhandeh, M., Marrocco, K., Genschik, P., and Ziegler-Graff, V. (2007). The Polerovirus F box protein P0 targets ARGONAUTE1 to suppress RNA silencing. *Curr. Biol.* 17, 1615–1621.

Boter, M., Amigues, B., Peart, J., Breuer, C., Kadota, Y., Casais, C., et al. (2007). Structural and functional analysis of SGT1 reveals that its interaction with HSP90 is required for the accumulation of Rx, an R protein involved in plant immunity. *Plant Cell* 19, 3791–3804.

Bukau, B., Weissman, J., and Horwich, A. (2006). Molecular chaperones and protein quality control. *Cell* 125, 443–451.

Cai, X. Z., Xu, Q. F., Wang, C. C., and Zheng, Z. (2006). Development of a virus-induced gene-silencing system for functional analysis of the RPS2-dependent resistance signalling pathways in Arabidopsis. *Plant Mol. Biol.* 62, 223–232.

Caplan, J. L., Zhu, X., Mamillapalli, P., Marathe, R., Anandalakshmi, R., and Dinesh-Kumar, S. P. (2009). Induced ER chaperones regulate a receptor-like kinase to mediate antiviral innate immune response in plants. *Cell Host Microbe* 6, 457–469.

Carr, T., Wang, Y., Huang, Z., Yeakley, J. M., Fan, J. B., and Whitham, S. A. (2006). Tobamovirus infection is independent of HSP101 mRNA induction and protein expression. *Virus Res.* 121, 33–41.

Chen, J., and Ahlquist, P. (2000). Brome mosaic virus polymerase-like protein 2a is directed to the endoplasmic reticulum by helicase-like viral protein 1a. *J. Virol.* 74, 4310–4318.

Chen, M. H., Tian, G. W., Gafni, Y., and Citovsky, V. (2005). Effects of calreticulin on viral cell-to-cell movement. *Plant Physiol.* 138, 1866–1876.

Chen, Z., Zhou, T., Wu, X., Hong, Y., Fan, Z., and Li, H. (2008). Influence of cytoplasmic heat shock protein 70 on viral infection of *Nicotiana benthamiana*. *Mol. Plant Pathol.* 9, 809–817.

Diaz, A., Gallei, A., and Ahlquist, P. (2012). Bromovirus RNA replication compartment formation requires concerted action of 1a's self-interacting RNA capping and helicase domains. *J. Virol.* 86, 821–834.

Dufresne, P. J., Thivierge, K., Cotton, S., Beauchemin, C., Ide, C., Ubalijoro, E., et al. (2008). Heat shock 70 protein interaction with Turnip mosaic virus RNA-dependent RNA polymerase within virus-induced membrane vesicles. *Virology* 374, 217–227.

Ellgaard, L., and Helenius, A. (2001). ER quality control: towards an understanding at the molecular level. *Curr. Opin. Cell Biol.* 13, 431–437.

Ellgaard, L., and Helenius, A. (2003). Quality control in the endoplasmic reticulum. *Nat. Rev. Mol. Cell Biol.* 4, 181–191.

Fu, D. Q., Ghabrial, S., and Kachroo, A. (2009). GmRAR1 and GmSGT1 are required for basal, R gene-mediated and systemic acquired resistance in soybean. *Mol. Plant Microbe Interact.* 22, 86–95.

Gallie, D. R. (2002). The 5′-leader of tobacco mosaic virus promotes translation through enhanced recruitment of eIF4F. *Nucleic Acids Res.* 30, 3401–3411.

Hafren, A., Hofius, D., Ronnholm, G., Sonnewald, U., and Makinen, K. (2010). HSP70 and its cochaperone CPIP promote potyvirus infection in *Nicotiana benthamiana* by regulating viral coat protein functions. *Plant Cell* 22, 523–535.

Haupt, S., Cowan, G. H., Ziegler, A., Roberts, A. G., Oparka, K. J., and Torrance, L. (2005). Two plant-viral movement proteins traffic in the endocytic recycling pathway. *Plant Cell* 17, 164–181.

Heath, C. M., Windsor, M., and Wileman, T. (2001). Aggresomes resemble sites specialized for virus assembly. *J. Cell Biol.* 153, 449–455.

Hein, I., Barciszewska-Pacak, M., Hrubikova, K., Williamson, S., Dinesen, M., Soenderby, I. E., et al. (2005). Virus-induced gene silencing-based functional characterization of genes associated with powdery mildew resistance in barley. *Plant Physiol.* 138, 2155–2164.

Hofius, D., Maier, A. T., Dietrich, C., Jungkunz, I., Bornke, F., Maiss, E., et al. (2007). Capsid protein-mediated recruitment of host DNAJ-like proteins is required for Potato virus Y infection in tobacco plants. *J. Virol.* 81, 11870–11880.

Huang, Y. W., Hu, C. C., Liou, M. R., Chang, B. Y., Tsai, C. H., Meng, M., et al. (2012). Hsp90 interacts specifically with viral RNA and differentially regulates replication initiation of Bamboo mosaic virus and associated satellite RNA. *PLoS Pathog.* 8:e1002726. doi: 10.1371/journal.ppat.1002726

Iwata, Y., and Koizumi, N. (2012). Plant transducers of the endoplasmic reticulum unfolded protein response. *Trends Plant Sci.* doi: 10.1016/j.tplants.2012.06.014 [Epub ahead of print].

Kadota, Y., Amigues, B., Ducassou, L., Madaoui, H., Ochsenbein, F., Guerois, R., et al. (2008). Structural and functional analysis of SGT1-HSP90 core complex required for innate immunity in plants. *EMBO Rep.* 9, 1209–1215.

Kadota, Y., and Shirasu, K. (2012). The HSP90 complex of plants. *Biochim. Biophys. Acta* 1823, 689–697.

Kadota, Y., Shirasu, K., and Guerois, R. (2010). NLR sensors meet at the SGT1-HSP90 crossroad. *Trends Biochem. Sci.* 35, 199–207.

Kampinga, H. H., and Craig, E. A. (2010). The HSP70 chaperone machinery: J proteins as drivers of functional specificity. *Nat. Rev. Mol. Cell Biol.* 11, 579–592.

Kampmueller, K. M., and Miller, D. J. (2005). The cellular chaperone heat shock protein 90 facilitates Flock House virus RNA replication in *Drosophila* cells. *J. Virol.* 79, 6827–6837.

Kim, M., Lee, U., Small, I., Des Francs-Small, C. C., and Vierling, E. (2012). Mutations in an Arabidopsis mitochondrial transcription termination factor-related protein enhance thermotolerance in the absence of the major molecular chaperone HSP101. *Plant Cell* 24, 3349–3365.

Komatsu, K., Hashimoto, M., Ozeki, J., Yamaji, Y., Maejima, K., Senshu, H., et al. (2010). Viral-induced systemic necrosis in plants involves both programmed cell death and the inhibition of viral multiplication, which are regulated by independent pathways. *Mol. Plant Microbe Interact.* 23, 283–293.

Leonard, S., Viel, C., Beauchemin, C., Daigneault, N., Fortin, M. G., and Laliberte, J. F. (2004). Interaction of VPg-Pro of turnip mosaic virus with the translation initiation factor 4E and the poly(A)-binding protein in planta. *J. Gen. Virol.* 85, 1055–1063.

Mathioudakis, M. M., Veiga, R., Ghita, M., Tsikou, D., Medina, V., Canto, T., et al. (2012). Pepino mosaic virus capsid protein interacts with a tomato heat shock protein cognate 70. *Virus Res.* 163, 28–39.

Mayer, M. P. (2010). Gymnastics of molecular chaperones. *Mol. Cell* 39, 321–331.

Mayer, M. P., and Bukau, B. (2005). Hsp70 chaperones: cellular functions and molecular mechanism. *Cell. Mol. Life Sci.* 62, 670–684.

Meunier, L., Usherwood, Y. K., Chung, K. T., and Hendershot, L. M. (2002). A subset of chaperones and folding enzymes form multiprotein complexes in endoplasmic reticulum to bind nascent proteins. *Mol. Biol. Cell* 13, 4456–4469.

Meusser, B., Hirsch, C., Jarosch, E., and Sommer, T. (2005). ERAD: the long road to destruction. *Nat. Cell Biol.* 7, 766–772.

Mine, A., Hyodo, K., Tajima, Y., Kusumanegara, K., Taniguchi, T., Kaido, M., et al. (2012). Differential roles of Hsp70 and Hsp90 in the assembly of the replicase complex of a positive-strand RNA plant virus. *J. Virol.* 86, 12091–12104.

Mine, A., Takeda, A., Taniguchi, T., Taniguchi, H., Kaido, M., Mise, K., et al. (2010). Identification and characterization of the 480-kilodalton template-specific RNA-dependent RNA polymerase complex of red clover necrotic mosaic virus. *J. Virol.* 84, 6070–6081.

Netherton, C., Moffat, K., Brooks, E., and Wileman, T. (2007). A guide to viral inclusions, membrane rearrangements, factories, and viroplasm produced during virus replication. *Adv. Virus Res.* 70, 101–182.

Nishikiori, M., Dohi, K., Mori, M., Meshi, T., Naito, S., and Ishikawa, M. (2006). Membrane-bound tomato mosaic virus replication proteins participate in RNA synthesis and are associated with host proteins in a pattern distinct from those that are not membrane bound. *J. Virol.* 80, 8459–8468.

Panavas, T., Hawkins, C. M., Panaviene, Z., and Nagy, P. D. (2005). The role of the p33:p33/p92 interaction domain in RNA replication and intracellular localization of p33 and p92 proteins of Cucumber necrosis tombusvirus. *Virology* 338, 81–95.

Parmar, V. M., and Schroder, M. (2012). Sensing endoplasmic reticulum stress. *Adv. Exp. Med. Biol.* 738, 153–168.

Pazhouhandeh, M., Dieterle, M., Marrocco, K., Lechner, E., Berry, B., Brault, V., et al. (2006). F-box-like domain in the polerovirus protein P0 is required for silencing suppressor function. *Proc. Natl. Acad. Sci. U.S.A.* 103, 1994–1999.

Pogany, J., Stork, J., Li, Z., and Nagy, P.D. (2008). *In vitro* assembly of the Tomato bushy stunt virus replicase requires the host Heat shock protein 70. *Proc. Natl. Acad. Sci. U.S.A.* 105, 19956–19961.

Satyanarayana, T., Gowda, S., Ayllon, M. A., and Dawson, W. O. (2004). Closterovirus bipolar virion: evidence for initiation of assembly by minor coat protein and its restriction to the genomic RNA 5′ region. *Proc. Natl. Acad. Sci. U.S.A.* 101, 799–804.

Satyanarayana, T., Gowda, S., Mawassi, M., Albiach-Marti, M. R., Ayllon, M. A., Robertson, C., et al. (2000). Closterovirus encoded HSP70 homolog and p61 in addition to both coat proteins function in efficient virion assembly. *Virology* 278, 253–265.

Senthil, G., Liu, H., Puram, V. G., Clark, A., Stromberg, A., and Goodin, M. M. (2005). Specific and common changes in *Nicotiana benthamiana* gene expression in response to infection by enveloped viruses. *J. Gen. Virol.* 86, 2615–2625.

Sharma, S. K., Christen, P., and Goloubinoff, P. (2009). Disaggregating chaperones: an unfolding story. *Curr. Protein Pept. Sci.* 10, 432–446.

Shirasu, K. (2009). The HSP90-SGT1 chaperone complex for NLR immune sensors. *Annu. Rev. Plant Biol.* 60, 139–164.

Shirasu, K., and Schulze-Lefert, P. (2003). Complex formation, promiscuity and multi-functionality: protein interactions in disease-resistance pathways. *Trends Plant Sci.* 8, 252–258.

Soellick, T., Uhrig, J. F., Bucher, G. L., Kellmann, J. W., and Schreier, P. H. (2000). The movement protein NSm of tomato spotted wilt tospovirus (TSWV): RNA binding, interaction with the TSWV N protein, and identification of interacting plant proteins. *Proc. Natl. Acad. Sci. U.S.A.* 97, 2373–2378.

Su, W., Liu, Y., Xia, Y., Hong, Z., and Li, J. (2011). Conserved endoplasmic reticulum-associated degradation system to eliminate mutated receptor-like kinases in Arabidopsis. *Proc. Natl. Acad. Sci. U.S.A.* 108, 870–875.

Takabatake, R., Ando, Y., Seo, S., Katou, S., Tsuda, S., Ohashi, Y., et al. (2007). MAP kinases function downstream of HSP90 and upstream of mitochondria in TMV resistance gene N-mediated hypersensitive cell death. *Plant Cell Physiol.* 48, 498–510.

Tatineni, S., Gowda, S., and Dawson, W. O. (2010). Heterologous minor coat proteins of Citrus tristeza virus strains affect encapsidation, but the coexpression of HSP70h and p61 restores encapsidation to wild-type levels. *Virology* 402, 262–270.

Tomita, Y., Mizuno, T., Diez, J., Naito, S., Ahlquist, P., and Ishikawa, M. (2003). Mutation of host DnaJ homolog inhibits brome mosaic virus negative-strand RNA synthesis. *J. Virol.* 77, 2990–2997.

Tonsor, S. J., Scott, C., Boumaza, I., Liss, T. R., Brodsky, J. L., and Vierling, E. (2008). Heat shock protein 101 effects in *A. thaliana*: genetic variation, fitness and pleiotropy in controlled temperature conditions. *Mol. Ecol.* 17, 1614–1626.

Tyedmers, J., Mogk, A., and Bukau, B. (2010). Cellular strategies for controlling protein aggregation. *Nat. Rev. Mol. Cell Biol.* 11, 777–788.

Verchot, J. (2011). Wrapping membranes around plant virus infection. *Curr. Opin. Virol.* 1, 388–395.

Wang, R. Y., Stork, J., and Nagy, P. D. (2009). A key role for heat shock protein 70 in the localization and insertion of tombusvirus replication proteins to intracellular membranes. *J. Virol.* 83, 3276–3287.

Weeks, S. A., and Miller, D. J. (2008). The heat shock protein 70 cochaperone YDJ1 is required for efficient membrane-specific flock house virus RNA replication complex assembly and function in *Saccharomyces cerevisiae*. *J. Virol.* 82, 2004–2012.

Weeks, S. A., Shield, W. P., Sahi, C., Craig, E. A., Rospert, S., and Miller, D. J. (2010). A targeted analysis of cellular chaperones reveals contrasting roles for heat shock protein 70 in flock house virus RNA replication. *J. Virol.* 84, 330–339.

Wells, D. R., Tanguay, R. L., Le, H., and Gallie, D. R. (1998). HSP101 functions as a specific translational regulatory protein whose activity is regulated by nutrient status. *Genes Dev.* 12, 3236–3251.

Wileman, T. (2007). Aggresomes and pericentriolar sites of virus assembly: cellular defense or viral design? *Annu. Rev. Microbiol.* 61, 149–167.

Ye, C., Chen, C., Payton, M., Dickman, M. B., and Verchot, J. (2012a). TGBp3 triggers the unfolded protein response and SKP1 dependent programmed cell death. *Mol. Plant Pathol.* doi: 10.1111/mpp.12000 [Epub ahead of print].

Ye, C. M., Kelly, V., Payton, M., Dickman, M. B., and Verchot, J. (2012b). SGT1 is induced by the Potato virus X TGBp3 and enhances virus accumulation in *Nicotiana benthamiana*. *Mol. Plant.* 5, 1151–1153.

Ye, C., Dickman, M. B., Whitham, S. A., Payton, M., and Verchot, J. (2011). The unfolded protein response is triggered by a plant viral movement protein. *Plant Physiol.* 156, 741–755.

Zhang, C., and Guy, C. L. (2005). Co-immunoprecipitation of Hsp101 with cytosolic Hsc70. *Plant Physiol. Biochem.* 43, 13–18.

Zhang, K., and Kaufman, R. J. (2006). The unfolded protein response: a stress signaling pathway critical for health and disease. *Neurology* 66, S102–S109.

Zhang, M., Kadota, Y., Prodromou, C., Shirasu, K., and Pearl, L. H. (2010). Structural basis for assembly of Hsp90-Sgt1-CHORD protein complexes: implications for chaperoning of NLR innate immunity receptors. *Mol. Cell* 39, 269–281.

Conflict of Interest Statement: The author declares that the research was conducted in the absence of any commercial or financial relationships that could be construed as a potential conflict of interest.

Received: 22 September 2012; accepted: 21 November 2012; published online: 06 December 2012.

Citation: Verchot J (2012) Cellular chaperones and folding enzymes are vital contributors to membrane bound replication and movement complexes during plant RNA virus infection. Front. Plant Sci. ***3****:275. doi: 10.3389/fpls.2012.00275*

This article was submitted to Frontiers in Plant-Microbe Interaction, a specialty of Frontiers in Plant Science.

frontiers in
PLANT SCIENCE

REVIEW ARTICLE
published: 28 December 2012
doi: 10.3389/fpls.2012.00293

Virus-induced ER stress and the unfolded protein response

Lingrui Zhang and Aiming Wang*

Southern Crop Protection and Food Research Centre, Agriculture and Agri-Food Canada, London, ON, Canada

Edited by:
James Schoelz, University of Missouri, USA

Reviewed by:
Sorina C. Popescu, Boyce Thompson Institute for Plant Research, USA
Jeanmarie Verchot, Oklahoma State University, USA

***Correspondence:**
Aiming Wang, Southern Crop Protection and Food Research Centre, Agriculture and Agri-Food Canada, 1391 Sandford St., London, ON N5V 4T3, Canada.
e-mail: aiming.wang@agr.gc.ca

The accumulation of unfolded or misfolded proteins in the lumen of the endoplasmic reticulum (ER) results in ER stress that triggers cytoprotective signaling pathways, termed the unfolded protein response (UPR), to restore and maintain homeostasis in the ER or to induce apoptosis if ER stress remains unmitigated. The UPR signaling network encompasses three core elements, i.e., PKR-like ER kinase (PERK), activating transcription factor 6 (ATF6), and inositol-requiring protein-1 (IRE1). Activation of these three branch pathways of the UPR leads to the translation arrest and degradation of misfolded proteins, the expression of ER molecular chaperones, and the expansion of the ER membrane to decrease the load of proteins and increase the protein-folding capacity in the ER. Recently, the essential roles of the UPR have been implicated in a number of mammalian diseases, particularly viral diseases. In virus-infected cells, the cellular translation machinery is hijacked by the infecting virus to produce large amounts of viral proteins, which inevitably perturbs ER homeostasis and causes ER stress. This review summarizes current knowledge about the UPR signaling pathways, highlights two identified UPR pathways in plants, and discuss progress in elucidating the UPR in virus-infected cells and its functional roles in viral infection.

Keywords: virus, endoplasmic reticulum, ER stress, unfolded protein response, signaling transduction

INTRODUCTION

The endoplasmic reticulum (ER) is a membrane-bound compartment that plays important roles in many cellular processes such as calcium homeostasis and protein processing (Kim et al., 2008; Hetz et al., 2011; Hetz, 2012). Secretory and membrane proteins are synthesized on ribosomes and translocated in an unfolded state into the ER lumen, where they undergo folding, organelle-specific post-translational modifications, and assembly into higher-order structures (Ellgaard and Helenius, 2003; He and Klionsky, 2009; Marcinak and Ron, 2010). As an organelle for folding and modifications of proteins, the ER is loaded with extremely high concentration of proteins (>100 mg/ml), a concentration at which co-aggregation between proteins and/or polypeptides is clearly promoted (Stevens and Argon, 1999). Therefore, the lumen of the ER needs a unique cellular environment that promotes processing and prevents aggregation (Anelli and Sitia, 2008; Kim et al., 2008; Hetz et al., 2011; Hetz, 2012). Indeed, as the major intracellular calcium pool, the ER is the proximal site of a signal transduction cascade that serves to keep cellular homeostasis (Hendershot, 2004; Kim et al., 2008; Hetz et al., 2011; Hetz, 2012). It is also rich in calcium-dependent ***molecular chaperones*** (see "Glossary") such as ER luminal binding proteins (BiP), calmodulin (CAM), and calreticulin (CRT), which assist in *de novo* folding or refolding of proteins with high fidelity (Navazio et al., 2001; Ellgaard and Helenius, 2003; Seo et al., 2008). Furthermore, the ER lumen has an oxidative environment, which is essential for ***protein disulphide isomerase*** (PDI)-mediated disulfide formation (see "Glossary"), a process required for the proper folding of a variety of proteins (Kim et al., 2008).

However, the load of client proteins may exceed the assigned processing capacity of the ER due to physiological fluctuations in the demand for protein synthesis and secretion (Zhang and Kaufman, 2006; Ron and Walter, 2007; Marcinak and Ron, 2010; Hetz et al., 2011). The resulting imbalance is referred to as ***ER stress*** (**Figure 1**) (see "Glossary"), which is a pervasive feature of eukaryotic cells (Gao et al., 2008; Liu and Howell, 2010; Marcinak and Ron, 2010; Hetz et al., 2011; Iwata and Koizumi, 2012). In yeast, animals, and plants, ER stress arises under various circumstances (**Figure 1**), including developmental processes that affect protein homeostasis networks and genetic mutations that erode the functionality of the ER (Brewer and Hendershot, 2004; Schröder and Kaufman, 2005; Balch et al., 2008; Kim et al., 2008; Marcinak and Ron, 2010; Hetz et al., 2011). In fact, a variety of external stimuli (abiotic and biotic stress) such as pathogen invasion, chemical insult, and energy or nutrient (glucose) deprivation have been shown to impose stress on the ER by leading to alterations of cellular redox equilibrium, disturbances of calcium homeostasis, failure of post-translational modifications, and a general increase in protein synthesis (**Figure 1**) (Dimcheff et al., 2004; Ye et al., 2011; Iwata and Koizumi, 2012). In general, perturbation of ER homeostasis causes unfolded proteins to accumulate in the lumen of the ER, triggering an evolutionarily conserved cytoprotective signaling pathway designated as the ***unfolded protein response*** (UPR) (**Figure 1**) (see "Glossary") (Zhang and Kaufman, 2006; Ron and Walter, 2007; Urade, 2007; Kim et al., 2008).

The initial intent of the UPR is to reestablish homeostasis, relieve stress exerted on the ER, and prevent the cytotoxic impact of malformed proteins via inhibition of mRNA translation and

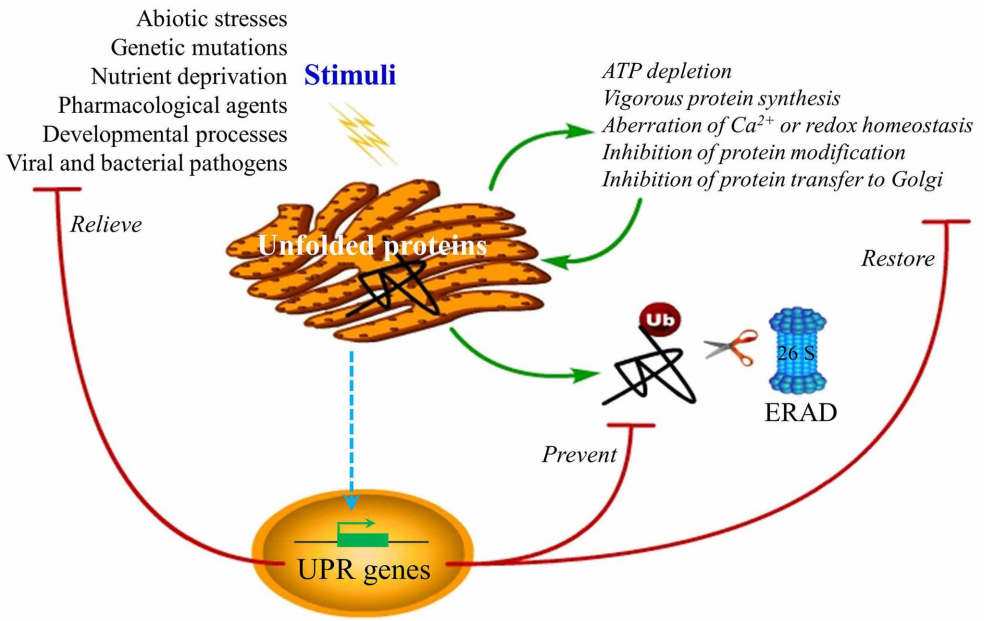

FIGURE 1 | ER stress and UPR functions. Disturbances of ER homeostasis cause overload of unfolded or misfolded protein in the ER lumen, a condition termed ER stress, triggering the UPR. The UPR may be induced by pharmacological chemicals, such as tunicamycin, thapsigargin, homocysteine, reductive/oxidative agents as well as non-steroidal anti-inflammatory agents, which impose stress on the ER by causing the vigorous protein synthesis, the imbalance of ER Ca^{2+} and redox, and the inhibition of protein modification or transfer to the Golgi body. In mammalian cells, ER stress also occurs under many circumstances, such as nutrient deprivation, developmental processes, genetic mutation, as well as pathogenic insult. The best-known example of ER stress arising from genetic mutation is the protein-misfolding diseases in human. Recent reports in plants have indicated a close connection between the UPR and environmental stimuli such as heat, salt, and drought stress as well as viral attack, although the underlying mechanisms are largely unknown. The purpose of the induced UPR is to restore the ER function and relive the stress exerted on the ER. In addition, the UPR also eliminates the cytotoxic malformed proteins, which are dislocated across the ER membrane for ubiquitination (Ub) and proteasome-mediated degradation through a pathway known as ERAD. However, if ER homeostasis or function cannot be re-established, programmed cell death will be activated by the UPR, presumably to protect the organism from the rogue cells that display misfolded proteins, which has not yet been confirmed in plants and is not shown in the diagram.

activation of adaptive mechanisms (**Figure 1**) (Xu, 2005; Kim et al., 2008; Preston et al., 2009; Ye et al., 2011). The adaptation effect predominantly refers to the upregulation of particular groups of genes to enhance the protein folding capacity of the ER and to promote ***ER-assisted degradation*** (ERAD) (see "Glossary") (Meusser et al., 2005; Kim et al., 2008). The signal-transduction events that are commonly associated with innate immunity and host defense, including mitogen-activated protein kinases (MAPKs), c-Jun N-terminal kinase (JNK), p38, and other kinases responsible for activation of nuclear factor-κB (NF-κB), are also induced, known as UPR-induced alarm mechanisms (Kaneko et al., 2003; Xu, 2005; Kim et al., 2008; Tabas and Ron, 2011). However, if the function of the ER cannot be reestablished especially under the conditions when the primary stimuli causing protein unfolding are excessive and/or protracted, a final mechanism called ***programmed cell death*** (also apoptosis in animals) (see "Glossary") is triggered, which presumably helps protect the organism from the expansion of potentially harmful substances produced by the damaged cells (Zhao and Ackerman, 2006; Ron and Walter, 2007; Kim et al., 2008; Tabas and Ron, 2011). The ER stress-induced cell death pathway is conserved throughout the plant and animal kingdoms (Urade, 2007; Qiang et al., 2012; Ye et al., 2012). In *Arabidopsis thaliana* roots, the mutualistic fungus *Piriformospora indica* induces ER stress but inhibits the adaptive UPR, resulting in a caspase 1-like mediated cell death, which is required for the establishment of the symbiosis (Qiang et al., 2012).

There is not only an increasing biomedical interest in but also a strong practical demand for investigating the molecular mechanisms underlying the UPR and the development of strategies to manipulate this pathway, due to the fact that chronic ER stress is involved in a number of mammalian diseases including cancers, neurodegeneration, diabetes, inflammation, atherosclerosis, and renal and viral diseases (He, 2006; Zhao and Ackerman, 2006; Yoshida, 2007; Hetz et al., 2011; Tabas and Ron, 2011). The molecular mechanism of the UPR has been investigated extensively in yeast and animals and to a much lesser extent in plants (Cox and Walter, 1996; Sidrauski and Walter, 1997; Oikawa et al., 2010). In mammalian cells, the UPR is mediated by two types of ER transmembrane proteins (ER stress sensors). The type I ER stress sensor consists of IRE1 (inositol-requiring transmembrane kinase/endonuclease) including two identifiable IRE1 isoforms IRE1α and IRE1β, and PERK (PKR-like ER kinase), whereas the type II ER stress sensor includes ATF6α and ATF6β (activating transcription factor 6) (Hetz et al., 2011). In contrast to animals, the UPR in yeast is controlled by only one

signaling pathway, the type I transmembrane ER protein IRE1p (Cox and Walter, 1996; Sidrauski and Walter, 1997; Oikawa et al., 2010).

In the past several years, the plant UPR signaling pathway has begun to be explored (Urade, 2007; Vitale and Boston, 2008; Deng et al., 2011; Nagashima et al., 2011). Thus far, two UPR pathways have been identified in plants, one mediated by IRE1-bZIP60 (basic leucine zipper), and the other by bZIP17/bZIP28 which is analogous to the animal ATF6 pathway (Urade, 2007; Vitale and Boston, 2008; Deng et al., 2011; Nagashima et al., 2011). In addition, an adaptive pathway mediated by plant-specific N-rich proteins, which diverges from the molecular chaperone-inducing branch of the UPR, was described as a novel branch of the ER stress response in plants that shares components with the osmotic stress signaling (Costa et al., 2008). Much of the work in plants has concentrated on ER stress induced by environmental cues (Iwata and Koizumi, 2012). For instance, in response to heat stress, two UPR pathways were found to be activated, indicated by bZIP28 proteolytic activation and bZIP60 mRNA splicing (Gao et al., 2008; Deng et al., 2011). The UPR and salt or drought stress have drawn attention from several laboratories (Irsigler et al., 2007; Liu et al., 2007; Costa et al., 2008; Liu and Howell, 2010). More recently, the essential role of the UPR in plants in response to viral attack has also been investigated (Ye and Verchot, 2011; Ye et al., 2011, 2012). In this review, we summarize in detail the current proposed models of how the ER transmembrane proteins sense the unfolded settings, and then address primarily the mechanistically distinct arms of the UPR as well as their relevance to viral infection in animals and plants. Some UPR related proteins such as cellular chaperons and folding enzymes may directly participate in the formation of membrane bound replication and movement complexes. Interested readers may refer to another review published in this special issue (Verchot, 2012). Finally, we discuss possible future directions of research on plant UPR, especially its roles in viral infection.

BiP: THE SUPPRESSOR OF THE UPR?

It is generally accepted that signaling in the UPR is initiated by UPR stress sensors, which are ER resident transmembrane proteins. They utilize their luminal portions to sense the protein-folding environment in the ER, and their cytoplasmic effector portions to interact with the transcriptional or translational apparatus (Ron and Walter, 2007). To date, several models have been proposed to explain how the unfolded protein load is detected by ER stress transducers (UPR stress sensors) to initiate the UPR activation (Parmar and Schröder, 2012).

INDIRECT RECOGNITION MODEL

The ER chaperone immunoglobulin heavy-chain BiP, also known as glucose-regulated protein 78 (GRP78), has been proposed as a master repressor of UPR (Hendershot, 2004; He, 2006; Zhang and Kaufman, 2006; Parmar and Schröder, 2012). It has been long known that BiP is more strongly induced by slowly folding proteins with a prolonged interaction with BiP than fast folding proteins (Gething et al., 1986; Watowich et al., 1991; Kohno et al., 1993). In normal cells, BiP keep UPR stress sensors in their inactive monomeric states through binding to their luminal domains (**Figure 2A**). Conversely, in cells undergoing ER stress, BiP is released when sequestered by unfolded proteins, leading to the activation of these ER stress sensors (**Figure 2A**) (Parmar and Schröder, 2012). Pivotal evidence for this chaperon-mediated model (indirect recognition model) comes from immunoprecipitation assay directly showing that, in unstressed acinar and fibroblasts cells, the luminal domains of PERK and IRE1 form a stable complex with the ER chaperone BiP, and the perturbation of protein folding promotes reversible dissociation of BiP from these two type-I transmembrane protein kinases, which correlates with the formation of activated PERK or IRE1 (Bertolotti et al., 2000). Consistently, in CHO cells stably overexpressing BiP, the amount of BiP being associated with PERK or IRE1 is considerably greater than that in parental CHO cells with normal levels of endogenous BiP (Bertolotti et al., 2000). Moreover, in BiP-overexpressing CHO cells, phosphorylation of PERK is delayed and incomplete, and activation of IRE1α by ER stress is absent (Dorner et al., 1992; Wang et al., 1996; Bertolotti et al., 2000). In fact, the UPR is attenuated by overexpression of only BiP rather than of other UPR molecular signatures (Dorner et al., 1990, 1992). As for the type-II transmembrane transducer, overexpression of wild-type BiP dramatically delays the translocation of ATF6 to the Golgi and leads to the lower amount of cleaved ATF6 in dithiothreitol (DTT)-treated Hela cell (Shen et al., 2002). A BiP mutant that bears a point mutation in its ATPase domain and loose ability to dissociate from ATF6 completely abolishes DTT-induced ATF6 activation (Shen et al., 2002). Collectively, these data suggest that the mechanisms of ER stress sensing by type-I transmembrane sensors may also operate in the control of type-II transmembrane sensor activation.

SEMI-DIRECT RECOGNITION MODEL

However, the indirect recognition model is challenged by an observation in yeast that deletion of the BiP-binding site renders IRE1p unaltered in ER stress inducibility, although it abolishes BiP binding (Kimata et al., 2004). The crystal structure of the yeast IRE1p luminal domain suggests that an IRE1p dimer creates a shared central groove formed by α-helices, with an architectural resemblance to the peptide binding domains of ***major histocompatibility complexes*** (MHCs) (see "Glossary") (Credle et al., 2005; Parmar and Schröder, 2012). Thus, IRE1 itself has the intrinsic ability to sense ER stress, and its activation may be initiated by BiP dissociation and further triggered by binding of unfolded proteins to its luminal domains (**Figure 2B**) (Kimata et al., 2004). This two-step activation model (semi-direct recognition model, **Figure 2B**) is proposed considering findings that BiP mutants locked in the ATP-bound state, but not the ADP-bound state interact with IRE1 (Kimata et al., 2003). Analysis of mutation in BiP ATPase domain further revealed that the conformational change in BiP induced by the binding of unfolded proteins to ATP-bound BiP leads to ATP hydrolysis, conversion of BiP to the ADP-bound state and release from IRE1 (Kimata et al., 2003; Todd-Corlett et al., 2007). This model is also supported by the fact that recombinant luminal domains of the yeast IRE1p is associated with unfolded proteins in a cell-free system (Kimata et al., 2007). However, this model remains controversial as there

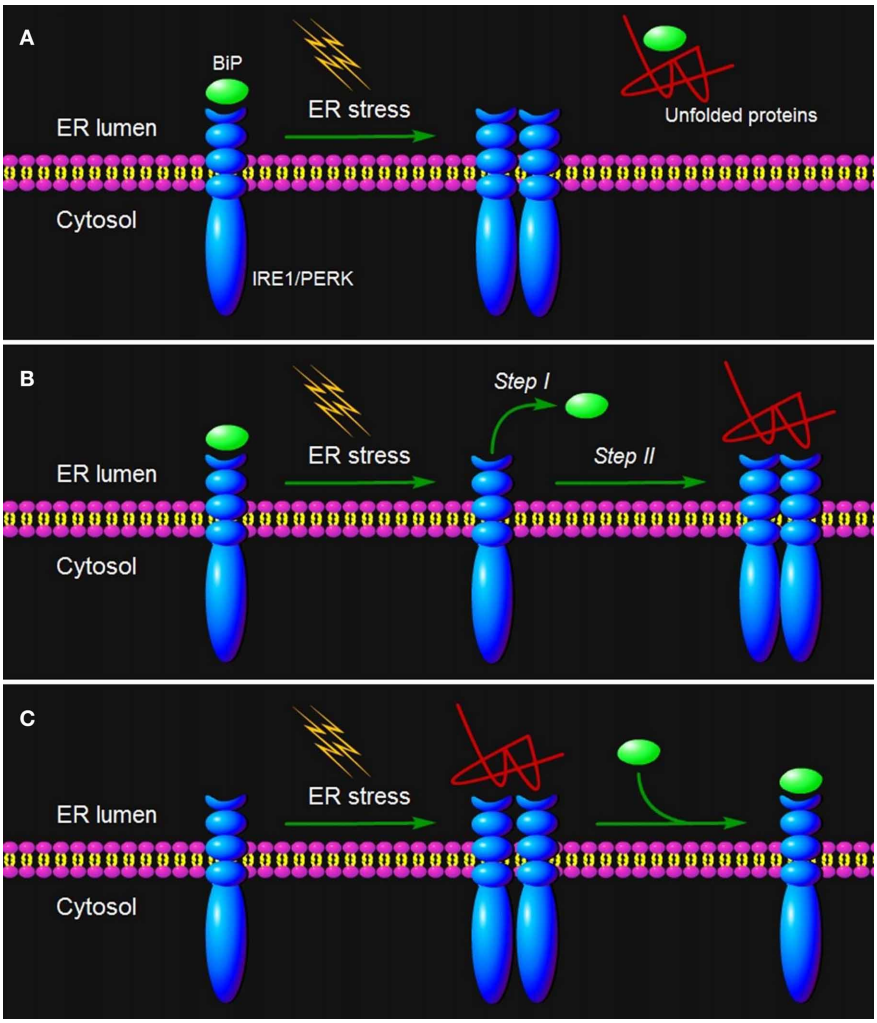

FIGURE 2 | ER stress sensing mechanism by IRE1/PERK. Three models are proposed to explain IRE1/PERK activation in response to the accumulation of unfolded proteins in the ER lumen. **(A)** The indirect recognition model proposes that BiP binding maintains IRE1/PERK in an inactive monomeric state. During ER stress, BiP is dissociated from its partners to bind unfolded proteins, which leads to the spontaneous dimerization of IRE1/PERK and activation of their RNase domains. In this case, BiP operates as the "UPR master control/ER stress sensor." The model may also operate in the control of ATF6 activation. **(B)** The semi-direct recognition model summarizes findings from studies of IRE1p in yeast and analyses of IRE1 crystal structure. This model proposes that the IRE1 is activated via two steps. In the first step, BiP dissociation from IRE1 leads to formation of higher order oligomers (called cluster). In the second step, direct interaction of unfolded proteins with IRE1 stabilizes the cytosolic domains of clustered IRE1 molecules and thus causes IRE1 activation. **(C)** A direct recognition model outlines recent studies in yeast. Three subpopulations of IRE1p co-exist within the cell: an inactive pool in equilibrium with an active unfolded protein-bound pool. The latter is sequestered by BiP binding, designated the third inactive set. In this model, BiP binding to or release from IRE1p does not activate the UPR, but it may serve as a buffer and a timer to adjust the sensitivity and dynamics of IRE1p activity. In turn, the unfolded protein binding to IRE1 is the single step of its activation.

lacks evidence that unfolded proteins bind to IRE1 *in vivo*, and there is no time-course analysis of BiP dissociation and binding of unfolded proteins to IRE1.

DIRECT RECOGNITION MODEL

Recently, based on time-resolved analysis of IRE1p signaling in yeast, Peter Walter's group has proposed a new quantitative model (direct recognition model, **Figure 2C**). In this dynamic UPR regulation model, IRE1 is in a dynamic equilibrium with BiP and unfolded proteins, and the unfolded protein binding to IRE1 is the single and sufficient step for activation of the UPR (Pincus et al., 2010). BiP binding to or release from IRE1 is ruled out as the primary switch that governs the UPR on or off as previously proposed, and it might act as a buffer and a timer to fine-tune the sensitivity and dynamics of the UPR, respectively (**Figure 2C**) (Pincus et al., 2010). The direct recognition model is strengthened by elegant biochemical assays showing that unfolded proteins are IRE1p-activating ligands that could directly induce the UPR in yeast cells (Gardner and Walter, 2011). Binding of unfolded proteins to IRE1 monomers induces dimerization via formation of the MHC-like peptide binding groove (Credle et al., 2005; Gardner and Walter, 2011). Moreover, considerable data suggest

that the cluster formation is a prerequisite for signaling by IRE1 (Credle et al., 2005; Kimata et al., 2007; Aragón et al., 2008; Korennykh et al., 2008). Nevertheless, the recombinant luminal regions of human IRE1 do not interact with unfolded proteins in a cell-free system (Oikawa et al., 2009), consistent with a previous prediction that, unlike yeast IRE1p, the MHC-like groove in the crystal structure of human IRE1 is too narrow for peptide binding (Zhou et al., 2006).

The difference in IRE1 structure between yeast and human reminds us that the complexity of ER stress sensing is far beyond our understanding and that structure-functional analysis in this field is far from complete. In the case of plants, the *Arabidopsis* and rice IRE1 proteins are the ER-resident proteins that possess kinase activity and have ability to sense ER stress with their luminal domain (Iwata and Koizumi, 2012). Although it has been known that overexpression of BiP in tobacco and soybean prevents activation of the UPR by ER stress inducers (Leborgne-Castel et al., 1999; Costa et al., 2008), the underlying mechanisms of ER stress sensing by plant IRE1 have not been investigated.

VIRAL INFECTION AND ER SENSING

In the recent decades, the importance of ER stress and UPR response in viral infection has been demonstrated in mammalian cells (Jordan et al., 2002; Baltzis et al., 2004; Netherton et al., 2004; Sun et al., 2004; Tardif et al., 2005). In a productive viral infection, large amounts of viral proteins are synthesized in infected cells, which lead to an overwhelming load of unfolded or misfolded proteins (Kim et al., 2008). Many mammalian viruses have evolved to manipulate host UPR signaling pathways to promote viral translation and persistence in infected cells. For example, flaviviruses such as Japanese encephalitis virus (JEV) and dengue viruses (DEN) trigger the specific UPR pathway, leading to enhanced protein folding abilities (Urano et al., 2000). Early studies with ***hemagglutinin-neuroamindase*** (HN) (see "Glossary") glycoproteins of influenza virus revealed that BiP associates transiently and non-covalently with the unfolded or immature glycoproteins (Hurtley et al., 1989). The misfolded, BiP-associated glycoproteins are not transported to the plasma membrane but persist as complexes in the ER for a long period of time before degradation (Hurtley et al., 1989). Similar observations have been reported with glycoprotein G of vesicular stomatitis virus, HN glycoproteins of paramyxovirus SV5, and glycoprotein of hepatitis C virus (HCV) (Ng et al., 1989; Machamer et al., 1990; Choukhi et al., 1998). Taken together, these data support the model in which interaction of BiP with unfolded viral proteins triggers the UPR response during viral infection.

Intriguingly, among 7 proteins encoded by simian virus 5, only the HN glycoprotein stimulates UPR response (Hurtley et al., 1989; Watowich et al., 1991). In virus-infected cells, the HN glycoprotein is inserted into the ER, and then transported to cell surface (He, 2006). Similarly, ectopic expression of the E2 protein, but not E1, core and NS3 proteins of HCV activates the expression of BiP (Liberman et al., 1999). HCV replicons expressing only non-structural proteins are also capable of stimulating BiP expression (Tardif et al., 2002). Infection of cytomegalovirus (CMV) causes a transient increase in BiP levels at the early phase of viral replication. Moreover, the expression of CMV *Us11* that physically interacts with BiP in mammalian cells is sufficient to trigger the UPR (Tirosh et al., 2005). In addition, several other studies have also suggested a connection between the UPR and viral replication. These include herpes simplex virus (HSV) 1, JEV, and HCV (Su et al., 2002; Cheng et al., 2005; Tardif et al., 2005). These studies suggest that either the process of viral replication or the production of a specific viral protein in the ER is capable of inducing UPR response.

Although how ER stress sensors sense viral infection to activate the UPR is not clear, a recent study with severe acute respiratory syndrome (SARS) coronavirus (SARS-CoV) has identified one of accessory proteins of SARS-CoV, the 8ab protein that could bind directly to the luminal domain of ATF6, the type II ER stress sensor (Sung et al., 2009). Ectopic expression of the 8ab protein in mammalian cells induces the proteolysis of ATF6 and the translocation of its cleaved DNA-binding and transcription-activation domains from the ER to nucleus (Sung et al., 2009). These findings suggest that viruses may exploit their own protein(s) to directly modulate UPR response.

As has been reported for animals, the most prominent phenomenon in plants induced by the UPR is the transcriptional induction of ER chaperone and protein-folding genes, such as BiP, CRT, and PDI (Schott et al., 2010). Recently, *Arabidopsis* stromal-derived factor 2 (SDF2) was identified as a crucial target of the plant UPR with a direct function in ER protein quality control (Schott et al., 2010). Using a combination of biochemical and cell biological methods, SDF2 was shown to respond to ER stress conditions and pathogen infestation in a manner similar to known molecular UPR markers (Wang et al., 2005; Schott et al., 2010). In plants, microarray-based analyses of gene expression have shown that BiP is upregulated in *Arabidopsis* in response to infections by *Turnip mosaic virus* (TuMV) and *Oilseed rape mosaic virus* (ORMV) (Whitham et al., 2003; Yang et al., 2007; García-Marcos et al., 2009). Similar upregulation of ER-resident chaperones has also been found in *Arabidopsis* and potato (*Solanum tuberosum*) during *Potato virus X* (PVX) infection (Whitham et al., 2003; Yang et al., 2007; García-Marcos et al., 2009). In PVX infection, a viral movement protein TGBp3, which resides in the ER, elicits the UPR in *Arabidopsis* and *Nicotiana benthamiana* as an early response to virus infection (Ye and Verchot, 2011; Ye et al., 2011). Similar to the ER-resident proteins encoded by flaviviruses or retroviruses such as HIV (Tardif et al., 2004; Chan and Egan, 2005; Sung et al., 2009), TGBp3 modulates the UPR signaling as a means to cope with robust viral protein synthesis (Ye and Verchot, 2011; Ye et al., 2011). In the case of HIV, the Vpu protein coded by HIV has been shown to trigger the degradation of the host CD4 protein by the 26S proteasome, and this degradation is vital for virion release (Schubert et al., 1998; Meusser et al., 2005; Nomaguchi et al., 2008). Considering the similarity of TGBp3 to Vpu in terms of molecular mass and subcellular localization, TGBp3 may have analogous functions to Vpu in targeting host proteins for ubiquitination and degradation to ensure virus spread (Ye et al., 2012). In addition, the TGBp3-elicited UPR effectively delays the host immune responses to aid PVX infection, including TGBp3-triggered programmed cell death (Ye et al., 2012). The induction of cell death pathway can be suppressed by

overexpression of BiP and is dependent on SKP1, a core subunit of the SCF (SKP1/Cullin1/F-box protein) ubiquitin E3 ligase complex (Ye et al., 2012). However, the mechanisms of the activation of the UPR by TGBp3 in PVX infection or by other viral proteins (if any) in infections by other plant viruses as well as the roles of the chaperone BiP in governing the UPR in virus-infected plants still remain unknown.

THREE PATHWAYS OF THE UPR

PERK PATHWAY AND PROTEIN SYNTHESIS CONTROL

PERK is a ER-localized type I transmembrane protein, with a catalytic kinase domain sharing substantial homology to other kinases of the ***eukaryotic translation initiation factor 2*** (eIF2) (see "Glossary") (Harding et al., 1999). In the early phase of ER stress, accumulation of unfolded or misfolded protein leads to oligomerization of PERK in the ER membranes, inducing its *trans*-autophosphorylation and kinase domain activation (He, 2006; Kim et al., 2008). ER stress-activated PERK phosphorylates eIF2α on Ser51, which inhibits the guanine nucleotide exchange factor eIF2B from recycling eIF2 to its active GTP-bound form (**Figure 3**). As a result, mRNA translation is shut off and the load of newly synthesized proteins is reduced that are destined to enter the already stressed ER lumen (**Figure 3**) (Hetz et al., 2006). An exceptional case to this general response is that certain mRNAs gain a selective advantage for translation under conditions in which eIF2α is phosphorylated (**Figure 3**) (Lu et al., 2004). The 5′ untranslated region of these mRNA contains short, inhibitory upstream open reading frames (uORFs) that prevent translation of their downstream encoding ORF in unstressed cells. When eIF2α activity is limited due to its phosphorylation in stressed cells, ribosomes skip the inhibitory uORFs so that they can be translated (Ron and Walter, 2007). Two of such genes that have been extensively studied include the transcription factor Gcn4 (general control non-depressible-4) in yeast and

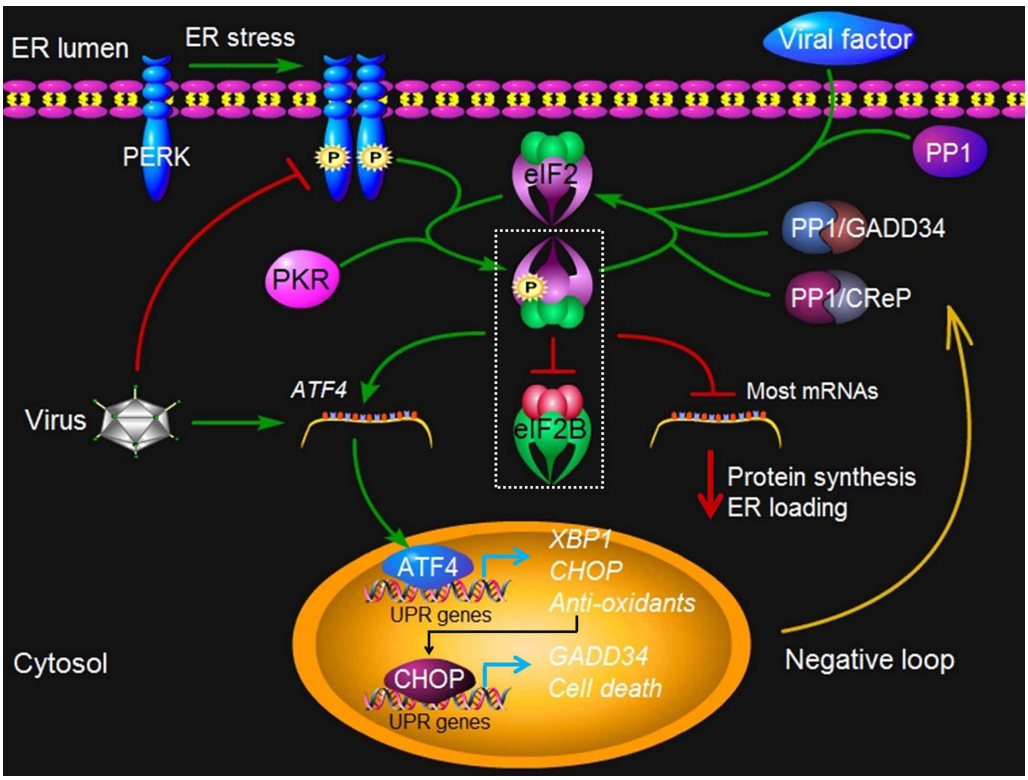

FIGURE 3 | PERK signaling under virus attack. Upon ER stress such as virus infection, protein kinase PERK oligomerizes in the ER membrane and is activated via *trans*-autophosphorylation. The activated PERK phosphorylates a subunit of eIF2, which inhibits the exchange factor eIF2B from recycling eIF2 to its active GTP-bound form. In addition, dsRNA-activated protein kinase R (PKR) can also activate this pathway independently of PERK. The resulting reduced activities of eIF2B and the eIF2 complex account for all of the important consequences of PERK activity, such as translation inhibition of most mRNAs, which reduces protein synthesis and lowers ER loading. However, some mRNA such as *ATF4* gains a selective advantage for translation via phosphorylated eIF2. ATF4 in turn contributes to the transcriptional activation of *CHOP*, *XBP1*, *GADD34*, and other genes involved oxidative stress and cell death. GADD34 is a regulatory subunit of protein phosphatase (PP) 1 that dephosphorylates eIF2α and recovers the activity of eIF2, constituting a negative feedback loop for regulation of PERK signaling. A constitutive phosphatase CreP also promotes eIF2 dephosphorylation. Viruses such as CMV may directly exploit the negative loop to terminate the PERK signaling pathway, via increasing the expression of ATF4, because the prolonged closure of protein synthesis is harmful to virus infection. Some viruses, such as HSV1 and ASFV, may produce a viral factor, which is homologous to host GADD34, to restore the activity of eIF2 along with PP1. Other viruses such as HCV may encode a viral protein that binds to PERK as a pseudosubstrate and thus, inhibits PERK activation. Finally, viruses such as LCMV may selectively activate the branches of the UPR to favor their replication. At present, no PERK-like pathway has been found in plants.

ATF4 in mammalian cells (**Figure 3**) (Hinnebusch and Natarajan, 2002; Lu et al., 2004; Vattem and Wek, 2004). ATF4 is responsible for stimulating the expression of a pro-apoptotic factor C/EBP homologous protein (CHOP), as well as growth arrest and DNA damage-inducible protein 34 (GADD34) (**Figure 3**) (Zinszner et al., 1998; Novoa et al., 2003).

A chemical inhibitor that sustains phosphorylation of eIF2α protects rat pheochromocytoma cell from ER stress, suggesting that the maintenance of eIF2α in an inactive state is somehow beneficial to cell survival during the circumstances that induce ER stress (Boyce et al., 2005). However, prolonged suppression of protein synthesis is typically incompatible with cell survival (Ron and Walter, 2007; Kim et al., 2008). Although the regulatory mechanisms and the phosphatase(s) involved are yet to be characterized, it has been reported that ER stress-induced PERK activation in pancreatic AR42J cells is rapidly reversible, and, upon removal of ER stress, activated PERK is dephosphorylated (Bertolotti et al., 2000; Jousse et al., 2003). In fact, it is well known that phosphorylated eIF2α is also subject to negative regulation (Ron and Walter, 2007). Somatic-cell genetic screen has identified two genes GADD34 and CReP (constitutive repressors of eIF2α phosphorylation) encoding the substrate targeting subunits of two phosphatase complexes that independently dephosphorylate eIF2α (**Figure 3**) (Connor et al., 2001; Jousse et al., 2003; Ma and Hendershot, 2003). CReP is constitutively expressed and contributes to baseline eIF2α dephosphorylation, whereas GADD34 is induced as part of the gene expression program activated by eIF2α phosphorylation and serves in a negative feedback loop that regulates eIF2α activity (**Figure 3**) (Jousse et al., 2003; Novoa et al., 2003).

In mammalian cells, a considerable body of evidence has indicated the association of viral replication with the PERK pathway (Jordan et al., 2002; Baltzis et al., 2004; Netherton et al., 2004; Sun et al., 2004; Boyce et al., 2005; Cheng et al., 2005; Isler et al., 2005). It becomes clear that the battle between the invading virus and the host cell in the ER is complicated. The repair of the ER function offered by PERK activation is beneficial to viral replication (He, 2006). On the other hand, the inhibition of protein synthesis mediated by the PERK pathway conversely regulates viral replication and maturation as all viruses depend on the cell translation machinery to synthesize viral proteins. Then one may wonder how viruses manage to overcome the translation inhibition imposed by the PERK pathway for the high speed production of viral proteins required for virus multiplication.

In human and mouse cells infected with the DNA virus HSV1, the production and processing of viral proteins in the ER presumably trigger the oligomerization of PERK, leading to the activation of PERK, as estimated by an increase in autophosphorylation of PERK (Cheng et al., 2005). Interestingly, in these cells with activated PERK, eIF2α remains in the unphosphorylated state, and viral polypeptide synthesis is thus normal. Obviously, the virus stimulates and then disarms the PERK activity. A virulence factor, the γ134.5 protein encoded by HSV1, has been shown to have a critical role in mediating eIF2α dephosphorylation in virus-infected cells (**Figure 3**) (He et al., 1997; Cheng et al., 2005). Furthermore, the γ134.5 protein can alleviate the translation arrest caused by the UPR inducing compounds DTT and thapsigargin (He et al., 1997; Cheng et al., 2005). Importantly, the γ134.5 protein also inhibits the activity of double-stranded RNA-dependent protein kinase R (PKR) by mediating eIF2α dephosphorylation (**Figure 3**) (He et al., 1997, 1998; Cheng et al., 2001). Indeed, the carboxyl-terminal domain of viral γ134.5 protein is highly homologous to the corresponding region of GADD34, suggesting the domain shared by the two proteins may perform a common function (He et al., 1997; Cheng et al., 2005). Like GADD34, the γ134.5 protein can recruit protein phosphatase 1 to dephosphorylate eIF2α and block translation shutoff during viral infection (**Figure 3**) (He et al., 1997; Cheng et al., 2005). Together, these findings suggest that the viral protein γ134.5 functions as an antagonist to the inhibitory activity of the PERK pathway on protein translation by maintaining the eIF2 activity during a productive HSV1 infection.

Although ER stress and the UPR are evident in the course of productive infection by African swine fever virus (ASFV, DNA virus), PERK activation seems not to be induced (Galindo et al., 2012). In Vero (African green monkey kidney) cells infected by ASFV, the eIF2α phosphorylation is maintained at a lower level in order to restore protein translation (Galindo et al., 2012). Furthermore, ASFV is capable of blocking the expression of CHOP induced by DTT, thapsigargin, and other agents (Netherton et al., 2004). ASFV also encodes the viral protein DP71L, a homolog to GADD34 (Zsak et al., 1996). However, it is not clear if DP71L also involves in the inhibition of PERK activation.

It is well documented that the human DNA virus CMV perturbs the PERK pathway (Netherton et al., 2004; Isler et al., 2005; Tirosh et al., 2005). Unlike HSV1, CMV replicates slowly and in an ordered temporal manner. It seems that CMV directly exploits the cellular negative feedback loop to inhibit PERK activities. In human foreskin fibroblasts (HFFs) cells infected with CMV, PERK is not phosphorylated in the early phase. As viral replication proceeds, there is an increase in the level of PERK phosphorylation. However, the amount of phosphorylated eIF2α is limited and translation attenuation does not occur (Netherton et al., 2004; Isler et al., 2005; Tirosh et al., 2005). Interestingly, translation of ATF4, which is dependent on eIF2α phosphorylation, is significantly increased (Netherton et al., 2004; Isler et al., 2005; Tirosh et al., 2005). Expression of ATF4 leads to the activation of target genes involved in the maintenance of metabolism and redox state, and thus may benefit CMV infection by maintaining a permissive cellular environment (**Figure 3**). It is worth to note that ATF4-induced GADD34 can act directly downstream of eIF2α phosphorylation to eliminate the negative effects of PERK activation (**Figure 3**) (Jousse et al., 2003; Novoa et al., 2003).

The PERK pathway is also associated with infections by RNA viruses. For example, a cytopathic strain of bovine viral diarrhea virus (BVDV), a member of flaviviruses, activates PERK and causes hyperphosphorylation of eIF2α (Jordan et al., 2002). However, it remains unclear as to how the translation attenuation resulting from PERK activation is overcome by BVDV. HCV encodes a viral E2 protein, which binds to PERK as a pseudosubstrate and may sequester it from its normal substrate eIF2α (**Figure 3**) (Pavio et al., 2003). Consistently, ectopic

expression of the E2 protein inhibits PERK phosphorylation and enhances translation, contributing to a persistent HCV infection. Additionally, viruses such as LCMV (lymphocytic choriomeningitis virus) bypass the PERK pathway to selectively activate the ATF6 pathway (Pasqual et al., 2011). Therefore, different viruses may adapt different strategies to cope with the PERK pathway for a productive infection. To date, no genes homologous to the animal PERK have been found in plants. It is reasonable to speculate that plants do not have the PERK pathway (Iwata and Koizumi, 2012).

IRE1 PATHWAY AND PROTEIN DEGRADATION

IRE1, the first UPR transducer identified by a mutation screen in yeast, is a bifunctional enzyme, i.e., a Ser/Thr protein kinase and a site-specific carboxyl-terminal endoribonuclease. Like PERK, IRE1 has an ER luminal amino-terminal domain and a transmembrane domain that anchors IRE1 to the ER membrane (**Figure 4**) (He, 2006). In response to ER stress, IRE1 is activated directly and/or indirectly by unfolded proteins as mentioned earlier. Unlike PERK, IRE1 signaling does not have selected downstream kinase targets because the only known substrate of the IRE1 kinase is IRE1 itself (Shamu and Walter, 1996; Papa et al., 2003). *Trans*-autophosphorylation of the kinase domain of IRE1 activates its unusual effector function that catalyzes the ***unconventional processing*** (see "Glossary") of the only known substrate (**Figure 4**): an mRNA that encodes a UPR transcriptional activator named Hac1 (homologous to ATF/CREB1) in yeast (Cox and Walter, 1996; Mori et al., 1996) or XBP1 (X-box BiP-1) in metazoans (Yoshida et al., 2001; Calfon et al., 2002).

The precursor XBP1 or Hac1 mRNA is cut twice by the activated IRE1, and a 26 nucleotide intron of *xbp1* mRNA is spliced out (Hetz et al., 2011). The 5′ and 3′ mRNA fragments are then re-ligated, producing a spliced mRNA that encodes a 41 kDa XBP1 protein, a bZIP family transcription factor (**Figure 4**) (Sidrauski et al., 1996; Stephens et al., 2005; Kim et al., 2008). The spliced version of XBP1 (termed XBP1s) upregulates a general population of UPR-related genes mainly involved in protein folding and ERAD (**Figure 4**) (Lee et al., 2003; Shaffer et al., 2004). Thus, the IRE1-XBP1 pathway directs both protein refolding and degradation in response to ER stress. Recently, the IRE1-dependent degradation of ER-associated mRNAs has also been observed in ER-stressed *Drosophila melanogaster* cells (Hollien and Weissman, 2006; Hollien et al., 2009), allowing to propose

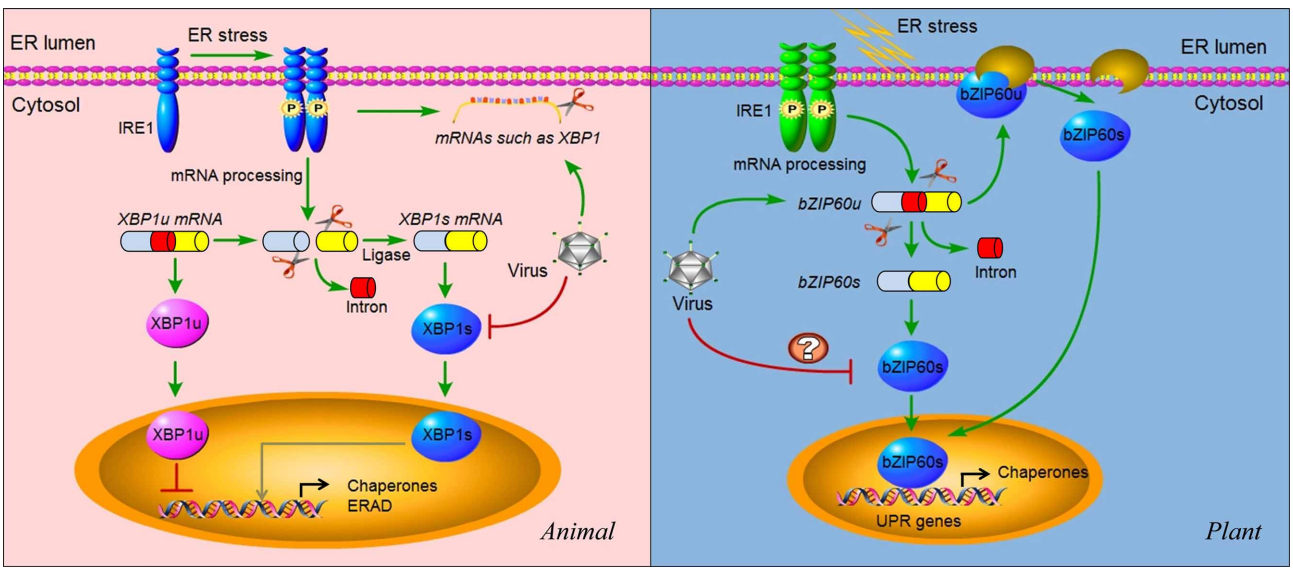

FIGURE 4 | IRE1 signaling and virus infection in animals and plants. In animals, IRE1 oligomerizes in the plane of the ER membrane in stressed cells, leading to *trans*-autophosphorylation and activation. Activated IRE1 mediates the sequence-specific cleavage of the XBP1 mRNA in higher eukaryotes, deleting a small RNA fragment (intron) and finally producing a spliced mRNA (*XBP1s*) with a frame shift in the coding sequence. Spliced *XBP1s* encodes a potent transcriptional activator (XBP1s), whereas the unspliced XBP1 mRNA (*XBP1u*) encodes an inhibitor of the UPR (XBP1u). In mammals, it seems that XBP1s regulates a subset of UPR genes that promote ERAD of misfolded proteins and refold proteins. In cultured *Drosophila melanogaster* cells, activated IRE1 can promote the cleavage of mRNAs, including *XBP1* mRNA, leading to their degradation. This reduces the load on the stressed ER and might facilitate reprogramming of the ER-associated protein synthesis and translocation machinery. In cells infected by viruses such as HCV, the IRE1 pathway is manipulated by the virus via repressing the transcriptional activity of XBP1s. In addition, some viruses might also promote the IRE1-dependent mRNA decay as a means to manipulate the IRE1 pathway. In plants, IRE1 homologs were detected in the genomes of *Arabidopsis* and rice a decade ago. However, the target of IRE1 was not identified until 2011. The mRNA of transcriptional factor bZIP60 is the substrate of IRE1 in plants. Similar to *XBP1* in animals, unspliced *bZIP60* (*bZIP60u*) is processed by activated IRE1. The protein product (bZIP60s) translated from the spliced *bZIP60* (*bZIPs*) is translocated into the nucleus to activate the expression of UPR genes such as chaperones. Different from XBP1u, plant bZIP60u protein, translated from *bZIP60u* mRNA, is retained in the ER membrane. Sensing unfolded proteins in the ER lumen, bZIP60u undergoes a proteolytic processing, releasing bZIP60s. A recent study has shown that the expression of bZIP60 was increased by PVX infection. However, the roles of the UPR pathway in virus infection have only begun to be investigated in plants. Critical unanswered questions need to be addressed in the future, such as whether viruses modulate the IRE1 pathway via inhibiting the transcriptional activity of bZIP60s (indicated by "?").

an XBP1-independent post-transcriptional mechanism for IRE1 to regulate gene expression that remodels the protein repertoire (**Figure 4**). However, it is unknown whether the mRNA degradation is promoted by IRE1 with its own endonuclease activity. In fact, in metazoans both the precursor and spliced form of XBP1 are translated (**Figure 4**) (Calfon et al., 2002; Yoshida et al., 2006). The XBP1s is more stable, working as a transactivator of UPR target genes, whereas the unspliced XBP1 (designated XBP1u) is labile and inhibits transcription of UPR target genes (**Figure 4**) (Yoshida et al., 2001; Calfon et al., 2002). By contrast, in yeast, the translation of unspliced HAC1 mRNA is repressed due to the presence of intron, and relief of this repression is the key step in activating the yeast UPR (Rüegsegger et al., 2001).

In human hepatoma cells expressing HCV subgenomic replicons, IRE1 is activated as indicated by elevated accumulation and expression of XBP1s (Tardif et al., 2004). However, the *trans*-activating activity of XBP1s is inhibited and the degradation of misfolded proteins is repressed due to the block of ERAD activity. In addition, in an IRE1-null cell line with a defective IRE1-XBP1 pathway, there is an elevated level of translation mediated by the HCV IRES (internal ribosome entry site), which directs the translation of HCV non-structural proteins (Tardif et al., 2004). Based on these data, it is concluded that HCV may suppress the IRE1-XBP1 pathway to stimulate HCV expression and to contribute to the persistence of the virus in infected hepatocytes (Tardif et al., 2004). However, the underlying mechanism of the repression of the transcriptional activity of XBP1s by HVC (**Figure 4**) is unclear. One possible explanation is that in cells carrying HCV replicons, XBP1 itself is targeted for proteasomal degradation, limiting its transcriptional regulation activity (Trujillo-Alonso et al., 2011). However, how HCV replicons direct XBP1 to be degraded remains to be understood. In addition to post-transcriptional modification by IRE1, HAC1 and XBP1 are also regulated by the UPR as transcriptional targets. In yeast, HAC1 mRNA production is induced by ER stress (Leber et al., 2004). In metazoan cells, levels of XBP1 mRNA also increase upon UPR induction (Yoshida et al., 2006), leading to accumulation of newly transcribed XBP1 mRNAs in their unspliced form. Therefore, the accumulated XBP1u mRNA may serve as an inhibitor to suppress the IRE1 signaling pathway since the XBP1u is a transcriptional repressor of UPR target genes (Yoshida et al., 2001; Calfon et al., 2002). Moreover, the XBP1u mRNA itself may also terminate the IRE1 signaling pathway by inhibitory heterodimerization with spliced XBP1 and/or competition for binding sites (Yoshida et al., 2006), conferring a switch-like property to XBP1-mediated gene regulation. Thus far, however, it is unknown if HCV infection increases the level of XBP1u mRNA and thus suppresses the transcriptional activity of XBP1s. Similar to the case of HCV, infection with human CMV or animal SARS-CoV also leads to a progressive increase in XBP1s mRNA; however, its target genes are not induced, suggesting that either the translation or the transcriptional regulation activity of XBP1s is blocked (Isler et al., 2005; Bechill et al., 2008).

A recent study in lung epithelial cell has showed that influenza A virus activates the IRE1 pathway with little or no concomitant activation of the PERK and ATF6 pathways, and inhibition of IRE1 activity leads to decreased viral replication, suggesting that IRE1 is a potential therapeutic target for influenza A virus (Hassan et al., 2012). In this study, influenza A virus replication also leads to an increase in XBP1 mRNA splicing, which can be blocked by the specific inhibitors of the IRE1 pathway. However, it is unclear if activation of IRE1 but inhibition of XBP1s is also used by influenza A virus as a strategy to cope with the IRE1 activation-mediated antiviral responses. In the case of West Nile Virus (WNV), the IRE1-XBP1 pathway is non-essential for its replication, although XBP1s is induced (Medigeshi et al., 2007). In *xbp1*$^{-/-}$ cells, WNV accumulation is similar to that in the wild type cells, suggesting a possibility that other UPR pathways can compensate for the absence of XBP1 in these cells (Medigeshi et al., 2007). In agreement with these findings, knockdown of XBP1 expression by small interfering RNA has minimal effects on cells' susceptibility to other flaviviruses such as JEV and DEN (Zhao and Ackerman, 2006), although IRE1-XBP1 pathway was activated during the two viruses infection, as evidenced by XBP1 mRNA splicing and protein expression, as well as induction of the downstream genes *ERdj4*, *EDEM1*, and *p58(IPK)* (Yu et al., 2006).

It has been almost one decade since IRE1 homologs were detected in the genomes of *Arabidopsis* and rice (Koizumi et al., 2001; Okushima et al., 2002). Now, it is clear that the mRNAs of *Arabidopsis* bZIP60 (AtbZIP60) and its rice ortholog OsbZIP50, collectively called bZIP60, are spliced by IRE1 (**Figure 4**) (Deng et al., 2011; Nagashima et al., 2011). The bZIP60 mRNA shares similar secondary structure with HAC1 and XBP1 mRNA, and they also share a similar splicing mechanism (**Figure 4**) (Iwata and Koizumi, 2012). Besides being processed conventionally as the mRNA targets of IRE1, which seems conserved in both plants and animals, plant bZIP60 has a unique post-translational modification (Iwata and Koizumi, 2005; Iwata et al., 2008). Plant bZIP60 (unspliced) is synthesized at a low level as a precursor protein, which is anchored in the ER membrane under normal conditions (**Figure 4**). Sensing ER stress by an as yet to be elucidated mechanism, the N-terminal domain of AtbZIP60 is cleaved and translocated to the nucleus (**Figure 4**) (Iwata and Koizumi, 2005; Iwata et al., 2008, 2009). In turn, the nuclear-localized AtbZIP60 forms a transcriptionally active protein complex of approximately 260 kDa to activate the transcription of UPR genes, such as BiP3, via the *cis*-elements plant-UPR element and ER stress response element (Urade, 2007; Iwata et al., 2009). However, the truncated species of bZIP60 has recently been suggested to be the product translated from the spliced mRNA mediated by IRE1, not the cleaved product of the full-length bZIP60 (Deng et al., 2011; Nagashima et al., 2011). Recently, the role of the bZIP60-mediated UPR has also been demonstrated for the first time in infection by a plant virus. In response to PVX infection or PVX TGBp3 induced-ER stress, bZIP60 is upregulated (**Figure 4**). Silencing *bZIP60* leads to the suppression of the UPR transcript levels and reduces PVX accumulation (Ye et al., 2011). It is suggested that the bZIP60-mediated UPR may be important to regulate cellular cytotoxicity and beneficial to PVX pathogenesis (Ye et al., 2011). However, the mechanism by which bZIP60 is manipulated by the virus and how bZIP60 operates in induction of the UPR are not clear.

ATF6 AND ER CHAPERONE EXPRESSION

ATF6α and ATF6β are the members of type II ER trasmembrane proteins that possess bZIP transcription factor domains in their cytosolic regions (Haze et al., 1999). They are synthesized as inactive precursors, tethered to the ER membrane by an ER-targeting hydrophobic sequence (**Figure 5**). Unlike PERK and IRE1 which oligomerize upon ER stress, ATF6 translocates from the ER into the Golgi apparatus (**Figure 5**). Once translocated to the Golgi, it is proteolytically processed by Golgi-resident intramembrane proteases, first by site 1 protease (S1P) and then in an intramembrane region by site 2 protease (S2P) (**Figure 5**) (Hetz et al., 2011). This proteolytic processing releases its cytoplasmic DNA-binding domain, ATF6f (a fragment of ATF6), which operates as a transcriptional activator that upregulates many UPR genes related to protein folding (**Figure 5**) (Haze et al., 1999; Lee et al., 2002; Yamamoto et al., 2007).

As mentioned above, replication of HCV subgenomic replicons suppresses the IRE1-XBP1 pathway (Tardif et al., 2002, 2004). However, in cells infected by HCV replicons, subgenomic replication results in the activation of the ATF6 pathway, indicated by the presence of a 50 kDa protein, a cleavage product corresponding to the DNA-binding domain of ATF6 (Tardif et al., 2002, 2004). As a result, there is an increased transcriptional level of chaperones such as BiP. At present, it remains elusive which non-structural viral protein(s) are involved in induction of ATF6, since HVC subgenomic replicons only express the structural proteins. Other experiments suggest that the accumulation of unfolded MHC class I, which is attributed to a decline in protein glycosylation caused by HCV replication, might account for the activation of ATF6 (Tardif and Siddiqui, 2003). Additionally, acute infection with LCMV or expression of its glycoprotein precursor results in a selective induction of the ATF6-regulated pathway of the UPR, whereas pathways controlled by PERK and IRE1 are silent (Pasqual et al., 2011). It seems that a selective induction of the ATF6-regulated branch of the UPR is likely beneficial for virus replication and cell viability, whereas the induction of PERK and IRE1 may be detrimental for the invading virus and the host cell (Pasqual et al., 2011). Similarly, in Vero cell, ASFV induces the ATF6 signaling pathway, but not the PERK or IRE1 pathways, which might benefit the virus by assisting protein folding and preventing early apoptosis (Galindo et al., 2012).

A different pattern has been reported in cells infected with Hepatitis B virus (HBV) (Li et al., 2007). In Hep3B cells, expression of the multifunctional regulatory protein of HBV (HBx protein) alone is sufficient to activate both the ATF6 and IRE1-XBP1 pathways, and silencing HBx blocks their activation induced by the constitutive replication of HBV (Li et al., 2007). Therefore, HBx-mediated activation of these two pathways probably promotes HBV replication in liver cells. Similarly, both the IRE1 and ATF6 pathways are activated during Rotavirus infection (Trujillo-Alonso et al., 2011). Another scenario has also been found in human lung adenocarcinoma cells where a global UPR activation occurs upon DEN infection (Umareddy et al., 2007). Selective perturbation of the UPR pathways considerably alters DEN infectivity (Umareddy et al., 2007). Although the molecular mechanisms by which DEN infection activates ER stress remain to be elucidated, the three branches of the UPR signaling cascades might be hijacked by DEN to produce a condition beneficial to the viral infection.

Similar to animals, plants have signaling components that function in parallel to the IRE1-bZIP60 signaling cascade (**Figure 5**) (Urade, 2007; Vitale and Boston, 2008; Deng et al., 2011; Nagashima et al., 2011; Iwata and Koizumi, 2012). In *Arabidopsis*, bZIP transcription factors bZIP17 and bZIP28 are also synthesized as a precursor protein and anchored in the ER (**Figure 5**) (Iwata et al., 2008; Seo et al., 2008). In response to

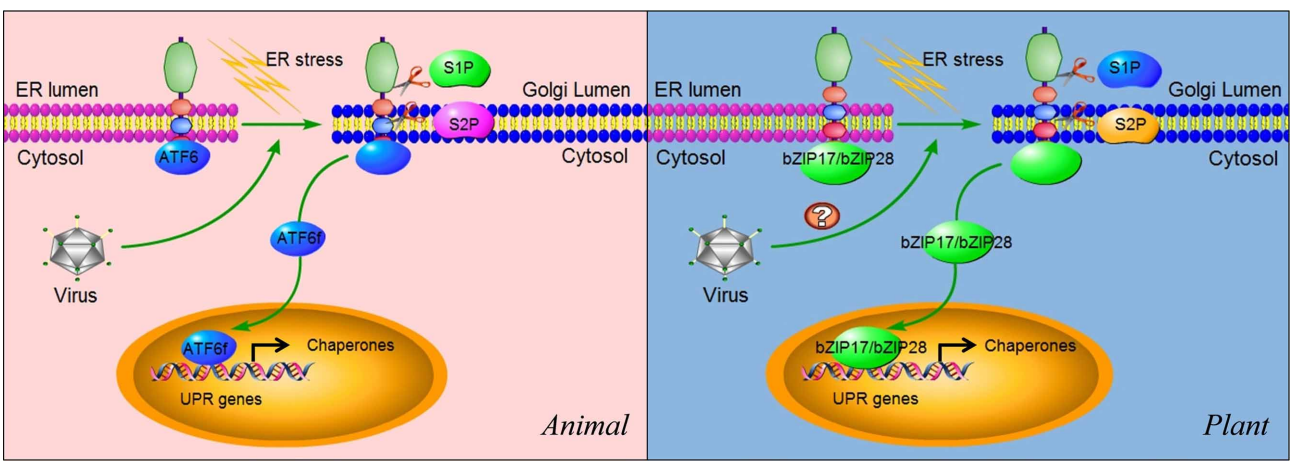

FIGURE 5 | ATF6 and bZIP17/bZIP28 pathways. In unstressed cells, ATF6 in animals and bZIP17/bZIP28 in plants reside in the ER membrane. They are delivered to the Golgi apparatus in an unknown mechanism upon sensing ER stress. In the Golgi apparatus, these proteins are subject to cleavage twice, first by the lumenal S1P and then the intra-membrane S2P, to release the cytosolic effector portions of the proteins (ATF6f). ATF6f then enters into the nucleus and probably activates a subset of UPR target genes, although these remain to be characterized. Some viruses such as ASFV have been shown to selectively activate the ATF6 pathway for their replication in animals. In plants, the cleaved N terminal portions of bZIP17 and bZIP28 also move into the nucleus and activate UPR genes. In plants, the functional roles of IRE1-bZIP17/bZIP28 in virus infection (indicated by "?") have yet to be elucidated.

ER stress, bZIP17 and bZIP28 undergo proteolytic processing and translocation in a manner similar to the animal ATF6-S1P/S2P system (**Figure 5**) (Iwata and Koizumi, 2012). Upon translocated into the nucleus, bZIP17 and bZIP28 activate genes involved in the UPR and other signaling pathways such as brassinosteroid signaling transduction (Che et al., 2010). Although the proteolytic activation of bZIP17 and bZIP28 has been shown to be triggered by heat stress (Urade, 2007; Vitale and Boston, 2008; Deng et al., 2011; Nagashima et al., 2011; Iwata and Koizumi, 2012), no information is available at present about their roles in viral infection. Therefore, our understanding of the plant UPR pathway is very limited, and more efforts are needed to characterize the bZIP17/bZIP28 pathway and its roles in physiological and pathological settings.

CROSSTALK BETWEEN THREE ARMS OF THE UPR

It is conceivable that IRE1, PERK, and ATF6 pathways communicate with each other extensively in many aspects, including activation, function, and feedback regulation. A seminal work discovering the crosstalk between these three arms comes from Hela cells, where XBP1 mRNA could be induced by ATF6 and spliced by IRE1 in response to ER stress (Yoshida et al., 2001). Moreover, transcriptional activation of XBP1 could be induced by the PERK signaling pathway as well, which might account for the broad effects of PERK during the UPR (Yoshida et al., 2001; Calfon et al., 2002). Besides PERK, IRE1 can also suppress protein translation via degrading mRNA (Hollien and Weissman, 2006; Hollien et al., 2009). In fact, a pro-apoptotic factor CHOP is regulated by both the ATF6 and PERK pathways (Schröder and Kaufman, 2005). While three arms of the UPR have their own specific functions in ER stress (**Figures 3, 4**, and **5**), mutant analyses in *C. elegans* have revealed that the IRE1-XBP1 and the ATF6 arms of the UPR might activate a common set of genes involved in stress tolerance and worm development, indicating a functional redundancy between these two arms (Shen et al., 2005). Furthermore, all the three arms could induce ERAD (Schröder and Kaufman, 2005), representing a common cellular process resulting from the three UPR branches.

These crosstalks further add to the complexity of the UPR induced by abiotic and biotic cues such viral infection. For example, some viruses, such as HBV, Rotavirus, and DEN, usually activate two or even three pathways to promote reproduction (Li et al., 2007; Umareddy et al., 2007; Trujillo-Alonso et al., 2011). The expression of CMV Us11 or CMV infection inhibits the ATF6 pathway but activates the IRE1 pathway as an alternative mechanism to upregulate the expression of chaperones. Meanwhile, the transcriptional activation of the XBP1 target genes (e.g., those encoding protein degradation factors) regulated by the IRE1 pathway is inhibited, presumably in order to keep viral proteins in the ER from being degraded (Tirosh et al., 2005). In this case, it is puzzling how the virus activates the most favorable pathway for its replication and deactivates the molecular signaling pathway that is probably detrimental for its accumulation in the host cell.

So far, two UPR pathways have been identified in plants. Their crosstalk, however, does exist and appear diverse. The expression of *AtPDI* genes was found to decrease in the *AtbZIP60* mutant but not in the *AtIRE1-2* mutant, indicating that the additional UPR signaling complements AtbZIP60 in the activation of *AtPDI* gene expression during ER stress (Lu and Christopher, 2008). The structural similarity, especially in the putative transmembrane domain of the bZIP60, bZIP17, and bZIP28 proteins (Iwata and Koizumi, 2012), suggests that these two pathways might collaborate closely in sensing ER stress. Indeed, bZIP28 proteolytic activation and bZIP60 mRNA splicing could be induced concomitantly in response to heat stress (Gao et al., 2008; Deng et al., 2011). This assumption is also in agreement with another recent observation that bZIP28 is capable of forming a heterodimer with bZIP60 (Iwata et al., 2009; Liu and Howell, 2010), a direct crosstalk between these two pathways.

CONCLUSION REMARKS

In higher eukaryotes, many critical biological processes are dependent on intercellular/intracellular communication, which requires relevant proteins timely and adequately expressed with high fidelity in folding. Therefore, the folding function of the ER and the signaling of the ER stress-induced UPR pathways have emerged as an important aspect of cell biology with broad implications to diverse physiological and pathological processes. Despite the recent advances made in understanding the UPR mechanisms implicated in abiotic and biotic stress such as viral infection, many critical questions still remain unanswered. The molecular and structural basis for recognition of the upstream signal by the ER stress sensors has only begun to be understood. Although several recognition models have been proposed mainly based on data using pharmacological chemicals and experimental stress conditions as the inducers of the UPR (**Figure 2**), we cannot empirically translate this knowledge into the case of viral infection. As discussed above, either virus replication or specific viral proteins (peptides) directly activate the UPR transducers, and different viruses may induce a specific UPR pathway(s). On the other hand, abiotic and biotic ER stress may also share some common UPR pathways that help host cells to defend against those adverse environmental stimuli. A good example is that virus infection can improve plant tolerance to abiotic stress (Xu et al., 2008). A key direction for future study in this field is to define how the ER stress is sensed and how those branched pathways are coordinated to function.

As a complex signal transduction network, the UPR protects the organisms against normal and unusual levels of ER stress by enhancing ER capacity, by reducing ER load, and by inducing programmed cell death. Different cell types may have different levels of sensitivity to ER stress. In response to specific viral infection and other stimuli, little is known about the regulation of UPR signaling in distinct cells, and how the kinetics and amplitude of signaling of each UPR branch is controlled. Our current knowledge about the roles of the downstream effectors of UPR transducers is also limited. For instance, it is unknown how the transcriptional activity of XBP1 is blocked in virus-infected cells (**Figure 5**). In plants, it is unclear whether the transcriptional activity of spliced bZIP60 is also a target by the invading virus, and whether there is an ERAD-like process responsible for removing spliced bZIP60 mRNA. As the plant IRE1 seems not only just to function through mediating bZIP60 mRNA splicing, its other downstream components remain to be characterized.

A comprehensive study on these questions will certainly shed new lights in the UPR pathways, and assist in a better understanding of host–virus interactions and, in the long run, developing novel antiviral strategies.

ACKNOWLEDGMENTS

This work was supported by grants from Agriculture and Agri-Food Canada and Natural Sciences and Engineering Research Council of Canada.

REFERENCES

Anelli, T., and Sitia, R. (2008). Protein quality control in the early secretory pathway. *EMBO J.* 27, 315–327.

Aragón, T., Van Anken, E., Pincus, D., Serafimova, I. M., Korennykh, A. V., Rubio, C. A., et al. (2008). Messenger RNA targeting to endoplasmic reticulum stress signalling sites. *Nature* 457, 736–740.

Balch, W. E., Morimoto, R. I., Dillin, A., and Kelly, J. W. (2008). Adapting proteostasis for disease intervention. *Science* 319, 916–919.

Baltzis, D., Qu, L. K., Papadopoulou, S., Blais, J. D., Bell, J. C., Sonenberg, N., et al. (2004). Resistance to vesicular stomatitis virus infection requires a functional cross talk between the eukaryotic translation initiation factor 2α kinases PERK and PKR. *J. Virol.* 78, 12747–12761.

Bechill, J., Chen, Z., Brewer, J. W., and Baker, S. C. (2008). Coronavirus infection modulates the unfolded protein response and mediates sustained translational repression. *J. Virol.* 82, 4492–4501.

Bertolotti, A., Zhang, Y., Hendershot, L. M., Harding, H. P., and Ron, D. (2000). Dynamic interaction of BiP and ER stress transducers in the unfolded-protein response. *Nat. Cell Biol.* 2, 326–332.

Boyce, M., Bryant, K. F., Jousse, C., Long, K., Harding, H. P., Scheuner, D., et al. (2005). A selective inhibitor of eIF2α dephosphorylation protects cells from ER stress. *Science* 307, 935.

Brewer, J. W., and Hendershot, L. M. (2004). Building an antibody factory: a job for the unfolded protein response. *Nat. Immunol.* 6, 23–29.

Calfon, M., Zeng, H., Urano, F., Till, J. H., Hubbard, S. R., Harding, H. P., et al. (2002). IRE1 couples endoplasmic reticulum load to secretory capacity by processing the *XBP-1* mRNA. *Nature* 415, 92–96.

Chan, S. W., and Egan, P. A. (2005). Hepatitis C virus envelope proteins regulate CHOP via induction of the unfolded protein response. *FASEB J.* 19, 1510–1512.

Che, P., Bussell, J. D., Zhou, W., Estavillo, G. M., Pogson, B. J., and Smith, S. M. (2010). Signaling from the endoplasmic reticulum activates brassinosteroid signaling and promotes acclimation to stress in *Arabidopsis*. *Sci. Signal.* 3:ra69. doi: 10.1126/scisignal.2001140

Cheng, G., Feng, Z., and He, B. (2005). Herpes simplex virus 1 infection activates the endoplasmic reticulum resident kinase PERK and mediates eIF-2α dephosphorylation by the γ134.5 protein. *J. Virol.* 79, 1379–1388.

Cheng, G., Gross, M., Brett, M. E., and He, B. (2001). AlaArg motif in the carboxyl terminus of the γ134.5 protein of herpes simplex virus type 1 is required for the formation of a high-molecular-weight complex that dephosphorylates eIF-2α. *J. Virol.* 75, 3666–3674.

Choukhi, A., Ung, S., Wychowski, C., and Dubuisson, J. (1998). Involvement of endoplasmic reticulum chaperones in the folding of hepatitis C virus glycoproteins. *J. Virol.* 72, 3851–3858.

Connor, J. H., Weiser, D. C., Li, S., Hallenbeck, J. M., and Shenolikar, S. (2001). Growth arrest and DNA damage-inducible protein GADD34 assembles a novel signaling complex containing protein phosphatase 1 and inhibitor 1. *Mol. Cell. Biol.* 21, 6841–6850.

Costa, M. D. L., Reis, P. A. B., Valente, M. A. S., Irsigler, A. S. T., Carvalho, C. M., Loureiro, M. E., et al. (2008). A new branch of endoplasmic reticulum stress signaling and the osmotic signal converge on plant-specific asparagine-rich proteins to promote cell death. *J. Biol. Chem.* 283, 20209–20219.

Cox, J. S., and Walter, P. (1996). A novel mechanism for regulating activity of a transcription factor that controls the unfolded protein response. *Cell* 87, 391–404.

Credle, J. J., Finer-Moore, J. S., Papa, F. R., Stroud, R. M., and Walter, P. (2005). On the mechanism of sensing unfolded protein in the endoplasmic reticulum. *Proc. Natl. Acad. Sci. U.S.A.* 102, 18773.

Deng, Y., Humbert, S., Liu, J. X., Srivastava, R., Rothstein, S. J., and Howell, S. H. (2011). Heat induces the splicing by IRE1 of a mRNA encoding a transcription factor involved in the unfolded protein response in *Arabidopsis*. *Proc. Natl. Acad. Sci. U.S.A.* 108, 7247.

Dimcheff, D. E., Faasse, M. A., McAtee, F. J., and Portis, J. L. (2004). Endoplasmic reticulum (ER) stress induced by a neurovirulent mouse retrovirus is associated with prolonged BiP binding and retention of a viral protein in the ER. *J. Biol. Chem.* 279, 33782.

Dorner, A. J., Wasley, L. C., and Kaufman, R. J. (1992). Overexpression of GRP78 mitigates stress induction of glucose regulated proteins and blocks secretion of selective proteins in Chinese hamster ovary cells. *EMBO J.* 11, 1563.

Dorner, A. J., Wasley, L. C., Raney, P., Haugejorden, S., Green, M., and Kaufman, R. J. (1990). The stress response in Chinese hamster ovary cells. Regulation of ERp72 and protein disulfide isomerase expression and secretion. *J. Biol. Chem.* 265, 22029–22034.

Ellgaard, L., and Helenius, A. (2003). Quality control in the endoplasmic reticulum. *Nat. Rev. Mol. Cell Biol.* 4, 181–191.

Galindo, I., Hernáez, B., Muñoz-Moreno, R., Cuesta-Geijo, M. A., Dalmau-Mena, I., and Alonso, C. (2012). The ATF6 branch of unfolded protein response and apoptosis are activated to promote African swine fever virus infection. *Cell Death Dis.* 3:e341. doi: 10.1038/cddis.2012.81

Gao, H., Brandizzi, F., Benning, C., and Larkin, R. M. (2008). A membrane-tethered transcription factor defines a branch of the heat stress response in *Arabidopsis thaliana*. *Proc. Natl. Acad. Sci. U.S.A.* 105, 16398–16403.

García-Marcos, A., Pacheco, R., Martiáñez, J., González-Jara, P., Díaz-Ruíz, J. R., and Tenllado, F. (2009). Transcriptional changes and oxidative stress associated with the synergistic interaction between *Potato virus X* and *Potato virus Y* and their relationship with symptom expression. *Mol. Plant Microbe Interact.* 22, 1431–1444.

Gardner, B. M., and Walter, P. (2011). Unfolded proteins are IRE1-activating ligands that directly induce the unfolded protein response. *Science* 333, 1891.

Gething, M. J., McCammon, K., and Sambrook, J. (1986). Expression of wild-type and mutant forms of influenza hemagglutinin: the role of folding in intracellular transport. *Cell* 46, 939–950.

Harding, H. P., Zhang, Y., and Ron, D. (1999). Protein translation and folding are coupled by an endoplasmic-reticulum-resident kinase. *Nature* 397, 271–274.

Hassan, I. H., Zhang, M. S., Powers, L. S., Shao, J. Q., Baltrusaitis, J., Rutkowski, D. T., et al. (2012). Influenza A viral replication is blocked by inhibition of the Inositol-requiring Enzyme 1 (IRE1) stress pathway. *J. Biol. Chem.* 287, 4679–4689.

Haze, K., Yoshida, H., Yanagi, H., Yura, T., and Mori, K. (1999). Mammalian transcription factor ATF6 is synthesized as a transmembrane protein and activated by proteolysis in response to endoplasmic reticulum stress. *Mol. Biol. Cell* 10, 3787–3799.

He, B. (2006). Viruses, endoplasmic reticulum stress, and interferon responses. *Cell Death Differ.* 13, 393–403.

He, B., Gross, M., and Roizman, B. (1997). The γ134.5 protein of herpes simplex virus 1 complexes with protein phosphatase 1α to dephosphorylate the α subunit of the eukaryotic translation initiation factor 2 and preclude the shutoff of protein synthesis by double-stranded RNA-activated protein kinase. *Proc. Natl. Acad. Sci. U.S.A.* 94, 843.

He, B., Gross, M., and Roizman, B. (1998). The γ134.5 protein of herpes simplex virus 1 has the structural and functional attributes of a protein phosphatase 1 regulatory subunit and is present in a high molecular weight complex with the enzyme in infected cells. *J. Biol. Chem.* 273, 20737–20743.

He, C., and Klionsky, D. J. (2009). Regulation mechanisms and signaling pathways of autophagy. *Annu. Rev. Genet.* 43, 67.

Hendershot, L. M. (2004). The ER function BiP is a master regulator of ER function. *Mt. Sinai J. Med.* 71, 289.

Hetz, C. (2012). The unfolded protein response: controlling cell fate decisions under ER stress and beyond. *Nat. Rev. Mol. Cell Biol.* 13, 89–102.

Hetz, C., Bernasconi, P., Fisher, J., Lee, A. H., Bassik, M. C., Antonsson, B., et al. (2006). Proapoptotic BAX and BAK modulate the unfolded protein response by a direct interaction with IRE1α. *Science* 312, 572.

Hetz, C., Martinon, F., Rodriguez, D., and Glimcher, L. H. (2011). The unfolded protein response: integrating stress signals through the stress sensor IRE1α. *Physiol. Rev.* 91, 1219–1243.

Hinnebusch, A. G., and Natarajan, K. (2002). Gcn4p, a master regulator of gene expression, is controlled at multiple levels by diverse signals of starvation and stress. *Eukaryot. Cell* 1, 22–32.

Hollien, J., Lin, J. H., Li, H., Stevens, N., Walter, P., and Weissman, J. S. (2009). Regulated IRE1-dependent decay of messenger RNAs in mammalian cells. *J. Cell Biol.* 186, 323–331.

Hollien, J., and Weissman, J. S. (2006). Decay of endoplasmic reticulum-localized mRNAs during the unfolded protein response. *Science* 313, 104.

Hurtley, S. M., Bole, D. G., Hoover-Litty, H., Helenius, A., and Copeland, C. S. (1989). Interactions of misfolded influenza virus hemagglutinin with binding protein (BiP). *J. Cell Biol.* 108, 2117–2126.

Irsigler, A., Costa, M., Zhang, P., Reis, P., Dewey, R., Boston, R., et al. (2007). Expression profiling on soybean leaves reveals integration of ER-and osmotic-stress pathways. *BMC Genomics* 8:431. doi: 10.1186/1471-2164-8-431

Isler, J. A., Skalet, A. H., and Alwine, J. C. (2005). Human cytomegalovirus infection activates and regulates the unfolded protein response. *J. Virol.* 79, 6890–6899.

Iwata, Y., Fedoroff, N. V., and Koizumi, N. (2008). *Arabidopsis* bZIP60 is a proteolysis-activated transcription factor involved in the endoplasmic reticulum stress response. *Plant Cell* 20, 3107–3121.

Iwata, Y., and Koizumi, N. (2005). An *Arabidopsis* transcription factor, AtbZIP60, regulates the endoplasmic reticulum stress response in a manner unique to plants. *Proc. Natl. Acad. Sci. U.S.A.* 102, 5280.

Iwata, Y., and Koizumi, N. (2012). Plant transducers of the endoplasmic reticulum unfolded protein response. *Trends Plant Sci*. 17, 720–727.

Iwata, Y., Yoneda, M., Yanagawa, Y., and Koizumi, N. (2009). Characteristics of the nuclear form of the *Arabidopsis* transcription factor AtbZIP60 during the endoplasmic reticulum stress response. *Biosci. Biotechnol. Biochem.* 73, 865–869.

Jordan, R., Wang, L., Graczyk, T. M., Block, T. M., and Romano, P. R. (2002). Replication of a cytopathic strain of bovine viral diarrhea virus activates PERK and induces endoplasmic reticulum stress-mediated apoptosis of MDBK cells. *J. Virol.* 76, 9588–9599.

Jousse, C., Oyadomari, S., Novoa, I., Lu, P., Zhang, Y., Harding, H. P., et al. (2003). Inhibition of a constitutive translation initiation factor 2α phosphatase, CReP, promotes survival of stressed cells. *J. Cell Biol.* 163, 767–775.

Kaneko, M., Niinuma, Y., and Nomura, Y. (2003). Activation signal of nuclear factor-κB in response to endoplasmic reticulum stress is transduced via IRE1 and tumor necrosis factor receptor-associated factor 2. *Biol. Pharm. Bull.* 26, 931–935.

Kim, I., Xu, W., and Reed, J. C. (2008). Cell death and endoplasmic reticulum stress: disease relevance and therapeutic opportunities. *Nat. Rev. Drug Discov.* 7, 1013–1030.

Kimata, Y., Ishiwata-Kimata, Y., Ito, T., Hirata, A., Suzuki, T., Oikawa, D., et al. (2007). Two regulatory steps of ER-stress sensor IRE1 involving its cluster formation and interaction with unfolded proteins. *J. Cell Biol.* 179, 75–86.

Kimata, Y., Kimata, Y. I., Shimizu, Y., Abe, H., Farcasanu, I. C., Takeuchi, M., et al. (2003). Genetic evidence for a role of BiP/Kar2 that regulates IRE1 in response to accumulation of unfolded proteins. *Mol. Biol. Cell* 14, 2559–2569.

Kimata, Y., Oikawa, D., Shimizu, Y., Ishiwata-Kimata, Y., and Kohno, K. (2004). A role for BiP as an adjustor for the endoplasmic reticulum stress-sensing protein IRE1. *J. Cell Biol.* 167, 445–456.

Kohno, K., Normington, K., Sambrook, J., Gething, M. J., and Mori, K. (1993). The promoter region of the yeast *KAR2* (*BiP*) gene contains a regulatory domain that responds to the presence of unfolded proteins in the endoplasmic reticulum. *Mol. Cell. Biol.* 13, 877–890.

Koizumi, N., Martinez, I. M., Kimata, Y., Kohno, K., Sano, H., and Chrispeels, M. J. (2001). Molecular characterization of two *Arabidopsis* IRE1 homologs, endoplasmic reticulum-located transmembrane protein kinases. *Plant Physiol.* 127, 949–962.

Korennykh, A. V., Egea, P. F., Korostelev, A. A., Finer-Moore, J., Zhang, C., Shokat, K. M., et al. (2008). The unfolded protein response signals through high-order assembly of IRE1. *Nature* 457, 687–693.

Leber, J. H., Bernales, S., and Walter, P. (2004). IRE1-independent gain control of the unfolded protein response. *PLoS Biol.* 2:e235. doi: 10.1371/journal.pbio.0020235

Leborgne-Castel, N., Jelitto-Van Dooren, E. P. W. M., Crofts, A. J., and Denecke, J. (1999). Overexpression of BiP in tobacco alleviates endoplasmic reticulum stress. *Plant Cell* 11, 459–469.

Lee, A. H., Iwakoshi, N. N., and Glimcher, L. H. (2003). XBP-1 regulates a subset of endoplasmic reticulum resident chaperone genes in the unfolded protein response. *Mol. Cell. Biol.* 23, 7448–7459.

Lee, K., Tirasophon, W., Shen, X., Michalak, M., Prywes, R., Okada, T., et al. (2002). IRE1-mediated unconventional mRNA splicing and S2P-mediated ATF6 cleavage merge to regulate XBP1 in signaling the unfolded protein response. *Genes Dev.* 16, 452–466.

Li, B., Gao, B., Ye, L., Han, X., Wang, W., Kong, L., et al. (2007). Hepatitis B virus X protein (HBx) activates ATF6 and IRE1-XBP1 pathways of unfolded protein response. *Virus Res.* 124, 44–49.

Liberman, E., Fong, Y. L., Selby, M. J., Choo, Q. L., Cousens, L., Houghton, M., et al. (1999). Activation of the grp78 andgrp94 Promoters by Hepatitis C Virus E2 Envelope Protein. *J. Virol.* 73, 3718–3722.

Liu, J. X., and Howell, S. H. (2010). bZIP28 and NF-Y transcription factors are activated by er stress and assemble into a transcriptional complex to regulate stress response genes in *Arabidopsis*. *Plant Cell* 22, 782–796.

Liu, J. X., Srivastava, R., Che, P., and Howell, S. H. (2007). Salt stress responses in *Arabidopsis* utilize a signal transduction pathway related to endoplasmic reticulum stress signaling. *Plant J.* 51, 897–909.

Lu, D. P., and Christopher, D. A. (2008). Endoplasmic reticulum stress activates the expression of a subgroup of protein disulfide isomerase genes and AtbZIP60 modulates the response in *Arabidopsis thaliana*. *Mol. Genet. Genomics* 280, 199–210.

Lu, P. D., Harding, H. P., and Ron, D. (2004). Translation reinitiation at alternative open reading frames regulates gene expression in an integrated stress response. *J. Cell Biol.* 167, 27–33.

Ma, Y., and Hendershot, L. M. (2003). Delineation of a negative feedback regulatory loop that controls protein translation during endoplasmic reticulum stress. *J. Biol. Chem.* 278, 34864–34873.

Machamer, C. E., Doms, R. W., Bole, D. G., Helenius, A., and Rose, J. K. (1990). Heavy chain binding protein recognizes incompletely disulfide-bonded forms of vesicular stomatitis virus G protein. *J. Biol. Chem.* 265, 6879–6883.

Marcinak, S. J., and Ron, D. (2010). The unfolded protein response in lung disease. *Proc. Am. Thorac. Soc.* 7, 356–362.

Medigeshi, G. R., Lancaster, A. M., Hirsch, A. J., Briese, T., Lipkin, W. I., DeFilippis, V., et al. (2007). West Nile virus infection activates the unfolded protein response, leading to CHOP induction and apoptosis. *J. Virol.* 81, 10849–10860.

Meusser, B., Hirsch, C., Jarosch, E., and Sommer, T. (2005). ERAD: the long road to destruction. *Nat. Cell Biol.* 7, 766–772.

Mori, K., Kawahara, T., Yoshida, H., Yanagi, H., and Yura, T. (1996). Signalling from endoplasmic reticulum to nucleus: transcription factor with a basic-leucine zipper motif is required for the unfolded protein-response pathway. *Genes Cells* 1, 803–817.

Nagashima, Y., Mishiba, K., Suzuki, E., Shimada, Y., Iwata, Y., and Koizumi, N. (2011). *Arabidopsis* IRE1 catalyses unconventional splicing of *bZIP60* mRNA to produce the active transcription factor. *Sci. Rep.* 1:29. doi: 10.1038/srep00029

Navazio, L., Mariani, P., and Sanders, D. (2001). Mobilization of Ca^{2+} by cyclic ADP-ribose from the endoplasmic reticulum of cauliflower florets. *Plant Physiol.* 125, 2129–2138.

Netherton, C. L., Parsley, J. C., and Wileman, T. (2004). African swine fever virus inhibits induction of the stress-induced proapoptotic transcription factor CHOP/GADD153. *J. Virol.* 78, 10825–10828.

Ng, D. T., Randall, R. E., and Lamb, R. A. (1989). Intracellular maturation and transport of the SV5 type II glycoprotein hemagglutinin-neuraminidase: specific and transient association with GRP78-BiP in the endoplasmic reticulum and extensive internalization from the cell surface. *J. Cell Biol.* 109, 3273–3289.

Nomaguchi, M., Fujita, M., and Adachi, A. (2008). Role of HIV-1 Vpu protein for virus spread and pathogenesis. *Microbes Infect.* 10, 960–967.

Novoa, I., Zhang, Y., Zeng, H., Jungreis, R., Harding, H. P., and Ron, D. (2003). Stress-induced gene expression requires programmed recovery from translational repression. *EMBO J.* 22, 1180–1187.

Oikawa, D., Kimata, Y., Kohno, K., and Iwawaki, T. (2009). Activation of mammalian IRE1α upon ER stress depends on dissociation of BiP rather than on direct interaction with unfolded proteins. *Exp. Cell Res.* 315, 2496–2504.

Oikawa, D., Tokuda, M., Hosoda, A., and Iwawaki, T. (2010). Identification of a consensus element recognized and cleaved by IRE1α. *Nucleic Acids Res.* 38, 6265–6273.

Okushima, Y., Koizumi, N., Yamaguchi, Y., Kimata, Y., Kohno, K., and Sano, H. (2002). Isolation and characterization of a putative transducer of endoplasmic reticulum stress in *Oryza sativa*. *Plant Cell Physiol.* 43, 532–539.

Papa, F. R., Zhang, C., Shokat, K., and Walter, P. (2003). Bypassing a kinase activity with an ATP-competitive drug. *Science* 302, 1533.

Parmar, V. M., and Schröder, M. (2012). Sensing endoplasmic reticulum stress. *Adv. Exp. Med. Biol.* 738, 153–168.

Pasqual, G., Burri, D. J., Pasquato, A., de la Torre, J. C., and Kunz, S. (2011). Role of the host cell's unfolded protein response in arenavirus infection. *J. Virol.* 85, 1662–1670.

Pavio, N., Romano, P. R., Graczyk, T. M., Feinstone, S. M., and Taylor, D. R. (2003). Protein synthesis and endoplasmic reticulum stress can be modulated by the hepatitis C virus envelope protein E2 through the eukaryotic initiation factor 2α kinase PERK. *J. Virol.* 77, 3578–3585.

Pincus, D., Chevalier, M. W., Aragón, T., Van Anken, E., Vidal, S. E., El-Samad, H., et al. (2010). BiP binding to the ER-stress sensor IRE1 tunes the homeostatic behavior of the unfolded protein response. *PLoS Biol.* 8:e1000415. doi: 10.1371/journal.pbio.1000415

Preston, A. M., Gurisik, E., Bartley, C., Laybutt, D. R., and Biden, T. J. (2009). Reduced endoplasmic reticulum (ER)-to-Golgi protein trafficking contributes to ER stress in lipotoxic mouse beta cells by promoting protein overload. *Diabetologia* 52, 2369–2373.

Qiang, X., Zechmann, B., Reitz, M. U., Kogel, K. H., and Schäfer, P. (2012). The mutualistic fungus Piriformospora indica colonizes *Arabidopsis* roots by inducing an endoplasmic reticulum stress-triggered caspase-dependent cell death. *Plant Cell* 24, 794–809.

Ron, D., and Walter, P. (2007). Signal integration in the endoplasmic reticulum unfolded protein response. *Nat. Rev. Mol. Cell Biol.* 8, 519–529.

Rüegsegger, U., Leber, J. H., and Walter, P. (2001). Block of *HAC1* mRNA translation by long-range base pairing is released by cytoplasmic splicing upon induction of the unfolded protein response. *Cell* 107, 103–114.

Schröder, M., and Kaufman, R. J. (2005). The mammalian unfolded protein response. *Annu. Rev. Biochem.* 74, 739–789.

Seo, P. J., Kim, S. G., and Park, C. M. (2008). Membrane-bound transcription factors in plants. *Trends Plant Sci.*13, 550–556.

Shaffer, A. L., Shapiro-Shelef, M., Iwakoshi, N. N., Lee, A. H., Qian, S. B., Zhao, H., et al. (2004). XBP1, downstream of Blimp-1, expands the secretory apparatus and other organelles, and increases protein synthesis in plasma cell differentiation. *Immunity* 21, 81–93.

Shamu, C. E., and Walter, P. (1996). Oligomerization and phosphorylation of the IRE1p kinase during intracellular signaling from the endoplasmic reticulum to the nucleus. *EMBO J.* 15, 3028.

Shen, J., Chen, X., Hendershot, L., and Prywes, R. (2002). ER stress regulation of ATF6 localization by dissociation of BiP/GRP78 binding and unmasking of Golgi localization signals. *Dev. Cell* 3, 99–111.

Shen, X., Ellis, R. E., Sakaki, K., and Kaufman, R. J. (2005). Genetic interactions due to constitutive and inducible gene regulation mediated by the unfolded protein response in *C.* elegans. *PLoS Genet.* 1:e37. doi: 10.1371/journal.pgen.0010037

Schott, A., Ravaud, S., Keller, S., Radzimanowski, J., Viotti, C., Hillmer, S., et al. (2010). *Arabidopsis* stromal-derived Factor 2 (SDF2) is a crucial target of the unfolded protein response in the endoplasmic reticulum. *J. Biol. Chem.* 285, 18113–18121.

Schubert, U., Antón, L. C., Baèík, I., Cox, J. H., Bour, S., Bennink, J. R., et al. (1998). CD4 glycoprotein degradation induced by human immunodeficiency virus type 1 Vpu protein requires the function of proteasomes and the ubiquitin-conjugating pathway. *J. Virol.* 72, 2280–2288.

Sidrauski, C., Cox, J. S., and Walter, P. (1996). tRNA ligase is required for regulated mRNA splicing in the unfolded protein response. *Cell* 87, 405–413.

Sidrauski, C., and Walter, P. (1997). The transmembrane kinase IRE1p is a site-specific endonuclease that initiates mRNA splicing in the unfolded protein response. *Cell* 90, 1031–1039.

Stephens, S. B., Dodd, R. D., Brewer, J. W., Lager, P. J., Keene, J. D., and Nicchitta, C. V. (2005). Stable ribosome binding to the endoplasmic reticulum enables compartment-specific regulation of mRNA translation. *Mol. Biol. Cell* 16, 5819–5831.

Stevens, F. J., and Argon, Y. (1999). Protein folding in the ER. *Semin. Cell Dev. Biol.* 10, 443–454.

Su, H. L., Liao, C. L., and Lin, Y. L. (2002). Japanese encephalitis virus infection initiates endoplasmic reticulum stress and an unfolded protein response. *J. Virol.* 76, 4162–4171.

Sun, M., Rothermel, T. A., Shuman, L., Aligo, J. A., Xu, S., Lin, Y., et al. (2004). Conserved cysteine-rich domain of paramyxovirus simian virus 5 V protein plays an important role in blocking apoptosis. *J. Virol.* 78, 5068–5078.

Sung, S. C., Chao, C. Y., Jeng, K. S., Yang, J. Y., and Lai, M. (2009). The 8ab protein of SARS-CoV is a luminal ER membrane-associated protein and induces the activation of ATF6. *Virology* 387, 402–413.

Tabas, I., and Ron, D. (2011). Integrating the mechanisms of apoptosis induced by endoplasmic reticulum stress. *Nat. Cell Biol.* 13, 184–190.

Tardif, K. D., Mori, K., Kaufman, R. J., and Siddiqui, A. (2004). Hepatitis C virus suppresses the IRE1-XBP1 pathway of the unfolded protein response. *J. Biol. Chem.* 279, 17158–17164.

Tardif, K. D., Mori, K., and Siddiqui, A. (2002). Hepatitis C virus subgenomic replicons induce endoplasmic reticulum stress activating an intracellular signaling pathway. *J. Virol.* 76, 7453–7459.

Tardif, K. D., and Siddiqui, A. (2003). Cell surface expression of major histocompatibility complex class I molecules is reduced in hepatitis C virus subgenomic replicon-expressing cells. *J. Virol.* 77, 11644–11650.

Tardif, K. D., Waris, G., and Siddiqui, A. (2005). Hepatitis C virus, ER stress, and oxidative stress. *Trends Microbiol.* 13, 159–163.

Tirosh, B., Iwakoshi, N. N., Lilley, B. N., Lee, A. H., Glimcher, L. H., and Ploegh, H. L. (2005). Human cytomegalovirus protein US11 provokes an unfolded protein response that may facilitate the degradation of class I major histocompatibility complex products. *J. Virol.* 79, 2768–2779.

Todd-Corlett, A., Jones, E., Seghers, C., and Gething, M. J. (2007). Lobe IB of the ATPase domain of Kar2p/BiP interacts with IER1p to negatively regulate the unfolded protein response in *Saccharomyces cerevisiae*. *J. Mol. Biol.* 367, 770–787.

Trujillo-Alonso, V., Maruri-Avidal, L., Arias, C. F., and López, S. (2011). Rotavirus infection induces the unfolded protein response of the cell and controls it through the nonstructural protein NSP3. *J. Virol.* 85, 12594–12604.

Umareddy, I., Pluquet, O., Wang, Q. Y., Vasudevan, S. G., Chevet, E., and Gu, F. (2007). Dengue virus serotype infection specifies the activation of the unfolded protein response. *Virol. J.* 4:91. doi: 10.1186/1743-422X-4-91

Urade, R. (2007). Cellular response to unfolded proteins in the endoplasmic reticulum of plants. *FEBS J.* 274, 1152–1171.

Urano, F., Wang, X. Z., Bertolotti, A., Zhang, Y., Chung, P., Harding, H. P., et al. (2000). Coupling of stress in the ER to activation of JNK protein kinases by transmembrane protein kinase IRE1. *Science* 287, 664.

Vattem, K. M., and Wek, R. C. (2004). Reinitiation involving upstream ORFs regulates ATF4 mRNA translation in mammalian cells. *Proc. Natl. Acad. Sci. U.S.A.* 101, 11269.

Verchot, J. (2012). Cellular chaperones and folding enzymes are vital contributors to membrane bound replicaiton and movement complexes during RNA virus infection. *Front. Plant Sci.* 3:275. doi: 10.3389/fpls.2012.00275

Vitale, A., and Boston, R. S. (2008). Endoplasmic reticulum quality control and the unfolded protein response: insights from plants. *Traffic* 9, 1581–1588.

Wang, D., Weaver, N. D., Kesarwani, M., and Dong, X. (2005). Induction of protein secretory pathway is required for systemic acquired resistance. *Science* 308, 1036.

Wang, X. Z., Lawson, B., Brewer, J. W., Zinszner, H., Sanjay, A., Mi, L. J., et al. (1996). Signals from the stressed endoplasmic reticulum induce C/EBP-homologous protein (CHOP/GADD153). *Mol. Cell. Biol.* 16, 4273–4280.

Watowich, S. S., Morimoto, R. I., and Lamb, R. A. (1991). Flux of the paramyxovirus hemagglutinin-neuraminidase glycoprotein through the endoplasmic reticulum activates transcription of the *GRP78-BiP* gene. *J. Virol.* 65, 3590–3597.

Whitham, S. A., Quan, S., Chang, H. S., Cooper, B., Estes, B., Zhu, T., et al. (2003). Diverse RNA viruses elicit the expression of common sets of genes in susceptible *Arabidopsis thaliana* plants. *Plant J.* 33, 271–283.

Xu, C. (2005). Endoplasmic reticulum stress: cell life and death decisions. *J. Clin. Invest.* 115, 2656–2664.

Xu, P., Chen, F., Mannas, J. P., Feldman, T., Sumner, L. W., and Roossinck, M. J. (2008). Virus infection improves drought tolerance. *New Phytol.* 180, 911–921.

Yamamoto, K., Sato, T., Matsui, T., Sato, M., Okada, T., Yoshida, H., et al. (2007). Transcriptional induction of mammalian er quality control proteins is mediated by single or combined action of ATF6α and XBP1. *Dev. Cell* 13, 365–376.

Yang, C., Guo, R., Jie, F., Nettleton, D., Peng, J., Carr, T., et al. (2007). Spatial analysis of *Arabidopsis thaliana* gene expression in response to Turnip mosaic virus infection. *Mol. Plant Microbe Interact.* 20, 358–370.

Ye, C., Chen, S., Payton, M., Dickman, M. B., and Verchot, J. (2012). TGBp3 triggers the unfolded protein response and SKP1-dependent programmed cell death. *Mol. Plant. Pathol.* [Online]. doi: 10.1111/mpp.12000

Ye, C., Dickman, M. B., Whitham, S. A., Payton, M., and Verchot, J. (2011). The unfolded protein response is triggered by a plant viral movement protein. *Plant Physiol.* 156, 741–755.

Ye, C., and Verchot, J. (2011). Role of unfolded protein response in plant virus infection. *Plant Signal. Behav.* 6, 1212–1215.

Yoshida, H. (2007). ER stress and diseases. *FEBS J.* 274, 630–658.

Yoshida, H., Matsui, T., Yamamoto, A., Okada, T., and Mori, K. (2001). XBP1 mRNA is induced by ATF6 and spliced by IRE1 in response to ER stress to produce a highly active transcription factor. *Cell* 107, 881–891.

Yoshida, H., Oku, M., Suzuki, M., and Mori, K. (2006). pXBP1 (U) encoded in XBP1 pre-mRNA negatively regulates unfolded protein response activator pXBP1 (S) in mammalian ER stress response. *J. Cell Biol.* 172, 565–575.

Yu, C. Y., Hsu, Y. W., Liao, C. L., and Lin, Y. L. (2006). Flavivirus infection activates the XBP1 pathway of the unfolded protein response to cope with endoplasmic reticulum stress. *J. Virol.* 80, 11868–11880.

Zhang, K., and Kaufman, R. J. (2006). The unfolded protein response: a stress signaling pathway critical for health and disease. *Neurology* 66, S102–S109.

Zhao, L., and Ackerman, S. L. (2006). Endoplasmic reticulum stress in health and disease. *Curr. Opin. Cell Biol.* 18, 444–452.

Zhou, J., Liu, C. Y., Back, S. H., Clark, R. L., Peisach, D., Xu, Z., et al. (2006). The crystal structure of human IRE1 luminal domain reveals a conserved dimerization interface required for activation of the unfolded protein response. *Proc. Natl. Acad. Sci. U.S.A.* 103, 14343–14348.

Zinszner, H., Kuroda, M., Wang, X. Z., Batchvarova, N., Lightfoot, R. T., Remotti, H., et al. (1998). CHOP is implicated in programmed cell death in response to impaired function of the endoplasmic reticulum. *Genes Dev.* 12, 982–995.

Zsak, L., Lu, Z., Kutish, G. F., Neilan, J. G., and Rock, D. L. (1996). An African swine fever virus virulence-associated gene NL-S with similarity to the herpes simplex virus *ICP34.* 5 gene. *J. Virol.* 70, 8865–8871.

Conflict of Interest Statement: The authors declare that the research was conducted in the absence of any commercial or financial relationships that could be construed as a potential conflict of interest.

Received: 25 September 2012; accepted: 08 December 2012; published online: 28 December 2012.

Citation: Zhang L and Wang A (2012) Virus-induced ER stress and the unfolded protein response. Front. Plant Sci. ***3****:293. doi: 10.3389/fpls.2012.00293*

This article was submitted to Frontiers in Plant-Microbe Interaction, a specialty of Frontiers in Plant Science.

GLOSSARY

***Molecular chaperone*:** A molecular chaperone is a protein that assists the folding/unfolding of other proteins. Some molecular chaperones reside in the lumen of the ER, such as BiP, also known as GRP78, a member of the Hsp70 family.

***Protein disulphide isomerase (PDI)*:** A cellular enzyme in the lumen of the ER of eukaryotes or the periplasmic region of prokaryotes catalyzes the formation and breakage of disulphide bonds between cysteine residues within proteins, allowing proteins to quickly find the correct arrangement of disulfide bonds in their fully folded state.

***ER stress*:** An organelles-initiated cell stress arises from mismatch between the load of unfolded or misfolded proteins in the lumen of the ER and the capacity of this cellular machinery.

***Unfolded protein response (UPR)*:** A highly conserved physiological response is induced by accumulation of unfolded proteins in the lumen of the ER. In mammals, the UPR is mediated by three ER stress sensors including IRE1, PERK, and ATF6. In yeast, the UPR is controlled by only one signaling pathway mediated by IRE1. Thus far, two UPR pathways have been identified in plants, one mediated by IRE1-bZIP60 and the other by bZIP17/bZIP28.

***ER-assisted degradation (ERAD)*:** ERAD is designated a cellular pathway, which translocates the unfolded proteins from the ER in a retrograde manner into the cytosol, where ER membrane associated ubiquitin ligases post-translationally modify the translocated proteins thereby targeting them for degradation, usually by the 26S proteasome.

***Programmed cell-death (PCD)*:** The term PCD defines any form of cell death resulting from an orderly cascade, mediated by intracellular death programs, regardless of the triggers or the hallmarks it exhibits. PCD serves fundamental functions in both plants, and metazoans where called apoptosis.

***Major histocompatibility complex (MHC)*:** An integral membrane protein complex has a characteristic groove as the binding site for the presentation of immunogenic peptides.

***Hemagglutinin-neuraminidase (HN)*:** A single viral envelope glycoprotein has both receptor-cleaving and receptor-binding activity, which is in contrast to the protein found in influenza, where both hemagglutinin and neuraminidase activities reside in two separate glycoproteins.

***Eukaryotic translation initiation factor 2 (eIF2)*:** The eIF2 complex is required in the translation initiation. It transfers Met-tRNA to the 40S submit of the ribosome to form the 43S pre-initiation complex in a GTP-dependent manner. eIF2 is a heterotrimer consisting of eIF2α, eIF2β, and eIF2γ. Phosphorylation of eIF2α by PERK inactivates eIF2α, resulting in inhibition of cap-dependent translation initiation.

***Unconventional processing*:** Conventional splicing is catalyzed by the spliceosome, which is composed of multiple proteins and small nuclear RNAs, and the cleavage reaction proceeds sequentially. The nucleotide sequence at the exon–intron border complies with Chambon's rule (GU-AG rule). In contrast, unconventional splicing is catalyzed by IRE1 and tRNA ligase, which is independent of the spliceosome, and the order of cleavage of the exon–intron junctions is not predetermined. A pair of characteristic stem–loop structures exists at the cleavage sites, which is recognized by IRE1, instead of a consensus sequence such as GU-AG.

frontiers in
PLANT SCIENCE

REVIEW ARTICLE
published: 26 March 2013
doi: 10.3389/fpls.2013.00068

Genetic recombination in plant-infecting messenger-sense RNA viruses: overview and research perspectives

Jozef J. Bujarski [1,2]*

[1] *Plant Molecular Biology Center and the Department of Biological Sciences, Northern Illinois University, DeKalb, IL, USA*
[2] *Laboratory of Molecular and Systems Biology, Institute of Bioorganic Chemistry, Polish Academy of Sciences, Poznan, Poland*

Edited by:
Jean-François Laliberté, Institut national de la recherche scientifique, Canada

Reviewed by:
F. Murilo Zerbini, Universidade Federal de Viçosa, Brazil
Justin Pita, Pennsylvania State University, USA

***Correspondence:**
Jozef J. Bujarski, Plant Molecular Biology Center and the Department of Biological Sciences, Northern Illinois University, Montgomery Hall, DeKalb, IL 60115, USA.
e-mail: jbujarski@niu.edu

RNA recombination is one of the driving forces of genetic variability in (+)-strand RNA viruses. Various types of RNA–RNA crossovers were described including crosses between the same or different viral RNAs or between viral and cellular RNAs. Likewise, a variety of molecular mechanisms are known to support RNA recombination, such as replicative events (based on internal or end-to-end replicase switchings) along with non-replicative joining among RNA fragments of viral and/or cellular origin. Such mechanisms as RNA decay or RNA interference are responsible for RNA fragmentation and *trans*-esterification reactions which are likely accountable for ligation of RNA fragments. Numerous host factors were found to affect the profiles of viral RNA recombinants and significant differences in recombination frequency were observed among various RNA viruses. Comparative analyses of viral sequences allowed for the development of evolutionary models in order to explain adaptive phenotypic changes and co-evolving sites. Many questions remain to be answered by forthcoming RNA recombination research. (1) How various factors modulate the ability of viral replicase to switch templates, (2) What is the intracellular location of RNA–RNA template switchings, (3) Mechanisms and factors responsible for non-replicative RNA recombination, (4) Mechanisms of integration of RNA viral sequences with cellular genomic DNA, and (5) What is the role of RNA splicing and ribozyme activity. From an evolutionary stand point, it is not known how RNA viruses parasitize new host species *via* recombination, nor is it obvious what the contribution of RNA recombination is among other RNA modification pathways. We do not understand why the frequency of RNA recombination varies so much among RNA viruses and the status of RNA recombination as a form of sex is not well documented.

Keywords: RNA recombination, viral replicase, template switching, non-replicative RNAs, host factors, cellular RNAs, ribonucleases, viral evolution

INTRODUCTION

Plus-stranded RNA viruses include some of the most dangerous pathogens for animals and humans. Moreover, a vast majority of plant viruses are (+) RNA viruses. RNA viruses demonstrate a large level of variability in their genetic information, due to either mutations, RNA–RNA crossovers (RNA recombination), or reassortment. RNA recombination was demonstrated for many RNA virus species, whether under natural or experimental conditions. Similar to genetic recombination in DNA-based organisms, viral RNA recombination is defined as the process of swapping RNA fragments among RNA molecules. If crossovers occur amongst the same RNA templates in a homologous fashion, the exchanges are functionally equivalent to DNA meiotic crossing-over. In some viruses, the frequency of homologous crossing-over is very high and practically every replicated viral RNA molecule can be considered as chimerical in nature, as we have demonstrated for brome mosaic virus (BMV) RNAs (Urbanowicz et al., 2005).

A variety of events have been described that contribute to the formation of RNA recombinants (**Figure 1**). Such events include crossovers between viruses belonging to the same or to different taxonomic groups, between viruses infecting different hosts, or from adopting genetic material from the host. Numerous questions about molecular mechanisms of RNA recombination remain unanswered. This review attempts to summarize the most important venues of RNA recombination research, their challenges and future directions in order to draw more accurate models for this important RNA virus phenomenon. Since this issue of Frontiers concerns plant pathology, most of the material discusses RNA recombination in plant viruses. However, the less advanced aspects of plant recombination studies have been illustrated with examples taken from animal/human RNA viruses in order to show mutual possibilities for model research.

REPLICATIVE MECHANISM OF RNA RECOMBINATION

The generally accepted mechanism of RNA recombination is currently explained by a copy-choice model where the viral RNA polymerase (RdRp) complex in mRNA viruses [reverse transcriptase (RT) in retroviruses] changes templates during synthesis of the nascent strand (Galetto et al., 2006). This swapping process generates recombinant RNA molecules of mixed ancestry. Although we begin to understand the nature of these processes, many questions are waiting for an answer. One group

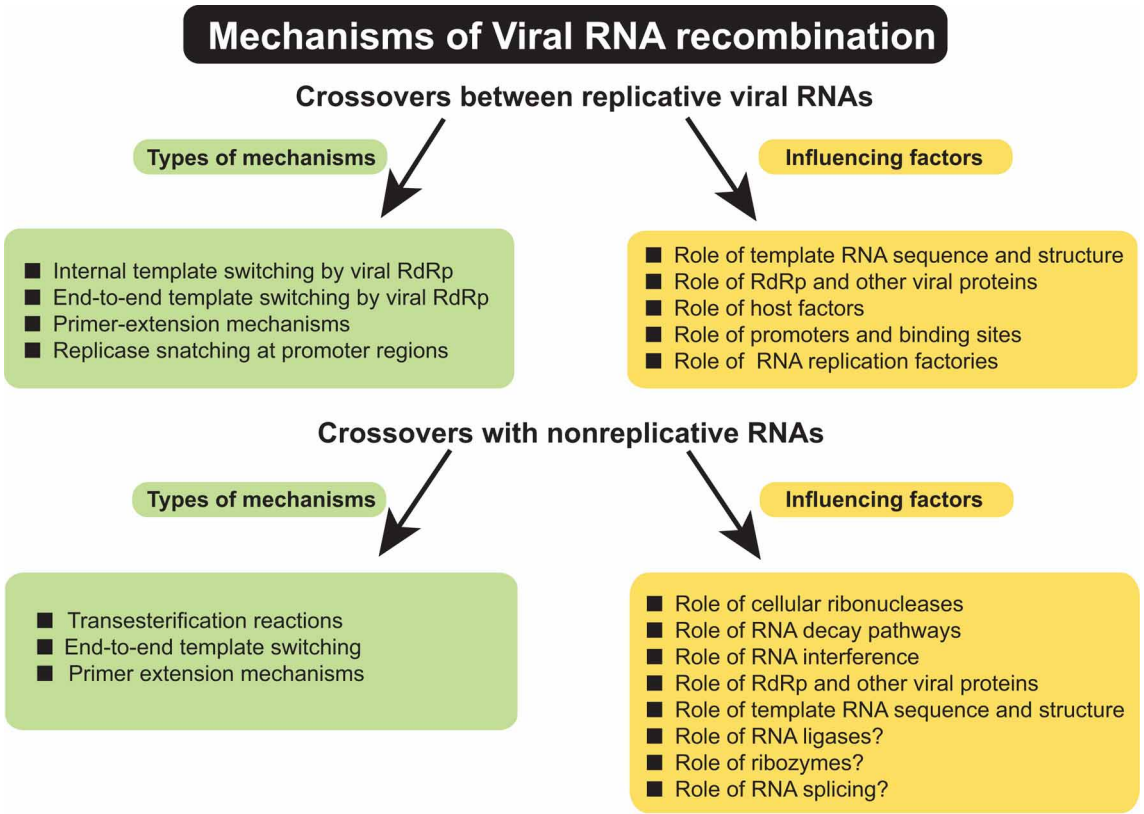

FIGURE 1 | Summary of types of mechanisms of genetic RNA recombination in (+) RNA viruses and factors influencing the RNA–RNA crossovers.

of questions revolves around the features that define the sites of crossovers. Among the factors known to promote replicase to switch are sequence homologies between recombination substrates along with secondary structures at the crossover sites, as demonstrated with the BMV and other systems (Figlerowicz and Bujarski, 1998; Nagy et al., 1999b). Also, the transcriptional activity seems to promote template switching. For instance, an efficient recombination hot spot has been mapped within the intercistronic region of BMV RNA3, the site carrying the promoter of transcription of subgenomic RNA4 (Wierzchoslawski et al., 2004). It is unknown what exactly facilitates crossovers at such sites. Possibilities include a snatching process of already bound RdRp complex to the promoter site, the premature termination of RNA synthesis and the replicase detachment–reattachment, or the effect of other bound viral and/or host factors (Sztuba-Solinska et al., 2011). These mechanisms may depend upon the type of template-switching process (whether the crosses occur internally or near the ends of the RNA templates) and on the involvement of crossover sequences in other processes, e.g., as a promoter of RNA replication or transcription.

Template switching was found to occur between related but also between unrelated RNA templates, generating legitimate (homologous) and illegitimate (nonhomologous) recombinants, respectively (Nagy and Simon, 1997). Since the latter involves sequences with little similarity, other factors must be important. Some data indicate that switches depend upon sequence composition, with the AU-rich regions promoting the RdRp detachment (Nagy et al., 1999a) and upon secondary structures (Galetto et al., 2006), along with protein or RNA binding activity. Switching may also depend upon the processivity (a measure of the average number of nucleotides copied per template association–disassociation cycle) features of the RdRp enzyme (Breyer and Matthews, 2001). A mandatory replicase breaking site is the end of any RNA template. End-to-end switching has been reported based upon *in vitro* results with RdRp enzymes from Bovine viral diarrhea virus (BVDV), BMV, Cucumber mosaic virus (CMV), and Cowpea chlorotic mottle virus (CCMV) (Kim and Kao, 2001). It is, however, not known how exactly such switches occur and whether the molecular mechanism is common among polymerases of different RNA viruses.

The strength of binding of the RdRp complex may play a key role during RNA template detachment–reattachment. With an increasing number of available RNA polymerase crystal structures, more is evident about the elements involved in RNA-replicase interactions. For instance, removal of a β-hairpin loop from the HCV RdRp protein increased *de novo* RNA synthesis and promoted RNA binding (Mosley et al., 2012). The RNA copying fidelity might be a matter of a nanosecond timescale complex dynamic in the RdRp enzyme that determines RNA

binding, nucleotide binding or catalysis (Moustafa et al., 2011) and thus needs to be experimentally determined. The use of engineered replicase variants in RNA recombination assays will shed new light onto the molecular details of template switching mechanisms.

Another, not well answered question is how RNA template substrates come together in order to facilitate the switch. One possibility is that secondary structure regions can hybridize in *trans* bringing the two RNA templates into a local interaction. Such data are available, for instance, based upon limited observations in BMV (Nagy and Bujarski, 1993; Dzianott et al., 1995) or analogously, during switches between dimeric RNAs (within kissing loops) during reverse transcription inside the Human immunodeficiency virus Type-1 (HIV-1) virions (Nikolaitchik et al., 2011), an atypical (+) sense RNA virus.

Yet, other data reveal that (+) RNA viruses are replicating in membranous structures called spherules or replication factories (Laliberté and Sanfaçon, 2010). Such host membrane-derived replication vesicles have limited loading capacity, but they may carry up to several positive and negative strand RNA molecules (den Boon et al., 2010). Recent advances reveal the assembly of replicase complexes within replication factories *via* highly orchestrated interactions between viral proteins, viral genomic RNAs, and co-opted host factors (Mine and Okuno, 2012). Such a micro-environment may secure tight packaging and thus the closeness of internalized viral RNA molecules. From the formal stand point then, one may consider RNA recombination switches in (+) RNA viruses inside replication factories as analogous to the switches that occur, e.g., during reverse transcription inside the HIV-1 virions.

Recently, we have demonstrated the participation of coat protein (CP) during BMV RNA recombination (Sztuba-Solinska et al., 2012). The nucleotide changes in *cis*-acting RNA motifs and the amino acid replacements within the corresponding CP binding sites—both debilitated the BMV RNA recombination. CP molecules likely mediate RNA crosses *via* dimerization/oligomerization of bound CP subunits. Indeed, the presence of BMV CP molecules has been demonstrated to be inside replication vesicles (Bamunusinghe et al., 2011). Another untested possibility predicts that a bound CP functions as a road block catalyzing the detachment of the replicase complex. The CP may also affect the properties of viral replicase. For instance, it has been shown recently that Norovirus RNA synthesis was enhanced by co-expressed structural protein VP1 (Subba-Reddy et al., 2012).

RECOMBINATION WITH NON-REPLICATIVE RNAs

Besides replicative copy-choice, the non-replicative mechanisms of viral RNA recombination have been described, mainly for animal/human RNA viruses, with almost no research focusing plant viruses. One of the best characterized non-replicative processes is demonstrated in the poliovirus where viable viruses were rescued in cells co-transfected with different pairs of viral RNA fragments (Gmyl et al., 1999). It is likely the recombinants may have resulted from transesterification reactions with the end structures similar to known ribozymes *via* intermediary formation of 2′,3′-cyclic phosphate. Indeed, *in vitro* data show that the transesterification reactions in the bacteriophage Qbeta RNA are guided by secondary structures that direct the attack of a 3′ hydroxyl onto the phosphodiester bonds (Chetverin et al., 1997). Later observations revealed enormous variability of the poliovirus genome and some variants may have been introduced by genetic errors due to non-replicative mechanisms (Agol, 2006). More recent results with partially-complementary RNA-oligonucleotides demonstrated the spontaneous formation of novel RNA molecules *via* 3′,5′-phosphodiester bonds (Lutay et al., 2007). These data show that viral RNA recombination can occur without participation of the RNA polymerase enzyme. The exact mechanisms of these non-replicative events are not completely understood and require further studies.

In contrast to poliovirus and other picornaviruses, bacteriophage Qbeta demonstrates low levels of recombination frequency. By using a cell-free system, Chetverin et al. (2005) have shown a high yield of primer-extension recombination with poliovirus replicase, but a low yield with Qbeta replicase. Thus, RNA recombination by poliovirus *vs.* Qbeta RdRps must be mechanistically different. Although both utilize transesterification reactions, the precise molecular bases for RNA swappings used by each of these enzymes are likely dissimilar reflecting different biochemical adaptations to the needs of individual viruses. It would be interesting to confirm experimentally the proposed transesterification models.

Among other examples of non-replicative recombination in mRNA viruses, the co-transfections of replicating and nonreplicating rubella virus (RUB) RNA transcripts containing nonoverlapping deletions did restore the infectious virus (Adams et al., 2003). Both, homologous and nonhomologous RNA recombinants emerged. The mechanism seemed to involve end-to-end replicase switching after initiation of minus-strand synthesis. However, the details of such mechanisms have not yet been confirmed. Another example of that sort involves recombination between BVDV and cellular RNAs, which can occur in the absence of viral replicase (see section "Recombination Between Viral and Cellular RNAs"). Analogous studies in the area of plant virology remain to be performed.

ROLE OF HOST FACTORS DURING RNA RECOMBINATION

An important subject of RNA recombination research is the role of host factors. While the involvement of viral RdRp proteins has been studied extensively, knowledge of the functions host components play is limited (Nagy and Pogany, 2011). One study was done with a model system of tomato bushy stunt virus (TBSV) that can recombine in yeast cells. The authors screened a yeast knockout library to identify over thirty different host genes suppressing or accelerating the TBSV RNA recombination (Serviene et al., 2005; Nagy, 2011). An interesting example is the gene PMR1 which encodes an ion pump (Pmr1p) controlling the Mn2+ concentration which may consequently affect the ability of TBSV replicase to change RNA binding/template switching events. Also stress signals, e.g., salt stress, affect viral recombination indirectly, by changing the concentration of recombination-essential proteins. Future studies are required to understand the interrelated network of cellular factors that define the final outcome of TBSV

RNA recombinants, not only in model yeast cells, but also in natural TBSV plant hosts. Moreover, these studies are limited to only one specific TBSV RNA experimental recombination system, and it is unclear if other RNA recombination events within the TBSV RNA follow similar mechanistic pathways.

In the copy choice mechanism, recombinant RNAs are formed due to switching of viral replicase among RNA templates. The switching properties likely depend on the co-recruited host factors. In BMV, a variety of host factors were found to be employed by the replicase complex (Noueiry and Ahlquist, 2003). Many of these factors facilitate the complex assembly, but some regulate viral gene expression or recruitment of BMV RNAs to the membrane replication factories. Yet, other factors modify lipid composition of the endoplasmic reticulum membrane which activates the replication complex. Many of these factors can potentially affect the co-recruitment of RNA recombination substrates and/or BMV replicase switching properties during recombination. BMV RNA recombination was reported to occur in yeast cells (Garcia-Ruiz and Ahlquist, 2006), but a systematic identification of host factors participating in BMV RNA recombination remains to be done. It will be interesting to find out whether these factors parallel those in the above tombusvirus recombination system. This data will broaden our knowledge about host pathways enabling RNA viruses to recombine their genetic information. As such, it will contribute to predictions made on the stability of the RNA viral genome in various hosts.

The functions of recruited host proteins and host membranes in different (+) RNA virus systems are now being progressively elucidated. Comparison among three plant RNA virus replication systems (TBSV, BMV, and dianthoviruses) reveals general patterns within the stepwise process of viral replicase complex assembly which requires concerted involvement of protein–protein, RNA–protein, and protein–lipid interactions (Mine and Okuno, 2012). However, each of these three plant virus systems recruits its own array of specific host factors. This suggests that each RNA virus has significantly unique ways of adapting to the cellular environment in order to assemble a functional RNA replication complex. This further suggests specific requirements are needed for RNA recombination in each individual RNA virus and therefore the recombination characteristics may significantly differ with each other among RNA viruses. Crystal structure studies help to reveal the complex and individual nature of viral replicases. Examples being the structure of Q{beta} phage polymerase, determined by Takeshita and Tomita (2010), or the analysis of the crystal structure of tomato mosaic virus helicase as a component of the viral replicase complex (Nishikiori et al., 2012).

RECOMBINATION BETWEEN VIRAL AND CELLULAR RNAs

RNA recombination events between viral and cellular RNAs have been observed for both plant and animal RNA viruses. One example is RNA recombination between the BVDV, a member of the pestivirus genus, and cellular RNA sequences. It occurs at the presence yet also in the absence of an active viral RdRp enzyme, implying that the mechanisms must be different from replicative template switching events (Becher and Tautz, 2011). The case of BVDV recombination has practical implications because the recombinant virus is lethal to its host. Normally, the virus is persistent, limiting the efficiency of RNA replication due to the dependency of a viral protease on limiting amounts of a cellular cofactor. In general, the uptake of a variety of cellular protein coding sequences at various positions in the pestiviral genomes has been reported, demonstrating that pestiviruses can gain access to the RNA pool of their hosts *via* RNA recombination. The example of BVDV shows us not only that recombination events with cellular RNAs cannot be excluded for other viruses, but also that the recombinant RNAs can be retro-transcribed and occasionally integrated into the host genome. The exact molecular mechanisms of the crossover events with cellular RNAs remain to be elucidated, as well as what factors target the crossover sites both to viral and to cellular RNAs.

Besides BVDV, HIV-1 is known to recombine effectively with host RNAs, e.g., with host tRNAs after introducing its strong secondary structure elements into the HIV RNA (Konstantinova et al., 2007). HIV-1 is capable of acquiring new genetic material, especially to the RT-encoding ORF (van der Hoek et al., 2005; Berkhout, 2011). Information about similar recombinant crosses with host RNAs in plant RNA viruses remains very limited, and their mechanisms are waiting to be elucidated.

One recombination process that was addressed with plant viruses has been the events between an invading virus and the transgene mRNAs in transgenic plants (Aaziz and Tepfer, 1999). One such example being recombination between two strains of CMV where one strain was expressed as a transgene while the other strain infected the transgenic plant (Turturo et al., 2008). This research group has also described recombination between related viruses (CMV and tomato aspermy virus TAV), with the population of recombinants being similar to each other in transgenic and in nontransgenic plants, suggesting similar molecular mechanisms of recombination (Jacquemond, 2012). In general, this demonstrates that transgene viral mRNAs enter the same pathway as do natural viral RNAs, most likely operating in the cytoplasm.

RNA recombination between viral and micro (mi)RNAs has not yet been reported. However, given the fact that this would be a useful source of already adapted elements to be acquired by the virus in order to secure the in-*trans* host-gene regulation, the lack of commonality of such an acquisition is surprising. Since (+) RNA viruses operate in the cytoplasm, as the miRNAs do, there are likely either structural and/or functional constrains against such snatching events. Future studies will certainly bring further insight to this question.

Recently, a reverse scenario was observed. Nonretroviral RNA sequences of Bornaviruses and other (−) strand RNA viruses were integrated into the host genome, including the human genome (Belyi et al., 2010; Horie et al., 2010). Also, mRNA viruses were described to leave their sequences in the cellular DNA of infected hosts (Crochu et al., 2004; Anne and Sela, 2005; Maori et al., 2007; Zemer et al., 2008; Geuking et al., 2009). These results demonstrate that RNA viruses can serve as a source of genetic innovation for their hosts. The RT activity encoded by retrotransposons is most likely responsible for reverse transcription and integration, yet further molecular studies are needed.

The above examples illustrate that the cytoplasmic RNA processing mechanisms are able to cross paths with viral replication

pathways inside the cell. Despite diverse examples of viral RNAs recombining with host RNA sequences (and *vice versa*), many unanswered questions remain to be addressed. They include, but are not limited to, the sub-cellular location of recombination events, the role and availability of host RNA degradome for recombination, or the link between the elements of RNA degradation pathways and viral RNA recombination. The molecular mechanisms of such crossover events are not well understood, especially whether template-switching or re-ligation processes are involved. More data, especially from plant RNA virus systems are required to assess the general nature of these processes in plant vs. animal/human tissues.

ROLE OF RIBONUCLEASES AND RNA INTERFERENCE PATHWAYS

Host RNAs undergo extensive degradation and turnover, as do viral RNAs (Lloyd, 2012). The participation of RNA decay pathways in viral RNA recombination has been studied in TBSV by the Nagy group (Jiang et al., 2010; Jaag et al., 2011). By testing eight known endoribonucleases, the authors have shown that mutations in the components of RNase MRP debilitated the production of endoribonucleolytically cleaved TBSV RNA in yeast. Also, by knocking down the RNase NME1 or silencing the Xrn4p exoribonuclease in *Nicotiana benthamiana*, the production of cleaved TBSV RNAs was debilitated, but recombination increased, suggesting the role of RNA intermediates in recombination (Jaag and Nagy, 2009). Similar effects promoting RNA recombination were observed in yeast for Xrn1p exoribonuclease (Serviene et al., 2005). It is noteworthy that deletions of the host Met22p/Hal2p bisphosphate-3′-nucleotidase (a known inhibitor of the Xmn1p ribonuclease) or the inhibition of this nucleotidase with LiCl or NaCl, also increased the frequency of TBSV RNA recombination in yeast (Jaag and Nagy, 2010). This shows that besides host factors, the salt stress can also affect viral RNA recombination. Whether other environmental conditions can influence viral RNA recombination needs further studies.

In contrary to RNA decay enzymes, we observed debilitating effects of the host RNA interference gene knockouts on BMV RNA recombination in *Arabidopsis thaliana*, and that BMV RNA fragments have recombined with BMV RNA progeny (Dzianott et al., 2012). It appeared that RNA silencing (RNAi) pathways participated in the rearrangement of genomic BMV RNAs. Therefore, BMV RNAs can recombine *via* several mechanisms including template-switching events along with RNAi-based sequence swapping. Similarly, the promoting role of RNAi in viral RNA recombination was reported for mycovirus infection in chestnut blight fungus cells (Sun et al., 2009; Nuss, 2011). These two examples show that the RNAi mechanisms can function as antiviral tools, but also that RNA silencing can promote additional variability to the viral RNA genome. Further studies are needed to determine the formation of viral RNA recombinants from RNAi-induced degradation products.

THE PHYLOGENETIC AND EVOLUTIONARY ROLE OF RNA RECOMBINATION

The biological diversity within both plant and animal RNA viruses is one of the largest found in all other forms of nature. RNA recombination is a main contributor to the ever evolving RNA viral genome. Comparative analyses of RNA viral sequences allow for the development of evolutionary models that demonstrate the associated adaptive phenotypic changes along with detecting the co-evolving sites within viral genomes (Pond et al., 2012).

The wide imprints of RNA recombination were found within natural populations of plant viruses. RNA recombination seems to be particularly frequent among members of the family *Potyviridae*, the largest family of plant RNA viruses. Frequent recombinational footprints were detected within the ORFs of both their structural and nonstructural proteins (Bousalem et al., 2000; Visser and Bellstedt, 2009; Yamasaki et al., 2010). Phylogenetic surveys indicate not only intraspecies and intragenus, but also intergenous recombination crossover's footprints in *Potyviridae* (Desbiez and Lecoq, 2004; Valli et al., 2007), supporting their apparent modular evolution. Recombination with host RNA was also detected, likely via retrotransposable elements (Tanne and Sela, 2005) demonstrating that, like animal viruses, plant viruses can expand their coding capacity via recombination with the host's messenger RNA pool (Chare and Holmes, 2006).

Also, the populations of plant viruses with genomes producing sgRNAs, e.g., *Closteroviridae*, *Luteoviridae*, or viruses with multipartite genomes, e.g., *Bromoviridae,* seem to accumulate recombinants readily. Evolutionary pathways were proposed for the emergence of members of *Luteoviridae* (Domier et al., 2002 and Moreno et al., 2004). Luteoviruses have mastered the process of modular swap (Pagán and Holmes, 2010) and the reconstructed phylogeny reveals their sequence evolution by intrafamilial as well as extrafamilial RNA recombination (Moonan et al., 2000). The most frequent swaps map to the junction between the CP and RdRp ORFs (Silva et al., 2008). In addition, some luteoviruses were found to recombine with host (chloroplast) sequences (Mayo and Jolly, 1991).

One extreme example of interspecies recombination is in circoviruses that arose by recombinants between plant DNA nanoviruses and mammalian RNA caliciviruses. In this case, the likely mediator has been a retrovirus that retro-transcribed the RNA into DNA (Davidson and Silva, 2008). Although likely, such events have not been experimentally confirmed and further research is required.

Among animal viruses, coronaviruses are highly recombinogenic (Woo et al., 2009) and natural RNA recombinant variants were described for flaviviruses (González-Candelas et al., 2011). By having one of the highest recombination rates among all viruses, retroviruses generate polymorphic sequences that increase their chances for survival under changing selection pressures (Delviks-Frankenberry et al., 2011). Besides retroviruses, picornaviruses are naturally highly recombinogenic (Lukashev, 2010). In fact, RNA recombination is their key genetic feature maintaining the global pool of variants from which the recombination snapshots generate new recombinant forms of picornaviruses. For instance, a model describing recombination between poliovirus and coxsackie virus was presented to illustrate the effects on viral emergence and evolution (Combelas et al., 2011). This and other studies reveal multiple mechanisms leading to genetic variability of polioviruses (Savolainen-Kopra

and Blomqvist, 2010), with significant contribution of homologous recombination events that fix advantageous mutations or remove deleterious ones. However, further research is required to understand the detailed evolution mechanisms of polioviruses.

The evolutionary genetics of emerging plant RNA viruses was studied by Elena et al. (2011). Apparently, devastating virus epidemics can spread from new plant virus variants that acquired new virulence factors. This study shows a multifaceted picture of virus emergence. Changes in ecological conditions bring together the reservoir viruses and their crop hosts, often as a result of interplay among the environment, genetic plasticity, and the required host factors. The stochastic processes contribute to the beginning of viral emergence in a new host species, followed by the adaptation phase. Also, vectors impose strong bottlenecks during host-to-host transmissions. The reservoir population seems to be the most important determinant of viral emergence, but little is known about viruses of wild plant species that work as reservoirs.

For all the mentioned RNA virus systems, of either plants or animals, detailed roles during virus evolution of RNA secondary structures, the function of sequence similarity or the impact of RNA co-packaging during RNA recombination, are all not well understood. Inaccuracies of viral RNA replication, damage from environmental factors, and attacks by RNA-modifying enzymes, all can contribute to RNA genome corruption and thus generate a question of how RNA viruses maintain their genetic integrity (Barr and Fearns, 2010). It seems that viral RdRps are sufficiently flexible to accommodate alternative initiation mechanisms, enabling terminal repair, terminal transferase activity, and recombinational crosses in the case of damaged key terminal sequences. Among a variety of mechanisms to protect RNA viral genome integrity, recombination allows for exchange of sequences between RNA templates, protecting not only their entire genome, but also their vulnerable termini. A typical example of efficient terminal crossover exchanges is seen within the 3′ noncoding region of BMV RNAs (Bujarski and Kaesberg, 1986). The differences in replicase architecture might affect the predilection of a particular virus for RNA recombination. The molecular aspects of the theory on "adaptable" viral RdRps have not been elucidated and structural studies will contribute to the answers.

METHODS FOR THE DETECTION OF RNA RECOMBINANTS

RNA recombination research concerns both virus evolution (where the most important subject is the detection of recombination imprints among natural viral RNA sequences) and the mechanism of recombination (by using the experimental systems of enhanced recombination frequency). As regards to the evolutionary studies, various computer programs are used for massive comparisons of viral sequences in order to reveal the recombination footprints. The examples of such software include, but are not limited to, Topali, RECCO, GARD, RDP, GENECONV, Chimaera, MaxChi, BOOTSCAN, SISCAN, PHYLPRO, DIPLOMO, SImPlot, Lard, and 3SEQ. These programs can identify the recombination sites among different viral strains, different viral species, and even between the virus and the host (Chare and Holmes, 2006). With advent of next-generation massive sequencing, the genetic diversity of viral RNA genomes can be characterized through the mapping of polymorphisms and measurement of mutation frequencies as well as by detection of recombination events to a single-nucleotide resolution (Routh et al., 2012). Such approach is very sensitive and unbiased, and it can identify hundreds of thousands of recombination events, allowing for a detailed description of RNA crossover profiles.

The detection of recombination events in the laboratory is challenging because RNA–RNA crossovers apparently are rare events and thus the main effort is to elaborate on experimental systems of engineered RNA templates of increased recombination activity. The efficient recovery of recombinants in mixed infections could be achieved by using temperature sensitive mutants, a long-term method used for animal RNA viruses (Hirst, 1962; Pringle, 1970). In whole plants, an important problem is that most recombinants are not competitive with the parental types and therefore disappear. One way to increase recombination rate is by using viral mutants bearing sequence modifications at their UTRs, which decreases the replication abilities of parental molecules, as was used to detect the BMV recombinants (Bujarski and Kaesberg, 1986). Another approach utilizes viral RNAs bearing silent markers or via mixed infections with two low-competing viral strains (e.g., as the used by us mixed infection with both type and Fescue strains of BMV). Other plant virus recombination systems employ mixtures of two parental RNAs with one component carrying a deleterious mutation, e.g., satellite and genomic RNAs of TCV (Zhang et al., 1991), or defective interfering and genomic RNAs of TBSV, Cucumber necrosis virus (CNV) (White and Morris, 1995), and Potato virus X (PVX) (Draghici and Varrelmann, 2010). All these types of recombination systems can be used in cell-free extracts (utilizing viral RdRp preparations), in single-cell (protoplast) hosts, in whole plant hosts, and even in yeast. Some of the systems make use of transient expression vectors by agro-infiltrating plant leaves (Kwon and Rao, 2012).

With these systems in hand, virologists can address such aspects of the RNA recombination process as the essential role of RNA sequence and structure, especially the role of RNA motifs, the function of viral replicase (RdRp) and other viral- and/or host-encoded proteins, or the mutual host–virus effects in short-term virus evolution. The main analytical effort in the recombination experiments is to identify RNA recombination products and to map the location of cross sites. Usually, viral RNAs are extracted and amplified by RT-PCR and the resulting cDNA products are cloned followed by sequencing and/or restriction digestion of a large number of clones. This way the crossovers are detected and mapped within the sequence markers, providing information about both frequency and distribution of recombination events. Proper controls are required to guard against RT-PCR generated recombinants.

FINAL REMARKS: UNANSWERED QUESTIONS AND PERSPECTIVES

Genetic RNA recombination is a major driving force for RNA virus diversity. By understanding the factors and the mechanisms that affect recombination, one can ultimately develop better means for controlling RNA virus infections. In this review I have described the current status of RNA virus recombination research and its future directions. I have also noted its progress over the

last several years emphasizing on some future research venues. Evidently, there is still much to be learned about the mechanistic details of RNA recombination. For example, it is not yet clear how various factors modulate the ability of viral replicase to switch templates, such as the role of RNA template structures, the molecular and structural features of replicase proteins, or the functions of other viral and host factors during cross-over events. Also, the intracellular location of the RNA–RNA template switching has not been confirmed. Besides copy-choice, RNA viruses can recombine with non-replicative RNAs. It is not exactly known what mechanism is responsible for ligation of viral RNA fragments, or where inside the cell this process occurs. RNA viruses were found to recombine with cellular RNAs, but again where in the cell and what factors enable such events, is not well known. And the opposite, the exact steps and the molecular mechanisms of the RNA viral sequence integration with the cellular DNA have not been untangled. Amongst other questions, not much is known about how splicing or active ribozymes can contribute to the RNA virus recombination (Edgell et al., 2011).

From the evolutionary stand point, RNA recombination seems to play a key function during virus speciation and emergence, but its shared contribution that parallels other RNA modification pathways has not yet been assessed. We do not fully understand how RNA viruses achieve their high potential of parasitizing new host species *via* recombination (Domingo, 2010). The entire population of RNA variants that are present in reservoir hosts can now be determined with the tools of next-generation sequencing so that the role of recombinants can be more precisely evaluated (Beerenwinkel et al., 2012).

The frequency of RNA crossing-over varies among RNA virus species and there is little evidence that recombination was favored by natural selection. Because of this and since recombination rates follow the patterns of RNA genome organization, Simon-Loriere and Holmes (2011) postulate that RNA recombination is a by-product of viral genome arrangement acting on selected aspects of the virus life cycle. Thus, according to the authors, RNA recombination does not seem to function as an obligatory form of sex in RNA viruses. Yet further studies are required, especially since Muller's ratchet effects were observed in RNA viruses (Turner, 2003) and the chimeric nature of viral RNAs due to frequent homologous RNA swaps was determined, e.g., in BMV (Urbanowicz et al., 2005).

Despite the above deficiencies, the so far accumulated knowledge about viral RNA recombination has already found some practical applications. For example, measures could be taken to reduce recombination while designing the antiviral resistance in transgenic plants with artificial micro RNAs (Fahim and Larkin, 2013) or with double stranded RNA-expressing transgenes (Zhang et al., 2011). Also, the potential instability and recovery of the wild-type virus *via* recombination can be reduced during construction of plant RNA viral vectors (Nagyová and Subr, 2007).

ACKNOWLEDGMENTS

The author thanks Margaret Bujarska for valuable comments on this manuscript. Jozef J. Bujarski was supported through a grant from the National Science Foundation (MCB-0920617) and through the Plant Molecular Biology Center at Northern Illinois University. The author apologizes to any author that has been omitted in this review for either space reasons or due to the nature of composition of this article.

REFERENCES

Aaziz, R., and Tepfer, M. (1999). Recombination in RNA viruses and in virus-resistant transgenic plants. *J. Gen. Virol.* 80, 1339–1346.

Adams, S. D., Tzeng, W. P., Chen, M. H., and Frey, T. K. (2003). Analysis of intermolecular RNA-RNA recombination by rubella virus. *Virology* 309, 258–271.

Agol, V. I. (2006). Molecular mechanisms of poliovirus variation and evolution. *Curr. Top. Microbiol. Immunol.* 299, 211–259.

Anne, E., and Sela, I. (2005). Occurrence of a DNA sequence of a non-retro RNA virus in a host plant genome and its expression: evidence for recombination between viral and host RNAs. *Virology* 332, 614–622.

Bamunusinghe, D., Seo, J. K., and Rao, A. L. (2011). Subcellular localization and rearrangement of endoplasmic reticulum by Brome mosaic virus capsid protein. *J. Virol.* 85, 2953–2963.

Barr, J. N., and Fearns, R. (2010). How RNA viruses maintain their genome integrity. *J. Gen. Virol.* 91, 1373–1387.

Becher, P., and Tautz, N. (2011). RNA recombination in pestiviruses: cellular RNA sequences in viral genomes highlight the role of host factors for viral persistence and lethal disease. *RNA Biol.* 8, 216–224.

Beerenwinkel, N., Günthard, H. F., VolkerRoth, and Metzner, K. J. (2012). Challenges and opportunities in estimating viral genetic diversity from next-generation sequencing data. *Front. Microbiol.* 3:329. doi: 10.3389/fmicb.2012.00329

Belyi, V. A., Levine, A. J., and Skalka, A. M. (2010). Unexpected inheritance: multiple integrations of ancient bornavirus and ebolavirus/marburgvirus sequences in vertebrate genomes. *PLoS Pathog.* 6:e1001030. doi: 10.1371/journal.ppat.1001030

Berkhout, B. (2011). HIV-1 as RNA evolution machine. *RNA Biol.* 8, 225–229.

Bousalem, M., Douzery, E. J. P., and Fargette, D. (2000). High genetic diversity, distant phylogenetic relationships and intraspecies recombination events among natural populations of Yam mosaic virus: a contribution to understanding potyvirus evolution. *J. Gen. Virol.* 81, 243–255.

Breyer, W. A., and Matthews, B. W. (2001). A structural basis for processivity. *Protein Sci.* 10, 1699–1711.

Bujarski, J. J., and Kaesberg, P. (1986). Genetic recombination between RNA components of a multipartite plant virus. *Nature* 321, 528–531.

Chare, E. R., and Holmes, E. C. (2006). A phylogenetic survey of recombination frequency in plant RNA viruses. *Arch. Virol.* 151, 933–946.

Chetverin, A. B., Chetverina, H. V., Demidenko, A. A., and Ugarov, V. I. (1997). Nonhomologous RNA recombination in a cell-free system: evidence for a transesterification-mechanism guided by secondary structure. *Cell* 88, 503–513.

Chetverin, A. B., Kopein, D. S., Chetverina, H. V., Demidenko, A. A., and Ugarov, V. I. (2005). Viral RNA-directed RNA polymerases use diverse mechanisms to promote recombination between RNA molecules. *J. Biol. Chem.* 280, 8748–8755.

Combelas, N., Holmblat, B., Joffret, M. L., Colbère-Garapin, F., and Delpeyroux, F. (2011). Recombination between poliovirus and coxsackie A viruses of species C: a model of viral genetic plasticity and emergence. *Viruses* 3, 1460–1484.

Crochu, S., Cook, S., Attoui, H., Charrel, R. N., De Chesse, R., Belhouchet, M., et al. (2004). Sequences of flavivirus-related RNA viruses persist in DNA form integrated in the genome of Aedes spp. mosquitoes. *J. Gen. Virol.* 85, 1971–1980.

Davidson, I., and Silva, R. F. (2008). Creation of diversity in the animal virus world by inter-species and intra-species recombinations: lessons learned from poultry viruses. *Virus Genes* 36, 1–9.

Delviks-Frankenberry, K., Galli, A., Nikolaitchik, O., Mens, H., Pathak, V. K., and Hu, W. S. (2011). Mechanisms and factors that

influence high frequency retroviral recombination. *Viruses* 3, 1650–1680.

den Boon, J. A., Diaz, A., and Ahlquist, P. (2010). Cytoplasmic viral replication complexes. *Cell Host Microbe.* 8, 77–85.

Desbiez, C., and Lecoq, H. (2004). The nucleotide sequence of watermelon mosaic virus (WMV, Potyvirus) reveals interspecific recombination between two related potyviruses in the 5_ part of the genome. *Arch. Virol.* 149, 1619–1632.

Domier, L. L., McCoppin, NK, Larsen, R. C., and D'Arcy, C. J. (2002). Nucleotide sequence shows that bean leafroll virus has a luteovirus-like genome organization. *J. Gen. Virol.* 83, 1791–1798.

Domingo, E. (2010). Mechanisms of viral emergence. *Vet. Res.* 41, 38–45.

Draghici, H.-K., and Varrelmann, M. (2010). Evidence for similarity-assisted recombination and predicted stemloop structure determinant in potato virus X RNA recombination. *J. Gen. Virol.* 91, 552–562.

Dzianott, A., Flasinski, S., and Bujarski, J. J. (1995). Foreign complementary sequences facilitate genetic RNA recombination in brome mosaic virus. *Virology* 208, 370–375.

Dzianott, A., Sztuba-Solinska, J., and Bujarski, J. J. (2012). Mutations in the antiviral RNAi defense pathway modify Brome mosaic virus RNA recombinant profiles. *Mol. Plant Microbe Interact.* 25, 97–106.

Edgell, D. R., Chalamcharla, V. R., and Belfort, M. (2011). Learning to live together: mutualism between self-slicing introns and their hosts. *BMC Biol.* 9:22. doi: 10.1186/1741-7007-9-22

Elena, S. F., Bedhomme, S., Carrasco, P., Cuevas, J. M., de la Iglesia, F., Lafforgue, G., et al. (2011). The evolutionary genetics of emerging plant RNA viruses. *Mol. Plant Microbe Interact.* 24, 287–293.

Fahim, M., and Larkin, P. J. (2013). Designing effective amiRNA and multimeric amiRNA against plant viruses. *Methods Mol. Biol.* 942, 357–377.

Figlerowicz, M., and Bujarski, J. J. (1998). RNA recombination in brome mosaic virus, a model plus strand RNA virus. *Acta Biochim. Pol.* 45, 847–868.

Galetto, R., Giacomoni, V., Véron, M., and Negroni, M. (2006). Dissection of a circumscribed recombination hot spot in HIV-1 after a single infectious cycle. *J. Biol. Chem.* 281, 2711–2720.

Garcia-Ruiz, H., and Ahlquist, P. (2006). Inducible yeast system for Viral RNA recombination reveals requirement for an RNA replication signal on both parental RNAs. *J. Virol.* 80, 8316–8328.

Geuking, M. B., Weber, J., Dewannieux, M., Gorelik, E., Heidmann, T., Hengartner, H., et al. (2009). Recombination of retrotransposon and exogenous RNA virus results in nonretroviral cDNA integration. *Science* 323, 393–396.

Gmyl, A. P., Belousov, E. V., Maslova, S. V., Khitrina, E. V., Chetverin, A. B., and Agol, V. I. (1999). Non-replicative RNA recombination in poliovirus. *J. Virol.* 73, 8958–8965.

González-Candelas, F., López-Labrador, F., and Bracho, M. A. (2011). Recombination in hepatitis C virus. *Viruses* 3, 2006–2024.

Hirst, G. K. (1962). Genetic recombination with Newcastle disease virus, polioviruses, and influenza. *Cold Spring Harb. Symp. Quant. Biol.* 27, 303–309.

Horie, M., Honda, T., Suzuki, Y., Kobayashi, Y., Daito, T., Oshida, T., et al. (2010). Endogenous non-retroviral RNA virus elements in mammalian genomes. *Nature* 463, 84–87.

Jaag, H. M., Lu, Q., Schmitt, M. E., and Nagy, P. D. (2011). Role of RNase MRP in viral RNA degradation and RNA recombination. *J. Virol.* 85, 243–253.

Jaag, H. M., and Nagy, P. D. (2009). Silencing of Nicotiana benthamiana Xrn4p exoribonuclease promotes tombusvirus RNAaccumulation and recombination. *Virology* 386, 344–352.

Jaag, H. M., and Nagy, P. D. (2010). The combined effect of environmental and host factors on the emergence of viral RNA recombinants. *PLoS Pathog.* 6:e1001156. doi: 10.1371/journal.ppat.1001156

Jacquemond, M. (2012). Cucumber mosaic virus. *Adv. Virus Res.* 84, 439–504.

Jiang, Y., Cheng, C. P., Serviene, E., Shapka, N., and Nagy, P. D. (2010). Repair of lost 5′ terminal sequences in tombusviruses: rapid recovery of promoter- and enhancer-like sequences in recombinant RNAs. *Virology* 404, 96–105.

Kim, M. J., and Kao, C. (2001). Factors regulating template switch *in vitro* by viral RNA-dependent RNA polymerases: implications for RNA-RNA recombination. *Proc. Natl. Acad. Sci. U.S.A.* 98, 4972–4977.

Konstantinova, P., ter Brake, O., Haasnoot, J., de Haan, P., and Berkhout, B. (2007). Trans-inhibition of HIV-1 by a long hairpin RNA expressed within the viral genome. *Retrovirology* 1, 4–15.

Kwon, S. J., and Rao, A. L. (2012). Emergence of distinct brome mosaic virus recombinants is determined by the polarity of the inoculum RNA. *J. Virol.* 86, 5204–5220.

Laliberté, J. F., and Sanfaçon, H. (2010). Cellular remodeling during plant virus infection. *Annu. Rev. Phytopathol.* 48, 69–91.

Lloyd, R. E. (2012). How do viruses interact with stress-associated RNA granules? *PLoS Pathog.* 8:e1002741. doi: 10.1371/journal.ppat.1002741

Lukashev, A. N. (2010). Recombination among picornaviruses. *Rev. Med. Virol.* 20, 327–337.

Lutay, A. V., Zenkova, M. A., and Vlassov, V. V. (2007). Nonenzymatic recombination of RNA: possible mechanism for the formation of novel sequences. *Chem. Biodivers.* 4, 762–767.

Maori, E., Lavi, S., Mozes-Koch, R., Gantman, Y., Peretz, Y., Edelbaum, O., et al. (2007). Isolation and characterization of Israeli acute paralysis virus, a dicistrovirus affecting honeybees in Israel: evidence for diversity due to intra- and inter-species recombination. *J. Gen. Virol.* 88, 3428–3438.

Mayo, M. A., and Jolly, C. A. (1991). The 5′-terminal sequence of potato leafroll virus RNA: evidence of recombination between virus and host RNA. *J. Gen. Virol.* 72, 2591–2595.

Mine, A., and Okuno, T. (2012). Composition of plant virus RNA replicase complexes. *Curr. Opin. Virol.* 2, 663–669.

Moonan, F., Molina, J., and Mirkov, T. E. (2000). Sugarcane yellow leaf virus: an emerging virus that has evolved by recombination between luteoviral and poleroviral ancestors. *Virology* 269, 156–171.

Moreno, I. M., Malpica, J. M., Díaz-Pendo, J. A., Moriones, E., Fraile, A., and Garcia-Arenal, F. (2004). Variability and genetic structure of the population of watermelon mosaic virus infecting melon in Spain. *Virology* 318, 451–460.

Mosley, R. T., Edwards, T. E., Murakami, E., Lam, A. M., Grice, R. L., Du, J., et al. (2012). Structure of hepatitis C virus polymerase in complex with primer-template RNA. *J. Virol.* 86, 6503–6511.

Moustafa, I. M., Shen, H., Morton, B., Colina, C. M., and Cameron, C. E. (2011). Molecular dynamics simulations of viral RNA polymerases link conserved and correlated motions of functional elements to fidelity. *J. Mol. Biol.* 410, 159–181.

Nagy, P. D. (2011). The roles of host factors in tombusvirus RNA recombination. *Adv. Virus Res.* 81, 63–84.

Nagy, P. D., and Bujarski, J. J. (1993). Targeting the site of RNA-RNA recombination in brome mosaic virus with antisense sequences. *Proc. Natl. Acad. Sci. U.S.A.* 90, 6390–6394.

Nagy, P. D., Ogiela, C., and Bujarski, J. J. (1999a). Mapping sequences active in homologous RNA recombination in brome mosaic virus: prediction of recombination hot spots. *Virology* 254, 92–104.

Nagy, P. D., Pogany, J., and Simon, A. E. (1999b). RNA elements required for RNA recombination function as replication enhancers *in vitro* and *in vivo* in a plus-strand RNA virus. *EMBO J.* 18, 5653–5665.

Nagy, P. D., and Pogany, J. (2011). The dependence of viral RNA replication on co-opted host factors. *Nat. Rev. Microbiol.* 10, 137–149.

Nagy, P. D., and Simon, A. E. (1997). New insights into the mechanisms of RNA recombination. *Virology* 235, 1–9.

Nagyová, A., and Subr, Z. (2007). Infectious full-length clones of plant viruses and their use for construction of viral vectors. *Acta Virol.* 51, 223–237.

Nikolaitchik, O. A., Galli, A., Moore, M. D., Pathak, V. K., and Hu, W.-S. (2011). Multiple Barriers to Recombination between Divergent HIV-1 Variants Revealed by a Dual-Marker recombination assay. *J. Mol. Biol.* 407, 521–531.

Nishikiori, M., Sugiyama, S., Xiang, H., Niiyama, M., Ishibashi, K., Inoue, T., et al. (2012). Crystal structure of the superfamily 1 helicase from Tomato mosaic virus. *J. Virol.* 86, 7565–7576.

Noueiry, A. O., and Ahlquist, P. (2003). Brome mosaic virus RNA replication: revealing the role of the host in RNA virus replication. *Annu. Rev. Phytopathol.* 41, 77–98.

Nuss, D. L. (2011). Mycoviruses, RNA silencing, and viral RNA recombination. *Adv. Virus Res.* 80, 25–48.

Pagán, I., and Holmes, E. C. (2010). Long-term evolution of the Luteoviridae: time scale and mode of virus speciation. *J. Virol.* 84, 6177–6187.

Pond, S. L., Murrell, B., and Poon, A. F. (2012). Evolution of viral genomes: interplay between selection, recombination, and other forces. *Methods Mol. Biol.* 856, 239–272.

Pringle, C. R. (1970). Genetic characteristics of conditional lethal

mutants of vesicular stomatitis virus induced by 5-fluorouracil, 5-azacytidine and ethyl methane sulfonate. *J. Virol.* 5, 559–567.

Routh, A., Ordoukhanian, P., and Johnson, J. E. (2012). Nucleotide-resolution profiling of RNA recombination in the encapsidated genome of a eukaryotic RNA virus by next-generation sequencing. *J. Mol. Biol.* 424, 257–269.

Savolainen-Kopra, C., and Blomqvist, S. (2010). Mechanisms of genetic variation in polioviruses. *Rev. Med. Virol.* 20, 358–371.

Serviene, E., Shapka, N., Cheng, C. P., Panavas, T., Phuangrat, B., Baker, J., et al. (2005). Genome-wide screen identifies host genes affecting viral RNA recombination. *Proc. Natl. Acad. Sci. U.S.A.* 102, 10545–10550.

Silva, T. F., Corrêa, R. L., Castilho, Y., Silvie, P., Bélot, J. L., and Vaslin, M. F. (2008). Widespread distribution and a new recombinant species of Brazilian virus associated with cotton blue disease. *Virol. J.* 5:123. doi: 10.1186/1743-422X-5-123

Simon-Loriere, E., and Holmes, E. C. (2011). Why do RNA viruses recombine? *Nat. Rev. Microbiol.* 9, 617–626.

Subba-Reddy, C. V., Yunus, M. A., Goodfellow, I. G., and Kao, C. C. (2012). Norovirus RNA synthesis is modulated by an interaction between the viral RNA-dependent RNA polymerase and the major capsid protein, VP1. *J. Virol.* 86, 10138–10149.

Sun, Q., Choi, G. H., and Nuss, D. L. (2009). A single Argonaute gene is required for induction of RNA silencing antiviral defense and promotes viral RNA recombination. *Proc. Natl. Acad. Sci. U.S.A.* 106, 17927–17932.

Sztuba-Solinska, J., Fanning, S. W., Horn, J. R., and Bujarski, J. J. (2012). Mutations in the coat protein-binding cis-acting RNA motifs debilitate RNA recombination of Brome mosaic virus. *Virus Res.* 170, 138–149.

Sztuba-Solinska, J., Urbanowicz, A., Figlerowicz, M., and Bujarski, J. J. (2011). RNA-RNA recombination in plant virus replication and evolution. *Annu. Rev. Phytopathol.* 49, 415–443.

Takeshita, D., and Tomita, K. (2010). Assembly of Q{beta} viral RNA polymerase with host translational elongation factors EF-Tu and -Ts. *Proc. Natl. Acad. Sci. U.S.A.* 107, 15733–15738.

Tanne, E., and Sela, I. (2005). Occurrence of a DNA sequence of a non-retro RNA virus in a host plant genome and its expression: evidence for recombination between viral and host RNAs. *Virology* 332, 614–622.

Turner, P. E. (2003). Searching for the advantages of virus sex. *Orig. Life Evol. Biosph.* 33, 95–108.

Turturo, C., Friscina, A., Gaubert, S., Jacquemond, M., Thompson, J. R., and Tepfer, M. (2008). Evaluation of potential risks associated with recombination in transgenic plants expressing viral sequences. *J. Gen. Virol.* 89, 327–335.

Urbanowicz, A., Alejska, M., Formanowicz, P., Blazewicz, J., Figlerowicz, M., and Bujarski, J. J. (2005). Homologous crossovers among molecules of brome mosaic bromovirus RNA1 or RNA2 segments *in vivo*. *J. Virol.* 79, 5732–5742.

Valli, A., López-Moya, J. J., and García, J. A. (2007). Recombination and gene duplication in the evolutionary diversification of P1 proteins in the family Potyviridae. *J. Gen. Virol.* 88, 1016–1028.

van der Hoek, L., Back, N., Jebbink, M. F., de Ronde, A., Bakker, M., Jurriaans, S., et al. (2005). Increased multinucleoside drug resistance and decreased replicative capacity of a human immunodeficiency virus type 1 variant with an 8-amino-Acid insert in the reverse transcriptase. *J. Virol.* 79, 3536–3543.

Visser, J. C., and Bellstedt, D. U. (2009). An assessment of molecular variability and recombination patterns in South African isolates of potato virus Y. *Arch. Virol.* 154, 1891–1900.

White, K. A., and Morris, T. J. (1995). RNA determinants of junction site selection in RNA virus recombinants and defective interfering RNAs. *RNA* 1, 1029–1040.

Wierzchoslawski, R., Dzianott, A., and Bujarski, J. (2004). Dissecting the requirement for subgenomic promoter sequences by RNA recombination of brome mosaic virus *in vivo*: evidence for functional separation of transcription and recombination. *J. Virol.* 78, 8552–8564.

Woo, P. C., Lau, S. K., Huang, Y., and Yuen, K. Y. (2009). Coronavirus diversity, phylogeny and interspecies jumping. *Exp. Biol. Med. (Maywood)* 234, 1117–1127.

Yamasaki, S., Sakai, J., Fuji, S., Kamisoyama, S., Emoto, K., Ohshima, K., et al. (2010). Comparisons among isolates of sweet potato feathery mottle virus using complete genomic RNA sequences. *Arch. Virol.* 155, 795–800.

Zemer, R., Kitay Cohen, Y., Naftaly, T., and Klein, A. (2008). Presence of hepatitis C virus DNA sequences in the DNA of infected patients. *Eur. J. Clin. Invest.* 38, 845–848.

Zhang, C. X., Cascone, P. J., and Simon, A. E. (1991). Recombination between satellite and genomic RNAs of turnip crinkle virus. *Virology* 184, 791–794.

Zhang, X., Sato, S., Ye, X., Dorrance, A. E., Morris, T. J., Clemente, T. E., et al. (2011). Robust RNAi-based resistance to mixed infection of three viruses in soybean plants expressing separate short hairpins from a single transgene. *Phytopathology* 101, 1264–1269.

Conflict of Interest Statement: The author declares that the research was conducted in the absence of any commercial or financial relationships that could be construed as a potential conflict of interest.

Received: 13 December 2012; accepted: 11 March 2013; published online: 26 March 2013.

*Citation: Bujarski JJ (2013) Genetic recombination in plant-infecting messenger-sense RNA viruses: overview and research perspectives. Front. Plant Sci. **4**:68. doi: 10.3389/fpls.2013.00068*

This article was submitted to Frontiers in Plant-Microbe Interaction, a specialty of Frontiers in Plant Science.